

NASA SP-7037 (319)
July 1995

p-133

AERONAUTICAL ENGINEERING

A CONTINUING BIBLIOGRAPHY WITH INDEXES

(NASA-SP-7037(319)) AERONAUTICAL
ENGINEERING: A CONTINUING
BIBLIOGRAPHY WITH INDEXES
(SUPPLEMENT 319) (NASA) 133 p

N96-10985

Unclass

00/01 0065431



National Aeronautics and
Space Administration

Scientific and Technical
Information Office

The NASA STI Office ... in Profile

Since its founding, NASA has been dedicated to the advancement of aeronautics and space science. The NASA Scientific and Technical Information (STI) Office plays a key part in helping NASA maintain this important role.

The NASA STI Office provides access to the NASA STI Database, the largest collection of aeronautical and space science STI in the world. The Office is also NASA's institutional mechanism for disseminating the results of its research and development activities.

Specialized services that help round out the Office's diverse offerings include creating custom thesauri, translating material to or from 34 foreign languages, building customized databases, organizing and publishing research results ... even providing videos.

For more information about the NASA STI Office, you can:

- **Phone** the NASA Access Help Desk at (301) 621-0390
- **Fax** your question to the NASA Access Help Desk at (301) 621-0134
- **E-mail** your question via the **Internet** to help@sti.nasa.gov
- **Write** to:

NASA Access Help Desk
NASA Center for AeroSpace Information
800 Elkridge Landing Road
Linthicum Heights, MD 21090-2934

NASA SP-7037 (319)

July 1995

AERONAUTICAL ENGINEERING

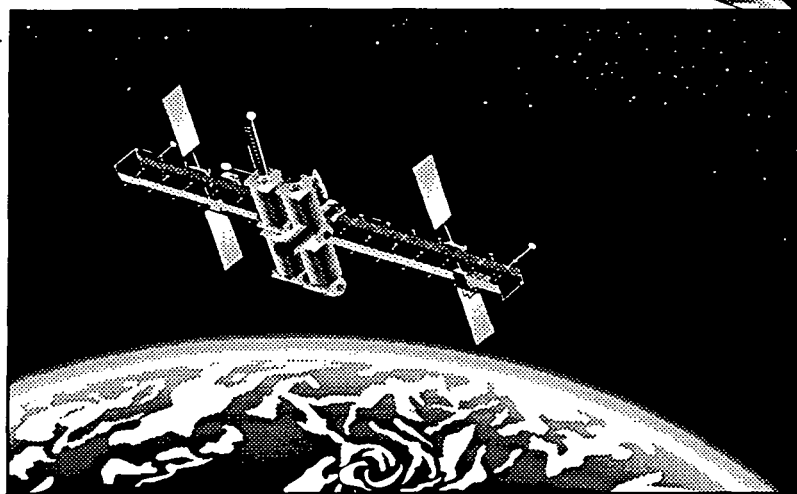
A CONTINUING BIBLIOGRAPHY WITH INDEXES



National Aeronautics and Space Administration
Scientific and Technical Information Office
Washington, DC

1995

The New NASA Video Catalog is Here



Free!

To order your free copy call
the NASA Access Help Desk at
(301) 621-0390 or
fax to (301) 621-0134 or
e-mail to helpdesk@sti.nasa.gov

EXPLORE THE UNIVERSE

This publication was prepared by the NASA Center for Aerospace Information,
800 Elkridge Landing Road, Linthicum Heights, MD 21090-2934, (301) 621-0390.

INTRODUCTION

This issue of *Aeronautical Engineering — A Continuing Bibliography with Indexes* (NASA SP-7037) lists 349 reports, journal articles, and other documents recently announced in the NASA STI Database.

Accession numbers cited in this issue include:

Scientific and Technical Aerospace Reports (STAR) (N-10000 Series)

Open Literature (A-60000 Series)

N95-22478 — N95-24194

A95-73327 — A95-77372

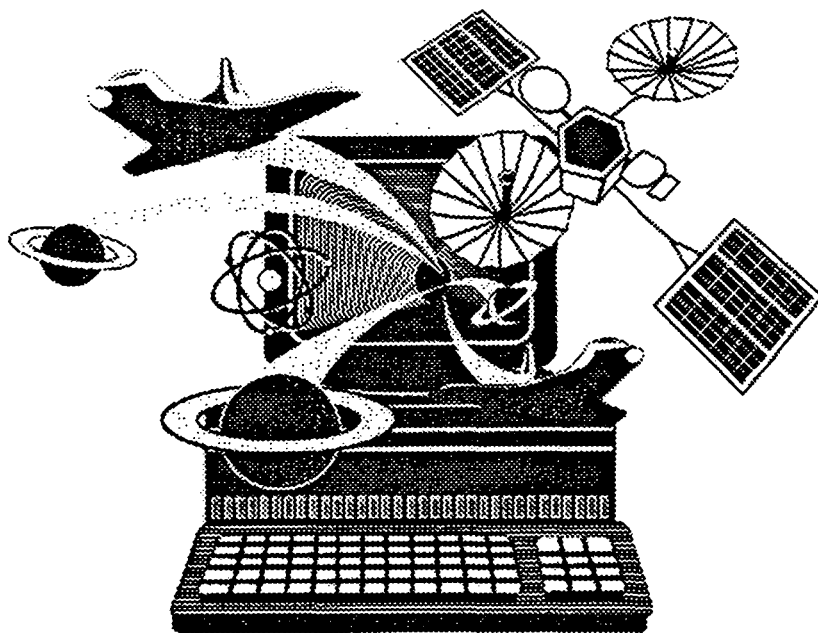
The coverage includes documents on the engineering and theoretical aspects of design, construction, evaluation, testing, operation, and performance of aircraft (including aircraft engines) and associated components, equipment, and systems. It also includes research and development in aerodynamics, aeronautics, and ground support equipment for aeronautical vehicles.

Each entry in the publication consists of a standard bibliographic citation accompanied, in most cases, by an abstract. The listing of the entries is arranged by the first nine *STAR* specific categories and the remaining *STAR* major categories. This arrangement offers the user the most advantageous breakdown for individual objectives. The citations include the original accession numbers from the respective announcement journals.

Seven indexes—subject, personal author, corporate source, foreign technology, contract number, report number, and accession number—are included.

A cumulative index for 1995 will be published in early 1996.

The NASA CASI price code table, addresses of organizations, and document availability information are located at the back of this issue.



SCAN Goes Electronic!

If you have NASA Mail or if you can access the Internet, you can get biweekly issues of *SCAN* delivered to your desk—top absolutely free!

Electronic SCAN takes advantage of computer technology to alert you to the latest aerospace-related, worldwide scientific and technical information that has been published.

No more waiting while the paper copy is printed and mailed to you. You can review *Electronic SCAN* the same day it is released! And you get all 191—or any combination of—subject areas of announcements with abstracts to browse at your leisure. When you locate a publication of interest, you can print the announcement or electronically add it to your publication order list.

Electronic SCAN
Timely
Flexible
Complete
Free!

For instant access via Internet:

<ftp.sti.nasa.gov>
<gopher.sti.nasa.gov>
listserv@sti.nasa.gov

For additional information:

e-mail: help@sti.nasa.gov
scan@sti.nasa.gov

(Enter this address on the "To" line. Leave the subject line blank and send. You will receive an automatic reply with instructions in minutes.)

Phone: (301) 621-0390 Fax: (301) 621-0134

Write: NASA Access Help Desk
NASA STI Office
NASA Center for AeroSpace Information
800 Elkridge Landing Road
Linthicum Heights, MD 21090-2934



National Aeronautics and
Space Administration

Scientific and Technical
Information Office

TABLE OF CONTENTS

Category 01	Aeronautics	261
Category 02	Aerodynamics Includes aerodynamics of bodies, combinations, wings, rotors, and control surfaces; and internal flow in ducts and turbomachinery.	262
Category 03	Air Transportation and Safety Includes passenger and cargo air transport operations; and aircraft accidents.	276
Category 04	Aircraft Communications and Navigation Includes digital and voice communication with aircraft; air navigation systems (satellite and ground based); and air traffic control.	278
Category 05	Aircraft Design, Testing and Performance Includes aircraft simulation technology.	280
Category 06	Aircraft Instrumentation Includes cockpit and cabin display devices; and flight instruments.	286
Category 07	Aircraft Propulsion and Power Includes prime propulsion systems and systems components, e.g., gas turbine engines and compressors; and onboard auxiliary power plants for aircraft.	288
Category 08	Aircraft Stability and Control Includes aircraft handling qualities; piloting; flight controls; and autopilots.	290
Category 09	Research and Support Facilities (Air) Includes airports, hangars and runways; aircraft repair and overhaul facilities; wind tunnels; shock tubes; and aircraft engine test stands.	295
Category 10	Astronautics Includes astronautics (general); astrodynamics; ground support systems and facilities (space); launch vehicles and space vehicles; space transportation; space communications, spacecraft communications, command and tracking; spacecraft design, testing and performance; spacecraft instrumentation; and spacecraft propulsion and power.	297
Category 11	Chemistry and Materials Includes chemistry and materials (general); composite materials; inorganic and physical chemistry; metallic materials; nonmetallic materials; propellants and fuels; and materials processing.	300
Category 12	Engineering Includes engineering (general); communications and radar; electronics and electri- cal engineering; fluid mechanics and heat transfer; instrumentation and photogra- phy; lasers and masers; mechanical engineering; quality assurance and reliability; and structural mechanics.	304

Category 13 Geosciences	316
Includes geosciences (general); earth resources and remote sensing; energy production and conversion; environment pollution; geophysics; meteorology and climatology; and oceanography.	
Category 14 Life Sciences	N.A.
Includes life sciences (general); aerospace medicine; behavioral sciences; man/system technology and life support; and space biology.	
Category 15 Mathematical and Computer Sciences	321
Includes mathematical and computer sciences (general); computer operations and hardware; computer programming and software; computer systems; cybernetics; numerical analysis; statistics and probability; systems analysis; and theoretical mathematics.	
Category 16 Physics	323
Includes physics (general); acoustics; atomic and molecular physics; nuclear and high-energy; optics; plasma physics; solid-state physics; and thermodynamics and statistical physics.	
Category 17 Social Sciences	N.A.
Includes social sciences (general); administration and management; documentation and information science; economics and cost analysis; law, political science, and space policy; and urban technology and transportation.	
Category 18 Space Sciences	N.A.
Includes space sciences (general); astronomy; astrophysics; lunar and planetary exploration; solar physics; and space radiation.	
Category 19 General	325

Subject Index	A-1
Personal Author Index	B-1
Corporate Source Index	C-1
Foreign Technology Index	D-1
Contract Number Index	E-1
Report Number Index	F-1
Accession Number Index	G-1
Appendix	APP-1

TYPICAL REPORT CITATION AND ABSTRACT

NASA SPONSORED

↓
ON MICROFICHE

ACCESSION NUMBER → N95-10318*# Dow Chemical Co., Midland, MI. ← CORPORATE SOURCE
 TITLE → NOVEL MATRIX RESINS FOR COMPOSITES FOR AIRCRAFT
 PRIMARY STRUCTURES, PHASE 1 Final Report, Apr. 1989 -
 Mar. 1992
 AUTHORS → EDMUND P. WOO, P. M. PUCKETT, S. MAYNARD, M. T. BISHOP,
 K. J. BRUZA, J. P. GODSCHALX, AND M. J. MULLINS Aug. 1992 ← PUBLICATION DATE
 164 p
 CONTRACT NUMBERS → (Contracts NAS1-18841; RTOP 510-02-11-02)
 REPORT NUMBERS → (NASA-CR-189657; NAS 1.26:189657) Avail: CASI HCA08/MFA02 ← AVAILABILITY AND
 PRICE CODE

The objective of the contract is the development of matrix resins with improved processability and properties for composites for primarily aircraft structures. To this end, several resins/systems were identified for subsonic and supersonic applications. For subsonic aircraft, a series of epoxy resins suitable for RTM and powder prepreg was shown to give composites with about 40 ksi compressive strength after impact (CAI) and 200 F/wet mechanical performance. For supersonic applications, a thermoplastic toughened cyanate prepreg system has demonstrated excellent resistance to heat aging at 360 F for 4000 hours, 40 ksi CAI and useful mechanical properties at greater than or equal to 310 F. An AB-BCB-maleimide resin was identified as a leading candidate for the HSCT. Composite panels fabricated by RTM show CAI of approximately 50 ksi, 350 F/wet performance and excellent retention of mechanical properties after aging at 400 F for 4000 hours. Author

TYPICAL JOURNAL ARTICLE CITATION AND ABSTRACT

NASA SPONSORED

↓

ACCESSION NUMBER → A95-60192* National Aeronautics and Space Administration. Ames. ← CORPORATE SOURCE
 Research Center, Moffett Field, CA.
 TITLE → AERODYNAMIC INTERACTIONS BETWEEN A ROTOR AND
 WING IN HOVER
 AUTHORS → FORT F. FELKER NASA. Ames Research Center, Moffett Field, ← AUTHOR'S AFFILIATION
 CA, US and JEFFREY S. LIGHT NASA. Ames Research Center,
 Moffett Field, CA, US Journal of the American Helicopter Society ← JOURNAL TITLE
 PUBLICATION DATE → 2 Jun. 1986 p. 53-61
 REPORT NUMBER → (HTN-94-00714) Copyright

An experimental investigation of rotor/wing aerodynamic interactions in hover is described. The investigation consisted of both a large-scale and a small-scale test. A 0.658-scale V-22 rotor and wing was used in the large-scale test. Wing download, wing surface pressure, rotor performance, and rotor downwash data from the large-scale test are presented. A small-scale experiment was conducted to determine how changes in the rotor/wing geometry affected the aerodynamic interactions. These geometry variations included the distance between the rotor and wing, wing incidence angle, wing flap angle, rotor rotation direction, and configurations both with the rotor axis at the tip of the wing (tilt rotor configuration) and with the rotor axis at the center of the wing (compound helicopter configuration). Author (Hemer)

AERONAUTICAL ENGINEERING

A Continuing Bibliography (Suppl. 319)

July 1995

01

AERONAUTICS (GENERAL)

A95-74042* National Aeronautics and Space Administration. Langley Research Center, Hampton, VA.

OPTIMIZATION OF CONTOURED HYPERSONIC SCRAMJET INLETS WITH A LEAST-SQUARES PARABOLIZED NAVIER-STOKES PROCEDURE

J. J. KORTE NASA. Langley Research Center, Hampton, VA, US and A. H. AUSLENDER Lockheed Engineering and Sciences Company, Hampton, VA, US Computing Systems in Engineering (ISSN 0956-0521) vol. 4, no. 1 February 1993 p. 13-26 (HTN-95-20976) Copyright

A new optimization procedure, in which a parabolized Navier-Stokes solver is coupled with a non-linear least-squares optimization algorithm, is applied to the design of a Mach 14, laminar two-dimensional hypersonic subscale flight inlet with an internal contraction ratio of 15:1 and a length-to-throat half-height ratio of 150:1. An automated numerical search of multiple geometric wall contours, which are defined by polynomial splines, results in an optimal geometry that yields the maximum total-pressure recovery for the compression process. Optimal inlet geometry is obtained for both inviscid and viscous flows, with the assumption that the gas is either calorically or thermally perfect. The analysis with a calorically perfect gas results in an optimized inviscid inlet design that is defined by two cubic splines and yields a mass-weighted total-pressure recovery of 0.787, which is a 23% improvement compared with the optimized shock-canceled two-ramp inlet design. Similarly, the design procedure obtains the optimized contour for a viscous calorically perfect gas to yield a mass-weighted total-pressure recovery value of 0.749. Additionally, an optimized contour for a viscous thermally perfect gas is obtained to yield a mass-weighted total-pressure recovery value of 0.768. The design methodology incorporates both complex fluid dynamic physics and optimal search techniques without an excessive compromise of computational speed; hence, this methodology is a practical technique that is applicable to optimal inlet design procedures. Author (Herner)

A95-75752

AUTOMATIC RIVETING CELL FOR COMMERCIAL AIRCRAFT FLOOR GRID ASSEMBLY

NIGEL R. ROCHE Deutsche Aerospace Airbus GmbH Aerospace Engineering (Warrendale, Pennsylvania) (ISSN 0736-2536) vol. 15, no. 1 January-February 1995 p. 7-10 (BTN-95-EIX95182617807) Copyright

A new floor grid structure assembly cell was created to allow manufacture of the A330/A340 widebody program into the Airbus manufacturing process. The cell is composed of three stations. Manufacturing in stations 1 and 3 is done manually, while operations are automated in station 2. The main part of the automatic station is a five-axis traveling-column robot with automatically changeable tools. These tools are Cherry Buck riveting machines and drilling machines. The riveting machines have a mass up to 350 kg, and perform drilling, sealing, installing, and closing operations in programmed sequences. EI

A95-75753

MAINTENANCE CHALLENGES AND TRENDS

LINDA E. TREGO Aerospace Engineering (Warrendale, Pennsylvania) (ISSN 0736-2536) vol. 15, no. 1 January-February 1995 p. 11-14

(BTN-95-EIX95182617808) Copyright

Airlines are faced with an increasing number of maintenance challenges. In the case of Delta Airlines, their approach to these challenges is a process of reengineering which consists of a review of all activities, and elimination of work that does add value to the process. This includes the examination of airlines's maintenance activities such as HMTVs (heavy maintenance visits, or 'D' checks) and engine overhauls, and revising processes to eliminate all unnecessary work. By changing the way HMTVs are performed, Delta eliminated the time needed to accomplish B-757 HMTVs by 20%, and reduced work hours to 20%. EI

A95-75754

MAINTENANCE PROGRAMS

LINDA E. TREGO Aerospace Engineering (Warrendale, Pennsylvania) (ISSN 0736-2536) vol. 15, no. 1 January-February 1995 p. 15-20

(BTN-95-EIX95182617809) Copyright

Although maintenance programs differ among airlines and for different aircraft, the same fundamental maintenance requirements apply to all. The method for determining the maintenance program for a system/powerplant including the APU is by using MSG-3, a progressive logic diagram that is applied to the aircraft's MSI (maintenance significant items). The basic planning requirements are derived from the Maintenance Steering Group (MSG-3), which is task oriented. MSIs are those significant items whose failure could 1) affect safety (on ground or flight) and 2) be undetectable or are not likely to be detected during operations, and/or 3) have significant operational impact, and/or 4) have significant economic impact. EI

A95-75756

CONDITION MONITORING AND DIAGNOSTICS

Aerospace Engineering (Warrendale, Pennsylvania) (ISSN 0736-2536) vol. 15, no. 1 January-February 1995 p. 25-26

(BTN-95-EIX95182617811) Copyright

Condition monitoring and diagnostics is being utilized by engineers to detect faults, maintain conditions within certain limits, predict possible future behavior, and improve the future design of aircraft and their subsystems. It has been defined as a field in which physical parameters of an operating machine are periodically or continuously sensed, measured, and recorded for the purpose of reducing, analyzing, comparing, and displaying data, and ultimately to support decisions related to the operation and maintenance of the machine. EI

A95-76765

CALCULATION OF WING-ALONE AERODYNAMICS TO HIGH ANGLES OF ATTACK

F. G. MOORE Naval Surface Warfare Cent, Dahlgren, VA, United States and R. M. MCINVILLE Journal of Spacecraft and Rockets (ISSN 0022-4650) vol. 32, no. 1 January-February 1995

A
B
S
T
R
A
C
T
S

01 AERONAUTICS (GENERAL)

p. 187-190 refs
(BTN-95-EIX95212645713) Copyright

A fourth-order semiempirical method has been developed to estimate wing-alone aerodynamics at all Mach numbers and angles of attack. The method utilizes the linearized theory approaches of the National Space Science Data Center (NSWCDD) Aeroprediction Code along with wing-alone data bases to evaluate constants needed in the fourth-order equation. In deriving the new method, many extrapolations were needed at low Mach numbers and high aspect ratios (ARs). As a result, additional accurate wing-alone wind-tunnel data are needed for $AR = 4.0$, $\lambda = 1.0$, at all Mach numbers and M less than 1.5, α greater than 30 deg, at all ARs.

EI

N95-23506# AVRO International Aerospace, Woodford (England). Engineering Test Facilities.

HEALTH AND USAGE MONITORING SYSTEMS: CORROSION SURVEILLANCE

J. D. SMART and D. C. WEETMAN (Real Time Corrosion Management Ltd., Grandby Row, England.) In AGARD, Corrosion Detection and Management of Advanced Airframe Materials 11 p Jan. 1995

Copyright Avail: CASI HC A03/MF A03

A predictive method of determining the inspection requirements for specific areas of individual aircraft could offer major advantages in terms of safety and maintenance and repair costs. An approach such as Health and Usage Monitoring in Service, in which the condition of components is monitored whilst in operation, would allow inspection requirements to be minimized and maintenance to be carried out as it becomes necessary. To use such an approach on aircraft would require very sensitive monitoring techniques. Modern electrochemical corrosion instrumentation could offer the required levels of sensitivity for detecting and characterizing the corrosion processes which precede the development of observable damage. This paper details a program carried out to assess the suitability of such electrochemical monitoring instrumentation for aerospace applications and to assess the feasibility of producing an aircraft system on which a predictive corrosion monitoring system could be based.

Author

N95-23519# Department of the Air Force, Tinker AFB, OK. OKLAHOMA CITY AIR LOGISTICS CENTER (USAF) AGING AIRCRAFT CORROSION PROGRAM

DONALD E. NIESER In AGARD, Corrosion Detection and Management of Advanced Airframe Materials 12 p Jan. 1995

Copyright Avail: CASI HC A03/MF A03

Because of projected reductions in future defense budgets, less money will be available for new aircraft acquisitions. Consequently, many of the current aircraft will have to be maintained well into the twenty-first century. As they continue to age, the time-dependent effects of material degradation, due to corrosion, will become more significant. Having to maintain aircraft three to four times their original design life presents a unique new set of complex technical problems and challenges. The primary concern is the reduction of airframe fatigue life and static strength due to widespread corrosion damage, fatigue, embrittlement, material loss due to corrosion, intergranular corrosion attack, fretting and stress concentrations. In an effort to ensure continued airworthiness and flight safety, an aggressive program plan has been developed and implemented at Tinker AFB to try to solve the corrosion problems and fatigue related problems to prevent the occurrence of catastrophic structural failures. The program consists of (1) invasive disassembly of a complete C/KC-135 and sections of B-52 and Boeing 707 aircraft, (2) corrosion documentation/information system development, (3) analysis and testing the effects of corrosion on structural integrity, as well as corrosion growth rates, (4) corrosion modeling and development of C/KC-135 service life extension strategies, (5) and comprehensive evaluation of nondestructive inspection/testing (NDI/NDT) equipment for hidden corrosion detection and quantification. This program has been extensively coordi-

nated with USAF Wright Labs, AFOSR, Naval Air Warfare Center, FAA Aging Aircraft Center, NASA Langley, industry and academia.

Author

N95-24025*# National Aeronautics and Space Administration. Lewis Research Center, Cleveland, OH.

RESEARCH AND TECHNOLOGY, 1994

Jan. 1995 171 p

(NASA-TM-106764; E-9207; NAS 1.15:106764) Avail: CASI HC A08/MF A02

This report selectively summarizes the NASA Lewis Research Center's research and technology accomplishments for the fiscal year 1994. It comprises approximately 200 short articles submitted by the staff members of the technical directorates. The report is organized into six major sections: Aeronautics, Aerospace Technology, Space Flight Systems, Engineering and Computational Support, Lewis Research Academy, and Technology Transfer. A table of contents and author index have been developed to assist the reader in finding articles of special interest. This report is not intended to be a comprehensive summary of all research and technology work done over the past fiscal year. Most of the work is reported in Lewis-published technical reports, journal articles, and presentations prepared by Lewis staff members and contractors. In addition, university grants have enabled faculty members and graduate students to engage in sponsored research that is reported at technical meetings or in journal articles. For each article in this report a Lewis contact person has been identified, and where possible, reference documents are listed so that additional information can be easily obtained. The diversity of topics attests to the breadth of research and technology being pursued and to the skill mix of the staff that makes it possible.

Author

02

AERODYNAMICS

Includes aerodynamics of bodies, combinations, wings, rotors, and control surfaces; and internal flow in ducts and turbomachinery.

A95-73441

TIME-OF-FLIGHT MASS SPECTROMETER FOR IMPULSE FACILITIES

K. A. SKINNER Univ of Queensland, St. Lucia, Australia and R. J. STALKER AIAA Journal (ISSN 0001-1452) vol. 32, no. 11 November 1994 p. 2325-2328 refs

(BTN-95-EIX95142553057) Copyright

A time-of-flight mass spectrometer has been coupled with a compact sampling system to measure species concentrations in hypersonic flows produced by an impulse facility. The ability to detect molecular species present at levels of only 2% by number has been shown.

EI

A95-73444

TWO-EQUATION TURBULENCE MODEL FOR UNSTEADY SEPARATED FLOWS AROUND AIRFOILS

G. JIN Inst de Mecanique des Fluides de Toulouse, Toulouse, France and M. BRAZA AIAA Journal (ISSN 0001-1452) vol. 32, no. 11 November 1994 p. 2316-2320 refs

(BTN-95-EIX95142553054) Copyright

The turbulent incompressible flow around an airfoil NACA 0012 at a Reynolds number range of $10(\exp 6)$ is simulated by an unsteady approach, using the phase-averaging decomposition. This decomposition provides the phase-averaged Navier-Stokes equations. The unsteady vorticity is introduced into the production term of turbulent energy to improve the behavior of the two-equation model with respect to the physics of the flow.

EI

A95-73461

LAPLACE INTERACTION LAW FOR THE COMPUTATION OF VISCOUS AIRFOIL FLOW IN LOW- AND HIGH-SPEED AERODYNAMICS

F. ARNOLD Deutsche Aerospace Airbus GmbH, Bremen, Germany, and F. THIELE AIAA Journal (ISSN 0001-1452) vol. 32, no. 11 November 1994 p. 2178-2185 refs (BTN-95-EIX95142553037) Copyright

A new interaction law that accelerates convergence of interactive boundary-layer methods is presented. The law is derived from the Laplace equation and allows the automatic implementation of the Kutta condition for lifting airfoil flows. The accurate influence coefficients of the Laplace interaction law (LIL) facilitate efficient prediction of high-lift flows about multi-element airfoils by direct numerical simulation. Taking into account suitable turbulent closure relations for boundary-layer equations, a fast and reliable computer code has been developed for industrial applications at Deutsche Aerospace Airbus. Very fast convergence and good agreement of calculated results with experiments are observed over a reasonable range of multi-element airfoil flows up to maximum lift. The LIL coupling technique can also be extended to transonic flows. A quasisimultaneous iteration procedure, similar to well-known thin-airfoil coupling techniques follows, and accelerated convergence is obtained using the more appropriate influence coefficients of LIL.

Author (EI)

A95-73462

EFFECTS OF EXPANSIONS ON A SUPERSONIC BOUNDARY LAYER: SURFACE PRESSURE MEASUREMENTS

JONATHAN A. DAWSON Ohio State Univ, Columbus, OH, United States, MO SAMIMY, and STEPHEN A. ARNETTE AIAA Journal (ISSN 0001-1452) vol. 32, no. 11 November 1994 p. 2169-2177 refs

(BTN-95-EIX95142553036) Copyright

Multipoint wall pressure measurements are used to investigate the response of a Mach 3, fully developed, compressible, turbulent boundary layer (Re_{θ} approximately = 25,000) to centered and gradual (R/δ approximately = 50) expansions, both of 7- and 14-deg deflection. Although rms fluctuation levels decrease across the expansions, the rms normalized by the local static pressure remains nominally constant. Just downstream of the expansions, normalized power spectra are more concentrated at low frequencies (f less than 10-15 kHz) than upstream, suggesting small-scale turbulence is quenched. This spectra alteration is more prominent for centered expansions and larger deflections. The spectra evolve very quickly after the centered expansions and very slowly after the gradual expansions. Downstream of the expansions, space-time correlations do not lend themselves to the derivation of convection velocities, signifying a severe distortion of the boundary layers. Measurements immediately after the gradual expansions compare well with those further downstream of the centered expansions of the same deflection, suggesting the distance from the beginning of the expansions is the appropriate length scale for characterizing the boundary-layer evolution. After the expansions, a band of elevated spanwise coherence (around 15-30 kHz) and elevated spanwise correlation levels emerge. Increases in streamwise coherence and correlation are less pronounced. At the last measurement stations, the boundary layers remain far from equilibrium.

Author (EI)

A95-73465

AERODYNAMIC SHAPE OPTIMIZATION USING PRECONDITIONED CONJUGATE GRADIENT METHODS

GREG W. BURGREN Old Dominion Univ, Norfolk, VA, United States and OKTAY BAYSAL AIAA Journal (ISSN 0001-1452) vol. 32, no. 11 November 1994 p. 2145-2152 refs (BTN-95-EIX95142553033) Copyright

In an effort to further improve upon the latest advancements made in aerodynamic shape optimization procedures, a systematic study is performed to examine several current solution methodologies as applied to various aspects of the optimization procedure. It is demonstrated that preconditioned conjugate gradient-like meth-

odologies dramatically decrease the computational efforts required for such procedures. The design problem investigated is the shape optimization of the upper and lower surfaces of an initially symmetric (NACA 0012) airfoil in inviscid transonic flow and at zero degrees angle of attack. The complete surface shape is represented using a Bezier-Bernstein polynomial. The present optimization method is demonstrated to automatically obtain super-critical airfoil shapes over a variety of freestream Mach numbers. Furthermore, the best optimization strategy examined resulted in a factor of 8 decrease in computational time as well as a factor of 4 decrease in memory over the most efficient strategies in current use.

Author (EI)

A95-73493

ANALYTICAL STUDY OF THE NEUTRAL STABILITY OF A MODEL HYPERSONIC BOUNDARY LAYER

DANIEL R. BOWER State Univ of New York at Buffalo, Buffalo, NY, United States and CHING SHI LIU AIAA Journal (ISSN 0001-1452) vol. 32, no. 12 December 1994 p. 2366-2371 refs (BTN-95-EIX95152577589) Copyright

The neutral modes of a hypersonic boundary layer flow over an adiabatic flat plate are considered. A formulation of the governing second-order linear equation for the pressure disturbance is developed that lends itself to the application of the WKB method over the entire boundary layer. This formulation provides analytic eigenvalues and eigenfunction relations for the pressure disturbances and is applicable to flows at moderate Mach numbers as well. Solutions are determined for the cases of the wave speed $c = 0$ and $c = 1$, and show good qualitative agreement with numerical computations as well as results in the limit $M(\text{sub } \infty)$ to infinity.

Author (EI)

A95-73494

COMPUTATION OF OSCILLATING AIRFOIL FLOWS WITH ONE- AND TWO-EQUATION TURBULENCE MODELS

J. A. EKATERINARIS Navy-NASA Joint Inst of Aeronautics, Moffett Field, CA, United States and F. R. MENTER AIAA Journal (ISSN 0001-1452) vol. 32, no. 12 December 1994 p. 2359-2365 refs (BTN-95-EIX95152577588) Copyright

The ability of one- and two-equation turbulence models to predict unsteady separated flows over airfoils is evaluated. An implicit, factorized, upwind-biased numerical scheme is used for the integration of the compressible, Reynolds-averaged Navier-Stokes equations. The turbulent eddy viscosity is obtained from the computed mean flowfield by integration of the turbulent field equations. One- and two-equation turbulence models are first tested for a separated airfoil flow at fixed angle of incidence. The same models are then applied to compute the unsteady flowfields about airfoils undergoing oscillatory motion at low subsonic Mach numbers. Experimental cases where the flow has been tripped at the leading-edge and where natural transition was allowed to occur naturally are considered. The more recently developed turbulence models capture the physics of unsteady separated flow significantly better than the standard k -epsilon and k -omega models. However, certain differences in the hysteresis effects are observed. For an untripped high-Reynolds-number flow, it was found necessary to take into account the leading-edge transitional flow region to capture the correct physical mechanism that leads to dynamic stall.

Author (EI)

A95-73495

COUPLED FEM-BEM APPROACH FOR MEAN FLOW EFFECTS ON VIBRO-ACOUSTIC BEHAVIOR OF PLANAR STRUCTURES

FRANCK SGARD Univ of Sherbrooke, Sherbrooke, Que, Canada, NOUREDDINE ATALLA, and JEAN NICOLAS AIAA Journal (ISSN 0001-1452) vol. 32, no. 12 December 1994 p. 2351-2358 refs (BTN-95-EIX95152577587) Copyright

The importance of the mean flow effects on the forced vibrational behavior of a baffled plate, as well as on its acoustic radiation patterns, is investigated for a plate with different kinds of boundary conditions. The analysis is based on a finite element method for the calculation of the plate transverse vibrations and the use of the

extended Kirchhoff's integral equation to account for fluid loading with mean flow. A variational boundary element method is used to compute the acoustic radiation impedance. The formulation shows explicitly the effects of mean flow in terms of added mass, stiffness and radiation damping. EI

A95-73496* National Aeronautics and Space Administration. Langley Research Center, Hampton, VA.

MACH WAVE EMISSION FROM A HIGH-TEMPERATURE SUPERSONIC JET

JOHN M. SEINER National Aeronautics and Space Administration. Langley Research Center, Hampton, VA, THONSE R. S. BHAT, and MICHAEL K. PONTON AIAA Journal (ISSN 0001-1452) vol. 32, no. 12 December 1994 p. 2345-2356 refs (BTN-95-EIX95152577586) Copyright

The paper considers the compressible Rayleigh equation as a model for the Mach wave emission mechanism associated with high-temperature supersonic jets. Solutions to the compressible Rayleigh equation reveal the existence of several families of supersonically convecting instability waves. These waves directly radiate noise to the jet far field. The predicted noise characteristics are compared to previously acquired experimental data for an axisymmetric Mach 2 fully pressure balanced jet (i.e., $P(\text{sub } e)/P(\text{sub } a) = 1.0$) operating over a range of jet total temperatures from ambient to 1370 K. The results of this comparison show that the first-order supersonic instability wave and the Kelvin-Helmholtz first-, second-, and third-order modes have directional radiation characteristics that are in agreement with observed data. The assumption of equal initial amplitudes for all of the waves leads to the conclusion that the flapping mode of instability dominates the noise radiation process of supersonic jets. At a jet temperature of 1370 K, supersonic instability waves are predicted to dominate the noise radiated at high frequency at narrow angles to the jet axis. Author (EI)

A95-73497 EFFICIENT SENSITIVITY ANALYSIS FOR ROTARY-WING AEROMECHANICAL PROBLEMS

ANNE MARIE SPENCE Univ of Maryland, College Park, MD, United States and ROBERTO CELI AIAA Journal (ISSN 0001-1452) vol. 32, no. 12 December 1994 p. 2337-2344 refs (BTN-95-EIX95152577585) Copyright

This paper describes a method for the calculation of the sensitivities of rotating blade root loads and hub loads to changes of blade design parameters using a chain rule differentiation approach. The algorithm exploits features of the formulation of the blade and fuselage equations of motion, and of the solution technique, to calculate the sensitivities at a fraction of the cost of an aeroelastic analysis. The mathematical model of the blade includes nonlinearities because of moderately large elastic deflections and the fuselage is described by nonlinear Euler equations, so that the resulting model is valid for both straight and turning flight. The results indicate that the semianalytical technique is very accurate and computationally efficient. Author (EI)

A95-73516 FLOW VISUALIZATION STUDIES ON SIDEWALL EFFECTS IN TWO-DIMENSIONAL TRANSONIC AIRFOIL TESTING

NORIKAZU SUDANI Natl Aerospace Lab, Tokyo, Japan, MAMORU SATO, HIROSHI KANDA, and KENICHI MATSUNO Journal of Aircraft (ISSN 0021-8669) vol. 31, no. 6 November-December 1994 p. 1233-1239 refs (BTN-95-EIX95152582313) Copyright

The effects of sidewall boundary layers in two-dimensional transonic airfoil testing were investigated using oil-flow or liquid crystal visualization techniques. Three different chord models were tested in order to clarify the sidewall effects and to seek a suitable aspect ratio of the airfoil. The oil-flow visualization data systematically reveal the surface flow patterns affected by the sidewalls and suggest a minimum aspect ratio for conducting reliable two-dimensional tests. The results of the liquid crystal visualization also show

the three dimensionality of the transition behavior and the necessity of the high aspect ratio. In addition, investigations on effects of the sidewall boundary-layer suction and application of a sidewall interference correction produce significant results for improvement of airfoil testing by removal of the sidewall effects. Author (EI)

A95-73518* National Aeronautics and Space Administration. Ames Research Center, Moffett Field, CA.

PROGRESS IN HIGH-LIFT AERODYNAMIC CALCULATIONS

STUART E. ROGERS National Aeronautics and Space Administration. Ames Research Center, Moffett Field, CA Journal of Aircraft (ISSN 0021-8669) vol. 31, no. 6 November-December 1994 p. 1244-1251 refs (BTN-95-EIX95152582315) Copyright

The current work presents progress in the effort to numerically simulate the flow over high-lift aerodynamic components, namely multielement airfoils in either a takeoff or landing configuration. The computational approach utilizes an incompressible flow solver and an overlaid chimera grid approach. A detailed grid resolution study is presented for flow over a three-element airfoil. Two turbulence models - a one-equation Baldwin-Barth model and a two-equation k-omega model - are compared. Excellent agreement with experiment is obtained for the lift coefficient at all angles of attack, including the prediction of maximum lift when using the two-equation model. Results for two other flap riggings are shown. Author (EI)

A95-73519 SIDEWASH ON THE VERTICAL TAIL IN SUBSONIC AND SUPERSONIC FLOWS

CHYN-SHAN CHIU China Junior Coll of Technology, Taipei, Taiwan, Province of China and I. J. LIN, Journal of Aircraft (ISSN 0021-8669) vol. 31, no. 6 November-December 1994 p. 1252-1256 refs (BTN-95-EIX95152582316) Copyright

A generalized vortex-lattice method is used for the investigation of sidewash on the single and twin vertical tails due to rolling wing in subsonic and supersonic flows. The current results of sidewash on the single vertical tail in incompressible inviscid flow are almost the same as Michael's calculations. The sidewash on the single vertical tail through high angle of attack is presented. The difference of sidewash on the single and twin vertical tail that is induced by the rolling wing in subsonic and supersonic flows is also studied. Author (EI)

A95-73520 LIMIT CYCLE PHENOMENA IN COMPUTATIONAL TRANSONIC AEROELASTICITY

KENNETH A. KOUSEN Univ of California, Los Angeles, CA, United States and ODDVAR O. BENDIKSEN Journal of Aircraft (ISSN 0021-8669) vol. 31, no. 6 November-December 1994 p. 1257-1263 refs (BTN-95-EIX95152582317) Copyright

Limit cycle behavior has been observed in past transonic flutter calculations by the authors, using a two degree-of-freedom typical section model coupled to an unsteady Euler equations solver. In this article, the structural nonlinearity of freeplay has been added to the typical section model, and its effects on the dynamic stability problem are assessed. In addition, limit cycle behavior in the swept-wing model of Isogai is demonstrated and related to the observed presence of multiple flutter points in the transonic dip region. Author (EI)

A95-73523 COMPUTATION OF THE POSTSTALL BEHAVIOR OF A CIRCULATION CONTROLLED AIRFOIL

SAMUEL W. LINTON Sterling Software at NASA Ames Research Cent, Moffett Field, CA, United States Journal of Aircraft (ISSN 0021-8669) vol. 31, no. 6 November-December 1994 p. 1273-1280 refs (BTN-95-EIX95152582320) Copyright

This article describes the numerical simulation of stalled and

uninstalled flows over a circulation controlled airfoil (CCA) using a fully implicit Navier-Stokes code, and the comparison with experimental results. Mach numbers of 0.3 and 0.5 and jet total to freestream pressure ratios of 1.4 and 1.8 are investigated. The Baldwin-Lomax and k-epsilon turbulence models are used, each modified to include the effect of strong streamline curvature. The numerical solutions of the poststall CCA show a highly regular unsteady periodic flowfield. This is the result of an alternation between adverse pressure gradient and shock-induced separation of the boundary layer on the airfoil trailing edge. Author (EI)

A95-73524
EXPERIMENTAL INVESTIGATION OF THE FLOWFIELD ABOUT AN UPSWEPT AFTERBODY

RONALD J. EPSTEIN von Karman Inst for Fluid Dynamics, Rhode-Saint-Genese, Belgium, MARIO C. CARONARO, and F. CAUDRON Journal of Aircraft (ISSN 0021-8669) vol. 31, no. 6 November-December 1994 p. 1281-1290 refs (BTN-95-EIX95152582321) Copyright

In general, the flowfield about the aft portion of an aircraft fuselage employing an upswept afterbody is complex and can have a detailed vortex structure. Directional pressure probe measurements show that the afterbody wake evolution is weakly dependent on the Reynolds number. Pressure taps are used to investigate the effect of base slant on the base pressure distribution. The base pressure distribution is found to increase along the upswept ramp in the freestream direction. Using oil flow visualizations general conclusions are drawn about the surface flow topology. Two distinct regions of flow separation are identified. An analytical model of the crossflow wake structure is developed from the experimental data. This model allows for conclusions to be drawn about the crossflow vortex structure and provides simple analytical expressions for the vorticity and swirl velocity distributions in the crossflow plane. Author (EI)

A95-73525
UNSTRUCTURED GRID SOLUTIONS TO A WING/PYLON/STORE CONFIGURATION

PARESH PARIKH VIGYAN, Inc, Hampton, VA, United States, SHAHYAR PIRZADEH, and NEAL T. FRINK Journal of Aircraft (ISSN 0021-8669) vol. 31, no. 6 November-December 1994 p. 1291-1296 refs (BTN-95-EIX95152582322) Copyright

The purpose of this article is to validate an inviscid flow solution package based on a new unstructured grid methodology using experimental data on a wing/pylon/tinned store configuration. The solution package consists of an advancing front grid generator, VGRID, and an efficient Euler equation solver, USM3D. Comparisons of computed data vs experimental data are made for two freestream Mach numbers at five store locations relative to the wing. Both rigid body aerodynamics and mutual interference effects are explored. A very good agreement is observed between computed and wind-tunnel data. Author (EI)

A95-73527
MOVING WALL EFFECT IN RELATION TO OTHER DYNAMIC STALL FLOW MECHANISMS

LARS E. ERICSSON Journal of Aircraft (ISSN 0021-8669) vol. 31, no. 6 November-December 1994 p. 1303-1309 refs (BTN-95-EIX95152582324) Copyright

An analysis is performed to determine the importance of the so-called moving wall effect relative to other unsteady flow mechanisms present in the dynamic stall process. Analysis of existing theoretical and experimental results indicates that the tangential moving wall effect on the initial boundary-layer development, close to the flow stagnation point, is not satisfactorily represented in current numerical methods. The analysis shows that this moving wall effect plays a dominant role in inducing self-excited oscillations, such as the wing rock of advanced aircraft, and also plays a significant role in so called supermaneuvers of these aircraft. Author (EI)

A95-73529* National Aeronautics and Space Administration. Langley Research Center, Hampton, VA.

SEPARATION CONTROL ON HIGH-LIFT AIRFOILS VIA MICRO-VORTEX GENERATORS

JOHN C. LIN National Aeronautical and Space Administration. Langley Research Center, Hampton, VA, STEPHEN K. ROBINSON, ROBERT J. MCGHEE, and WALTER O. VALAREZO Journal of Aircraft (ISSN 0021-8669) vol. 31, no. 6 November-December 1994 p. 1317-1323 refs

(BTN-95-EIX95152582326) Copyright

An experimental investigation has been conducted to evaluate boundary-layer separation control on a two-dimensional single-flap, three-element, high-lift system at near-flight Reynolds numbers with small surface-mounted vortex generators. The wind-tunnel testing was carried out in the NASA Langley Low-Turbulence Pressure Tunnel as part of a cooperative program between McDonnell Douglas Aerospace and NASA Langley Research Center to develop code validation data bases and to improve physical understanding of multielement airfoil flows. This article describes results obtained for small (subboundary-layer) vane-type vortex generators mounted on a multielement airfoil in a landing configuration. Measurements include lift, drag, surface pressure, wake profile, and fluctuating surface heat fluxes. The results reveal that vortex generators as small as 0.18% of reference (slat and flap stowed) wing chord ('micro-vortex generators') can effectively reduce boundary-layer separation on the flap for landing configurations. Reduction of flap separation can significantly improve performance of the high-lift system by reducing drag and increasing lift for a given approach angle of attack. At their optimum chordwise placement on the flap, the micro-vortex generators are hidden inside the wing when the flap is retracted, thus extracting no cruise drag penalty. Author (EI)

A95-73530
STUDY OF AN AIRFOIL WITH A FLAP AND SPOILER

ABDULLAH AL SHABIBI Sultan Qaboos Univ, Muscat, Oman, MUNIR ALI HAMMADI, and JOSEPH MATHEW Journal of Aircraft (ISSN 0021-8669) vol. 31, no. 6 November-December 1994 p. 1324-1327 refs

(BTN-95-EIX95152582327) Copyright

An experimental investigation of an airfoil with a spoiler and flap was carried out. Results of these studies are presented. The coefficient of lift was seen to decline sharply in the range of spoiler angles ranging from 0 to 15 deg, due to the early separation that the spoiler introduces on the airfoil. Experiments with wing-flap combinations for flap angles ranging from 0 to 45 deg showed that there is an optimum wing-flap gap for a wing-flap configuration. A considerable increase in the intensities of turbulences were seen at higher flap angles that should contribute to the sharp increase in the drag at the higher flap angles. A wake frequency spectrum for varying angles of attack has been made and is presented. Author (EI)

A95-73532* National Aeronautics and Space Administration. Langley Research Center, Hampton, VA.

ANALYSIS OF A HIGHER HARMONIC CONTROL TEST TO REDUCE BLADE VORTEX INTERACTION NOISE

THOMAS F. BROOKS National Aeronautics and Space Administration. Langley Research Center, Hampton, VA, EARL R. BOOTH, JR., D. DOUGLAS BOYD, JR., WOLF R. SPLETTSTOESSER, KLAUS-J. SCHULTZ, ROLAND KUBE, GEORG H. NIESL, and OLIVIER STREBY Journal of Aircraft (ISSN 0021-8669) vol. 31, no. 6 November-December 1994 p. 1341-1349 refs (BTN-95-EIX95152582330) Copyright

A noise study using an aeroelastically scaled BO-105 rotor was conducted in the German-Dutch Wind Tunnel to examine the use of higher harmonic control (HHC) of blade pitch to reduce impulsive blade-vortex interaction (BVI) noise. The noise directivity was measured over a large plane underneath the rotor using a traversing inflow microphone array. Noise and vibration measurements were made for a range of matched rotor operating conditions where prescribed (or open loop) HHC pitch, at various amplitudes and phases, was superimposed on normal (baseline) collective and

02 AERODYNAMICS

cyclic trim pitch. Acoustic data are presented for 3, 4, and 5P HHC applied to a typical landing approach rotor operating condition where BVI noise is normally intense. Noise reductions of up to 6 dB were found for the advancing side BVI noise radiating upstream of the rotor, and also for the retreating side BVI noise radiating below and downstream of the rotor. The relative levels between the sides were modified by HHC control phase. To help give insight to the physics of the HHC/BVI noise problem, high-resolution loading and noise prediction results are presented for comparison to the data. The predictions are based on a new high-resolution version of the CAMRAD rotor performance program under development at Langley, called HIREs. Author (EI)

A95-73539

POSTINSTABILITY BEHAVIOR OF A TWO-DIMENSIONAL AIRFOIL WITH A STRUCTURAL NONLINEARITY

S. J. PRICE McGill Univ, Montreal, Que, Canada, B. H. K. LEE, and H. ALIGHANBARI Journal of Aircraft (ISSN 0021-8669) vol. 31, no. 6 November-December 1994 p. 1395-1401 refs (BTN-95-EIX95152582337) Copyright

A two-dimensional airfoil with a free-play nonlinearity in pitch subject to incompressible flow has been analyzed. The aerodynamic forces on the airfoil were evaluated using Wagner's function and the resulting equations integrated numerically to give time histories of the airfoil motion. Regions of limit cycle oscillation are detected for velocities well below the linear flutter boundary, and the existence of these regions is strongly dependent on the initial conditions and properties of the airfoil. Furthermore, for small structural preloads, narrow regions of chaotic motion are obtained, as suggested by power spectral densities, phase-plane plots, and Poincare sections of the airfoil time histories. The existence of this chaotic motion is strongly dependent on a number of airfoil parameters, including, mass, frequency ratio, structural damping, and preload.

Author (EI)

A95-73541

STATIC PRESSURE DISTRIBUTION IN THE INLET OF A HELICOPTER TURBINE COMPRESSOR

JOHANNES P. VANDERWALT Univ of the Witwatersrand, Johannesburg, South Africa and ALAN NURICK Journal of Aircraft (ISSN 0021-8669) vol. 31, no. 6 November-December 1994 p. 1411-1413 refs (BTN-95-EIX95152582339) Copyright

The parallel compressor model was used to demonstrate that when the airflow into a compressor is distorted, the velocity at the inlet to the compressor will be virtually constant with consequent variations in the static pressure. Refined parallel compressor models have been proposed in which it is assumed that the compressor tends to induce a constant air inlet velocity with static pressure gradients that are in sympathy with the total pressure gradients. Four basic elements have been identified to be important for distortion measurement: (1) circumferential intensity; (2) extent; (3) multiple-per-rev elements defined at constant radius; and (4) a radial intensity element. EI

A95-73546

FLOW STUDY OF SUPERSONIC WING-NACELLE CONFIGURATION

KASIM BIBER Wichita State Univ, Wichita, KS, United States and JOEL MENDOZA Journal of Aircraft (ISSN 0021-8669) vol. 31, no. 6 November-December 1994 p. 1424-1426 refs (BTN-95-EIX95152582344) Copyright

Nacelle/airframe integration is of major importance for aerodynamically efficient supersonic transport aircraft design and development. When the nacelle is integrated with an aircraft wing, its flowfield is affected by the wing boundary layer, depending on the nacelle proximity to the wing surface. The shock-boundary layer flow interaction between the nacelle and wing is studied, as well as the wing interference effects on the nacelle flowfield. The nacelle leading-edge shock wave appears to be steady and attached to the inlet lip for all test cases. The boundary layer on the wing lower

surface is turbulent and the shock expansion waves from the nacelle do not have a significant impingement effect on its character. EI

A95-73547

ANALYTIC PREDICTION OF LIFT FOR DELTA WINGS WITH PARTIAL LEADING-EDGE THRUST

LANCE W. TRAUB Univ of the Witwatersrand, Johannesburg, South Africa Journal of Aircraft (ISSN 0021-8669) vol. 31, no. 6 November-December 1994 p. 1426-1429 refs (BTN-95-EIX95152582345) Copyright

Expressions were derived to analytically determine the lift and drag coefficients of delta wings with partial leading-edge thrust in subsonic flow. The method uses the suction analogy, with an assumed theoretical leading-edge thrust distribution. Separate expressions to estimate the effective thrust based on the empirical method of Carlson and Mack and the method of Kulfan were derived. Some airfoil and wing geometric parameters, as well as the potential constant, are required in the equations. The two methods were compared with experimental results, and good agreement was shown at moderate angles of attack which improves as the wing aspect ratio was reduced. EI

A95-73548* National Aeronautics and Space Administration, Langley Research Center, Hampton, VA.

COMPUTATIONAL STUDY OF PLUME-INDUCED SEPARATION ON A HYPERSONIC POWERED MODEL

L. D. HUEBNER National Aeronautics and Space Administration, Langley Research Center, Hampton, VA Journal of Aircraft (ISSN 0021-8669) vol. 31, no. 6 November-December 1994 p. 1429-1431 refs (BTN-95-EIX95152582346) Copyright

The computation of hypersonic air-breathing vehicle flowfields were studied under simulated powered conditions. Two-dimensional parabolized Navier-Stokes (PNS) and full Reynolds-averaged Navier-Stokes (RANS) calculations were performed to predict the possible existence and effects of flow separation on the cowl of a hypersonic airbreathing model employing scramjet exhaust flow simulation at representative Mach 10 wind tunnel conditions. Flow separation resulted in a negligible difference in lift and thrust, while there was a small increase in pitching moment. If the cowl trailing edge was at a position such that part of the cowl was an expansion surface, the separation would likely be greater, as would the impact on lift and thrust. EI

A95-73552* National Aeronautics and Space Administration, Langley Research Center, Hampton, VA.

AERODYNAMIC CHARACTERISTICS OF A HYPERSONIC VISCOUS OPTIMIZED WAVERIDER AT HIGH ALTITUDES

DIDIER F. G. RAULT National Aeronautics and Space Administration, Langley Research Center, Hampton, VA Journal of Spacecraft and Rockets (ISSN 0022-4650) vol. 31, no. 5 September-October 1994 p. 719-727 refs (BTN-95-EIX95152583251) Copyright

The aerodynamic characteristics of a University of Maryland viscous optimized waverider are studied at altitudes ranging from 97 to 145 km and incidence angles of 0 to 30 deg. The direct simulation Monte Carlo method is used to simulate and analyze the flowfield around the waverider and evaluate surface loads. It is shown that the vehicle lift-to-drag ratio decreases rapidly as flight altitude is increased, and is confined to values less than 0.3. At high altitudes, the waverider is surrounded by a thick viscous shock layer, and the friction forces, which are typically large at high Knudsen numbers, are shown to significantly reduce lift and increase drag. Author (EI)

A95-73557

BASE DRAG PREDICTION ON MISSILE CONFIGURATIONS

F. G. MOORE Naval Surface Warfare Cent, Dahlgren, VA, United States, F. WILCOX, and T. HYMER Journal of Spacecraft and Rockets (ISSN 0022-4650) vol. 31, no. 5 September-October 1994 p. 759-765 refs (BTN-95-EIX95152583256) Copyright

New wind-tunnel data have been taken, and a new empirical model has been developed for predicting base drag on missile configurations. The new wind-tunnel data were taken at NASA Langley Research Center in the unitary wind tunnel at Mach numbers from 2.0 to 4.5, angles of attack to 16 deg, fin control deflections, up to 20 deg, fin thickness-to-chord ratio of 0.05 to 0.15, and fin locations flush with the base to two chord lengths upstream of the base. The newly developed empirical model uses these data along with previous wind-tunnel data. It estimates base drag as a function of all the preceding variables along with boattail and power-on or power-off effects. In comparing the new empirical model to that used in the former aeroprediction code, the new model gives improved accuracy compared to wind-tunnel data. The new model also is more robust due to inclusion of additional variables. On the other hand, additional wind-tunnel data are needed to validate or modify the current empirical model in areas where data are not available.

Author (EI)

A95-73558

AERODYNAMIC CHARACTERISTICS OF A CANARD-CONTROLLED MISSILE AT HIGH ANGLES OF ATTACK

EDMUND H. SMITH Naval Air Warfare Cent, China Lake, CA, United States, SHESHAGIRI HEBBAR, and MAX F. PLATZER Journal of Spacecraft and Rockets (ISSN 0022-4650) vol. 31, no. 5 September-October 1994 p. 766-772 refs (BTN-95-EIX95152583257) Copyright

A low-speed wind-tunnel investigation was conducted to examine the aerodynamic characteristics of a one-third-scale model of a canard-controlled missile at high angles of attack using force and moment measurements. The data were taken at a nominal Mach number of 0.2 for angles of attack up to 50 deg at three different canard deflection settings. The test runs were limited to 0- and 45-deg missile roll angles (symmetric configurations) and two sets of tails (aft fins), one with the full area including the roll damping tabs (rollerons) and the other without the rollerons. The data indicate that the rollerons act as an effective fin area at low speeds and high angles of attack, and make the missile more stable. The test data were also used to validate the aerodynamic characteristics of the missile as predicted by the Missile Datcom program. The agreement between the Datcom predictions and the test data is fairly good, with the latter indicating a slightly higher static stability. Author (EI)

A95-73560

THREE-DIMENSIONAL STRUCTURE OF A SUPERSONIC JET IMPINGING ON AN INCLINED PLATE

KYOUNG-HO KIM Hyundai Motor Co and KEUN-SHIK CHANG Journal of Spacecraft and Rockets (ISSN 0022-4650) vol. 31, no. 5 September-October 1994 p. 778-782 refs (BTN-95-EIX95152583259) Copyright

The flow structure of an underexpanded supersonic jet impinging on an inclined flat plate has been numerically investigated using a total-variation-diminishing scheme for the Euler equations. The impinging jet is characterized by many discontinuities, such as barrel shock, exhaust gas jet boundary, Mach disk, reflected shock, plate shock, subtail shock, contact surface, and sometimes a stagnation bubble. Furthermore, if the plate is inclined, the jet structure becomes three-dimensional and severely distorted. The effect of plate inclination has been investigated in the present paper by studying the formation of the asymmetric stagnation bubble and the magnitude and location of the maximum wall pressure. Comparison with the existing experimental results over a broad range of data sets on pressure and shock structure has led to the conclusion that the present inviscid numerical model can offer fairly good prediction of the impinging jet for moderate plate inclinations. The maximum wall pressure was found to be larger on the inclined plate than on the normal plate. Author (EI)

A95-73561

IMPROVED VERSION OF THE NAVAL SURFACE WARFARE CENTER AEROPREDICTION CODE (AP93)

F. G. MOORE Naval Surface Warfare Cent, Dahlgren, VA, United

States, T. HYMER, and R. MCINVILLE Journal of Spacecraft and Rockets (ISSN 0022-4650) vol. 31, no. 5 September-October 1994 p. 783-791 refs (BTN-95-EIX95152583260) Copyright

A new and improved version of the naval Surface Warfare Center, Dahlgren Division aeroprediction code has been developed. The new code, AP93, contains new technology that allows planar aerodynamics of axisymmetric solid-rocket-type weapons to be computed over the entire Mach-number range that weapons fly and for angles of attack up to 30 deg. Comparisons of the new AP93 code with the AP81 show that the AP93 on the average reduces the normal force and center-of-pressure errors of the AP81 code almost by half, and gives a slight improvement in axial force errors. EI

A95-75097* National Aeronautics and Space Administration. Langley Research Center, Hampton, VA.

SENSITIVITY OF ACOUSTIC PREDICTIONS TO VARIATION OF INPUT PARAMETERS

KENNETH S. BRENTNER NASA. Langley Research Center, Hampton, VA, US, CASEY L. BURLEY NASA. Langley Research Center, Hampton, VA, US, and MICHAEL A. MARCOLINI NASA. Langley Research Center, Hampton, VA, US American Helicopter Society, Journal (ISSN 0002-8711) vol. 39, no. 3 July 1994 p. 43-52 (HTN-95-80855) Copyright

Rotor noise prediction codes predict the thickness and loading noise produced by a helicopter rotor, given the blade motion, rotor operating conditions, and fluctuating force distribution over the blade surface. However, the criticality of these various inputs, and their respective effects on the predicted acoustic field, have never been fully addressed. This paper examines the importance of these inputs, and the sensitivity of the acoustic predictions to a variation of each parameter. The effects of collective and cyclic pitch, as well as coning and cyclic flapping, are presented. Blade loading inputs are examined to determine the necessary spatial and temporal resolution, as well as the importance of the chordwise distribution. The acoustic predictions show regions in the acoustic field where significant errors occur when simplified blade motions or blade loadings are used. An assessment of the variation in the predicted acoustic field is balanced by a consideration of Central Processing Unit (CPU) time necessary for the various approximations.

Author (Herner)

A95-75101

THE INFLUENCE OF ALTERNATE INTER-BLADE CONNECTIONS ON GROUND RESONANCE

N. M. SELA Technion-Israel Institute of Technology, Haifa, Israel and A. ROSEN Technion-Israel Institute of Technology, Haifa, Israel American Helicopter Society, Journal (ISSN 0002-8711) vol. 39, no. 3 July 1994 p. 73-78 (HTN-95-80859) Copyright

The present analysis is an extension to a previous work by the authors where the ground resonance problem of a helicopter with a rotor incorporating inter-connected blades was analyzed. As before the blades are inter-connected with springs and dampers, but in the present analysis the direction of inter-blade connections is opposite to that analyzed previously. Using the Modified Multiblade Coordinate Transformation (MMCT), a set of constant coefficient equations is obtained. Examination of the equations reveals that the present arrangement of the inter-connecting springs and dampers is less effective than the previous one for three-bladed rotors, equally effective for four-bladed rotors, and more effective for rotors incorporating five blades or more.

Author (Herner)

A95-75728

DETERMINATION OF WALL BOUNDARY CONDITIONS FOR HIGH-SPEED-RATIO DIRECT SIMULATION MONTE CARLO CALCULATIONS

FRANK G. COLLINS Univ of Tennessee Space Inst, Tullahoma, TN, United States and E. C. KNOX Journal of Spacecraft and Rockets (ISSN 0022-4650) vol. 31, no. 6 November-December 1994 p. 965-970 refs

(BTN-95-EIX95182617457) Copyright

A procedure for determining the velocity distribution function for the molecules that are reflected from an element of surface when a vehicle is moving in the transition or free-molecule flow regimes at high speed ratios is described. This distribution function could be used as the boundary condition for DSMC calculations. The method uses measurements of the momentum accommodation coefficients to determine the parameters for the Nocilla model of the reflected velocity distribution function. The use of this function as a boundary condition with the DSMC method would yield more accurate predictions of flow fields than are presently obtained using the assumption of diffuse scattering from the body surface. Several sets of Nocilla model parameters are determined as examples of the application of the procedure.

Author (EI)

A95-75729* National Aeronautics and Space Administration. Langley Research Center, Hampton, VA.

ZONALLY DECOUPLED DIRECT SIMULATION MONTE CARLO SOLUTIONS OF HYPERSONIC BLUNT-BODY WAKE FLOWS

RICHARD G. WILMOTH National Aeronautics and Space Administration, Langley Research Center, Hampton, VA, ROBERT A. MITCHELTREE, JAMES N. MOSS, and VIRENDRA K. DOGRA Journal of Spacecraft and Rockets (ISSN 0022-4650) vol. 31, no. 6 November-December 1994 p. 971-979 refs (BTN-95-EIX95182617458) Copyright

Direct simulation Monte Carlo (DSMC) solutions are presented for the hypersonic flow behind a blunt body in which the wake region is solved in a zonally decoupled manner. The forebody flow is solved separately using either a DSMC or a Navier-Stokes method, and the forebody exit-plane solution is specified as the inflow condition to the decoupled DSMC solution of the wake region. Results are presented for a 70-deg, blunted cone at flow conditions that can be accommodated in existing low-density wind tunnels with the Knudsen number (based on the base diameter) ranging from 0.03 to 0.001. The zonally decoupled solutions show good agreement with fully coupled DSMC solutions of the wake flow densities and velocities. The wake closure predicted by the zonally decoupled solutions is in better agreement with fully coupled results than that predicted by a fully coupled Navier-Stokes method, indicating the need to account for rarefaction in the wake for the cases considered. The combined use of Navier-Stokes for the forebody with a decoupled DSMC solution for the wake provides an efficient method for solving transitional blunt-body flows where the forebody flow is continuum and the wake is rarefied.

Author (EI)

**A95-75731
CONVECTIVE AND RADIATIVE HEAT TRANSFER ANALYSIS FOR THE FIRE 2 FOREBODY**

ROBERT B. GREENDYKE ViGYAN, Inc, Hampton, VA, United States and LIN C. HARTUNG Journal of Spacecraft and Rockets (ISSN 0022-4650) vol. 31, no. 6 November-December 1994 p. 986-992 refs (BTN-95-EIX95182617460) Copyright

A Navier-Stokes flowfield solution method using finite-rate chemistry and two-temperature thermal nonequilibrium was used in combination with two nonequilibrium radiative heat transfer codes to calculate heating for the FIRE II vehicle. An axisymmetric model of the actual body shape was used. One radiative heating code was used in uncoupled fashion with the flowfield solver's energy equations, while the other code was used in both coupled and uncoupled variations. Several trajectory points ranging from highly nonequilibrium flow to near-equilibrium flow were used for a study of both convective and radiative heating over the vehicle. Considerable variation in radiative heating was seen at the extremes, while agreement was good in the intermediate trajectory points. Total heat transfer calculations gave good comparison until the peak heating trajectory points were encountered and returned to good agreement for the last two equilibrium points.

Author (EI)

A95-75733

WING VERTICAL POSITION EFFECTS ON WING-BODY CARRYOVER FOR NONCIRCULAR MISSILES

BRIAN E. EST Univ of Missouri-Rolla, Rolla, MO, United States and H. F. NELSON Journal of Spacecraft and Rockets (ISSN 0022-4650) vol. 31, no. 6 November-December 1994 p. 999-1006 refs (BTN-95-EIX95182617462) Copyright

The preliminary design component buildup factor $K(\text{sub } W(B))$, a measure of the wing-body interference caused by upwash, is investigated for unbanked, supersonic missiles with noncircular body cross section. The aerodynamic effects of wing vertical location relative to the missile fuselage centerline, Mach number, and fuselage cross-sectional shape are parametrically varied to develop a preliminary design data base of $K(\text{sub } W(B))$ values for circular, square, and triangular missile bodies. A spatial marching Euler code ZEUS is used to determine the delta-wing normal force in the presence of the body. Euler $K(\text{sub } W(B))$ predictions are compared to the slender body theory presently used for computing low angle-of-attack $K(\text{sub } W(B))$ in missile preliminary design engineering methods. Euler values of $K(\text{sub } W(B))$ exhibit sensitivity to wing vertical position, Mach number, and body cross-sectional shape, whereas slender body theory is a function of wing semispan to body radius ratios, S/R , only. Euler values of $K(\text{sub } W(B))$ are generally found to differ from slender body theory values by less than 15% for smaller S/R , and they approach slender body theory values at larger S/R .

Author (EI)

A95-75736

SUPERSONIC NEAR-WAKE AFTERBODY BOATTAILING EFFECTS ON AXISYMMETRIC BODIES

J. L. HERRIN Univ of Illinois at Urbana-Champaign, Urbana, IL, United States and J. C. DUTTON Journal of Spacecraft and Rockets (ISSN 0022-4650) vol. 31, no. 6 November-December 1994 p. 1021-1028 refs (BTN-95-EIX95182617465) Copyright

An experimental investigation of the near-wake flowfield downstream of a conical boattailed afterbody in supersonic flow is presented. The afterbody investigated is typical of those for conventional boattailed missiles and projectiles in unpowered flight. Flow visualization, mean static pressure measurements, and three-component laser Doppler velocimeter data have been obtained throughout the near wake of the body. The effects of afterbody boattailing on the physics of the near-wake flow are determined by comparing the present data with similar data obtained on a cylindrical afterbody. Results indicate that a net afterbody drag reduction of 21% is achieved with the current boattailed afterbody for a freestream Mach number of 2.46. The shear-layer growth rate, and therefore mass entrainment from the recirculation region behind the base, is shown to be significantly reduced by afterbody boattailing due to the reduction in turbulence levels throughout the near wake as compared to the cylindrical afterbody.

Author (EI)

A95-75758

TRANSIENT STRUCTURE OF VORTEX BREAKDOWN ON A DELTA WING

J. -C. LIN Lehigh Univ, Bethlehem, PA, United States and D. ROCKWELL AIAA Journal (ISSN 0001-1452) vol. 33, no. 1 January 1995 p. 6-12 refs (BTN-95-EIX95182619073) Copyright

The transient relaxation process of the leading-edge vortex on a delta wing pitched to high angle of attack is quantitatively characterized using high-image density particle image velocimetry. Instantaneous distributions of azimuthal vorticity and patterns of sectional streamlines over an entire plane allow definition of a new, rapidly evolving mechanism at the onset of vortex breakdown; it marks the transition from a relatively high to low upstream propagation speed of the breakdown.

Author (EI)

A95-75761* National Aeronautics and Space Administration. Ames Research Center, Moffett Field, CA.

AEROACOUSTIC MODEL FOR WEAK SHOCK WAVES BASED ON BURGERS EQUATION

SANFORD S. DAVIS National Aeronautics and Space Administration, Ames Research Center, Moffett Field, CA AIAA Journal (ISSN 0001-1452) vol. 33, no. 1 January 1995 p. 27-32 refs (BTN-95-EIX95182619076) Copyright

The adiabatic form of the Euler equations are cast in a form emphasizing its signal propagation properties and solved using an approximate eigenfunction analysis. Second-order rarefaction waves appear as direct eigenfunction solutions. The underlying scalar equation describing nonlinear shock wave evolution is rederived as a first-order Burgers equation. The characteristic sonic boom N waves are predicted using an implicit aeroacoustic-based finite-difference algorithm with numerical damping designed to suppress spurious oscillations at shock-wave discontinuities. The evolution of these sonic-boom-type signals to the mid- and far field are computed directly with the numerical method. Author (EI)

A95-75763

TURBULENT TRANSONIC AIRFOIL FLOW SIMULATION USING A PRESSURE-BASED ALGORITHM

GANG ZHOU Chalmers Univ of Technology, Gothenburg, Sweden, LARS DAVIDSON, and ERIK OLSSON AIAA Journal (ISSN 0001-1452) vol. 33, no. 1 January 1995 p. 42-47 refs (BTN-95-EIX95182619078) Copyright

There are few successful computational reports for transonic airfoil flow worked out with the pressure-based method. In this study, an advanced approach based on a pressure correction scheme is developed to solve the Reynolds-averaged Navier-Stokes equations for turbulent transonic flow around the airfoil RAE 2822. An implicit numerical dissipation model is adopted to create a dissipation mechanism based on pressure gradients to damp the destabilizing numerical effects, without smearing the physical discontinuity at shocks. The standard k-epsilon turbulence closure with a near-wall one-equation model is used. The computational results are compared with experimental data. Several discretization schemes such as the second-order upwind, hybrid, and MUSCL schemes for convection terms are investigated. The computational results show that the proposed pressure-based method has a resolution comparable to, or better than, the traditional time-marching methods. Author (EI)

A95-75765

SIMULATION OF TRANSVERSE GAS INJECTION IN TURBULENT SUPERSONIC AIR FLOWS

F. GRASSO Univ of Rome 'La Sapienza', Rome, Italy and V. MAGI AIAA Journal (ISSN 0001-1452) vol. 33, no. 1 January 1995 p. 56-62 refs (BTN-95-EIX95182619080) Copyright

The present paper deals with the simulation of the fluid dynamic behavior of transverse gas injection in turbulent supersonic air streams. The Favre-averaged Navier-Stokes equations are solved for a multicomponent mixture of gases. A two-equation k-epsilon turbulence model is employed that properly accounts for low Reynolds effects. The governing equations are solved by a finite volume approach with the k-epsilon model equations fully coupled with those of the mean flow, and an implicit treatment of the source terms. Several test cases are considered and the results are compared with available experimental measurements. Author (EI)

A95-75778

VISCOUS-INVISCID INTERACTION METHOD FOR UNSTEADY LOW-SPEED AIRFOIL FLOWS

ISMAIL H. TUNCER Naval Postgraduate Sch, Monterey, CA, United States, JOHN A. EKATERINARIS, and MAX F. PLATZER AIAA Journal (ISSN 0001-1452) vol. 33, no. 1 January 1995 p. 151-154 refs (BTN-95-EIX95182619093) Copyright

A Reynolds-averaged Navier-Stokes solver was coupled with

a potential flow panel code in an attempt to split the flowfield into viscous and inviscid flow zones. The objective was to reduce the computational domain in which Navier-Stokes equations are solved. This method confines the Navier-Stokes computations to the close proximity of the vortical boundary-layer and the wake regions. It is capable of predicting low Mach number, attached or mildly separated flowfields as accurately as the full-domain Navier-Stokes solutions. For a typical flowfield, the Navier-Stokes/potential flow interactive solution method is about 40% more efficient than the full Navier-Stokes method in terms of CPU times. EI

A95-76589

SCALING OF INCIPIENT SEPARATION IN SUPERSONIC/TRANSONIC SPEED LAMINAR FLOWS

GEORGE R. INGER Iowa State Univ, Ames, IA, United States AIAA Journal (ISSN 0001-1452) vol. 33, no. 1 January 1995 p. 178-181 refs (BTN-95-EIX95182619104) Copyright

Interactions between oblique shock waves and boundary layers must be understood to predict the performance of aerodynamic devices such as flaps, spoilers, and inlets. These involve strong viscous/inviscid interaction flow with a large local adverse pressure gradient that often provokes boundary-layer separation. The prediction of the onset of such separation and the delineation of the underlying scaling laws that govern it continue to be important in aerodynamic studies of high speed aircraft and missiles, these vehicles operate and are tested over a wide range of Mach and Reynolds numbers. This paper re-examines the fundamental similarity rules pertaining to the laminar (high-altitude) flight regime of supersonic vehicles, with the goal of establishing a single unified scaling law for both supersonic and moderately hypersonic Mach numbers. EI

A95-76590

SIMPLE METHOD OF SUPERSONIC FLOW VISUALIZATION USING WATERTABLE

A. K. PAL Jadavpur Univ, Calcutta, India and B. BOSE AIAA Journal (ISSN 0001-1452) vol. 33, no. 1 January 1995 p. 181-182 refs (BTN-95-EIX95182619105) Copyright

A simple and novel optical method for the quantitative evaluation of physical flow variables in a high-speed flow has been obtained from photographs of the flow pattern, obtained in a watertable using the established theory of hydraulic analogy. Here, the photographic method for flow visualization is demonstrated at supersonic speeds. It is also shown that it may be extended to study different model configurations. EI

A95-76605

MULTIAXIS PILOT RATINGS FOR DAMAGED AIRCRAFT

YAUG-FEA JENG Oklahoma State Univ, Stillwater, OK, United States and ROBERT L. SWAIM Journal of Guidance, Control, and Dynamics (ISSN 0731-5090) vol. 17, no. 6 November-December 1994 p. 1241-1244 refs (BTN-95-EIX95182619128) Copyright

A systematic methodology for the prediction of loss of control for various maneuvers performed by a specific aircraft with various types and degrees of damage is presented. The study monitors the development of loss of control while the scale of the specific damage is increasing. This study also investigates the sensitivity of the specific aircraft to different types of damage while a specific maneuver is being performed. The result shows the existence of the critical degrees of specific damage that cause the pilot to lose control as represented by a pilot opinion rating (POR) of greater than 9 on the Cooper-Harper rating scale. Author (EI)

A95-76615

ANALYTICAL AEROPROPULSIVE/AEROELASTIC HYPERSONIC-VEHICLE MODEL WITH DYNAMIC ANALYSIS

FRANK R. CHAVEZ Univ of Maryland at Coll Park, College Park, MD, United States and DAVID K. SCHMIDT Journal of Guidance,

Control, and Dynamics (ISSN 0731-5090) vol. 17, no. 6 November-December 1994 p. 1308-1319 refs (BTN-95-EIX95182619138) Copyright

Dynamic characteristics determination of hypersonic vehicles needs an integrated approach since the propulsion system and airframe are so highly coupled. A first step toward the development of an integrated approach that is intentionally generic and basic is presented. Further, analytical expressions are developed to allow for characterization of the vehicle's dynamics early in the design cycle, so that configuration trade-off may be performed with some cognizance of the attitude dynamics. It is shown that the vehicle's aerodynamics and propulsive forces are both very significant in the evaluation of key derivatives that dictate the vehicle's dynamic characteristics. It is also shown that the vehicle selected is highly unstable in pitch and exhibits strong airframe/engine/elastic coupling in the aeroelastic and attitude dynamics. EI

A95-76636* National Aeronautics and Space Administration. Langley Research Center, Hampton, VA.

APPLICATION OF TRANSONIC SMALL DISTURBANCE THEORY TO THE ACTIVE FLEXIBLE WING MODEL

WALTER A. SILVA National Aeronautics and Space Administration, Langley Research Center, Hampton, VA and ROBERT M. BENNETT Journal of Aircraft (ISSN 0021-8669) vol. 32, no. 1 January-February 1995 p. 16-22 refs (BTN-95-EIX95182619210) Copyright

The CAP-TSD code, developed at the NASA Langley Research Center, is applied to the active flexible wing wind-tunnel model for prediction of transonic aeroelastic behavior. A semispan computational model is used for evaluation of symmetric motions, and a full-span model is used for evaluation of antisymmetric motions. Static aeroelastic solutions using the computational aeroelasticity program-transonic small disturbance, are computed. Dynamic (flutter) analyses are then performed as perturbations about the static aeroelastic deformations and presented as flutter boundaries in terms of Mach number and dynamic pressure. Flutter boundaries that take into account modal refinements, vorticity and entropy corrections, antisymmetric motions, and sensitivity to the modeling of the wingtip ballast stores are also presented and compared with experimental flutter results. Author (EI)

A95-76643* National Aeronautics and Space Administration. Langley Research Center, Hampton, VA.

ROLLING MANEUVER LOAD ALLEVIATION USING ACTIVE CONTROLS

JESSICA A. WOODS-VEDELER National Aeronautics and Space Administration, Langley Research Center, Hampton, VA, ANTHONY S. POTOTZKY, and SHERWOOD T. HOADLEY Journal of Aircraft (ISSN 0021-8669) vol. 32, no. 1 January-February 1995 p. 68-76 refs

(BTN-95-EIX95182619217) Copyright

Rolling maneuver load alleviation (RMLA) has been demonstrated on the Active Flexible Wing wind-tunnel model in the NASA Langley Transonic Dynamics Tunnel (TDT). The objective was to develop a systematic approach for designing active control laws to alleviate wing loads generated during rolling maneuvers. Two RMLA control laws were developed that utilized outboard control surface pairs (leading and trailing edge) to counteract the loads and used inboard trailing-edge control surface pairs to maintain roll performance. Rolling maneuver load tests were performed in the TDT at several dynamic pressures including two below and one 11% above the open-loop flutter dynamic pressure. Above open-loop flutter, the RMLA system was operated simultaneously with an active flutter suppression system. At all dynamic pressures for which baseline results were obtained, torsion moment loads were reduced for both RMLA control laws. Results for bending moment load reductions were mixed; however, design equations developed in this study provided conservative estimates of load reduction in all cases. Author (EI)

A95-76646

DYNAMIC INVESTIGATION OF THE ANGULAR MOTION OF A

ROTATING BODY-PARACHUTE SYSTEM

D. LEVIN Technion - Israel Inst of Technology, Haifa, Israel and Z. SHPUND Journal of Aircraft (ISSN 0021-8669) vol. 32, no. 1 January-February 1995 p. 93-99 refs (BTN-95-EIX95182619220) Copyright

The modern design of parachute-payload systems that undergo specific trajectories has to cope with dynamic behavior characteristics, which were of secondary importance in the past. Static and dynamic measurements, as well as computational simulations, are being employed to help the designers in converging to an optimal solution. However, some aerodynamic dynamic data are often impossible to obtain either computationally or experimentally through direct measurement. Novel experimental techniques have to be implemented in order to expand the analysis capability or to validate the design of specific configurations. A test technique that allows three degrees of freedom for investigating experimentally the dynamic behavior of parachute-payload systems is presented. The system is utilized to investigate the effect of the parachute geometrical variables on the dynamic stability of the parachute-payload system. The cross-type parachute-payload systems that were tested exhibit three zones of different dynamic stability modes and the occurrence of dynamic instability for statically stable configurations. These results show the need for obtaining more dynamic data for the complete understanding of the dynamic behavior of closely coupled parachute-payload configurations. Author (EI)

A95-76651

STABILITY DERIVATIVES OF A FLAPPED PLATE IN UNSTEADY GROUND EFFECT

A. O. NUHAIT King Saud Univ, Riyadh, Saudi Arabia and M. F. ZEDAN Journal of Aircraft (ISSN 0021-8669) vol. 32, no. 1 January-February 1995 p. 124-129 refs (BTN-95-EIX95182619225) Copyright

The stability derivatives of a flapped plate moving in ground proximity are evaluated using an unsteady ground effect model. The model, which has been developed previously, was extended to account for the flap. The results show that ground proximity has a substantial effect on the derivatives of the aerodynamic coefficients. The derivatives obtained by the present unsteady model disagree with those obtained by the customary steady ground effect model, especially very close to the ground. The effect of the flight-path angle (in addition to the pitch angle or angle of attack) on aerodynamic coefficients is found to be substantial and, therefore, their derivatives with respect to it are very important. Because of its own nature, the steady approach fails to account for the flight-path angle and, therefore, it cannot provide the derivatives with respect to this angle near ground. Author (EI)

A95-76653

AERODYNAMICS OF A FINITE WING WITH SIMULATED ICE

A. KHODADOUST Univ of Illinois at Urbana-Champaign, Urbana, IL, United States and M. B. BRAGG Journal of Aircraft (ISSN 0021-8669) vol. 32, no. 1 January-February 1995 p. 137-144 refs (BTN-95-EIX95182619227) Copyright

The flowfield about a semispan finite wing with a simulated leading-edge ice accretion is studied experimentally. The finite wing was tested in both a straight and swept wing configuration. Surface pressures, fluorescent oil flow visualization, and helium bubble flow visualization studies of the flowfield are reported. The presence of the simulated ice accretion produces a large leading-edge separation bubble which results in a global change of the pressure field, reduction of lift, and increase in drag. Fluorescent oil flow visualization and pressure distributions from the centerline of the straight wing at low angles of attack show a predominantly two-dimensional flowfield on the wing's upper surface. Three-dimensional effects due to the tip-induced vortex and root-wall interaction become important at high angles of attack. Oil flow visualization shows that wall suction near the wing root drastically changes the flowfield near the root. The measured span loads on the straight wing compare well with the computational results when the endwall is properly modeled. The swept wing has a highly three-dimensional flowfield. Pressure distributions indicate higher lift near the root and lower lift near the

tip. Helium bubble traces show a strong spanwise flow component on the swept wing. These results are in good qualitative agreement with Navier-Stokes calculations. Author (EI)

A95-76656

AERODYNAMIC CHARACTERISTICS OF EXTERNAL STORE CONFIGURATIONS AT LOW SPEEDS

O. OZCAN Istanbul Technical Univ, Istanbul, Turkey, M. F. UNAL, A. R. ASLAN, Y. BOZKURT, and N. H. AYDIN Journal of Aircraft (ISSN 0021-8669) vol. 32, no. 1 January-February 1995 p. 161-170 refs

(BTN-95-EIX95182619230) Copyright

Aerodynamic characteristics of external store configurations used on interceptor aircraft were investigated experimentally and computationally. Balance measurements, flow visualization, and static pressure measurements were made in a low-speed wind tunnel. The experimental and computational data revealed the global structure of the flow around a basic configuration. Six groups of models were used in the present study. This article discusses the results for the first and second group of models. The incompressible flow over a limited number of models was computed by solving the Navier-Stokes equations. The solution method is based on the Galerkin finite element discretization of space and the fractional step discretization of time. Reasonably good agreement was observed between the experimental and computational static pressure distributions on a basic geometry. The computational data, which revealed details of reverse flow regions, supported and supplemented the experimental data. Author (EI)

A95-76659

UNSTEADY GROUND EFFECTS ON AERODYNAMIC COEFFICIENTS OF FINITE WINGS WITH CAMBER

A. O. NUHAIT King Saud Univ, Riyadh, Saudi Arabia Journal of Aircraft (ISSN 0021-8669) vol. 32, no. 1 January-February 1995 p. 186-192 refs

(BTN-95-EIX95182619233) Copyright

A numerical investigation on finite thin cambered wings moving near ground in unsteady flow was conducted. The numerical model is based on the general three-dimensional vortex-lattice method in which the wake is computed as part of the solution. The image technique is used to simulate the ground effects. The computed results indicate that the percentage changes in the aerodynamic coefficients ($C_{\text{sub L}}$ and $C_{\text{sub M}}$) increase with proximity to the ground. The greater the sink rate, the weaker the increase, which is consistent with the trend shown by other experimental investigators for flat wings. Increasing the aspect ratio increases the ground effect, causing wings to start feeling the ground at higher positions. The ground effects are weaker as the camber ratio increases, consistent with the results of two-dimensional plates. Moving the position of maximum camber backward has a similar effect. Meanlines of NACA five-digit series showed bigger increase in $C_{\text{sub L}}$ and $C_{\text{sub M}}$ compared to NACA four-digit and six-digit series meanlines. Increasing the angle of attack increases the ground effects in conflict with the results of two-dimensional plates. Author (EI)

A95-76661

STUDY OF THE DROPLET SPRAY CHARACTERISTICS OF A SUBSONIC WIND TUNNEL

MICHAEL B. BRAGG Univ of Illinois at Urbana-Champaign, Urbana, IL, United States and ABDOLLAH KHODADOUST Journal of Aircraft (ISSN 0021-8669) vol. 32, no. 1 January-February 1995 p. 199-204 refs

(BTN-95-EIX95182619235) Copyright

A finite difference, two-dimensional potential flow solver, and a three-dimensional particle trajectory code have been written to compute water droplet trajectories in a subsonic incompressible flow wind tunnel. This method was used to study the spray cloud in the test section of a two-dimensional wind tunnel resulting from the injection of a distribution of water droplets in the settling chamber ahead of the inlet. The results of this computational study showed that the trajectories of the larger water droplets were affected by the droplet inertia and gravity

more dramatically than that for the smaller particles. The calculated liquid water content across the test section indicated a high concentration near the tunnel centerline. The largest droplets were present at the test section only in the center one-third of the wind tunnel, whereas the smaller droplets spanned almost the entire test section width. This resulted in a computed droplet size distribution skewed toward the larger droplets in comparison with the initial Langmuir-D distribution. The distribution of particle sizes and concentrations required at the droplet injection point in the settling chamber for a Langmuir-D distribution of uniform liquid water content in the center third of the test section was computed. Author (EI)

A95-76740

REVIEW AND DEVELOPMENT OF BASE PRESSURE AND BASE HEATING CORRELATIONS IN SUPERSONIC FLOW

J. PARKER LAMB Univ of Texas at Austin, Austin, TX, United States and WILLIAM L. OBERKAMPF Journal of Spacecraft and Rockets (ISSN 0022-4650) vol. 32, no. 1 January-February 1995 p. 8-23 refs

(BTN-95-EIX95212645688) Copyright

A comprehensive review of experimental base pressure and base heating data related to supersonic and hypersonic flight vehicles is presented. Particular attention is paid to free-flight data as well as to wind-tunnel data for models without rear sting support. Using theoretically based correlation parameters, a series of internally consistent, empirical predictions are developed for planar and axisymmetric geometries (wedges, cones, and cylinders). These equations encompass the speed range from low supersonic to hypersonic flow and laminar and turbulent forebody boundary layers. A wide range of cone and wedge angles and cone bluntness ratios is included in the data base used to develop the correlations. The present investigation also includes an analysis of the effect of the angle of attack and the specific-heat ratio of the gas. Angle-of-attack effects are considered on sharp and blunted cones and cylindrical afterbodies. Author (EI)

A95-76742

NUMERICAL INVESTIGATION OF SUPERSONIC FLOWS AROUND A SPIKED BLUNT BODY

MASAFUMI YAMAUCHI Tokyo Noko Univ, Tokyo, Japan, KOZO FUJII, and FUMIO HIGASHINO Journal of Spacecraft and Rockets (ISSN 0022-4650) vol. 32, no. 1 January-February 1995 p. 32-42 refs

(BTN-95-EIX95212645690) Copyright

In supersonic flow, a spike attached to the nose reduces the drag of a blunt body. Supersonic flows around a spiked blunt body are numerically simulated to examine the effects of the spike length, Mach number, and angle of attack. Three-dimensional thin-layer compressible Navier-Stokes equations are solved using a high-resolution upwind scheme with LU-ADI time-integration algorithm. The computed results show that the drag of the spiked blunt body is significantly influenced by the spike length, Mach number, and angle of attack. Scales of the separated region are not significantly influenced by the freestream Mach number. For the spiked blunt body at angle of attack, the flowfield becomes complex with spiral flows. The computed results are in reasonable agreement with experimental data. Author (EI)

A95-76744

INTEGRATED DESIGN OF HYPERSONIC WAVERIDERS INCLUDING INLETS AND TAILFINS

SHEAM-CHYUN LIN Natl Taiwan Inst of Technology, Taipei, Taiwan, Province of China and YU-SHAN LUO Journal of Spacecraft and Rockets (ISSN 0022-4650) vol. 32, no. 1 January-February 1995 p. 48-54 refs

(BTN-95-EIX95212645692) Copyright

A generic aerospace vehicle including an airframe, inlet, and tail-wings is developed by means of the waverider concept. The stream surfaces of the hypersonic flow past a cone with both transverse and longitudinal curvatures are used to design the forebody configuration. By suitably choosing the even polynomial

02 AERODYNAMICS

stream surfaces, the airframe, horizontal stabilizers, and inlet can be constructed together. In addition, several small caret-waveriders are patched on this configuration as the vertical fins for the furnishing of a hypersonic vehicle. Also calculated are the mass flow rate, lift, drag, and lift-to-drag ratio. Moreover, effects of the various parameters on the shape and aerodynamic performance of this high-speed vehicle are found and discussed in detail. Hence, an overall aerodynamic design of a hypersonic vehicle is established in a simple and systematic way. Author (EI)

A95-76746* National Aeronautics and Space Administration. Lewis Research Center, Cleveland, OH.

NUMERICAL ANALYSIS OF HYPERSONIC LOW-DENSITY SCRAMJET INLET FLOW

CHAN H. CHUNG National Aeronautics and Space Administration. Lewis Research Center, Cleveland, OH, SUK C. KIM, KENNETH J. DEWITT, and HENRY T. NAGAMATSU Journal of Spacecraft and Rockets (ISSN 0022-4650) vol. 32, no. 1 January-February 1995 p. 60-66 refs
(BTN-95-EIX95212645694) Copyright

Hypersonic low-density flow around a two-dimensional scramjet inlet model has been analyzed using the direct simulation Monte Carlo (DSMC) method. The predominant features of hypersonic flows, such as a thick viscous layer due to the low-density fluid together with shock-boundary-layer interaction and shock impingement as well as shock-induced separation, are encountered in this type of flowfield. Three hypersonic flowfields with different degrees of rarefaction are investigated. The freestream Knudsen numbers of the flowfields based on the height of the duct passage are in the range of 0.02-0.12. Conventional continuum gas dynamics based on the concept of a local equilibrium may not be adequate to describe this type of flowfield accurately. The pressures obtained by the DSMC simulation are compared with available experimental data. Good agreement is obtained with previous experimental data and with theoretical solutions for similar wedge flow cases near the leading edge of the ramp centerbody. Good agreement is observed with the experimental data of Minucci and Nagamatsu except for some discrepancies, especially in the lower-density cases, which may be partially attributed to three-dimensional effects and/or to experimental uncertainty. Author (EI)

A95-76747

ANALYTICAL SOLUTION AND PARAMETER ESTIMATION OF PROJECTILE DYNAMICS

SUSANNE WEISS DLR, German Aerospace Research Establishment, Braunschweig, Germany, KARL-FRIEDRICH DOHERR, and HARTMUT SCHILLING Journal of Spacecraft and Rockets (ISSN 0022-4650) vol. 32, no. 1 January-February 1995 p. 67-74 refs
(BTN-95-EIX95212645695) Copyright

For the determination of the pitch, yaw, and roll characteristics of conventional projectiles an approach is presented that allows fast estimation of the projectile parameters from test data. To avoid numerical integration and the corresponding integration errors and convergence problems, an analytical solution of the six-degree-of-freedom differential equations of motion is introduced. Here, instead of time, the arc length of the flight path is taken as the independent variable. Also, linear aerodynamics without Magnus effects is assumed. The projectile parameters are determined by minimizing the squared sum of the differences between the measured and the simulated trajectory using a nongradient direct search method. As an example, yaw-card measurements from tests with KE rods (high-kinetic-energy projectiles) are analyzed. It is shown that the main aerodynamic coefficients can be extracted from these data. In addition, it is possible to identify the size and the location of the muzzle jump as well as the jump due to sabot separation.

Author (EI)

A95-76764

LASER VELOCIMETRY SEED-PARTICLE BEHAVIOR IN SHEAR LAYERS AT MACH 12

J. D. SCHMISSEUR Wright Lab, Wright-Patterson Air Force Base,

OH, United States and M. S. MAURICE Journal of Spacecraft and Rockets (ISSN 0022-4650) vol. 32, no. 1 January-February 1995 p. 185-187 refs

(BTN-95-EIX95212645712) Copyright

The seed particle behavior in a Mach 12 flowfield was examined through laser velocimetry measurements in the Aeromechanics Division Twenty-Inch Hypersonic Wind Tunnel. Data were collected in the shear layer generated by the nozzle wall at the nozzle exit plane. Two diameters of alumina, nominally 0.3 and 1.0 micron, were used as seed material to investigate the particle response characteristics. EI

N95-22666*# National Aeronautics and Space Administration. Ames Research Center, Moffett Field, CA.

FLOW VISUALIZATION STUDIES OF VTOL AIRCRAFT MODELS DURING HOVER IN GROUND EFFECT

NIKOS J. MOURTOS (San Jose State Univ., CA.), STEPHANE COUILLAUD (San Jose State Univ., CA.), DALE CARTER (San Jose State Univ., CA.), CRAIG HANGE, DOUG WARDWELL, and RICHARD J. MARGASON Jan. 1995 48 p Original contains color illustrations

(Contract(s)/Grant(s): RTOP 505-68-32)

(NASA-TM-108860; A-95025; NAS 1.15:108860) Avail: CASI HC A03/MF A01; 28 functional color pages

A flow visualization study of several configurations of a jet-powered vertical takeoff and landing (VTOL) aircraft model during hover in ground effect was conducted. A surface oil flow technique was used to observe the flow patterns on the lower surfaces of the model. There were significant configuration effects. Wing height with respect to fuselage, the presence of an engine inlet duct beside the fuselage, and nozzle pressure ratio are seen to have strong effects on the surface flow angles on the lower surface of the wing. This test was part of a program to improve the methods for predicting the hot gas ingestion (HGI) for jet-powered vertical/short takeoff and landing (V/STOL) aircraft. The tests were performed at the Jet Calibration and Hover Test (JCAHT) Facility at Ames Research Center.

Author

N95-22802*# National Aeronautics and Space Administration. Langley Research Center, Hampton, VA.

WING PRESSURE DISTRIBUTIONS FROM SUBSONIC TESTS OF A HIGH-WING TRANSPORT MODEL

ZACHARY T. APPLIN, GARL L. GENTRY, JR., and M. A. TAKALLU (Lockheed Engineering and Sciences Co., Hampton, VA.) Jan. 1995 442 p

(Contract(s)/Grant(s): RTOP 505-59-10-13)

(NASA-TM-4583; L-17380; NAS 1.15:4583) Avail: CASI HC A19/MF A04

A wind tunnel investigation was conducted on a generic, high-wing transport model in the Langley 14- by 22-Foot Subsonic Tunnel. This report contains pressure data that document effects of various model configurations and free-stream conditions on wing pressure distributions. The untwisted wing incorporated a full-span, leading-edge Krueger flap and a part-span, double-slotted trailing-edge flap system. The trailing-edge flap was tested at four different deflection angles (20 deg, 30 deg, 40 deg, and 60 deg). Four wing configurations were tested: cruise, flaps only, Krueger flap only, and high lift (Krueger flap and flaps deployed). Tests were conducted at free-stream dynamic pressures of 20 psf to 60 psf with corresponding chord Reynolds numbers of 1.22×10^6 to 2.11×10^6 and Mach numbers of 0.12 to 0.20. The angles of attack presented range from 0 deg to 20 deg and were determined by wing configuration. The angle of sideslip ranged from minus 20 deg to 20 deg. In general, pressure distributions were relatively insensitive to free-stream speed with exceptions primarily at high angles of attack or high flap deflections. Increasing trailing-edge Krueger flap significantly reduced peak suction pressures and steep gradients on the wing at high angles of attack. Installation of the empennage had no effect on wing pressure distributions. Unpowered engine nacelles reduced suction pressures on the wing and the flaps. Author

**N95-22917*# Lockheed-Fort Worth Co., Fort Worth, TX.
EULER TECHNOLOGY ASSESSMENT PROGRAM FOR
PRELIMINARY AIRCRAFT DESIGN EMPLOYING SPLITFLOW
CODE WITH CARTESIAN UNSTRUCTURED GRID METHOD
Report, 1 Feb. - 1 Aug. 1994**

DENNIS B. FINLEY Mar. 1995 100 p
(Contract(s)/Grant(s): NAS1-19000; RTOP 505-68-30-03)
(NASA-CR-4649; NAS 1.26:4649) Avail: CASI HC A05/MF A02

This report documents results from the Euler Technology Assessment program. The objective was to evaluate the efficacy of Euler computational fluid dynamics (CFD) codes for use in preliminary aircraft design. Both the accuracy of the predictions and the rapidity of calculations were to be assessed. This portion of the study was conducted by Lockheed Fort Worth Company, using a recently developed in-house Cartesian-grid code called SPLITFLOW. The Cartesian grid technique offers several advantages for this study, including ease of volume grid generation and reduced number of cells compared to other grid schemes. SPLITFLOW also includes grid adaptation of the volume grid during the solution convergence to resolve high-gradient flow regions. This proved beneficial in resolving the large vortical structures in the flow for several configurations examined in the present study. The SPLITFLOW code predictions of the configuration forces and moments are shown to be adequate for preliminary design analysis, including predictions of sideslip effects and the effects of geometry variations at low and high angles of attack. The time required to generate the results from initial surface definition is on the order of several hours, including grid generation, which is compatible with the needs of the design environment. Author

**N95-23095*# Boeing Defense and Space Group, Seattle, WA.
EULER TECHNOLOGY ASSESSMENT FOR PRELIMINARY
AIRCRAFT DESIGN EMPLOYING OVERFLOW CODE WITH
MULTIBLOCK STRUCTURED-GRID METHOD Technical
Report, 1 Feb. - 1 Aug. 1994**

DAVID A. TREIBER and DENNIS A. MUILENBURG Hampton, VA
NASA Mar. 1995 66 p
(Contract(s)/Grant(s): NAS1-18762; RTOP 505-68-30-03)
(NASA-CR-4651; NAS 1.26:4651) Avail: CASI HC A04/MF A01

The viability of applying a state-of-the-art Euler code to calculate the aerodynamic forces and moments through maximum lift coefficient for a generic sharp-edge configuration is assessed. The OVERFLOW code, a method employing overset (Chimera) grids, was used to conduct mesh refinement studies, a wind-tunnel wall sensitivity study, and a 22-run computational matrix of flow conditions, including sideslip runs and geometry variations. The subject configuration was a generic wing-body-tail geometry with chined forebody, swept wing leading-edge, and deflected part-span leading-edge flap. The analysis showed that the Euler method is adequate for capturing some of the non-linear aerodynamic effects resulting from leading-edge and forebody vortices produced at high angle-of-attack through C_{sub} Lmax). Computed forces and moments, as well as surface pressures, match well enough useful preliminary design information to be extracted. Vortex burst effects and vortex interactions with the configuration are also investigated. Author

N95-23182*# Wayne State Univ., Detroit, MI. Dept. of Mathematics.

**ACTIVE CONTROL OF PANEL VIBRATIONS INDUCED BY A
BOUNDARY LAYER FLOW Technical Report, 31 Aug. 1990 -
31 Oct. 1994**

PAO-LIU CHOW 24 Jan. 1995 30 p
(Contract(s)/Grant(s): NAG1-1175)
(NASA-CR-197867; NAS 1.26:197867) Avail: CASI HC A03/MF A01

The problems of active and passive control of sound and vibration has been investigated by many researchers for a number of years. However, few of the articles are concerned with the sound and vibration with flow-structure interaction. Experimental and numerical studies on the coupling between panel vibration and acoustic radiation due to flow excitation have been done by Maestrello and his associates at NASA/Langley Research Center. Since the coupled

system of nonlinear partial differential equations is formidable, an analytical solution to the full problem seems impossible. For this reason, we have to simplify the problem to that of the nonlinear panel vibration induced by a uniform flow or a boundary-layer flow with a given wall pressure distribution. Based on this simplified model, we have been able to consider the control and stabilization of the nonlinear panel vibration, which have not been treated satisfactorily by other authors. Although the sound radiation has not been included, the vibration suppression will clearly reduce the sound radiation power from the panel. The major research findings are presented in three sections. In section two we describe results on the boundary control of nonlinear panel vibration, with or without flow excitation. Sections three and four are concerned with some analytical and numerical results in the optimal control of the linear and nonlinear panel vibrations, respectively, excited by the flow pressure fluctuations. Finally, in section five, we draw some conclusions from research findings. Derived from text

**N95-23185*# Lockheed Aeronautical Systems Co., Marietta, GA.
AN ASSESSMENT OF VISCOUS EFFECTS IN
COMPUTATIONAL SIMULATION OF BENIGN AND BURST
VORTEX FLOWS ON GENERIC FIGHTER WIND-TUNNEL
MODELS USING TEAM CODE Contractor Report, 1 Feb. - 1
Aug. 1994**

TIM A. KINARD, BRENDA W. HARRIS, and PRADEEP RAJ Hampton, VA NASA Mar. 1995 82 p
(Contract(s)/Grant(s): NAS1-19000; RTOP 505-68-30-03)
(NASA-CR-4650; NAS 1.26:4650) Avail: CASI HC A05/MF A01

Vortex flows on a twin-tail and a single-tail modular transonic vortex interaction (MTVI) model, representative of a generic fighter configuration, are computationally simulated in this study using the Three-dimensional Euler/Navier-Stokes Aerodynamic Method (TEAM). The primary objective is to provide an assessment of viscous effects on benign (10 deg angle of attack) and burst (35 deg angle of attack) vortex flow solutions. This study was conducted in support of a NASA project aimed at assessing the viability of using Euler technology to predict aerodynamic characteristics of aircraft configurations at moderate-to-high angles of attack in a preliminary design environment. The TEAM code solves the Euler and Reynolds-average Navier-Stokes equations on patched multiblock structured grids. Its algorithm is based on a cell-centered finite-volume formulation with multistage time-stepping scheme. Viscous effects are assessed by comparing the computed inviscid and viscous solutions with each other and experimental data. Also, results of Euler solution sensitivity to grid density and numerical dissipation are presented for the twin-tail model. The results show that proper accounting of viscous effects is necessary for detailed design and optimization but Euler solutions can provide meaningful guidelines for preliminary design of flight vehicles which exhibit vortex flows in parts of their flight envelope. Author

**N95-23193*# Joint Inst. for Advancement of Flight Sciences,
Hampton, VA.**

**AN APPROXIMATE THEORETICAL METHOD FOR MODELING
THE STATIC THRUST PERFORMANCE OF NON-
AXISYMMETRIC TWO-DIMENSIONAL CONVERGENT-
DIVERGENT NOZZLES M.S. Thesis - George Washington
Univ.**

CRAIG A. HUNTER Mar. 1995 51 p
(Contract(s)/Grant(s): NCC1-14; NCC1-24; RTOP 537-07-20)
(NASA-CR-195050; NAS 1.26:195050) Avail: CASI HC A04/MF A01

An analytical/numerical method has been developed to predict the static thrust performance of non-axisymmetric, two-dimensional convergent-divergent exhaust nozzles. Thermodynamic nozzle performance effects due to over- and underexpansion are modeled using one-dimensional compressible flow theory. Boundary layer development and skin friction losses are calculated using an approximate integral momentum method based on the classic Karman-Polhausen solution. Angularity effects are included with these two models in a computational Nozzle Performance Analysis Code,

02 AERODYNAMICS

NPAC. In four different case studies, results from NPAC are compared to experimental data obtained from subscale nozzle testing to demonstrate the capabilities and limitations of the NPAC method. In several cases, the NPAC prediction matched experimental gross thrust efficiency data to within 0.1 percent at a design NPR, and to within 0.5 percent at off-design conditions. Author

N95-23218*# Old Dominion Univ., Norfolk, VA. Dept. of Aerospace Engineering.

AERODYNAMIC DESIGN OPTIMIZATION WITH SENSITIVITY ANALYSIS AND COMPUTATIONAL FLUID DYNAMICS Final Report, period ending 31 May 1995

OKTAY BAYSAL Mar. 1995 8 p

(Contract(s)/Grant(s): NAG1-1188)

(NASA-CR-197419; NAS 1.26:197419) Avail: CASI HC A02/MF A01

An investigation was conducted from October 1, 1990 to May 31, 1994 on the development of methodologies to improve the designs (more specifically, the shape) of aerodynamic surfaces of coupling optimization algorithms (OA) with Computational Fluid Dynamics (CFD) algorithms via sensitivity analyses (SA). The study produced several promising methodologies and their proof-of-concept cases, which have been reported in the open literature. Author

N95-23250*# National Aeronautics and Space Administration. Ames Research Center, Moffett Field, CA.

EXPERIMENTAL RESULTS FOR A HYPERSONIC NOZZLE/ AFTERBODY FLOW FIELD

FRANK W. SPAID (McDonnell-Douglas Aerospace, Saint Louis, MO.), EARL R. KEENER (Eloret Corp., Palo Alto, CA.), and FRANK C. L. HUI Mar. 1995 106 p

(Contract(s)/Grant(s): RTOP 505-70-62)

(NASA-TM-4638; A-94119; NAS 1.15:4638) Avail: CASI HC A06/MF A02

This study was conducted to experimentally characterize the flow field created by the interaction of a single-expansion ramp-nozzle (SERN) flow with a hypersonic external stream. Data were obtained from a generic nozzle/afterbody model in the 3.5 Foot Hypersonic Wind Tunnel at the NASA Ames Research Center, in a cooperative experimental program involving Ames and McDonnell Douglas Aerospace. The model design and test planning were performed in close cooperation with members of the Ames computational fluid dynamics (CFD) team for the National Aerospace Plane (NASP) program. This paper presents experimental results consisting of oil-flow and shadow graph flow-visualization photographs, afterbody surface-pressure distributions, rake boundary-layer measurements, Preston-tube skin-friction measurements, and flow field surveys with five-hole and thermocouple probes. The probe data consist of impact pressure, flow direction, and total temperature profiles in the interaction flow field. Author

N95-23283*# Mississippi State Univ., Mississippi State, MS. Dept. of Aerospace Engineering.

CROSSFLOW INSTABILITY CONTROL ON A SWEEP-WING: PRELIMINARY STUDIES Abstract Only

DAVID H. BRIDGES In Hampton Univ., 1994 NASA-HU American Society for Engineering Education (ASEE) Summer Faculty Fellowship Program p 63 Dec. 1994

Avail: CASI HC A01/MF A02

The pressure distribution on a swept wing causes the streamlines at the edge of the boundary layer to be curved. This pressure gradient normal to the external streamline creates a velocity component normal to the external streamline within the boundary layer which is referred to as the crossflow velocity. Because the crossflow velocity profile perpendicular to the wing surface has an inflection point, the profile is unstable. The stationary instability mode takes the form of crossflow vortices. Under these conditions, the boundary layer on the

wing is extremely unstable and transition to turbulent flow takes place much closer to the leading edge of the wing than it would on an unswept wing. Higher skin friction drag is associated with turbulent flow, and so better aircraft performance could be obtained if the crossflow could be eliminated. One method of controlling crossflow that is being investigated is boundary-layer suction. An extensive airfoil suction experiment in the 8 feet Transonic Pressure Tunnel (TPT) at NASA Langley Research Center will begin late in 1994. Because of the size, complexity, and expense associated with this test, a number of 'risk-reduction' tests are currently being conducted. The 20 x 28 in. Shear Flow Control Tunnel at NASA Langley is being used for some of these tests. Prior to the summer of 1994, a flat plate with a swept leading edge was installed in the 20 x 28 in. tunnel, with a displacement body mounted on the tunnel ceiling that created a pressure distribution on the plate similar to the pressure distribution on a swept wing. The flow over the plate was investigated during the summer of 1994 using a laser Doppler velocimeter (LDV) system. The LDV measurements indicated the possible presence of multiple disturbance modes, a rarely-seen phenomena since, in most tests, one disturbance mode dominates. The possible existence of multiple disturbance modes in the flat plate boundary layer, however, means that the flow in the 20 x 28 in. tunnel is of interest itself, and will be investigated more thoroughly in the future. With a view to these investigations, the boundary layer traverse mechanism in the 20 x 28 in. tunnel was modified to improve its performance, and strain gauges were mounted on the traverse in order to monitor its deflection during a test. Other preliminary work conducted in the 20 x 28 in. tunnel included the use of an infrared camera system. Previous work with this system showed that transition indeed could be detected, but the signal produced by the crossflow vortices was too weak to be detected. It was hoped that spraying the flat plate with naphthalene would augment the heat transfer associated with the crossflow vortices so that they would show up in a IR image; however, experiments showed that this would not work. Another set of tests was conducted in the 20 x 28 in. tunnel to determine the tripping requirements for a set of airfoil-shaped struts that will be used in the 8 feet TPT experiment. Since the Reynolds number associated with these struts is small, a laminar boundary layer would separate early, causing large fluctuations in the flow field. A turbulent boundary layer would remain attached further back, but tripping from laminar to turbulent flow at low Reynolds number is very difficult. However, trip strip configurations were found that should effectively trip the boundary layer at the required conditions. Currently underway is an investigation of the data acquisition requirements for the 8 feet TPT experiment, with the purpose of the finding the minimum amount of data needed to characterize sufficiently the swept-wing boundary layer. This study is being conducted using a numerically generated data set. Author

N95-23294*# Texas A&M Univ., College Station, TX. Dept. of Aerospace Engineering.

CONTROL OF FLOW SEPARATION IN AIRFOIL/WING DESIGN APPLICATIONS Abstract Only

THOMAS A. GALLY In Hampton Univ., 1994 NASA-HU American Society for Engineering Education (ASEE) Summer Faculty Fellowship Program p 75 Dec. 1994

Avail: CASI HC A01/MF A02

Existing aerodynamic design methods have generally concentrated on the optimization of airfoil or wing shapes to produce a minimum drag while satisfying some basic constraints such as lift, pitching moment, or thickness. Since the minimization of drag almost always precludes the existence of separated flow, the evaluation and validation of these design methods for their robustness and accuracy when separated flow is present has not been aggressively pursued. However, two new applications for these design tools may be expected to include separated flow and the issues of aerodynamic design with this feature must be addressed. The first application of the aerodynamic design tools is the design of airfoils or wings to provide an optimal performance over a wide range of flight conditions (multipoint

design). While the definition of 'optimal performance' in the multipoint setting is currently being hashed out, it is recognized that given a wide enough range of flight conditions, it will not be possible to ensure a minimum drag constraint at all conditions, and in fact some amount of separated flow (presumably small) may have to be allowed at the more demanding flight conditions. Thus a multipoint design method must be tolerant of the existence of separated flow and may include some controls upon its extent. The second application is in the design of wings with extended high speed buffet boundaries of their flight envelopes. Buffet occurs on a wing when regions of flow separation have grown to the extent that their time varying pressures induce possible destructive effects upon the wing structure or adversely effect either the aircraft controllability or the passenger comfort. A conservative approach to the expansion of the buffet flight boundary is to simply expand the flight envelope of nonseparated flow under the assumption that buffet will also thus be alleviated. However, having the ability to design a wing with separated flow and thus to control the location, extent, and severity of the separated flow regions may allow aircraft manufacturers to gain an advantage in the early design stages of an aircraft, when configuration changes are relatively inexpensive to make. Continuing the work begun last year, an airfoil design package has been modified to provide some control over the existence and extent of flow separation. This package consists of a 2-D Navier-Stokes flow solver which is coupled to the CDISC (constrained direct/iterative surface curvature) design method. The first modification is a prediction method for determining whether separation is likely based solely upon a given pressure distribution. If separation is predicted but is undesirable, the new routines will modify the pressure distribution to alleviate the problem. This new pressure distribution is then used in the design method to generate a new aerodynamic shape. Since separation may be acceptable in some cases, particularly if the separation does not extend to the trailing edge, another added logic estimates the extent of separation based upon a correlation with calculated separated flow cases. If the flow behind a shock induced separation is not predicted to reattach before the trailing edge, the logic weakens the shock strength and otherwise alters the pressure distribution in order to promote reattachment. This later addition is as yet unreliable due to secondary separation effects, but additional work is being pursued to improve the method.

Author

N95-23333*# California Univ., Davis, CA. Dept. of Mechanical and Aeronautical Engineering.

HIGH-LIFT FLOW-PHYSICS FLIGHT EXPERIMENTS ON A SUBSONIC CIVIL TRANSPORT AIRCRAFT (B737-100)

Abstract Only

CORNELIS P. VANDAM In Hampton Univ., 1994 NASA-HU American Society for Engineering Education (ASEE) Summer Faculty Fellowship Program p 115 Dec. 1994
 Avail: CASI HC A01/MF A02

As part of the subsonic transport high-lift program, flight experiments are being conducted using NASA Langley's B737-100 to measure the flow characteristics of the multi-element high-lift system at full-scale high-Reynolds-number conditions. The instrumentation consists of hot-film anemometers to measure boundary-layer states, an infra-red camera to detect transition from laminar to turbulent flow, Preston tubes to measure wall shear stress, boundary-layer rakes to measure off-surface velocity profiles, and pressure orifices to measure surface pressure distributions. The initial phase of this research project was recently concluded with two flights on July 14. This phase consisted of a total of twenty flights over a period of about ten weeks. In the coming months the data obtained in this initial set of flight experiments will be analyzed and the results will be used to finalize the instrumentation layout for the next set of flight experiments scheduled for Winter and Spring of 1995. The main goal of these upcoming flights will be: (1) to measure more detailed surface pressure distributions across the wing for a range of flight conditions and flap settings; (2) to visualize the

surface flows across the multi-element wing at high-lift conditions using fluorescent mini tufts; and (3) to measure in more detail the changes in boundary-layer state on the various flap elements as a result of changes in flight condition and flap deflection. These flight measured results are being correlated with experimental data measured in ground-based facilities as well as with computational data calculated with methods based on the Navier-Stokes equations or a reduced set of these equations. Also these results provide insight into the extent of laminar flow that exists on actual multi-element lifting surfaces at full-scale high-life conditions. Preliminary results indicate that depending on the deflection angle, the slat and flap elements have significant regions of laminar flow over a wide range of angles of attack. Boundary-layer transition mechanisms that were observed include attachment-line contamination on the slat and inflectional instability on the slat and fore flap. Also, the results agree fairly well with the predictions reported in a paper presented at last year's AIAA Fluid Dynamics Conference. The fact that extended regions of laminar flow are shown to exist on the various elements of the high-lift system raises the question what the effect is of loss of laminar flow as a result of insect contamination, rain or ice accumulation on high-life performance.

Author

N95-23462*# Toledo Univ., OH.

ENHANCED ANALYSIS AND USERS MANUAL FOR RADIAL-INFLOW TURBINE CONCEPTUAL DESIGN CODE RTD Final Contractor Report

ARTHUR J. GLASSMAN Cleveland NASA Mar. 1995 24 p
 (Contract(s)/Grant(s): NAG3-1165; RTOP 505-69-50)
 (NASA-CR-195454; E-9538; NAS 1.26:195454) Avail: CASI HC A03/MF A01

Modeling enhancements made to a radial-inflow turbine conceptual design code are documented in this report. A stator-endwall clearance-flow model was added for use with pivoting vanes. The rotor calculations were modified to account for swept blades and splitter blades. Stator and rotor trailing-edge losses and a vaneless-space loss were added to the loss model. Changes were made to the disk-friction and rotor-clearance loss calculations. The loss model was then calibrated based on experimental turbine performance. A complete description of code input and output along with sample cases are included in the report.

Author

N95-23669*# Tennessee Univ., Tullahoma, TN. Space Inst.

SUPERSONIC LAMINAR FLOW CONTROL RESEARCH

Semiannual Report No. 2, Jul. - Dec. 1994

C. F. LO Dec. 1994 64 p
 (Contract(s)/Grant(s): NAG2-881)
 (NASA-CR-197938; NAS 1.26:197938) Avail: CASI HC A04/MF A01

The objective of the research is to understand supersonic laminar flow stability, transition and active control. Some prediction techniques will be developed or modified to analyze laminar flow stability. The effects of super laminar flow with distributed heating and cooling on active control will be studied. The primary tasks of the research applying to the NASA/Ames Proof of Concept (POC) and Laminar Flow Supersonic Wind Tunnel (LFSWT) nozzle design with laminar flow control are as follows: (1) predictions of supersonic laminar boundary layer stability and transition; (2) effects of wall heating and cooling for supersonic laminar flow control; and (3) performance evaluation of POC and LFSWT nozzles design with wall heating and cooling effects applying at different locations and various length. A paper addressing the effect of heating and cooling strips on boundary layer stability of nozzles and test sections of supersonic wind tunnels is included as an appendix.

Derived from text

AIR TRANSPORTATION AND SAFETY

Includes passenger and cargo air transport operations; and aircraft accidents.

A95-73522

DESIGN CONSTRAINTS IN THE PAYLOAD-RANGE DIAGRAM OF ULTRAHIGH CAPACITY TRANSPORT AIRPLANES

RODRIGO MARTINEZ-VAL Universidad Politecnica de Madrid, Madrid, Spain, EMILIO PEREZ, TOMAS MUNOZ, and CRISTINA CUERNO *Journal of Aircraft* (ISSN 0021-8669) vol. 31, no. 6 November-December 1994 p. 1268-1272 refs (BTN-95-EIX95152582319) Copyright

The economic and productivity potential of ultrahigh capacity airplanes, assessed through the payload-range diagram and the direct operating cost, is considered in the present work from a designer's viewpoint. Two different scenarios are envisaged: first, with current requirements and constraints; and second, after including some achievable improvements. The design constraints analyzed are maximum takeoff weight-based wing loading, maximum wingspan, minimum aspect ratio, maximum zero fuel weight-based wing loading, and maximum fuel capacity. Furthermore, to account for possible advantages of unconventional concepts, the common wing-tailplane and a three-surface arrangement are dealt with in parallel yielding a total of four cases: two configurations in two scenarios. The payload-range diagrams obtained are compatible with very dense, transatlantic, and transpacific routes; however, the three-surface solution in the second scenario exhibits very poor payload vs range flexibility. The benefits of the four cases are considered by computing the direct operating cost relative to that of a B747-400, providing clear economic arguments in favor of these ultrahigh capacity aircraft. Author (EI)

A95-73536

EFFECT OF UNDERWING FROST ON A TRANSPORT AIRCRAFT AIRFOIL AT FLIGHT REYNOLDS NUMBER

M. B. BRAGG Univ of Illinois at Urbana-Champaign, Urbana, IL, United States, D. C. HEINRICH, W. O. VALAREZO, and R. J. MCGHEE *Journal of Aircraft* (ISSN 0021-8669) vol. 31, no. 6 November-December 1994 p. 1372-1379 refs (BTN-95-EIX95152582334) Copyright

The effect of underwing frost on a transport aircraft airfoil in a takeoff configuration was studied. Underwing frost can occur when the lower surface of the wing is cooled by fuel cold-soaked in the wing tanks during cruise. Frost may accrete on the wing lower surface while the aircraft is awaiting takeoff. A two-dimensional test was performed in the NASA Langley Low-Turbulence Pressure Tunnel on a representative high-lift airfoil with a leading-edge slat and trailing-edge flap. Frost was simulated on the lower surface using distributed roughness particles. The test was conducted at $M = 0.2$ and $Re = 5 \times 10^6$ (exp 6) to 1.6×10^7 (exp 7). The effects of the frost on performance were generally small, with the largest effects occurring for the open-slat case with the frost starting at 12% chord. In this situation, it was found that the frost contaminated the upper surface boundary layer at high angles of attack, increasing drag and reducing maximum lift. Author (EI)

A95-73588

MULTIPLE SITE FATIGUE DAMAGE IN FUSELAGE SKIN SPLICES: EXPERIMENTAL SIMULATION AND THEORETICAL PREDICTION

GRAEME F. EASTAUGH Carleton Univ, PAUL V. STRAZNICKY, and DAVID L. SIMPSON *Canadian Aeronautics and Space Journal* (ISSN 0008-2821) vol. 40, no. 4 December 1994 p. 151-159 refs (BTN-95-EIX95152584676) Copyright

The results of experimental and theoretical research into multiple site fatigue damage (MSD) in the skin splices of pressurized fuselages are described. First, a special coupon-type splice test specimen has been designed that approximates on-aircraft condi-

tions and enables realistic MSD to be created and studied in a laboratory environment. The coupon specimens usually used in industry and research are not suitable for studying MSD crack growth because the net section stress increases atypically as the cracks progress and because the specimens tend to fail before MSD has developed adequately. The specimen concept described in this paper is intended to overcome these problems. Second, an efficient computer program for predicting MSD crack growth within a frame-bay has been developed. Rooke's technique of compounding stress intensity factors is applied in a new way, and graphical output of multiple crack growth curves can be produced in a few minutes on a SUN computer workstation. In an initial evaluation, the program agreed well with experimental results. Author (EI)

A95-76604

OPTIMAL LATERAL-ESCAPE MANEUVERS FOR MICROBURST ENCOUNTERS DURING FINAL APPROACH

H. G. VISSER Delft Univ of Technology, Delft, Netherlands *Journal of Guidance, Control, and Dynamics* (ISSN 0731-5090) vol. 17, no. 6 November-December 1994 p. 1234-1240 refs (BTN-95-EIX95182619127) Copyright

The optimization of lateral-escape trajectories in a microburst wind field for an aircraft on final approach is studied to minimize the peak value of altitude drop. To investigate the characteristics of open-loop extremal solutions for various locations of the microburst, an extensive numerical effort is performed. The results show that a lateral-escape maneuver may significantly improve an aircraft's survivability, in comparison to an escape maneuver restricted to the vertical plane. One of the most significant observations is that, in contrast to nonturning escape maneuvers, lateral-escape maneuvers often exhibit a climb, rather than a descent, in the initial phase. It is hoped that the insight obtained may help the development of near-optimal lateral-escape guidance strategies for onboard application. EI

A95-76645

EFFECT OF CURVATURE IN THE NUMERICAL SIMULATION OF AN ELECTROTHERMAL DE-ICER PAD

J. R. HUANG Univ of Toledo, Toledo, OH, United States, THEO G. KEITH, JR., and KENNETH J. DEWITT *Journal of Aircraft* (ISSN 0021-8669) vol. 32, no. 1 January-February 1995 p. 84-92 refs (BTN-95-EIX95182619219) Copyright

A finite element method, which incorporates an assumed phase state technique, is presented for the solution of one- and two-dimensional heat conduction problems with phase change. A simulation of an electrothermal de-iced aircraft surface is made using this method. The major interest of this study is the effect of the surface curvature on the numerical results. Comparison of predicted temperatures within a rectangular simulation and those within an airfoil reveals the extent and importance of modeling curvature effects. When surface curvature is less than 0.25, curvature effects may be neglected and a rectangular shape may be used instead of the actual geometry. Author (EI)

N95-23201# Manchester Univ. (England). Dept. of Pure and Applied Physics.

COLLABORATIVE RESEARCH ON AIRCRAFT ICING AND CHARGING PROCESSES IN ICE Final Annual Technical Report, 1 Sep. 1992 - 31 Aug. 1994

C. P. SAUNDERS 1 Sep. 1994 44 p (Contract(s)/Grant(s): AF-AFOSR-0376-91) (AD-A285102; EOARD-TR-94-07) Avail: CASI HC A03/MF A01

This study is into the electrification processes that occur when ice crystals collide with other bodies. The work is of relevance to the charging of ice pellets falling in thunderstorms when they collide with ice crystals, and to the charging of aircraft when they fly through ice phase precipitation. The study relates the thunderstorm field measurements made over recent years to the laboratory simulations of thunderstorm conditions. Charging is shown to be dependent on the water content in the cloud, on the ice crystal sizes, on the speed of impact, and on the temperature. Several theories to account for this

charge transfer behavior are discussed, including measurements of a charge layer at an ice interface that may be indicative of charge being available for transfer during ice particle collisions. The major conclusion is that all the proposed mechanisms have problems in accounting for the observed charging behavior. Further field studies are needed in which the growth or sublimation state of ice pellets in thunderstorms may be identified so that laboratory simulations can be made more relevant. DTIC

N95-23598# National Transportation Safety Board, Washington, DC.

REPORT OF PROCEEDINGS: AVIATION ACCIDENT INVESTIGATION SYMPOSIUM. VOLUME 2: PARTICIPANT PRESENTATIONS

1994 331 p Symposium held in Tysons Corner, VA, 29-31 Mar. 1994
(PB94-917007; NTSB/RP-94/02-VOL-2) Avail: CASI HC A15/MF A03

Volume 2 contains presentations made by participants in the Safety Board's Aviation Accident Investigation Symposium held at Tysons Corner, Virginia, from March 29 through 31, 1994. Volume 1 contains the Safety Board's responses to a number of recommendations made by the aviation industry during the symposium. The symposium provided a forum for the aviation industry to discuss and critique Safety Board programs and practices, as well as procedures used during aviation accident investigations. Participants included representatives from U.S. air carriers, airframe and engine manufacturers, aviation associations and unions, government officials and interested parties, as well as foreign investigative authorities and manufacturers. Author

N95-23609# National Transportation Safety Board, Washington, DC.

AIRCRAFT ACCIDENT REPORT. RUNWAY OVERRUN FOLLOWING REJECTED TAKEOFF. CONTINENTAL AIRLINES FLIGHT 795, MCDONNELL DOUGLAS MD-82, N18835, LAGUARDIA AIRPORT, FLUSHING, NY, 2 MARCH 1994

1995 89 p
(PB95-910401; NTSB/AAR-95/01) Avail: CASI HC A05/MF A01

This report explains the accident involving Continental Airlines flight 795, an MD-82 airplane, which experienced a runway overrun following a rejected takeoff from runway 13 at LaGuardia Airport, Flushing, New York, on March 2, 1994. Safety issues discussed in the report include the availability of takeoff performance data for flightcrews, the proper functioning of pitot/static heat systems, the duration of cockpit voice recordings, and problems associated with passenger evacuations from airplanes. Safety recommendations concerning these issues were addressed to the Federal Aviation Administration and to Continental Airlines, Inc. Author

N95-24012# Wichita State Univ., Wichita, KS.

THE AIRLINE QUALITY REPORT, 1994

BRENT D. BOWEN (Nebraska Univ., Omaha, NE.) and DEAN E. HEADLEY Apr. 1994 48 p
(NIAR-94-11) Avail: CASI HC A03/MF A01

The Airline Quality Rating was developed and first announced in early 1991 as an objective method of comparing airline performance on combined multiple factors important to consumers. Development history and calculation details for the AQR rating system are detailed in The Airline Quality Rating (NIAR Report 91-11) issued in April, 1991, by the National Institute for Aviation Research at Wichita State University. A full reporting of the monthly Airline Quality Rating scores for 1991 and 1992 is available in Airline Quality Report 1992 (NIAR Report 92-11) and Airline Quality Rating Report 1993 (NIAR Report 93-11) by contacting Wichita State University. The Airline Quality Rating 1994 (NIAR Report 94-11) is a summary of month-by-month quality ratings for the nine major domestic U.S. airlines operating during 1993. Using the Airline Quality Rating (AQR) system and monthly performance data for each airline for the calendar year of 1993, individual and comparative ratings are reported. This research monograph, NIAR Report 94-11, contains a

brief summary of the AQR methodology, detailed data and charts that track comparative quality for major domestic airlines across the 12 month period of 1993, and industry average results. Also, comparative Airline quality Rating data for 1992 is included to provide a longer term view of quality in the industry. Author

N95-24024# Civil Aeromedical Inst., Oklahoma City, OK.

AIRCRAFT FIRES, SMOKE TOXICITY, AND SURVIVAL: AN OVERVIEW Final Report

ARVIND K. CHATURVEDI and DONALD C. SANDERS Feb. 1995 7 p
(DOT/FAA/AM-95/8) Avail: CASI HC A02/MF A01

In-flight fires in modern aircraft are rare, but post-crash fires do occur. Cabin occupants frequently survive initial forces of such crashes but are incapacitated from smoke inhalation. According to an international study, there were 95 fire-related civil passenger aircraft accidents world-wide over a 26-year period, claiming approximately 2400 lives. Between 1985-1991, about 16% (32) of all US transport aircraft accidents involved fire and 22% (140) of the deaths in these accidents resulted from fire/smoke toxicity. Our laboratory database (1967-1993) indicates that 360 individuals in 134 fatal fire-related civil aircraft (air carrier and general aviation) accidents had carboxyhemoglobin saturation levels, with or without cyanide in blood, high enough to impair performance. Combustion toxicology is now moving from a descriptive to a mechanistic phase. Methods for gas analyses have been developed and combustion/animal-exposure assemblies have been constructed. Material/fire-retardant toxicity and interactions between smoke gases are being studied. Relationships between gas exposure concentrations, blood levels, and incapacitation onset are being established in animal models. Continuing basic research in smoke toxicity will be necessary to understand its complexities, and thus enhance aviation safety and fire survival chances. Author

N95-24050# Wichita State Univ., Wichita, KS. National Inst. for Aviation Research.

A MULTIBODY/FINITE ELEMENT ANALYSIS APPROACH FOR MODELING OF CRASH DYNAMIC RESPONSES

DEREN MA Apr. 1994 210 p
(NIAR-94-3) Avail: CASI HC A10/MF A03

Occupant models are robust tools for gaining insight into the gross motion of ground vehicle or aircraft occupants and evaluating loads and deformations of their critical parts in the studies of crashworthiness. One of the most important issues in occupant modeling is how the large motion of rigid segments of occupants such as the limbs and the small deformations of flexible bodies such as the spine column are handled. In this dissertation, mathematical models of the occupants with a finite element model of the spine are developed based on the principles of the rigid/flexible multibody dynamics and finite element methods along with numerical techniques. An exhaustive study of the occupant modeling and post-crash dynamic behavior of the vehicle occupants under various crash environments is performed by both experimental and analytical means. With the validated occupant model containing the lumbar spine, the gross motion of occupant segments, including displacements, velocities and accelerations are evaluated. The spinal axial loads, bending moments, shear forces, internal forces, nodal forces, and deformation time histories are also determined. In addition, variables such as Head Injury Criteria (HIC), Severity Index (SI) and Dynamic Response Index (DRI) are evaluated to determine possibilities of the injuries in particular crash scenario. This detailed information helps assess the level of spinal injury, determine mechanisms of spinal injury, and design and develop better occupant safety devices. Derived from text

N95-24065# Federal Aviation Administration, Washington, DC. Flight Standards Service.

OCEANIC OPERATIONS: AN AUTHORITATIVE GUIDE TO OCEANIC OPERATIONS

Sep. 1994 243 p
(FAA-AFS-550; FAA-AC-91-70) Avail: CASI HC A11/MF A03

This advisory circular (AC) contains information and guidance to be used by operators and pilots planning oceanic flights. Information is presented on the following topics: United States aviation and the International Civil Aviation Organization; oceanic operations for all aircraft in all geographic areas; North Atlantic operations; Northern Pacific operations; Southern Pacific operations; Caribbean operations; Gulf of Mexico operations; long-range navigation; helicopter oceanic operations; crew training for oceanic operations; general aviation short-range aircraft oceanic operations; polar flights; and oceanic operations to the former Soviet Union and other Soviet Block nations. CASI

**N95-24071# Civil Aeromedical Inst., Oklahoma City, OK.
A REVIEW OF CIVIL AVIATION FATAL ACCIDENTS IN WHICH
LOST/DISORIENTED WAS A CAUSE/FACTOR: 1981-1990**

Final Report

WILLIAM E. COLLINS Jan. 1995 11 p
(DOT/FAA/AM-95/1) Avail: CASI HC A03/MF A01

The National Transportation Safety Board (NTSB) analyzes circumstances and data from civil aviation accidents and describes one or more causes and/or related factors to help explain each accident. Among the formally accepted NTSB categories of accident causation is one termed 'lost/disoriented,' that term generally differs from 'spatial disorientation' and refers more to a loss of geographic awareness and, perhaps, resulting confusion on the part of the pilot. The present study was undertaken to provide information regarding the circumstances surrounding these fatal general aviation accidents in recent years, and to define demographic and behavioral characteristics of the 'lost/disoriented' pilots. Those reports were examined and analyzed in terms of type of accident, age and experience of pilots, actions of pilots, night or day, and other conditions. The computer search yielded a total of 120 accidents in which 'lost/disoriented' was among the findings noted by investigators of general aviation accidents for the 10-year period. Those accidents resulted in 169 fatalities. Related causes and circumstances associated with the accidents were analyzed and categorized. 'Lost/disoriented' accident frequency for the 1981-90 period peaked at 22 fatal accidents in 1985 and declined steadily thereafter. 75% of the pilots had no instrument rating, 64% of the accidents were associated with adverse weather, and just over half occurred at night. Other analyses suggest that educational efforts should continue to emphasize proper flight planning and the flight hazards of adverse weather conditions so that the recently lowered rates of 'lost/disoriented' accidents can be maintained or improved. Author

N95-24105# National Transportation Safety Board, Washington, DC.

AVIATION ACCIDENT INVESTIGATION SYMPOSIUM.

VOLUME 1: INDUSTRY RECOMMENDATIONS AND SAFETY BOARD RESPONSES

17 Mar. 1994 73 p Symposium held in Tysons Corner, VA, 29-31 Mar. 1994
(PB94-917005; NTSB/RP-94/01-VOL-1) Avail: CASI HC A04/MF A01

Volume 1 contains the Safety Board's responses to a number of recommendations made by the aviation industry during the Safety Board's Aviation Accident Investigation Symposium. The symposium provided a forum for the aviation industry to discuss and critique Safety Board programs and practices, as well as procedures used during aviation accident investigations. Participants included representatives from U.S. air carriers, airframe and engine manufacturers, aviation associations and unions, government officials and interested parties, as well as foreign investigative authorities and manufacturers. Author (revised)

AIRCRAFT COMMUNICATIONS AND NAVIGATION

Includes digital and voice communication with aircraft; air navigation systems (satellite and ground based); and air traffic control.

A95-73433

ON THE EXACT SOLUTIONS OF PSEUDORANGE EQUATIONS

JAMES CHAFFEE JChaffee & Associates, Austin, TX, United States and JONATHAN ABEL IEEE Transactions on Aerospace and Electronic Systems (ISSN 0018-9251) vol. 30, no. 4 October 1994 p. 1021-1030 refs
(BTN-95-EIX95142555477) Copyright

Three formulations of exact solution algorithms to the system of determined pseudorange equations are derived. It is demonstrated that pseudorange equations are hyperbolic in nature and may have two solutions, even when the emitter configuration is nonsingular. Conditions for uniqueness and for the existence of multiple solutions are derived in terms of the Lorentz inner product. The bifurcation parameter for systems of pseudorange equations is also expressed in terms of the Lorentz functional. The solution is expressed as a product of the geometric dilution of precision (GDOP) matrix, representing the linear part of the solution, and a vector of nonlinear terms. Using this formulation, stability of solutions is discussed. Author (EI)

A95-73435

ENHANCING FILTER ROBUSTNESS IN CASCADED GPS-INS INTEGRATIONS

SPIRO P. KARATSINIDES Smiths Industries, Grand Rapids, MI, United States IEEE Transactions on Aerospace and Electronic Systems (ISSN 0018-9251) vol. 30, no. 4 October 1994 p. 1001-1008 refs
(BTN-95-EIX95142555475) Copyright

Filter robustness is defined as the ability of the global positioning system/inertial navigation system (GPS/INS) Kalman filter to cope with adverse environments and input conditions, to successfully identify such conditions, and to take evasive action. A formulation of two techniques for a cascaded GPS-INS Kalman filter integration is discussed. This is an integration in which the navigation solution from a GPS receiver is used as a measurement in the filter to estimate inertial errors and instrument biases. A method of suppressing transients is also presented together with a method of formulating the filter noise statistics dynamically based on the inputs from the GPS and the INS. EI

A95-73571

THERMAL FORCE MODELING FOR GLOBAL POSITIONING SYSTEM SATELLITES USING THE FINITE ELEMENT METHOD

YVONNE VIGUE California Inst of Technology, Pasadena, CA, United States, BOB E. SCHUTZ, and P. A. M. ABUSALI Journal of Spacecraft and Rockets (ISSN 0022-4650) vol. 31, no. 5 September-October 1994 p. 855-859 refs
(BTN-95-EIX95152583270) Copyright

Geophysical applications of the Global Positioning System (GPS) require the capability to estimate and propagate satellite orbits with high precision. An accurate model of all the forces acting on a satellite is an essential part of achieving high orbit accuracy. Methods of analyzing the perturbation due to thermal radiation and determining its effects on the long-term orbital behaviour of GPS satellites are presented. The thermal imbalance force, a nongravitational orbit perturbation previously considered negligible, is the focus of this paper. The Earth's shadowing of a satellite in orbit causes periodic changes in the satellite's thermal environment. Simulations show that neglecting thermal imbalance in the satellite force model gives orbit errors larger than 10 m over several days for eclipsing satellites. This orbit mismodeling can limit accuracy in orbit determination and in estimation of baselines used for geophysical applications. Author (EI)

A95-75714

REAL-TIME NAVIGATION USING THE GLOBAL POSITIONING SYSTEM

DAN SIMON TRW Test Lab, Mesa, AZ, United States and HOSSNY EL-SHERIEF IEEE Aerospace and Electronic Systems Magazine (ISSN 0885-8985) vol. 10, no. 1 January 1995 p. 31-37 refs (BTN-95-EIX95172595298) Copyright

This paper presents the results of an investigation of the application of the Global Positioning System (GPS) to real-time integrated missile navigation. We present quantifiable measures of navigation accuracy as a function of GPS user segment parameters. These user segment parameters include antenna phase response accuracy, single versus dual frequency, and Kalman filter structure and size. We also formulate some new phase-locked loop (PLL) filter designs for application in GPS receivers, and demonstrate their superiority over more conventional filters. Author (EI)

A95-76622

SWITCHED BIAS PROPORTIONAL NAVIGATION FOR HOMING GUIDANCE AGAINST HIGHLY MANEUVERING TARGETS

K. RAVINDRABABU Indian Inst of Science, Bangalore, India, I. G. SARMA, and K. N. SWAMY Journal of Guidance, Control, and Dynamics (ISSN 0731-5090) vol. 17, no. 6 November-December 1994 p. 1357-1363 refs (BTN-95-EIX95182619145) Copyright

A new form of the proportional navigation (PN) guidance law for short-range homing missiles is proposed. Named the Switched Bias Proportional Navigation (SBPN) law, it is derived by invoking sliding-mode control theory and is structured around the basic PN, with an additive switched bias term. This additional term depends only on the polarity of the line-of-sight rate, which is readily available with a seeker. It is shown that the bias term acts as an estimate of the target acceleration and other unmodeled dynamics. An adaptive procedure is suggested to select the gain of this term, which results in improved performance. The SBPN is almost as simple to implement as the PN law itself, as it does not require any additional information related to the engagement, in the form of either measurements or estimates. Simulation results show that the acceleration profiles of SBPN closely follow those of augmented PN guidance law, after a short initial transient. They further demonstrate the robustness of the proposed SBPN in the presence of missile velocity variation. Author (EI)

A95-76631

DRAG FUNCTION MODELING FOR AIR TRAFFIC SIMULATION

MARK R. ANDERSON Virginia Polytechnic Inst and State Univ, Blacksburg, VA, United States and DANIEL E. SCHAB Journal of Guidance, Control, and Dynamics (ISSN 0731-5090) vol. 17, no. 6 November-December 1994 p. 1383-1385 refs (BTN-95-EIX95182619154) Copyright

A new approach to developing a drag function expression for commercial air traffic or combat aircraft threat models is presented. The idea is to determine parameters of a simplified drag coefficient function so that the performance of the modeled aircraft closely matches that of the actual aircraft. The drag function parameters are varied using a form of parameter identification or multidimensional curve fitting. In other words, the parameters of the air traffic model drag function are actually extracted from performance data rather than estimated from wind tunnel data. Thus, the performance of the air traffic model will match the actual aircraft. EI

A95-76674

SIMULATION ON THE 3-D TURBULENT FLOW IN THE PASSAGES OF FINOCYL GRAIN

YU LIU Northwestern Polytechnical Univ, Xi'an, China, HONGQING HE, XINPING WU, and TIMIN CAI Tuijin Jishu/Journal of Propulsion Technology (ISSN 1001-4055) no. 6 December 1994 p. 10-17 In CHINESE refs (BTN-95-EIX95202638962) Copyright

The SIMPLE algorithm was used to simulate the 3-D flow in the

chamber of solid propellant rocket engine with the following physical factors taken into account: finocyl grain, 3-D mass addition and incompressible turbulent flow, moving boundaries of propellant burning surfaces, and heat radiation of gas, etc. The equations used are: 3-D continuity, momentum, and energy equations; k-epsilon equations of turbulent model; and 3-D flux equations of heat radiation, etc. In addition, the tracking technique with marked grid was used to treat the moving boundaries of burning surfaces. Our results show that the geometry matches between the fin-canals and main passage, and the degree of propellant mass addition, will significantly influence the parameter distribution of flow field and sometimes even returning flow and eddy flow may occur. Author (revised by EI)

A95-76676

NEW FAILURE DETECTION APPROACH AND ITS APPLICATION TO GPS AUTONOMOUS INTEGRITY MONITORING

REN DA American GNC Corp, Canoga Park, CA, United States and CHING-FANG LIN IEEE Transactions on Aerospace and Electronic Systems (ISSN 0018-9251) vol. 31, no. 1 January 1995 p. 499-506 refs (BTN-95-EIX95202637613) Copyright

This investigation presents a new approach for detecting failures which affect only subsets of system measurements. In addition to a main Kalman filter, which processes all the measurements to give the optimal state estimate, a bank of auxiliary Kalman filters is also used, which process subsets of the measurements to provide the state estimates which serve as failure detection references. After the statistical property of the differences between the state estimate of the main Kalman filter and those of the auxiliaries is derived with an application of the orthogonal projection theory, failure detection is undertaken by checking the consistency between the state estimate of the main Kalman filter and those of the auxiliaries by means of the chi-square statistical hypothesis test. The effectiveness of the proposed procedure is illustrated in a problem of GPS (Global Positioning System) autonomous integrity monitoring for a GPS/SDINS (Strapdown Inertial Navigation System) integrated navigation system. Author (EI)

A95-76683

SOLUTIONS OF GENERALIZED PROPORTIONAL NAVIGATION WITH MANEUVERING AND NONMANEUVERING TARGETS

PIN-JAR YUAN Chung Shan Inst of Science and Technology, Lungtan, Taiwan, Province of China and SHIH-CHE HSU IEEE Transactions on Aerospace and Electronic Systems (ISSN 0018-9251) vol. 31, no. 1 January 1995 p. 469-474 refs (BTN-95-EIX95202637606) Copyright

In this generalized proportional navigation (GPN), the commanded acceleration is applied in a direction with a bias angle to the normal direction of line-of-sight (LOS) and its magnitude is proportional to the product of closing speed and LOS rate between interceptor and its target. Some solutions of GPN were obtained before under the assumption that the magnitude of commanded acceleration is proportional to the LOS rate only. Now in this article, the exact and complete closed-form solutions are derived under this modified guidance scheme for both maneuvering and nonmaneuvering targets. Some related important characteristics, such as capture capability and energy cost, are investigated and discussed. The variation of bias angle will induce the change of capture area and energy cost required. Also, a typical example of target maneuver is introduced to describe the effect of target maneuver easily. It shows that the target maneuver will decrease the capture area and increase the energy cost for effective intercept of target. Author (EI)

A95-76697

COVARIANCE ANALYSIS OF STRAPDOWN INS CONSIDERING GYROCOMPASS CHARACTERISTICS

HEUNG WON PARK Seoul Natl Univ, Seoul, Korea, Republic of, JANG GYU LEE, and CHAN GOOK PARK IEEE Transactions on

04 AIRCRAFT COMMUNICATIONS AND NAVIGATION

Aerospace and Electronic Systems (ISSN 0018-9251) vol. 31, no. 1 January 1995 p. 320-328 refs (BTN-95-EIX95202637592) Copyright

A complete error covariance analysis for strapdown inertial navigation system (SDINS) is presented. The authors have found that in SDINS the cross-coupling terms in gyrocompass alignment errors can significantly influence the SDINS error propagation. Initial heading error has a close correlation with the east component of gyro bias error, while initial level tilt errors are closely related to accelerometer bias errors. In addition, pseudostate variables are introduced in covariance analysis for SDINS utilizing the characteristics of gyrocompass alignment errors. This approach simplifies the covariance analysis because it makes the initial error covariance matrix to a diagonal form. Thus a real implementation becomes easier. The approach is conformed by comparing the results for a simplified case with the covariance analysis obtained from the conventional SDINS error model. Author (EI)

N95-23318* Saint Cloud State Coll., MN. Dept. of Electrical Engineering.

DIFFERENTIAL GPS AND SYSTEM INTEGRATION OF THE LOW VISIBILITY LANDING AND SURFACE OPERATIONS (LVLASO) DEMONSTRATION Abstract Only

JAMES M. RANKIN In Hampton Univ., 1994 NASA-HU American Society for Engineering Education (ASEE) Summer Faculty Fellowship Program p 100 Dec. 1994

Avail: CASI HC A01/MF A02

The LVLASO Flight Demonstration of ASTA concepts (FDAC) integrates NASA-Langley's electronic moving map display and Transport Systems Research Vehicle (TSRV) (a modified Boeing 737 aircraft); ARINC's VHF data link, GPS ground station, and automated controller workstation; and Norden's surface radar/airport movement safety system. Aircraft location is shown on the electronic map display in the cockpit. An approved taxi route as well as other aircraft and surface traffic are also displayed. An Ashtech Z12 Global Positioning System (GPS) receiver on the TSRV estimates the aircraft's position. In Differential mode (DPS), the Ashtech receiver accepts differential C/A code pseudorange corrections from a GPS ground station. The GPS ground station provides corrections up to ten satellites. The corrections are transmitted on a VHF data link at a 1 Hz. rate using the RTCM-104 format. DGPS position estimates will be within 5 meters of actual aircraft position. DGPS position estimates are blended with position, velocity, acceleration, and heading data from the TSRV Air Data/Inertial Reference System (ADIRS). The ADIRS data is accurate in the short-term, but drifts over time. The DGPS data is used to keep the ADIRS position accurate. Ownship position, velocity, heading, and turn rate are sent at a 20 Hz. rate to the electronic map display. Airport traffic is detected by the airport surface radar system. Aircraft and vehicles such as fuel trucks and baggage carts are detected. The traffic's location, velocity, and heading are sent to the TSRV. To prevent traffic symbology from jumping each second when a location update arrives, velocity and heading are used to predict a new traffic location for each display update. Possible runway incursions and collisions can be shown on the electronic map. Integrating the different systems used in the FDAC requires attention to the underlying coordinate systems. The airport diagram displayed on the electronic map is obtained from published navigational charts. The charts reference the North American Datum of 1927 (NAD27) or a local state-plane coordinate system. GPS uses the World Geodetic Standard of 1984 (WGS84). Both NAD27 and WGS84 model the Earth as an ellipsoid, however, they use a different origin and different size ellipsoids. Latitudes and longitudes given in these systems can be converted to a Cartesian system with the origin at the Earth's center. The surface radar detects traffic in a locally-level, rho-theta coordinate system. The electronic airport diagram is stored using a flat XY coordinate system. The map origin is at the tower and is referenced as True North up. All ownship and other traffic positions must be converted to the electronic map's frame of reference for display. Author

N95-23393* National Aeronautics and Space Administration. Ames Research Center, Moffett Field, CA.

CUEING LIGHT CONFIGURATION FOR AIRCRAFT NAVIGATION Patent

MARY K. KAISER, inventor (to NASA) and WALTER J. JOHNSON, inventor (to NASA) 24 May 1994 9 p Filed 27 Aug. 1992 (NASA-CASE-ARC-11982-1; US-PATENT-5,315,296; US-PATENT-APPL-SN-935939; US-PATENT-CLASS-340-946; US-PATENT-CLASS-73-178H; US-PATENT-CLASS-340-953; US-PATENT-CLASS-340-961; US-PATENT-CLASS-340-981; US-PATENT-CLASS-362-62; INT-PATENT-CLASS-G08B-21/00) Avail: US Patent and Trademark Office

A pattern of light is projected from multiple sources located on an aircraft to form two clusters. The pattern of each cluster changes as the aircraft flies above and below a predetermined nominal altitude. The initial patterns are two horizontal, spaced apart lines. Each is capable of changing to a delta formation as either the altitude or the terrain varies. The direction of the delta cues the pilot as to the direction of corrective action.

Official Gazette of the U.S. Patent and Trademark Office

N95-23565# Civil Aeromedical Inst., Oklahoma City, OK.

THE ROLE OF FLIGHT PROGRESS STRIPS IN EN ROUTE AIR TRAFFIC CONTROL: A TIME-SERIES ANALYSIS Final Report

MARK B. EDWARDS (Oklahoma Univ., Oklahoma City, OK.), DANA FULLER (Oklahoma Univ., Oklahoma City, OK.), O. U. VORTAC (Oklahoma Univ., Oklahoma City, OK.), and CAROL A. MANNING Jan. 1995 13 p

(DOT/FAA/AM-95/4) Avail: CASI HC A03/MF A01

Paper flight progress strips (FPS's) are currently used in the United States en route air traffic control system to document flight information. Impending automation will replace these paper strips with electronic flight data entries. In this observational study, control actions, communication events, and computer interactions were recorded and analyzed using time-series regression models. Regression models were developed to predict FPS activities (Writing, Manipulating, Looking) at different levels of traffic complexity, for individuals and teams of air traffic controllers. The ability to predict FPS manipulations was modest, but prediction of looking at FPS's was poor. Overall, these data indicate that: (1) flight strip activities were similar for individuals and for the data-side controllers in the team (whose primary responsibility is the strips); and (2) flight strip activity for teams was predictable from the radar-side controller's actions, but not the data-side controller's actions. Author

05

AIRCRAFT DESIGN, TESTING AND PERFORMANCE

Includes aircraft simulation technology.

A95-73437

LABS BEHIND BOEING'S NEW 777

ART BROWN Boeing Commercial Airplanes Group, TOM MOORE, MATT MILLER, and MARK LAPIN Aerospace Engineering (Warrendale, Pennsylvania) (ISSN 0736-2536) vol. 14, no. 12 December 1994 p. 17-20 (BTN-95-EIX95142562403) Copyright

Boeing's 777 twinjet transport is innovative in many ways, the most important of which is the extent to which its onboard systems for flight control, navigation, communication, climate control, and passenger comfort are integrated and interdependent. This aircraft has taken systems interdependence to an entirely new level, which could not be achieved without a new type of test laboratory. IASL will conduct all-encompassing integration testing to verify that interdependent aircraft systems function together as intended. EI

A95-73526**NONLINEAR ANGLE OF TWIST OF ADVANCED COMPOSITE WING BOXES UNDER PURE TORSION**

GIULIO ROMEO, GIACOMO FRULLA, and MARIO BUSTO *Journal of Aircraft* (ISSN 0021-8669) vol. 31, no. 6 November-December 1994 p. 1297-1302 refs
(BTN-95-EIX95152582323) Copyright

This article reports both the theoretical analysis and experimental results performed on advanced composite wing boxes under pure torsion. By taking into account the nonlinear effective shear modulus of skin panels operating during postbuckling, it is possible to obtain good correlation between the theoretical and the experimental behavior. An incomplete diagonal shear stress field is used to calculate the effective shear modulus that can be reduced by up to 50% in comparison to the unbuckled panels. This causes a drastic reduction in the wing box's torsional stiffness. At a shear load triple that of buckling, our results revealed angles of twist up to 50% greater than those predicted by the linear analysis. Author (EI)

A95-73531* National Aeronautics and Space Administration. Ames Research Center, Moffett Field, CA.

NAVIER-STOKES PREDICTION OF LARGE-AMPLITUDE DELTA-WING ROLL OSCILLATIONS

NEAL M. CHADERJIAN National Aeronautics and Space Administration. Ames Research Center, Moffett Field, CA *Journal of Aircraft* (ISSN 0021-8669) vol. 31, no. 6 November-December 1994 p. 1333-1340 refs
(BTN-95-EIX95152582329) Copyright

Vertical flow about a 65-deg sweep delta wing at 15-deg angle of attack is numerically simulated for static roll and forced roll oscillations using the time-dependent, three-dimensional, Reynolds-averaged, Navier-Stokes (RANS) equations. This is a first step towards the development of an experimentally validated computational method for simulating wing rock with the RANS equations. Turbulent computations are presented for static roll angles up through 42 deg. The effects of roll angle on the vortex aerodynamics are discussed, and solution accuracy is evaluated by comparison with experimental data. The effects of grid refinement and zonal boundary condition treatment are assessed at zero roll angle. Computational results for a large-amplitude ($\Phi(\text{sub max}) = 40$ deg), high-rate ($f = 7$ Hz) forced roll motion is also presented. Computed static and dynamic surface-pressure coefficients, rolling-moment coefficients, normal-force coefficients, and streamwise c.p. locations compare very well with experimental data. The static rolling-moment coefficients indicate the wing is statically stable under the present flow conditions. Moreover, the dynamic rolling-moment coefficients indicate that the fluid extracts energy from the wing motion, i.e., the wing is positively damped. The computed and experimental damping energy agree within 3%. Author (EI)

A95-73533**FURTHER ANALYSIS OF HIGH-RATE ROLLING EXPERIMENTS OF A 65-DEG DELTA WING**

LARS E. ERICSSON and ERNEST S. HANFF *Journal of Aircraft* (ISSN 0021-8669) vol. 31, no. 6 November-December 1994 p. 1350-1357 refs
(BTN-95-EIX95152582331) Copyright

Further analyses have been performed of the experimental results obtained in the roll oscillation tests of a 65-deg sharp-edged delta wing at 30-deg inclination of the roll axis in order to uncover the fluid mechanical phenomena causing the unusual, highly nonlinear vehicle dynamics. It was found in an earlier analysis that in addition to the expected effect of convective flow time lag, the test results show highly nonlinear effects on vortex breakdown of the oscillatory rate. The present analysis reveals that these effects are themselves influenced by convective flow time lag. As a result, the past time history of the oscillatory response can in some cases have a strong influence on the final trim condition. Author (EI)

A95-73535* National Aeronautics and Space Administration. Ames Research Center, Moffett Field, CA.

FOREBODY FLOW CONTROL ON A FULL-SCALE F/A-18 AIRCRAFT

WENDY R. LANSER National Aeronautics and Space Administration. Ames Research Center, Moffett Field, CA and LARRY A. MEYN *Journal of Aircraft* (ISSN 0021-8669) vol. 31, no. 6 November-December 1994 p. 1365-1371 refs
(BTN-95-EIX95152582333) Copyright

A full-scale F/A-18 was tested in the 80- by 120-ft Wind Tunnel at NASA Ames Research Center to measure the effectiveness of pneumatic forebody vortex control devices. By altering the forebody vortex flow, yaw control can be maintained to angles of attack greater than 50 deg. Two forebody vortex control devices were tested: (1) a discrete circular jet; and (2) a tangential blowing slot. The tests were conducted for angles of attack between 25-50 deg, and angles of sideslip from - 15 to 15 deg. The Reynolds number based on wing mean aerodynamic chord ranged from 4.5 to 12.0 x 10⁶ (exp 6). The time-averaged yawing moments, along with both time-averaged and time-dependent pressures on the forebody of the aircraft, are presented here for various configurations. Of particular interest was the result that the tangentially blowing slot had a greater effect on the yawing moment than the discrete circular jet. Additionally, it was found that blowing very close to the radome apex was not as effective as blowing slightly farther aft on the radome, and that a 16-in.-long slot was more effective than either an 8- or 48-in.-long slot. Author (EI)

A95-73537**PNEUMATIC CONCEPT FOR TIP-STALL CONTROL OF CRANKED-ARROW WINGS**

DHANVADA M. RAO ViGYAN, Inc, Hampton, VA, United States *Journal of Aircraft* (ISSN 0021-8669) vol. 31, no. 6 November-December 1994 p. 1380-1386 refs
(BTN-95-EIX95152582335) Copyright

A novel blowing concept aimed at controlling the tip stall of cranked-arrow wings was experimentally investigated. The concept employs a tangential jet sheet blown spanwise on the tip-panel upper surface, from a chordwise slot located at the leading-edge break. The blown sheet interacts three dimensionally with the external flow, forming a controllable vortex that powerfully influences the tip-panel upper-surface flowfield leading to local lift improvement and stall delay. As a consequence, simultaneous blowing on both the tips alleviates pitch-up, whereas one-side blowing provides roll control; a concurrent overall lift increase occurs in both cases due to vortex augmentation. Low-speed wind-tunnel flow visualizations, pressure measurements, and six-component balance data were acquired on a generic cranked-arrow configuration to verify the concept and obtain preliminary indications of its aerodynamic control potential. Author (EI)

A95-73540**DYNAMIC ANALYSIS OF BEARINGLESS TAIL ROTOR BLADES BASED ON NONLINEAR SHELL MODES**

OLIVIER A. BAUCHAU Rensselaer Polytechnic Inst, Troy, NY, United States and WUYING CHIANG *Journal of Aircraft* (ISSN 0021-8669) vol. 31, no. 6 November-December 1994 p. 1402-1410 refs
(BTN-95-EIX95152582338) Copyright

The unique structural features of helicopter bearingless rotors call for the development of design and modeling methodologies for laminated composite flex-structures. Indeed, the flex-structure should be flexible enough to replace the flap, lead-lag, and feathering bearings, while maintaining high strength and stiffness in the axial direction. Laminated composite materials are a material of choice for such an application. Chordwise deformations, transitional zones between different cross sections and localized compressive stresses are all likely to be present in the flex-structure, rendering the validity of a beam model questionable. In this article a nonlinear anisotropic shallow shell model is developed that accommodates transverse shearing deformations, and arbitrarily large displacements and rotations, but strains are assumed to remain small. The displacement-based shell model has six degrees of freedom at each node

and allows for an automatic compatibility of the shell and beam models. The model is validated by comparing its predictions with several benchmark problems. A four-bladed composite bearingless tail rotor system is analyzed in detail using the shell model and compared with the predictions of a beam model. Significant differences are observed between the two models, especially in the torsional behavior. Author (EI)

A95-73542

STATIC AEROELASTIC CHARACTERISTICS OF A COMPOSITE WING

IN LEE Korea Advanced Inst of Science and Technology, Taejon, Korea, Republic of, SEUNG-HO KIM, and HIROKAZU MIURA Journal of Aircraft (ISSN 0021-8669) vol. 31, no. 6 November-December 1994 p. 1413-1416 refs (BTN-95-EIX95152582340) Copyright

The effect of fiber orientation on the deformation pattern and aerodynamic coefficients of the cantilevered composite wing is investigated. The wing structure is assumed as a plate-like wing. The finite element method that accounts for the transverse shear deformation has been used for the structural analysis. The vortex lattice method has been applied to the various-shaped thin wings for the aerodynamic analysis. The aerodynamic forces are interpolated to the structural nodal forces by the surface spline method. The deformed shape of a wing and redistributed aerodynamic forces are obtained from an iteration procedure. Various-shaped thin wings are analyzed and the flexibility effect of the laminated composite wing is investigated. EI

A95-73544

METHOD FOR THE PREDICTION OF THE ONSET OF WING ROCK

BRAD S. LIEBST Air Force Inst of Technology, Wright-Patterson Air Force Base, OH, United States and ROBERT C. NOLAN Journal of Aircraft (ISSN 0021-8669) vol. 31, no. 6 November-December 1994 p. 1419-1421 refs (BTN-95-EIX95152582342) Copyright

The rolling oscillations that are commonly referred to as wing rock are actually unstable dutch-roll motions developing into a limit cycle. Dutch-roll motion may consist of considerable yaw, and sideslip at low angle of attack (AOA). The trigger parameter has been developed to predict the onset of wing rock for a swept-wing fighter design. The procedure appears to be accurate within one degree AOA as verified with flight test data. EI

A95-73549

EFFECT OF LEEWARD FLOW DIVIDERS ON THE WING ROCK OF A DELTA WING

T. TERRY NG Univ of Toledo, Toledo, OH, United States, TONY SKAFF, and JOHN KOUNTZ Journal of Aircraft (ISSN 0021-8669) vol. 31, no. 6 November-December 1994 p. 1431-1433 refs (BTN-95-EIX95152582347) Copyright

The effects of a flow divider placed on the leeward side of an 80 degree sharp-edged delta wing were studied. Effects of divider geometry, sizes, and placement were investigated. Measurements indicate that the divider increases the rolling moment at sideslip condition for the angle-of-attack range where wing rock is promoted by the divider. Flow visualization shows that this is due to an increase in the vortex position asymmetry. The static stability is increased moderately, but the dynamic stability is reduced correspondingly. The divider therefore enhances the tendency for wing rock. At higher angles of attack where wing rock is suppressed by the divider, the rolling moment at sideslip is reduced by the divider. EI

A95-73587

ANALYTICAL SOLUTION FOR CONTROLS, HEATS, AND STATES OF FLIGHT TRAJECTORIES

AHMED Z. AL-GARNI King Fahd Univ of Petroleum and Minerals, Dhahran, Saudi Arabia Journal of Spacecraft and Rockets (ISSN 0022-4650) vol. 31, no. 5 September-October 1994 p. 924-928 refs

(BTN-95-EIX95152583286) Copyright

A new closed-form analytical solution for the nonlinear aerodynamic and thrust controls in feedback form for high angle of attack is presented. Three cases are presented for each of a given pair of constraints, including analytical solutions for heat rate and heat load and for most of the state variables. Comparisons with numerical results show good agreement. It is suggested that the results obtained for the three cases can be used during several intervals of the trajectory to simulate and approximate the more general case. EI

A95-73589

VALIDATION OF AN EFFECTIVE FLAT CRUCIFORM-SHAPED SPECIMEN TO STUDY CFRP COMPOSITE LAMINATES UNDER BIAXIAL LOADING

Y. YOUSSEF Universite de Sherbrooke, Sherbrooke, Que, Canada, S. LABONTE, C. ROY, and D. LEFEBVRE Canadian Aeronautics and Space Journal (ISSN 0008-2821) vol. 40, no. 4 December 1994 p. 158-162 refs

(BTN-95-EIX95152584677) Copyright

A global research project covering different topics related to biaxial testing and characterization of composite laminates is being carried out at the Universite de Sherbrooke. Optimization of a specimen design, fabrication procedures and techniques, strain/stress measuring methods, damage monitoring, and failure theories are some of the aspects being investigated. This paper describes how the optimization of a flat cruciform-shaped specimen has been achieved by a simple testing procedure. Typical results from static biaxial tests demonstrate the effectiveness of the specimen to provide a better understanding of the strength of composite laminates. Author (EI)

A95-73590

EVALUATION OF ADVANCED AEROSPACE MATERIALS BY DEPTH SENSING INDENTATION AND SCRATCH METHODS

R. BERRICHE Materials and Propulsion Lab, Ottawa, Ont, Canada Canadian Aeronautics and Space Journal (ISSN 0008-2821) vol. 40, no. 4 December 1994 p. 163-170 refs

(BTN-95-EIX95152584678) Copyright

Depth Sensing Indentation (DSI) instruments have been proven very useful for evaluating the mechanical properties of various materials on a small scale. In this paper, a newly developed DSI instrument called the NanoMechanical Probe (NMP) is described. Methods for measuring various micro-mechanical properties, such as hardness, elastic modulus, coating-substrate adhesion, and fiber-matrix interfacial strength, are reviewed. In addition, the results of recent tests conducted on coatings and other materials for aerospace applications are presented and discussed. Author (EI)

A95-73591

IMPROVING PREDICTION: THE INCORPORATION OF SIMPLIFIED ROTOR DYNAMICS IN A MATHEMATICAL MODEL OF THE BELL 412HP

KENNETH HUI Flight Research Lab, Ottawa, Ont, Canada and STEWART BAILLIE Canadian Aeronautics and Space Journal (ISSN 0008-2821) vol. 40, no. 4 December 1994 p. 171-177 refs (BTN-95-EIX95152584679) Copyright

The development of a mathematical model of the Flight Research Laboratory (FRL) Bell 412HP helicopter is described. This mathematical model, based on project-dedicated flight test data, will be used to support the flight mechanics research program of the FRL. All models analyzed in this paper were developed using the NRC-modified version of NASA's MMLE3 program: a time domain parameter estimation routine. Because the quasi-steady six degree of freedom rigid body model resulted in a poor representation of the Bell 412HP, a rotor dynamics model has been appended to the six degree of freedom model structure to form a hybrid model. These two modelling approaches, where rotor dynamic effects were included and excluded from the estimation model, were compared for two Bell 412HP flight test cases. The incorporation of simplified rotor

dynamic effects in the hybrid model results in a Bell 412HP model with improved prediction capabilities. Author (EI)

A95-75098

H-76B FANTAIL DEMONSTRATER COMPOSITE FAN BLADE FABRICATION

THOMAS FALASCO Boeing Defense & Space Group, Philadelphia, PA, US, EDWARD ZACHAR Boeing Defense & Space Group, Philadelphia, PA, US, and ART LALLO Boeing Defense & Space Group, Philadelphia, PA, US American Helicopter Society, Journal (ISSN 0002-8711) vol. 39, no. 3 July 1994 p. 53-57 (HTN-95-80856) Copyright

The Boeing Sikorsky First Team jointly developed a modified H-76B helicopter as a demonstrator aircraft for the LH Fantail (TM) antitorque system. A significant achievement was the development and fabrication of the occurred composite Fantail (TM) blades in 15 months between program start in 1989 and aircraft completion in March 1990. The Fantail (TM) blade manufacturing concept utilizes a single cure technique which completely eliminates the requirement for multiple cure cycles and air bladders. Author (Herner)

A95-75099* National Aeronautics and Space Administration. Langley Research Center, Hampton, VA.

AN ANALYTICAL AND EXPERIMENTAL INVESTIGATION OF THE RESPONSE OF THE CURVED, COMPOSITE FRAME/SKIN SPECIMENS

EDUARDO MOAS Analytical Services and Materials, Inc., Hampton, VA, US, RICHARD L. BOITNOTT U.S. Army Research Laboratory, Hampton, VA, US, and O. HAYDEN GRIFFIN, JR. Virginia Polytechnic Institute, Blacksburg, VA, US American Helicopter Society, Journal (ISSN 0002-8711) vol. 39, no. 3 July 1994 p. 58-66

(Contract(s)/Grant(s): NAG1-343; NAG1-19317) (HTN-95-80857) Copyright

Six-foot diameter, semicircular graphite/epoxy specimens representative of generic aircraft frames were loaded quasi-statistically to determine their load response and failure mechanisms for large deflections that occur in airplanes crashes. These frame/skin specimens consisted of a cylindrical skin section co-cured with a semicircular I-frame. The skin provided the necessary lateral stiffness to keep deformations in the plane of the frame in order to realistically represent deformations as they occur in actual fuselage structures. Various frame laminate stacking sequences and geometries were evaluated by statically loading the specimen until multiple failures occurred. Two analytical methods were compared for modeling the frame/skin specimens: a two-dimensional shell finite element analysis and a one-dimensional, closed-form, curved beam solution derived using an energy method. Flange effectivities were included in the beam analysis to account for the curling phenomenon that occurs in thin flanges of curved beams. Good correlation was obtained between experimental results and the analytical predictions of the linear response of the frames prior to the initial failure. The specimens were found to be useful for evaluating composite frame designs. Author (Herner)

A95-75100

AN UNMANNED AIR VEHICLE CONCEPT WITH TIPJET DRIVE

ALAN W. SCHWARTZ Naval Surface Warfare Center, Bethesda, MD, US, KENNETH R. READER Naval Surface Warfare Center, Bethesda, MD, US, and ERNEST O. ROGERS Naval Surface Warfare Center, Bethesda, MD, US American Helicopter Society, Journal (ISSN 0002-8711) vol. 39, no. 3 July 1994 p. 67-74 (HTN-95-80858) Copyright

A new concept is developed for an unmanned aerial vehicle (UAV) configured with a tipjet-driven, two-bladed, stoppable rotor and circulation control airfoils. The vehicle's high-aspect ratio wing 'converts' to a tipjet-driven helicopter rotor for vertical takeoff and landing (VTOL). The conceptual design is presented for a 1200-lb Tipjet VTOL UAV that is suitable for performing various Navy UAV missions. Vehicle performance predictions are included for the key flight regimes of hover, low-speed rotary-wing flight, and conversion

between rotary-wing and fixed-wing flight. Results of standard mission performance analyses indicate that the 1200-lb Tipjet VTOL UAV is a viable candidate vehicle for the designated Navy UAV missions. Moreover, the Tipjet concept is directly applicable to much larger UAVs that will greatly enhance naval warfare capabilities.

Author (Herner)

A95-75773

EXPERIMENTAL EVALUATION OF A BOX BEAM

SPECIFICALLY TAILORED FOR CHORDWISE DEFORMATION

LAWRENCE W. REHFELD Univ of California, Davis, CA, United States, PETER J. ZISCHKA, STEPHEN CHANG, MICHAEL L. FENTRESS, and DAMODAR R. AMBUR AIAA Journal (ISSN 0001-1452) vol. 33, no. 1 January 1995 p. 116-119 refs (BTN-95-EIX95182619088) Copyright

This paper describes an experimental methodology based upon the use of a flexible sling support and load application system that has been created and utilized to evaluate a box beam that incorporates an elastic tailoring technology. The design technique used here for elastically tailoring the composite box beam structure is to produce exaggerated chordwise camber deformation of substantial magnitude to be of practical use in the new composite aircraft wings. The traditional methods such as a four-point bend test to apply constant bending moment with rigid fixtures inhibit the desired chordwise deformation from occurring, hence the need for the new test method. The experimental results for global camber and spanwise bending compliances correlate well with theoretical predictions based on a beamlike model. Author (EI)

A95-76390

CYPHER MOVES TOWARD AUTONOMOUS FLIGHT

STANLEY W. KANDEBO Aviation Week & Space Technology (ISSN 0005-2175) vol. 140, no. 10 March 7, 1994 p. 42-45 (HTN-95-41394) Copyright

Sikorsky aircraft expects to resume flight test of its Cypher unmanned aerial vehicle (UAV) this week following several months of retrofits aimed at advancing the autonomous capabilities of the aircraft. Cypher is a 6.5-ft-diameter, doughnut-shaped UAV driven by two independent coaxial rotors that are powered by a 52-hp, 2-cycle, rotary Aldis engine. A brief discussion of design, performance tests, and other aspects of the aircraft is presented. Herner

A95-76582

COMPARISON OF LINEAR STABILITY RESULTS WITH FLIGHT TRANSITION DATA

J. A. MASAD High Technology Corp, Hampton, VA, United States and M. R. MALIK AIAA Journal (ISSN 0001-1452) vol. 33, no. 1 January 1995 p. 161-163 refs (BTN-95-EIX95182619097) Copyright

There is a need for an accurate and efficient method of predicting the location of transition on aerodynamic surfaces. Currently, the most common approach is the empirical $e(\exp N)$ method which utilizes linear stability theory. In the work described here, the results of the $e(\exp N)$ method were compared with the experimental flight data of Fisher and Dougherty for compressible flow past a sharp cone. The comparisons demonstrate the effect of mild heat transfer at subsonic freestream Mach numbers and the effect of compressibility for freestream Mach numbers up to 2. EI

A95-76635* National Aeronautics and Space Administration. Langley Research Center, Hampton, VA.

SUMMARY OF AN ACTIVE FLEXIBLE WING PROGRAM

BOYD PERRY, III National Aeronautics and Space Administration, Langley Research Center, Hampton, VA, STANLEY R. COLE, and GERALD D. MILLER Journal of Aircraft (ISSN 0021-8669) vol. 32, no. 1 January-February 1995 p. 10-15 refs (BTN-95-EIX95182619209) Copyright

This article presents a summary of a NASA/Rockwell Active Flexible Wing program. Major elements of the program are presented. Key program accomplishments included single- and multiple-mode flutter suppression, load alleviation and load control

during rapid roll maneuvers, and multi-input/multi-output multiple-function active controls tests above the open-loop flutter boundary.

Author (EI)

A95-76644

APPLICATION OF NAVIER-STOKES AEROELASTIC METHODS TO IMPROVE FIGHTER WING MANEUVER PERFORMANCE

DAVID M. SCHUSTER Lockheed Engineering and Sciences Co., Inc., Hampton, VA, United States Journal of Aircraft (ISSN 0021-8669) vol. 32, no. 1 January-February 1995 p. 77-83 refs (BTN-95-EIX95182619218) Copyright

An aeroelastic analysis method, based on three-dimensional Navier-Stokes aerodynamics, has been applied to improve the performance of fighter wings operating at sustained maneuver flight conditions. The scheme reduces the trimmed pressure drag of wings performing high-g maneuvers through a simultaneous application of control surface deflection and aeroelastic twist. The aerodynamic and structural interactions are decoupled by assuming an aeroelastic twist mode shape and optimizing the aerodynamic performance based on this aeroelastic mode. The wing structural stiffness properties are then determined through an inverse scheme based on the aerodynamic loads and desired twist at the maneuver flight condition. The decoupled technique is verified by performing a fully coupled aeroelastic analysis. One of the more important features of this application, over and above improved maneuver flight performance, is that the wing performance at cruise conditions is not compromised. Thus, this method represents a multiple-point wing design capability utilizing computational aerodynamics methods and aeroelastic tailoring.

Author (EI)

A95-76654

RESPONSE OF A NONROTATING ROTOR BLADE TO LATERAL TURBULENCE. PART 1: THEORY

D. M. TANG Duke Univ, Durham, NC, United States and E. H. DOWELL Journal of Aircraft (ISSN 0021-8669) vol. 32, no. 1 January-February 1995 p. 145-153 refs (BTN-95-EIX95182619228) Copyright

Theoretical simulation of a rotor blade in forward flight by a nonrotating rotor blade in a longitudinal sinusoidal pulsating flow, and the flapping and torsional response of a flexible nonrotating rotor blade model to lateral turbulence, have been investigated. A direct time domain computational method using a modified linear ONERA aerodynamic model and a time-frequency approach using the classical aerodynamic model have been proposed. A theoretical lift comparison between the classical aerodynamic theory and the modified ONERA model is made. The numerical calculations indicate that the statistically quantitative agreement for both flap and torsional variance responses between the linear ONERA and classical aerodynamic models is reasonably good. The effects of random parametric excitation (when the longitudinal flow includes a turbulence component) and parameter variations are discussed. The numerical results are used to confirm the validity of a new experimental method presented as a companion paper.

Author (EI)

A95-76655

RESPONSE OF A NONROTATING ROTOR BLADE TO LATERAL TURBULENCE. PART 2: EXPERIMENT

D. M. TANG Duke Univ, Durham, NC, United States and E. H. DOWELL Journal of Aircraft (ISSN 0021-8669) vol. 32, no. 1 January-February 1995 p. 154-160 refs (BTN-95-EIX95182619229) Copyright

In Part 1 of this work, a theoretical simulation study of rotor blade response to turbulence in forward flight is presented. For verification of this theoretical computational method, a new experimental method based on a special gust field generated by a rotating slotted cylinder with an airfoil (RSC/airfoil) in a wind tunnel is developed to simulate the aerodynamic environment of a rotating rotor blade in forward flight. This gust generator can produce a single harmonic gust wave and also turbulence with uniform power spectral density over a certain frequency band in the lateral and longitudinal

directions. In this article, quantitative comparisons are also made with theoretical results for both random and nonrandom parametric excitation. The quantitative agreement between theory and experiment indicates that this experimental method is useful.

Author (EI)

N95-22510# Army Research Lab., Watertown, MA. Materials Directorate.

RATIONALE FOR THE MODULAR AIR-SYSTEM VULNERABILITY ESTIMATION NETWORK (MAVEN) METHODOLOGY Final Report, Jan. - Jun. 1994

LISA K. ROACH Sep. 1994 26 p (Contract(s)/Grant(s): DA PROJ. 1L1-62618-AH-80) (AD-A285797; ARL-TR-581) Avail: CASI HC A03/MF A01

The air community has long had a need for a new vulnerability/ lethality (V/L) methodology, one usable by the triservice community. Current methods range from manual calculations of total vulnerable area (A_v) to complex models of incendiary functioning, fragment penetration, and fire initiation with component fault tree damage modes. Most, if not all, of these models make use of expected value, or deterministic, methods which do not accurately reflect the actual, observed phenomenology. In addition, technological advances in system design and weapon lethality have outpaced the growth of these models. While the community has tried to come to grips with these more complex systems and phenomenology, clearly, the existing models have not. The purpose of this report is to describe the rationale behind the development of a new stochastic, point-burst vulnerability model for air systems which supports the myriad of analyses the air community must perform, as well as to discuss, in general, the technical requirements which generated this need.

DTIC

N95-22806*# National Aeronautics and Space Administration. Flight Research Center, Edwards, CA.

FLIGHT TEST OF THE X-29A AT HIGH ANGLE OF ATTACK: FLIGHT DYNAMICS AND CONTROLS

JEFFREY E. BAUER, ROBERT CLARKE, and JOHN J. BURKEN Washington Feb. 1995 70 p (Contract(s)/Grant(s): RTOP 505-64-30) (NASA-TP-3537; H-1984; NAS 1.60:3537) Avail: CASI HC A04/MF A01

The NASA Dryden Flight Research Center has flight tested two X-29A aircraft at low and high angles of attack. The high-angle-of-attack tests evaluate the feasibility of integrated X-29A technologies. More specific objectives focus on evaluating the high-angle-of-attack flying qualities, defining multiaxis controllability limits, and determining the maximum pitch-pointing capability. A pilot-selectable gain system allows examination of tradeoffs in airplane stability and maneuverability. Basic fighter maneuvers provide qualitative evaluation. Bank angle captures permit qualitative data analysis. This paper discusses the design goals and approach for high-angle-of-attack control laws and provides results from the envelope expansion and handling qualities testing at intermediate angles of attack. Comparisons of the flight test results to the predictions are made where appropriate. The pitch rate command structure of the longitudinal control system is shown to be a valid design for high-angle-of-attack control laws. Flight test results show that wing rock amplitude was overpredicted and aileron and rudder effectiveness were underpredicted. Flight tests show the X-29A airplane to be a good aircraft up to 40 deg angle of attack.

Author

N95-22829*# National Aeronautics and Space Administration. Flight Research Center, Edwards, CA.

DIRECT ADAPTIVE PERFORMANCE OPTIMIZATION OF SUBSONIC TRANSPORTS: A PERIODIC PERTURBATION TECHNIQUE

MARTIN D. ESPANA and GLENN GILYARD Washington Mar. 1995 45 p (Contract(s)/Grant(s): RTOP 505-69-10) (NASA-TM-4676; H-2040; NAS 1.15:4676) Avail: CASI HC A03/MF A01

Aircraft performance can be optimized at the flight condition by using available redundancy among actuators. Effective use of this potential allows improved performance beyond limits imposed by design compromises. Optimization based on nominal models does not result in the best performance of the actual aircraft at the actual flight condition. An adaptive algorithm for optimizing performance parameters, such as speed or fuel flow, in flight based exclusively on flight data is proposed. The algorithm is inherently insensitive to model inaccuracies and measurement noise and biases and can optimize several decision variables at the same time. An adaptive constraint controller integrated into the algorithm regulates the optimization constraints, such as altitude or speed, without requiring and prior knowledge of the autopilot design. The algorithm has a modular structure which allows easy incorporation (or removal) of optimization constraints or decision variables to the optimization problem. An important part of the contribution is the development of analytical tools enabling convergence analysis of the algorithm and the establishment of simple design rules. The fuel-flow minimization and velocity maximization modes of the algorithm are demonstrated on the NASA Dryden B-720 nonlinear flight simulator for the single- and multi-effector optimization cases. Author

N95-22949*# Old Dominion Univ., Norfolk, VA. Dept. of Aerospace Engineering.

A CFD STUDY OF COMPLEX MISSILE AND STORE CONFIGURATIONS IN RELATIVE MOTION Final Report, period ending 30 Sep. 1994

OKTAY BAYSAL Mar. 1995 6 p
(Contract(s)/Grant(s): NAG1-1150)
(NASA-CR-197912; NAS 1.26:197912) Avail: CASI HC A02/MF A01

An investigation was conducted from May 16, 1990 to August 31, 1994 on the development of computational fluid dynamics (CFD) methodologies for complex missiles and the store separation problem. These flowfields involved multiple-component configurations, where at least one of the objects was engaged in relative motion. The two most important issues that had to be addressed were: (1) the unsteadiness of the flowfields (time-accurate and efficient CFD algorithms for the unsteady equations), and (2) the generation of grid systems which would permit multiple and moving bodies in the computational domain (dynamic domain decomposition). The study produced two competing and promising methodologies, and their proof-of-concept cases, which have been reported in the open literature: (1) Unsteady solutions on dynamic, overlapped grids, which may also be perceived as moving, locally-structured grids, and (2) Unsteady solutions on dynamic, unstructured grids. Author

N95-22953*# National Aeronautics and Space Administration. Langley Research Center, Hampton, VA.

INTEGRATED AERODYNAMIC/DYNAMIC/STRUCTURAL OPTIMIZATION OF HELICOPTER ROTOR BLADES USING MULTILEVEL DECOMPOSITION

JOANNE L. WALSH, KATHERINE C. YOUNG, JOCELYN I. PRITCHARD (Army Vehicle Structures Lab., Hampton, VA.), HOWARD M. ADELMAN, and WAYNE R. MANTAY (Army Aviation Systems Command, Hampton, VA.) Jan. 1995 52 p
(Contract(s)/Grant(s): RTOP 505-63-36-06; DA PROJ. 1L1-6241-A-47-AB)
(NASA-TP-3465; L-17233; NAS 1.60:3465; ARL-TR-518) Avail: CASI HC A04/MF A01

This paper describes an integrated aerodynamic/dynamic/structural (IADS) optimization procedure for helicopter rotor blades. The procedure combines performance, dynamics, and structural analyses with a general-purpose optimizer using multilevel decomposition techniques. At the upper level, the structure is defined in terms of global quantities (stiffness, mass, and average strains). At the lower level, the structure is defined in terms of local quantities (detailed dimensions of the blade structure and stresses). The IADS procedure provides an optimization technique that is compatible with industrial design practices in which the aerodynamic and dynamic designs are performed at a global level and the structural

design is carried out at a detailed level with considerable dialog and compromise among the aerodynamic, dynamic, and structural groups. The IADS procedure is demonstrated for several examples.

Author

N95-23161# National Aerospace Lab., Amsterdam (Netherlands). **REVIEW OF AERONAUTICAL FATIGUE INVESTIGATION IN THE NETHERLANDS DURING THE PERIOD MARCH 1991-MARCH 1993 Technical Paper**

J. B. DEJONGE 16 Mar. 1993 33 p See also PB92-223437 (PB95-139184; NLR-TP-93109-U) Avail: CASI HC A03/MF A01

A brief review is given of work performed in the Netherlands in the field of aeronautical fatigue. Where possible, applicable references have been presented. NTIS

N95-23217*# Princeton Univ., NJ. Dept. of Mechanical and Aerospace Engineering.

AN INVESTIGATION OF HELICOPTER DYNAMIC COUPLING USING AN ANALYTICAL MODEL Final Report

JEFFREY D. KELLER 7 Mar. 1995 23 p
(Contract(s)/Grant(s): NAG2-561)
(NASA-CR-197420; NAS 1.26:197420) Avail: CASI HC A03/MF A01

Many attempts have been made in recent years to predict the off-axis response of a helicopter to control inputs, and most have had little success. Since physical insight is limited by the complexity of numerical simulation models, this paper examines the off-axis response problem using an analytical model, with the goal of understanding the mechanics of the coupling. A new induced velocity model is extended to include the effects of wake distortion from pitch rate. It is shown that the inclusion of these results in a significant change in the lateral flap response to a steady pitch rate. The proposed inflow model is coupled with the full rotor/body dynamics, and comparisons are made between the model and flight test data for a UH-60 in hover. Results show that inclusion of induced velocity variations due to shaft rate improves correlation in the pitch response to lateral cycle inputs. Author

N95-23317*# Mississippi State Univ., Mississippi State, MS. Dept. of Aerospace Engineering.

THIN TAILORED COMPOSITE WING FOR CIVIL TILTROTOR Abstract Only

MASOUD RAIS-ROHANI In Hampton Univ., 1994 NASA-HU American Society for Engineering Education (ASEE) Summer Faculty Fellowship Program p 99 Dec. 1994
Avail: CASI HC A01/MF A02

The tiltrotor aircraft is a flight vehicle which combines the efficient low speed (i.e., take-off, landing, and hover) characteristics of a helicopter with the efficient cruise speed of a turboprop airplane. A well-known example of such vehicle is the Bell-Boeing V-22 Osprey. The high cruise speed and range constraints placed on the civil tiltrotor require a relatively thin wing to increase the drag-divergence Mach number which translates into lower compressibility drag. It is required to reduce the wing maximum thickness-to-chord ratio t/c from 23% (i.e., V-22 wing) to 18%. While a reduction in wing thickness results in improved aerodynamic efficiency, it has an adverse effect on the wing structure and it tends to reduce structural stiffness. If ignored, the reduction in wing stiffness leads to susceptibility to aeroelastic and dynamic instabilities which may consequently cause a catastrophic failure. By taking advantage of the directional stiffness characteristics of composite materials the wing structure may be tailored to have the necessary stiffness, at a lower thickness, while keeping the weight low. The goal of this study is to design a wing structure for minimum weight subject to structural, dynamic and aeroelastic constraints. The structural constraints are in terms of strength and buckling allowables. The dynamic constraints are in terms of wing natural frequencies in vertical and horizontal bending and torsion. The aeroelastic constraints are in terms of frequency placement of the wing structure relative to those of the rotor system. The wing-rotor-pylon aeroelastic and dynamic interactions are limited in this design study by holding the cruise

05 AIRCRAFT COMMUNICATIONS AND NAVIGATION

speed, rotor-pylon system, and wing geometric attributes fixed. To assure that the wing-rotor stability margins are maintained a more rigorous analysis based on a detailed model of the rotor system will need to ensue following the design study. The skin-stringer-rib type architecture is used for the wing-box structure. The design variables include upper and lower skin ply thicknesses and orientation angles, spar and rib web thicknesses and cap areas, and stringer cross-sectional areas. These design variables will allow the maximum tailoring of the structure to meet the design requirements most efficiently. Initial dynamic analysis has been conducted using MSC/NASTRAN to determine the baseline wing's frequencies and mode shapes. For the design study we intend to use the finite-element based code called WIDOWAC (Wing Design Optimization With Aerodynamic Constraints) that was developed at NASA Langley in early 1970's for airplane wing structural analysis and preliminary design. Currently, the focus is on modification and validation of this code which will be used for the civil tiltrotor design efforts. Author

N95-23390* National Aeronautics and Space Administration. Ames Research Center, Moffett Field, CA.

AERODYNAMIC SURFACE DISTENSION SYSTEM FOR HIGH ANGLE OF ATTACK FOREBODY VORTEX CONTROL Patent
PETER T. ZELL, inventor (to NASA) 5 Jul. 1994 10 p Filed 8 Feb. 1993

(NASA-CASE-ARC-11979-1; US-PATENT-5,326,050; US-PATENT-APPL-SN-014584; US-PATENT-CLASS-244-75R; US-PATENT-CLASS-244-199; INT-PATENT-CLASS-B64C-5/00) Avail: US Patent and Trademark Office

A deployable system is introduced for assisting flight control under certain flight conditions, such as at high angles of attack, whereby two inflatable membranes are located on the forebody portion of an aircraft on opposite sides thereof. The members form control surfaces for effecting lateral control forces if one is inflated and longitudinal control forces if both are inflated.

Official Gazette of the U.S. Patent and Trademark Office

N95-23395* National Aeronautics and Space Administration. Ames Research Center, Moffett Field, CA.

LIFT ENHANCING TABS FOR AIRFOILS Patent
JAMES C. ROSS, inventor (to NASA) 15 Mar. 1994 9 p Filed 8 Feb. 1993

(NASA-CASE-ARC-11990-1; US-PATENT-5,294,080; US-PATENT-APPL-SN-014581; US-PATENT-CLASS-244-215; US-PATENT-CLASS-244-216; INT-PATENT-CLASS-B64C-9/16) Avail: US Patent and Trademark Office

A tab deployable from the trailing edge of a main airfoil element forces flow onto a following airfoil element, such as a flap, to keep the flow attached and thus enhance lift. For aircraft wings with high lift systems that include leading edge slats, the slats may also be provided with tabs to turn the flow onto the following main element.

Official Gazette of the U.S. Patent and Trademark Office

N95-23666 Defence Science and Technology Organisation, Melbourne (Australia). Air Operations Div.

ENHANCEMENT OF F/A-18 OPERATIONAL FLIGHT MEASUREMENTS: DATA REPORT FOR PHASE 1

B. A. WOODYATT, J. BENNETT, and S. D. HILL Aug. 1994 73 p (DSTO-TR-0049; AR-008-910) Copyright Avail: Issuing Activity (DSTO Aeronautical and Maritime Research Lab., GPO Box 4331, Melbourne, Victoria 3001, Australia)

This report describes the procedures used in the processing of approximately 300 hours of flight maintenance data from the F/A-18's Maintenance Status Display and Recording System (MSDRS). A Flight Path Reconstruction (FPR) program and a modified F/A-18 mathematical model from the US Naval Air Warfare Center Aircraft Division (NAWC-AD) were used to enhance these flight data in resolution and frequency. DSTO's Airframes and Engines Division (AED) will use these enhanced flight data to obtain a representative flight load spectrum. The load spectrum will be used in a full scale

fatigue test of the empennage and aft fuselage of an F/A-18, the Australian contribution to the International Follow-On Structural Test Program (IFOSTP). IFOSTP is a joint collaboration between the Canadian Forces (CF) and the Royal Australian Air Force (RAAF) to appraise structural modifications to the F/A-18 designed to achieve a service life of 6000 hours. Author

N95-24091# General Accounting Office, Washington, DC. National Security and International Affairs Div.

REPORT TO THE SECRETARY OF DEFENSE. UNMANNED AERIAL VEHICLES: NO MORE HUNTER SYSTEMS SHOULD BE BOUGHT UNTIL PROBLEMS ARE FIXED

Mar. 1995 19 p

(GAO/NSIAD-95-52; B-259256) Avail: CASI HC A03/MF A01; GAO, PO Box 6015, Gaithersburg, MD 20877 HC

The Department of Defense is acquiring the Hunter Short-Range Unmanned Aerial Vehicle (UAV) for use by the Army, Navy and Marine Corps. The Hunter is a pilotless aircraft resembling a small airplane that is controlled from a ground station. It is intended to perform reconnaissance, target acquisition, and other military missions by flying over enemy territory and transmitting video imagery back to ground stations for use by military commanders. This report reviews the Hunter program to determine: (1) whether it has been demonstrated to be logistically supportable; (2) whether performance deficiencies found in prior testing have been resolved; and (3) whether it represents a valid joint-service effort as mandated by Congress. Derived from text

06

AIRCRAFT INSTRUMENTATION

Includes cockpit and cabin display devices; and flight instruments.

A95-73438

FLIGHT-DECK DISPLAYS ON THE BOEING 777

JEAN M. CRANE Boeing Commercial Airplane Group, ERIC S. BANG, and MARTIN C. HARTEL Aerospace Engineering (Warrendale, Pennsylvania) (ISSN 0736-2536) vol. 14, no. 12 December 1994 p. 11-16

(BTN-95-EIX95142562402) Copyright

Two new functions incorporated onto the Boeing 777 flight deck, the electronic checklist function (ECL) and the flight deck communication function (FDCF), can be accessed interactively on multifunctional displays. Using an integrated design approach, wherein the design and operational requirements of both were developed with CCds and a CUI, engineers were able to maximize ease of training and operation. Before the functions could be integrated to the flight deck, decisions regarding where information would be displayed, how pilot would interact with the functions, and where the controls would be located were made. Boeing 777 applied an integrated approach that maintained the existing flight-deck philosophies and did not add new technologies simply for technologies' sake. EI

A95-73451

GROWTH OF MULTIPLE CRACKS AND THEIR LINKUP IN A FUSELAGE LAP JOINT

RIPUDAMAN SINGH Georgia Inst of Technology, Atlanta, GA, United States, JAI H. PARK, and SATYA N. ATLURI AIAA Journal (ISSN 0001-1452) vol. 32, no. 11 November 1994 p. 2260-2268 refs

(BTN-95-EIX95142553047) Copyright

An issue of concern in aging aircraft is the growth of multiple cracks emanating from a row of fastener holes, typically in a pressurized aircraft fuselage lap splice. This multisite damage (MSD), or widespread fatigue damage, if allowed to progress, can suddenly become catastrophic. The understanding of the failure

behavior dictates the level of compromise between safety and economy. The complexity of the structure due to various stiffening elements makes it unamenable to a simple direct analysis. A two-step elastic finite element fatigue analysis combining a conventional finite element method and the Schwartz-Neumann alternating method, with analytical solutions is developed to understand fatigue growth of multiple cracks and to obtain a first estimate of the residual life of a stiffened fuselage shell structure with MSD in the riveted lap joint. The analysis procedure is validated by simulating a laboratory fatigue test on a lap joint in a flat coupon. Both the coupon and the shell panel are found to have fatigue lives only up to the first linkup of neighboring crack tips. Author (EI)

A95-75716

CASS: DESIGN FOR SUPPORTABILITY

ANDREW C. MENA Martin Marietta Corp, Daytona Beach, FL, United States IEEE Aerospace and Electronic Systems Magazine (ISSN 0885-8985) vol. 10, no. 1 January 1995 p. 23-27 refs (BTN-95-EIX95172595296) Copyright

All configurations of the CASS test set are designed around a common HYBRID core. The five configurations of CASS provide the heart of all known present and future requirements for Automatic Test Equipment (ATE). Additional testing requirements are fulfilled by CASS through ancillary equipment such as inertial navigation systems, advanced communication bus interfaces, fiber optic data bus, high-speed data bus, and pneumatics capabilities. The high-power device test subsystem, currently in its conceptual phase, is another ancillary addition which can be connected to any RF or CNI configuration to support all high-power RF requirements. Building all capabilities around a common core eliminates many of the problems associated with previously fielded ATE systems. One of the major problems that has been reduced is the negative impact on systems being supported when the test set fails. EI

A95-75717

CONTAINING MILITARY AUTOTEST COST GROWTH THROUGH THE USE OF COMMERCIAL STANDARD EQUIPMENT ARCHITECTURES

R. E. KNOFF Collins Avionics & Communications Div, Cedar Rapids, IA, United States IEEE Aerospace and Electronic Systems Magazine (ISSN 0885-8985) vol. 10, no. 1 January 1995 p. 19-22

(BTN-95-EIX95172595295) Copyright

The recent past has been stressful for commercial airline industry: fierce competition has caused the demise of several carriers. The resulting drive to slash operating expenses has bolstered development of avionics industry standards for automated test equipment. Rockwell's Collins Air Transport Division (CATD) has begun to market compliant test gear that airline maintenance departments wishing to acquire modern high performance test systems without the development cost penalty has eagerly received. A similar situation now confronts the military. The various branches can no longer justify the maintenance of independent autotest architectures. This paper describes the CATD implementation of the commercial-standard architecture; shows how we have designed the system to avoid obsolescence; and indicates the considerations that are necessary for adapting it to military scenarios. Author (EI)

A95-75718

ATE ENABLING TECHNOLOGIES

LARRY V. KIRKLAND OO-ALC/TISA, Hill AFB, UT, United States and JEFFREY S. DEAN IEEE Aerospace and Electronic Systems Magazine (ISSN 0885-8985) vol. 10, no. 1 January 1995 p. 14-18 refs

(BTN-95-EIX95172595294) Copyright

A discussion of the current and emerging core technologies and philosophies that will enable Air Force personnel to quickly, accurately and intuitively diagnose faults in increasingly complex systems. Author (EI)

A95-75720

NEW COMMERCIAL OFF-THE-SHELF TESTERS ARE AUTOMATIC AND INTELLIGENT

HENRY OMAN IEEE Aerospace and Electronic Systems Magazine (ISSN 0885-8985) vol. 10, no. 1 January 1995 p. 3-8 refs (BTN-95-EIX95172595292) Copyright

A typical commercial off-the-shelf (COTS) automatic tester is based on a 60-MHz 486 PC with a 1-Gb hard disk. It uses open-architecture operating systems. The test engineer can create his own test programs, using packages such as LABVIEW, ATLAS, and SMART. He does not need support from a team of computer programmers. This is the direction in which commercial airlines are going. The COTS tester can have an IEEE Standard 'VXI' box. Into it can be plugged virtual-instrument circuit cards. New automatic-testing technology ranges from multi-media presentations of test advice to the trouble-shooting technician, to 3-D video displays. This technology, plus orders for Department of Defense agencies to use COTS, presents to the armed services these choices: (1) continue buying and using 1980's technology, or (2) go to the lower-cost, high-performance COTS that were shown and described at AUTOTESTCON '93 by the test-equipment industry. EI

A95-76734

OVERVIEW OF ALLIEDSIGNAL'S AVIONICS DEVELOPMENT IN THE CIS

FRANK M. G. DORENBERG AlliedSignal Commercial Avionics Systems and LEO G. LAFORGE IEEE Aerospace and Electronic Systems Magazine (ISSN 0885-8985) vol. 10, no. 2 February 1995 p. 8-12 refs

(BTN-95-EIX95212641069) Copyright

Comprised of 12 independent countries, the Commonwealth of Independent States (CIS), successor to the Soviet Union, has a large aerospace industry. In pursuing its objectives as a global supplier, AlliedSignal Aerospace has adopted a strategy for conducting business in the CIS which is based upon forming long-term partnerships with domestic suppliers, to jointly develop products and services for this large and growing market. This paper describes the CIS aviation industry and infrastructure, and gives an overview of the development of the ARIA-200 system - a project of AlliedSignal to provide air transports with internationally accepted levels of operational capabilities and state-of-the-art equipment, functionality, and reliability. A description of one such air transport, the BE-200, is given. It is a multirole amphibious aircraft designed primarily for fire fighting. EI

A95-76735

DESIGN OF WIDE ANGLE HEAD UP DISPLAYS FOR SYNTHETIC VISION

PAUL L. WISELY GEC Marconi Avionic Ltd, Kent, United Kingdom IEEE Aerospace and Electronic Systems Magazine (ISSN 0885-8985) vol. 10, no. 2 February 1995 p. 13-18 refs

(BTN-95-EIX95212641070) Copyright

With the current interest by aircraft manufacturers and operators in both enhanced and synthetic vision has come increased interest by industry in designing and producing suitable head up displays to help realize such systems. Author (EI)

A95-76736

FLIGHT TEST EVALUATION OF A 35 GHZ FORWARD LOOKING ALTIMETER FOR TERRAIN AVOIDANCE

ROBERT C. BECKER Honeywell Technology Cent, Minneapolis, MN, United States and LARRY D. ALMSTED IEEE Aerospace and Electronic Systems Magazine (ISSN 0885-8985) vol. 10, no. 2 February 1995 p. 19-22

(BTN-95-EIX95212641071) Copyright

Honeywell has conducted a series of flight tests of a 35 GHz digital microprocessor controlled forward looking radar altimeter. A Bell 206L Jet Ranger helicopter was used to evaluate the capability of the sensor as a detector of various types of terrain collision hazards. The sensor was composed of a covert, spread spectrum radar altimeter processor driving a 35 GHz converter and antenna

06 AIRCRAFT PROPULSION AND POWER

assembly mounted on a steerable platform. Excellent correlation between predicted performance and observed performance was obtained. Author (EI)

N95-22578* National Aeronautics and Space Administration. Pasadena Office, CA.

VIRTUAL REALITY FLIGHT CONTROL DISPLAY WITH SIX-DEGREE-OF-FREEDOM CONTROLLER AND SPHERICAL ORIENTATION OVERLAY Patent

BRIAN C. BECKMAN, inventor (to NASA) (Jet Propulsion Lab., California Inst. of Tech., Pasadena, CA.) 14 Feb. 1995 14 p. Filed 23 Apr. 1993 Supersedes N93-30416 (31 - 11, p. 3251)

(Contract(s)/Grant(s): NAS7-918)

(NASA-CASE-NPO-18733-1-CU; US-PATENT-5,388,990; US-PATENT-APPL-SN-056503; US-PATENT-CLASS-434-38; US-PATENT-CLASS-434-43; US-PATENT-CLASS-434-307R; US-PATENT-CLASS-434-372; US-PATENT-CLASS-364-578; US-PATENT-CLASS-395-152; US-PATENT-CLASS-345-8) Avail: US Patent and Trademark Office

A virtual reality flight control system displays to the pilot the image of a scene surrounding a vehicle or pod having six degrees of freedom of acceleration or velocity control by the pilot and traveling through inertial space, the image itself including a superimposed figure providing the pilot an instant reference of orientation consisting of superimposed sets of geometric figures whose relative orientations provide the pilot an instantaneous feel or sense of orientation changes with respect to some fixed coordinate system. They include a first set of geometric figures whose orientations are fixed to the pilot's vehicle and a second set of geometric figures whose orientations are fixed with respect to a fixed or interstellar coordinate system. The first set of figures is a first set of orthogonal great circles about the three orthogonal axes of the flight vehicle or pod and centered at and surrounding the pilot's head, while the second set of figures is a second set of orthogonal great circles about the three orthogonal axes of a fixed or interstellar coordinate system, also centered at and surrounding the pilot's head.

Official Gazette of the U.S. Patent and Trademark Office

N95-24030* National Aeronautics and Space Administration. Ames Research Center, Moffett Field, CA.

TRISTAR 1: EVALUATION METHODS FOR TESTING HEAD-UP DISPLAY (HUD) FLIGHT SYMBOLOGY

R. L. NEWMAN (Crew Systems Consultants, San Marcos, TX.), L. A. HAWORTH, G. K. KESSLER (Naval Air Test Center, Patuxent River, MD.), D. J. EKSUZIAN (Naval Air Development Center, Warminster, PA.), W. R. ERCOLINE (Krug Life Sciences, Inc., Houston, TX.), R. H. EVANS (Air Force Instrument Flight Center, Randolph AFB, TX.), T. C. HUGHES (Aeronautical Systems Div., Wright-Patterson AFB, OH.), and L. F. WEINSTEIN (Krug Life Sciences, Inc., Houston, TX.) Feb. 1995 88 p

(Contract(s)/Grant(s): RTOP 505-64-36)

(NASA-TM-4665; A-94141; NAS 1.15:4665; TR-94-A-019; NAWCADPAX-95-10-RTR; AL-CF-TR-1994-0159) Avail: CASI HC A05/MF A01

The first in a series of piloted head-up display (HUD) flight symbology studies (TRISTAR) measuring pilot task performance was conducted at the NASA Ames Research Center by the Tri-Service Flight Symbology Working Group (FSWG). Sponsored by the U.S. Army Aeroflightdynamics Directorate, this study served as a focal point for the FSWG to examine HUD test methodology and flight symbology presentations. HUD climb-dive marker dynamics and climb-dive ladder presentations were examined as pilots performed air-to-air (A/A), air-to-ground (A/G), instrument landing system (ILS), and unusual attitude (UA) recover tasks. Symbolic presentations resembled pitch ladder variations used by the U.S. Air Force (USAF), U.S. Navy (USN), and Royal Air Force (RAF). The study was initiated by the FSWG to address HUD flight symbology deficiencies, standardization, issue identification, and test methodologies. It provided the mechanism by which the USAF, USN, RAF, and USA could integrate organizational ideas and reduce differences for comparisons. Specifically it examined flight symbology

issues collectively identified by each organization and the use of objective and subjective text methodology and flight tasking proposed by the FSWG. Author

07

AIRCRAFT PROPULSION AND POWER

Includes prime propulsion systems and systems components, e.g., gas turbine engines and compressors; and on-board auxiliary power plants for aircraft.

A95-75757

ARTIFICIAL INTELLIGENCE FOR TURBOPROP ENGINE MAINTENANCE

Aerospace Engineering (Warrendale, Pennsylvania) (ISSN 0736-2536) vol. 15, no. 1 January-February 1995 p. 27-31 (BTN-95-EIX95182617812) Copyright

Long-term maintenance operations, causing the unit to out of action, may seem economical - but they result in reduced operating readiness. Offsetting that concern, careless, hurried maintenance reduces margins of safety and reliability. Any tool that improves maintenance without causing a sharp increase in cost is valuable. Artificial intelligence (AI) is one of the tools. Expert system and neural networks are two different areas of AI that show promise for turboprop engine maintenance. EI

A95-76389

LYCOMING TO TEST NEW ENGINE CORE

STANLEY W. KANDEBO Aviation Week & Space Technology (ISSN 0005-2175) vol. 140, no. 10 March 7, 1994 p. 32-33 (HTN-95-41393) Copyright

Textron Lycoming plans to develop a new family of engines based on a common core. The core engine for the new Lycoming engine family, designated the 500 series, is an increased efficiency, improved performance derivative based on the core used in the company's T55, ALF502, and LF507 engines. A brief description of engine design, performance, and Textron Lycoming business plans is given. Hemer

A95-76616

DERIVATION OF SYSTEM MATRICES FROM NONLINEAR DYNAMIC SIMULATION OF JET ENGINES

N. SUGIYAMA Natl Aerospace Lab, Chofu, Japan Journal of Guidance, Control, and Dynamics (ISSN 0731-5090) vol. 17, no. 6 November-December 1994 p. 1320-1326 refs (BTN-95-EIX95182619139) Copyright

Most multivariable control design methodologies are linear theories and utilize a linearized plant model. Since accuracy of a linearized plant model affects the quality of a control system designed by those methods, a reasonable linearized plant model that adequately simulates the plant must be prepared. This paper describes a derivation method of such a model in the form of ABCD system matrices from nonlinear dynamic simulation. System matrices of a two-spool turbofan engine are derived and compared to the actual engine data. The effect of perturbation size and linearization formula over a linearized model are discussed. A corrected form of the system matrices is introduced to extend the data base to the whole flight envelope. Author (EI)

A95-76648

EROSION OF DUST-FILTERED HELICOPTER TURBINE ENGINES. PART 1: BASIC THEORETICAL CONSIDERATIONS

JOHANNES P. VANDERWALT Univ of the Witwatersrand, Johannesburg, South Africa and ALAN NURICK Journal of Aircraft (ISSN 0021-8669) vol. 32, no. 1 January-February 1995 p. 106-111 refs (BTN-95-EIX95182619222) Copyright

A theoretical model has been developed for predicting the effects of the erosion of helicopter engines and their performance as

a result of ingesting sparse dust concentrations. In such concentrations particle-on-particle interactions are negligible, and most particles have diameters less than 100 micron. These dust distributions may be found in engines fitted with filters comprised of banks of centrifugal separators. The model includes the effects of particle size distribution, particle velocity, and dust concentration. Author (EI)

A95-76649

EROSION OF DUST-FILTERED HELICOPTER TURBINE ENGINES. PART 2: EROSION REDUCTION

JOHANNES P. VANDERWALT Univ of the Witwatersrand, Johannesburg, South Africa and ALAN NURICK Journal of Aircraft (ISSN 0021-8669) vol. 32, no. 1 January-February 1995 p. 112-117 refs

(BTN-95-EIX95182619223) Copyright

The effects of erosion of filtered and unfiltered dusts ingested by a helicopter gas turbine engine are investigated for the case where particle-on-particle interactions are negligible. The effects of the particle size distribution of the dust in the ingested airstream on engine life are included in the analysis. An erosion reduction factor, which may be used to predict the increase in life of a gas turbine engine in terms of a filtration efficiency factor and the effective particle sizes of the filtered and unfiltered dusts is presented. The method is validated using experimental results obtained on a Turmo 4B gas turbine engine. Author (EI)

A95-76650

LIFE PREDICTION OF HELICOPTER ENGINES FITTED WITH DUST FILTERS

JOHANNES P. VANDERWALT Univ of the Witwatersrand, Johannesburg, South Africa and ALAN NURICK Journal of Aircraft (ISSN 0021-8669) vol. 32, no. 1 January-February 1995 p. 118-123 refs

(BTN-95-EIX95182619224) Copyright

Engine erosion in environments such as those that may be encountered by helicopters during hover, nap-of-the-Earth flight, dust storms, and generally dusty atmospheres can have significant effects on engine performance and life, resulting from the degradation of the first-stage compressor. Ingestion of dust into a turbine engine may be limited by means of dust filters fitted to the engine intakes. Efficient filtration of the dust results in a sparse dust concentration entering the engine that is comprised essentially of particles that have a diameter of less than 100 micron, and indicated negligible particle-on-particle interactions. The dependence of engine performance on the erosion of the first-stage compressor by sparse dust concentrations may be extended to enable the life of an engine to be predicted for a typical flight in a specific dust environment. The methodology for predicting engine life is presented. Author (EI)

A95-76673

A NEW TYPE OF SIMULATOR FOR SIMULATING THE FLOW-FIELD DISTORTION OF ENGINE INLET

CHENGYI PENG Nanjing Univ of Aeronautics & Astronautics, Nanjing, China, JIAJU MA, and JUFENFEI YING Tuijin Jishu/Journal of Propulsion Technology (ISSN 1001-4055) no. 6 December 1994 p. 18-22 In CHINESE refs

(BTN-95-EIX95202638963) Copyright

The need of innovation in the art of engine-face flow-field simulation is expounded, and a new type of simulator is presented. The design concept, principle and construction, special features, and test results of the simulator are also discussed. Owing to its capability in simulating the distortion of steady and dynamic pressure as well as the swirling flow-field, it is suitable to research on: (1) their comprehensive influence on the performance of engine or compressor; (2) evaluating the compatibility between engine and its inlet; and (3) the tolerant limit of engine or compressor for distortion. EI

N95-23088* Colorado Univ., Boulder, CO. Dept. of Aerospace Engineering Sciences.

HIGH-PERFORMANCE PARALLEL ANALYSIS OF COUPLED

PROBLEMS FOR AIRCRAFT PROPULSION Progress Report, Jun. 1994 - Jan. 1995

C. A. FELIPPA, C. FARHAT, P.-S. CHEN, U. GUMASTE, M. LEOINNE, and P. STERN Feb. 1995 51 p Original contains color illustrations

(Contract(s)/Grant(s): NAG3-1273)

(NASA-CR-197440; CU-CAS-95-03; NAS 1.26:197440) Avail: CASI HC A04/MF A01 4 functional color pages

This research program deals with the application of high-performance computing methods to the numerical simulation of complete jet engines. The program was initiated in 1993 by applying two-dimensional parallel aeroelastic codes to the interior gas flow problem of a by-pass jet engine. The fluid mesh generation, domain decomposition and solution capabilities were successfully tested. Attention was then focused on methodology for the partitioned analysis of the interaction of the gas flow with a flexible structure and with the fluid mesh motion driven by these structural displacements. The latter is treated by an ALE technique that models the fluid mesh motion as that of a fictitious mechanical network laid along the edges of near-field fluid elements. New partitioned analysis procedures to treat this coupled 3-component problem were developed in 1994. These procedures involved delayed corrections and subcycling, and have been successfully tested on several massively parallel computers. For the global steady-state axisymmetric analysis of a complete engine we have decided to use the NASA-sponsored ENG10 program, which uses a regular FV-multiblock-grid discretization in conjunction with circumferential averaging to include effects of blade forces, loss, combustor heat addition, blockage, bleeds and convective mixing. A load-balancing preprocessor for parallel versions of ENG10 has been developed. It is planned to use the steady-state global solution provided by ENG10 as input to a localized three-dimensional FSI analysis for engine regions where aeroelastic effects may be important. Author

N95-23222* Moller International, Inc., Davis, CA.

EVALUATION OF THERMAL BARRIER AND PS-200 SELF-LUBRICATING COATINGS IN AN AIR-COOLED ROTARY ENGINE Final Contractor Report

PAUL S. MOLLER Cleveland, OH NASA Mar. 1995 39 p

(Contract(s)/Grant(s): NAS3-26309; RTOP 324-02-00)

(NASA-CR-195445; E-9493; NAS 1.26:195445) Avail: CASI HC A03/MF A01

This project provides an evaluation of the feasibility and desirability of applying a thermal barrier coating overlaid with a wear coating on the internal surfaces of the combustion area of rotary engines. Many experiments were conducted with different combinations of coatings applied to engine components of aluminum, iron and titanium, and the engines were run on a well-instrumented test stand. Significant improvements in specific fuel consumption were achieved and the wear coating, PS-200, which was invented at NASA's Lewis Research Center, held up well under severe test conditions. Author

N95-23550* National Aeronautics and Space Administration. Lewis Research Center, Cleveland, OH.

SENSITIVITY OF COMBUSTION-ACOUSTIC INSTABILITIES TO BOUNDARY CONDITIONS FOR PREMIXED GAS TURBINE COMBUSTORS

DOUGLAS DARLING, KRISHNAN RADHAKRISHNAN (NYMA, Inc., Brook Park, OH.), and AYO OYEDIRAN (AYT Corp., Brook Park, OH.) Mar. 1995 8 p Presented at the Central/Western States Sections Joint Technical Meeting, San Antonio, TX, 23-26 Apr. 1995; sponsored by the Combustion Institute

(Contract(s)/Grant(s): NAS3-27186; RTOP 537-02-21)

(NASA-TM-106890; E-9530; NAS 1.15:106890) Avail: CASI HC A02/MF A01

Premixed combustors, which are being considered for low NOx engines, are susceptible to instabilities due to feedback between pressure perturbations and combustion. This feedback can cause damaging mechanical vibrations of the system as well as degrade the emissions characteristics and combustion efficiency. In a lean

07 AIRCRAFT PROPULSION AND POWER

combustor instabilities can also lead to blowout. A model was developed to perform linear combustion-acoustic stability analysis using detailed chemical kinetic mechanisms. The Lewis Kinetics and Sensitivity Analysis Code, LSENS, was used to calculate the sensitivities of the heat release rate to perturbations in density and temperature. In the present work, an assumption was made that the mean flow velocity was small relative to the speed of sound. Results of this model showed the regions of growth of perturbations to be most sensitive to the reflectivity of the boundary when reflectivities were close to unity. Author

N95-24053* Union Carbide Industrial Gases, Inc., Tonawanda, NY. Linde Div.

AIRBORNE ROTARY AIR SEPARATOR STUDY Interim Report
A. ACHARYA, C. F. GOTTZMANN, and J. J. NOWOBILSKI Cleveland, OH NASA Dec. 1990 64 p
(Contract(s)/Grant(s): NAS3-25560)
(NASA-CR-189099; E-9583; NAS 1.26:189099) Avail: CASI HC A04/MF A01

Several air breathing propulsion concepts for future earth-to-orbit transport vehicles utilize air collection and enrichment, and subsequent storage of liquid oxygen for later use in the vehicle emission. Work performed during the 1960's established the feasibility of substantially reducing weight and volume of a distillation type air separator system by operating the distillation elements in high 'g' fields obtained by rotating the separator assembly. This contract studied the capability test and hydraulic behavior of a novel structured or ordered distillation packing in a rotating device using air and water. Pressure drop and flood points were measured for different air and water flow rates in gravitational fields of up to 700 g. Behavior of the packing follows the correlations previously derived from tests at normal gravity. The novel ordered packing can take the place of trays in a rotating air separation column with the promise of substantial reduction in pressure drop, volume, and system weight. The results obtained in the program are used to predict design and performance of rotary separators for air collection and enrichment systems of interest for past and present concepts of air breathing propulsion (single or two-stage to orbit) systems. Author

08

AIRCRAFT STABILITY AND CONTROL

Includes aircraft handling qualities; piloting; flight controls; and autopilots.

A95-75093

IDENTIFICATION OF HIGHER ORDER HELICOPTER DYNAMICS USING LINEAR MODELING METHODS

BIMAL L. APOUNSO Systems Technologies, Inc., Hawthorne, CA, US, DONALD E. JOHNSTON Systems Technologies, Inc., Hawthorne, CA, US, WALTER A. JOHNSON Systems Technologies, Inc., Hawthorne, CA, US, and RAYMOND E. MAGDELANEO Systems Technologies, Inc., Hawthorne, CA, US American Helicopter Society, Journal (ISSN 0002-8711) vol. 39, no. 3 July 1994 p. 3-11

(Contract(s)/Grant(s): NO0019-87-C-0195)
(HTN-95-80851) Copyright

The higher order dynamics of the helicopter are dominated by rotor and structural modes. Accurate modeling of these high-order dynamics is essential if high bandwidth, robust control systems are to be implemented in modern helicopters. An analytically based, higher-order linear model has been developed and compared with frequency domain flight data for a Sikorsky CH-53E helicopter at hover. Flight test data showed that the helicopter to be remarkably linear in its responses. The linear model proved capable of modeling the higher-order dynamics of the helicopter in hover with an adequate degree of accuracy. Correlation between the model and flight data for the cyclic response in the pitch and roll axes was improved

by adjusting model parameters specific to the rotor lag degree-of-freedom dynamics were different from those predicted by theory. The model was used to identify the dominant high-order modes in the helicopter responses. Author (Herner)

A95-75094

EFFECTS OF HIGH ORDER DYNAMICS ON HELICOPTER FLIGHT CONTROL LAW DESIGN

STEVEN J. INGLE Boeing Defense and Space Group, Philadelphia, PA, US and ROBERTO CELI Univ. of Maryland, College Park, MD, US American Helicopter Society, Journal (ISSN 0002-8711) vol. 39, no. 3 July 1994 p. 12-23
(Contract(s)/Grant(s): NSF CDR-88-03012)
(HTN-95-80852) Copyright

The main objective of the study is to assess the effects of incorporating higher order dynamics such as rotor and inflow dynamics when designing a flight control system to satisfy handling qualities specifications such as Aeronautical Design Standard (ADS)-33C. The control methodologies examined are Linear Quadratic Gaussian (LQG), Eigenstructure Assignment (EA), and H(sub infinity). The UH-60 in hover is used as a test case to which a representative subset of the ADS-33C requirements, for a Rate Command Attitude Hold response type, is applied. The results indicate that acceptable controllers can be designed using EA with a rigid body model of the helicopter; however the control activity is high and the controller is not robust. An H(sub infinity) design requires the modeling of higher order dynamics; the resulting controller is higher order but more robust, and the control activity is lower. It was not possible to determine a suitable LQG based controller that would satisfy all the requirements. Author (Herner)

A95-75095* National Aeronautics and Space Administration. Ames Research Center, Moffett Field, CA.

INVESTIGATION OF THE EFFECTS OF BANDWIDTH AND TIME DELAY ON HELICOPTER ROLL-AXIS HANDLING QUALITIES

CHRIS L. BLANKEN NASA. Ames Research Center, Moffett Field, CA, US and HEINZ-JURGEN PAUSDER Institut fuer Flumechanik, Braunschweig, Germany American Helicopter Society, Journal (ISSN 0002-8711) vol. 39, no. 3 July 1994 p. 24-33
(HTN-95-80853) Copyright

Several years of cooperative research conducted under the U.S./German Memorandum of Understanding (MOU) in helicopter aeromechanics have recently resulted in a successful handling qualities study. The focus of this cooperative research has been the effect of time delays in a high bandwidth vehicle on handling qualities. The jointly performed study included the use of U.S. ground-based simulation and German in-flight simulation facilities. The NASA-Ames Vertical Motion Simulator (VMS) was used to develop a high bandwidth slalom tracking task which took into consideration the constraints of the facilities. The VMS was used to define a range of the test parameters and to perform initial handling qualities evaluations. The flight tests were conducted using DLR's variable-stability BO 105 S3 Advanced Technology Testing Helicopter System (ATHeS). Configurations included a rate command and an attitude command response system with added time delays of up to 160 milliseconds over the baseline and band width values between 1.5 and 4.5 rad/sec. Sixty-six evaluations were performed in about 25 hours of flight time during ten days of testing. The results indicate a need to more tightly constrain the allowable roll axis phase delay for the Level 1 and Level 2 requirements in the U.S. Army's specification for helicopter handling qualities Aeronautical Design Standard (ADS)-33C. Author (Herner)

A95-75096* National Aeronautics and Space Administration. Lewis Research Center, Cleveland, OH.

INTEGRATED FLIGHT/PROPULSION CONTROL FOR HELICOPTERS

STEPHEN M. ROCK Stanford Univ., Stanford, CA, US and KEN NEIGHBORS Stanford Univ., Stanford, CA, US American Helicopter Society, Journal (ISSN 0002-8711) vol. 39, no. 3 July 1994 p.

34-42

(Contract(s)/Grant(s): NAG3-1177)
(HTN-95-80854) Copyright

Presented is a procedure for improving the communication of requirements and specifications in the early design phases of an integrated helicopter/engine control system. The procedure is based on establishing a bound on a transfer matrix that relates blade cyclic and collective inputs to rotor speed variations. This bound becomes a new specification for the propulsion control system designer that embodies the mission-level performance goals of the helicopter. An example application of the procedure is provided for a Blackhawk/700 system undergoing vertical accelerations from hover.

Author (Herner)

A95-75772

FLUTTER OF AN INFINITELY LONG PANEL IN A DUCT

RONALD J. EPSTEIN Duke Univ, Durham, NC, United States, RAMAKRISHNA SRINIVASAN, and EARL H. DOWELL AIAA Journal (ISSN 0001-1452) vol. 33, no. 1 January 1995 p. 109-115 refs

(BTN-95-EIX95182619087) Copyright

The aeroelastic stability is examined of an infinitely long panel of finite width enclosed in a duct such that both the upper and lower surfaces of the panel are exposed to an inviscid and compressible flow. The panel behavior is accounted for by small deflection plate theory, whereas the aerodynamic forces acting on the panel are described by the classical linearized small disturbance potential theory. As such, a self-consistent theoretical model is constructed for the asymptotic behavior of the panel. Two panel boundary conditions are considered; the panel is assumed to be either simply supported or clamped along the side edges. For the simply supported case, rather extensive numerical results have been obtained. The effects of Mach number, air/panel mass ratio, and duct dimension on the flutter velocity are determined.

Author (EI)

A95-76603

KINEMATICS AND AERODYNAMICS OF VELOCITY-VECTOR ROLL

WAYNE C. DURHAM Virginia Polytechnic Inst and State Univ, Blacksburg, VA, United States, FREDERICK H. LUTZE, and WILLIAM MASON Journal of Guidance, Control, and Dynamics (ISSN 0731-5090) vol. 17, no. 6 November-December 1994 p. 1228-1233 (BTN-95-EIX95182619126) Copyright

The velocity-vector roll is an angular rotation of an airplane about its instantaneous velocity vector, constrained to be performed at a constant angle of attack (AOA), no sideslip, and constant velocity. The body-axis rotations and the constraints are used in the moment equations to determine the aerodynamic moments required to perform the velocity-vector roll. The total aerodynamic moments are analyzed to know the conditions under which their maximum occur. For representative tactical airplanes, it is shown that the conditions for maximum pitching moment are strongly a function of the orientation of the airplane. Maximum required pitching moment occurs at peak roll rate and is achieved at an AOA in excess of 45 deg. The conditions for maximum rolling moment depend on the value of the roll mode time constant. Lastly, results are compared with those obtained using conventional assumptions of zero pitch and yaw rates. Significant improvement is observed, especially in the prediction of maximum pitching-moment requirements.

EI

A95-76606* National Aeronautics and Space Administration. Ames Research Center, Moffett Field, CA.

H-INFINITY HELICOPTER FLIGHT CONTROL LAW DESIGN WITH AND WITHOUT ROTOR STATE FEEDBACK

MARC D. TAKAHASHI National Aeronautics and Space Administration, Ames Research Center, Moffett Field, CA Journal of Guidance, Control, and Dynamics (ISSN 0731-5090) vol. 17, no. 6 November-December 1994 p. 1245-1251 refs

(BTN-95-EIX95182619129) Copyright

An H-infinity formulation to design pitch-roll flight control laws for hovering helicopter is proposed. Using this formulation, control law designs were developed to examine the effect of using rotor state feedback. Two laws developed for an articulated helicopter math model in low-speed flight include a compensator using rigid-body measurements and one using body plus rotor statements. The design with no rotor state feedback has the potential to pass approximately twice as much noise to the actuators near the 1/rev frequency as the design with rotor state feedback. In addition, the response of the controller with no rotor state feedback was more sensitive to gain variations. Due to this sensitivity, the design with no rotor state feedback showed more high-frequency oscillation in roll.

EI

A95-76607* National Aeronautics and Space Administration. Ames Research Center, Moffett Field, CA.

AUTOMATIC GUIDANCE AND CONTROL FOR HELICOPTER OBSTACLE AVOIDANCE

VICTOR H. L. CHENG National Aeronautics and Space Administration, Ames Research Center, Moffett Field, CA and T. LAM Journal of Guidance, Control, and Dynamics (ISSN 0731-5090) vol. 17, no. 6 November-December 1994 p. 1252-1259 refs (BTN-95-EIX95182619130) Copyright

The helicopter nap-of-the-earth flight problem has previously been discussed in various papers. The concept of automatic guidance involving obstacle avoidance requires a sophisticated obstacle detection system to provide three-dimensional obstacle and terrain data in flight in a hostile and unknown environment. Passive imaging sensors, augmented by selective use of low-detectability active sensors, will likely be needed to maximize covertness and safety, thus necessitating data fusion. The sensor data, limited by intervisibility constraints of the environment, suggest the use of heuristic arguments in flight-path planning over conventional analytic techniques. In addition, explicit consideration of vehicle capability is essential in the autopilot design to assure safe flight in such close proximity to the ground. This paper describes the automatic obstacle avoidance guidance and control functions and the implementation of these functions and a mock obstacle detection system in a graphical simulation for evaluation.

Author (EI)

A95-76608

DIRECT-LIFT DESIGN STRATEGY FOR LONGITUDINAL CONTROL OF HYPERSONIC AIRCRAFT

PHUONG VU California Polytechnic State Univ, San Luis Obispo, CA, United States and DANIEL J. BIEZAD Journal of Guidance, Control, and Dynamics (ISSN 0731-5090) vol. 17, no. 6 November-December 1994 p. 1260-1266 refs (BTN-95-EIX95182619131) Copyright

A longitudinal control design called the G-command, alpha follow-up is described that significantly improves the lag between pitch angle and flight-path angle responses associated with hypersonic flight. The design technique relies on classical, successive loop closures to determine the control architecture and introduces a direct-lift control strategy to design dynamic compensation. This dynamic compensation constrains and 'washes out' body-flap input to avoid excessive flap deflection and associated heating while providing angle-of-attack control at the engine inlet. The final design was implemented on a generic hypersonic aircraft simulation at NASA Dryden and evaluated by a NASA test pilot familiar with the SR-71. The pilot flew turning and altitude change maneuvers using the implemented control law and verified the ability to track flight path with ease and precision. Finally, evidence is presented that supports a flying qualities metric for longitudinal, hypersonic flight based on the bandwidth of the flight-path-angle-to-stick-frequency response.

Author (EI)

A95-76609

MULTIRATE FLUTTER SUPPRESSION SYSTEM DESIGN FOR A MODEL WING

GREGORY S. MASON Seattle Univ, Seattle, WA, United States and MARTIN C. BERG Journal of Guidance, Control, and Dynamics (ISSN 0731-5090) vol. 17, no. 6 November-December 1994 p. 1267-1274 refs

(BTN-95-EIX95182619132) Copyright

A new methodology for multirate control system design is described. It accommodates a general multiple-input, multiple-output control law structure that allows the sampling rates for the plant sensor output signals, the update rates for the processor states, and the update rates for the plant control input signals to be independently specified. It includes a capability to design for multiple plant conditions so as to achieve robustness to plant parameter variations. Its analysis components include a method for determining conventional gain and phase margins, a method for determining a bound on the smallest destabilizing uncertainty, and a method for determining the maximum root-mean-square (rms) gain of a multirate system. The methodology is demonstrated by application to the design of a multirate flutter suppression system for a model wing.

Author (EI)

A95-76630

AUTOMATIC FORMATION FLIGHT CONTROL

M. PACHTER Air Force Inst of Technology, Wright-Patterson AFB, OH, United States, J. J. D'AZZO, and J. L. DARGAN Journal of Guidance, Control, and Dynamics (ISSN 0731-5090) vol. 17, no. 6 November-December 1994 p. 1380-1383

(BTN-95-EIX95182619153) Copyright

The control design problem of an automatic pilot for formation flight control has been analyzed and decomposed into two uncoupled linear single-input, two-output dynamic tracking control system design problems. This, in turn, results in the efficient design of a PI formation-hold autopilot that uses a mix of separation errors and maneuver errors. The formation flight control problem considered here is significant in view of its direct operational importance: It affords the automation of the coordination of a leader/wingman flight, the design of a robotic wingman, and the automatic control of aircraft during maneuvers such as aerial refueling.

EI

A95-76640* National Aeronautics and Space Administration. Langley Research Center, Hampton, VA.

FLUTTER SUPPRESSION CONTROL LAW DESIGN AND TESTING FOR THE ACTIVE FLEXIBLE WING

VIVEK MUKHOPADHYAY National Aeronautics and Space Administration, Langley Research Center, Hampton, VA Journal of Aircraft (ISSN 0021-8669) vol. 32, no. 1 January-February 1995 p. 45-51 refs

(BTN-95-EIX95182619214) Copyright

Design of a control law for simultaneously suppressing the symmetric and antisymmetric flutter modes of a sting-mounted, fixed-in-roll aeroelastic wind-tunnel model is described. The flutter suppression control law was designed using linear quadratic Gaussian theory, and involved control law order reduction, a gain root-locus study, and use of previous experimental results. A 23% increase in the open-loop flutter dynamic pressure was demonstrated during the wind-tunnel test. Rapid roll maneuvers at 11% above the symmetric flutter boundary were also performed when the model was in a free-to-roll configuration.

Author (EI)

A95-76641* National Aeronautics and Space Administration. Langley Research Center, Hampton, VA.

DESIGN AND MULTIFUNCTION TESTS OF A FREQUENCY DOMAIN-BASED ACTIVE FLUTTER SUPPRESSION SYSTEM

WILLIAM M. ADAMS, JR. National Aeronautics and Space Administration, Langley Research Center, Hampton, VA and DAVID M. CHRISTHILF Journal of Aircraft (ISSN 0021-8669) vol. 32, no. 1 January-February 1995 p. 52-60 refs

(BTN-95-EIX95182619215) Copyright

This article describes the process of analysis, design, digital

implementation, and subsonic testing of an active controls flutter suppression system for a full-span, free-to-roll, wind-tunnel model of an advanced fighter concept. A frequency domain representation of the plant was employed, and a robust multiinput/multioutput controller was generated by using optimization techniques to maximize singular value robustness criteria and insensitivity to uncertainty in the flutter frequency. During testing in a fixed-in-roll configuration, simultaneous suppression of both symmetric and antisymmetric flutter was successfully demonstrated. For a free-to-roll configuration, symmetric flutter was suppressed to the limit of the tunnel test envelope. During aggressive rolling maneuvers above the open-loop flutter boundary, simultaneous flutter suppression and maneuver load control were demonstrated. Finally, the flutter suppression controller was reoptimized during the test using combined experimental and analytical frequency domain data, resulting in improved stability robustness. The reoptimization, accomplished overnight, shows the potential, with a much faster computer, to apply the design procedure to a tuning-type adaptive active flutter suppression controller.

Author (EI)

A95-76642* National Aeronautics and Space Administration. Langley Research Center, Hampton, VA.

FLUTTER SUPPRESSION FOR THE ACTIVE FLEXIBLE WING: A CLASSICAL DESIGN

M. R. WASZAK National Aeronautics and Space Administration, Langley Research Center, Hampton, VA and S. SRINATHKUMAR Journal of Aircraft (ISSN 0021-8669) vol. 32, no. 1 January-February 1995 p. 61-67 refs

(BTN-95-EIX95182619216) Copyright

The synthesis and experimental validation of a control law for an active flutter suppression system for the active flexible wing wind-tunnel model is presented. The design was accomplished with traditional root locus methods making extensive use of interactive computer graphics tools and simulation-based analysis. The design approach relied on a fundamental understanding of the flutter mechanism to formulate a very simple control law structure resulting in a filter with an 'inverted notch' characteristic. This unusual filter characteristic was required to compensate for adverse zero locations in the frequency range near flutter. Wind-tunnel tests of the flutter suppression controller demonstrated simultaneous suppression of two flutter modes, significantly increasing the flutter dynamic pressure. The flutter suppression controller was also successfully operated in combination with a rolling maneuver controller to perform flutter suppression during rapid rolling maneuver.

Author (EI)

A95-76681

ROBUSTLY STABLE PRELIMINARY CONTROL SYSTEMS DESIGN FOR THE YF-16 CCV AIRCRAFT

IEEE Transactions on Aerospace and Electronic Systems (ISSN 0018-9251) vol. 31, no. 1 January 1995 p. 479-486 refs

(BTN-95-EIX95202637608) Copyright

A preliminary control system design for the YF-16 CCV aircraft in its longitudinal mode satisfying its flying qualities specifications is investigated. The design is shown to be robustly stable when the actuator model and the unstable pole in the airframe model of the aircraft are subjected to structured uncertainties. Very recent tools of robust stability analysis are utilized to accomplish this goal.

Author (EI)

N95-22674*# McDonnell-Douglas Aerospace, Long Beach, CA. Transport Aircraft.

GUIDANCE AND CONTROL REQUIREMENTS FOR HIGH-SPEED ROLLOUT AND TURNOFF (ROTO) Final Report

STEVE H. GOLDTHORPE, ALAN C. KERNIK, LARRY S. MCBEE, and ORV W. PRESTON Jan. 1995 127 p

(Contract(s)/Grant(s): NAS1-19703; RTOP 538-04-13-01)

(NASA-CR-195026; NAS 1.26:195026) Avail: CASI HC A07/MF A02

This report defines the initial requirements for designing a research high-speed rollout and turnoff (ROTO) guidance and control system applicable to transport class aircraft whose purpose

is to reduce the average runway occupancy time (ROT) for aircraft operations. The requirements will be used to develop a ROTO system for both automatic and manual piloted operation under normal and reduced visibility conditions. Requirements were determined for nose wheel/rudder steering, braking/reverse thrust, and the navigation system with the aid of a non-real time, three degree-of-freedom MD-11 simulation program incorporating airframe and gear dynamics. The requirements were developed for speeds up to 70 knots using 30 ft exit geometries under dry and wet surface conditions. The requirements were generated under the assumptions that the aircraft landing system meets the current Category III touchdown dispersion requirements and that aircraft interarrival spacing is 2 nautical miles. This effort determined that auto-asymmetric braking is needed to assist steering for aft center-of-gravity aircraft. This report shows various time-history plots of the aircraft performance for the ROTO operation. This effort also investigated the state-of-the-art in the measurement of the runway coefficient of friction for various runway conditions. Author

N95-22908* Massachusetts Inst. of Tech., Cambridge, MA. Dept. of Aeronautics and Astronautics.

DESIGN OF HIGH PERFORMANCE MULTIVARIABLE CONTROL SYSTEMS FOR SUPERMANEUVERABLE AIRCRAFT AT HIGH ANGLE OF ATTACK Final Report

LENA VALAVANI 1995 3 p

(Contract(s)/Grant(s): NAG1-1088)

(NASA-CR-197661; NAS 1.26:197661) Avail: CASI HC A01/MF A01

The main motivation for the work under the present grant was to use nonlinear feedback linearization methods to further enhance performance capabilities of the aircraft, and robustify its response throughout its operating envelope. The idea was to use these methods in lieu of standard Taylor series linearization, in order to obtain a well behaved linearized plant, in its entire operational regime. Thus, feedback linearization was going to constitute an 'inner loop', which would then define a 'design plant model' to be compensated for robustness and guaranteed performance in an 'outer loop' application of modern linear control methods. The motivation for this was twofold; first, earlier work had shown that by appropriately conditioning the plant through conventional, simple feedback in an 'inner loop', the resulting overall compensated plant design enjoyed considerable enhancement of performance robustness in the presence of parametric uncertainty. Second, the nonlinear techniques did not have any proven robustness properties in the presence of unstructured uncertainty; a definition of robustness (and performance) is very difficult to achieve outside the frequency domain; to date, none is available for the purposes of control system design. Thus, by proper design of the outer loop, such properties could still be 'injected' in the overall system. Author

N95-22954* National Aeronautics and Space Administration. Lewis Research Center, Cleveland, OH.

STABLE H(INFINITY) CONTROLLER DESIGN FOR THE LONGITUDINAL DYNAMICS OF AN AIRCRAFT

HITAY OEZBAY (Ohio State Univ., Columbus, OH.) and SANJAY GARG Feb. 1995 53 p

(Contract(s)/Grant(s): RTOP 505-62-50)

(NASA-TM-106847; E-9421; NAS 1.15:106847) Avail: CASI HC A04/MF A01

This report discusses different approaches to stable H infinity controller design applied to the problem of augmenting the longitudinal dynamics of an aircraft. Stability of the H infinity controller is investigated by analyzing the effects of changes in the performance index weights, and modifications in the measured outputs. The existence of a stable suboptimal controller is also investigated. It is shown that this is equivalent to finding a stable controller, whose infinity norm is less than a specified bound, for an unstable plant which is determined from parametrization of all H infinity controllers. Examples are given for a gust alleviation and a command tracking problem. Author

N95-23297* California Univ., Davis, CA. Dept. of Mechanical and Aeronautical Engineering.

ANALYSIS OF THE LONGITUDINAL HANDLING QUALITIES

AND PILOT-INDUCED-OSCILLATION TENDENCIES OF THE HIGH-ANGLE-OF-ATTACK RESEARCH VEHICLE (HARV)

Abstract Only

RONALD A. HESS In Hampton Univ., 1994 NASA-HU American Society for Engineering Education (ASEE) Summer Faculty Fellowship Program p 79 Dec. 1994

Avail: CASI HC A01/MF A02

The NASA High-Angle-of Attack Research Vehicle (HARV), a modified F-18 aircraft, experienced handling qualities problems in recent flight tests at NASA Dryden Research Center. Foremost in these problems was the tendency of the pilot-aircraft system to exhibit a potentially dangerous phenomenon known as a pilot-induced oscillation (PIO). When they occur, PIO's can severely restrict performance, sharply diminish mission capabilities, and can even result in aircraft loss. A pilot/vehicle analysis was undertaken with the goal of reducing these PIO tendencies and improving the overall vehicle handling qualities with as few changes as possible to the existing feedback/feedforward flight control laws. Utilizing a pair of analytical pilot models developed by the author, a pilot/vehicle analysis of the existing longitudinal flight control system was undertaken. The analysis included prediction of overall handling qualities levels and PIO susceptibility. The analysis indicated that improvement in the flight control system was warranted and led to the formulation of a simple control stick command shaping filter. Analysis of the pilot/vehicle system with the shaping filter indicated significant improvements in handling qualities and PIO tendencies could be achieved. A non-real time simulation of the modified control system was undertaken with a realistic, nonlinear model of the current HARV. Special emphasis was placed upon those details of the command filter implementation which could effect safety of flight. The modified system is currently awaiting evaluation in the real-time, pilot-in-the-loop, Dual-Maneuvering-Simulator (DMS) facility at Langley. Author

N95-23314* Old Dominion Coll., Norfolk, VA. Dept. of Aerospace Engineering.

INNER LOOP FLIGHT CONTROL FOR THE HIGH-SPEED CIVIL TRANSPORT Abstract Only

BRETT A. NEWMAN In Hampton Univ., 1994 NASA-HU American Society for Engineering Education (ASEE) Summer Faculty Fellowship Program p 96 Dec. 1994

Avail: CASI HC A01/MF A02

High-speed aerospace vehicles which employ high strength, light weight, yet deformable materials may exhibit significant interaction between the rigid-body and vibrational dynamics. Preliminary High-Speed Civil Transport (HSCT) configurations are a prime example. Traditionally, separate control systems have been used to augment the rigid-body and vibrational dynamics. In the HSCT arena, the highly coupled motions may not allow this design freedom. The research activity addresses two specific issues associated with the design and development of an integrated flight control system (FCS) for HSCT configurations, which are discussed next. The HSCT is expected to have a short period instability at subsonic speeds. Flight vehicles with this characteristic (i.e., F-16, F-22, X-29, Space Shuttle) are stabilized with what is called a superaugmented pitch rate loop. One concern is 'Will this stability augmentation logic work for a HSCT?' Studies show that an idealized pitch rate design would be acceptable, but is not realistic. Investigations using a contaminated pitch rate design reveal serious hurdles to overcome in the FCS design. Mounting location for the pitch rate sensor is critical. Results indicate a forward location leads to destabilizing pick-up of aeroelastic modes, while aft locations lead to undesirable coupling of the dominate pitch mode with the first aeroelastic mode. Intermediate locations for the sensor may not be acceptable. The source of the problem is the presence of low frequency aeroelastic modes in HSCT configurations, which are not present in vehicles currently using the superaugmented logic. To say the least, a conventional superaugmented pitch rate loop strategy may have undesirable characteristics. An unconventional strategy, which attempts to eliminate the above deficiencies by blending several pitch rate signals, indicates an improvement in the FCS architecture feasibility, but is still lacking in some respects. The HSCT configu-

ration does not have aerodynamic surfaces in the vicinity of the nose (i.e., no canard or vane). A second concern is 'Can the fuselage bending/torsion aeroelastic modes be effectively augmented without sufficient control input near the vehicle nose?' The supraaugmented FCS results above may be suggesting the necessity of a secondary feedback loop to achieve an acceptable integrated FCS. Preliminary analysis of HSCT aeroelastic mode shapes indicate the use of existing wing leading edge devices as a second control input may be lacking in control authority for the rigid-body attitude and aeroelastic modes. An effort is underway to incorporate generic wing leading edge devices and canards into a generic HSCT model for the purpose of assessing additional control authority and its use in candidate FCS designs. A generic HSCT mathematical model was necessary for the studies above. A HSCT category model is available in NASA-CR-172201. This model describes the linear, longitudinal dynamics about the following flight condition: ascent, $W = 730,000$ lbs, $h = 6,500$ ft, $M = 0.6$. The model incorporates the full rigid-body variable set, as well as eighteen aeroelastic modes. Elevator deflection serves as the control input. Modifications to the model include the incorporation of relaxed static stability (i.e., static margin from -7.3% to +10%) and additional control inputs. Author

N95-23319* Saint Louis Univ., Cahokia, IL. Dept. of Aerospace Engineering.

PRELIMINARY IDENTIFICATION OF BUFFET PROBLEMS IN HIGH SPEED CIVIL TRANSPORT Abstract Only

KRISHNASWAMY RAVINDRA In Hampton Univ., 1994 NASA-HU American Society for Engineering Education (ASEE) Summer Faculty Fellowship Program p 101 Dec. 1994
Avail: CASI HC A01/MF A02

In the present study, some effort is made to identify whether empennage buffet is a relevant factor in the design and operation of the High Speed Civil Transport (HSCT). Based on some results of the only operational supersonic transport, Concorde and the innumerable studies that exist on the tail buffet of high performance airplanes, CFD analyses on the HSCT as well as low speed wind tunnel tests on models, it appears as though buffet will be a factor that needs attention in the proper design of empennage structure. Utilizing the existing empirical relation between the reduced frequency of the leading edge vortices and the geometric parameters, it is estimated that the characteristic frequencies of the vortices from the wing cranks are in the range of certain fundamental frequencies of the wing-fuselage-empennage structure. Buffet is believed to be critical during take-off, climb, descent and landing. Computational and experimental data available in open literature indicate coherent vortex flow structure in the empennage region at supersonic cruise speeds. This raises further concern on the fatigue life of the empennage structure. Three second generation supersonic transport designs taken from open literature are briefly compared with the 'empennage buffet' in mind. Future research efforts relating to buffet studies on the HSCT are summarized. A bibliography pertaining to the present research, including relevant studies on the first generation supersonic transport is presented. The effect of rounded wing leading edges on the present frequency estimates needs further study. The effect of engine exhaust on the flow field in the empennage region also needs further study. Author

N95-23325*# Tennessee Univ. Space Inst., Tullahoma, TN. HANDLING QUALITIES OF THE HIGH SPEED CIVIL TRANSPORT Abstract Only

U. PETER SOLIES In Hampton Univ., 1994 NASA-HU American Society for Engineering Education (ASEE) Summer Faculty Fellowship Program p 107 Dec. 1994
Avail: CASI HC A01/MF A02

The low speed handling qualities of a High Speed Civil Transport class aircraft have been investigated by using data of the former Advanced Supersonic Transport (AST) 105. The operation of such vehicles in the airport terminal area is characterized by 'backside' performance. Main objectives of this research effort were: (Q) determination of the nature and magnitude of the speed instability associated with the backside of the thrust required curve; (2)

confirmation of the validity of existing MIL-SPEC handling qualities criteria; (3) safety of operation of the vehicle in the event of autothrottle failure; and (4) correlation of required engine responsiveness with level of speed instability. Preliminary findings comprise the following: (1) The critical velocity for speed instability was determined to be 196 knots, well above the projected approach speed of 155 knots. This puts the vehicle far on the backside of its thrust required curve. While the aircraft can be configured to have static and dynamic stability at this trim point, a significant speed instability emerges, if a pilot or autopilot attempts flight path control with elevator and/or canard control surfaces only. This requires a properly configured autothrottle and/or variable aerodynamic drag devices which can provide speed stability; (2) An AST 105 type vehicle meets MIL-SPEC criteria only in part. While the damping criteria for phugoid and short period motion are met easily, the AST 105 falls short of the required minimum short period frequency, meaning that the HSCT is too sluggish in pitch to meet the military criteria. Obviously the military specification do not consider a vehicle with such high pitch inertia. With regard to speed stability and flight path stability criteria, the vehicle meets levels 2 and 3 of the military requirements, indicating that it would be landed safely with manual controls in case of an autothrottle failure, even though the pilot workload would be high; and (3) This requires quick thrust response to throttle adjustment, however. If the engine responsiveness is slow, the aircraft handling qualities are further deteriorated. Progress has been made in correlating required engine responses dynamics with the given level of speed instability of the vehicle.

Author (revised)

N95-23389* National Aeronautics and Space Administration. Ames Research Center, Moffett Field, CA.

ENGINES-ONLY FLIGHT CONTROL SYSTEM Patent

FRANK W. BURCHAM, inventor (to NASA), GLENN B GILYARD, inventor (to NASA), JOSEPH L. CONLEY, inventor (to NASA), JAMES F. STEWART, inventor (to NASA), and CHARLES G. FULLERTON, inventor (to NASA) 19 Jul. 1994 18 p Filed 28 May 1992

(NASA-CASE-ARC-11944-1; US-PATENT-5,330,131; US-PATENT-APPL-SN-889347; US-PATENT-CLASS-244-75R; US-PATENT-CLASS-244-7R; US-PATENT-CLASS-244-182; US-PATENT-CLASS-244-51; INT-PATENT-CLASS-B64C-19/00) Avail: US Patent and Trademark Office

A backup flight control system for controlling the flightpath of a multi-engine airplane using the main drive engines is introduced. The backup flight control system comprises an input device for generating a control command indicative of a desired flightpath, a feedback sensor for generating a feedback signal indicative of at least one of pitch rate, pitch attitude, roll rate and roll attitude, and a control device for changing the output power of at least one of the main drive engines on each side of the airplane in response to the control command and the feedback signal.

Official Gazette of the U.S. Patent and Trademark Office

N95-23392* Georgia Tech Research Inst., Atlanta, GA. Contracting Support Div.

FLUTTER ANALYSIS OF COMPOSITE BOX BEAMS Final Administrative Report, 21 Sep. 1993 - 20 Sep. 1994

DEWEY H. HODGES and MATTHEW GREENMAN 21 Feb. 1995 14 p

(Contract(s)/Grant(s): NGT-50981)

(NASA-CR-197931; NAS 1.26:197931) Avail: CASI HC A03/MF A01

The dynamic aeroelastic instability of flutter is an important factor in the design of modern high-speed, flexible aircraft. The current trend is toward the creative use of composites to delay flutter. To obtain an optimum design, we need an accurate as well as efficient model. As a first step towards this goal, flutter analysis is carried out for an unswept composite box beam using a linear structural model and Theodorsen's unsteady aerodynamic theory. Structurally, the wing was modeled as a thin-walled box-beam of rectangular cross section. Theodorsen's theory was used to get 2-

D unsteady aerodynamic forces, which were integrated over the span. A free-vibration analysis is carried out. These fundamental modes are used to get the flutter solution using the V-g method. Future work is intended to build on this foundation. Author

N95-23410* Minnesota Univ., Minneapolis, MN. Dept. of Aerospace Engineering and Mechanics.
FEEDBACK CONTROL LAWS FOR HIGHLY MANEUVERABLE AIRCRAFT Annual Report, 1 Feb. 1995 - 31 Jan. 1996
 WILLIAM L. GARRARD and GARY J. BALAS 31 Jan. 1995 11 p
 (Contract(s)/Grant(s): NAG1-1380)
 (NASA-CR-197944; NAS 1.26:197944) Avail: CASI HC A03/MF A01

During this year, we concentrated our efforts on the design of controllers for lateral/directional control using mu synthesis. This proved to be a more difficult task than we anticipated and we are still working on the designs. In the lateral-directional control problem, the inputs are pilot lateral stick and pedal commands and the outputs are roll rate about the velocity vector and side slip angle. The control effectors are ailerons, rudder deflection, and directional thrust vectoring vane deflection which produces a yawing moment about the body axis. Our math model does not contain any provision for thrust vectoring of rolling moment. This has resulted in limitations of performance at high angles of attack. During 1994-95, the following tasks for the lateral-directional controllers were accomplished: (1) Designed both inner and outer loop dynamic inversion controllers. These controllers are implemented using accelerometer outputs rather than an a priori model of the vehicle aerodynamics; (2) Used classical techniques to design controllers for the system linearized by dynamics inversion. These controllers acted to control roll rate and Dutch roll response; (3) Implemented the inner loop dynamic inversion and classical controllers on the six DOF simulation; (4) Developed a lateral-directional control allocation scheme based on minimizing required control effort among the ailerons, rudder, and directional thrust vectoring; and (5) Developed mu outer loop controllers combined with classical inner loop controllers.

Derived from text

N95-23671* National Aeronautics and Space Administration, Lewis Research Center, Cleveland, OH.
MOTOR DRIVE TECHNOLOGIES FOR THE POWER-BY-WIRE (PBW) PROGRAM: OPTIONS, TRENDS AND TRADEOFFS
 MALIK E. ELBULUK (Akron Univ., Akron, OH.) and M. DAVID KANKAM Mar. 1995 14 p Presented at the National Aerospace and Electronics Conference, Wright-Patterson AFB, OH, 23-27 May 1995; cosponsored by the IEEE and the Aerospace and Electronics Systems Society
 (Contract(s)/Grant(s): RTOP 233-02-03)
 (NASA-TM-106885; E-9521; NAS 1.15:106885) Avail: CASI HC A03/MF A01

Power-By-Wire (PBW) is a program involving the replacement of hydraulic and pneumatic systems currently used in aircraft with an all-electric secondary power system. One of the largest loads of the all-electric secondary power system will be the motor loads which include pumps, compressors and Electrical Actuators (EA's). Issues of improved reliability, reduced maintenance and efficiency, among other advantages, are the motivation for replacing the existing aircraft actuators with electrical actuators. An EA system contains four major components. These are the motor, the power electronic converters, the actuator and the control system, including the sensors. This paper is a comparative literature review in motor drive technologies, with a focus on the trends and tradeoffs involved in the selection of a particular motor drive technology. The reported research comprises three motor drive technologies. These are the induction motor (IM), the brushless dc motor (BLDCM) and the switched reluctance motor (SRM). Each of the three drives has the potential for application in the PBW program. Many issues remain to be investigated and compared between the three motor drives, using actual mechanical loads expected in the PBW program.

Author

09

RESEARCH AND SUPPORT FACILITIES (AIR)

Includes airports, hangars and runways; aircraft repair and overhaul facilities; wind tunnels; shock tube facilities; and engine test blocks.

A95-74554
MEASUREMENT OF PARTICLE EMISSIONS FROM CLEAN ROOM GAS-HANDLING COMPONENTS

R. PERIASAMY Research Triangle Inst, Research Triangle Park, NC, United States, D. S. ENSOR, R. P. DONOVAN, A. C. CLAYTON, and J. RIDDLE Journal of the Electrochemical Society (ISSN 0013-4651) vol. 141, no. 6 June 1994 p. 1649-1653 refs
 (BTN-94-EIX94381359040) Copyright

Particle emissions from clean room gas-handling components were measured by following a test method developed recently by SEMATECH. Three types of tests, namely, the static, the dynamic, and the impact tests were conducted to determine particle emissions from the components tested. Particles emitted by the components such as valves, point-of-use filters and inline pressure regulators were measured using a condensation nucleus particle counter. The number of particles emitted by the valve was influenced by the actuator pressure used to open and close the test valve. That is, the higher the actuator pressure the higher the number of particles released from the automatic valve. Particle contributions measured from valves, filters, and regulators are presented here. Author (EI)

A95-74629
MEASUREMENT OF MOISTURE AND TOTAL HYDROCARBON CONTRIBUTIONS BY VALVES USED IN CLEAN ROOM GAS-DELIVERY SYSTEMS

R. PERIASAMY Research Triangle Inst, Research Triangle Park, NC, United States, J. R. NEWSOME, D. S. ENSOR, R. P. DONOVAN, and J. RIDDLE Journal of the Electrochemical Society (ISSN 0013-4651) vol. 141, no. 6 June 1994 p. 1653-1657 refs
 (BTN-94-EIX94381359041) Copyright

Moisture and total hydrocarbon (THC) emissions from valves used in clean room gas-distribution systems were measured by following two test methods developed recently by SEMATECH. Each test method consists of two types of tests: a purge test and a bakeout test. The apparatus specified in each test method is similar except for the detector. Simply by switching the detectors, the same apparatus may be used for both test methods. We report measurements of THC and moisture made with this apparatus and carried out on both manual and automatic all metal stainless steel valves with either Kel-F or tetrafluoroethylene gaskets, some new (fresh out of the bag) and some used. Author (EI)

A95-76584
APPLICATION OF A CONTROL-VOLUME-BASED FINITE-ELEMENT FORMULATION TO THE SHOCK TUBE PROBLEM

S. M. H. KARIMIAN Univ of Waterloo, Waterloo, Ont, Canada and G. E. SCHNEIDER AIAA Journal (ISSN 0001-1452) vol. 33, no. 1 January 1995 p. 165-167 refs
 (BTN-95-EIX95182619099) Copyright

The performance of a newly developed pressure-based method for incompressible/compressible flow calculation is investigated by solving the shock tube problem, which has served as a benchmark case in literature. It is demonstrated that the present method is capable of solving transient and compressible flows incorporating strong discontinuities. EI

A95-76637* National Aeronautics and Space Administration, Langley Research Center, Hampton, VA.

SIMULATION AND MODEL REDUCTION FOR THE ACTIVE FLEXIBLE WING PROGRAM

CAREY BUTTRILL National Aeronautics and Space Administration, Langley Research Center, Hampton, VA, BARTON BACON, JENNIFER HEEG, JACOB HOUCK, and DAVID WOOD Journal of Aircraft (ISSN 0021-8669) vol. 32, no. 1 January-February 1995 p. 23-31

09 RESEARCH AND SUPPORT FACILITIES (AIR)

refs

(BTN-95-EIX95182619211) Copyright

The simulation methodology used in the Active Flexible Wing wind-tunnel test program is described. An overview of the aeroservoelastic modeling used in building the required batch and hot-bench simulations is presented. Successful hot-bench implementation required that the full mathematical model be significantly reduced while assuring that accuracy be maintained for all combinations of 10 inputs and 56 outputs. The reduction was accomplished by using a method based on internally balanced realizations and by focusing on the linear, aeroelastic portion of the full mathematical model. The error-bound properties of the internally balanced realization significantly contribute to its utility in the model reduction process. The reduction method and the results achieved are described. Author (EI)

A95-76639* National Aeronautics and Space Administration. Langley Research Center, Hampton, VA.

ON-LINE ANALYSIS CAPABILITIES DEVELOPED TO SUPPORT THE ACTIVE FLEXIBLE WING WIND-TUNNEL TESTS

CAROL D. WIESEMAN National Aeronautics and Space Administration, Langley Research Center, Hampton, VA, SHERWOOD T. HOADLEY, and SANDRA M. MCGRAW Journal of Aircraft (ISSN 0021-8669) vol. 32, no. 1 January-February 1995 p. 39-44 refs (BTN-95-EIX95182619213) Copyright

A variety of on-line analysis tools were developed to support two active flexible wing (AFW) wind-tunnel tests. These tools were developed to verify control law execution, to satisfy analysis requirements of the control law designers, to provide measures of system stability in a real-time environment, and to provide project managers with a quantitative measure of controller performance. Descriptions and purposes of capabilities that were developed are presented in this article along with examples. Procedures for saving and transferring data for near real-time analysis, and descriptions of the corresponding data interface programs, are also presented. Although much of the on-line analysis capabilities described herein are not technically new, the implementation for near real-time analysis to verify and evaluate controller performance is new, and is included in this special Journal of Aircraft issue for completeness in describing the AFW wind-tunnel testing. The on-line analysis tools worked well before, during, and after the wind-tunnel tests, and proved to be a vital and important part of the entire test effort. part of the entire test effort. Author (EI)

N95-23011* National Aeronautics and Space Administration. Langley Research Center, Hampton, VA.

DYNAMIC RESPONSE TESTS OF INERTIAL AND OPTICAL WIND-TUNNEL MODEL ATTITUDE MEASUREMENT DEVICES

R. D. BUEHRLE, C. P. YOUNG, JR. (North Carolina State Univ., Raleigh, NC.), A. W. BURNER, J. S. TRIPP, P. TCHENG, T. D. FINLEY, and T. G. POPERNACK, JR. Feb. 1995 44 p (Contract(s)/Grant(s): RTOP 505-59-54-01) (NASA-TM-109182; NAS 1.15:109182) Avail: CASI HC A03/MF A01

Results are presented for an experimental study of the response of inertial and optical wind-tunnel model attitude measurement systems in a wind-off simulated dynamic environment. This study is part of an ongoing activity at the NASA Langley Research Center to develop high accuracy, advanced model attitude measurement systems that can be used in a dynamic wind-tunnel environment. This activity was prompted by the inertial model attitude sensor response observed during high levels of model vibration which results in a model attitude measurement bias error. Significant bias errors in model attitude measurement were found for the measurement using the inertial device during wind-off dynamic testing of a model-system. The amount of bias present during wind-tunnel tests will depend on the amplitudes of the model dynamic response and the modal characteristics of the model system.

Correction models are presented that predict the vibration-induced bias errors to a high degree of accuracy for the vibration modes characterized in the simulated dynamic environment. The optical system results were uncorrupted by model vibration in the laboratory setup. Author

N95-23192* National Aeronautics and Space Administration. Lewis Research Center, Cleveland, OH.

NASA LOW-SPEED AXIAL COMPRESSOR FOR FUNDAMENTAL RESEARCH

CHARLES A. WASSERBAUER (Sverdrup Technology, Inc., Brook Park, OH.), HAROLD F. WEAVER, and RICHARD G. SENYITKO (Sverdrup Technology, Inc., Brook Park, OH.) Feb. 1995 13 p (Contract(s)/Grant(s): NAS3-25266; RTOP 505-62-52) (NASA-TM-4635; E-9016; NAS 1.15:4635) Avail: CASI HC A03/MF A01

A low-speed multistage axial compressor built by the NASA Lewis Research Center is described. The purpose of this compressor is to increase the understanding of the complex flow phenomena within multistage axial compressors and to obtain detailed data from a multistage compressor environment for use in developing and verifying models for computational fluid dynamic code assessment. The compressor has extensive pressure instrumentation in both stationary and rotating frames of reference, and has provisions for flow visualization and laser velocimetry. The compressor will accommodate rotational speeds to 1050 rpm and is rated at a pressure ratio of 1.042. Author

N95-23299* Old Dominion Coll., Norfolk, VA. Dept. of Mechanical Engineering.

SYSTEM IDENTIFICATION OF THE LARGE-ANGLE MAGNETIC SUSPENSION TEST FIXTURE (LAMSTF) Abstract Only

JEN-KUANG HUANG In Hampton Univ., 1994 NASA-HU American Society for Engineering Education (ASEE) Summer Faculty Fellowship Program p 81 Dec. 1994 Avail: CASI HC A01/MF A02

The Large-Angle Magnetic Suspension Test Fixture (LAMSTF), a laboratory-scale research project to demonstrate the magnetic suspension of objects over wide ranges of attitudes, has been developed. This system represents a scaled model of a planned Large-Gap Magnetic Suspension System (LGMSS). The LAMSTF consists of a small cylindrical permanent magnet suspended element which is levitated above a planar array of five electromagnets mounted in a circular configuration. The cylinder is a rigid body and can be controlled to move in five independent degrees of freedom. Six position variables are sensed indirectly by using infrared light-emitting diodes and light-receiving phototransistors. The motion of the suspended cylinder is in general nonlinear and hence only the linear, time-invariant perturbed motion about an equilibrium state is considered. One of the main challenges in this project is the control of the suspended element over a wide range of orientations. An accurate dynamic model plays an essential role in controller design. The analytical model is first derived and open-loop characteristics discussed. The system is shown to be highly unstable and requires feedback control for system identification. Projection filters are first proposed to identify the state space model from closed-loop input/output test data in the time domain. This method is then extended to identify linear systems from the frequency test data. A canonical transformation matrix is also derived to transform the identified state space model into the physical coordinate. The LAMSTF system is stabilized by using a linear quadratic regulator (LQR) feedback controller for closed-loop identification. The rate information is obtained by calculating the back difference of the sensed position signals. Only the closed-loop random input/output data are recorded. Preliminary results from numerical simulations demonstrate that the identified system model is fairly accurate from either time domain or frequency-domain data. Experiments will be performed to validate the proposed closed-loop identification algorithms. Author

N95-23304* Old Dominion Coll., Norfolk, VA. Dept. of Mechanical Engineering.

OPTIMIZED DESIGN OF A HYPERSONIC NOZZLE Abstract Only

RAMESH KRISHNAMURTHY *In* Hampton Univ., 1994 NASA-HU American Society for Engineering Education (ASEE) Summer Faculty Fellowship Program p 86 Dec. 1994
 Avail: CASI HC A01/MF A02

Conventional procedures for designing nozzles involve the design of an inviscid contour (using the method of characteristics) that is corrected with a displacement thickness calculated from boundary-layer theory. However, nozzles designed using this classical procedure have been shown to exhibit poor flow quality at Mach numbers characteristic of hypersonic applications. The nozzle to be designed will be a part of the NASA HYPULSE facility which is being used for hypervelocity flight research. Thus, the flow quality of the nozzle is a critical question that needs to be addressed. Design of nozzles for hypersonic applications requires a proper assessment of the effects of the thick boundary layer on the inviscid flowfield. Since the flow field is largely supersonic, the parabolized form of the Navier-Stokes (PNS) equations can be used. The requirement of a uniform flow at the exit plane of the nozzle can be used to define an objective function as part of an optimization procedure. The design procedure used in this study involves the coupling of a nonlinear (least-squares) optimization algorithm with an efficient, explicit PNS solver. The thick boundary layers growing on the walls of the nozzle limit the extent of the usable core region (region with uniform flow) for testing models (especially rectangular). In order to maximize the region of uniform flow, it was decided to have the exit plane of this nozzle to be (nearly) rectangular. Thus, an additional constraint on the nozzle shape resulted, namely the nozzle will have a shape transitioning from a circular one at the inlet to that of a rectangle at the exit. In order to provide for a smooth shape transition, the cross sectional contour of the nozzle is defined by a superellipse. The nozzle is taken to be a meter in length. The axial variations of the major and minor radii of the superellipse are governed by cubic splines. The design parameters are the coefficients of the splines associated with the local nozzle wall slopes. Extensive calculations have been made (with a three-dimensional Euler code) to understand the effects of various parameters such as location of the knot points of the spline function, different ways of characterizing the uniformity of the flow in the exit plane, as well as the effect of constraining the area of the nozzle to be invariant. Turbulent flow (measurements indicate that the flow at the nozzle inlet is turbulent) calculations are now being performed (with the inviscidly designed nozzle contours) to assess the flow quality. Author (revised)

N95-23309* New Jersey Inst. of Tech., Newark, NJ. Dept. of Chemical Engineering, Chemistry and Environmental Science.

DESIGN OF A VARIABLE AREA DIFFUSER FOR A 15-INCH MACH 6 OPEN-JET TUNNEL Abstract Only

NORMAN W. LONEY *In* Hampton Univ., 1994 NASA-HU American Society for Engineering Education (ASEE) Summer Faculty Fellowship Program p 91 Dec. 1994
 Avail: CASI HC A01/MF A02

The Langley 15-inch Mach 6 High Temperature Tunnel was recently converted from a Mach 10 Hypersonic Flow Apparatus. This conversion was effected to improve the capability of testing in Mach 6 air at relatively high reservoir temperatures not previously possible at Langley. Elevated temperatures allow the matching of the Mach numbers, Reynolds numbers, and ratio of wall-to-adiabatic-wall temperatures (TW/Taw) between this and the Langley 20-inch Mach 6 CF4 Tunnel. This ratio is also matched for Langley's 31-inch Mach 10 Tunnel and is an important parameter useful in the simulation of slender bodies such as National Aerospace Plane (NASP) configurations currently being studied. Having established the nozzle's operating characteristics, the decision was made to install another test section to provide model injection capability. This test section is an open-jet type, with an injection system capable of injecting a model from retracted position to nozzle centerline between 0.5 and

2 seconds. Preliminary calibrations with the new test section resulted in Tunnel blockage. This blockage phenomenon was eliminated when the conical center body in the diffuser was replaced. The issue then, is to provide a new and more efficient variable area diffuser configuration with the capability to withstand testing of larger models without sending the Tunnel into an unstart condition. Use of the 1-dimensional steady flow equation with due regard to friction and heat transfer was employed to estimate the required area ratios (exit area / throat area) in a variable area diffuser. Correlations between diffuser exit Mach number and area ratios, relative to the stagnation pressure ratios and diffuser inlet Mach number were derived. From these correlations, one can set upper and lower operating pressures and temperatures for a given diffuser throat area. In addition, they will provide appropriate input conditions for the full 3-dimensional computational fluid dynamics (CFD) code for further simulation studies. Author

N95-24019# Los Alamos National Lab., NM.

NTS-SPILL TEST FACILITY WIND TUNNEL EXHAUST PLUME CHARACTERIZATION

R. KERR, H. GOLDWIRE, D. SMITH, J. RAWLINGS, T. SCHAFER, and J. ROBSON Jul. 1994 8 p Presented at the 1994 Chemical Analysis By Laser Interrogation of Proliferation Effluents (CALIOPE ITR) Interim Technical Review, Livermore, CA, 26-28 Apr. 1994 (Contract(s)/Grant(s): W-7405-ENG-48) (DE95-003630; UCRL-JC-118476; CONF-9404162-14) Avail: CASI HC A02/MF A01

The exhaust plume of the NTS-STF wind tunnel has been characterized to demonstrate its suitability as a target for CALIOPE experiments. Smoke from grenades has been released in multiple quantities and at different positions inside the tunnel. The smoke plumes have been recorded on video tape. The wind velocity profile has also been determined with a moveable array of miniature vane anemometers. These measurements will be used to determine the vapor concentration pathlength as part of the ground truth. DOE

10

ASTRONAUTICS

Includes astronautics (general); astrodynamics; ground support systems and facilities (space); launch vehicles and space vehicles; space transportation; spacecraft communications, command and tracking; spacecraft design, testing and performance; spacecraft instrumentation; and spacecraft propulsion and power.

A95-73559

PREDICTING EXHAUST PLUME BOUNDARIES WITH SUPERSONIC EXTERNAL FLOWS

KYLE L. NASH Mevatec Corp, Huntsville, AL, United States, KEVIN W. WHITAKER, and L. MICHAEL FREEMAN *Journal of Spacecraft and Rockets* (ISSN 0022-4650) vol. 31, no. 5 September-October 1994 p. 773-777 refs
 (BTN-95-EIX95152583258) Copyright

Several methods for predicting exhaust plume boundaries with a surrounding external flow currently exist. Unfortunately, these methods are usually cumbersome and often expensive, since they may be computationally intensive. Also, these methods typically provide many flowfield details in addition to the plume boundary location. If only the latter is desired, then calculation of these other details is wasted effort. This concern resulted in the development of a simplified plume boundary prediction method capable of analyzing underexpanded nozzle flow exhausting into a supersonic external flow. This new method is based upon the well-established Latvala method and uses an iterative scheme that employs two-dimensional flowfield assumptions. However, the method is still applicable to axisymmetric plumes, and its simplicity permits efficient operation on personal computers. Predictions of boundaries for axisymmetric plumes surrounded by various high-speed external flows exhibit

excellent agreement with empirical data, and parametric studies indicate that trends are correctly predicted. Author (EI)

A95-73564

FUNCTIONAL DEPENDENCE OF TRAJECTORY DISPERSION ON INITIAL CONDITION ERRORS

ROBERT A. LAFARGE Sandia Natl Lab, Albuquerque, NM, United States and ROY S. BATY Journal of Spacecraft and Rockets (ISSN 0022-4650) vol. 31, no. 5 September-October 1994 p. 806-813 refs

(BTN-95-EIX95152583263) Copyright

This article proposes numerical techniques to approximate dispersion bounds and burst patterns for Monte Carlo trajectory simulations. The algorithms developed approximate trajectory dispersion bounds and burst patterns caused by the errors in initial conditions in 1/100th of the computational expense of full Monte Carlo analyses. The proposed techniques are based on the properties that the six-degree-of-freedom equations of motion produce solutions that vary continuously with initial conditions and preserve the statistical distribution of the initial conditions. The continuity of solutions in initial conditions is studied numerically by performing a stability analysis. Numerical experiments simulating a fuse effectiveness study for two generic re-entry bodies are exhibited. The dispersion bounds and burst patterns predicted using the proposed algorithms are compared to the dispersion bounds and burst patterns predicted using full Monte Carlo simulations. The agreement is excellent. Author (EI)

A95-73568

FOURTH-GENERATION MARS VEHICLE CONCEPTS

BRENT SHERWOOD Boeing Defense & Space Group, Huntsville, AL, United States Journal of Spacecraft and Rockets (ISSN 0022-4650) vol. 31, no. 5 September-October 1994 p. 834-841 refs (BTN-95-EIX95152583267) Copyright

Conceptual designs for fourth-generation crew-carrying Mars transfer and excursion vehicles, fully integrated to state-of-the-art standards, are presented. The resulting vehicle concepts are sized for six crew members, and can support all opposition and conjunction opportunities in or after 2014. The modular, reusable transfer ship is launched to Earth orbit on six 185-ton-class boosters and assembled there robotically. Its dual nuclear-thermal rocket engines use liquid hydrogen propellant. The payload consists of a microgravity habitation system and an expendable lift-to-drag = 1.6 lander capable of aeromaneuvering to sites within +/- 20 deg of the equator. This lander can deliver either an expendable, storable-bipropellant crew-carrying ascent vehicle, or 40 tons of cargo, and it is capable of limited surface mobility to support base buildup. Multiple cargo landers sent ahead on robotic transfer vehicles deliver the supplies and equipment required for long-duration surface missions. EI

A95-73577

EFFECTS OF SATELLITE BUNCHING ON THE PROBABILITY OF COLLISION IN GEOSYNCHRONOUS ORBIT

V. A. CHOBOTOV Aerospace Corp, El Segundo, CA, United States and C. G. JOHNSON Journal of Spacecraft and Rockets (ISSN 0022-4650) vol. 31, no. 5 September-October 1994 p. 895-899 refs

(BTN-95-EIX95152583276) Copyright

The rapid increase in the satellite population in geostationary Earth orbit is a matter of international concern, in part because of increased collision hazard. Collocated satellite pairs in GEO experience natural drift requiring periodic station-keeping impulses, leading to similar trajectories and close encounters. To assess this risk, a procedure was devised that ranks satellite pairs in GEO according to the highest number of encounters over an extended time interval. Probability of collision was determined by a geometric and a statistical approach. It was found that many pairs of satellites in GEO remain in close proximity and experience many close approaches over time. The top 10 pairs in terms of closest encounters were identified, and mean-time-to-collision based on encounter statistics was determined. Results of the study suggest that the

bunching of active or inactive satellites at certain longitudes is a significant effect to be considered in the assessment of the collision hazard in the geosynchronous ring. Author (EI)

A95-73583

DYNAMICAL INSTABILITY OF THE AEROGRAVITY ASSIST MANEUVER

COLIN R. MCINNER Univ of Glasgow, Glasgow, United Kingdom Journal of Spacecraft and Rockets (ISSN 0022-4650) vol. 31, no. 5 September-October 1994 p. 916-918 refs

(BTN-95-EIX95152583282) Copyright

Fundamental dynamical equations are used to form a single expression for vertical acceleration. It is shown that the AGA (aerogravity assist) maneuver is dynamically unstable with respect to altitude errors. However, this instability can be controlled using feedback linearization. The existence of instability further emphasizes the need for robust guidance during the atmospheric pass. EI

A95-75725* National Aeronautics and Space Administration, Langley Research Center, Hampton, VA.

AERODYNAMICS OF THE SHUTTLE ORBITER AT HIGH ALTITUDES

DIDIER F. G. RAULT National Aeronautics and Space Administration, Langley Research Center, Hampton, VA Journal of Spacecraft and Rockets (ISSN 0022-4650) vol. 31, no. 6 November-December 1994 p. 944-952 refs

(BTN-95-EIX95182617454) Copyright

The high-altitude, high-Knudsen-number aerodynamics of the Shuttle Orbiter are computed from low Earth orbit down to 100 km using three-dimensional direct simulation Monte Carlo and free-molecule codes. Results are compared with the latest Shuttle aerodynamic model, which is based on in-flight accelerometer measurements, and bridging-formula models. Good comparison is observed, except for the normal-force and pitching-moment coefficients. The present results were obtained for a generic Shuttle geometry configuration corresponding to a zero deflection for all control surfaces. Author (EI)

A95-75734

AERODYNAMIC DESIGN OF PEGASUS: CONCEPT TO FLIGHT WITH COMPUTATIONAL FLUID DYNAMICS

MICHAEL R. MENDENHALL Nielsen Engineering & Research Inc, Mountain View, CA, United States, DANIEL J. LESIEUTRE, STEVEN C. CARUSO, MARNIX F. E. DILLENIUS, and GARY D. KUHN Journal of Spacecraft and Rockets (ISSN 0022-4650) vol. 31, no. 6 November-December 1994 p. 1007-1015 refs

(BTN-95-EIX95182617463) Copyright

Pegasus, a three-stage, air-launched, winged space booster, was developed to provide fast and efficient commercial launch services for small satellites. The aerodynamic design and analysis of the vehicle were conducted without wind-tunnel and subscale model testing, using only computational aerodynamic and fluid-dynamic methods. All levels of codes, ranging in complexity from empirical database methods to three-dimensional Navier-Stokes codes, were used in the design. This article describes the design and analysis requirements, the unique and conservative design philosophy, and the analysis methods considered for the various technical areas of interest and concern. Author (EI)

A95-75735

SOME ASPECTS OF THE AERODYNAMICS OF SEPARATING STRAP-ONS

K. K. BISWAS Vikram Sarabhai Space Cent, Thiruvananthapuram, India and C. G. KRISHNAN Journal of Spacecraft and Rockets (ISSN 0022-4650) vol. 31, no. 6 November-December 1994 p. 1016-1020 refs

(BTN-95-EIX95182617464) Copyright

An aerodynamics model for analyzing strap-on separation is proposed. This model comprises both interference aerodynamics and free-body aerodynamics. The interference aerodynamics is

primarily due to the close proximity of core and strap-ons. The free-body aerodynamics is solely due to the body geometry of the strap-ons. Using this aerodynamic model, the dynamics of separating strap-ons has been simulated in a six-degree-of-freedom mode to determine if a collision occurs. This aerodynamic model is very handy for various off-design studies relating to separating strap-ons.

Author (EI)

A95-76621

SHUTTLE ENTRY GUIDANCE REVISITED USING NONLINEAR GEOMETRIC METHODS

KENNETH D. MEASE Univ of California, Irvine, CA, United States and JEAN-PAUL KREMER Journal of Guidance, Control, and Dynamics (ISSN 0731-5090) vol. 17, no. 6 November-December 1994 p. 1350-1356 refs

(BTN-95-EIX95182619144) Copyright

The entry guidance law for the space shuttle orbiter is revisited using nonlinear geometric methods. The shuttle guidance concept is to track a reference drag trajectory that has been designed to lead a specified range and velocity. It is shown that the approach taken in the original derivation of the shuttle entry guidance has much in common with the more recently developed feedback linearization method of differential geometric control. Using the feedback linearization method, however, an alternative, potentially superior, guidance law was formulated. Comparing the two guidance laws based performance domains in state space, taking into account the nonlinear dynamics, the alternative guidance law achieves the desired performance over larger domains in state space; the stability domain of the laws are similar. With larger operating domain for the shuttle or some other entry vehicle, the alternative guidance law should be considered.

EI

A95-76758

FUEL-OPTIMAL BANK-ANGLE CONTROL FOR LUNAR-RETURN AEROCAPTURE

J. L. MEYER North Carolina State Univ, Raleigh, NC, United States, L. SILVERBERG, and G. D. WALBERG Journal of Spacecraft and Rockets (ISSN 0022-4650) vol. 32, no. 1 January-February 1995 p. 149-155 refs

(BTN-95-EIX95212645706) Copyright

Aerocapture is defined as the deceleration of a spacecraft due to drag produced on it by a planet's atmosphere such that the vehicle is captured into orbit about the planet. This is accomplished by varying the direction of the vehicle's lift vector through bank-angle modulation. This paper examines the application of four optimal-control approaches to aerocapture. The first is a minimization of a pseudo fuel cost function, which yields continuous controls. The second is bang-bang control, which minimizes the time associated with bank-angle modulation. Next, an absolute fuel function is minimized, which results in controls in the form of impulses. A fourth approach is a modification to impulsive control, where impulses are approximated by pulses of finite duration. All of the approaches are applied to a single-pass aerocapture problem. The modified impulsive-control approach is applied to a two-pass aerocapture scenario. Recommendations on the practical implementation of these control approaches in the presence of vehicle and atmospheric uncertainties are given.

Author (EI)

A95-76759

MINIMUM-MASS DESIGN OF SANDWICH AEROBRAKES FOR A LUNAR TRANSFER VEHICLE

K. N. SHIVAKUMAR North Carolina A&T State Univ, Greensboro, NC, United States and J. C. RIDDICK Journal of Spacecraft and Rockets (ISSN 0022-4650) vol. 32, no. 1 January-February 1995 p. 156-161 refs

(BTN-95-EIX95212645707) Copyright

A structural mass optimization study of a sandwich aerobrake for a lunar transfer vehicle (LTV) was conducted. The proposed spherical aerobrake had a base diameter of 15.2 m and radius of 13.6 m. A hot thermal protection system (TPS) and cold structure were used in the design. Honeycomb sandwich aerobrake structures made up of four

different materials - aluminum alloy, titanium alloy, graphite-epoxy, and graphite-polyimide - were considered. Cases of aerodynamic load, equivalent uniform pressure, and aerodynamic plus thermal load were analyzed. Both linear stress and buckling analyses were conducted for a range of skin and core thicknesses. A graphical optimization procedure was used to determine the skin and core thicknesses of a minimum-mass aerobrake. The design criteria used were material strength, global buckling, and TPS tile deformation. Among them, the TPS deformation criterion was the most critical. The graphite-epoxy aerobrake was the lightest among the four materials studied. Its total mass is about 12.3% of the LTV mass, for supports at 75% span. Equivalent uniform loading produced smaller deformations, stresses, and buckling loads than did the more realistic aerodynamic loading for the same aerobrake configuration. Thermally induced stresses countered the aerodynamically induced stresses and hence had a beneficial effect on the deformation and buckling of the aerobrake.

Author (EI)

N95-23532# Sandia National Labs., Albuquerque, NM.

MOVING MASS TRIM CONTROL FOR AEROSPACE VEHICLES

R. D. ROBINETT, B. A. RAINWATER, and S. A. KERR 1994 17 p Presented at the American Institute of Aeronautics and Astronautics Missile Sciences Conference, Monterey, CA, 7-9 Nov. 1994 (Contract(s)/Grant(s): DE-AC04-94AL-85000)

(DE95-002602; SAND-94-2746C; CONF-9411142-4) Avail: CASI HC A03/MF A01

A moving mass trim controller increases the accuracy of axisymmetric, ballistic vehicles. The MMTC is different than other moving mass schemes because it generates an angle-of-attack (AOA) directly from the mass motion. The nonlinear equations of motion for a ballistic vehicle with one moving point mass are derived and provide the basis for a detailed simulation model. The full nonlinear equations are linearized to produce a set of linear, time-varying autopilot equations. These autopilot equations are analyzed and used to develop theoretical design tools for the creation of MMTC's for both fast and slow spinning vehicles. A fast spinning MMTC is designed for a generic artillery rocket that uses principal axis misalignment to generate trim AOA. A slow spinning is designed for a generic reentry vehicle that generates a trim AOA with a center of mass offset and aerodynamic drag. The performance of both MMTC's are evaluated with the detailed simulation.

DOE

N95-23761*# Honeywell Technology Center, Minneapolis, MN.

EMPIRICAL RESULTS ON SCHEDULING AND DYNAMIC BACKTRACKING

MARK S. BODDY and ROBERT P. GOLDMAN In JPL, Third International Symposium on Artificial Intelligence, Robotics, and Automation for Space 1994 p 431-434 Oct. 1994

Avail: CASI HC A01/MF A03

At the Honeywell Technology Center (HTC), we have been working on a scheduling problem related to commercial avionics. This application is large, complex, and hard to solve. To be a little more concrete: 'large' means almost 20,000 activities, 'complex' means several activity types, periodic behavior, and assorted types of temporal constraints, and 'hard to solve' means that we have been unable to eliminate backtracking through the use of search heuristics. At this point, we can generate solutions, where solutions exist, or report failure and sometimes why the system failed. To the best of our knowledge, this is among the largest and most complex scheduling problems to have been solved as a constraint satisfaction problem, at least that has appeared in the published literature. This abstract is a preliminary report on what we have done and how. In the next section, we present our approach to treating scheduling as a constraint satisfaction problem. The following sections present the application in more detail and describe how we solve scheduling problems in the application domain. The implemented system makes use of Ginsberg's Dynamic Backtracking algorithm, with some minor extensions to improve its utility for scheduling. We describe those extensions and the performance of the resulting system. The paper concludes with some general remarks, open questions and plans for future work.

Derived from text

N95-23781# Massachusetts Inst. of Tech., Lexington, MA. Lincoln Lab.

CALCULATION OF SATELLITE DRAG COEFFICIENTS

EDWARD M. GAPOSCHKIN 18 Jul. 1994 57 p
(Contract(s)/Grant(s): F19628-90-C-0002)
(AD-A285118; MIT-TR-998; ESC-TR-93-293) Avail: CASI HC A04/MF A01

Calculation of Cd for satellites using accommodation coefficients is reviewed. A phenomenological model for accommodation coefficients due to Hurlbut, Sherman, and Nocilla is used to obtain values for the accommodation coefficients for average satellite materials, thermosphere constituents and temperatures, and satellite velocities using a number of laboratory measurements. There is a significant difference between these results and the traditional method of calculating Cd. These differences contribute as much as 20% error in use of thermosphere models for calculation of satellite drag. DTIC

N95-24032*# Auburn Univ., AL. Dept. of Aerospace Engineering. **AERODYNAMIC FLIGHT CONTROL TO INCREASE PAYLOAD CAPABILITY OF FUTURE LAUNCH VEHICLES Final Report**, 20 Jan. 1994 - 19 Jan. 1995

JOHN E. COCHRAN, JR. 28 Feb. 1995 9 p
(Contract(s)/Grant(s): NAS8-39131)
(NASA-CR-197704; NAS 1.26:197704) Avail: CASI HC A02/MF A01

The development of new launch vehicles will require that designers use innovative approaches to achieve greater performance in terms of payload capability. The objective of the work performed under this delivery order was to provide technical assistance to the Contract Officer's Technical Representative (COTR) in the development of ideas and concepts for increasing the payload capability of launch vehicles by incorporating aerodynamic controls. Although aerodynamic controls, such as moveable fins, are currently used on relatively small missiles, the evolution of large launch vehicles has been moving away from aerodynamic control. The COTR reasoned that a closer investigation of the use of aerodynamic controls on large vehicles was warranted. Derived from text

11

CHEMISTRY AND MATERIALS

Includes chemistry and materials (general); composite materials; inorganic and physical chemistry; metallic materials; nonmetallic materials; and propellants and fuels.

A95-73345

MIL-HDBK-5 DESIGN ALLOWABLES FOR FIBRE/METAL LAMINATES: ARALL 2 AND ARALL 3

H. F. WU Alcoa Technical Cent, Alcoa Cent, PA, United States and L. L. WU Journal of Materials Science Letters (ISSN 0261-8028) vol. 13, no. 8 April 15, 1994 p. 582-585
(BTN-94-EIX94371346933) Copyright

Fiber/metal laminates are a new aircraft material showing great potential where both strength and fatigue resistance are required and in certain non-structural application. In view of their comparative weight saving of over 20% in typical applications, fiber/metal laminates can replace monolithic aluminium alloys in over 30% of aircraft structures. Consideration of fiber/metal laminates for aerospace applications will require the generation of these basic strength property design allowables. The work in this article sets a precedent in that fiber/metal laminates represent the first emerging classes of hybrid materials to be incorporated into MIL-HDBK-5 as modified metals. EI

A95-75755

AIRCRAFT STRIPPING AND PAINTING

STUART BIRCH and LINDA E. TREGO Aerospace Engineering (Warrendale, Pennsylvania) (ISSN 0736-2536) vol. 15, no. 1 January-February 1995 p. 21-23
(BTN-95-EIX95182617810) Copyright

Many researchers are studying different stripping processes and paint that will improve coating duration, decrease maintenance time, and be environmentally friendly. Particularly, FLS Aerospace is assessing two possible solutions for its future needs: Envirostrip, a biodegradable, nontoxic polymer stripper designed to remove paint and primer from metal composites surfaces, and Flashjet, using a dry-ice-particle stream which uses pulse light energy and is fully automated. EI

N95-22689# Oak Ridge National Lab., TN.

EVOLUTION OF OXIDATION AND CREEP DAMAGE MECHANISMS IN HIPED SILICON NITRIDE MATERIALS

A. A. WERESZCZAK, M. K. FERBER, T. P. KIRKLAND, and K. L. MORE 1994 14 p Presented at the Conference on Plastic Deformation of Ceramics, Snowbird, UT, 7-12 Aug. 1994
(Contract(s)/Grant(s): DE-AC05-84OR-21400)
(DE95-001360; CONF-940865-4) Avail: CASI HC A03/MF A01

Several yttria-fluxed, hot-isostatically pressed (HIPed) silicon nitrides have been tensile creep tested at temperatures representative of gas turbine engines. Creep and oxidation assisted damage mechanisms concurrently evolve when these materials are tested at high temperatures and low stresses (i.e., long exposure times at temperature). Atmospheric creep testing results in creation of oxygen and yttrium gradients across the radial dimension. High concentrations of oxygen and yttrium coincide with dense populations of lenticular-shaped cavities near the surface of crept specimens. The center of the tensile specimens was devoid of oxygen or yttrium; in addition, lenticular cavities were rare. The gradient in lenticular-cavity concentration is coincident with the oxygen and yttrium gradients. Stress corrosion cracking (SCC) also occurs in these HIPed silicon nitrides when they are subjected to stress at high temperatures in ambient air. The size of this damage zone increases when the temperature is higher and/or the applied stress is lower. Stress-corrosion cracking initiates at the surface of the tensile specimen and advances radially inwards. What nucleates SCC has not yet been identified, but it is believed to result from a stress-concentrator (e.g., machining damage) at the surface and its growth is a result of coalescence of microcracks and cavities. The higher concentration of oxygen and yttrium in the grain boundaries near the specimen's surface lessens the local high temperature mechanical integrity; this is believed to be associated with the growth of the SCC zone. This SCC zone continues to grow in size during tensile loading until it reaches a critical size which causes fracture. DOE

N95-22764# Argonne National Lab., IL.

EVALUATION OF NEUTRON TECHNIQUES FOR ILLICIT SUBSTANCE DETECTION

C. L. FINK, B. J. MICKLICH, T. J. YULE, P. HUMM, L. SAGALOVSKY, and M. M. MARTIN 1994 5 p Presented at the 13th International Conference on the Application of Accelerators in Research and Industry, Denton, TX, 7-10 Nov. 1994
(Contract(s)/Grant(s): W-31-109-ENG-38)
(DE95-002988; ANL/TD/CP-83462; CONF-941129-9) Avail: CASI HC A01/MF A01

The authors are studying inspection systems based on the use of fast neutrons for detecting illicit substances such as explosives and drugs in luggage and cargo containers. Fast neutron techniques can determine the quantities of light elements such as carbon, nitrogen, and oxygen in a volume element. Illicit substances containing these elements are characterized by distinctive elemental densities or density ratios. They discuss modeling and tomographic reconstruction studies for fast-neutron transmission spectroscopy. DOE

N95-23031* Air Force Systems Command, McClellan AFB, CA. Advanced Composites Program Office.

MISHAP RISK CONTROL FOR ADVANCED AEROSPACE/ COMPOSITE MATERIALS

JOHN M. OLSON *In* NASA. Goddard Space Flight Center, Environmental, Safety, and Health Considerations: Composite Materials in the Aerospace Industry p 107-120 Oct. 1994
 Avail: CASI HC A03/MF A03

Although advanced aerospace materials and advanced composites provide outstanding performance, they also present several unique post-mishap environmental, safety, and health concerns. The purpose of this paper is to provide information on some of the unique hazards and concerns associated with these materials when damaged by fire, explosion, or high-energy impact. Additionally, recommended procedures and precautions are addressed as they pertain to all phases of a composite aircraft mishap response, including fire-fighting, investigation, recovery, clean-up, and guidelines are general in nature and not application-specific. The goal of this project is to provide factual and realistic information which can be used to develop consistent and effective procedures and policies to minimize the potential environmental, safety, and health impacts of a composite aircraft mishap response effort. Author

N95-23038* Air Force Inst. of Tech., Wright-Patterson AFB, OH. **MODELING AEROSOL EMISSIONS FROM THE COMBUSTION OF COMPOSITE MATERIALS**

J. A. ROOP, D. J. CALDWELL, and K. J. KUHLMANN *In* NASA. Goddard Space Flight Center, Environmental, Safety, and Health Considerations: Composite Materials in the Aerospace Industry p 219-230 Oct. 1994
 Avail: CASI HC A03/MF A03

The use of advanced composite materials (ACM) in the B-2 bomber, composite armored vehicle, and F-22 advanced tactical fighter has rekindled interest concerning the health risk of burned or burning ACM. The objective of this work was to determine smoke production from burning ACM and its toxicity. A commercial version of the UPITT II combustion toxicity method developed at the University of Pittsburgh, and subsequently refined through a US Army-funded basic research project, was used to establish controlled combustion conditions which were selected to evaluate real-world exposure scenarios. Production and yield of toxic species varied with the combustion conditions. Previous work with this method showed that the combustion conditions directly influenced the toxicity of the decomposition products from a variety of materials. Author

N95-23179* Virginia Polytechnic Inst., Blacksburg, VA. Dept. of Engineering Science and Mechanics.

DEVELOPMENT AND VERIFICATION OF A RESIN FILM INFUSION/RESIN TRANSFER MOLDING SIMULATION MODEL FOR FABRICATION OF ADVANCED TEXTILE COMPOSITES
Interim Report 99, Jan 1992 - Dec. 1994

JOHN DOUGLAS MACRAE, ALFRED C. LOOS, H. BENSON DEXTER (National Aeronautics and Space Administration. Langley Research Center, Hampton, VA.), JERRY W. DEATON (National Aeronautics and Space Administration. Langley Research Center, Hampton, VA.), and GREGORY H. HASKO (Lockheed Engineering and Sciences Co., Hampton, VA.) Dec. 1994 176 p
 (Contract(s)/Grant(s): NAG1-343)
 (NASA-CR-197439; NAS 1.26:197439; CCMS-95-01; VPI-E-94-09)
 Avail: CASI HC A09/MF A02

The objective of this study was to develop a two-dimensional computer model for the simulation of the resin transfer molding/resin film infusion processing of advanced composite materials. This computer simulation model is designed to provide aircraft structure and tool designers with a method of predicting the infiltration and curing behavior of a composite material component. For a given specified cure cycle, the computer model can be used to calculate the resin infiltration, resin viscosity, resin advancement, heat transfer within the component/tool assembly during processing and preform compaction. Formulations of the resin flow problem are

given using the finite element/control volume technique based on Darcy's Law of flow through porous media. This technique allows for the efficient numerical calculation of the advancing resin front within the preform materials. The heat transfer in the fabric preform and tooling is analyzed using a transient finite element method which included the effects of convection on the tooling surfaces. Compaction behavior of the tooling assembly is analyzed using a simplified isotropic form of the plane elasticity equations. All of these solutions were coupled together in a quasi-steady state non-linear fashion inside the computer code. Simulation model verifications were carried out on individual components of the computer model. A verification of the flow model is carried out by a comparison with experiments reported in literature as well as two dimensional visualization studies performed for a center-port injection of a flat plate. The heat transfer model was verified using the experimental results of a thick section composite laminate processing. Verification of the compaction model were limited to the comparison of the final part dimensions. Two computer simulations were performed on two resin infusion cycles of a single blade-stiffened composite panel. The simulation model results of the two cycles were used to assist in the development of an alternative cycle for the composite manufacturing of a three blade stiffened panel. The results demonstrated the importance of a sufficient minimum viscosity region in the cycle in order to allow the resin to completely infiltrate the fabric preform of the structure. Predictions of the viscosities and degree of cure profiles within the single blade stiffened panel illustrated the uniformity of these parameters during the curing cycle. Author

N95-23277* Iowa State Univ. of Science and Technology, Ames, IA. Dept. of Aerospace Engineering and Engineering Mechanics.

IDEALIZED TEXTILE COMPOSITES FOR EXPERIMENTAL/ ANALYTICAL CORRELATION Abstract Only

DANIEL O. ADAMS *In* Hampton Univ., 1994 NASA-HU American Society for Engineering Education (ASEE) Summer Faculty Fellowship Program p 57 Dec. 1994

Avail: CASI HC A01/MF A02

Textile composites are fiber reinforced materials produced by weaving, braiding, knitting, or stitching. These materials offer possible reductions in manufacturing costs compared to conventional laminated composites. Thus, they are attractive candidate materials for aircraft structures. To date, numerous experimental studies have been performed to characterize the mechanical performance of specific textile architectures. Since many materials and architectures are of interest, there is a need for analytical models to predict the mechanical properties of a specific textile composite material. Models of varying sophistication have been proposed based on mechanics of materials, classical laminated plate theory, and the finite element method. These modeling approaches assume an idealized textile architecture and generally consider a single unit cell. Due to randomness of the textile architectures produced using conventional processing techniques, experimental data obtained has been of limited use for verifying the accuracy of these analytical approaches. This research is focused on fabricating woven textile composites with highly aligned and accurately placed fiber tows that closely represent the idealized architectures assumed in analytical models. These idealized textile composites have been fabricated with three types of layer nesting configurations: stacked, diagonal, and split-span. Compression testing results have identified strength variations as a function of nesting. Moire interferometry experiments are being used to determine localized deformations for detailed correlation with model predictions. Author

N95-23300* Florida Univ., Gainesville, FL. Dept. of Aerospace Engineering, Mechanical and Engineering Science.

INTERLAMINAR SHEAR TEST METHOD DEVELOPMENT FOR LONG TERM DURABILITY TESTING OF COMPOSITES

Abstract Only

PETER G. IFJU *In* Hampton Univ., 1994 NASA-HU American Society for Engineering Education (ASEE) Summer Faculty Fellowship Program p 82 Dec. 1994

Avail: CASI HC A01/MF A02

The high speed civil transport is a commercial aircraft that is expected to carry 300 passengers at Mach 2.4 over a range of more than 6000 nautical miles. With the existing commercial structural material technology (i.e., aluminum) the performance characteristics of the high speed civil transport would not be realized. Therefore there has been a concerted effort in the development of light weight materials capable of withstanding elevated temperatures for long duration. Thermoplastic composite materials are such candidate materials and the understanding of how these materials perform over the long term under harsh environments is essential to safe and effective design. The matrix dominated properties of thermoplastic composites are most affected by both time and temperature. There is currently an effort to perform short term testing to predict long term behavior of in-plane mechanical properties E22 (transverse modulus of elasticity) and G12 (shear modulus). Out-of-plane properties such as E33, G13, and G23 are inherently more difficult to characterize. This is especially true for the out-of-plane shear modulus G23 and hence there is no existing acceptable standard test method. Since G23 is the most matrix dominated property, it is essential that a test method be developed. A shear test methodology is developed to do just that. The test method, called the double notched specimen, along with the previously developed shear gage was tested at room temperature. Mechanical testing confirmed the attributes of the methodology. A finite element parametric study was conducted for specimen optimization. Moire interferometry, a high sensitivity laser optical method, was used for full-field analysis of the specimen. From this work, material parameters will be determined and thus enable the prediction of long term material behavior of laminates subjected to general loading states.

Author (revised)

N95-23496# Advisory Group for Aerospace Research and Development, Neuilly-Sur-Seine (France). Structures and Materials Panel. **CORROSION DETECTION AND MANAGEMENT OF ADVANCED AIRFRAME MATERIALS [LA DETECTION DE LA CORROSION ET LA GESTION DES MATERIAUX AVANCES ENTRANT DANS LA CONSTRUCTION DES CELLULES]** Jan. 1995 240 p In ENGLISH and FRENCH Presented at the 79th Meeting of the AGARD Structures and Materials Panel, Seville, Spain, 5-6 Oct. 1994 Original contains color illustrations (AGARD-CP-565; ISBN-92-836-1011-3) Copyright Avail: CASI HC A11/MF A03

A Specialists' Meeting on Corrosion Detection and Management of Advanced Airframe Materials was held to present the current knowledge base of corrosion, degradation, detection and prevention and to identify the research and development issues which must be addressed in order to ensure long service life and low maintenance costs of NATO aircraft. The Meeting concentrated on corrosion detection, test methodology for environmental assessment, mechanistic evaluation, corrosion prevention methods, and materials selection and design to prevent environmental degradation. For individual titles, see N95-23497 through N95-23519.

N95-23497# Defence Research Agency, Farnborough, Hampshire (England). Structural Materials Centre.

THE CORROSION AND PROTECTION OF ADVANCED ALUMINIUM - LITHIUM AIRFRAME ALLOYS

C. J. E. SMITH, D. L. BARTLETT, and J. A. GRAY In AGARD, Corrosion Detection and Management of Advanced Airframe Materials 9 p Jan. 1995

Copyright Avail: CASI HC A02/MF A03

The corrosion and stress corrosion cracking behavior of 8090-T81 and 2091-T84 sheet and 8090-T8171 plate aluminum-lithium alloys tested under laboratory and marine exposure conditions are compared with aerospace aluminium alloys currently in service. Initial results are also presented on the corrosion performance of a metal matrix composite aluminium alloy. The corrosion protection of aluminium-lithium alloys is discussed and progress on the development of chromate-free systems and their application to advanced aluminium alloys is described.

Author

N95-23500# Naval Air Warfare Center, Warminster, PA. Aircraft Div.

CORROSION OF LANDING GEAR STEELS

E. U. LEE, J. KOZOL, J. B. BOODEY, and J. WALDMAN In AGARD, Corrosion Detection and Management of Advanced Airframe Materials 12 p Jan. 1995

Copyright Avail: CASI HC A03/MF A03

A study was conducted on the corrosion behavior of landing gear steels, AerMet 100, 300M, AF1410, HYTUF and 4340. This study included investigations of stress corrosion cracking and immersion corrosion in an aqueous 3.5 percent NaCl solution, salt spray corrosion in a fog chamber of atomized aqueous 5 percent NaCl solution, humidity corrosion in an atmosphere of vapor from distilled water and hydrogen embrittlement. AF1410 steel is most resistant to stress corrosion cracking, and it is followed by AerMet 100, 0.20C AF1410, HYTUF, 300M and 4340 steels. The immersion corrosion and salt spray corrosion rates of an AerMet 100 steel are 33-40 percent and 13-20 percent those of a 300M steel. In a humidity chamber, AerMet 100 steel is not corrodible in 110 days, whereas 300M steel is quite susceptible to humidity corrosion. Compared to 300M steel, AerMet 100 steel is less susceptible to hydrogen embrittlement.

Author

N95-23508# Belgian Center for Corrosion Study, Brussels (Belgium). Center for Corrosion Study.

IN-SITU DETECTION OF SURFACE PASSIVATION OR ACTIVATION AND OF LOCALIZED CORROSION: EXPERIENCES AND PROSPECTIVES IN AIRCRAFT

A. POURBAIX In AGARD, Corrosion Detection and Management of Advanced Airframe Materials 5 p Jan. 1995

Copyright Avail: CASI HC A01/MF A03

The surveillance of the actual conditions of materials in aircrafts and the analysis of the influence of flight or standby conditions require detection methods that give quantitative and instantaneous results and that are related to the real degradation process. Electrochemical methods derived from methods used in laboratory have proven to be of interest. The scientific concepts and the instrumentation are generally easily applicable to field conditions; some effort is necessary to develop relevant sensors. The first example applies to the phosphating of carbon steels before painting. The characterization of surface passivation or reactivity can be of interest before and during the surface conversion processes. The second example applies to the detection of crevice corrosion, as may occur in riveted joints.

Author

N95-23509# Belgian Center for Corrosion Study, Brussels (Belgium). Center for Corrosion Study.

TEST METHOD AND TEST RESULTS FOR ENVIRONMENTAL ASSESSMENT OF AIRCRAFT MATERIALS

A. POURBAIX In AGARD, Corrosion Detection and Management of Advanced Airframe Materials 4 p Jan. 1995

(Contract(s)/Grant(s): DAJA45-83-C-0011; DAJA45-83-C-0041)

Copyright Avail: CASI HC A01/MF A03

A study was conducted to identify whether life prediction of high strength aluminum alloys for aircrafts can be determined from short term accelerated atmospheric corrosion tests. The method used is a wet and dry method with electrochemical measurements to characterize the formation or destruction of passive layers. The materials tested include high strength steel 4130, precipitation hardening 15-7 Mo-PH steel and aluminum alloys 6061, 7075 and 2024 with different heat treatments and surface conditions. It appears that the ranking of different Al alloys depends on the type of atmosphere (chloride or acid). The method also clearly showed the detrimental effect of chromated cadmium plating on the hydrogen embrittlement of high strength steel. Corrosion processes of aluminum and high strength steels were clearly identified and useful recommendations could be derived from such tests.

Author

**N95-23510# Deutsche Aerospace A.G., Munich (Germany).
CORROSION PROTECTION MEASURES FOR CFC/METAL
JOINTS OF FUEL INTEGRAL TANK STRUCTURES OF
ADVANCED MILITARY AIRCRAFT**

CLAUS D. HAMM *In* AGARD, Corrosion Detection and Management of Advanced Airframe Materials 11 p Jan. 1995
Copyright Avail: CASI HC A03/MF A03

Assembly of carbon fiber composites (CFC) and aluminum structures shall be avoided in unprotected conditions. The more noble CFC could cause fatal galvanic corrosion on the aluminum part. Adequate protection methods for electrical isolation of these dissimilar materials shall be adopted. Adhesion of the coatings on both the CFC and aluminum substrate during exposure to the simulated fuel tank environment is an essential requirement for corrosion protection and fuel tightness of the joint. In a sequence of material and functional tests for selection of adequate coatings and associated materials as well as galvanic corrosion and integral tank aspects have been taken into account. Additional to the static panel test for paint adhesion corrosion tests under dynamic loading and corrosive environment were performed. Based on the experience of these investigations the selected combinations of the coatings, sealants and associated materials were applied on structural tank box for final evaluation. This test article represented the section of a fuselage integral fuel tank structure. For simulation of the complete in-service spectrum, during the life of an aircraft structure, static and dynamic loads were induced. The internal tank environment was simulated by water as fuel replacement and by pressurization of the compartment. Resistance of the CFC/aluminum joint to galvanic corrosion and liquid tightness of the selected integral tank concept proved excellent under simulated conditions. Author

**N95-23513# Air Products and Chemicals, Inc., Allentown, PA.
ORGANIC COATING TECHNOLOGY FOR THE PROTECTION
OF AIRCRAFT AGAINST CORROSION**

CHARLES R. HEGEDUS, STEPHEN J. SPADAFORA, and ANTHONY T. ENG (Naval Air Warfare Center, Warminster, PA.) *In* AGARD, Corrosion Detection and Management of Advanced Airframe Materials 12 p Jan. 1995 Original contains color illustrations
Copyright Avail: CASI HC A03/MF A03

Coating systems on military and commercial aircraft perform a variety of functions. Clearly, the most critical of these is the protection of aircraft structures from environmental degradation. Protective coatings serve as the primary defense against corrosion of aircraft metallic alloys, as well as degradation of other materials such as polymeric composites. Traditional coatings for aircraft include epoxy primers and polyurethane topcoats. Primers normally contain high concentrations of corrosion inhibitors, such as chromates, and they are designed to provide superior adhesion and corrosion protection. Polyurethane topcoats are formulated to enhance protection and durability; they also provide desired optical effects (i.e., anesthetics or camouflage). More recently, alternative coatings have been developed, such as self-priming topcoats, flexible primers, temporary and multi-functional coatings. These new developments reflect trends in protective coatings technology, changes in aircraft operational requirements/capabilities, and, most dramatically, concerns over environmental protection and worker safety. This issue has created a drive toward coatings with low (possibly zero) concentrations of volatile organic compounds (VOC's) and non-toxic corrosion inhibitors. In turn, these changes have led to concerns over long-term performance, especially protection against corrosion. This paper reviews current organic coatings technology for the protection of aircraft structures and discusses future needs and trends based on advancing technology, environmental concerns, and operational requirements. Author

N95-23515# Naval Air Warfare Center, Warminster, PA. Aircraft Div.

CORROSION DETECTION AND MONITORING OF AIRCRAFT STRUCTURES: AN OVERVIEW

V. S. AGARWALA, P. K. BHAGAT (Federal Aviation Administration, Atlantic City, NJ.), and G. L. HARDY (Wright Lab., Wright-Patterson AFB, OH.) *In* AGARD, Corrosion Detection and Management of

Advanced Airframe Materials 6 p Jan. 1995

Copyright Avail: CASI HC A02/MF A03

Corrosion occurs on both military and civilian aircraft as a result of operation in corrosive environments and utilization of less than optimum corrosion preventive measures during fabrication. For low usage rate systems such as military aircraft, corrosion treatment constitutes a high cost maintenance action because corrosion effects can be life limiting mainly due to the fact that current techniques require extensive material loss for reliable detection of corrosion. For high usage systems such as commercial aircraft, corrosion may constitute a safety problem. A recent study by the U.S. Air Force at Tinker Air Force Base has demonstrated that while off-the-shelf nondestructive inspection equipment has some capability for detecting and quantifying aircraft corrosion, significant improvements in both detection and quantification are still required. Results of this study will be briefly reviewed along with discussions relating to some new and innovative inspection technology for detecting corrosion. New concepts and techniques for corrosion monitoring, i.e., detection of onset of corrosion or breakdown of corrosion protection system, will also be discussed. Advances in electrochemical measurements, thermal imaging, and optical scanning for chemical changes are providing some new research and development opportunities. Finally, concepts relating to damage-revealing chemicals and coatings which may revolutionize the detection and management of corrosion in our systems will be discussed. Author

**N95-23516# Deutsche Aerospace A.G., Munich (Germany).
EXPERIENCE OF IN-SERVICE CORROSION ON MILITARY
AIRCRAFT**

H. J. VOSS *In* AGARD, Corrosion Detection and Management of Advanced Airframe Materials 18 p Jan. 1995
Copyright Avail: CASI HC A03/MF A03

To prevent corrosion of military aircraft the design has to be performed with respect to a careful material selection and an effective surface protection treatment of the materials. Protective treatment on aircraft against moisture, humidity, salty atmosphere, industrial environment, hydraulic fluids, fuel, de-icing fluids, combat chemicals etc. is necessary to meet the operation requirements of the aircraft throughout its operational life. Occurring corrosion detected during maintenance shows that not in every case the requirements above can avoid corrosion problems. This report will show some selected examples of in-service corrosion under investigation of the causes. Inspection and repair methods are shown; further recommendations for corrosion prevention and control to reduce corrosion problems based on practical experiences will be given. Author

N95-23517# Naval Air Station, Norfolk, VA.

**US NAVY OPERATING EXPERIENCE WITH NEW AIRCRAFT
CONSTRUCTION MATERIALS**

G. T. BROWNE *In* AGARD, Corrosion Detection and Management of Advanced Airframe Materials 19 p Jan. 1995
Copyright Avail: CASI HC A03/MF A03

This paper addresses the U.S. Navy's experience and problems encountered with new aircraft construction material in the highly corrosive naval operating environment, including: experience with carbon bismaleimide (BMI) and epoxy matrices composite, new aluminum alloys and metal to composite joint repair of honeycomb and monolithic composite structure in fleet activities ashore and afloat; problems experienced with electromagnetic interference (EMI) protection, systems currently in use, and the development of corrosion inhibiting conductive (EMI) sealant; and fastener compatibility for joining carbon composite to metals, H-60 and H-53 helicopter problems, and corrective actions. Author

N95-23518# Aerospatiale, Toulouse (France). Avions Div.

CORROSION IN SERVICE EXPERIENCE WITH AIRCRAFT IN FRANCE

M. J. FRUSTIE and P. GAUTHIER (CTMS, Toulouse, France.) *In* AGARD, Corrosion Detection and Management of Advanced Air-

frame Materials 7 p Jan. 1995 In FRENCH
Copyright Avail: CASI HC A02/MF A03

The objective of this communication is to present from a comparison of observed corrosions on modern airplanes (Airbus, ATR) and corrosions on older airplanes (Transall, Caravelle) the progress realized in the control of corrosion, based on the adaption of materials and better performing protection. It's necessary today to adapt the techniques and constraints of the new legislative dispositions concerning the environment which bring to research the new materials and protection system. Transl. by CASI

N95-23981# Oak Ridge National Lab., TN.

CU DEPOSITION USING A PERMANENT MAGNET ELECTRON CYCLOTRON RESONANCE MICROWAVE PLASMA SOURCE

L. A. BERRY, S. M. GORBATKIN, and R. L. RHOADES 1994 14 p Presented at the International Conference on Metallurgical Coatings and Thin Films, San Diego, CA, 25-29 Apr. 1994

(Contract(s)/Grant(s): DE-AC05-84OR-21400)

(DE94-017768; CONF-940440-5) Avail: CASI HC A03/MF A01

An electron cyclotron resonance (ECR) plasma has been used in conjunction with a solid metal sputter target for Cu deposition over 200-mm diameters. The goal is to develop a deposition process suitable for filling submicron, high aspect ratio features used for ultralarge scale integration. The system uses a permanent magnet for creation of the magnetic field necessary for ECR and is significantly more compact than systems equipped with electromagnets. A custom launcher design allows remote microwave injection with the microwave entrance window shielded from the Cu flux. Cu deposition rates up to 100 nm/min were observed and film resistivities were typically in the low to mid 2 micro-ohm-cm range. Based on deposition rate measurements at two radial sample position, uniformities of a few percent over 200-mm diameters should be attainable.

DOE

12

ENGINEERING

Includes engineering (general); communications; electronics and electrical engineering; fluid mechanics and heat transfer; instrumentation and photography; lasers and masers; mechanical engineering; quality assurance and reliability; and structural mechanics.

A95-73439

COMPLIANT INTERLAYER

G. P. JARRABET Technetics Corp Aerospace Engineering (Warrendale, Pennsylvania) (ISSN 0736-2536) vol. 14, no. 12 December 1994 p. 7-10

(BTN-95-EIX95142562401) Copyright

Although ceramics withstand extremely high temperatures that would destroy most other engineering materials, these are most likely to fail catastrophically; thus, they must be processed and applied carefully to avoid flaws and operating loads that stress them beyond their operating failure. These problems are avoided with the use of a fiber-metal compliant interlayer between the ceramic and the metal, hence reducing thermal cycling stresses that lead to failure. Typical applications include high-temperature gas-turbine engine seals and combustors, and internal-combustion engine components and insulators. EI

A95-73452

MECHANICAL SYSTEM RELIABILITY AND RISK ASSESSMENT

T. A. CRUSE Vanderbilt Univ, Nashville, TN, United States, S. MAHADEVAN, Q. HUANG, and S. MEHTA AIAA Journal (ISSN 0001-1452) vol. 32, no. 11 November 1994 p. 2249-2259 refs (BTN-95-EIX95142553046) Copyright

A new methodology is reported for the prediction of the reliability of mechanical structures subject to multiple failure modes, including noncritical damage. The reduction of system reliability due

to accumulated damage is quantitatively estimated by updating the critical system failure states at each level of damage. Correlated design variables are automatically accounted for in the system reliability calculations. Second-order reliability bounds are reported which are unbiased to the ordering of the events. A system risk assessment methodology is also reported that accounts for the cost of multiple types of failure modes and includes the effect of inspection success on reducing the consequences of system failure. Application of the new technology is illustrated for a simplified system model of an aeropropulsion rotor system. However, the methodology is general and is applicable to any engineering system. Author (EI)

A95-73454* National Aeronautics and Space Administration. Lewis Research Center, Cleveland, OH.

FLOW STRUCTURE IN THE WAKE OF A WISHBONE VORTEX GENERATOR

B. J. WENDT National Aeronautics and Space Administration, Lewis Research Center, Cleveland, OH and W. R. HINGST AIAA Journal (ISSN 0001-1452) vol. 32, no. 11 November 1994 p. 2234-2240 refs

(BTN-95-EIX95142553044) Copyright

The results of an experimental examination of the vortex structures shed from a low-profile 'wishbone' generator are presented. The vortex generator height relative to the turbulent boundary layer was varied by testing two differently sized models. Measurements of the mean three-dimensional velocity field were conducted in cross-stream planes downstream of the vortex generators. In all cases a counter-rotating vortex pair was observed. Individual vortices were characterized by three descriptors derived from the velocity data: circulation, peak vorticity, and cross-stream location of peak vorticity. Measurements in the cross plane at two axial locations behind the smaller wishbone characterize the downstream development of the vortex pairs. A single region of streamwise velocity deficit is shared by both vortex cores. This is in contrast to conventional generators, where each core coincides with a region of velocity deficit. The measured cross-stream velocities for each case are compared with an Oseen model with matching descriptors. The best comparison occurs with the data from the larger wishbone. Author (EI)

A95-73457

SIMULATION OF TURBULENT FLUCTUATIONS

GIOVANNI MENGALI Univ of Pisa, Pisa, Italy and MARCO MICHELI AIAA Journal (ISSN 0001-1452) vol. 32, no. 11 November 1994 p. 2210-2216 refs

(BTN-95-EIX95142553041) Copyright

A simulation technique is used to generate three signals representing the time variation of the velocity components in turbulent flows. This technique makes use of a bank of linear filters driven by non-Gaussian white noises. The filter impulse responses are chosen so as to obtain specified second-order (spectral) characteristics at the filter outputs. Higher order moments can also be accommodated by further specifying the statistical properties of the driving noises. The signals generated in this way may be employed to solve various engineering problems such as, testing the adequacy of measurement methods based on hot-wire anemometry or obtaining gust velocity components suitable for applications in flight simulators. Author (EI)

A95-73458

MAIN FEATURES OF OVEREXPANDED TRIPLE JETS

GAMAL H. MOUSTAFA Menoufia Univ, Shbien El-Kom, Egypt AIAA Journal (ISSN 0001-1452) vol. 32, no. 11 November 1994 p. 2205-2209 refs

(BTN-95-EIX95142553040) Copyright

The flowfield of an overexpanded triple free jet has been investigated. The flowfield was generated by three Laval nozzles set in a common end wall with equal spacing in a triangular configuration. Total pressure measurements were made for three exit Mach numbers of 1.5, 2, and 2.5 with the range of stagnation pressure from

2.9 to 4.5 atmospheres. The spacing between the nozzles based on the throat diameter was varied as 2.8, 3.6, 4.4, and 6. The triple jet has been compared to a single jet operating at the same initial flow conditions. It is shown that the triple jet in triangular configuration undergoes a transformation in its shape and axis orientation. The triple jet spreads at the base side more than at the top side. The differential spreading rate generates more flow disturbance and, therefore, enhances the mixing process. Author (EI)

A95-73460

ADAPTIVE FINITE ELEMENT METHOD FOR TURBULENT FLOW NEAR A PROPELLER

DOMINIQUE PELLETIER Ecole Polytechnique de Montreal, Montreal, Que, Canada, FLORIN ILINCA, and JEAN-FRANCOIS HETU AIAA Journal (ISSN 0001-1452) vol. 32, no. 11 November 1994 p. 2186-2193 refs (BTN-95-EIX95142553038) Copyright

This paper presents an adaptive finite element method based on remeshing to solve incompressible turbulent free shear flow near a propeller. Solutions are obtained in primitive variables using a highly accurate finite element approximation on unstructured grids. Turbulence is modeled by a mixing length formulation. Two general purpose error estimators, which take into account swirl and the variation of the eddy viscosity, are presented and applied to the turbulent wake of a propeller. Predictions compare well with experimental measurements. The proposed adaptive scheme is robust, reliable and cost effective. Author (EI)

A95-73477

SHOCK TUNNEL MEASUREMENTS OF HYPERVELOCITY BLUNTED CONE DRAG

L. M. PORTER Univ of Queensland, St. Lucia, Australia, A. PAULL, D. J. MEE, and J. M. SIMMONS AIAA Journal (ISSN 0001-1452) vol. 32, no. 12 December 1994 p. 2476-2477 refs (BTN-95-EIX95152577606) Copyright

Presented here are results obtained from an investigation into the effects of nose bluntness on slender cone drag in the hypervelocity flight regime. The results indicate that, for small cone angles, the drag of a blunt cone is reasonably well predicted by the Newtonian sine-square law modified for blunt bodies. This suggests the absence of any real gas effects on the total drag. The effect of nose bluntness at the smaller bluntness ratios is relatively small. This is encouraging for the design of a hypervelocity space plane or a centerbody for an axisymmetric scramjet where a slightly blunted nose is required to reduce stagnation point heating. EI

A95-73479

EFFECTS OF SPATIAL ORDER OF ACCURACY ON THE COMPUTATION OF VORTICAL FLOWFIELDS

J. A. EKATERINARIS Navy-NASA Joint Inst of Aeronautics, Moffett Field, CA, United States AIAA Journal (ISSN 0001-1452) vol. 32, no. 12 December 1994 p. 2471-2474 refs (BTN-95-EIX95152577604) Copyright

A high-order accurate method on general curvilinear meshes was used to improve the numerical solutions of complex, three-dimensional, vortical flowfields over a sharp-edged double-delta wing at high incidence. The inviscid fluxes computed from the flowfield were evaluated using third-, fourth-, and fifth-order upwind-biased formulas. Result showed that a higher order of accuracy enables better convection of vorticity, yields stronger vortices, and produces closer agreement with the measured surface pressures. EI

A95-73486

EIGENANALYSIS OF UNSTEADY FLOWS ABOUT AIRFOILS, CASCADES, AND WINGS

KENNETH C. HALL Duke Univ, Durham, NC, United States AIAA Journal (ISSN 0001-1452) vol. 32, no. 12 December 1994 p. 2426-2432 refs (BTN-95-EIX95152577597) Copyright

A general technique for constructing reduced order models of

unsteady aerodynamic flows about two-dimensional isolated airfoils, cascades of airfoils, and three-dimensional wings is developed. The starting point is a time domain computational model of the unsteady small disturbance flow. For illustration purposes, we apply the technique to an unsteady incompressible vortex lattice model. The eigenmodes of the system, which may be thought of as aerodynamic states, are computed and subsequently used to construct computationally efficient, reduced order models of the unsteady flowfield. Only a handful of the most dominant eigenmodes are retained in the reduced order model. The effect of the remaining eigenmodes is included approximately using a static correction technique. An important advantage of the present method is that once the eigenmode information has been computed, reduced order models can be constructed for any number of arbitrary modes of airfoil motion very inexpensively. Numerical examples are presented that demonstrate the accuracy and computational efficiency of the present method. Finally, we show how the reduced order model may be incorporated into an aeroelastic flutter model. Author (EI)

A95-73498

DEVELOPMENT OF AERONAUTICAL MOBILE SATELLITE SERVICES OVER THE PAST THIRTY YEARS

GUANGREN CHEN Civil Aviation Inst of China, Tianjin, China and FUQIN XIONG IEEE Aerospace and Electronic Systems Magazine (ISSN 0885-8985) vol. 9, no. 12 December 1994 p. 25-36 refs (BTN-95-EIX95152569458) Copyright

This paper presents an overview of the development of aeronautical mobile satellite services (AMSS) over the past 30 years. The inherent shortcomings of present air-ground HF communications have hindered the development of civil aviation, but according to the Future Air Navigation Systems (FANS) concept aeronautical satellite communication - including Automatic Dependent Surveillance (ADS) - will be the key to eliminating the shortcomings of HF communication systems. Satellite-based communication and surveillance will significantly improve air traffic control (ATC) over the oceanic and remote terrestrial airspace, and it will benefit civil aviation authorities, airlines as well as passengers. This paper discusses the availability of system elements, and world wide trials, demonstrations and preoperational use of aeronautical satellite communications over past years are described. Future satellite systems possible for aeronautical communications are also discussed. Author (EI)

A95-73551

HYPERSONIC RAREFIED FLOW PAST SPHERES INCLUDING WAKE STRUCTURE

VIRENDRA K. DOGRA ViGYAN, Inc, Hampton, VA, United States, JAMES N. MOSS, RICHARD G. WILMOTH, and JOSEPH M. PRICE Journal of Spacecraft and Rockets (ISSN 0022-4650) vol. 31, no. 5 September-October 1994 p. 713-718 refs (BTN-95-EIX95152583250) Copyright

Results of a numerical study using the direct simulation Monte Carlo method are presented for hypersonic rarefied flow past spheres. The flow conditions considered are those corresponding to low-density wind-tunnel test conditions. The set of the experimental conditions for the calculations encompasses the transitional to near-continuum flow regimes. Comparison of the calculated drag with experimental results shows good agreement to well within the experimental error. Particular attention is focused on the wake structure. Calculations show that the wake is very rarefied with considerable thermal nonequilibrium for all the cases considered. No flow separation is observed in the wake for the near-continuum case where a vortex has been predicted by Navier-Stokes-type calculations. Author (EI)

A95-73553* National Aeronautics and Space Administration. Ames Research Center, Moffett Field, CA.

HYPERSONIC NONEQUILIBRIUM NAVIER-STOKES SOLUTIONS OVER AN ABLATING GRAPHITE NOSETIP

Y.-K. CHEN National Aeronautics and Space Administration, Ames

Research Center, Moffett Field, CA and W. D. HENLINE Journal of Spacecraft and Rockets (ISSN 0022-4650) vol. 31, no. 5 September-October 1994 p. 728-734 refs
(BTN-95-EIX95152583252) Copyright

The general boundary conditions, including mass and energy balances, of chemically equilibrated or nonequilibrated gas adjacent to ablating surfaces have been derived. A computer procedure based on these conditions was developed and interfaced with the Navier-Stokes solver GASP (General Aerodynamics Simulation Program). A test case with a proposed hypersonic test-vehicle configuration and associated freestream conditions was developed. The solutions of the GASP code with various surface boundary conditions were obtained and compared with those of the ASCC (ABRES Shape Change) code, and the effect of nonequilibrium gas as well as surface chemistry on surface heating and ablation rate were examined. Author (EI)

A95-73554* National Aeronautics and Space Administration. Ames Research Center, Moffett Field, CA.
HYPersonic CONVECTIVE HEAT TRANSFER OVER 140-DEG BLUNT CONES IN DIFFERENT GASES

D. A. STEWART National Aeronautics and Space Administration, Ames Research Center, Moffett Field, CA and Y. K. CHEN Journal of Spacecraft and Rockets (ISSN 0022-4650) vol. 31, no. 5 September-October 1994 p. 735-743 refs
(BTN-95-EIX95152583253) Copyright

Large-angle blunt cones, with various corner radii, were tested in dissociated air, CO₂, and CO₂-Ar gas mixtures. These experiments were conducted at angles of attack from 0 to 20 deg. The heating distribution data and how shock-waved geometry were obtained during the cone's exposure to the three gases. The data can be used to partially validate two-dimensional (2-D) axisymmetric and three-dimensional Navier-Stokes solutions of the heating distribution over a 140-deg blunt cone in a simulated Martian atmosphere. The predicted heating distribution over the cones and estimated bow shock standoff distances using a 2-D axisymmetric Navier-Stokes code were compared with test data taken at zero angle of attack. Author (EI)

A95-73555* National Aeronautics and Space Administration. Langley Research Center, Hampton, VA.
APPLICATION OF THE MULTIGRID SOLUTION TECHNIQUE TO HYPersonic ENTRY VEHICLES

FRANCIS A. GREENE National Aeronautics and Space Administration, Langley Research Center, Hampton, VA Journal of Spacecraft and Rockets (ISSN 0022-4650) vol. 31, no. 5 September-October 1994 p. 744-750 refs
(BTN-95-EIX95152583254) Copyright

Multigrid techniques have been incorporated into an existing hypersonic flow analysis code, the Langley aerothermodynamic upwind relaxation algorithm. The multigrid scheme is based on the full approximation storage approach and uses full multigrid to obtain a well-defined fine-mesh starting solution. Predictions were obtained using standard transfer operators, and a V cycle was used to control grid sequencing. Computed hypersonic flow solutions, compared with experimental data for a 15-deg blunted sphere-cone and a blended-wing body, are presented. It is shown that the algorithm predicts heating rates accurately, and computes solutions in one-third the computational time of the nonmultigrid algorithm. Author (EI)

A95-73556* National Aeronautics and Space Administration. Langley Research Center, Hampton, VA.
HIGHER-ORDER VISCOUS SHOCK-LAYER SOLUTIONS FOR HIGH-ALTITUDE FLOWS

ROOP N. GUPTA National Aeronautics and Space Administration, Langley Research Center, Hampton, VA, ERNEST V. ZOBY, SUDHEER N. NAYANI, and KAM-PUI LEE Journal of Spacecraft and Rockets (ISSN 0022-4650) vol. 31, no. 5 September-October 1994 p. 751-758 refs
(BTN-95-EIX95152583255) Copyright

A higher-order viscous-shock-layer method has been developed and is used to obtain physically consistent results under varying degrees of low-density conditions for perfect-gas and

nonequilibrium flows past slender bodies. The method of solution is a spatial-marching, implicit finite-difference technique, which employs a Vigneron pressure condition in the subsonic nose region. Higher-order body and shock slip conditions are employed with the method to obtain solutions for the low-density flows. Detailed comparisons with the direct simulation Monte Carlo method and Navier-Stokes calculations clearly show that the higher-order terms included in the HVSL equations are required to predict comparable values of surface pressure and heat transfer rate at higher altitude. The deficiency of the standard viscous shock-layer method in predicting low-density flows can not be corrected by the slip conditions alone as considered by earlier researchers. Author (EI)

A95-73584

SUPERSONIC AXISYMMETRIC CONICAL FLOW SOLUTIONS FOR DIFFERENT RATIOS OF SPECIFIC HEATS

BHAVESH B. PATEL Mississippi State Univ, Mississippi State, MS, United States, B. K. HODGE, and KEITH KOENIG Journal of Spacecraft and Rockets (ISSN 0022-4650) vol. 31, no. 5 September-October 1994 p. 918-920 refs
(BTN-95-EIX95152583283) Copyright

The aim of this study is to summarize the salient behavioural characteristics of calorically perfect conical supersonic flows for different values of the ratio of specific heats. Although the computation of the conical flow is relatively straightforward, some effort is required to assemble a useful set of information for a variety of values of gamma. Over the range of ratio of specific heats, 1.0(+) less than gamma less than 1.67, the characteristics demonstrate considerable variations. EI

A95-74496

SEM REPRESENTATION OF THE EARLY AND LATE TIME FIELDS SCATTERED FROM WIRE TARGETS

MICHAEL A. RICHARDS Nichols Research Corp, Shalimar, FL, United States IEEE Transactions on Antennas and Propagation (ISSN 0018-926X) vol. 42, no. 4 April 1994 p. 564-566 refs
(BTN-94-EIX94381353142) Copyright

In this communication, the singularity expansion method (SEM) is used to express the field scattered from an arbitrary thin-wire target. Explicit expressions are given for both the class-1 and class-2 representations of the scattered field due to step excitations. Numerical results are given for the early-time transient fields scattered from both a straight wire and a simple swept-wing aircraft model. The results of the SEM computations are compared to fields obtained by Fourier inversion techniques. It is shown that the class-2 representation yields a significant improvement over the class-1 result during the early-time interval, albeit at the expense of a more complex computation. Author (EI)

A95-74612

FINITE ELEMENT MODEL FOR A FLEXIBLE NON-SYMMETRIC ROTOR ON DISTRIBUTED BEARING: A STABILITY STUDY

A. G. TAYLOR Univ of Alberta, Edmonton, Alberta, Canada and A. CRAGGS Journal of Sound and Vibration (ISSN 0022-460X) vol. 173, no. 1 May 26, 1994 p. 1-21 refs
(BTN-94-EIX94381352212) Copyright

A finite element model is presented for a flexible, non-axisymmetric shaft-rotor system supported in distributed bearings. The stability of this model is analyzed over a normal rotation speed range and the results are compared with analytical and numerical studies carried out on rigid and simpler flexible models. The same types of regions of instabilities are found for the finite element, flexible shaft-rotor model, and the role of shear deflection is particularly significant in one of the mechanisms. Author (EI)

A95-74702

TRANSIENT ANALYSIS OF A CRACKED ROTOR PASSING THROUGH CRITICAL SPEED

A. S. SEKHAR Indian Inst of Technology Madras, Madras, India and B. S. PRABHU Journal of Sound and Vibration (ISSN 0022-460X)

vol. 173, no. 3 June 9, 1994 p. 415-421 refs
(BTN-94-EIX94401360022) Copyright

The past several years have seen growing interest in the dynamic behavior of rotor bearing systems with cracked shafts. Vibration monitoring is considered as a possible means of detecting the presence of growth of cracks, which can otherwise lead to catastrophic failure. The transient vibration response of a cracked rotor passing through its critical speed is analyzed in the context of crack detection and monitoring. EI

A95-75516

FATIGUE STRENGTH OF HIGH-TEMPERATURE ALLOYS UNDER CONDITIONS OF CYCLIC TEMPERATURE VARIATION. COMMUNICATION 1: EXPERIMENTAL PROCEDURE AND RESULTS

V. T. TROSHCHENKO Inst Problem Prochnosti AN Ukrainy, Kiev, Ukraine, B. A. GRYAZNOV, and YU. B. YAMSHANOV Problemy Prochnosti (ISSN 0556-171X) no. 3 March 1994 p. 13-20 In RUSSIAN refs
(BTN-94-EIX94401363884) Copyright

Determination of the serviceability of the material of gas-turbine engine blades, one of the most loaded elements of the engine, critical for the reliability of the turbine, is discussed. The NUM-3 setup, intended for studying fatigue strength of high-temperature alloys under conditions simulating service ones, is briefly described. The results of the investigation into the fatigue of alloys EP962 and EI698 under isothermal conditions and complex thermal-mechanical loading are presented. The analysis of the findings revealed a number of regularities in the effect of thermal cycling and resulting varying thermal stresses on the fatigue strength of the materials studied. EI

A95-75760

NUMERICAL STUDY OF SOUND GENERATION DUE TO A SPINNING VORTEX PAIR

DUCK JOO LEE Korea Advanced Inst of Science and Technology, Taejeon, Korea, Republic of and SAM OK KOO AIAA Journal (ISSN 0001-1452) vol. 33, no. 1 January 1995 p. 20-26 refs
(BTN-95-EIX95182619075) Copyright

A numerical approach for the calculation of an acoustic field is applied to the case of a spinning vortex pair to investigate the sound generation by quadrupole sources in unsteady vortical flows. Based on the unsteady hydrodynamic information from the known incompressible flowfield, the perturbed compressible acoustic terms derived from the Euler equations are calculated. Nonreflecting boundary conditions are developed to obtain highly stable solutions. Calculated results are compared with analytical solutions obtained by the method of matched asymptotic expansions. The possibility of predicting the effect of convective mean flow is also tested. It is concluded that the sound generated by the quadrupole sources of unsteady vortical flows without a sound-generating body or surface can be calculated by using the source terms of hydrodynamic flow fluctuations. Author (EI)

A95-75762

APPLICATION OF WALL FUNCTIONS TO GENERALIZED NONORTHOGONAL CURVILINEAR COORDINATE SYSTEMS

DOUGLAS L. SONDAK United Technologies Research Cent, East Hartford, CT, United States and RICHARD H. PLETCHER AIAA Journal (ISSN 0001-1452) vol. 33, no. 1 January 1995 p. 33-41 refs
(BTN-95-EIX95182619077) Copyright

A method has been developed for the application of wall functions to generalized curvilinear coordinate systems with nonorthogonal grids. Two test cases have been computed using this method with the k-epsilon turbulence model: flow over a flat plate at 0-deg angle of attack using a nonorthogonal grid at the wall and flow over a prolate hemispheroid with a hemispherical nose cap at 0-deg angle of attack. All results are compared with experimental data. In addition, the hemispheroid results are compared with computations

using the Baldwin-Lomax algebraic turbulence model and the Chien low-Reynolds-number k-epsilon turbulence model. Author (EI)

A95-76484* National Aeronautics and Space Administration. Langley Research Center, Hampton, VA.

MULTIGRID SOLUTION OF COMPRESSIBLE TURBULENT FLOW ON UNSTRUCTURED MESHES USING A TWO-EQUATION MODEL

D. J. MAVRIPLIS National Aeronautics and Space Administration Langley Research Center, Hampton, VA, United States and L. MATINELLI International Journal for Numerical Methods in Fluids (ISSN 0271-2091) vol. 18, no. 10 May 30, 1994 p. 887-914 refs
(BTN-94-EIX94401378794) Copyright

The steady state solution of the system of equations consisting of the full Navier-Stokes equations and two turbulence equations has been obtained using a multigrid strategy of unstructured meshes. The flow equations and turbulence equations are solved in a loosely coupled manner. The flow equations are advanced in time using a multistage Runge-Kutta time-stepping scheme with a stability-bound local time step, while turbulence equations are advanced in a point-implicit scheme with a time step which guarantees stability and positivity. Low-Reynolds-number modifications to the original two-equation model are incorporated in a manner which results in well-behaved equations for arbitrarily small wall distances. A variety of aerodynamic flows are solved, initializing all quantities with uniform freestream values. Rapid and uniform convergence rates for the flow and turbulence equations are observed. Author (EI)

A95-76489

INFLUENCE OF STREAMWISE CURVATURE ON LONGITUDINAL VORTICES IMBEDDED IN TURBULENT BOUNDARY LAYERS

W. J. KIM Univ of Iowa, Iowa City, IA, United States and V. C. PATEL Computers & Fluids (ISSN 0045-7930) vol. 23, no. 5 June 1994 p. 647-673 refs
(BTN-94-EIX94401378820) Copyright

Numerical experiments were conducted to study the fate of artificially introduced vortex pairs in an otherwise two-dimensional turbulent boundary layer, with emphasis on the influence of streamwise surface curvature. The Reynolds-averaged Navier-Stokes equations for three-dimensional turbulent flows, together with a two-layer turbulence model to resolve the near-wall flow, were solved by a numerical method for a configuration for which some measurements are available from recent experiments. EI

A95-76491

GRID REFINEMENT TEST OF TIME-PERIODIC FLOWS OVER BLUFF BODIES

MOSHE ROSENFELD Tel Aviv Univ, Tel Aviv, Israel Computers & Fluids (ISSN 0045-7930) vol. 23, no. 5 June 1994 p. 693-709 refs
(BTN-94-EIX94401378822) Copyright

A grid refinement study of the time-periodic flow over a circular cylinder at $Re = 200$ is presented. An efficient numerical solution method of the time-dependent incompressible Navier-Stokes equations allowed the solution of the problem on several meshes up to 513×513 points. The time-periodic solution was presented in the frequency domain by expanding it into a Fourier series in time. The dependence of the solution on the mesh size has been studied both in the physical and Fourier domains. In the physical domain, very fine meshes are needed to obtain a spatially converged solution, i.e. a solution that varies with the mesh size as the spatial accuracy of the scheme. EI

A95-76585

SIMULATING HEAT ADDITION VIA MASS ADDITION IN CONSTANT AREA COMPRESSIBLE FLOWS

W. H. HEISER U.S. Air Force Acad, CO, United States, W. B. MCCLURE, and C. W. WOOD AIAA Journal (ISSN 0001-1452) vol. 33, no. 1 January 1995 p. 167-171 refs
(BTN-95-EIX95182619100) Copyright

A study conducted demonstrated the striking similarity between the influence of heat addition and mass addition on compressible flows. These results encourage the belief that relatively modest laboratory experiments employing mass addition can be devised that will reproduce the leading phenomena of heat addition, such as the axial variation of properties, choking, and wall-boundary-layer separation. These suggest that some aspects of the complex behavior of dual-mode ramjet/scramjet combustors could be experimentally evaluated or demonstrated by replacing combustion with less expensive, more easily controlled, and safer mass addition.

EI

A95-76586**EFFECT OF AMBIENT TURBULENCE INTENSITY ON SPHERE WAKES AT INTERMEDIATE REYNOLDS NUMBERS**

J.-S. WU Univ of Michigan, Ann Arbor, MI, United States and G. M. FAETH AIAA Journal (ISSN 0001-1452) vol. 33, no. 1 January 1995 p. 171-173 refs
(BTN-95-EIX95182619101) Copyright

In order to resolve the effects of ambient turbulence intensity variations on sphere wakes at intermediate Reynolds numbers ($Re = 125-1560$), the effect of Re on vortex shedding, the mean streamwise velocities, and the effects of vortex shedding, wake turbulence, and ambient turbulence on effective turbulent viscosities have been determined.

EI

A95-76647**TRACKING OF RAINDROPS IN FLOW OVER AN AIRFOIL**

JAMES R. VALENTINE Univ of Utah, Salt Lake City, UT, United States and RAND A. DECKER Journal of Aircraft (ISSN 0021-8669) vol. 32, no. 1 January-February 1995 p. 100-105 refs
(BTN-95-EIX95182619221) Copyright

The splashback that occurs when raindrops impact an airfoil results in an 'ejecta fog' of small droplets near the leading edge. Acceleration of these droplets by the air flowfield is a momentum sink for the airflow and has been hypothesized to contribute to the degradation of airfoil performance in heavy rain. Presented here is a one-way coupled Lagrangian particle tracking scheme to evaluate droplet concentrations and the associated momentum sink around a NACA 64-210 airfoil section for three rainfall rates. A laminar air flowfield is determined with a standard CFD code and is used as input to the particle tracking algorithm. Raindrops are assumed to be noninteracting, nondeforming, nonevaporating, and nonspinning spheres, and are tracked through the same curvilinear grid used by the airflow code. A simple model is used to simulate impacts and the resulting splashback on the airfoil surface.

Author (EI)

A95-76652**NATURAL LAMINAR FLOW WING CONCEPT FOR SUPERSONIC TRANSPORTS**

BERRY T. GIBSON Northrop Grumman Corp, Pico Rivera, CA, United States and HEINZ A. GERHARDT Journal of Aircraft (ISSN 0021-8669) vol. 32, no. 1 January-February 1995 p. 130-136 refs
(BTN-95-EIX95182619226) Copyright

A 'reverse' delta wing, having a straight leading edge and forward-swept trailing edges, is shown to be capable of achieving extended runs of natural laminar flow during supersonic flight. Euler calculations at supersonic Mach number confirm that the flow over a reverse delta wing is nominally two dimensional, in contrast to delta wing flow that exhibits large spanwise flow gradients, particularly near the leading edge. The data suggest that crossflow and attachment line instabilities, the primary modes of transition on swept wings, are minimal on a reverse delta wing. Predicted forces on 2% thick delta wings are in accord with the principles of reciprocal flow theory because lift-curve slope, wave drag, and drag-due-to-lift are nearly identical. The reverse delta wing has a large aerodynamic center shift as Mach number increases from subsonic to supersonic. Subsonic wind-tunnel tests were conducted with a variety of leading-

and trailing-edge flap planforms to assess the longitudinal characteristics of a reverse delta wing. The experimental data show that leading-edge flaps are highly effective at increasing maximum lift and decreasing drag at moderate angles of attack. Trailing-edge flaps were up to 90% as effective as delta wing flaps in generating untrimmed lift increments.

Author (EI)

A95-76658**NEURAL NETWORK PREDICTION OF THREE-DIMENSIONAL UNSTEADY SEPARATED FLOWFIELDS**

SCOTT J. SCHRECK U.S. Air Force Acad, CO, United States, WILLIAM E. FALLER, and MARVIN W. LUTTGES Journal of Aircraft (ISSN 0021-8669) vol. 32, no. 1 January-February 1995 p. 178-185 refs
(BTN-95-EIX95182619232) Copyright

Unsteady surface pressures were measured on a wing pitching beyond static stall. Surface pressure measurements confirmed that the pitching wing generated a rapidly evolving, three-dimensional unsteady surface pressure field. Using these data, both linear and nonlinear neural networks were developed. A novel quasilinear activation function enabled extraction of a linear equation system from the weight matrices of the linear network. This equation set was used to predict unsteady surface pressures and unsteady aerodynamic loads. Neural network predictions were compared directly to measured surface pressures and aerodynamic loads. The neural network accurately predicted both temporal and spatial variations for the unsteady separated flowfield as well as for the aerodynamic loads. Consistent results were obtained using either the linear or nonlinear neural network. In addition, fluid mechanics modeled by the linear equation set were consistent with established vorticity dynamics principles.

Author (EI)

A95-76660* National Aeronautics and Space Administration. Ames Research Center, Moffett Field, CA.

CFD OPTIMIZATION OF A THEORETICAL MINIMUM-DRAG BODY

SAMSON CHEUNG National Aeronautics and Space Administration, Ames Research Center, Moffett Field, CA, PHILIP AARONSON, and THOMAS EDWARDS Journal of Aircraft (ISSN 0021-8669) vol. 32, no. 1 January-February 1995 p. 193-198 refs
(BTN-95-EIX95182619234) Copyright

This article describes a methodology behind coupling a fast, parabolized Navier-Stokes flow solver to a nonlinear constrained optimizer. The design parameters, constraints, grid refinement, behavior of the optimizer, and flow physics related to the CFD calculations are discussed. Pressure drag reduction in the supersonic regime of a theoretical minimum-drag body of revolution is performed. Careful selection of design variables allows the optimization process to improve the aerodynamic performance. A calculation including nonlinear and viscous effects produces a different minimum drag geometry than linear theory and results in a drag reduction of approximately 4%. Effect of grid density on the optimization process is also studied. In order to obtain accurate optimization results, CFD calculations must model physical phenomena that contribute to the optimization parameters.

Author (EI)

A95-76686**DESCRIPTION OF A GNSS AVAILABILITY MODEL AND ITS USE IN DEVELOPING REQUIREMENTS**

WALTER A. POOR MITRE Corp, McLean, VA, United States IEEE Transactions on Aerospace and Electronic Systems (ISSN 0018-9251) vol. 31, no. 1 January 1995 p. 436-446 refs
(BTN-95-EIX95202637603) Copyright

The Global Navigation Satellite System (GNSS) Air Traffic Operations Model (GATOM) calculates a variety of statistical measures of the required services at locations specified by the user. A description of the current version of the model is presented. Results of the analysis which addresses Global Positioning System (GPS) constellations of 24 to 32 satellites as well as augmentation with

baro-altimeter and geostationary satellites conducted with respect to availability during category 1 and nonprecision approaches, are discussed. EI

N95-22481* Eloret Corp., Palo Alto, CA.

PARTICLE KINETIC SIMULATION OF HIGH ALTITUDE

HYPERVELOCITY FLIGHT Report, 1 Jan. 1989 - 31 Jan. 1994

IAIN BOYD and BRIAN L. HAAS 19 Apr. 1994 9 p

(Contract(s)/Grant(s): NCC2-582)

(NASA-CR-197383; NAS 1.26:197383) Avail: CASI HC A02/MF A01

Rarefied flows about hypersonic vehicles entering the upper atmosphere or through nozzles expanding into a near vacuum may only be simulated accurately with a direct simulation Monte Carlo (DSMC) method. Under this grant, researchers enhanced the models employed in the DSMC method and performed simulations in support of existing NASA projects or missions. DSMC models were developed and validated for simulating rotational, vibrational, and chemical relaxation in high-temperature flows, including effects of quantized anharmonic oscillators and temperature-dependent relaxation rates. State-of-the-art advancements were made in simulating coupled vibration - dissociation - recombination for post-shock flows. Models were also developed to compute vehicle surface temperatures directly in the code rather than requiring isothermal estimates. These codes were instrumental in simulating aerobraking of NASA's Magellan spacecraft during orbital maneuvers to assess heat transfer and aerodynamic properties of the delicate satellite. NASA also depended upon simulations of entry of the Galileo probe into the atmosphere of Jupiter to provide drag and flow field information essential for accurate interpretation of an onboard experiment. Finally, the codes have been used extensively to simulate expanding nozzle flows in low-power thrusters in support of propulsion activities at NASA-Lewis. Detailed comparisons between continuum calculations and DSMC results helped to quantify the limitations of continuum CFD codes in rarefied applications. Author

N95-22669* National Aeronautics and Space Administration. Lewis Research Center, Cleveland, OH.

ADDITIONAL IMPROVEMENTS TO THE NASA LEWIS ICE ACCRETION CODE LEWICE

WILLIAM B. WRIGHT (NYMA, Inc., Brook Park, OH.) and COLIN S. BIDWELL Mar. 1995 14 p Presented at the 33rd Aerospace Sciences Meeting and Exhibit, Reno, NV, 9-12 Jan. 1995; sponsored by AIAA

(Contract(s)/Grant(s): NAS3-27186; RTOP 505-68-10)

(NASA-TM-106849; E-9425; NAS 1.15:106849; AIAA PAPER 95-0752) Avail: CASI HC A03/MF A01

Due to the feedback of the user community, three major features have been added to the NASA Lewis ice accretion code LEWICE. These features include: first, further improvements to the numerics of the code so that more time steps can be run and so that the code is more stable; second, inclusion and refinement of the roughness prediction model described in an earlier paper; third, inclusion of multi-element trajectory and ice accretion capabilities to LEWICE. This paper will describe each of these advancements in full and make comparisons with the experimental data available. Further refinement of these features and inclusion of additional features will be performed as more feedback is received. Author

N95-22804* National Aeronautics and Space Administration. Ames Research Center, Moffett Field, CA.

NONLINEAR SYSTEM GUIDANCE IN THE PRESENCE OF TRANSMISSION ZERO DYNAMICS

G. MEYER, L. R. HUNT, and R. SU Jan. 1995 42 p

(Contract(s)/Grant(s): RTOP 505-64-52)

(NASA-TM-4661; A-95014; NAS 1.15:4661) Avail: CASI HC A03/MF A01

An iterative procedure is proposed for computing the commanded state trajectories and controls that guide a possibly multiaxis, time-varying, nonlinear system with transmission zero dynamics through a given arbitrary sequence of control points. The procedure

is initialized by the system inverse with the transmission zero effects nulled out. Then the 'steady state' solution of the perturbation model with the transmission zero dynamics intact is computed and used to correct the initial zero-free solution. Both time domain and frequency domain methods are presented for computing the steady state solutions of the possibly nonminimum phase transmission zero dynamics. The procedure is illustrated by means of linear and nonlinear examples. Author

N95-23015* National Aeronautics and Space Administration. Langley Research Center, Hampton, VA.

MACH 10 COMPUTATIONAL STUDY OF A THREE-DIMENSIONAL SCRAMJET INLET FLOW FIELD

SCOTT D. HOLLAND Mar. 1995 32 p

(Contract(s)/Grant(s): RTOP 506-40-41-02)

(NASA-TM-4602; L-17348; NAS 1.15:4602) Avail: CASI HC A03/MF A01

The present work documents the computational results for a combined computational and experimental parametric study of the internal aerodynamics of a generic three-dimensional sidewall-compression scramjet inlet configuration at Mach 10. The three-dimensional Navier-Stokes code SCRAMIN was chosen for the computational portion of the study because it uses a well-known and well-proven numerical scheme and has shown favorable comparison with experiment at Mach numbers between 2 and 6. One advantage of CFD was that it provided flow field data for a detailed examination of the internal flow characteristics in addition to the surface properties. The experimental test matrix at mach 10 included three geometric contraction ratios (3, 5, and 9), three Reynolds numbers (0.55×10^6 (exp 6) per foot, 1.14×10^6 (exp 6) per foot, and 2.15×10^6 (exp 6) per foot), and three cowl positions (at the throat and two forward positions). Computational data for two of these configurations (the contraction ratio of 3, $Re = 2.15 \times 10^6$ (exp 6) per foot, at two cowl positions) are presented along with a detailed analysis of the flow interactions in successive computational planes. Author

N95-23183* Tennessee Univ., Tullahoma, TN. Center for Space Transportation and Applied Research.

A WALL INTERFERENCE ASSESSMENT/CORRECTION

SYSTEM Final Report, Jun. 1991 - Jun. 1994

C. F. LO Jun. 1994 10 p

(Contract(s)/Grant(s): NAG2-733)

(NASA-CR-197421; NAS 1.26:197421) Avail: CASI HC A02/MF A01

A Wall Signature method originally developed by Hackett has been selected to be adapted for the Ames 12-ft Wind Tunnel WIAC system in the project. This method uses limited measurements of the static pressure at the wall, in conjunction with the solid wall boundary condition, to determine the strength and distribution of singularities representing the test article. The singularities are used in turn for estimating wall interference at the model location. The development and implementation of a working prototype will be completed, delivered and documented with a software manual. The WIAC code will be validated by conducting numerically simulated experiments rather than actual wind tunnel experiments. The simulations will be used to generate both free-air and confined wind-tunnel flow fields for each of the test articles over a range of test configurations. Specifically, the pressure signature at the test section wall will be computed for the tunnel case to provide the simulated 'measured' data. These data will serve as the input for the WIAC method—Wall Signature method. The performance of the WIAC method then may be evaluated by comparing the corrected parameters with those for the free-air simulation. The following two additional tasks are included: (1) On-line wall interference calculation: The developed wall signature method (modified Hackett's method) for Ames 12-ft Tunnel will be the pre-computed coefficients which facilitate the on-line calculation of wall interference, and (2) Support system effects estimation: The effects on the wall pressure measurements due to the presence of the model support systems will be evaluated. Author

N95-23190* Auburn Univ., AL. Dept. of Mechanical Engineering.
INFLUENCE OF BACKUP BEARINGS AND SUPPORT STRUCTURE DYNAMICS ON THE BEHAVIOR OF ROTORS WITH ACTIVE SUPPORTS Semiannual Status Report
 GEORGE T. FLOWERS Feb. 1995 5 p
 (Contract(s)/Grant(s): NAG3-1507)
 (NASA-CR-197438; NAS 1.26:197438) Avail: CASI HC A01/MF A01

This semiannual status report lists specific accomplishments made on the research of the influence of backup bearings and support structure dynamics on the behavior of rotors with active supports. Papers have been presented representing work done on the T-501 engine model; an experimental/simulation study of auxiliary bearing rotordynamics; and a description of a rotordynamical model for a magnetic bearing supported rotor system, including auxiliary bearing effects. A finite element model for a foil bearing has been developed. Additional studies of rotor/bearing/housing dynamics are currently being performed as are studies of the effects of sideloads on auxiliary bearing rotordynamics using the magnetic bearing supported rotor model. Derived from text

N95-23210* National Aeronautics and Space Administration.
 Langley Research Center, Hampton, VA.
MACH 10 COMPUTATIONAL STUDY OF A THREE-DIMENSIONAL SCRAMJET INLET FLOW FIELD
 SCOTT D. HOLLAND Mar. 1995 30 p
 (Contract(s)/Grant(s): RTOP 506-40-41-02)
 (NASA-TM-4602; L-17348; NAS 1.15:4602) Avail: CASI HC A03/MF A01

The present work documents the computational results for a combined computational and experimental parametric study of the internal aerodynamics of a generic three-dimensional sidewall-compression scramjet inlet configuration at Mach 10. The three-dimensional Navier-Stokes code SCRAMIN was chosen for the computational portion of the study because it uses a well-known and well-proven numerical scheme and has shown favorable comparison with experiment at Mach numbers between 2 and 6. One advantage of CFD was that it provided flow field data for a detailed examination of the internal flow characteristics in addition to the surface properties. The experimental test matrix at Mach 10 included three geometric contraction ratios (3, 5, and 9), three Reynolds numbers (0.55×10^6 per foot, 1.14×10^6 per foot, and 2.15×10^6 per foot), and three cowl positions (at the throat and two forward positions). Computational data for two of these configurations (the contraction ratio of 3, $Re = 2.15 \times 10^6$ per foot, at two cowl positions) are presented along with a detailed analysis of the flow interactions in successive computational planes.

Author

N95-23257* Vigyan Research Associates, Inc., Hampton, VA.
PERFORMANCE OF THE 0.3-METER TRANSONIC CRYOGENIC TUNNEL WITH AIR, NITROGEN, AND SULFUR HEXAFLUORIDE MEDIA UNDER CLOSED LOOP AUTOMATIC CONTROL
 S. BALAKRISHNA and W. ALLEN KILGORE Jan. 1995 35 p
 (Contract(s)/Grant(s): NAS1-19672; RTOP 505-59-50-02)
 (NASA-CR-195052; NAS 1.26:195052) Avail: CASI HC A03/MF A01

The NASA Langley 0.3-m Transonic Cryogenic Tunnel was modified in 1994, to operate with any one of the three test gas media viz., air, cryogenic nitrogen gas, or sulfur hexafluoride gas. This document provides the initial test results with respect to the tunnel performance and tunnel control, as a part of the commissioning activities on the microcomputer based controller. The tunnel can provide precise and stable control of temperature to less than or equal to ± 0.3 K in the range 80-320 K in cyro mode or 300-320 K in air/SF6 mode, pressure to ± 0.01 psia in the range 15-88 psia and Mach number to ± 0.0015 in the range 0.150 to transonic Mach numbers up to 1.000. A new heat exchanger has been included in the tunnel circuit and is performing adequately. The tunnel airfoil testing benefits considerably by precise control of tunnel states and helps

in generating high quality aerodynamic test data from the 0.3-m TCT. Author

N95-23287* Illinois Univ., Chicago, IL.
HOLOGRAPHIC INTERFEROMETRIC TOMOGRAPHY FOR RECONSTRUCTING FLOW FIELDS Abstract Only
 SOYOUNG S. CHA In Hampton Univ., 1994 NASA-HU American Society for Engineering Education (ASEE) Summer Faculty Fellowship Program p 68 Dec. 1994
 Avail: CASI HC A01/MF A02

Holographic interferometric tomography is a technique for instantaneously capturing and quantitatively reconstructing three-dimensional flow fields. It has a very useful application potential for high-speed aerodynamics. However, three major challenging tasks need to be accomplished before its practical applications. First, fluid flows are mostly unsteady or at least non repeatable. Consequently, a means for instantaneously recording three-dimensional flow fields, that is, a simple holographic technique for simultaneously recording multi-directional projections, needs to be developed. Second, while holographic interferometry provides enormous data storage capabilities, expeditious data extraction from complicated interferograms is very important for timely near real-time applications. Third, unlike medical applications, flow tomography does not provide complete data sets but instead involves ill-posed reconstruction problems of incomplete projection and limited angular scanning. During this summer research period, new experimental techniques and corresponding hardware were developed and tested to address the above mentioned tasks. The first task was achieved by diffuser illumination. This concept allows instantaneous capture of many projections with a conventional setup for single-projection recording. For the second task, a phase-shifting technique was incorporated. This technique allows one to acquire multiple phase-stepped interferograms for a single projection and thus to extract phase information from intensity data almost at real-time. For the third task, the research that has been extensively conducted previously was utilized. In this research period, a complete experimental setup that provides the above three major capabilities was designed, built, and tested by integrating all the techniques. A simple laboratory experiment for simulating wind-tunnel testing was then conducted. A test flow was produced by employing a relatively simple device that generated a gravity-driven flow. The flow was then experimentally investigated to check the viability of the holographic interferometric tomographic technique before wind-tunnel application. Author

N95-23290* Rochester Univ., NY. Dept. of Imaging and Photographic Technology.
SCIENTIFIC AND TECHNICAL PHOTOGRAPHY AT NASA LANGLEY RESEARCH CENTER Abstract Only
 ANDREW DAVIDHAZY In Hampton Univ., 1994 NASA-HU American Society for Engineering Education (ASEE) Summer Faculty Fellowship Program Dec. 1994
 Avail: CASI HC A01/MF A02

As part of my assignment connected with the Scientific and Technical Photography & Lab (STPL) at the NASA Langley Research Center I conducted a series of interviews and observed the day to day operations of the STPL with the ultimate objective of becoming exposed first hand to a scientific and technical photo/imaging department for which my school prepares its graduates. I was also asked to share my observations with the staff in order that these comments and observations might assist the STPL to better serve its customers. Meetings with several individuals responsible for various wind tunnels and with a group that provides photo-optical instrumentation services at the Center gave me an overview of the services provided by the Lab and possible areas for development. In summary form these are some of the observations that resulted from the interviews and daily contact with the STPL facility. (1) The STPL is perceived as a valuable and almost indispensable service group within the organization. This comment was invariably made by everyone. Everyone also seemed to support the idea that the STPL continue to provide its current level of service and quality. (2) The STPL generally is not perceived to be a highly technically oriented

group but rather as a provider of high quality photographic illustration and documentation services. In spite of the importance and high marks assigned to the STPL there are several observations that merit consideration and evaluation for possible inclusion into the STPL's scope of expertise and future operating practices. (1) While the care and concern for artistic rendition of subjects is seen as laudable and sometimes valuable, the time that this often requires is seen as interfering with keeping the tunnels operating at maximum productivity. Tunnel managers would like to shorten down-time due to photography, have services available during evening hours and on short notice. It may be of interest to the STPL that tunnel managers are incorporating ever greater imaging capabilities in their facilities. To some extent this could mean a reduced demand for traditional photographic services. (2) The photographic archive is seen as a Center resource. Archiving of images, as well as data, is a matter of concern to the investigators. The early holdings of the Photographic Archives are quickly deteriorating. The relative inaccessibility of the material held in the archives is problematic. (3) In certain cases delivery or preparation of digital image files instead of, or along with, hardcopy is already being perceived by the STPL's customers as desirable. The STPL should make this option available, and the fact that it has, or will have this capability widely known. (4) The STPL needs to continue to provide expert advice and technical imaging support in terms of application information to users of traditional photographic and new electronic imaging systems. Cooperative demo projects might be undertaken to maintain or improve the capabilities of the Lab. (5) STPL personnel do not yet have significant electronic imaging or electronic communication skills and improvements in this is an area could potentially have a positive impact on the Center. (6) High speed photographic or imaging services are often mentioned by the STPL as being of primary importance to their mission but the lab supports very few projects calling for high speed imaging services. Much high speed equipment is in poor state of repair. It is interesting to note that when the operation of lasers, digital imaging or quantitative techniques are requested these are directed to another NASA department. Could joint activities be initiated to solve problems? (7). The STPL could acquire more technical assignments if examples of the areas where they possess expertise would be circulated around the center. The fact that the STPL owns high speed video capability could be 'advertised' among its customer base if there truly was an interest in building up a customer base in this area. The STPL could participate in events like TOPS as an exhibitor, as well as a documenter, of the event. Author

N95-23311* Arizona Univ., Tucson, AZ. Dept. of Aerospace and Mechanical Engineering.

RESIDUAL STRENGTH OF THIN PANELS WITH CRACKS

Abstract Only

ERDOGAN MADENCI In Hampton Univ., 1994 NASA-HU American Society for Engineering Education (ASEE) Summer Faculty Fellowship Program p 93 Dec. 1994

Avail: CASI HC A01/MF A02

The previous design philosophies involving safe life, fail-safe and damage tolerance concepts become inadequate for assuring the safety of aging aircraft structures. For example, the failure mechanism for the Aloha Airline accident involved the coalescence of undetected small cracks at the rivet holes causing a section of the fuselage to peel open during flight. Therefore, the fuselage structure should be designed to have sufficient residual strength under worst case crack configurations and in-flight load conditions. Residual strength is interpreted as the maximum load carrying capacity prior to unstable crack growth. Internal pressure and bending moment constitute the two major components of the external loads on the fuselage section during flight. Although the stiffeners in the form of stringers, frames and tear straps sustain part of the external loads, the significant portion of the load is taken up by the skin. In the presence of a large crack in the skin, the crack lips bulge out with considerable yielding; thus, the geometric and material nonlinearities must be included in the analysis for predicting residual strength. Also, these nonlinearities do not permit the decoupling of in-plane

and out-of-plane bending deformations. The failure criterion combining the concepts of absorbed specific energy and strain energy density addresses the aforementioned concerns. The critical absorbed specific energy (local toughness) for the material is determined from the global specimen response and deformation geometry based on the uniaxial tensile test data and detailed finite element modeling of the specimen response. The use of the local toughness and stress-strain response at the continuum level eliminates the size effect. With this critical parameter and stress-strain response, the finite element analysis of the component by using STAGS along with the application of this failure criterion provides the stable crack growth calculations for residual strength predictions. Author

N95-23377* National Aeronautics and Space Administration. Ames Research Center, Moffett Field, CA.

SYSTEM FOR DETERMINING AERODYNAMIC IMBALANCE Patent

GARY B. CHURCHILL, inventor (to NASA) and BENNY K. CHEUNG, inventor (to NASA) 4 Oct. 1994 7 p Filed 7 Aug. 1992 (NASA-CASE-ARC-11913-1; US-PATENT-5,352,090; US-PATENT-APPL-SN-926117; US-PATENT-CLASS-416-61; US-PATENT-CLASS-416-34; INT-PATENT-CLASS-B64C-1/100) Avail: US Patent and Trademark Office

A system is provided for determining tracking error in a propeller or rotor driven aircraft by determining differences in the aerodynamic loading on the propeller or rotor blades of the aircraft. The system includes a microphone disposed relative to the blades during the rotation thereof so as to receive separate pressure pulses produced by each of the blades during the passage thereof by the microphone. A low pass filter filters the output signal produced by the microphone, the low pass filter having an upper cut-off frequency set below the frequency at which the blades pass by the microphone. A sensor produces an output signal after each complete revolution of the blades, and a recording display device displays the outputs of the low pass filter and sensor so as to enable evaluation of the relative magnitudes of the pressure pulses produced by passage of the blades by the microphone during each complete revolution of the blades. Official Gazette of the U.S. Patent and Trademark Office

N95-23423*# Sverdrup Technology, Inc., Brook Park, OH. THREE-DIMENSIONAL NAVIER-STOKES ANALYSIS AND REDESIGN OF AN IMBEDDED BELLMOUTH NOZZLE IN A TURBINE CASCADE INLET SECTION

P. W. GIEL and J. R. SIRBAUGH In NASA. Marshall Space Flight Center, Eleventh Workshop for Computational Fluid Dynamic Applications in Rocket Propulsion p 1239-1257 Jul. 1993

Avail: CASI HC A03/MF A10

Verification of proposed turbopump blading performance will involve evaluation of candidate blades in cascade test facilities. It is necessary to be able to predict the flow fields within these cascades for the results to be applicable to actual engine environments. This work presents the results of a study to predict the flow field for the NASA Lewis Transonic Turbine Blade Cascade Facility, which is similar to those used to evaluate rocket propulsion turbines. A pitchwise nonuniform total pressure distribution was observed at the blade row leading edge plane. A CFD analysis was used to show that the cause of the flow nonuniformity was a pair of vortices that originated in an embedded bellmouth inlet. Further CFD analysis was used to verify that a redesigned inlet section resulted in a flow with acceptable uniformity. A computational analysis was chosen because physical accessibility to the inlet section was limited, and because a computational approach also allows one to examine design changes cheaper and more quickly than an experimental approach would. The PARC code, a general purpose, three-dimensional, Navier-Stokes code with multiblock solution capability, was chosen for the present study. Results are presented detailing the computational requirements needed to accurately predict flows of this nature. Calculations of the original geometry showed total pressure loss regions consistent in strength and in location to experimental measurements. An examination of the results shows that the distortions are caused by a pair of vortices that originate as

a result of the interaction of the flow with the imbedded bellmouth. Computations were performed for an inlet geometry which eliminated the imbedded bellmouth by bridging the region between it and the upstream wall. This analysis indicated that eliminating the imbedded bellmouth eliminates the troublesome pair of vortices, resulting in a flow with much greater pitchwise uniformity. Author

N95-23425*# MCAT Inst., Moffett Field, CA.

THREE-DIMENSIONAL UNSTEADY FLOW CALCULATIONS IN AN ADVANCED GAS GENERATOR TURBINE

AKIL A. RANGWALLA *In* NASA. Marshall Space Flight Center, Eleventh Workshop for Computational Fluid Dynamic Applications in Rocket Propulsion p 1287-1320 Jul. 1993

Avail: CASI HC A03/MF A10

This paper deals with the application of a three-dimensional, unsteady Navier-Stokes code for predicting the unsteady flow in a single stage of an advanced gas generator turbine. The numerical method solves the three-dimensional thin-layer Navier-Stokes equations, using a system of overlaid grids, which allow for relative motion between the rotor and stator airfoils. Results in the form of time averaged pressures and pressure amplitudes on the airfoil surfaces will be shown. In addition, instantaneous contours of pressure, Mach number, etc. will be presented in order to provide a greater understanding of the inviscid as well as the viscous aspects of the flowfield. Also, relevant secondary flow features such as cross-plane velocity vectors and total pressure contours will be presented. Prior work in two-dimensions has indicated that for the advanced designs, the unsteady interactions can play a significant role in turbine performance. These interactions affect not only the stage efficiency but can substantially alter the time-averaged features of the flow. This work is a natural extension of the work done in two-dimensions and hopes to address some of the issues raised by the two-dimensional calculations. These calculations are being performed as an integral part of an actual design process and demonstrate the value of unsteady rotor-stator interaction calculations in the design of turbomachines. Author

N95-23429*# Virginia Polytechnic Inst. and State Univ., Blacksburg, VA. Dept. of Mechanical Engineering.

SUPERSONIC FLOW AND SHOCK FORMATION IN TURBINE TIP GAPS

JOHN MOORE *In* NASA. Marshall Space Flight Center, Eleventh Workshop for Computational Fluid Dynamic Applications in Rocket Propulsion p 1423-1433 Jul. 1993

Avail: CASI HC A03/MF A10

Shock formation due to overexpansion of supersonic flow at the inlet to the tip clearance gap of a turbomachine has been studied. As the flow enters the tip gap, it accelerates around the blade pressure-side corner creating a region of minimum static pressure. The 'free streamline' separates from the wall at the corner; and, for Mach numbers greater than about 1.3, it curves back to intersect the blade tip. At this point, the freestream flow is abruptly turned parallel to the surface, giving rise to an oblique shock. The results are consistent with compressible sharp-edged orifice flow calculations found in the literature and with the theory of oblique shock wave formation in supersonic flow over a wedge. For freestream Mach numbers of 1.4 to 1.8, wave angles are 43 to 54 deg, and turning angles are 9 to 20 deg; as the Mach number increases, the angle of turn also increases. It appears that in a turbine, after separating from the inlet corner, the flow reattaches on the blade tip and an oblique shock is formed at 0.4-1.4 tip gap heights into the clearance gap. The resulting shock-boundary layer interaction may contribute to further enhancement of already high heat transfer to the blade tip in this region. This in turn could lead to higher blade temperatures and adversely affect blade life and turbine efficiency. Author

N95-23435*# Pratt and Whitney Aircraft, West Palm Beach, FL. **AERODYNAMIC DESIGN AND ANALYSIS OF A HIGHLY LOADED TURBINE EXHAUST**

F. W. HUBER, X. A. MONTESDEOCA, and R. J. ROWEY *In* NASA. Marshall Space Flight Center, Eleventh Workshop for Computa-

tional Fluid Dynamic Applications in Rocket Propulsion p 1535-1553 Jul. 1993

Avail: CASI HC A03/MF A10

The aerodynamic design and analysis of a turbine exhaust volute manifold is described. This turbine exhaust system will be used with an advanced gas generator oxidizer turbine designed for very high specific work. The elevated turbine stage loading results in increased discharge Mach number and swirl velocity which, along with the need for minimal circumferential variation of fluid properties at the turbine exit, represent challenging volute design requirements. The design approach, candidate geometries analyzed, and steady state/unsteady CFD analysis results are presented. Author

N95-23436*# Rockwell International Corp., Canoga Park, CA. Rocketdyne Div.

CFD ANALYSIS OF TURBOPUMP VOLUTES

EDWARD P. ASCOLI, DANIEL C. CHAN, ARMEN DARIAN, WAYNE W. HSU, and KEN TRAN *In* NASA. Marshall Space Flight Center, Eleventh Workshop for Computational Fluid Dynamic Applications in Rocket Propulsion p 1555-1578 Jul. 1993

Avail: CASI HC A03/MF A10

An effort is underway to develop a procedure for the regular use of CFD analysis in the design of turbopump volutes. Airflow data to be taken at NASA Marshall will be used to validate the CFD code and overall procedure. Initial focus has been on preprocessing (geometry creation, translation, and grid generation). Volute geometries have been acquired electronically and imported into the CATIA CAD system and RAGGS (Rockwell Automated Grid Generation System) via the IGES standard. An initial grid topology has been identified and grids have been constructed for turbine inlet and discharge volutes. For CFD analysis of volutes to be used regularly, a procedure must be defined to meet engineering design needs in a timely manner. Thus, a compromise must be established between making geometric approximations, the selection of grid topologies, and possible CFD code enhancements. While the initial grid developed approximated the volute tongue with a zero thickness, final computations should more accurately account for the geometry in this region. Additionally, grid topologies will be explored to minimize skewness and high aspect ratio cells that can affect solution accuracy and slow code convergence. Finally, as appropriate, code modifications will be made to allow for new grid topologies in an effort to expedite the overall CFD analysis process. Author

N95-23438*# Pratt and Whitney Aircraft, West Palm Beach, FL.

PHASE 2: HGM AIR FLOW TESTS IN SUPPORT OF HEX VANE INVESTIGATION

G. B. COX, JR., L. L. STEELE, and D. W. EISENHART *In* NASA. Marshall Space Flight Center, Eleventh Workshop for Computational Fluid Dynamic Applications in Rocket Propulsion p 1607-1618 Jul. 1993

(Contract(s)/Grant(s): NAS8-36801)

Avail: CASI HC A03/MF A10

Following the start of SSME certification testing for the Pratt and Whitney Alternate Turbopump Development (ATD) High Pressure Oxidizer Turbopump (HPOTP), cracking of the leading edge of the inner HEX vane was experienced. The HEX vane, at the inlet of the oxidizer bowl in the Hot Gas Manifold (HGM), accepts the HPOTP turbine discharge flow and turns it toward the Gaseous Oxidizer Heat Exchanger (GOX HEX) coil. The cracking consistently initiated over a specific circumferential region of the hex vane, with other circumferential locations appearing with increased run time. Since cracking had not to date been seen with the baseline HPOTP, a fluid-structural interaction involving the ATD HPOTP turbine exit flowfield and the HEX inner vane was suspected. As part of NASA contract NAS8-36801, Pratt and Whitney conducted air flow tests of the ATD HPOTP turbine turnaround duct flowpath in the MSFC Phase 2 HGM air flow model. These tests included HEX vane strain gages and additional fluctuating pressure gages in the turnaround duct and HEX vane flowpath area. Three-dimensional flow probe measurements at two stations downstream of the turbine simulator exit plane were also made. Modifications to the HPOTP turbine

simulator investigated the effects on turbine exit flow profile and velocity components, with the objective of reproducing flow conditions calculated for the actual ATD HPOTP hardware. Testing was done at the MSFC SSME Dynamic Fluid Air Flow (Dual-Leg) Facility, at air supply pressures between 50 and 250 psia. Combinations of turbine exit Mach number and pressure level were run to investigate the effect of flow regime. Information presented includes: (1) Descriptions of turbine simulator modifications to produce the desired flow environment; (2) Types and locations for instrumentation added to the flow model for improved diagnostic capability; (3) Evaluation of the effect of changes to the turbine simulator flowpath on the turbine exit flow environment; and (4) Comparison of the experimental turbine exit flow environment to the environment calculated for the ATD HPOTP.

Author

N95-23440* Rockwell International Corp., Canoga Park, CA. Rocketdyne Div.

IMPELLER FLOW FIELD CHARACTERIZATION WITH A LASER TWO-FOCUS VELOCIMETER

L. A. BROZOWSKI, T. V. FERGUSON, and L. ROJAS *In NASA, Marshall Space Flight Center, Eleventh Workshop for Computational Fluid Dynamic Applications in Rocket Propulsion p 1635-1688 Jul. 1993*

(Contract(s)/Grant(s): NAS8-38864)

Avail: CASI HC A04/MF A10

Use of Computational Fluid Dynamics (CFD) codes, prevalent in the rocket engine turbomachinery industry, necessitates data of sufficient quality and quantity to benchmark computational codes. Existing data bases for typical rocket engine configurations, in particular impellers, are limited. In addition, traditional data acquisition methods have several limitations: typically transducer uncertainties are 0.5% of transducer full scale and traditional pressure probes are unable to provide flow characteristics in the circumferential (blade-to-blade) direction. Laser velocimetry circumvents these limitations by providing +0.5% uncertainty in flow velocity and +0.5% uncertainty in flow angle. The percent of uncertainty in flow velocity is based on the measured value, not full range capability. The laser electronics multiple partitioning capability allows data acquired between blades as the impeller rotates, to be analyzed separately, thus providing blade-to-blade flow characterization. Unlike some probes, the non-intrusive measurements made with the laser velocimeter does not disturb the flow. To this end, and under Contract (NAS8-38864) to the National Aeronautics and Space Administration (NASA) at Marshall Space Flight Center (MSFC), an extensive test program was undertaken at Rocketdyne. Impellers from two different generic rocket engine pump configurations were examined. The impellers represent different spectrums of pump design: the Space Shuttle Main Engine (SSME) high pressure fuel turbopump (HPFTP) impeller was designed in the 1970's the Consortium for CFD application in Propulsion Technology Pump Stage Technology Team (Pump Consortium) optimized impeller was designed with the aid of modern computing techniques. The tester configuration for each of the impellers consisted of an axial inlet, an inducer, a diffuser, and a crossover discharge. While the tested configurations were carefully chosen to be representative of generic rocket engine pumps, several features of both testers were intentionally atypical. A crossover discharge, downstream of the impeller, rather than a volute discharge was used to minimize asymmetric flow conditions that might be reflected in the impeller discharge flow data. Impeller shroud wear ring radial clearances were purposely close to minimize leakage flow, thus increasing confidence in using the inlet data as an input to CFD programs. The empirical study extensively examined the flow fields of the two impellers via performance of laser two-focus velocimeter surveys in an axial plane upstream of the impellers and in multiple radial planes downstream of the impellers. Both studies were performed at the impeller design flow coefficients. Inlet laser surveys that provide CFD code inlet boundary conditions were performed in one axial plane, with ten radial locations surveyed. Three wall static pressures, positioned circumferentially around the impeller inlet, were used to identify asymmetrical pressure distribu-

tions in the inlet survey plane. The impeller discharge flow characterization consisted of three radial planes for the SSME HPFTP impeller and two radial planes for the Pump Consortium optimized impeller. Housing wall static pressures were placed to correspond to the radial locations surveyed with the laser velocimeter. Between five and thirteen axial stations across the discharge channel width were examined in each radial plane during the extensive flow mapping. The largely successful empirical flow characterization of two different impellers resulted in a substantial contribution to the limited existing data base, and yielded accurate data for CFD code benchmarking.

Author

N95-23444* Pennsylvania State Univ., University Park, PA. Dept. of Aerospace Engineering.

NUMERICAL COMPUTATION OF AERODYNAMICS AND HEAT TRANSFER IN A TURBINE CASCADE AND A TURN-AROUND DUCT USING ADVANCED TURBULENCE MODELS

B. LAKSHMINARAYANA and J. LUO *In NASA, Marshall Space Flight Center, Eleventh Workshop for Computational Fluid Dynamic Applications in Rocket Propulsion p 1773-1806 Jul. 1993*

Avail: CASI HC A03/MF A10

The objective of this research is to develop turbulence models to predict the flow and heat transfer fields dominated by the curvature effect such as those encountered in turbine cascades and turn-around ducts. A Navier-Stokes code has been developed using an explicit Runge-Kutta method with a two layer k-epsilon/ARSM (Algebraic Reynolds Stress Model), Chien's Low Reynolds Number (LRN) k-epsilon model and Coakley's LRN q-omega model. The near wall pressure strain correlation term was included in the ARSM. The formulation is applied to Favre-averaged N-S equations and no thin-layer approximations are made in either the mean flow or turbulence transport equations. Anisotropic scaling of artificial dissipation terms was used. Locally variable timestep was also used to improve convergence. Detailed comparisons were made between computations and data measured in a turbine cascade by Arts et al. at Von Karman Institute. The surface pressure distributions and wake profiles were predicted well by all the models. The blade heat transfer is predicted well by k-epsilon/ARSM model, as well as the k-epsilon model. It's found that the onset of boundary layer transition on both surfaces is highly dependent upon the level of local freestream turbulence intensity, which is strongly influenced by the streamline curvature. Detailed computation of the flow in the turn around duct has been carried out and validated against the data by Monson as well as Sandborn. The computed results at various streamwise locations both on the concave and convex sides are compared with flow and turbulence data including the separation zone on the inner wall. The k-epsilon/ARSM model yielded relatively better results than the two-equation turbulence models. A detailed assessment of the turbulence models has been made with regard to their applicability to curved flows.

Author

N95-23446* Pennsylvania State Univ., University Park, PA. Propulsion Engineering Research Center.

CONVERGENCE ACCELERATION OF IMPLICIT SCHEMES IN THE PRESENCE OF HIGH ASPECT RATIO GRID CELLS

B. E. O. BUELOW, S. VENKATESWARAN, and C. L. MERKLE *In NASA, Marshall Space Flight Center, Eleventh Workshop for Computational Fluid Dynamic Applications in Rocket Propulsion p 1829-1855 Jul. 1993*

Avail: CASI HC A03/MF A10

The performance of Navier-Stokes codes are influenced by several phenomena. For example, the robustness of the code may be compromised by the lack of grid resolution, by a need for more precise initial conditions or because all or part of the flowfield lies outside the flow regime in which the algorithm converges efficiently. A primary example of the latter effect is the presence of extended low Mach number and/or low Reynolds number regions which cause convergence deterioration of time marching algorithms. Recent research into this problem by several workers including the present authors has largely negated this difficulty through the introduction of

time-derivative preconditioning. In the present paper, we employ the preconditioned algorithm to address convergence difficulties arising from sensitivity to grid stretching and high aspect ratio grid cells. Strong grid stretching is particularly characteristic of turbulent flow calculations where the grid must be refined very tightly in the dimension normal to the wall, without a similar refinement in the tangential direction. High aspect ratio grid cells also arise in problems that involve high aspect ratio domains such as combustor coolant channels. In both situations, the high aspect ratio cells can lead to extreme deterioration in convergence. It is the purpose of the present paper to address the reasons for this adverse response to grid stretching and to suggest methods for enhancing convergence under such circumstances. Numerical algorithms typically possess a maximum allowable or optimum value for the time step size, expressed in non-dimensional terms as a CFL number or vonNeumann number (VNN). In the presence of high aspect ratio cells, the smallest dimension of the grid cell controls the time step size causing it to be extremely small, which in turn results in the deterioration of convergence behavior. For explicit schemes, this time step limitation cannot be exceeded without violating stability restrictions of the scheme. On the other hand, for implicit schemes, which are typically unconditionally stable, there appears to be room for improvement through careful tailoring of the time step definition based on results of linear stability analyses. In the present paper, we focus on the central-differenced alternating direction implicit (ADI) scheme. The understanding garnered from this analyses can then be applied to other implicit schemes. In order to systematically study the effects of aspect ratio and the methods of mitigating the associated problems, we use a two pronged approach. We use stability analyses as a tool for predicting numerical convergence behavior and numerical experiments on simple model problems to verify predicted trends. Based on these analyses, we determine that efficient convergence may be obtained at all aspect ratios by getting a combination of things right. Primary among these are the proper definition of the time step size, proper selection of viscous preconditioner and the precise treatment of boundary conditions. These algorithmic improvements are then applied to a variety of test cases to demonstrate uniform convergence at all aspect ratios.

Author

N95-23447* National Aeronautics and Space Administration. Lewis Research Center, Cleveland, OH.

A TIME-ACCURATE FINITE VOLUME METHOD VALID AT ALL FLOW VELOCITIES

S.-W. KIM In NASA. Marshall Space Flight Center, Eleventh Workshop for Computational Fluid Dynamic Applications in Rocket Propulsion p 1857-1887 Jul. 1993
 Avail: CASI HC A03/MF A10

A finite volume method to solve the Navier-Stokes equations at all flow velocities (e.g., incompressible, subsonic, transonic, supersonic and hypersonic flows) is presented. The numerical method is based on a finite volume method that incorporates a pressure-staggered mesh and an incremental pressure equation for the conservation of mass. Comparison of three generally accepted time-advancing schemes, i.e., Simplified Marker-and-Cell (SMAC), Pressure-Implicit-Splitting of Operators (PISO), and Iterative-Time-Advancing (ITA) scheme, are made by solving a lid-driven polar cavity flow and self-sustained oscillatory flows over circular and square cylinders. Calculated results show that the ITA is the most stable numerically and yields the most accurate results. The SMAC is the most efficient computationally and is as stable as the ITA. It is shown that the PISO is the most weakly convergent and it exhibits an undesirable strong dependence on the time-step size. The degenerated numerical results obtained using the PISO are attributed to its second corrector step that cause the numerical results to deviate further from a divergence free velocity field. The accurate numerical results obtained using the ITA is attributed to its capability to resolve the nonlinearity of the Navier-Stokes equations. The present numerical method that incorporates the ITA is used to solve an unsteady transitional flow over an oscillating airfoil and a chemically reacting flow of hydrogen in a vitiated supersonic airstream.

The turbulence fields in these flow cases are described using multiple-time-scale turbulence equations. For the unsteady transitional over an oscillating airfoil, the fluid flow is described using ensemble-averaged Navier-Stokes equations defined on the Lagrangian-Eulerian coordinates. It is shown that the numerical method successfully predicts the large dynamic stall vortex (DSV) and the trailing edge vortex (TEV) that are periodically generated by the oscillating airfoil. The calculated streaklines are in very good comparison with the experimentally obtained smoke picture. The calculated turbulent viscosity contours show that the transition from laminar to turbulent state and the relaminarization occur widely in space as well as in time. The ensemble-averaged velocity profiles are also in good agreement with the measured data and the good comparison indicates that the numerical method as well as the multiple-time-scale turbulence equations successfully predict the unsteady transitional turbulence field. The chemical reactions for the hydrogen in the vitiated supersonic airstream are described using 9 chemical species and 48 reaction-steps. Consider that a fast chemistry can not be used to describe the fine details (such as the instability) of chemically reacting flows while a reduced chemical kinetics can not be used confidently due to the uncertainty contained in the reaction mechanisms. However, the use of a detailed finite rate chemistry may make it difficult to obtain a fully converged solution due to the coupling between the large number of flow, turbulence, and chemical equations. The numerical results obtained in the present study are in good agreement with the measured data. The good comparison is attributed to the numerical method that can yield strongly converged results for the reacting flow and to the use of the multiple-time-scale turbulence equations that can accurately describe the mixing of the fuel and the oxidant.

Author

N95-23466* Institute for Computer Applications in Science and Engineering, Hampton, VA.

A STUDY OF THE VORTEX FLOW OVER 76/40-DEG DOUBLE-DELTA WING Final Report

N. G. VERHAAGEN (Technische Hogeschool, Delft, Netherlands.), L. N. JENKINS (National Aeronautics and Space Administration. Langley Research Center, Hampton, VA.), S. B. KERN (Naval Air Warfare Center, Warminster, PA.), and A. E. WASHBURN (Vigyan Research Associates, Inc., Hampton, VA.) NASA Feb. 1995 34 p (Contract(s)/Grant(s): NAS1-19480; RTOP 505-90-52-01) (NASA-CR-195032; NAS 1.26:195032; ICASE-95-5; AIAA PAPER 95-0560) Avail: CASI HC A03/MF A01

A low-speed wind-tunnel study of the flow about a 76/40-deg double-delta wing is described for angles of attack ranging from -10 to 25 deg and Reynolds numbers ranging from 0.5 to 1.5 Million. The study was conducted to provide data for the purpose of understanding the vortical flow behavior and for validating Computational Fluid Dynamics methods. Flow visualization tests have provided insight into the effect of the angle of attack and Reynolds number of the vortex-dominated flow both on and off of the surface of the double-delta wing. Upper surface pressure recordings from pressure orifices and Pressure Sensitive Paint have provided data on the pressures induced by the vortices. Flowfield surveys were carried out at an angle of attack of 10 deg by using a thin 5-hole probe. Numerical solutions of the compressible thin-layer Navier-Stokes equations were conducted and compared to the experimental data.

Author

N95-23505# Defence Research Agency, Farnborough, Hampshire (England). Structural Materials Centre.

NON-DESTRUCTIVE DETECTION OF CORROSION FOR LIFE MANAGEMENT

DAVID A. BRUCE In AGARD, Corrosion Detection and Management of Advanced Airframe Materials 8 p Jan. 1995
 Copyright Avail: CASI HC A02/MF A03

In recent years, aircraft operators have been driven to increased use of Non-Destructive Evaluation (NDE) to ensure airworthiness during life extensions for ageing aircraft or as an integral part of a damage tolerant lifting philosophy. Major airframe static and fatigue tests are routinely used to highlight problem areas on

airframes where design limitations or changes of usage may lead to early failures. The results of such tests become progressively less reliable as the age of the airframe increases and the operating conditions diverge from those under which the tests were conducted. Increased inspection, whether by visual or other means is usually the only alternative to wholesale refurbishment or replacement of aircraft or components. Almost all of the development to date of NDE techniques for corrosion detection and characterization has been concentrated on existing airframe materials, principally Aluminum alloys and steels. The current capabilities of corrosion detection techniques will be reviewed and current research aimed at areas where there is a requirement for improved detection capability will be described. New materials, such as Polymer Matrix Composites, will experience different types of 'corrosive' deterioration. The capability of NDE methods to detect material degradation in new composite materials will be discussed. Finally, reliance on NDE, choice of NDE technique and optimal scheduling of inspections all require an assessment of the reliability of NDE methods. It will be shown that a range of NDE techniques with differing capabilities and characteristics will be required to ensure compatibility with maintenance schedules if full use is to be made of NDE for life management of structures which may be subject to corrosion. Author

N95-23507# National Aerospace Lab., Amsterdam (Netherlands). EDDY CURRENT DETECTION OF PITTING CORROSION AROUND FASTENER HOLES

J. H. HEIDA and W. G. J. THART *In* AGARD, Corrosion Detection and Management of Advanced Airframe Materials 10 p Jan. 1995 Sponsored by Royal Netherlands Air Force Copyright Avail: CASI HC A02/MF A03

An evaluation of the eddy current technique for the detection and depth assessment of corrosion around fastener holes in F-16 lower wing skins is described. The corrosion type in this structure is pitting corrosion at the countersink edge of the fastener holes. Due to a corrosion clean-up limit of only 1.5 - 2.5 percent, a maximum thickness reduction in the range of 0.08 - 0.32 mm is allowed (depending on local skin thickness). This specifies the needed sensitivity for in-service corrosion inspection. In the evaluation use was made of specimens cut out of the F-16 lower wing skin structure. In total twelve specimens were exposed to an accelerated corrosion test (EXCO-test). Eddy current inspection of the specimens with installed fasteners was performed with a standard eddy scope and four different eddy current probes. After the eddy current inspection cross-sections of the twelve-specimens were made to determine the extent of pitting corrosion at the countersink edges. After evaluation of the inspection results the following conclusions can be drawn: for in-service detection of countersink edge corrosion standard visual inspection is the preferred technique regarding the simplicity, sensitivity and reliability of inspection; and for the purpose of depth assessment the eddy current technique is capable of detecting countersink edge corrosion with a depth from about 0.1 mm. Due to the corrosion clean-up limit of only 1.5 - 2.5 percent (0.08 - 0.32 mm), however, the eddy current technique is considered not applicable for in-service depth assessment of countersink edge corrosion in F-16 lower wing skins. Author

N95-23512# National Aeronautics and Space Administration. Langley Research Center, Hampton, VA.

NEW NONDESTRUCTIVE TECHNIQUES FOR THE DETECTION AND QUANTIFICATION OF CORROSION IN AIRCRAFT STRUCTURES

W. P. WINFREE, K. E. CRAMER, P. H. JOHNSTON, and M. NAMKUNG *In* AGARD, Corrosion Detection and Management of Advanced Airframe Materials 6 p Jan. 1995 Copyright Avail: CASI HC A02/MF A03

An overview is presented of several techniques under development at NASA Langley Research Center for detection and quantification of corrosion in aircraft structures. The techniques have been developed as part of the NASA Airframe Structural Integrity Program. The techniques focus on the detection of subsurface corrosion in thin laminated structures. Results are presented on specimens

with both manufactured defects, for calibration of the techniques, and on specimens removed from aircraft. Author

N95-23602# Advisory Group for Aeronautical Research and Development, Oxford (England). Structures and Materials Panel. POD ASSESSMENT OF NDI PROCEDURES USING A ROUND ROBIN TEST [LES TESTS COMPARATIFS INTER-LABORATOIRES POUR L'EVALUATION DE LA PROBABILITE DE DETECTION (POD) DES PROCEDURES NDI]

Jan. 1995 40 p (AGARD-R-809; ISBN-92-836-1010-5) Copyright Avail: CASI HC A03/MF A01

Under the auspices of the AGARD Structures and Materials Panel R&D Cooperation Program, a round-robin NDI demonstration has been carried out. Six laboratories in four NATO countries participated in the project. The aim of the project was to determine the sensitivity and reliability of NDI procedures presently employed by the participating laboratories and to establish whether or not the procedures would be adequate for the implementation of a damage-tolerance based maintenance approach or whether improved methods are required. Author

N95-23630*# Pennsylvania State Univ., State College, PA. Propulsion Engineering Research Center.

CAVITATION MODELING IN EULER AND NAVIER-STOKES CODES

MANISH DESHPANDE, JINZHANG FENG, and CHARLES L. MERKLE *In* NASA. Marshall Space Flight Center, Eleventh Workshop for Computational Fluid Dynamic Applications in Rocket Propulsion, Part 1 p 377-401 Jul. 1993 Avail: CASI HC A03/MF A10

Many previous researchers have modeled sheet cavitation by means of a constant pressure solution in the cavity region coupled with a velocity potential formulation for the outer flow. The present paper discusses the issues involved in extending these cavitation models to Euler or Navier-Stokes codes. The approach taken is to start from a velocity potential model to ensure our results are compatible with those of previous researchers and available experimental data, and then to implement this model in both Euler and Navier-Stokes codes. The model is then augmented in the Navier-Stokes code by the inclusion of the energy equation which allows the effect of subcooling in the vicinity of the cavity interface to be modeled to take into account the experimentally observed reduction in cavity pressures that occurs in cryogenic fluids such as liquid hydrogen. Although our goal is to assess the practicality of implementing these cavitation models in existing three-dimensional, turbomachinery codes, the emphasis in the present paper will center on two-dimensional computations, most specifically isolated airfoils and cascades. Comparisons between velocity potential, Euler and Navier-Stokes implementations indicate they all produce consistent predictions. Comparisons with experimental results also indicate that the predictions are qualitatively correct and give a reasonable first estimate of sheet cavitation effects in both cryogenic and non-cryogenic fluids. The impact on CPU time and the code modifications required suggests that these models are appropriate for incorporation in current generation turbomachinery codes. Author

N95-23652*# National Aeronautics and Space Administration. Marshall Space Flight Center, Huntsville, AL.

VALIDATION OF A COMPUTATIONAL FLUID DYNAMICS (CFD) CODE FOR SUPERSONIC AXISYMMETRIC BASE FLOW

P. KEVIN TUCKER *In* its Eleventh Workshop for Computational Fluid Dynamic Applications in Rocket Propulsion, Part 1 p 879-901 Jul. 1993

Avail: CASI HC A03/MF A10

The ability to accurately and efficiently calculate the flow structure in the base region of bodies of revolution in supersonic flight is a significant step in CFD code validation for applications ranging from base heating for rockets to drag for protectives. The FDNS code is used to compute such a flow and the results are

12 ENGINEERING

compared to benchmark quality experimental data. Flowfield calculations are presented for a cylindrical afterbody at $M = 2.46$ and angle of attack $\alpha = 0$. Grid independent solutions are compared to mean velocity profiles in the separated wake area and downstream of the reattachment point. Additionally, quantities such as turbulent kinetic energy and shear layer growth rates are compared to the data. Finally, the computed base pressures are compared to the measured values. An effort is made to elucidate the role of turbulence models in the flowfield predictions. The level of turbulent eddy viscosity, and its origin, are used to contrast the various turbulence models and compare the results to the experimental data. Author

N95-23662# Technion - Israel Inst. of Tech., Haifa (Israel). Faculty of Aerospace Engineering.

REVIEW OF SOME RESULTS OF THE AUTHOR'S FATIGUE INVESTIGATIONS WITH APPLICATIONS IN ENGINEERING AND MATERIAL SCIENCE

A. BUCH Apr. 1994 61 p

(TAE-698) Avail: CASI HC A04/MF A01

This document deals with research results mainly connected with the problem of fatigue calculations and various aspects of fatigue. It contains the following topics: Correlation between fatigue limits and ultimate tensile strength, Fatigue properties of pure metals, Analytical approach to notch-size effects in fatigue of aircraft sheet materials, Torsional fatigue life of axle shafts under program loading, Fatigue properties of aircraft lugs with interference fit, Comparison of various aircraft loading test results with the aid of Relative-Miner-Rule, The Relative Method in the case of Local-Strain-Approach, and Prediction of fatigue life. CASI

N95-23670# Clemson Univ., SC. Radar Systems Lab.

MAXIMUM-LIKELIHOOD SPECTRAL ESTIMATION AND ADAPTIVE FILTERING TECHNIQUES WITH APPLICATION TO AIRBORNE DOPPLER WEATHER RADAR Thesis Technical Report No. 20

JONATHAN Y. LAI 28 Nov. 1994 88 p

(Contract(s)/Grant(s): NAG1-928)

(NASA-CR-197699; NAS 1.26:197699; TR-112894-3570P) Avail: CASI HC A05/MF A01

This dissertation focuses on the signal processing problems associated with the detection of hazardous windshears using airborne Doppler radar when weak weather returns are in the presence of strong clutter returns. In light of the frequent inadequacy of spectral-processing oriented clutter suppression methods, we model a clutter signal as multiple sinusoids plus Gaussian noise, and propose adaptive filtering approaches that better capture the temporal characteristics of the signal process. This idea leads to two research topics in signal processing: (1) signal modeling and parameter estimation, and (2) adaptive filtering in this particular signal environment. A high-resolution, low SNR threshold maximum likelihood (ML) frequency estimation and signal modeling algorithm is devised and proves capable of delineating both the spectral and temporal nature of the clutter return. Furthermore, the Least Mean Square (LMS)-based adaptive filter's performance for the proposed signal model is investigated, and promising simulation results have testified to its potential for clutter rejection leading to more accurate estimation of windspeed thus obtaining a better assessment of the windshear hazard. Author

N95-23792# Technology Integration and Development Group, Inc., Bedford, MA.

GEARBOX VIBRATION DIAGNOSTIC ANALYZER Final Report

Cleveland, OH NASA Apr. 1992 19 p

(Contract(s)/Grant(s): NAS3-26134; RTOP 505-63-36)

(NASA-CR-189141; E-9589; NAS 1.26:189141; TII-R9201-001-RD)

Avail: CASI HC A03/MF A01

This report describes the Gearbox Vibration Diagnostic Analyzer installed in the NASA Lewis Research Center's 500 HP Helicopter Transmission Test Stand to monitor gearbox testing. The vibration of the gearbox is analyzed using diagnostic algorithms to calculate a parameter indicating damaged components. Author

N95-24189# Toledo Univ., OH. Dept. of Mechanical Engineering.

USER'S GUIDE FOR ECAP2D: AN EULER UNSTEADY AERODYNAMIC AND AEROELASTIC ANALYSIS PROGRAM FOR TWO DIMENSIONAL OSCILLATING CASCADES, VERSION 1.0

T. S. R. REDDY Cleveland, OH NASA Apr. 1995 71 p

(Contract(s)/Grant(s): NAG3-1137; RTOP 538-06-13)

(NASA-CR-189146; E-9552; NAS 1.26:189146) Avail: CASI HC A04/MF A01

This guide describes the input data required for using ECAP2D (Euler Cascade Aeroelastic Program-Two Dimensional). ECAP2D can be used for steady or unsteady aerodynamic and aeroelastic analysis of two dimensional cascades. Euler equations are used to obtain aerodynamic forces. The structural dynamic equations are written for a rigid typical section undergoing pitching (torsion) and plunging (bending) motion. The solution methods include harmonic oscillation method, influence coefficient method, pulse response method, and time integration method. For harmonic oscillation method, example inputs and outputs are provided for pitching motion and plunging motion. For the rest of the methods, input and output for pitching motion only are given. Author

13

GEOSCIENCES

Includes geosciences (general); earth resources; energy production and conversion; environment pollution; geophysics; meteorology and climatology; and oceanography.

A95-73517

PILOT WEATHER ADVISOR SYSTEM

SHASHI SETH VIGYAN, Inc, Hampton, VA, United States and NORMAN L. CRABILL Journal of Aircraft (ISSN 0021-8669) vol. 31, no. 6 November-December 1994 p. 1240-1243 refs

(BTN-95-EIX95152582314) Copyright

We are currently developing a system called the Pilot Weather Advisor, which will shortly provide pilots with graphical weather depictions using color laptop computers, and eventually will be a part of an advanced technology flight management system. Through the use of broadcast satellite communications the PWxA system provides near real-time graphic depictions of weather information in the cockpit of aircraft in flight. The purpose of this system is to improve the safety and utility of general aviation and commercial aircraft operations. The concept of providing pilots with graphic depictions of weather conditions, overlaid on maps with geographical and navigational information, is extremely powerful. We have demonstrated the feasibility of using satellite communications to provide significant amounts of weather data to aircraft in flight. We have also demonstrated the usefulness of providing weather data in graphic form which increases efficiency and decreases pilot workload.

Author (EI)

A95-73521

POLAR PATROL BALLOON

JUN NISHIMURA Inst of Space and Astronautical Science, Tokyo, Japan, NOBUYUKI YAJIMA, HIROMITSU AKIYAMA, and S. KOKUBUN Journal of Aircraft (ISSN 0021-8669) vol. 31, no. 6 November-December 1994 p. 1264-1267 refs

(BTN-95-EIX95152582318) Copyright

From late December of 1990 to early January of 1991, the National Institute of Polar Research, in collaboration with the Institute of Space and Astronautical Science, launched two large zero-pressure balloons from Syowa Station, which is the Japanese research base in Antarctica. The balloon launched on December 25 returned near Syowa Station after 15 days of flight, keeping a constant altitude of about 30 km. It finally accomplished almost a one and half circumpolar flight. The total flight duration was about 40

days. This article will describe the balloon system and the flight behavior of the balloon.

Author (EI)

A95-75031* National Aeronautics and Space Administration. Goddard Space Flight Center, Greenbelt, MD.
TRAJECTORY MODELING OF EMISSIONS FROM LOWER STRATOSPHERIC AIRCRAFT

LYNN C. SPARLING Hughes STX, Lanham, MD, US, MARK R. SCHOEBERL NASA. Goddard Space Flight Center, Greenbelt, MD, US, ANNE R. DOUGLASS NASA. Goddard Space Flight Center, Greenbelt, MD, US, CLARK J. WEAVER Applied Research Corporation, Landover, MD, US, PAUL A. NEWMAN NASA. Goddard Space Flight Center, Greenbelt, MD, US, and LESLIE R. LAIT Hughes STX, Lanham, MD, US Journal of Geophysical Research (ISSN 0148-0227) vol. 100, no. D1 January 20, 1995 p. 1427-1438 (HTN-95-41219) Copyright

A series of isentropic trajectory calculations has been performed for emissions by stratospheric aircraft moving across the northern midlatitude oceanic flight corridors. Emission of exhaust is simulated by the daily initialization of air parcels along a flight path on the 500 K isentropic surface. Parcels are tracked during the first three weeks of each January from 1980 to 1994 in order to determine the interannual variability in the spatial distribution of the exhaust and the likelihood of exposure to cold temperatures. Few parcels emitted along these flight paths at this time of year had experienced nitric acid trihydrate (NAT) formation temperatures, except for the particularly cold Januaries 1986, 1987, and 1992. Large zonal fluctuations in the distribution of the emissions are typical for this time year and are strongly dependent on flight path. An extended 6-month (January-June) run in which parcels were released daily along the New York-London route shows that emissions in the flight corridor increase at a time-averaged rate which is nearly twice the rate at which the zonal average increases. In addition, local fluctuations of pollutant density can be several times higher than the zonal average and can persist for several weeks. A rapid buildup of emissions occurred during the summer months. These elevated emission levels must be considered in the interpretation of environmental impact assessments based on two-dimensional transport models.

Author (Herner)

A95-75035
THUNDERCLOUD ELECTRIC FIELD MODELING FOR THE IONOSPHERE-EARTH REGION. 1: DEPENDENCE ON CLOUD CHARGE DISTRIBUTION

PETER I. Y. VELINOV Bulgarian Academy of Sciences, Sofia, Bulgaria and PETER T. TONEV Bulgarian Academy of Sciences, Sofia, Bulgaria Journal of Geophysical Research (ISSN 0148-0227) vol. 100, no. D1 January 20, 1995 p. 1477-1485 Research sponsored by the Bulgarian National Science Foundation (HTN-95-41223) Copyright

The transmission of DC electric fields by thunderclouds with charge distributions is investigated analytically for the region between the ionosphere and the Earth surface. In such a way the hitherto existing presentations of thunderclouds by electric charge centers (monopole presentation) are generalized to much more adequate three-dimensional model charge regions. A modified ellipsoidal Gaussian profile for the charge distribution of the electrified cloud is accepted. The electrical conductivities are approximated by piecewise exponential functions of altitude. An assumption is made that the geomagnetic field lines in the lower and middle atmosphere are straight and vertical. Analytical solutions to Maxwell equations for the electric potential U and field E are obtained. The effect of the spatial distribution of the charge on E is investigated. The variations of the electric fields at the ionospheric and surface levels, which are caused by different charge distributions, horizontal sizes, and heights of the electrified clouds, are analyzed.

Author (Herner)

A95-75532
A NEW GENERATION OF INSTRUMENTS FOR FLYING LABORATORIES

A. V. LITNETSKIY, V. V. VOLKOV, and YU. A. SEREGIN Meteorologiya i Gidrologiya (ISSN 0130-2906) no. 3 March 1994 p. 103-109 In RUSSIAN refs (BTN-94-EIX94401363947) Copyright

Technical possibilities of the measurement-computational complexes 'Cyclon-1' and 'Cyclon-2' designed for airplanes-meteorological laboratories and timely airplanes carrying out the works on cloud seeding to bring about additional precipitation are analyzed. The complexes have been installed on the AN-26 and Yak-40 airplanes, and passed the flying tests. Technical characteristics of the complexes are presented and the prospects of their improvement are discussed.

EI

A95-75976
POSSIBLE EFFECTS OF CO₂ INCREASE ON THE HIGH-SPEED CIVIL TRANSPORT IMPACT ON OZONE

G. PITARI Univ. degli Studi, L'Aquila, Italy and G. VISCONTI Univ. degli Studi, L'Aquila, Italy Journal of Geophysical Research (ISSN 0148-0227) vol. 99, no. D8 August 20, 1994 p. 16,879-16,896 Research sponsored by the Italian Space Agency and the Commission of European Communities (HTN-95-60779) Copyright

The role of heterogeneous chemistry on the potential impact on ozone of a commercial fleet of high speed civil transport aircraft (HSCT) has been recently studied with assessment models. Here an attempt is made to model the effects of the carbon dioxide increase which is predicted in the future atmosphere when HSCT should be operational. For this purpose we have first used a three-dimensional model for the radiative and dynamical calculations and then a photochemical two-dimensional model including an explicit gas-particle interaction in the process of aerosol formation. The denoxification and denitrification associated with the formation of nitric acid trihydrate (NAT) aerosols is shown to significantly affect the partition of chemical families. The radiative perturbation introduced by the CO₂ increase is shown to perturb the stratospheric dynamics in such a way that the lower stratospheric residual circulation is enhanced. This has the effect of reducing by about 15% the stratospheric residence time of odd nitrogen injected by the aircraft, so that the overall perturbation of stratospheric chemistry due to HSCT is mitigated with respect to the reference case in which CO₂ is kept at the present level. Another effect is found to be produced by the stratospheric temperature cooling following the CO₂ increase. Our model predicts a large enhancement of the surface area density of NAT aerosols in the arctic region, so that the additional denitrification produces a further decrease of the relative role of the NO(X) catalytic cycle for ozone destruction in the lower stratosphere. For this reason, the ClO and OH decreases associated with the HSCT-induced NO(X) increase are found to be dominant in the ozone budget, thus producing a global ozone increase in the case of 500 ppmv CO₂ (+0.27% for mach 2.4 and NO(X), emission index 15). The balance between the different tendencies of ClO, NO(X), and OH cycles is found to be closer in the reference case of 335 ppmv CO₂, where a small column ozone depletion by HSCT is predicted (-0.53% globally).

Author (Herner)

A95-76265* National Aeronautics and Space Administration. Ames Research Center, Moffett Field, CA.

ESTIMATES OF TOTAL ORGANIC AND INORGANIC CHLORINE IN THE LOWER STRATOSPHERE FROM IN SITU AND FLASK MEASUREMENTS DURING AASE 2

E. L. WOODBRIDGE National Oceanic and Atmospheric Administration, Boulder, CO, US, J. W. ELKINS National Oceanic and Atmospheric Administration, Boulder, CO, US, D. W. FAHEY National Oceanic and Atmospheric Administration, Boulder, CO, US, L. E. HEIDT National Center for Atmospheric Research, Boulder, CO, US, S. SOLOMON National Oceanic and Atmospheric Administration, Boulder, CO, US, T. J. BARING Colorado Univ., Boulder, CO, US, T. M. GILPIN National Center for Atmospheric Research, Boulder, CO, US, W. H. POLLACK National Center for Atmospheric Research, Boulder, CO, US, S. M. SCHAUFFLER National Center for Atmospheric Research, Boulder, CO, US, E. L. ATLAS National

Center for Atmospheric Research, Boulder, CO, US et al. *Journal of Geophysical Research* (ISSN 0148-0227) vol. 100, no. D2 February 20, 1995 p. 3057-3064 Research sponsored by NASA. Ames Research Center and JPL (HTN-95-A0861) Copyright

Aircraft sampling has provided extensive in situ and flask measurements of organic chlorine species in the lower stratosphere. The recent Airborne Arctic Stratospheric Expedition 2 (AASE 2) included two independent measurements of organic chlorine species using whole air sample and real-time techniques. From the whole air sample measurements we derive directly the burden of total organic chlorine (CCl(y)) in the lower stratosphere. From the more limited real-time measurements we estimate the CCl(y) burden using mixing ratios and growth rates of the principal CCl(y) species in the troposphere in conjunction with results from a two-dimensional photochemical model. Since stratospheric chlorine is tropospheric in origin and tropospheric mixing ratios are increasing, it is necessary to establish the average age of a stratospheric air parcel to assess its total chlorine (Cl(sub Total)) abundance. Total inorganic chlorine (Cl(y)) in the parcel is then estimated by the simple difference, $Cl(y) = Cl(sub Total) - CCl(y)$. The consistency of the results from these two quite different techniques suggests that we can determine the CCl(y) and Cl(y) in the lower stratosphere with confidence. Such estimates of organic and inorganic chlorine are crucial in evaluating the photochemistry controlling chlorine partitioning and hence ozone loss processes in the lower stratosphere.

Author (Herner)

A95-76266* National Aeronautics and Space Administration. Ames Research Center, Moffett Field, CA.

IN SITU OBSERVATIONS IN AIRCRAFT EXHAUST PLUMES IN THE LOWER STRATOSPHERE AT MIDLATITUDES

D. W. FAHEY National Oceanic and Atmospheric Administration, Boulder, CO, US, E. R. KEIM National Oceanic and Atmospheric Administration, Boulder, CO, US, E. L. WOODBRIDGE National Oceanic and Atmospheric Administration, Boulder, CO, US, R. S. GAO National Oceanic and Atmospheric Administration, Boulder, CO, US, K. A. BOERING Harvard Univ., Cambridge, MA, US, B. C. DAUBE Harvard Univ., Cambridge, MA, US, S. C. WOFSY Harvard Univ., Cambridge, MA, US, R. P. LOHMANN Pratt & Whitney, East Hartford, CT, US, E. J. HINTSA Harvard Univ., Cambridge, MA, US, A. E. DESSLER Harvard Univ., Cambridge, MA, US et al. *Journal of Geophysical Research* (ISSN 0148-0227) vol. 100, no. D2 February 20, 1995 p. 3065-3074 Research sponsored by NASA. Ames Research Center, JPL, and NAS-NRC (HTN-95-A0862) Copyright

Instrumentation on the NASA ER-2 high-altitude aircraft has been used to observe engine exhaust from the same aircraft while operating in the lower stratosphere. Encounters with the exhaust plume occurred approximately 10 min after emission with spatial scales near 2 km and durations of up to 10 s. Measurements include total reactive nitrogen, NO(y), the component species NO and NO₂, CO₂, H₂O, CO, N₂O, condensation nuclei, and meteorological parameters. The integrated amounts of CO₂ and H₂O during the encounters are consistent with the stoichiometry of fuel combustion (1:1 molar). Emission indices (EI) for NO(x) (= NO + NO₂), CO, and N₂O are calculated using simultaneous measurements of CO₂. EI values for NO(x) near 4 g/(kg fuel) are in good agreement with values scaled from limited ground-based tests of the ER-2 engine. Non-NO(x) species comprise less than about 20% of emitted reactive nitrogen, consistent with model evaluations. In addition to demonstrating the feasibility of aircraft plume detection, these results increase confidence in the projection of emissions from current and proposed supersonic aircraft fleets and hence in the assessment of potential long-term changes in the atmosphere. Author (Herner)

A95-76267* National Aeronautics and Space Administration. Goddard Space Flight Center, Greenbelt, MD.

SENSITIVITY OF TWO-DIMENSIONAL MODEL PREDICTIONS OF OZONE RESPONSE TO STRATOSPHERIC AIRCRAFT: AN

UPDATE

DAVID B. CONSIDINE Applied Research Corp., Landover, MD, US, ANNE R. DOUGLASS NASA. Goddard Space Flight Center, Greenbelt, MD, US, and CHARLES H. JACKMAN NASA. Goddard Space Flight Center, Greenbelt, MD, US *Journal of Geophysical Research* (ISSN 0148-0227) vol. 100, no. D2 February 20, 1995 p. 3075-3090

(HTN-95-A0863) Copyright

The Goddard Space Flight Center (GSFC) two-dimensional model of stratospheric photochemistry and dynamics has been used to calculate the O₃ response to stratospheric aircraft (high-speed civil transport (HSCT)) emissions. The sensitivity of the model O₃ response was examined for systematic variations of five parameters and two reaction rates over a wide range, expanding on calculations by various modeling groups for the NASA High Speed Research Program and the World Meteorological Organization. In all, 448 model runs were required to test the effects of variations in the latitude, altitude, and magnitude of the aircraft emissions perturbation, the background chlorine levels, the background sulfate aerosol surface area densities, and the rates of two key reactions. No deviation from previous conclusions concerning the response of O₃ to HSCTs was found in this more exhaustive exploration of parameter space. Maximum O₃ depletions occur for high-altitude, low altitude HSCT perturbations. Small increases in global total O₃ can occur for low-altitude, high-altitude injections. Decreasing aerosol surface area densities and background chlorine levels increases the sensitivity of model O₃ to the HSCT perturbations. The location of the aircraft emissions is the most important determinant of the model response. Response to the location of the HSCT emissions is not changed qualitatively by changes in background chlorine and aerosol loading. The response is also not very sensitive to changes in the rates of the reactions NO + HO₂ yields NO₂ + OH and HO₂ + O₃ yields OH + 2O₂ over the limits of their respective uncertainties. Finally, levels of lower stratospheric HO(sub x) generally decrease when the HSCT perturbation is included, even though there are large increases in H₂O due to the perturbation. Author (Herner)

A95-76394

DIURNAL VARIATION OF LEE VORTICES IN TAIWAN AND THE SURROUNDING AREA

WEN-YIH SUN Purdue University, West Lafayette, IN, US and JIUN-DAR CHERN Purdue University, West Lafayette, IN, US *Journal of the Atmospheric Sciences* (ISSN 0022-4928) vol. 50, no. 20 October 15, 1993 p. 3404-3430 (Contract(s)/Grant(s): NSF ATMS-86-11729; NSF ATMS-89-07881) (HTN-95-91363) Copyright

Lee vortices have been frequently observed in the wake of mesoscale mountains under a low Froude number flow regime. During the Taiwan Area Mesoscale Experiment (TAMEX), a cyclonic vortex was observed to the lee of Taiwan by a P-3 aircraft. In this paper a numerical simulation is carried out to study this event. It is shown that the numerical results are capable of recapturing the detailed features as observed by airplane and surface analysis. The simulated surface pressure, wind field, and lee vortex are in good agreement with observations. The diurnal oscillation of cloudiness and precipitation in Taiwan is also consistent with the observations under undisturbed conditions during the TAMEX period. Under a prevailing southwesterly - to - westerly summer monsoon flow, numerical results demonstrate that the observed cyclonic vortex initially develops to the southeast of Taiwan after sunset, then drifts northeastward. The diurnal forcing not only generates land/sea breezes but also controls the vortex shedding. A sensitivity test without diurnal forcing indicates that the intrinsic vortex shedding period of Taiwan island is about 54 hours under the same initial condition. Due to the influence of diurnal forcing, however, the vortex shedding period becomes 24 hours, with the cyclonic vortex forming at 1700 LST and the anticyclonic vortex forming at 0500 LST. Moreover, the diurnal effect also influences the propagation of vortices, especially near the surface. The results of a vorticity budget study show that the tilting term is important to generate vorticity over

the Central Mountain Range. However, the stretching and advection terms are responsible for carrying and enhancing the vorticity to the lee side and are directly related to the initial development of the vortex. Each term in the vorticity budget is quite complicated due to the existence of clouds, boundary-layer forcing, and the circulation of land/sea breezes.

Author (Herner)

A95-76657

REAL-TIME ESTIMATION OF ATMOSPHERIC TURBULENCE SEVERITY FROM IN-SITU AIRCRAFT MEASUREMENTS

LARRY B. CORNMAN Natl Cent for Atmospheric Research, Boulder, CO, United States, CORINNE S. MORSE, and GARY CUNNING Journal of Aircraft (ISSN 0021-8669) vol. 32, no. 1 January-February 1995 p. 171-177 refs

(BTN-95-EIX95182619231) Copyright

The quality of atmospheric turbulence detection and forecast information for the operational meteorology and aviation communities is directly linked to the quality of real-time measurements. Currently, the only direct data are subjective, qualitative, and intermittent pilot reports. This article describes techniques, suitable for real-time application on commercial transport aircraft, to generate quantitative and comprehensive turbulence measurements. These algorithms build on standard methods used in the analysis of aircraft response to turbulence, but are specifically designed to address the limitations of the available on-board data and computational resources.

Author (EI)

A95-76737

2 MICRON LIDAR FOR LASER-BASED REMOTE SENSING: FLIGHT DEMONSTRATION AND APPLICATION SURVEY

THOMAS J. WAGENER Honeywell Technology Cent, Bloomington, MN, United States, NICK DEMMA, JEFFREY D. KMETEC, and TRACY S. KUBO IEEE Aerospace and Electronic Systems Magazine (ISSN 0885-8985) vol. 10, no. 2 February 1995 p. 23-28 refs

(BTN-95-EIX95212641072) Copyright

A flight test of a diode-pumped solid-state 2 micron Doppler Light Detection And Ranging (LIDAR) system was conducted on-board the NASA Ames DC-8 Airborne Laboratory. This was the first ever airborne demonstration of a 2 micron diode-pumped solid-state Doppler LIDAR. The LIDAR performance was verified by comparing the true-airspeed (TAS) estimate with that found using the pneumatic air data system; excellent agreement was found. The capabilities of this pulsed 2 micron Doppler LIDAR system include high bandwidth air data determination without the need for extensive forebody calibration, remote wind profiling as far as several kilometers away from the aircraft, eye-safe laser transmission at 2 micron, and diode-pumped solid-state design for compact construction and reliable performance.

Author (EI)

A95-77000

A COMPARISON OF SOME AERODYNAMIC RESISTANCE METHODS USING MEASUREMENTS OVER COTTON AND GRASS FROM THE 1991 CALIFORNIA OZONE DEPOSITION EXPERIMENT

J. PADRO Atmospheric Environment Service, Downsview, Ontario, Canada, W. J. MASSMAN USDA/Forest Service, Fort Collins, CO, US, R. H. SHAW Univ. of California, Davis, CA, US, A. DELANY NCAR, Boulder, CO, US, and S. P. ONCLEY NCAR, Boulder, CO, US Boundary-Layer Meteorology (ISSN 0006-8314) vol. 71, no. 4 December 1994 p. 327-339

(HTN-95-11295) Copyright

Measurements of dry deposition velocities ($V_{\text{sub d}}$) of O₃ (using the eddy correlation technique) made over a cotton field and senescent grass near Fresno California during July and August 1991 were used to test some dry deposition velocity models. Over the cotton field, the observed maximum daytime $V_{\text{sub d}}$ was about

0.8 cm/s and the average nighttime value was about 0.2 cm/s. Over the grass, daytime values averaged about 0.2 cm/s and nighttime values about 0.05 cm/s. Application of a site-specific model known as ADOM (Acid Deposition and Oxidant Model) over the cotton field generally overestimated the observations except for a few hours in the afternoon when the observations were underestimated. The overestimation was attributed to inadequacies in the surface resistance formulation and the underestimation to uncertainties in the aerodynamic formulation. Unlike previous studies which focused on the role of surface resistance, we perform additional tests using a large variety of aerodynamic resistance formulae, in addition to those in ADOM, to determine their influence on the modelled $V_{\text{sub d}}$ of O₃ over cotton. Over grass, ADOM considerably overestimated the observations but showed improvement when other surface resistance formulations were applied.

Author (Herner)

A95-77009

GEOID LINEATIONS OF 1000 KM WAVELENGTH OVER THE CENTRAL PACIFIC

A. CAZENAVE GRGS-CNES, Toulouse, France, B. PARSONS Univ. of Oxford, Oxford, UK, and P. CALCAGNO GRGS-CNES, Toulouse, France Geophysical Research Letters (ISSN 0094-8276) vol. 22, no. 2 January 15, 1995 p. 97-100 Research sponsored by the Centre National d'Etudes Spatiales (HTN-95-11304) Copyright

Altimeter profiles of the ERS-1 and Topex-Poseidon satellites have been used to compute a geoid surface from which we have extracted medium-wavelength geoid anomalies over the central Pacific. In this region, the geoid shows prominent elongated anomalies of 20-40 cm in amplitude, with a spacing of approx. 1000 km and oriented N60 deg W. In the south central Pacific, the Polynesian hotspot swells seem to be located on the linear geoid highs. However, the latter extend much farther eastward, preceeding the active hotspots. To the north, other geoid lines are visible but they do not coincide with known tectonic features. The wavelet transform applied to raw geoid data clearly detects a strong signal at the 1000-1200 km wavelength. The amplitude of the lineations increases with age, by a factor of 3 between 10 and 50 my. Analysis of seafloor topography corrected for age and sediments reveals topography anomalies correlated with the geoid lineations. Admittance and coherence calculations give high coherence (0.9) in the 1000-1200 km waveband and admittance values of 1.5 m/km at 10 my and 3 m/km at 60 my. The mechanism producing the lineations is unclear. Their characteristics however are not incompatible with a convective origin.

Author (Herner)

A95-77334

TRANSPORT OF EXHAUST PRODUCTS IN THE NEAR TRAIL OF A JET ENGINE UNDER ATMOSPHERIC CONDITIONS

B. KARCHER Universitat Muenchen, Freising, Germany Journal of Geophysical Research (ISSN 0148-0227) vol. 99, no. D7 July 20, 1994 p. 14,509-14,517 Research sponsored by the Bundesministerium fuer Forschung und Technologie, Germany (HTN-95-91421) Copyright

The transport of exhaust effluents and the possibility of water ice contrail formation are investigated under the specific fluid dynamical conditions in the near exhaust trail of a subsonic jet aircraft at cruise altitude. By means of a computational model describing the two-dimensional turbulent mixing of a single jet of hot exhaust gas with the atmosphere, representative results are discussed on the temperature and saturation ratio evolutions of air parcels in the jet flow field as well as on radial distributions of exhaust effluents undergoing chemical reactions behind the nozzle exit with prescribed, typical net reaction rates. The results underline the importance of a simultaneous treatment of spatially resolved jet expansion together with microphysical and chemical processes, because this coupling leads to distinct concentration patterns for various classes of chemical reactants and is essential for the detailed prediction of contrails.

Author (Herner)

N95-23009* National Aeronautics and Space Administration. Langley Research Center, Hampton, VA.

COMPENDIUM OF NASA DATA BASE FOR THE GLOBAL TROPOSPHERIC EXPERIMENT'S PACIFIC EXPLORATORY MISSION WEST-A (PEM WEST-A)

G. L. GREGORY and A. D. SCOTT, JR. Feb. 1995 140 p
(Contract(s)/Grant(s): RTOP 464-54-03-70)
(NASA-TM-109177; NAS 1.15:109177) Avail: CASI HC A07/MF A02

This compendium describes aircraft data that are available from NASA's Pacific Exploratory Mission West-A (PEM West-A). PEM West is a component of the International Global Atmospheric Chemistry's (IGAC) East Asia/North Pacific Regional Study (APARE) project. The PEM- West program encompassed two expeditions to study contrasting meteorological regimes in the Pacific. Objectives of PEM West are to investigate the atmospheric chemistry of ozone over the northwest Pacific — natural budgets and the impact of anthropogenic sources; and to investigate sulfur chemistry — continental versus marine sulfur sources. PEM West-A was conducted in September 1991 during which the predominance of tropospheric air is from the mid-Pacific (marine) regions, but (at times) is modified/mixed with Asian continental outflow. PEM West-B was conducted during February 1994, a period characterized by maximum continental outflow. PEM-B data (not included) will become public domain during the Summer of 1995. PEM West-A flight experiments were based at Japan, Hong Kong, and Guam. This document provides a representation of NASA DC-8 aircraft data that are available from NASA Langley's Distributed Active Archive Center (DAAC), which include numerous data such as meteorological observations, modeling products, results from surface studies, satellite observations, and sonde releases. Author

N95-23259* National Aeronautics and Space Administration. Lewis Research Center, Cleveland, OH.

DESIGN OF A GAAS/GE SOLAR ARRAY FOR UNMANNED AERIAL VEHICLES

DAVID A. SCHEIMAN (NYMA, Inc., Brook Park, OH.), DAVID J. BRINKER, DAVID J. BENTS, and ANTHONY J. COLOZZA (NYMA, Inc., Brook Park, OH.) Mar. 1995 6 p Presented at the First World Conference on Photovoltaic Energy Conversion, Waikoloa, HI, 5-9 Dec. 1994; cosponsored by IEEE, PVSEC-Japan, and PVSEC-Europe

(Contract(s)/Grant(s): NAS3-27186; RTOP 233-02-0A)
(NASA-TM-106870; E-9489; NAS 1.15:106870) Avail: CASI HC A02/MF A01

Unmanned Aerial Vehicles (UAV) are being proposed for many applications including surveillance, mapping and atmospheric studies. These applications require a lightweight, low speed, medium to long duration airplane. Due to the weight, speed, and altitude constraints imposed on such aircraft, solar array generated electric power is a viable alternative to air-breathing engines. Development of such aircraft is currently being funded under the Environmental Research Aircraft and Sensor Technology (ERAST) program. NASA Lewis Research Center (LeRC) is currently building a Solar Electric Airplane to demonstrate UAV technology. This aircraft utilizes high efficiency Applied Solar Energy Corporation (ASEC) GaAs/Ge space solar cells. The cells have been provided by the Air Force through the ManTech Office. Expected completion of the plane is early 1995, with the airplane currently undergoing flight testing using battery power. Author

N95-23766* Woods Hole Oceanographic Inst., MA. Dept. of Applied Ocean Physics and Engineering.

ASSIMILATION OF ALTIMETER DATA IN A QUASI-GEOSTROPHIC MODEL OF THE GULF STREAM SYSTEM: A DYNAMICAL PERSPECTIVE Ph.D. Thesis - MIT

ANTONIETTA CAPOTONDI Jun. 1993 243 p Limited Reproducibility: More than 20% of this document may be affected by microfiche quality
(Contract(s)/Grant(s): JPL-958208)
(NASA-CR-196313; NAS 1.26:196313; AD-A279436; WHOI-93-29)

Avail: Issuing Activity (Defense Technical Information Center (DTIC))

The dynamical aspects involved in the assimilation of altimeter data in a numerical ocean model have been investigated. The model used for this study is a quasi-geostrophic model of the Gulf Stream region. The data that have been assimilated are maps of sea surface height which have been obtained as the superposition of sea surface height variability deduced from the Geosat altimeter measurements and a mean field constructed from historical hydrographic data. The method used for assimilating the data is the nudging technique. Nudging has been implemented in such a way as to achieve a high degree of convergence of the surface model fields toward the observations. We have analyzed the mechanisms of the model adjustment, and the final statistical equilibrium characteristics of the model simulation when the surface data are assimilated. Since the surface data are the superposition of a mean component and an eddy component, in order to understand the relative role of these two components in determining the characteristics of the final statistical steady state, we have considered two different experiments: in the first experiment only the climatological mean field is assimilated, while in the second experiment the total surface streamfunction field (mean + eddies) has been used. We have found that the mean component of the surface data determines, to a large extent, the structure of the flow field in the subsurface layers, while the eddy field, as well as the inflow/outflow conditions at the open boundaries, affect its intensity. In particular, if surface eddies are not assimilated only a weak flow develops in the two deeper model layers where no inflow/outflow is prescribed at the boundaries. DTIC

N95-23940* Consiglio Nazionale delle Ricerche, Rome (Italy).

MAX-91: POLARIMETRIC SAR RESULTS ON MONTESPERTOLI SITE

S. BARONTI, S. LUCIANI (Tor Vergata Univ., Rome, Italy.), S. MORETTI (Florence Univ., Italy.), S. PALOSCIA, G. SCHIAVON (Tor Vergata Univ., Rome, Italy.), and S. SIGISMONDI (Florence Univ., Italy.) In JPL, Summaries of the 4th Annual JPL Airborne Geoscience Workshop. Volume 3: AIRSAR Workshop p 5-8 25 Oct. 1993 Sponsored by Italian Space Agency
Avail: CASI HC A01/MF A01

The polarimetric Synthetic Aperture Radar (SAR) is a powerful sensor for high resolution ocean and land mapping and particularly for monitoring hydrological parameters in large watersheds. There is currently much research in progress to assess the SAR operational capability as well as to estimate the accuracy achievable in the measurements of geophysical parameters with the presently available airborne and spaceborne sensors. An important goal of this research is to improve our understanding of the basic mechanisms that control the interaction of electro-magnetic waves with soil and vegetation. This can be done both by developing electromagnetic models and by analyzing statistical relations between backscattering and ground truth data. A systematic investigation, which aims at a better understanding of the information obtainable from the multi-frequency polarimetric SAR to be used in agro-hydrology, is in progress by our groups within the framework of SIR-C/X-SAR Project and has achieved a most significant milestone with the NASA/JPL Aircraft Campaign named MAC-91. Indeed this experiment allowed us to collect a large and meaningful data set including multi-temporal multi-frequency polarimetric SAR measurements and ground truth. This paper presents some significant results obtained over an agricultural flat area within the Montespertoli site, where intensive ground measurements were carried out. The results are critically discussed with special regard to the information associated with polarimetric data. Author

N95-23947* Naval Research Lab., Washington, DC. Remote Sensing Div.

STATISTICS OF MULTI-LOOK AIRSAR IMAGERY: A COMPARISON OF THEORY WITH MEASUREMENTS

J. S. LEE, K. W. HOPPEL, and S. A. MANGO In JPL, Summaries of the 4th Annual JPL Airborne Geoscience Workshop. Volume 3: AIRSAR Workshop p 33-36 25 Oct. 1993
Avail: CASI HC A01/MF A01

The intensity and amplitude statistics of SAR images, such as L-Band HH for SEASAT and SIR-B, and C-Band VV for ERS-1 have been extensively investigated for various terrain, ground cover and ocean surfaces. Less well-known are the statistics between multiple channels of polarimetric of interferometric SAR's, especially for the multi-look processed data. In this paper, we investigate the probability density functions (PDF's) of phase differences, the magnitude of complex products and the amplitude ratios, between polarization channels (i.e. HH, HV, and VV) using 1-look and 4-look AIRSAR polarimetric data. Measured histograms are compared with theoretical PDF's which were recently derived based on a complex Gaussian model.

Author

N95-23948* New South Wales Univ., Kensington (Australia). Center for Remote Sensing and GIS.

AIRSAR DEPLOYMENT IN AUSTRALIA, SEPTEMBER 1993: MANAGEMENT AND OBJECTIVES

A. K. MILNE and I. J. TAPLEY (Commonwealth Scientific and Industrial Research Organization, Wembley, Australia.) In JPL, Summaries of the 4th Annual JPL Airborne Geoscience Workshop. Volume 3: AIRSAR Workshop p 37-40 25 Oct. 1993
 Avail: CASI HC A01/MF A01

Past co-operation between the NASA Earth Science and Applications Division and the CSIRO and Australian university researchers has led to a number of mutually beneficial activities. These include the deployment of the C-130 aircraft with TIMS, AIS, and NS001 sensors in Australia in 1985; collaboration between scientists from the USA and Australia in soils research which has extended for the past decade; and in the development of imaging spectroscopy where DSIRO and NASA have worked closely together and regularly exchanged visiting scientists. In May this year TIMS was flown in eastern Australia on board a CSIRO-owned aircraft together with a CSIRO-designed CO2 laser spectrometer. The Science Investigation Team for the Shuttle Imaging Radar (SIRC-C) Program includes one Australian Principal Investigator and ten Australian co-investigators who will work on nine projects related to studying land and near-shore surfaces after the Shuttle flight scheduled for April 1994. This long-term continued joint collaboration was progressed further with the deployment of AIRSAR downunder in September 1993. During a five week period, the DC-8 aircraft flew in all Australian states and collected data from some 65 individual test sites.

Derived from text

15

MATHEMATICAL AND COMPUTER SCIENCES

Includes mathematical and computer sciences (general); computer operations and hardware; computer programming and software; computer systems; cybernetics; numerical analysis; statistics and probability; systems analysis; and theoretical mathematics.

A95-73471

PRECONDITIONED DOMAIN DECOMPOSITION SCHEME FOR THREE-DIMENSIONAL AERODYNAMIC SENSITIVITY ANALYSIS

MOHAMED E. ELESCHAKY Old Dominion Univ, Norfolk, VA, United States and OKTAY BAYSAL AIAA Journal (ISSN 0001-1452) vol. 32, no. 12 December 1994 p. 2489-2491 refs
 (BTN-95-EIX95152577612) Copyright

A preconditioned domain decomposition scheme is introduced for the solution of 3-D aerodynamic sensitivity equation. To reduce the memory requirement and ensure its convergence, this scheme uses the restarting GMRES procedure with preconditioners to solve the effective sensitivity equation of the boundary-interface cells in the SADD scheme. It is found that the commonly used preconditioners do not provide a converged solution for the present approach. However, excluding the dense matrices and the effect of cross terms between boundary interfaces produces an efficient and effective

preconditioning matrix. Excluding only the dense matrix and using the complete LU factorization of the coefficient matrix of the boundary-interface cells produce a more effective preconditioning matrix with 58% increase in the computer memory requirement. EI

A95-76588

OBSERVATIONS ON USING EXPERIMENTAL DATA AS BOUNDARY CONDITIONS FOR COMPUTATIONS

PAUL D. ORKWIS Univ of Cincinnati, Cincinnati, OH, United States, CHUNG-JEN TAM, and PETER J. DISIMILE AIAA Journal (ISSN 0001-1452) vol. 33, no. 1 January 1995 p. 176-178 refs
 (BTN-95-EIX95182619103) Copyright

Many computational efforts have been undertaken to simulate experiments of open cavity flows. These computations have attempted to match the conditions of the experiment by employing the same nondimensional flowfield parameters and identical geometries. However, without intimate knowledge of the experimental procedures and apparatus, it is impossible to match all of the boundary conditions for these flow fields. In this paper, a procedure to determine the computational boundary conditions from an experimental supersonic open cavity flow field study is presented. The approach produces valid quantitative and qualitative field and surface property information that can be used to uncover the dynamic mechanisms that drive open cavity flow fields. EI

A95-76592

AEROELASTIC VEHICLE MULTIVARIABLE CONTROL SYNTHESIS WITH ANALYTICAL ROBUSTNESS EVALUATION

BRETT NEWMAN Old Dominion Univ, Norfolk, VA, United States and DAVID K. SCHMIDT Journal of Guidance, Control, and Dynamics (ISSN 0731-5090) vol. 17, no. 6 November-December 1994 p. 1145-1153 refs
 (BTN-95-EIX95182619115) Copyright

An aeroelastic vehicle model is briefly presented and deficiencies in the vehicle dynamics are noted. A new approach to model-following control synthesis is briefly discussed and applied to the vehicle model. A conventional or classical control synthesis approach is also considered for the purposes of comparison. The resulting compensators and closed-loop systems are analyzed with an analytical model to expose sources of system characteristics that limit the closed-loop system stability robustness. It is shown, that major among these critical characteristics are the frequency and damping of the vehicle first aeroelastic mode dipole; and closed-form expressions for these terms are presented as functions of the vehicle stability derivatives and vibrational characteristics. EI

A95-76598

FUNCTIONAL AGILITY METRICS AND OPTIMAL TRAJECTORY ANALYSIS

GEORGE W. RYAN, III Univ of Kansas, Lawrence, KS, United States and DAVID R. DOWNING Journal of Guidance, Control, and Dynamics (ISSN 0731-5090) vol. 17, no. 6 November-December 1994 p. 1193-1197 refs
 (BTN-95-EIX95182619121) Copyright

This paper examines several functional fighter agility metrics using optimal and nonoptimal maneuvers for a generic F-18-type aircraft to investigate the sensitivity of these metrics to the control strategy used to test them. The maneuvers tested are 180 deg heading changes. The metrics tested are the combat cycle time, the dynamic speed turn agility plots, and the relative energy state metric. Significant improvements in the measured agility metrics are possible if an optimal control strategy is used to test them. For example, reductions in combat cycle time of 60% with subsequent reductions in speed bleed rate of 80% are possible if an optimal maneuver is flown instead of a typical flight test maneuver. The specific agility improvements are vehicle airframe and control system dependent. However, the techniques used in this study are applicable to any aircraft and could provide insight into flight control system design and design tactics for maximizing performance during air combat engagements. Author (EI)

A95-76602

MULTIVARIABLE STABILITY AND ROBUSTNESS OF SEQUENTIALLY DESIGNED FEEDBACK SYSTEMS

BRETT NEWMAN Old Dominion Univ, Norfolk, VA, United States and DAVID K. SCHMIDT Journal of Guidance, Control, and Dynamics (ISSN 0731-5090) vol. 17, no. 6 November-December 1994 p. 1219-1227 refs
(BTN-95-EIX95182619125) Copyright

In sequential loop closure, the importance of evaluating the stability and stability robustness at the intermediate loop closures is well known. However, knowledge concerning how the intermediate loop closures, as well as the final loop closures, contribute to the stability and stability robustness of the overall feedback system holds special significance to the analysis and design of multivariable feedback systems. An analysis of the complete feedback system reveals the multivariable Nyquist contributions from the intermediate loop closures. It is also shown that the results greatly simplify if frequency separation exists between the intermediate loops. The analysis is presented with a two-step loop closure procedure using 'inner' and 'outer' loops that can be generalized to multistep situations. The control of the longitudinal dynamics of an aircraft is addressed to further clarify and demonstrate the results. Author (EI)

A95-76626

ATTAINABLE MOMENTS FOR THE CONSTRAINED CONTROL ALLOCATION PROBLEM

WAYNE C. DURHAM Virginia Polytechnic Inst and State Univ, Blacksburg, VA, United States Journal of Guidance, Control, and Dynamics (ISSN 0731-5090) vol. 17, no. 6 November-December 1994 p. 1371-1373 refs
(BTN-95-EIX95182619149) Copyright

Modern tactical aircraft are being designed with more than the classical set of control effectors. The effective allocation, or blending, of these controls to achieve specific objectives is the control allocation problem. A means of determining the subset of attainable moments that will yield a description of the boundary that contains the necessary information for the determination of controls in the allocation problem is therefore needed. Here, an algorithm is presented that is computationally simple, requiring only the inversion of a 2×2 matrix and a subsequent multiplication of an m -dimensional control vector (where m is the number of controls) by the control effectiveness matrix to calculate the coordinates of each vertex in moment space. EI

A95-76638* National Aeronautics and Space Administration, Langley Research Center, Hampton, VA.

MULTIPLE-FUNCTION DIGITAL CONTROLLER SYSTEM FOR ACTIVE FLEXIBLE WING WIND-TUNNEL MODEL

SHERWOOD T. HOADLEY National Aeronautics and Space Administration, Langley Research Center, Hampton, VA and SANDRA M. MCGRAW Journal of Aircraft (ISSN 0021-8669) vol. 32, no. 1 January-February 1995 p. 32-38 refs
(BTN-95-EIX95182619212) Copyright

A real-time multiple-function digital controller system was developed for the Active Flexible Wing program, which demonstrated through wind-tunnel tests that digital control can be used with great versatility to perform a multifunction task such as suppressing flutter and reducing loads during rolling maneuvers. The digital controller system (DCS) allowed simultaneous execution of two control laws: (1) flutter suppression and (2) either roll trim or a rolling maneuver load control. The DCS operated within, but independently of, a slower host operating system environment, at regulated speeds up to 200 Hz. It also coordinated the acquisition, storage, and transfer of data for near real-time controller performance evaluation and both open- and closed-loop plant estimation. It synchronized the operation of four different processing units, allowing flexibility in the number, form, functionality, and order of control laws, and variability in selection of sensors and actuators employed. Most importantly, the DCS enabled successful demonstration of active flutter suppression to conditions approximately 26% (in dynamic pressure) above the open-loop boundary in cases when the model was fixed-in-roll,

and up to 23% when it was free-to-roll. Aggressive roll maneuvers with load control were achieved above the flutter boundary. The purpose of this article is to present the development, validation, and wind-tunnel testing of this multiple-function digital controller system.

Author (EI)

N95-23308*# Kansas Univ., Lawrence, KS. Dept. of Aerospace Engineering.

ON-LINE, ADAPTIVE STATE ESTIMATOR FOR ACTIVE NOISE CONTROL Abstract Only

TAE W. LIM /n Hampton Univ., 1994 NASA-HU American Society for Engineering Education (ASEE) Summer Faculty Fellowship Program p 90 Dec. 1994
Avail: CASI HC A01/MF A02

Dynamic characteristics of airframe structures are expected to vary as aircraft flight conditions change. Accurate knowledge of the changing dynamic characteristics is crucial to enhancing the performance of the active noise control system using feedback control. This research investigates the development of an adaptive, on-line state estimator using a neural network concept to conduct active noise control. In this research, an algorithm has been developed that can be used to estimate displacement and velocity responses at any locations on the structure from a limited number of acceleration measurements and input force information. The algorithm employs band-pass filters to extract from the measurement signal the frequency contents corresponding to a desired mode. The filtered signal is then used to train a neural network which consists of a linear neuron with three weights. The structure of the neural network is designed as simple as possible to increase the sampling frequency as much as possible. The weights obtained through neural network training are then used to construct the transfer function of a mode in z -domain and to identify modal properties of each mode. By using the identified transfer function and interpolating the mode shape obtained at sensor locations, the displacement and velocity responses are estimated with reasonable accuracy at any locations on the structure. The accuracy of the response estimates depends on the number of modes incorporated in the estimates and the number of sensors employed to conduct mode shape interpolation. Computer simulation demonstrates that the algorithm is capable of adapting to the varying dynamic characteristics of structural properties. Experimental implementation of the algorithm on a DSP (digital signal processing) board for a plate structure is underway. The algorithm is expected to reach the sampling frequency range of about 10 kHz to 20 kHz which needs to be maintained for a typical active noise control application. Author

N95-23419*# Mississippi State Univ., Mississippi State, MS. Center for Computational Field Simulation.

TIGER: A USER-FRIENDLY INTERACTIVE GRID GENERATION SYSTEM FOR COMPLICATED TURBOMACHINERY AND AXIS-SYMMETRIC CONFIGURATIONS

MING H. SHIH and BHARAT K. SONI /n NASA, Marshall Space Flight Center, Eleventh Workshop for Computational Fluid Dynamic Applications in Rocket Propulsion p 1149-1161 Jul. 1993 Sponsored by NASA, Lewis Research Center
Avail: CASI HC A03/MF A10

The issue of time efficiency in grid generation is addressed by developing a user friendly graphical interface for interactive/automatic construction of structured grids around complex turbomachinery/axis-symmetric configurations. The accuracy of geometry modeling and its fidelity is accomplished by adapting the nonuniform rational b-spline (NURBS) representation. A customized interactive grid generation code, TIGER, has been developed to facilitate the grid generation process for complicated internal, external, and internal-external turbomachinery fields simulations. The FORMS Library is utilized to build user-friendly graphical interface. The algorithm allows a user to redistribute grid points interactively on curves/surfaces using NURBS formulation with accurate geometric definition. TIGER's features include multiblock, multiduct/shroud, multiblade row, uneven blade count, and patched/overlapping block

interfaces. It has been applied to generate grids for various complicated turbomachinery geometries, as well as rocket and missile configurations. Author (revised)

N95-23603# Civil Aeromedical Inst., Oklahoma City, OK.
DEVELOPMENT OF QUALIFICATION GUIDELINES FOR PERSONAL COMPUTER-BASED AVIATION TRAINING DEVICES Final Report
 KEVIN W. WILLIAMS and ROBERT E. BLANCHARD Feb. 1995 28 p
 (DOT/FAA/AM-95/6) Avail: CASI HC A03/MF A01

Recent advances in the capabilities of personal computers have resulted in an increase in the number of flight simulation programs made available as Personal Computer-Based Aviation Training Devices (PCATD's). The potential benefits of PCATD's have been recognized by researchers and software/hardware developers alike. The purpose of this report is twofold: (1) present a conceptual approach based upon human learning principles and available flight training data for use in the development and evaluation of PCATD's; and (2) provide a detailed technical plan for an initial effort to develop and test guidelines for assessing the use of PCATD's in a training curriculum of a flight school conducted in accordance with the regulations stated in FAR Part 141. Author

16

PHYSICS

Includes physics (general); acoustics; atomic and molecular physics; nuclear and high-energy physics; optics; plasma physics; solid-state physics; and thermodynamics and statistical physics.

A95-73538
STRUCTURAL ACOUSTIC CALCULATIONS IN THE LOW-FREQUENCY RANGE

S. DEROSA CIRA SpA, Capua, Italy, G. PEZZULLO, L. LECCE, and F. MARULO Journal of Aircraft (ISSN 0021-8669) vol. 31, no. 6 November-December 1994 p. 1387-1394 refs
 (BTN-95-EIX95152582336) Copyright

The structural acoustic research activities pursued at the Aircraft Design Institute in collaboration with the Italian Aerospace Research Center during the last 5 yr are collected and summarized in this article. The fluid-structural interaction is approached from several viewpoints, paying attention to the theoretical analysis of the problem, as well as to its practical and realistic applications. The research results are presented with a view to outline both the future necessary developments of the theoretical approach, mainly looking at the possible extension of the deterministic approach, and the actual numerical-experimental comparisons that have been completed for gaining a necessary confidence level of the methodologies when facing real design problems. Author (EI)

A95-75494
EFFECTS OF AMB PARAMETERS ON THE DYNAMIC STABILITY OF THE ROTOR

HONGLI WANG Tianjin Univ, Tianjin, China and ZHIQIANG WU Applied Mathematics and Mechanics (English Edition) (ISSN 0253-4827) vol. 15, no. 4 April 1994 p. 347-351 refs
 (BTN-94-EIX94381353450) Copyright

The motion equation of the rotor suspended by active magnetic bearing (AMB) was derived in which the nonlinear characteristics of the force was taken into account. Then the response equation was also derived, and based on the response equation, the functions of jump range and the effects of AMB parameters were discussed. It is shown that the jumps will appear as the eccentricity of the rotor is suitably chosen. In addition, the smaller the gap of the magnetic field, the smaller the ratio of the characteristic currents, or the larger the linearized range of the magnetic force. These results can be

used to improve the properties of electromagnetic bearings and controlling them. EI

N95-22675*# Cambridge Acoustical Associates, Inc., Cambridge, MA.

THE USE OF COWL CAMBER AND TAPER TO REDUCE ROTOR/STATOR INTERACTION NOISE Final Report

R. MARTINEZ Cleveland, OH NASA Feb. 1995 89 p
 (Contract(s)/Grant(s): NAS3-27229; RTOP 535-03-10)
 (NASA-CR-195421; E-9364; NAS 1.26:195421) Avail: CASI HC A05/MF A01

The project had two specific technical objectives: (1) to develop a realistic three-dimensional model of tonal noise due to rotor/stator interaction, as the input field for predictions of diffraction and dissipation by a lined cowl; and (2) to determine whether the generator curve of that cowl, or duct, could be 'steered' to yield substantially lower values of propulsor noise along the engine's fore and aft open sectors. The more general and important aim of their research is to provide the commercial aircraft industry with a useful predictive tool to help it meet its noise-reduction goals. The work has produced a tractable and yet realistic model of rotor/stator interaction noise. The blades in the fan stage are radially divergent, twisted, and of realistically wide chords to match the high frequencies and speeds of the sound-production process. The resulting three-dimensional acoustic nearfield insonifies the interior wall of the diffracting cowl, whose shape, incidentally, does not affect fore or aft noise significantly (but other factors do). Author

N95-23178*# National Aeronautics and Space Administration. Lewis Research Center, Cleveland, OH.

SUPERSONIC JET NOISE REDUCTIONS PREDICTED WITH INCREASED JET SPREADING RATE

MILO D. DAHL and PHILIP J. MORRIS (Pennsylvania State Univ., University Park, PA.) Mar. 1995 8 p Presented at the Joint Fluids Engineering Conference, Hilton Head, SC, 13-18 Aug. 1995; co-sponsored by the ASME and the Japan Society of Mechanical Engineers

(Contract(s)/Grant(s): RTOP 505-62-52)
 (NASA-TM-106872; E-9491; NAS 1.15:106872) Avail: CASI HC A02/MF A01

In this paper, predictions are made of noise radiation from single, supersonic, axisymmetric jets. We examine the effects of changes in operating conditions and the effects of simulated enhanced mixing that would increase the spreading rate of the jet shear layer on radiated noise levels. The radiated noise in the downstream direction is dominated by mixing noise and it is well described by the instability wave noise radiation analysis. A numerical prediction scheme is used for the mean flow providing an efficient method to obtain the mean flow development for various operating conditions and to simulate the enhanced mixing. Using far field radiated noise measurements as a reference, the calculations predict that enhanced jet spreading results in a reduction of radiated noise. Author

N95-23503# Institute for Aerospace Research, Ottawa (Ontario). Structures, Materials and Propulsion Lab.

DOUBLE PASS RETROREFLECTION FOR CORROSION DETECTION IN AIRCRAFT STRUCTURES

J. P. KOMOROWSKI, S. KRISHNAKUMAR, R. W. GOULD, N. C. BELLINGER, F. KARPALA (Diffracto Ltd., Windsor, Ontario.), and O. L. HAGENIERS (Diffracto Ltd., Windsor, Ontario.) In AGARD, Corrosion Detection and Management of Advanced Airframe Materials 12 p Jan. 1995

Copyright Avail: CASI HC A03/MF A03

An optical double pass retroreflection surface inspection technique (D Sight) used for visualizing surface distortions, depressions or protrusions has been adapted as a rapid, enhanced visual inspection method inspection of large external aircraft surfaces. A project to fully characterize the D Sight indications of corrosion damage in lap splices is currently active. Over 150 large transport aircraft fuselage lap splice specimens have been collected. D Sight

Aircraft Inspection System - (DAIS) 250C has been developed and tested both in the laboratory and in the field. In laboratory tests lap splices retrieved from retired aircraft and subjected to accelerated corrosion and lap splices naturally corroded in-service were inspected with DAIS, eddy current, X-ray, shadow moire and subjected to tear down. It has been shown that the DAIS 250C is capable of locating corrosion pillowing indicative of a thickness loss as low as 2 percent. The first field trial of the DAIS 250C was based on two service bulletins requiring inspection of longitudinal and circumferential lap splices on the 737-200 aircraft from BS 259.5 to BS 1016. The DAIS 250C inspection, including analysis and report, took 36 man-hours. The recommended technique in the SB was close visual inspection and the time required according to the service bulletins, was 278 man-hours. Author

N95-24076# Los Alamos National Lab., NM.
PHONON CHARACTERISTICS OF HIGH (T SUB C) SUPERCONDUCTORS FROM NEUTRON DOPPLER BROADENING MEASUREMENTS

W. J. TRELA, G. H. KWEI, J. E. LYNN, and K. MEGGERS (Kiel Univ., Germany.) 1994 9 p Presented at the 1994 Fall Meeting of the Materials Research Society (MRS), Boston, MA, 28 Nov. - 2 Dec. 1994

(Contract(s)/Grant(s): W-7405-ENG-36)
 (DE95-003703; LA-UR-94-3872; CONF-941144-14) Avail: CASI HC A02/MF A01

Statistical information on the phonon frequency spectrum of materials can be measured by neutron transmission techniques if they contain nuclei with low energy resonances, narrow enough to be Doppler-broadened, in their neutron cross sections. The authors have carried out some measurements using this technique for materials of the lanthanum barium cuprate class, $\text{La}(2-x)\text{Ba}(x)\text{CuO}_4$. Two samples with slightly different concentrations of oxygen, one being superconductive, the other not, were examined. Pure lanthanum cuprate was also measured. Lanthanum, barium and copper all have relatively low energy narrow resonances. Thus it should be possible to detect differences in the phonons carried by different kinds of atom in the lattice. Neutron cross section measurements have been made with high energy resolution and statistical precision on the 59 m flight path of LANSCE, the pulsed spallation neutron source at Los Alamos National Laboratory. Measurements on all three materials were made over a range of temperatures from 15 to 300 K, with small steps through the critical temperature region near 27 K. No significant changes in the mean phonon energy of the lanthanum atoms were observed near the critical temperature of the superconducting material. It appears however that the mean phonon energy of lanthanum in the superconductor is considerably higher than that in the non-superconductors. The samples used in this series of experiments were too thin in barium and copper to determine anything significant about their phonon spectra. DOE

N95-23168# Defense Advanced Research Projects Agency, Arlington, VA.

TECHNOLOGY REINVESTMENT PROJECT'S FOCUS AREA: AFFORDABLE POLYMER MATRIX COMPOSITES FOR AIRFRAME STRUCTURES

1994 202 p Workshops held in Seattle, WA, 16 Nov. 1994; and Oakland, CA, 18 Nov. 1994

(PB95-136032) Avail: CASI HC A10/MF A03

The mission of the Technology Reinvestment Project (TRP) is to stimulate the transition to a growing, integrated, national industrial capability that provides the most advanced, affordable military systems and the most competitive commercial products. Programs are structured to expand high quality employment opportunities in dual-use technologies that demonstrably enhance U.S. competitiveness and national security. The publication contains the transparencies from the TRP workshops held in Seattle, WA and Oakland, CA in November, 1994. It includes general sessions on TRP, Technology Development, Regional Technology Alliances, and

Manufacturing Education and Training, as well as the break out session on Affordable Polymer Matrix Composites for Airframe Structures. Also included are registration forms for both workshops. NTIS

N95-23284*# Arkansas Univ., Pine Bluff, AR. Dept. of Mathematics and Computer Science.

AUTOMATION TECHNOLOGY USING GEOGRAPHIC INFORMATION SYSTEM (GIS) Abstract Only

CYNTHIA L. BROOKS In Hampton Univ., 1994 NASA-HU American Society for Engineering Education (ASEE) Summer Faculty Fellowship Program p 64 Dec. 1994

Avail: CASI HC A01/MF A02

Airport Surface Movement Area is but one of the actions taken to increase the capacity and safety of existing airport facilities. The System Integration Branch (SIB) has designed an integrated system consisting of an electronic moving display in the cockpit, and includes display of taxi routes which will warn controllers and pilots of the position of other traffic and warning information automatically. Although, this system has in test simulation proven to be accurate and helpful; the initial process of obtaining an airport layout of the taxi-routes and designing each of them is a very tedious and time-consuming process. Other methods of preparing the display maps are being researched. One such method is the use of the Geographical Information System (GIS). GIS is an integrated system of computer hardware and software linking topographical, demographic and other resource data that is being referenced. The software can support many areas of work with virtually unlimited information compatibility due to the system's open architecture. GIS will allow us to work faster with increased efficiency and accuracy while providing decision making capabilities. GIS is currently being used at the Langley Research Center with other applications and has been validated as an accurate system for that task. GIS usage for our task will involve digitizing aerial photographs of the topology for each taxi-runway and identifying each position according to its specific spatial coordinates. The information currently being used can be integrated with the GIS system, due to its ability to provide a wide variety of user interfaces. Much more research and data analysis will be needed before this technique will be used, however we are hopeful this will lead to better usage of man-power and technological capabilities for the future. Author

N95-23320*# College of William and Mary, Williamsburg, VA. Dept. of Mathematics.

PREPARATION OF COURSE MATERIALS: ELEMENTARY MATHEMATICS OF POWERED FLIGHT Abstract Only

GEORGE T. RUBLEIN In Hampton Univ., 1994 NASA-HU American Society for Engineering Education (ASEE) Summer Faculty Fellowship Program p 102 Dec. 1994

Avail: CASI HC A01/MF A02

Non-science students at William and Mary will soon be required to take a mathematics course in order to earn a bachelor's degree. A standard menu of technique courses is the usual way in which universities provide for this requirement: Trigonometry, probability, geometry for teachers, and the like. In this work, we attempt to break away from these largely unsuccessful choices. Our intent is to prepare material that sets a variety of simple mathematical procedures in the context of a commonly experienced part of students' lives: riding in commercial airplanes. The work, begun last summer at Langley, is now close to completion and trial in upcoming fall term at William and Mary. As of this writing, the narrative is complete for 12 to 14 projected sections. We have prepared material on wind triangles, wind roses, navigation maps, drag induced loss of velocity for unpowered missiles (tennis balls), luggage and its effect on center of gravity, localized magnetic declination and VOR orientation, geometry of great circles, terminal velocity for falling bodies, pressure vessels: tires and balloons and blimps, global structure of declination lines, map projections (mercator, azimuthal equidistant, Lambert), ears and their reaction to altitude change. The next

section will treat lift, drag and thrust. The last will treat control surfaces. The entire approach avoids any effort to investigate mathematical topics that arise in the solution of problems. And by the same token, we avoid any organized attempt to explain aeronautical engineering, even on an elementary level. We look only at enough mathematics to do a problem and we select only engineering topics that permit some kind of (elementary) mathematical analysis. In the end, we will think of the material as successful if two things happen: Students must come away with some confidence that even lay people can quantify parts of their surroundings. Other potential instructors must be willing to gain enough familiarity with the physical content of the material so that it can be used at other universities.

Author

N95-23872*# National Aeronautics and Space Administration. Ames Research Center, Moffett Field, CA.

AVIRIS AND TMS DATA PROCESSING AND DISTRIBUTION AT THE LAND PROCESSES DISTRIBUTED ACTIVE ARCHIVE CENTER

G. R. MAH and J. MYERS *In* JPL, Summaries of the 4th Annual JPL Airborne Geoscience Workshop. Volume 1: AVIRIS Workshop p 109-112 25 Oct. 1993

Avail: CASI HC A01/MF A03

The U.S. Government has initiated the Global Change Research program, a systematic study of the Earth as a complete system. NASA's contribution of the Global Change Research Program is the Earth Observing System (EOS), a series of orbital sensor platforms and an associated data processing and distribution system. The EOS Data and Information System (EOSDIS) is the archiving, production, and distribution system for data collected by the EOS space segment and uses a multilayer architecture for processing, archiving, and distributing EOS data. The first layer consists of the spacecraft ground stations and processing facilities that receive the raw data from the orbiting platforms and then separate the data by individual sensors. The second layer consists of Distributed Active Archive Centers (DAAC) that process, distribute, and archive the sensor data. The third layer consists of a user science processing network. The EOSDIS is being developed in a phased implementation. The initial phase, Version 0, is a prototype of the operational system. Version 0 activities are based upon existing systems and are designed to provide an EOSDIS-like capability for information management and distribution. An important science support task is the creation of simulated data sets for EOS instruments from precursor aircraft or satellite data. The Land Processes DAAC, at the EROS Data Center (EDC), is responsible for archiving and processing EOS precursor data from airborne instruments such as the Thermal Infrared Multispectral Scanner (TMS), the Thematic Mapper Simulator (TMS), and Airborne Visible and Infrared Imaging Spectrometer (AVIRIS). AVIRIS, TMS, and TMS are flown by the NASA-Ames Research Center (ARC) on an ER-2. The ER-2 flies at 65000 feet and can carry up to three sensors simultaneously. Most jointly collected data sets are somewhat boresighted and roughly registered. The instrument data are being used to construct data sets that simulate the spectral and spatial characteristics of the Advanced Spaceborne Thermal Emission and Reflection Radiometer (ASTER) instrument scheduled to be flown on the first EOS-AM spacecraft. The ASTER is designed to acquire 14 channels of land science data in the visible and near-IR (VNIR), shortwave-IR (SWIR), and thermal-IR (TIR) regions from 0.52 micron to 11.65 micron at high spatial resolutions of 15 m to 90 m. Stereo data will also be acquired in the VNIR region in a single band. The AVIRIS and TMS cover the ASTER VNIR and SWIR bands, and the TMS covers the TIR bands. Simulated ASTER data sets have been generated over Death Valley, California, Cuprite, Nevada, and the Drum Mountains, Utah using a combination of AVIRIS, TMS, and TMS data, and existing digital elevation models (DEM) for the topographic information.

Author

19

GENERAL

N95-23276*# Hampton Univ., VA. Dept. of Architecture. 1994 NASA-HU AMERICAN SOCIETY FOR ENGINEERING EDUCATION (ASEE) SUMMER FACULTY FELLOWSHIP PROGRAM Abstracts Only

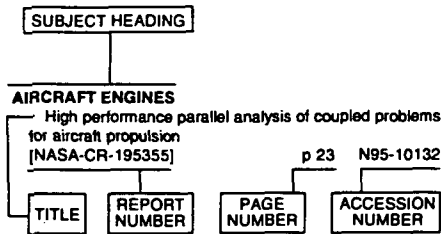
JOHN H. SPENCER, comp. and DEBORAH B. YOUNG, comp. (Old Dominion Coll., Norfolk, VA.) Dec. 1994 155 p Program held in Hampton, VA, 6 Jun. - 12 Aug. 1994

(Contract(s)/Grant(s): NGT-47-020-800)

(NASA-CR-194972; NAS 1.26:194972) Avail: CASI HC A08/MF A02

Since 1964, the National Aeronautics and Space Administration (NASA) has supported a program of summer faculty fellowships for engineering and science educators. In a series of collaborations between NASA research and development centers and nearby universities, engineering faculty members spend 10 weeks working with professional peers on research. The Summer Faculty Program Committee of the American Society for Engineering Education supervises the programs. Objectives: (1) To further the professional knowledge of qualified engineering and science faculty members; (2) To stimulate and exchange ideas between participants and NASA; (3) To enrich and refresh the research and teaching activities of participants' institutions; (4) To contribute to the research objectives of the NASA center. For individual titles, see N95-23277 through N95-23333.

Typical Subject Index Listing



The subject heading is a key to the subject content of the document. The title is used to provide a description of the subject matter. When the title is insufficiently descriptive of document content, a title extension is added, separated from the title by three hyphens. The accession number and the page number are included in each entry to assist the user in locating the abstract in the abstract section. If applicable, a report number is also included as an aid in identifying the document. Under any one subject heading, the accession numbers are arranged in sequence.

A

- ABLATION**
Hypersonic nonequilibrium Navier-Stokes solutions over an ablating graphite nosetip
[BTN-95-EIX95152583252] p 305 A95-73553
- ACCELERATED LIFE TESTS**
Interlaminar shear test method development for long term durability testing of composites
p 301 N95-23300
Eddy current detection of pitting corrosion around fastener holes
p 315 N95-23507
Test method and test results for environmental assessment of aircraft materials
p 302 N95-23509
- ACCELERATION (PHYSICS)**
Dynamical instability of the aerogravity assist maneuver
[BTN-95-EIX95152583282] p 298 A95-73583
- ACCELEROMETERS**
Covariance analysis of strapdown INS considering gyrocompass characteristics
[BTN-95-EIX9520637592] p 279 A95-76697
- ACCIDENT PREVENTION**
Mishap risk control for advanced aerospace/composite materials
p 301 N95-23031
- ACCOMMODATION COEFFICIENT**
Calculation of satellite drag coefficients
[AD-A285118] p 300 N95-23781
- ACOUSTIC EMISSION**
Mach wave emission from a high-temperature supersonic jet
[BTN-95-EIX95152577586] p 264 A95-73496
- ACOUSTIC MEASUREMENT**
Structural acoustic calculations in the low-frequency range
[BTN-95-EIX95152582336] p 323 A95-73538
- ACTIVE CONTROL**
Grid refinement test of time-periodic flows over bluff bodies
[BTN-94-EIX94401378822] p 307 A95-76491
- Summary of an active flexible wing program
[BTN-95-EIX95182619209] p 283 A95-76635
Simulation and model reduction for the active flexible wing program
[BTN-95-EIX95182619211] p 295 A95-76637
Multiple-function digital controller system for active flexible wing wind-tunnel model
[BTN-95-EIX95182619212] p 322 A95-76638
On-line analysis capabilities developed to support the active flexible wing wind-tunnel tests
[BTN-95-EIX95182619213] p 296 A95-76639
Flutter suppression control law design and testing for the active flexible wing
[BTN-95-EIX95182619214] p 292 A95-76640
Design and multifunction tests of a frequency domain-based active flutter suppression system
[BTN-95-EIX95182619215] p 292 A95-76641
Rolling maneuver load alleviation using active controls
[BTN-95-EIX95182619217] p 270 A95-76643
Active control of panel vibrations induced by a boundary layer flow
[NASA-CR-197867] p 273 N95-23182
On-line, adaptive state estimator for active noise control
p 322 N95-23308
Supersonic laminar flow control research
[NASA-CR-197938] p 275 N95-23669
- ACTIVE SATELLITES**
Effects of satellite bunching on the probability of collision in geosynchronous orbit
[BTN-95-EIX95152583276] p 298 A95-73577
- ACTUATORS**
Motor drive technologies for the power-by-wire (PBW) program: Options, trends and tradeoffs
[NASA-TM-106885] p 295 N95-23671
- ADAPTIVE CONTROL**
Adaptive finite element method for turbulent flow near a propeller
[BTN-95-EIX95142553038] p 305 A95-73460
Direct adaptive performance optimization of subsonic transports: A periodic perturbation technique
[NASA-TM-4676] p 284 N95-22829
- ADAPTIVE FILTERS**
Maximum-likelihood spectral estimation and adaptive filtering techniques with application to airborne Doppler weather radar
[NASA-CR-197699] p 316 N95-23670
- ADHESION TESTS**
Evaluation of advanced aerospace materials by depth sensing indentation and scratch methods
[BTN-95-EIX95152584678] p 282 A95-73590
Corrosion protection measures for CFC/metal joints of fuel integral tank structures of advanced military aircraft
p 303 N95-23510
- ADHESIVE BONDING**
Evaluation of advanced aerospace materials by depth sensing indentation and scratch methods
[BTN-95-EIX95152584678] p 282 A95-73590
- AEROACOUSTICS**
Analysis of a higher harmonic control test to reduce blade vortex interaction noise
[BTN-95-EIX95152582330] p 265 A95-73532
Numerical study of sound generation due to a spinning vortex pair
[BTN-95-EIX95182619075] p 307 A95-75760
Aeroacoustic model for weak shock waves based on Burgers equation
[BTN-95-EIX95182619076] p 269 A95-75761
Supersonic jet noise reductions predicted with increased jet spreading rate
[NASA-TM-106872] p 323 N95-23178
- AEROBRAKING**
Minimum-mass design of sandwich aerobreaks for a lunar transfer vehicle
[BTN-95-EIX95212645707] p 299 A95-76759
- AEROCAPTURE**
Fuel-optimal bank-angle control for lunar-return aerocapture
[BTN-95-EIX95212645706] p 299 A95-76758
- AERODYNAMIC BALANCE**
System for determining aerodynamic imbalance
[NASA-CASE-ARC-11913-1] p 311 N95-23377
- AERODYNAMIC BRAKES**
Minimum-mass design of sandwich aerobreaks for a lunar transfer vehicle
[BTN-95-EIX95212645707] p 299 A95-76759
- AERODYNAMIC CHARACTERISTICS**
Aerodynamic characteristics of a hypersonic viscous optimized waverider at high altitudes
[BTN-95-EIX95152583251] p 266 A95-73552
Aerodynamic characteristics of a canard-controlled missile at high angles of attack
[BTN-95-EIX95152583257] p 267 A95-73558
Aerodynamic characteristics of external store configurations at low speeds
[BTN-95-EIX95182619230] p 271 A95-76656
Thin tailored composite wing for civil tiltrotor
p 285 N95-23317
Aerodynamic flight control to increase payload capability of future launch vehicles
[NASA-CR-197704] p 300 N95-24032
- AERODYNAMIC COEFFICIENTS**
Navier-Stokes prediction of large-amplitude delta-wing roll oscillations
[BTN-95-EIX95152582329] p 281 A95-73531
Analytic prediction of lift for delta wings with partial leading-edge thrust
[BTN-95-EIX95152582345] p 266 A95-73547
Drag function modeling for air traffic simulation
[BTN-95-EIX95182619154] p 279 A95-76631
Unsteady ground effects on aerodynamic coefficients of finite wings with camber
[BTN-95-EIX95182619233] p 271 A95-76659
Calculation of satellite drag coefficients
[AD-A285118] p 300 N95-23781
- AERODYNAMIC CONFIGURATIONS**
Aerodynamic shape optimization using preconditioned conjugate gradient methods
[BTN-95-EIX95142553033] p 263 A95-73465
Base drag prediction on missile configurations
[BTN-95-EIX95152583256] p 266 A95-73557
Aerodynamic characteristics of a canard-controlled missile at high angles of attack
[BTN-95-EIX95152583257] p 267 A95-73558
Impeller flow field characterization with a laser two-focus velocimeter
p 313 N95-23440
- AERODYNAMIC DRAG**
Analytic prediction of lift for delta wings with partial leading-edge thrust
[BTN-95-EIX95152582345] p 266 A95-73547
Base drag prediction on missile configurations
[BTN-95-EIX95152583256] p 266 A95-73557
Improved version of the Naval Surface Warfare Center aeroprediction code (AP93)
[BTN-95-EIX95152583260] p 267 A95-73561
Drag function modeling for air traffic simulation
[BTN-95-EIX95182619154] p 279 A95-76631
Application of Navier-Stokes aeroelastic methods to improve fighter wing maneuver performance
[BTN-95-EIX95182619218] p 284 A95-76644
Numerical investigation of supersonic flows around a spiked blunt body
[BTN-95-EIX95212645690] p 271 A95-76742
A comparison of some aerodynamic resistance methods using measurements over cotton and grass from the 1991 California ozone deposition experiment
[HTN-95-11295] p 319 A95-77000
Calculation of satellite drag coefficients
[AD-A285118] p 300 N95-23781
- AERODYNAMIC FORCES**
Static aeroelastic characteristics of a composite wing
[BTN-95-EIX95152582340] p 282 A95-73542
Flutter of an infinitely long panel in a duct
[BTN-95-EIX95182619087] p 291 A95-75772
- AERODYNAMIC HEAT TRANSFER**
Numerical computation of aerodynamics and heat transfer in a turbine cascade and a turn-around duct using advanced turbulence models
p 313 N95-23444
- AERODYNAMIC HEATING**
Hypersonic convective heat transfer over 140-deg blunt cones in different gases
[BTN-95-EIX95152583253] p 306 A95-73554

- Convective and radiative heat transfer analysis for the
Ire 2 forebody
[BTN-95-EIX95182617460] p 268 A95-75731
- AERODYNAMIC INTERFERENCE**
Wing vertical position effects on wing-body carryover
for noncircular missiles
[BTN-95-EIX95182617462] p 268 A95-75733
Some aspects of the aerodynamics of separating
strap-ons
[BTN-95-EIX95182617464] p 298 A95-75735
A wall interference assessment/correction system
[NASA-CR-197421] p 309 N95-23183
- AERODYNAMIC LOADS**
Design constraints in the payload-range diagram of
ultrahigh capacity transport airplanes
[BTN-95-EIX95152582319] p 276 A95-73522
Hypersonic rarefied flow past spheres including wake
structure
[BTN-95-EIX95152583250] p 305 A95-73551
Summary of an active flexible wing program
[BTN-95-EIX95182619209] p 283 A95-76635
Rolling maneuver load alleviation using active controls
[BTN-95-EIX95182619217] p 270 A95-76643
Minimum-mass design of sandwich aerobrakes for a
lunar transfer vehicle
[BTN-95-EIX95212645707] p 299 A95-76759
System for determining aerodynamic imbalance
[NASA-CASE-ARC-11913-1] p 311 N95-23377
Review of some results of the author's fatigue
investigations with applications in engineering and material
science
[TAE-698] p 316 N95-23662
- AERODYNAMIC NOISE**
Numerical study of sound generation due to a spinning
vortex pair
[BTN-95-EIX95182619075] p 307 A95-75760
Supersonic jet noise reductions predicted with increased
jet spreading rate
[NASA-TM-106872] p 323 N95-23178
- AERODYNAMIC STABILITY**
Analytical study of the neutral stability of a model
hypersonic boundary layer
[BTN-95-EIX95152577589] p 263 A95-73493
Navier-Stokes prediction of large-amplitude delta-wing
roll oscillations
[BTN-95-EIX95152582329] p 281 A95-73531
Further analysis of high-rate rolling experiments of a
65-deg delta wing
[BTN-95-EIX95152582331] p 281 A95-73533
The influence of alternate inter-blade connections on
ground resonance
[HTN-95-80859] p 267 A95-75101
Dynamic investigation of the angular motion of a rotating
body-parachute system
[BTN-95-EIX95182619220] p 270 A95-76646
- AERODYNAMIC STALLING**
Computation of the poststall behavior of a circulation
controlled airfoil
[BTN-95-EIX95152582320] p 264 A95-73523
Moving wall effect in relation to other dynamic stall flow
mechanisms
[BTN-95-EIX95152582324] p 265 A95-73527
- AERODYNAMICS**
Mechanical system reliability and risk assessment
[BTN-95-EIX95142553046] p 304 A95-73452
Simulation of turbulent fluctuations
[BTN-95-EIX95142553041] p 304 A95-73457
Laplace interaction law for the computation of viscous
airfoil flow in low- and high-speed aerodynamics
[BTN-95-EIX95142553037] p 263 A95-73461
Preconditioned domain decomposition scheme for
three-dimensional aerodynamic sensitivity analysis
[BTN-95-EIX95152577612] p 321 A95-73471
Shock tunnel measurements of hypervelocity blunted
cone drag
[BTN-95-EIX95152577606] p 305 A95-73477
Eigenanalysis of unsteady flows about airfoils, cascades,
and wings
[BTN-95-EIX95152577597] p 305 A95-73486
Progress in high-lift aerodynamic calculations
[BTN-95-EIX95152582315] p 264 A95-73518
Unstructured grid solutions to a wing/pylon/store
configuration
[BTN-95-EIX95152582322] p 265 A95-73525
Moving wall effect in relation to other dynamic stall flow
mechanisms
[BTN-95-EIX95152582324] p 265 A95-73527
Navier-Stokes prediction of large-amplitude delta-wing
roll oscillations
[BTN-95-EIX95152582329] p 281 A95-73531
Further analysis of high-rate rolling experiments of a
65-deg delta wing
[BTN-95-EIX95152582331] p 281 A95-73533
Pneumatic concept for tip-stall control of cranked-arrow
wings
[BTN-95-EIX95152582335] p 281 A95-73537
- Higher-order viscous shock-layer solutions for
high-altitude flows
[BTN-95-EIX95152583255] p 306 A95-73556
Aerodynamic characteristics of a canard-controlled
missile at high angles of attack
[BTN-95-EIX95152583257] p 267 A95-73558
Improved version of the Naval Surface Warfare Center
aeroprediction code (AP93)
[BTN-95-EIX95152583260] p 267 A95-73561
Functional dependence of trajectory dispersion on initial
condition errors
[BTN-95-EIX95152583263] p 298 A95-73564
Supersonic axisymmetric conical flow solutions for
different ratios of specific heats
[BTN-95-EIX95152583283] p 306 A95-73584
Analytical solution for controls, heats, and states of flight
trajectories
[BTN-95-EIX95152583286] p 282 A95-73587
Aerodynamics of the Shuttle Orbiter at high altitudes
[BTN-95-EIX95182617454] p 298 A95-75725
Some aspects of the aerodynamics of separating
strap-ons
[BTN-95-EIX95182617464] p 298 A95-75735
Comparison of linear stability results with flight transition
data
[BTN-95-EIX95182619097] p 283 A95-76582
Aeroelastic vehicle multivariable control synthesis with
analytical robustness evaluation
[BTN-95-EIX95182619115] p 321 A95-76592
Functional agility metrics and optimal trajectory
analysis
[BTN-95-EIX95182619121] p 321 A95-76598
Analytical solution and parameter estimation of projectile
dynamics
[BTN-95-EIX95212645695] p 272 A95-76747
Calculation of wing-alone aerodynamics to high angles
of attack
[BTN-95-EIX95212645713] p 261 A95-76765
Mach 10 computational study of a three-dimensional
scramjet inlet flow field
[NASA-TM-4602] p 310 N95-23210
Aerodynamic design optimization with sensitivity analysis
and computational fluid dynamics
[NASA-CR-197419] p 274 N95-23218
Aerodynamic surface distension system for high angle
of attack forebody vortex control
[NASA-CASE-ARC-11979-1] p 286 N95-23390
Aerodynamic design and analysis of a highly loaded
turbine exhaust
p 312 N95-23435
Numerical computation of aerodynamics and heat
transfer in a turbine cascade and a turn-around duct using
advanced turbulence models
p 313 N95-23444
NTS-spill test facility wind tunnel exhaust plume
characterization
[DE95-003630] p 297 N95-24019
- AEROELASTICITY**
Eigenanalysis of unsteady flows about airfoils, cascades,
and wings
[BTN-95-EIX95152577597] p 305 A95-73486
Efficient sensitivity analysis for rotary-wing
aeromechanical problems
[BTN-95-EIX95152577585] p 264 A95-73497
Limit cycle phenomena in computational transonic
aeroelasticity
[BTN-95-EIX95152582317] p 264 A95-73520
Static aeroelastic characteristics of a composite wing
[BTN-95-EIX95152582340] p 282 A95-73542
Flutter of an infinitely long panel in a duct
[BTN-95-EIX95182619087] p 291 A95-75772
Aeroelastic vehicle multivariable control synthesis with
analytical robustness evaluation
[BTN-95-EIX95182619115] p 321 A95-76592
Analytical aeropropulsive/aeroelastic
hypersonic-vehicle model with dynamic analysis
[BTN-95-EIX95182619138] p 269 A95-76615
Application of transonic small disturbance theory to the
active flexible wing model
[BTN-95-EIX95182619210] p 270 A95-76636
Application of Navier-Stokes aeroelastic methods to
improve fighter wing maneuver performance
[BTN-95-EIX95182619218] p 284 A95-76644
High-performance parallel analysis of coupled problems
for aircraft propulsion
[NASA-CR-197440] p 289 N95-23088
Flutter analysis of composite box beams
[NASA-CR-197931] p 294 N95-23392
User's guide for ECAP2D: An Euler unsteady
aerodynamic and aeroelastic analysis program for two
dimensional oscillating cascades, version 1.0
[NASA-CR-189146] p 316 N95-24189
- AERONAUTICAL ENGINEERING**
Research and Technology, 1994
[NASA-TM-106764] p 262 N95-24025
- AERONAUTICAL SATELLITES**
Development of aeronautical mobile satellite services
over the past thirty years
[BTN-95-EIX95152569458] p 305 A95-73498
- AEROSERVOELASTICITY**
Simulation and model reduction for the active flexible
wing program
[BTN-95-EIX95182619211] p 295 A95-76637
- AEROSOLS**
Modeling aerosol emissions from the combustion of
composite materials
p 301 N95-23038
- AEROSPACE ENGINEERING**
Research and Technology, 1994
[NASA-TM-106764] p 262 N95-24025
- AEROSPACE INDUSTRY**
Overview of AlliedSignal's avionics development in the
CIS
[BTN-95-EIX95212641069] p 287 A95-76734
- AEROSPACE VEHICLES**
Application of the multigrad solution technique to
hypersonic entry vehicles
[BTN-95-EIX95152583254] p 306 A95-73555
Integrated design of hypersonic waveriders including
inlets and tailfins
[BTN-95-EIX95212645692] p 271 A95-76744
Moving mass trim control for aerospace vehicles
[DE95-002602] p 299 N95-23532
- AEROTHERMOCHEMISTRY**
Hypersonic nonequilibrium Navier-Stokes solutions over
an ablating graphite nosetip
[BTN-95-EIX95152583252] p 305 A95-73553
- AEROTHERMODYNAMICS**
Hypersonic nonequilibrium Navier-Stokes solutions over
an ablating graphite nosetip
[BTN-95-EIX95152583252] p 305 A95-73553
Hypersonic convective heat transfer over 140-deg blunt
cones in different gases
[BTN-95-EIX95152583253] p 306 A95-73554
- AFTERBODIES**
Experimental investigation of the flowfield about an
upswep afterbody
[BTN-95-EIX95152582321] p 265 A95-73524
Supersonic near-wake afterbody boattailing effects on
axisymmetric bodies
[BTN-95-EIX95182617465] p 268 A95-75736
Experimental results for a hypersonic nozzle/afterbody
flow field
[NASA-TM-4638] p 274 N95-23250
Validation of a Computational Fluid Dynamics (CFD)
code for supersonic axisymmetric base flow
p 315 N95-23652
- AGING (MATERIALS)**
Oklahoma City air logistics center (USAF) aging aircraft
corrosion program
p 262 N95-23519
- AGRICULTURE**
MAX-91: Polarimetric SAR results on Montespetoli
site
p 320 N95-23940
- AIR**
Airborne rotary air separator study
[NASA-CR-189099] p 290 N95-24053
- AIR BREATHING ENGINES**
Computational study of plume-induced separation on a
hypersonic powered model
[BTN-95-EIX95152582346] p 266 A95-73548
Airborne rotary air separator study
[NASA-CR-189099] p 290 N95-24053
- AIR COOLING**
Evaluation of thermal barrier and PS-200 self-lubricating
coatings in an air-cooled rotary engine
[NASA-CR-195445] p 289 N95-23222
- AIR FILTERS**
Erosion of dust-filtered helicopter turbine engines. Part
2: Erosion reduction
[BTN-95-EIX95182619223] p 289 A95-76649
Life prediction of helicopter engines fitted with dust
filters
[BTN-95-EIX95182619224] p 289 A95-76650
Airborne rotary air separator study
[NASA-CR-189099] p 290 N95-24053
- AIR FLOW**
Simulation of transverse gas injection in turbulent
supersonic air flows
[BTN-95-EIX95182619080] p 269 A95-75765
Tracking of raindrops in flow over an airfoil
[BTN-95-EIX95182619221] p 308 A95-76647
CFD analysis of turbopump volutes
p 312 N95-23436
Phase 2: HGM air flow tests in support of HEX vane
investigation
p 312 N95-23438
- AIR INTAKES**
Three-dimensional Navier-Stokes analysis and redesign
of an imbedded bellmouth nozzle in a turbine cascade
inlet section
p 311 N95-23423

AIR JETS

- Simulation of transverse gas injection in turbulent supersonic air flows
[BTN-95-EIX95182619080] p 269 A95-75765

AIR LAUNCHING

- Aerodynamic design of pegasus: Concept to flight with computational fluid dynamics
[BTN-95-EIX95182617463] p 298 A95-75734

AIR LAW

- Oceanic operations: An authoritative guide to oceanic operations
[FAA-AFS-550] p 277 N95-24065

AIR NAVIGATION

- Development of aeronautical mobile satellite services over the past thirty years
[BTN-95-EIX95152569458] p 305 A95-73498
Real-time navigation using the global positioning system
[BTN-95-EIX95172595298] p 279 A95-75714
Cueing light configuration for aircraft navigation
[NASA-CASE-ARC-11982-1] p 280 N95-23393
Oceanic operations: An authoritative guide to oceanic operations
[FAA-AFS-550] p 277 N95-24065

AIR POLLUTION

- In situ observations in aircraft exhaust plumes in the lower stratosphere at midlatitudes
[HTN-95-A0862] p 318 A95-76266
Transport of exhaust products in the near trail of a jet engine under atmospheric conditions
[HTN-95-91421] p 319 A95-77334

AIR SAMPLING

- Estimates of total organic and inorganic chlorine in the lower stratosphere from in situ and flask measurements during AASE 2
[HTN-95-A0861] p 317 A95-76265

AIR TRAFFIC CONTROL

- Development of aeronautical mobile satellite services over the past thirty years
[BTN-95-EIX95152569458] p 305 A95-73498
Description of a GNSS availability model and its use in developing requirements
[BTN-95-EIX95202637603] p 308 A95-76686
The role of flight progress strips in en route air traffic control: A time-series analysis
[DOT/FAA/AM-95/4] p 280 N95-23565

AIR TRAFFIC CONTROLLERS (PERSONNEL)

- The role of flight progress strips in en route air traffic control: A time-series analysis
[DOT/FAA/AM-95/4] p 280 N95-23565

AIR TRANSPORTATION

- Maintenance challenges and trends
[BTN-95-EIX95182617808] p 261 A95-75753
Report of proceedings: Aviation Accident Investigation Symposium. Volume 2: Participant presentations
[PB94-917007] p 277 N95-23598
Oceanic operations: An authoritative guide to oceanic operations
[FAA-AFS-550] p 277 N95-24065

AIRBORNE RADAR

- 2 micron LIDAR for laser-based remote sensing: Flight demonstration and application survey
[BTN-95-EIX95212641072] p 319 A95-76737
MAX-91: Polarimetric SAR results on Montespertoli site
p 320 N95-23940

AIRCRAFT ACCIDENT INVESTIGATION

- Report of proceedings: Aviation Accident Investigation Symposium. Volume 2: Participant presentations
[PB94-917007] p 277 N95-23598
Aircraft accident report. Runway overrun following rejected takeoff. Continental airlines flight 795, McDonnell Douglas MD-82, N18835, LaGuardia Airport, Flushing, NY, 2 March 1994
[PB95-910401] p 277 N95-23609
Aviation Accident Investigation Symposium. Volume 1: Industry recommendations and Safety Board responses
[PB94-917005] p 278 N95-24105

AIRCRAFT ACCIDENTS

- Mishap risk control for advanced aerospace/composite materials
p 301 N95-23031
Aircraft accident report. Runway overrun following rejected takeoff. Continental airlines flight 795, McDonnell Douglas MD-82, N18835, LaGuardia Airport, Flushing, NY, 2 March 1994
[PB95-910401] p 277 N95-23609
Aircraft fires, smoke toxicity, and survival: An overview
[DOT/FAA/AM-95/8] p 277 N95-24024
A review of civil aviation fatal accidents in which lost/oriented was a cause/factor: 1981-1990
[DOT/FAA/AM-95/1] p 278 N95-24071

AIRCRAFT APPROACH SPACING

- Guidance and control requirements for high-speed Rollout and Turnoff (ROTO)
[NASA-CR-195026] p 292 N95-22674

AIRCRAFT CONFIGURATIONS

- Unstructured grid solutions to a wing/pylon/store configuration
[BTN-95-EIX95152582322] p 265 A95-73525

AIRCRAFT CONSTRUCTION MATERIALS

- MIL-HDBK-5 design allowables for fibre/metal laminates: ARALL 2 and ARALL 3
[BTN-94-EIX94371346933] p 300 A95-73345
Evaluation of advanced aerospace materials by depth sensing indentation and scratch methods
[BTN-95-EIX95152584678] p 282 A95-73590
H-76B fantail demonstrator composite fan blade fabrication
[HTN-95-80856] p 283 A95-75098
Mishap risk control for advanced aerospace/composite materials
p 301 N95-23031
Technology reinvestment project's focus area: Affordable polymer matrix composites for airframe structures
[PB95-136032] p 324 N95-23168
Development and verification of a resin film infusion/resin transfer molding simulation model for fabrication of advanced textile composites
[NASA-CR-197439] p 301 N95-23179
Test method and test results for environmental assessment of aircraft materials
p 302 N95-23509
US Navy operating experience with new aircraft construction materials
p 303 N95-23517
Review of some results of the author's fatigue investigations with applications in engineering and material science
[TAE-698] p 316 N95-23662

AIRCRAFT CONTROL

- Cypher moves toward autonomous flight
[HTN-95-41394] p 283 A95-76390
Functional agility metrics and optimal trajectory analysis
[BTN-95-EIX95182619121] p 321 A95-76598
Multiaxis pilot ratings for damaged aircraft
[BTN-95-EIX95182619128] p 269 A95-76605
Direct-lift design strategy for longitudinal control of hypersonic aircraft
[BTN-95-EIX95182619131] p 291 A95-76608
Attainable moments for the constrained control allocation problem
[BTN-95-EIX95182619149] p 322 A95-76626
Automatic formation flight control
[BTN-95-EIX95182619153] p 292 A95-76630
Multiple-function digital controller system for active flexible wing wind-tunnel model
[BTN-95-EIX95182619212] p 322 A95-76638
Robustly stable preliminary control systems design for the YF-16 CCV aircraft
[BTN-95-EIX95202637608] p 292 A95-76681
Guidance and control requirements for high-speed Rollout and Turnoff (ROTO)
[NASA-CR-195026] p 292 N95-22674
Nonlinear system guidance in the presence of transmission zero dynamics
[NASA-TM-4661] p 309 N95-22804
Flight test of the X-29A at high angle of attack: Flight dynamics and controls
[NASA-TP-3537] p 284 N95-22806
Design of high performance multivariable control systems for supermaneuverable aircraft at high angle of attack
[NASA-CR-197661] p 293 N95-22908
Stable H(infinity) controller design for the longitudinal dynamics of an aircraft
[NASA-TM-106847] p 293 N95-22954
Analysis of the longitudinal handling qualities and pilot-induced-oscillation tendencies of the High-Angle-of-Attack Research Vehicle (HARV)
p 293 N95-23297
Handling qualities of the High Speed Civil Transport
p 294 N95-23325

- Feedback control laws for highly maneuverable aircraft
[NASA-CR-197944] p 295 N95-23410

AIRCRAFT DESIGN

- Flight-deck displays on the Boeing 777
[BTN-95-EIX95142562402] p 286 A95-73438
Structural acoustic calculations in the low-frequency range
[BTN-95-EIX95152582336] p 323 A95-73538
Flow study of supersonic wing-nacelle configuration
[BTN-95-EIX95152582344] p 266 A95-73546
An analytical and experimental investigation of the response of the curved, composite frame/skin specimens
[HTN-95-80857] p 283 A95-75099
An unmanned air vehicle concept with tipjet drive
[HTN-95-80858] p 283 A95-75100
Integrated design of hypersonic waveriders including inlets and tailfins
[BTN-95-EIX95212645692] p 271 A95-76744

- Euler Technology Assessment program for preliminary aircraft design employing SPLITFLOW code with Cartesian unstructured grid method
[NASA-CR-4649] p 273 N95-22917

- Euler technology assessment for preliminary aircraft design employing OVERFLOW code with multiblock structured-grid method
[NASA-CR-4651] p 273 N95-23095
Control of flow separation in airfoil/wing design applications
p 274 N95-23294
Thin tailored composite wing for civil tiltrotor
p 285 N95-23317

AIRCRAFT ENGINES

- Artificial intelligence for turboprop engine maintenance
[BTN-95-EIX95182617812] p 288 A95-75757
Lycoming to test new engine core
[HTN-95-41393] p 288 A95-76389
A new type of simulator for simulating the flow-field distortion of engine inlet
[BTN-95-EIX95202638963] p 289 A95-76673
High-performance parallel analysis of coupled problems for aircraft propulsion
[NASA-CR-197440] p 289 N95-23088
Engines-only flight control system
[NASA-CASE-ARC-11944-1] p 294 N95-23389

AIRCRAFT FUELS

- Trajectory modeling of emissions from lower stratospheric aircraft
[HTN-95-41219] p 317 A95-75031
In situ observations in aircraft exhaust plumes in the lower stratosphere at midlatitudes
[HTN-95-A0862] p 318 A95-76266
Sensitivity of two-dimensional model predictions of ozone response to stratospheric aircraft: An update
[HTN-95-A0863] p 318 A95-76267

AIRCRAFT GUIDANCE

- Analytical solution for controls, heats, and states of flight trajectories
[BTN-95-EIX95152583286] p 282 A95-73587
Guidance and control requirements for high-speed Rollout and Turnoff (ROTO)
[NASA-CR-195026] p 292 N95-22674
Nonlinear system guidance in the presence of transmission zero dynamics
[NASA-TM-4661] p 309 N95-22804

AIRCRAFT HAZARDS

- Thundercloud electric field modeling for the ionosphere-Earth region. 1: Dependence on cloud charge distribution
[HTN-95-41223] p 317 A95-75035

AIRCRAFT ICING

- Effect of curvature in the numerical simulation of an electrothermal deicer pad
[BTN-95-EIX95182619219] p 276 A95-76645
Aerodynamics of a finite wing with simulated ice
[BTN-95-EIX95182619227] p 270 A95-76653
Additional improvements to the NASA Lewis ice accretion code LEWICE
[NASA-TM-106849] p 309 N95-22669
Collaborative research on aircraft icing and charging processes in ice
[AD-A285102] p 276 N95-23201

AIRCRAFT INDUSTRY

- Report of proceedings: Aviation Accident Investigation Symposium. Volume 2: Participant presentations
[PB94-917007] p 277 N95-23598

AIRCRAFT INSTRUMENTS

- Flight-deck displays on the Boeing 777
[BTN-95-EIX95142562402] p 286 A95-73438
Flight test evaluation of a 35 GHz forward looking altimeter for terrain avoidance
[BTN-95-EIX95212641071] p 287 A95-76736

AIRCRAFT LANDING

- Progress in high-lift aerodynamic calculations
[BTN-95-EIX95152582315] p 264 A95-73518

AIRCRAFT MAINTENANCE

- Maintenance challenges and trends
[BTN-95-EIX95182617808] p 261 A95-75753
Maintenance programs
[BTN-95-EIX95182617809] p 261 A95-75754
Aircraft stripping and painting
[BTN-95-EIX95182617810] p 300 A95-75755
Condition monitoring and diagnostics
[BTN-95-EIX95182617811] p 261 A95-75756
Artificial intelligence for turboprop engine maintenance
[BTN-95-EIX95182617812] p 288 A95-75757
POD assessment of NDI procedures using a round robin test
[AGARD-R-809] p 315 N95-23602
Enhancement of F/A-18 operational flight measurements: Data report for phase 1
[DSTO-TR-0049] p 286 N95-23666

AIRCRAFT MANEUVERS

- Functional agility metrics and optimal trajectory analysis
[BTN-95-EIX95182619121] p 321 A95-76598

- Kinematics and aerodynamics of velocity-vector roll
[BTN-95-EIX95182619126] p 291 A95-76603
- Optimal lateral-escape maneuvers for microburst encounters during final approach
[BTN-95-EIX95182619127] p 276 A95-76604
- Multiaxis pilot ratings for damaged aircraft
[BTN-95-EIX95182619128] p 269 A95-76605
- Automatic formation flight control
[BTN-95-EIX95182619153] p 292 A95-76630
- Rolling maneuver load alleviation using active controls
[BTN-95-EIX9518261917] p 270 A95-76643
- Application of Navier-Stokes aeroelastic methods to improve fighter wing maneuver performance
[BTN-95-EIX95182619218] p 284 A95-76644

AIRCRAFT MODELS

- SEM representation of the early and late time fields scattered from wire targets
[BTN-94-EIX94381353142] p 306 A95-74496
- Some aspects of the aerodynamics of separating strap-ons
[BTN-95-EIX95182617464] p 298 A95-75735
- Aeroelastic vehicle multivariable control synthesis with analytical robustness evaluation
[BTN-95-EIX95182619115] p 321 A95-76592
- Drag function modeling for air traffic simulation
[BTN-95-EIX95182619154] p 279 A95-76631
- An investigation of helicopter dynamic coupling using an analytical model
[NASA-CR-197420] p 285 N95-23217
- Inner loop flight control for the High-Speed Civil Transport
p 293 N95-23314

AIRCRAFT NOISE

- The use of cowl camber and taper to reduce rotor/stator interaction noise
[NASA-CR-195421] p 323 N95-22675

AIRCRAFT PARTS

- Review of some results of the author's fatigue investigations with applications in engineering and material science
[TAE-698] p 316 N95-23662

AIRCRAFT PERFORMANCE

- An unmanned air vehicle concept with tipjet drive
[HTN-95-80858] p 283 A95-75100
- Multiaxis pilot ratings for damaged aircraft
[BTN-95-EIX95182619128] p 269 A95-76605
- Drag function modeling for air traffic simulation
[BTN-95-EIX95182619154] p 279 A95-76631
- Application of Navier-Stokes aeroelastic methods to improve fighter wing maneuver performance
[BTN-95-EIX95182619218] p 284 A95-76644
- Tracking of raindrops in flow over an airfoil
[BTN-95-EIX95182619221] p 308 A95-76647
- Guidance and control requirements for high-speed Rollout and Turnoff (ROTO)
[NASA-CR-195026] p 292 N95-22674
- Direct adaptive performance optimization of subsonic transports: A periodic perturbation technique
[NASA-TM-4676] p 284 N95-22829
- Design of high performance multivariable control systems for supermaneuverable aircraft at high angle of attack
[NASA-CR-197661] p 293 N95-22908

AIRCRAFT POWER SUPPLIES

- Motor drive technologies for the power-by-wire (PBW) program: Options, trends and tradeoffs
[NASA-TM-106885] p 295 N95-23671

AIRCRAFT PRODUCTION

- Automatic riveting cell for commercial aircraft floor grid assembly
[BTN-95-EIX95182617807] p 261 A95-75752

AIRCRAFT RELIABILITY

- Labs behind Boeing's new 777
[BTN-95-EIX95142562403] p 280 A95-73437
- Oklahoma City air logistics center (USAF) aging aircraft corrosion program
p 262 N95-23519

AIRCRAFT SAFETY

- Maintenance programs
[BTN-95-EIX95182617809] p 261 A95-75754
- Additional improvements to the NASA Lewis ice accretion code LEWICE
[NASA-TM-106849] p 309 N95-22669
- Handling qualities of the High Speed Civil Transport
p 294 N95-23325
- Report of proceedings: Aviation Accident Investigation Symposium. Volume 2: Participant presentations
[PB94-917007] p 277 N95-23598
- Aircraft fires, smoke toxicity, and survival: An overview
[DOT/FAA/AM-95/8] p 277 N95-24024
- A multibody/finite element analysis approach for modeling of crash dynamic responses
[NIAR-94-3] p 277 N95-24050
- Aviation Accident Investigation Symposium. Volume 1: Industry recommendations and Safety Board responses
[PB94-917005] p 278 N95-24105

AIRCRAFT SPECIFICATIONS

- Integrated flight/propulsion control for helicopters
[HTN-95-80854] p 290 A95-75096

AIRCRAFT STABILITY

- Postinstability behavior of a two-dimensional airfoil with a structural nonlinearity
[BTN-95-EIX95152582337] p 266 A95-73539
- Method for the prediction of the onset of wing rock
[BTN-95-EIX95152582342] p 282 A95-73544
- Effect of leeward flow dividers on the wing rock of a delta wing
[BTN-95-EIX95152582347] p 282 A95-73549
- System for determining aerodynamic imbalance
[NASA-CASE-ARC-11913-1] p 311 N95-23377
- Aerodynamic flight control to increase payload capability of future launch vehicles
[NASA-CR-197704] p 300 N95-24032

AIRCRAFT STRUCTURES

- MIL-HDBK-5 design allowables for fibre/metal laminates: ARALL 2 and ARALL 3
[BTN-94-EIX94371346933] p 300 A95-73345
- Experimental evaluation of a box beam specifically tailored for chordwise deformation
[BTN-95-EIX95182619088] p 283 A95-75773
- Review of aeronautical fatigue investigation in the Netherlands during the period March 1991-March 1993
[PB95-139184] p 285 N95-23161
- Double pass retroreflection for corrosion detection in aircraft structures
p 323 N95-23503
- Non-destructive detection of corrosion for life management
p 314 N95-23505
- Health and usage monitoring systems: Corrosion surveillance
p 262 N95-23506
- New nondestructive techniques for the detection and quantification of corrosion in aircraft structures
p 315 N95-23512
- Organic coating technology for the protection of aircraft against corrosion
p 303 N95-23513
- Corrosion detection and monitoring of aircraft structures: An overview
p 303 N95-23515
- Experience of in-service corrosion on military aircraft
p 303 N95-23516
- US Navy operating experience with new aircraft construction materials
p 303 N95-23517
- Oklahoma City air logistics center (USAF) aging aircraft corrosion program
p 262 N95-23519

AIRCRAFT WAKES

- Unsteady ground effects on aerodynamic coefficients of finite wings with camber
[BTN-95-EIX95182619233] p 271 A95-76659

AIRFIELD SURFACE MOVEMENTS

- Automation technology using Geographic Information System (GIS)
p 324 N95-23284

AIRFOIL OSCILLATIONS

- Computation of oscillating airfoil flows with one- and two-equation turbulence models
[BTN-95-EIX95152577588] p 263 A95-73494

AIRFOIL PROFILES

- Forebody flow control on a full-scale F/A-18 aircraft
[BTN-95-EIX95152582333] p 281 A95-73535
- Effect of curvature in the numerical simulation of an electrothermal de-icer pad
[BTN-95-EIX95182619219] p 276 A95-76645
- Control of flow separation in airfoil/wing design applications
p 274 N95-23294

AIRFOILS

- Two-equation turbulence model for unsteady separated flows around airfoils
[BTN-95-EIX95142553054] p 262 A95-73444
- Laplace interaction law for the computation of viscous airfoil flow in low- and high-speed aerodynamics
[BTN-95-EIX95142553037] p 263 A95-73461
- Aerodynamic shape optimization using preconditioned conjugate gradient methods
[BTN-95-EIX95142553033] p 263 A95-73465
- Eigenanalysis of unsteady flows about airfoils, cascades, and wings
[BTN-95-EIX95152577597] p 305 A95-73486
- Computation of oscillating airfoil flows with one- and two-equation turbulence models
[BTN-95-EIX95152577588] p 263 A95-73494
- Flow visualization studies on sidewall effects in two-dimensional transonic airfoil testing
[BTN-95-EIX95152582313] p 264 A95-73516
- Progress in high-lift aerodynamic calculations
[BTN-95-EIX95152582315] p 264 A95-73518
- Computation of the poststall behavior of a circulation controlled airfoil
[BTN-95-EIX95152582320] p 264 A95-73523
- Separation control on high-lift airfoils via micro-vortex generators
[BTN-95-EIX95152582326] p 265 A95-73529
- Study of an airfoil with a flap and spoiler
[BTN-95-EIX95152582327] p 265 A95-73530

- Effect of underwing frost on a transport aircraft airfoil at flight Reynolds number
[BTN-95-EIX95152582334] p 276 A95-73536
- Postinstability behavior of a two-dimensional airfoil with a structural nonlinearity
[BTN-95-EIX95152582337] p 266 A95-73539
- Turbulent transonic airfoil flow simulation using a pressure-based algorithm
[BTN-95-EIX95182619078] p 269 A95-75763
- Viscous-inviscid interaction method for unsteady low-speed airfoil flows
[BTN-95-EIX95182619093] p 269 A95-75778
- Tracking of raindrops in flow over an airfoil
[BTN-95-EIX95182619221] p 308 A95-76647
- Response of a nonrotating rotor blade to lateral turbulence. Part 2: Experiment
[BTN-95-EIX95182619229] p 284 A95-76655

AIRFRAME MATERIALS

- Technology reinvestment project's focus area: Affordable polymer matrix composites for airframe structures
[PB95-136032] p 324 N95-23168
- Corrosion detection and management of advanced airframe materials
[AGARD-CP-565] p 302 N95-23496
- The corrosion and protection of advanced aluminum-lithium airframe alloys
p 302 N95-23497
- Non-destructive detection of corrosion for life management
p 314 N95-23505
- New nondestructive techniques for the detection and quantification of corrosion in aircraft structures
p 315 N95-23512

AIRFRAMES

- An analytical and experimental investigation of the response of the curved, composite frame/skin specimens
[HTN-95-80857] p 283 A95-75099
- Integrated design of hypersonic waveriders including inlets and tailfins
[BTN-95-EIX9512645692] p 271 A95-76744
- Oklahoma City air logistics center (USAF) aging aircraft corrosion program
p 262 N95-23519

AIRLINE OPERATIONS

- Development of aeronautical mobile satellite services over the past thirty years
[BTN-95-EIX95152569458] p 305 A95-73498
- Containing military autotest cost growth through the use of commercial standard equipment architectures
[BTN-95-EIX95172595295] p 287 A95-75717
- Maintenance challenges and trends
[BTN-95-EIX95182617808] p 261 A95-75753
- Maintenance programs
[BTN-95-EIX95182617809] p 261 A95-75754
- Aircraft accident report. Runway overrun following rejected takeoff. Continental Airlines flight 795, McDonnell Douglas MD-82, N18835, LaGuardia Airport, Flushing, NY, 2 March 1994
[PB95-910401] p 277 N95-23609
- The airline quality report, 1994
[NIAR-94-11] p 277 N95-24012

AIRPORTS

- Evaluation of neutron techniques for illicit substance detection
[DE95-002988] p 300 N95-22764
- Automation technology using Geographic Information System (GIS)
p 324 N95-23284

AIRSPACE

- Oceanic operations: An authoritative guide to oceanic operations
[FAA-AFS-550] p 277 N95-24065

ALGORITHMS

- Efficient sensitivity analysis for rotary-wing aeromechanical problems
[BTN-95-EIX95152577585] p 264 A95-73497
- Application of the multigrid solution technique to hypersonic entry vehicles
[BTN-95-EIX95152583254] p 306 A95-73555
- Functional dependence of trajectory dispersion on initial condition errors
[BTN-95-EIX95152583263] p 298 A95-73564
- Optimization of contoured hypersonic scramjet inlets with a least-squares parabolized Navier-Stokes procedure
[HTN-95-20976] p 261 A95-74042
- Real-time estimation of atmospheric turbulence severity from in-situ aircraft measurements
[BTN-95-EIX95182619231] p 319 A95-76657
- Aerodynamic design optimization with sensitivity analysis and computational fluid dynamics
[NASA-CR-197419] p 274 N95-23218
- On-line, adaptive state estimator for active noise control
p 322 N95-23308
- Empirical results on scheduling and dynamic backtracking
p 299 N95-23761

ALTERNATING DIRECTION IMPLICIT METHODS

Convergence acceleration of implicit schemes in the presence of high aspect ratio grid cells p 313 N95-23446

ALTIMETERS

Assimilation of altimeter data in a quasi-geostrophic model of the Gulf Stream system: A dynamical perspective [NASA-CR-196313] p 320 N95-23766

ALTIMETRY

Geoid lineations of 1000 km wavelength over the central Pacific [HTN-95-11304] p 319 A95-77009

ALUMINUM

Corrosion protection measures for CFC/metal joints of fuel integral tank structures of advanced military aircraft p 303 N95-23510

ALUMINUM ALLOYS

Test method and test results for environmental assessment of aircraft materials p 302 N95-23509

ALUMINUM-LITHIUM ALLOYS

The corrosion and protection of advanced aluminum-lithium airframe alloys p 302 N95-23497

ANGLE OF ATTACK

Aerodynamic characteristics of a canard-controlled missile at high angles of attack [BTN-95-EIX95152583257] p 267 A95-73558

Improved version of the Naval Surface Warfare Center aeroprediction code (AP93) [BTN-95-EIX95152583260] p 267 A95-73561

Transient structure of vortex breakdown on a delta wing [BTN-95-EIX95182619073] p 268 A95-75758

Kinematics and aerodynamics of velocity-vector roll [BTN-95-EIX95182619126] p 291 A95-76603

Review and development of base pressure and base heating correlations in supersonic flow [BTN-95-EIX95212645688] p 271 A95-76740

Numerical investigation of supersonic flows around a spiked blunt body [BTN-95-EIX95212645690] p 271 A95-76742

Calculation of wing-alone aerodynamics to high angles of attack [BTN-95-EIX95212645713] p 261 A95-76765

Wing pressure distributions from subsonic tests of a high-wing transport model --- in the Langley 14- by 22-Foot Subsonic Wind Tunnel [NASA-TM-4583] p 272 N95-22802

Flight test of the X-29A at high angle of attack: Flight dynamics and controls [NASA-TP-3537] p 284 N95-22806

An assessment of viscous effects in computational simulation of benign and burst vortex flows on generic fighter wind-tunnel models using TEAM code [NASA-CR-4650] p 273 N95-23185

Aerodynamic surface distension system for high angle of attack forebody vortex control [NASA-CASE-ARC-11979-1] p 286 N95-23390

ANNUAL VARIATIONS

Possible effects of CO₂ increase on the high-speed civil transport impact on ozone [HTN-95-60779] p 317 A95-75976

ANTI-AIRCRAFT MISSILES

Switched bias proportional navigation for homing guidance against highly maneuvering targets [BTN-95-EIX95182619145] p 279 A95-76622

APPLICATIONS OF MATHEMATICS

Preparation of course materials: Elementary mathematics of powered flight p 324 N95-23320

APPROACH

Optimal lateral-escape maneuvers for microburst encounters during final approach [BTN-95-EIX95182619127] p 276 A95-76604

APPROXIMATION

Adaptive finite element method for turbulent flow near a propeller [BTN-95-EIX95142553038] p 305 A95-73460

Application of the multigrid solution technique to hypersonic entry vehicles [BTN-95-EIX95152583254] p 306 A95-73555

Multiple site fatigue damage in fuselage skin splices: Experimental simulation and theoretical prediction [BTN-95-EIX95152584676] p 276 A95-73588

Application of a control-volume-based finite-element formulation to the shock tube problem [BTN-95-EIX95182619099] p 295 A95-76584

ARAMID FIBER COMPOSITES

MIL-HDBK-5 design allowables for fibre/metal laminates: ARALL 2 and ARALL 3 [BTN-94-EIX94371346933] p 300 A95-73345

ARCHITECTURE (COMPUTERS)

New commercial off-the-shelf testers are automatic and intelligent [BTN-95-EIX95172595292] p 287 A95-75720

ARGON

Hypersonic convective heat transfer over 140-deg blunt cones in different gases [BTN-95-EIX95152583253] p 306 A95-73554

ARTIFICIAL INTELLIGENCE

New commercial off-the-shelf testers are automatic and intelligent [BTN-95-EIX95172595292] p 287 A95-75720

Artificial intelligence for turboprop engine maintenance [BTN-95-EIX95182617812] p 288 A95-75757

ARTIFICIAL SATELLITES

Calculation of satellite drag coefficients [AD-A285118] p 300 N95-23781

ASCENT PROPULSION SYSTEMS

Fourth-generation Mars vehicle concepts [BTN-95-EIX95152583267] p 298 A95-73568

ASCENT TRAJECTORIES

Dynamical instability of the aerogravity assist maneuver [BTN-95-EIX95152583282] p 298 A95-73583

ASPECT RATIO

Calculation of wing-alone aerodynamics to high angles of attack [BTN-95-EIX95212645713] p 261 A95-76765

ASSIMILATION

Assimilation of altimeter data in a quasi-geostrophic model of the Gulf Stream system: A dynamical perspective [NASA-CR-196313] p 320 N95-23766

ATLANTIC OCEAN

Oceanic operations: An authoritative guide to oceanic operations [FAA-AFS-550] p 277 N95-24065

ATMOSPHERIC CHEMISTRY

Possible effects of CO₂ increase on the high-speed civil transport impact on ozone [HTN-95-60779] p 317 A95-75976

Compendium of NASA data base for the Global Tropospheric Experiment's Pacific Exploratory Mission West-A (PEM West-A) [NASA-TM-109177] p 320 N95-23009

ATMOSPHERIC COMPOSITION

Possible effects of CO₂ increase on the high-speed civil transport impact on ozone [HTN-95-60779] p 317 A95-75976

Compendium of NASA data base for the Global Tropospheric Experiment's Pacific Exploratory Mission West-A (PEM West-A) [NASA-TM-109177] p 320 N95-23009

ATMOSPHERIC EFFECTS

Test method and test results for environmental assessment of aircraft materials p 302 N95-23509

ATMOSPHERIC ENTRY

Application of the multigrid solution technique to hypersonic entry vehicles [BTN-95-EIX95152583254] p 306 A95-73555

ATMOSPHERIC MODELS

Hypersonic convective heat transfer over 140-deg blunt cones in different gases [BTN-95-EIX95152583253] p 306 A95-73554

Thundercloud electric field modeling for the ionosphere-Earth region. 1: Dependence on cloud charge distribution [HTN-95-41223] p 317 A95-75035

Possible effects of CO₂ increase on the high-speed civil transport impact on ozone [HTN-95-60779] p 317 A95-75976

Estimates of total organic and inorganic chlorine in the lower stratosphere from in situ and flask measurements during AASE 2 [HTN-95-A0861] p 317 A95-76265

Sensitivity of two-dimensional model predictions of ozone response to stratospheric aircraft: An update [HTN-95-A0863] p 318 A95-76267

Diurnal variation of lee vortices in Taiwan and the surrounding area [HTN-95-91363] p 318 A95-76394

Assimilation of altimeter data in a quasi-geostrophic model of the Gulf Stream system: A dynamical perspective [NASA-CR-196313] p 320 N95-23766

ATMOSPHERIC TURBULENCE

Response of a nonrotating rotor blade to lateral turbulence. Part 2: Experiment [BTN-95-EIX95182619229] p 284 A95-76655

Real-time estimation of atmospheric turbulence severity from in-situ aircraft measurements [BTN-95-EIX95182619231] p 319 A95-76657

ATTITUDE (INCLINATION)

Dynamic response tests of inertial and optical wind-tunnel model attitude measurement devices [NASA-TM-109182] p 296 N95-23011

ATTITUDE CONTROL

Moving mass trim control for aerospace vehicles [DE95-002602] p 299 N95-23532

ATTITUDE INDICATORS

Dynamic response tests of inertial and optical wind-tunnel model attitude measurement devices [NASA-TM-109182] p 296 N95-23011

AUSTRALIA

AIRSAAR deployment in Australia, September 1993: Management and objectives p 321 N95-23948

AUTOMATED PILOT ADVISORY SYSTEM

Differential GPS and system integration of the Low Visibility Landing and Surface Operations (LVLASO) demonstration p 280 N95-23318

AUTOMATIC CONTROL

Automatic rrveting cell for commercial aircraft floor grid assembly [BTN-95-EIX95182617807] p 261 A95-75752

Cypher moves toward autonomous flight [HTN-95-41394] p 283 A95-76390

Automatic guidance and control for helicopter obstacle avoidance [BTN-95-EIX95182619130] p 291 A95-76607

Nonlinear system guidance in the presence of transmission zero dynamics [NASA-TM-4661] p 309 N95-22804

Performance of the 0.3-meter transonic cryogenic tunnel with air, nitrogen, and sulfur hexafluoride media under closed loop automatic control [NASA-CR-195052] p 310 N95-23257

AUTOMATIC FLIGHT CONTROL

Automatic formation flight control [BTN-95-EIX95182619153] p 292 A95-76630

AUTOMATIC PILOTS

Automatic guidance and control for helicopter obstacle avoidance [BTN-95-EIX95182619130] p 291 A95-76607

Automatic formation flight control [BTN-95-EIX95182619153] p 292 A95-76630

AUTOMATIC TEST EQUIPMENT

CASS: Design for supportability [BTN-95-EIX95172595296] p 287 A95-75716

Containing military autotest cost growth through the use of commercial standard equipment architectures [BTN-95-EIX95172595295] p 287 A95-75717

ATE enabling technologies [BTN-95-EIX95172595294] p 287 A95-75718

New commercial off-the-shelf testers are automatic and intelligent [BTN-95-EIX95172595292] p 287 A95-75720

AUTONOMOUS

New commercial off-the-shelf testers are automatic and intelligent [BTN-95-EIX95172595292] p 287 A95-75720

The role of flight progress strips in en route air traffic control: A time-series analysis [DOT/FAA/AM-95/4] p 280 N95-23565

AUTONOMOUS NAVIGATION

Cypher moves toward autonomous flight [HTN-95-41394] p 283 A95-76390

AUXILIARY POWER SOURCES

Motor drive technologies for the power-by-wire (PBW) program: Options, trends and tradeoffs [NASA-TM-106885] p 295 N95-23671

AVIONICS

Labs behind Boeing's new 777 [BTN-95-EIX95142562403] p 280 A95-73437

CASS: Design for supportability [BTN-95-EIX95172595296] p 287 A95-75716

Containing military autotest cost growth through the use of commercial standard equipment architectures [BTN-95-EIX95172595295] p 287 A95-75717

ATE enabling technologies [BTN-95-EIX95172595294] p 287 A95-75718

New commercial off-the-shelf testers are automatic and intelligent [BTN-95-EIX95172595292] p 287 A95-75720

Overview of AlliedSignal's avionics development in the CIS [BTN-95-EIX95212641069] p 287 A95-76734

Design of wide angle head up displays for synthetic vision [BTN-95-EIX95212641070] p 287 A95-76735

AXIAL LOADS

Validation of an effective flat cruciform-shaped specimen to study CFRP composite laminates under biaxial loading [BTN-95-EIX95152584677] p 282 A95-73589

AXISYMMETRIC BODIES

Supersonic near-wake afterbody boattailing effects on axisymmetric bodies [BTN-95-EIX95182617465] p 268 A95-75736

AXISYMMETRIC FLOW

Supersonic axisymmetric conical flow solutions for different ratios of specific heats [BTN-95-EIX95152583283] p 306 A95-73584

Supersonic jet noise reductions predicted with increased jet spreading rate [NASA-TM-106872] p 323 N95-23178

TIGER: A user-friendly interactive grid generation system for complicated turbomachinery and axis-symmetric configurations p 322 N95-23419
Validation of a Computational Fluid Dynamics (CFD) code for supersonic axisymmetric base flow p 315 N95-23652

B

BACKWASH

Sidewash on the vertical tail in subsonic and supersonic flows
[BTN-95-EIX95152582316] p 264 A95-73519

BAFFLES

Coupled FEM-BEM approach for mean flow effects on vibro-acoustic behavior of planar structures
[BTN-95-EIX95152577587] p 263 A95-73495

BALLISTIC TRAJECTORIES

Analytical solution and parameter estimation of projectile dynamics
[BTN-95-EIX95212645695] p 272 A95-76747

BALLISTIC VEHICLES

Moving mass trim control for aerospace vehicles
[DE95-002602] p 299 N95-23532

BALLISTICS

Analytical solution and parameter estimation of projectile dynamics
[BTN-95-EIX95212645695] p 272 A95-76747

BALLOON FLIGHT

Polar Patrol Balloon
[BTN-95-EIX95152582318] p 316 A95-73521

BANDWIDTH

Identification of higher order helicopter dynamics using linear modeling methods
[HTN-95-80851] p 290 A95-75093
Investigation of the effects of bandwidth and time delay on helicopter roll-axis handling qualities
[HTN-95-80853] p 290 A95-75095

BARIUM OXIDES

Phonon characteristics of high (T sub c) superconductors from neutron Doppler broadening measurements
[DE95-003703] p 324 N95-24076

BASE FLOW

Base drag prediction on missile configurations
[BTN-95-EIX95152583256] p 266 A95-73557
Validation of a Computational Fluid Dynamics (CFD) code for supersonic axisymmetric base flow p 315 N95-23652

BASE HEATING

Review and development of base pressure and base heating correlations in supersonic flow
[BTN-95-EIX95212645688] p 271 A95-76740

BASE PRESSURE

Review and development of base pressure and base heating correlations in supersonic flow
[BTN-95-EIX95212645688] p 271 A95-76740

BEACONS

Cueing light configuration for aircraft navigation
[NASA-CASE-ARC-11982-1] p 280 N95-23393

BEARINGLESS ROTORS

Dynamic analysis of bearingless tail rotor blades based on nonlinear shell modes
[BTN-95-EIX95152582338] p 281 A95-73540

BEARINGS

Finite element model for a flexible non-symmetric rotor on distributed bearing: A stability study
[BTN-94-EIX94381352212] p 306 A95-74612

BELL AIRCRAFT

Improving prediction: The incorporation of simplified rotor dynamics in a mathematical model of the bell 412HP
[BTN-95-EIX95152584679] p 282 A95-73591

BEND TESTS

Experimental evaluation of a box beam specifically tailored for chordwise deformation
[BTN-95-EIX95182619088] p 283 A95-75773

BENDING

Experimental evaluation of a box beam specifically tailored for chordwise deformation
[BTN-95-EIX95182619088] p 283 A95-75773

BLADE SLAP NOISE

Sensitivity of acoustic predictions to variation of input parameters
[HTN-95-80855] p 267 A95-75097

BLADE TIPS

Supersonic flow and shock formation in turbine tip gaps p 312 N95-23429

BLADE-VORTEX INTERACTION

Analysis of a higher harmonic control test to reduce blade vortex interaction noise
[BTN-95-EIX95152582330] p 265 A95-73532

BLOWING

Forebody flow control on a full-scale F/A-18 aircraft
[BTN-95-EIX95152582333] p 281 A95-73535

Pneumatic concept for tip-stall control of cranked-arrow wings
[BTN-95-EIX95152582335] p 281 A95-73537

BLUFF BODIES

Grid refinement test of time-periodic flows over bluff bodies
[BTN-94-EIX94401378822] p 307 A95-76491

BLUNT BODIES

Shock tunnel measurements of hypervelocity blunted cone drag
[BTN-95-EIX95152577606] p 305 A95-73477
Zonally decoupled direct simulation Monte Carlo solutions of hypersonic blunt-body wake flows
[BTN-95-EIX95182617458] p 268 A95-75729
Numerical investigation of supersonic flows around a spiked blunt body
[BTN-95-EIX95212645690] p 271 A95-76742

BO-105 HELICOPTER

Analysis of a higher harmonic control test to reduce blade vortex interaction noise
[BTN-95-EIX95152582330] p 265 A95-73532

BODIES OF REVOLUTION

CFD optimization of a theoretical minimum-drag body
[BTN-95-EIX95182619234] p 308 A95-76660

BODY-WING CONFIGURATIONS

Improved version of the Naval Surface Warfare Center aeroprediction code (AP93)
[BTN-95-EIX95152583260] p 267 A95-73561
Wing vertical position effects on wing-body carryover for noncircular missiles
[BTN-95-EIX95182617462] p 268 A95-75733

BOEING AIRCRAFT

H-76B fantail demonstrator composite fan blade fabrication
[HTN-95-80856] p 283 A95-75098

BOEING 737 AIRCRAFT

Differential GPS and system integration of the Low Visibility Landing and Surface Operations (LVLASO) demonstration p 280 N95-23318

BOEING 777 AIRCRAFT

Labs behind Boeing's new 777
[BTN-95-EIX95142562403] p 280 A95-73437
Flight-deck displays on the Boeing 777
[BTN-95-EIX95142562402] p 286 A95-73438

BOMBS (ORDNANCE)

Aerodynamic characteristics of external store configurations at low speeds
[BTN-95-EIX95182619230] p 271 A95-76656

BOOSTER ROCKET ENGINES

Aerodynamic design of pegasus: Concept to flight with computational fluid dynamics
[BTN-95-EIX95182617463] p 298 A95-75734
Some aspects of the aerodynamics of separating strap-ons
[BTN-95-EIX95182617464] p 298 A95-75735

BOUNDARY CONDITIONS

Determination of wall boundary conditions for high-speed-ratio direct simulation Monte Carlo calculations
[BTN-95-EIX95182617457] p 267 A95-75728
Observations on using experimental data as boundary conditions for computations
[BTN-95-EIX95182619103] p 321 A95-76588
Sensitivity of combustion-acoustic instabilities to boundary conditions for premixed gas turbine combustors
[NASA-TM-106890] p 289 N95-23550

BOUNDARY ELEMENT METHOD

Coupled FEM-BEM approach for mean flow effects on vibro-acoustic behavior of planar structures
[BTN-95-EIX95152577587] p 263 A95-73495

BOUNDARY LAYER CONTROL

Flow structure in the wake of a wishbone vortex generator
[BTN-95-EIX95142553044] p 304 A95-73454
Separation control on high-lift airfoils via micro-vortex generators
[BTN-95-EIX95152582326] p 265 A95-73529
Forebody flow control on a full-scale F/A-18 aircraft
[BTN-95-EIX95152582333] p 281 A95-73535
Supersonic laminar flow control research
[NASA-CR-197938] p 275 N95-23669

BOUNDARY LAYER EQUATIONS

An approximate theoretical method for modeling the static thrust performance of non-axisymmetric two-dimensional convergent-divergent nozzles
[NASA-CR-195050] p 273 N95-23193

BOUNDARY LAYER FLOW

Analytical study of the neutral stability of a model hypersonic boundary layer
[BTN-95-EIX95152577589] p 263 A95-73493
Flow visualization studies on sidewall effects in two-dimensional transonic airfoil testing
[BTN-95-EIX95152582313] p 264 A95-73516
Flow study of supersonic wing-nacelle configuration
[BTN-95-EIX95152582344] p 266 A95-73546

Active control of panel vibrations induced by a boundary layer flow
[NASA-CR-197867] p 273 N95-23182

BOUNDARY LAYER SEPARATION

Computation of the poststall behavior of a circulation controlled airfoil
[BTN-95-EIX95152582320] p 264 A95-73523
Experimental investigation of the flowfield about an upswept afterbody
[BTN-95-EIX95152582321] p 265 A95-73524
Separation control on high-lift airfoils via micro-vortex generators
[BTN-95-EIX95152582326] p 265 A95-73529
Study of an airfoil with a flap and spoiler
[BTN-95-EIX95152582327] p 265 A95-73530
Computational study of plume-induced separation on a hypersonic powered model
[BTN-95-EIX95152582346] p 266 A95-73548
Scaling of incipient separation in supersonic/transonic speed laminar flows
[BTN-95-EIX95182619104] p 269 A95-76589
Aerodynamics of a finite wing with simulated ice
[BTN-95-EIX95182619227] p 270 A95-76653
Control of flow separation in airfoil/wing design applications p 274 N95-23294

BOUNDARY LAYER STABILITY

Supersonic laminar flow control research
[NASA-CR-197938] p 275 N95-23669

BOUNDARY LAYER TRANSITION

Hypersonic rarefied flow past spheres including wake structure
[BTN-95-EIX95152583250] p 305 A95-73551
Scaling of incipient separation in supersonic/transonic speed laminar flows
[BTN-95-EIX95182619104] p 269 A95-76589
Crossflow instability control on a swept-wing: Preliminary studies p 274 N95-23283
High-lift flow-physics flight experiments on a subsonic civil transport aircraft (B737-100) p 275 N95-23333
Supersonic laminar flow control research
[NASA-CR-197938] p 275 N95-23669

BOUNDARY LAYERS

Laplace interaction law for the computation of viscous airfoil flow in low- and high-speed aerodynamics
[BTN-95-EIX95142553037] p 263 A95-73461
Simulating heat addition via mass addition in constant area compressible flows
[BTN-95-EIX95182619100] p 307 A95-76585
Scaling of incipient separation in supersonic/transonic speed laminar flows
[BTN-95-EIX95182619104] p 269 A95-76589
Optimized design of a hypersonic nozzle p 297 N95-23304

BOX BEAMS

Experimental evaluation of a box beam specifically tailored for chordwise deformation
[BTN-95-EIX95182619088] p 283 A95-75773
Flutter analysis of composite box beams
[NASA-CR-197931] p 294 N95-23392

BUFFETING

Preliminary identification of buffet problems in high speed civil transport p 294 N95-23319

BUNCHING

Effects of satellite bunching on the probability of collision in geosynchronous orbit
[BTN-95-EIX95152583276] p 298 A95-73577

BURGER EQUATION

Aeroacoustic model for weak shock waves based on Burgers equation
[BTN-95-EIX95182619076] p 269 A95-75761

C

CALIBRATING

Design of a variable area diffuser for a 15-inch Mach 6 open-jet tunnel p 297 N95-23309

CALIFORNIA

A comparison of some aerodynamic resistance methods using measurements over cotton and grass from the 1991 California ozone deposition experiment
[HTN-95-11295] p 319 A95-77000

CAMBER

The use of cowl camber and taper to reduce rotor/stator interaction noise
[NASA-CR-195421] p 323 N95-22675

CAMBERED WINGS

Unsteady ground effects on aerodynamic coefficients of finite wings with camber
[BTN-95-EIX95182619233] p 271 A95-76659

CANARD CONFIGURATIONS

Aerodynamic characteristics of a canard-controlled missile at high angles of attack
[BTN-95-EIX95152583257] p 267 A95-73558
Inner loop flight control for the High-Speed Civil Transport p 293 N95-23314

CARBON DIOXIDE

Hypersonic convective heat transfer over 140-deg blunt cones in different gases

[BTN-95-EIX95152583253] p 306 A95-73554

Possible effects of CO₂ increase on the high-speed civil transport impact on ozone

[HTN-95-60779] p 317 A95-75976

CARBON FIBER REINFORCED PLASTICS

Mishap risk control for advanced aerospace/composite materials

p 301 N95-23031

CARBON FIBERS

Corrosion protection measures for CFC/metal joints of fuel integral tank structures of advanced military aircraft

p 303 N95-23510

CARBON STEELS

In-situ detection of surface passivation or activation and of localized corrosion: Experiences and prospectives in aircraft

p 302 N95-23508

CARGO

Evaluation of neutron techniques for illicit substance detection

[DE95-002988] p 300 N95-22764

CARIBBEAN REGION

Oceanic operations: An authoritative guide to oceanic operations

[FAA-AFS-550] p 277 N95-24065

CASCADE FLOW

Eigenanalysis of unsteady flows about airfoils, cascades, and wings

[BTN-95-EIX95152577597] p 305 A95-73486

Numerical computation of aerodynamics and heat transfer in a turbine cascade and a turn-around duct using advanced turbulence models

p 313 N95-23444

User's guide for ECAP2D: An Euler unsteady aerodynamic and aeroelastic analysis program for two dimensional oscillating cascades, version 1.0

[NASA-CR-189146] p 316 N95-24189

CASES (CONTAINERS)

NASA low-speed axial compressor for fundamental research

[NASA-TM-4635] p 296 N95-23192

CAVITATION FLOW

Cavitation modeling in Euler and Navier-Stokes codes

p 315 N95-23630

CAVITIES

Cavitation modeling in Euler and Navier-Stokes codes

p 315 N95-23630

CAVITY FLOW

Observations on using experimental data as boundary conditions for computations

[BTN-95-EIX95182619103] p 321 A95-76588

A time-accurate finite volume method valid at all flow velocities

p 314 N95-23447

CERAMIC COATINGS

Compliant interlayer

[BTN-95-EIX95142562401] p 304 A95-73439

CERAMICS

Compliant interlayer

[BTN-95-EIX95142562401] p 304 A95-73439

CHANGE DETECTION

Real-time estimation of atmospheric turbulence severity from in-situ aircraft measurements

[BTN-95-EIX95182619231] p 319 A95-76657

CHARGE DISTRIBUTION

Thundercloud electric field modeling for the ionosphere-Earth region. 1: Dependence on cloud charge distribution

[HTN-95-41223] p 317 A95-75035

CHARGE TRANSFER

Collaborative research on aircraft icing and charging processes in ice

[AD-A285102] p 276 N95-23201

CHEMICAL COMPOSITION

Possible effects of CO₂ increase on the high-speed civil transport impact on ozone

[HTN-95-60779] p 317 A95-75976

CHEMICAL EXPLOSIONS

Evaluation of neutron techniques for illicit substance detection

[DE95-002988] p 300 N95-22764

CHLORINE COMPOUNDS

Estimates of total organic and inorganic chlorine in the lower stratosphere from in situ and flask measurements during AASE 2

[HTN-95-A0861] p 317 A95-76265

CIVIL AVIATION

Development of aeronautical mobile satellite services over the past thirty years

[BTN-95-EIX95152569458] p 305 A95-73498

Containing military autotest cost growth through the use of commercial standard equipment architectures

[BTN-95-EIX95172595295] p 287 A95-75717

Maintenance challenges and trends

[BTN-95-EIX95182617808] p 261 A95-75753

Maintenance programs

[BTN-95-EIX95182617809] p 261 A95-75754

Possible effects of CO₂ increase on the high-speed civil transport impact on ozone

[HTN-95-60779] p 317 A95-75976

Inner loop flight control for the High-Speed Civil Transport

p 293 N95-23314

Handling qualities of the High Speed Civil Transport

p 294 N95-23325

The airline quality report, 1994

[NIAR-94-11] p 277 N95-24012

Oceanic operations: An authoritative guide to oceanic operations

[FAA-AFS-550] p 277 N95-24065

A review of civil aviation fatal accidents in which lost/disoriented was a cause/factor: 1981-1990

[DOT/FAA/AM-95/1] p 278 N95-24071

CLEAN ROOMS

Measurement of particle emissions from clean room gas-handling components

[BTN-94-EIX94381359040] p 295 A95-74554

Measurement of moisture and total hydrocarbon contributions by valves used in clean room gas-delivery systems

[BTN-94-EIX94381359041] p 295 A95-74629

CLOUD COVER

Diurnal variation of lee vortices in Taiwan and the surrounding area

[HTN-95-91363] p 318 A95-76394

CLOUD SEEDING

A new generation of instruments for flying laboratories

[BTN-94-EIX94401363947] p 317 A95-75532

CLUTTER

Maximum-likelihood spectral estimation and adaptive filtering techniques with application to airborne Doppler weather radar

[NASA-CR-197699] p 316 N95-23670

COATING

Organic coating technology for the protection of aircraft against corrosion

p 303 N95-23513

Corrosion in service experience with aircraft in France

p 303 N95-23518

COCKPITS

Flight-deck displays on the Boeing 777

[BTN-95-EIX95142562402] p 286 A95-73438

Differential GPS and system integration of the Low Visibility Landing and Surface Operations (LVLASO) demonstration

p 280 N95-23318

COLLISION AVOIDANCE

Automatic guidance and control for helicopter obstacle avoidance

[BTN-95-EIX95182619130] p 291 A95-76607

Flight test evaluation of a 35 GHz forward looking altimeter for terrain avoidance

[BTN-95-EIX95212641071] p 287 A95-76736

COLLISIONS

Effects of satellite bunching on the probability of collision in geosynchronous orbit

[BTN-95-EIX95152583276] p 298 A95-73577

COMBUSTION

Modeling aerosol emissions from the combustion of composite materials

p 301 N95-23038

COMBUSTION CHAMBERS

Simulating heat addition via mass addition in constant area compressible flows

[BTN-95-EIX95182619100] p 307 A95-76585

Sensitivity of combustion-acoustic instabilities to boundary conditions for premixed gas turbine combustors

[NASA-TM-106890] p 289 N95-23550

COMBUSTION EFFICIENCY

Sensitivity of combustion-acoustic instabilities to boundary conditions for premixed gas turbine combustors

[NASA-TM-106890] p 289 N95-23550

COMBUSTION PRODUCTS

Aircraft fires, smoke toxicity, and survival: An overview

[DOT/FAA/AM-95/8] p 277 N95-24024

COMBUSTION STABILITY

Sensitivity of combustion-acoustic instabilities to boundary conditions for premixed gas turbine combustors

[NASA-TM-106890] p 289 N95-23550

COMMERCIAL AIRCRAFT

Automatic riveting cell for commercial aircraft floor grid assembly

[BTN-95-EIX95182617807] p 261 A95-75752

Maintenance challenges and trends

[BTN-95-EIX95182617808] p 261 A95-75753

Maintenance programs

[BTN-95-EIX95182617809] p 261 A95-75754

Preparation of course materials: Elementary mathematics of powered flight

p 324 N95-23320

Aircraft accident report. Runway overrun following rejected takeoff. Continental airlines flight 795, McDonnell Douglas MD-82, N18835, LaGuardia Airport, Flushing, NY, 2 March 1994

[PB95-910401] p 277 N95-23609

COMMONWEALTH OF INDEPENDENT STATES

Overview of AlliedSignal's avionics development in the CIS

[BTN-95-EIX95212641069] p 287 A95-76734

COMPONENT RELIABILITY

Mechanical system reliability and risk assessment

[BTN-95-EIX95142553046] p 304 A95-73452

COMPOSITE MATERIALS

Modeling aerosol emissions from the combustion of composite materials

p 301 N95-23038

Review of aeronautical fatigue investigation in the Netherlands during the period March 1991-March 1993

[PB95-139184] p 285 N95-23161

COMPOSITE STRUCTURES

Nonlinear angle of twist of advanced composite wing boxes under pure torsion

[BTN-95-EIX95152582323] p 281 A95-73526

Static aeroelastic characteristics of a composite wing

[BTN-95-EIX95152582340] p 282 A95-73542

H-76B fantail demonstrator composite fan blade fabrication

[HTN-95-80856] p 283 A95-75098

Experimental evaluation of a box beam specifically tailored for chordwise deformation

[BTN-95-EIX95182619088] p 283 A95-75773

Mishap risk control for advanced aerospace/composite materials

p 301 N95-23031

Development and verification of a resin film infusion/resin transfer molding simulation model for fabrication of advanced textile composites

[NASA-CR-197439] p 301 N95-23179

Thin tailored composite wing for civil tiltrotor

p 285 N95-23317

US Navy operating experience with new aircraft construction materials

p 303 N95-23517

COMPRESSIBLE BOUNDARY LAYER

Effects of expansions on a supersonic boundary layer: Surface pressure measurements

[BTN-95-EIX95142553036] p 263 A95-73462

COMPRESSIBLE FLOW

Computation of oscillating airfoil flows with one- and two-equation turbulence models

[BTN-95-EIX95152577588] p 263 A95-73494

Supersonic axisymmetric conical flow solutions for different ratios of specific heats

[BTN-95-EIX95152583283] p 306 A95-73584

Multigrid solution of compressible turbulent flow on unstructured meshes using a two-equation model

[BTN-94-EIX94401378794] p 307 A95-76484

Comparison of linear stability results with flight transition data

[BTN-95-EIX95182619097] p 283 A95-76582

Application of a control-volume-based finite-element formulation to the shock tube problem

[BTN-95-EIX95182619099] p 295 A95-76584

An approximate theoretical method for modeling the static thrust performance of non-axisymmetric two-dimensional convergent-divergent nozzles

[NASA-CR-195050] p 273 N95-23193

COMPRESSOR BLADES

NASA low-speed axial compressor for fundamental research

[NASA-TM-4635] p 296 N95-23192

COMPRESSORS

Static pressure distribution in the inlet of a helicopter turbine compressor

[BTN-95-EIX95152582339] p 266 A95-73541

COMPUTATIONAL FLUID DYNAMICS

Adaptive finite element method for turbulent flow near a propeller

[BTN-95-EIX95142553038] p 305 A95-73460

Laplace interaction law for the computation of viscous airfoil flow in low- and high-speed aerodynamics

[BTN-95-EIX95142553037] p 263 A95-73461

Effects of spatial order of accuracy on the computation of vortical flowfields

[BTN-95-EIX95152577604] p 305 A95-73479

Eigenanalysis of unsteady flows about airfoils, cascades, and wings

[BTN-95-EIX95152577597] p 305 A95-73486

Progress in high-lift aerodynamic calculations

[BTN-95-EIX95152582315] p 264 A95-73518

Higher-order viscous shock-layer solutions for high-altitude flows

[BTN-95-EIX95152583255] p 306 A95-73556

Base drag prediction on missile configurations

[BTN-95-EIX95152583256] p 266 A95-73557

Predicting exhaust plume boundaries with supersonic external flows

[BTN-95-EIX95152583258] p 297 A95-73559

Three-dimensional structure of a supersonic jet impinging on an inclined plate

[BTN-95-EIX95152583259] p 267 A95-73560

- Optimization of contoured hypersonic scramjet inlets with a least-squares parabolized Navier-Stokes procedure
[HTN-95-20976] p 261 A95-74042
- Zonally decoupled direct simulation Monte Carlo solutions of hypersonic blunt-body wake flows
[BTN-95-EIX95182617458] p 268 A95-75729
- Convective and radiative heat transfer analysis for the fire 2 forebody
[BTN-95-EIX95182617460] p 268 A95-75731
- Aerodynamic design of pegasus: Concept to flight with computational fluid dynamics
[BTN-95-EIX95182617463] p 298 A95-75734
- Application of wall functions to generalized nonorthogonal curvilinear coordinate systems
[BTN-95-EIX95182619077] p 307 A95-75762
- Turbulent transonic airfoil flow simulation using a pressure-based algorithm
[BTN-95-EIX95182619078] p 269 A95-75763
- Simulation of transverse gas injection in turbulent supersonic air flows
[BTN-95-EIX95182619080] p 269 A95-75765
- Viscous-inviscid interaction method for unsteady low-speed airfoil flows
[BTN-95-EIX95182619093] p 269 A95-75778
- Multigrid solution of compressible turbulent flow on unstructured meshes using a two-equation model
[BTN-94-EIX94401378794] p 307 A95-76484
- Grid refinement test of time-periodic flows over bluff bodies
[BTN-94-EIX94401378822] p 307 A95-76491
- Comparison of linear stability results with flight transition data
[BTN-95-EIX95182619097] p 283 A95-76582
- Application of a control-volume-based finite-element formulation to the shock tube problem
[BTN-95-EIX95182619099] p 295 A95-76584
- CFD optimization of a theoretical minimum-drag body
[BTN-95-EIX95182619234] p 308 A95-76660
- Simulation on the 3-D turbulent flow in the passages of finocyl grain
[BTN-95-EIX95202638962] p 279 A95-76674
- Particle kinetic simulation of high altitude hypervelocity flight
[NASA-CR-197383] p 309 N95-22481
- Euler Technology Assessment program for preliminary aircraft design employing SPLITFLOW code with Cartesian unstructured grid method
[NASA-CR-4649] p 273 N95-22917
- A CFD study of complex missile and store configurations in relative motion
[NASA-CR-197912] p 285 N95-22949
- Mach 10 computational study of a three-dimensional scramjet inlet flow field
[NASA-TM-4602] p 309 N95-23015
- Euler technology assessment for preliminary aircraft design employing OVERFLOW code with multiblock structured-grid method
[NASA-CR-4651] p 273 N95-23095
- An assessment of viscous effects in computational simulation of benign and burst vortex flows on generic fighter wind-tunnel models using TEAM code
[NASA-CR-4650] p 273 N95-23185
- Mach 10 computational study of a three-dimensional scramjet inlet flow field
[NASA-TM-4602] p 310 N95-23210
- Aerodynamic design optimization with sensitivity analysis and computational fluid dynamics
[NASA-CR-197419] p 274 N95-23218
- TIGER: A user-friendly interactive grid generation system for complicated turbomachinery and axis-symmetric configurations
p 322 N95-23419
- Three-dimensional Navier-Stokes analysis and redesign of an imbedded bellmouth nozzle in a turbine cascade inlet section
p 311 N95-23423
- Supersonic flow and shock formation in turbine tip gaps
p 312 N95-23429
- CFD analysis of turbopump volutes
p 312 N95-23436
- Convergence acceleration of implicit schemes in the presence of high aspect ratio grid cells
p 313 N95-23446
- A time-accurate finite volume method valid at all flow velocities
p 314 N95-23447
- A study of the vortex flow over 76/40-deg double-delta wing
[NASA-CR-195032] p 314 N95-23466
- Validation of a Computational Fluid Dynamics (CFD) code for supersonic axisymmetric base flow
p 315 N95-23652
- Supersonic laminar flow control research
[NASA-CR-197938] p 275 N95-23669
- COMPUTATIONAL GRIDS**
Adaptive finite element method for turbulent flow near a propeller
[BTN-95-EIX95142553038] p 305 A95-73460
- Laplace interaction law for the computation of viscous airfoil flow in low- and high-speed aerodynamics
[BTN-95-EIX95142553037] p 263 A95-73461
- Effects of spatial order of accuracy on the computation of vortical flowfields
[BTN-95-EIX95152577604] p 305 A95-73479
- Eigenanalysis of unsteady flows about airfoils, cascades, and wings
[BTN-95-EIX95152577597] p 305 A95-73486
- Progress in high-lift aerodynamic calculations
[BTN-95-EIX95152582315] p 264 A95-73518
- Unstructured grid solutions to a wing/pylon/store configuration
[BTN-95-EIX95152582322] p 265 A95-73525
- Navier-Stokes prediction of large-amplitude delta-wing roll oscillations
[BTN-95-EIX95152582329] p 281 A95-73531
- Application of the multigrid solution technique to hypersonic entry vehicles
[BTN-95-EIX95152583254] p 306 A95-73555
- Application of wall functions to generalized nonorthogonal curvilinear coordinate systems
[BTN-95-EIX95182619077] p 307 A95-75762
- Viscous-inviscid interaction method for unsteady low-speed airfoil flows
[BTN-95-EIX95182619093] p 269 A95-75778
- Grid refinement test of time-periodic flows over bluff bodies
[BTN-94-EIX94401378822] p 307 A95-76491
- Observations on using experimental data as boundary conditions for computations
[BTN-95-EIX95182619103] p 321 A95-76588
- CFD optimization of a theoretical minimum-drag body
[BTN-95-EIX95182619234] p 308 A95-76660
- A CFD study of complex missile and store configurations in relative motion
[NASA-CR-197912] p 285 N95-22949
- Mach 10 computational study of a three-dimensional scramjet inlet flow field
[NASA-TM-4602] p 310 N95-23210
- TIGER: A user-friendly interactive grid generation system for complicated turbomachinery and axis-symmetric configurations
p 322 N95-23419
- CFD analysis of turbopump volutes
p 312 N95-23436
- Convergence acceleration of implicit schemes in the presence of high aspect ratio grid cells
p 313 N95-23446
- COMPUTER AIDED DESIGN**
Functional agility metrics and optimal trajectory analysis
[BTN-95-EIX95182619121] p 321 A95-76598
- Euler Technology Assessment program for preliminary aircraft design employing SPLITFLOW code with Cartesian unstructured grid method
[NASA-CR-4649] p 273 N95-22917
- Euler technology assessment for preliminary aircraft design employing OVERFLOW code with multiblock structured-grid method
[NASA-CR-4651] p 273 N95-23095
- Control of flow separation in airfoil/wing design applications
p 274 N95-23294
- Thin tailored composite wing for civil tiltrotor
p 285 N95-23317
- CFD analysis of turbopump volutes
p 312 N95-23436
- COMPUTER GRAPHICS**
Pilot Weather Advisor system
[BTN-95-EIX95152582314] p 316 A95-73517
- COMPUTER PROGRAMS**
Unstructured grid solutions to a wing/pylon/store configuration
[BTN-95-EIX95152582322] p 265 A95-73525
- Improved version of the Naval Surface Warfare Center aeroprediction code (AP93)
[BTN-95-EIX95152583260] p 267 A95-73561
- Multiple site fatigue damage in fuselage skin splices: Experimental simulation and theoretical prediction
[BTN-95-EIX95152584676] p 276 A95-73588
- Aerodynamic design of pegasus: Concept to flight with computational fluid dynamics
[BTN-95-EIX95182617463] p 298 A95-75734
- CFD optimization of a theoretical minimum-drag body
[BTN-95-EIX95182619234] p 308 A95-76660
- Additional improvements to the NASA Lewis ice accretion code LEWICE
[NASA-TM-106849] p 309 N95-22669
- Automation technology using Geographic Information System (GIS)
p 324 N95-23284
- Residual strength of thin panels with cracks
p 311 N95-23311
- CFD analysis of turbopump volutes
p 312 N95-23436
- Enhanced analysis and users manual for radial-inflow turbine conceptual design code RTD
[NASA-CR-195454] p 275 N95-23462

- User's guide for ECAP2D: An Euler unsteady aerodynamic and aeroelastic analysis program for two dimensional oscillating cascades, version 1.0
[NASA-CR-189146] p 316 N95-24189
- COMPUTER SYSTEMS DESIGN**
CASS: Design for supportability
[BTN-95-EIX95172595296] p 287 A95-75716
- Containing military autotest cost growth through the use of commercial standard equipment architectures
[BTN-95-EIX95172595295] p 287 A95-75717
- ATE enabling technologies
[BTN-95-EIX95172595294] p 287 A95-75718
- New commercial off-the-shelf testers are automatic and intelligent
[BTN-95-EIX95172595292] p 287 A95-75720
- On-line, adaptive state estimator for active noise control
p 322 N95-23308
- COMPUTER SYSTEMS PERFORMANCE**
CASS: Design for supportability
[BTN-95-EIX95172595296] p 287 A95-75716
- COMPUTERIZED SIMULATION**
Navier-Stokes prediction of large-amplitude delta-wing roll oscillations
[BTN-95-EIX95152582329] p 281 A95-73531
- Aerodynamic characteristics of a hypersonic viscous optimized waverider at high altitudes
[BTN-95-EIX95152583251] p 266 A95-73552
- Hypersonic convective heat transfer over 140-deg blunt cones in different gases
[BTN-95-EIX95152583253] p 306 A95-73554
- Predicting exhaust plume boundaries with supersonic external flows
[BTN-95-EIX95152583258] p 297 A95-73559
- Improving prediction: The incorporation of simplified rotor dynamics in a mathematical model of the bell 412HP
[BTN-95-EIX95152584679] p 282 A95-73591
- New commercial off-the-shelf testers are automatic and intelligent
[BTN-95-EIX95172595292] p 287 A95-75720
- Determination of wall boundary conditions for high-speed-ratio direct simulation Monte Carlo calculations
[BTN-95-EIX95182617457] p 267 A95-75728
- Zonally decoupled direct simulation Monte Carlo solutions of hypersonic blunt-body wake flows
[BTN-95-EIX95182617458] p 268 A95-75729
- Simulating heat addition via mass addition in constant area compressible flows
[BTN-95-EIX95182619100] p 307 A95-76585
- Functional agility metrics and optimal trajectory analysis
[BTN-95-EIX95182619121] p 321 A95-76598
- Response of a nonrotating rotor blade to lateral turbulence. Part 2: Experiment
[BTN-95-EIX95182619229] p 284 A95-76655
- Unsteady ground effects on aerodynamic coefficients of finite wings with camber
[BTN-95-EIX95182619233] p 271 A95-76659
- Particle kinetic simulation of high altitude hypervelocity flight
[NASA-CR-197383] p 309 N95-22481
- High-performance parallel analysis of coupled problems for aircraft propulsion
[NASA-CR-197440] p 289 N95-23088
- Development and verification of a resin film infusion/resin transfer molding simulation model for fabrication of advanced textile composites
[NASA-CR-197439] p 301 N95-23179
- A wall interference assessment/correction system
[NASA-CR-197421] p 309 N95-23183
- Design of a variable area diffuser for a 15-inch Mach 6 open-jet tunnel
p 297 N95-23309
- Development of qualification guidelines for personal computer-based aviation training devices
[DOT/FAA/AM-95/6] p 323 N95-23603
- CONCENTRATION (COMPOSITION)**
Time-of-flight mass spectrometer for impulse facilities
[BTN-95-EIX95142553057] p 262 A95-73441
- Erosion of dust-filtered helicopter turbine engines. Part 1: Basic theoretical considerations
[BTN-95-EIX95182619222] p 288 A95-76648
- CONCORDE AIRCRAFT**
Preliminary identification of buffet problems in high speed civil transport
p 294 N95-23319
- CONDUCTIVE HEAT TRANSFER**
Effect of curvature in the numerical simulation of an electrothermal de-icer pad
[BTN-95-EIX95182619219] p 276 A95-76645
- CONFERENCES**
Corrosion detection and management of advanced airframe materials
[AGARD-CP-565] p 302 N95-23496
- Report of proceedings: Aviation Accident Investigation Symposium, Volume 2: Participant presentations
[PB94-917007] p 277 N95-23598

- Aviation Accident Investigation Symposium, Volume 1: Industry recommendations and Safety Board responses [PB94-917005] p 278 N95-24105
- CONGRESSIONAL REPORTS**
- Report to the Secretary of Defense. Unmanned aerial vehicles: No more Hunter systems should be bought until problems are fixed [GAO/NSIAD-95-52] p 286 N95-24091
- CONICAL FLOW**
- Supersonic axisymmetric conical flow solutions for different ratios of specific heats [BTN-95-EIX95152583283] p 306 A95-73584
- CONJUGATE GRADIENT METHOD**
- Aerodynamic shape optimization using preconditioned conjugate gradient methods [BTN-95-EIX95142553033] p 263 A95-73465
- CONSERVATION LAWS**
- A time-accurate finite volume method valid at all flow velocities p 314 N95-23447
- CONSTRAINTS**
- Empirical results on scheduling and dynamic backtracking p 299 N95-23761
- CONTAMINATION**
- Measurement of moisture and total hydrocarbon contributions by valves used in clean room gas-delivery systems [BTN-94-EIX94381359041] p 295 A95-74629
- CONTINUUM FLOW**
- Hypersonic rarefied flow past spheres including wake structure [BTN-95-EIX95152583250] p 305 A95-73551
- CONTRAILS**
- Transport of exhaust products in the near trail of a jet engine under atmospheric conditions [HTN-95-91421] p 319 A95-77334
- CONTROL EQUIPMENT**
- Engines-only flight control system [NASA-CASE-ARC-11944-1] p 294 N95-23389
- CONTROL SIMULATION**
- Investigation of the effects of bandwidth and time delay on helicopter roll-axis handling qualities [HTN-95-80853] p 290 A95-75095
- CONTROL STABILITY**
- Multivariable stability and robustness of sequentially designed feedback systems [BTN-95-EIX95182619125] p 322 A95-76602
- Robustly stable preliminary control systems design for the YF-16 CCV aircraft [BTN-95-EIX95202637608] p 292 A95-76681
- Stable H(infinity) controller design for the longitudinal dynamics of an aircraft [NASA-TM-106847] p 293 N95-22954
- CONTROL SURFACES**
- Comparison of linear stability results with flight transition data [BTN-95-EIX95182619097] p 283 A95-76582
- Attainable moments for the constrained control allocation problem [BTN-95-EIX95182619149] p 322 A95-76626
- Rolling maneuver load alleviation using active controls [BTN-95-EIX95182619217] p 270 A95-76643
- Aerodynamic surface distension system for high angle of attack forebody vortex control [NASA-CASE-ARC-11979-1] p 286 N95-23390
- CONTROL SYSTEMS DESIGN**
- Effects of high order dynamics on helicopter flight control law design [HTN-95-80852] p 290 A95-75094
- Integrated flight/propulsion control for helicopters [HTN-95-80854] p 290 A95-75096
- Multivariable stability and robustness of sequentially designed feedback systems [BTN-95-EIX95182619125] p 322 A95-76602
- H-infinity helicopter flight control law design with and without rotor state feedback [BTN-95-EIX95182619129] p 291 A95-76606
- Direct-lift design strategy for longitudinal control of hypersonic aircraft [BTN-95-EIX95182619131] p 291 A95-76608
- Multirate flutter suppression system design for a model wing [BTN-95-EIX95182619132] p 292 A95-76609
- Derivation of system matrices from nonlinear dynamic simulation of jet engines [BTN-95-EIX95182619139] p 288 A95-76616
- Attainable moments for the constrained control allocation problem [BTN-95-EIX95182619149] p 322 A95-76626
- Automatic formation flight control [BTN-95-EIX95182619153] p 292 A95-76630
- Flutter suppression control law design and testing for the active flexible wing [BTN-95-EIX95182619214] p 292 A95-76640
- Design and multifunction tests of a frequency domain-based active flutter suppression system [BTN-95-EIX95182619215] p 292 A95-76641
- Flutter suppression for the active flexible wing: A classical design [BTN-95-EIX95182619216] p 292 A95-76642
- Rolling maneuver load alleviation using active controls [BTN-95-EIX95182619217] p 270 A95-76643
- Robustly stable preliminary control systems design for the YF-16 CCV aircraft [BTN-95-EIX95202637608] p 292 A95-76681
- Design of high performance multivariable control systems for supermaneuverable aircraft at high angle of attack [NASA-CR-197661] p 293 N95-22908
- Stable H(infinity) controller design for the longitudinal dynamics of an aircraft [NASA-TM-106847] p 293 N95-22954
- System identification of the Large-Angle Magnetic Suspension Test Fixture (LAMSTF) p 296 N95-23299
- Engines-only flight control system [NASA-CASE-ARC-11944-1] p 294 N95-23389
- Feedback control laws for highly maneuverable aircraft [NASA-CR-197944] p 295 N95-23410
- CONTROL THEORY**
- Shuttle entry guidance revisited using nonlinear geometric methods [BTN-95-EIX95182619144] p 299 A95-76621
- Switched bias proportional navigation for homing guidance against highly maneuvering targets [BTN-95-EIX95182619145] p 279 A95-76622
- Stable H(infinity) controller design for the longitudinal dynamics of an aircraft [NASA-TM-106847] p 293 N95-22954
- CONTROLLABILITY**
- Flight test of the X-29A at high angle of attack: Flight dynamics and controls [NASA-TP-3537] p 284 N95-22806
- Analysis of the longitudinal handling qualities and pilot-induced-oscillation tendencies of the High-Angle-of-Attack Research Vehicle (HARV) p 293 N95-23297
- CONTROLLERS**
- Multiple-function digital controller system for active flexible wing wind-tunnel model [BTN-95-EIX95182619212] p 322 A95-76638
- On-line analysis capabilities developed to support the active flexible wing wind-tunnel tests [BTN-95-EIX95182619213] p 296 A95-76639
- Stable H(infinity) controller design for the longitudinal dynamics of an aircraft [NASA-TM-106847] p 293 N95-22954
- CONVECTIVE FLOW**
- Further analysis of high-rate rolling experiments of a 65-deg delta wing [BTN-95-EIX95152582331] p 281 A95-73533
- CONVECTIVE HEAT TRANSFER**
- Hypersonic convective heat transfer over 140-deg blunt cones in different gases [BTN-95-EIX95152583253] p 306 A95-73554
- Convective and radiative heat transfer analysis for the fire 2 forebody [BTN-95-EIX95182617460] p 268 A95-75731
- CONVERGENCE**
- Preconditioned domain decomposition scheme for three-dimensional aerodynamic sensitivity analysis [BTN-95-EIX95152577612] p 321 A95-73471
- Analytical solution for controls, heats, and states of flight trajectories [BTN-95-EIX95152583286] p 282 A95-73587
- Convergence acceleration of implicit schemes in the presence of high aspect ratio grid cells p 313 N95-23446
- CONVERGENT-DIVERGENT NOZZLES**
- Main features of overexpanded triple jets [BTN-95-EIX95142553040] p 304 A95-73458
- An approximate theoretical method for modeling the static thrust performance of non-axisymmetric two-dimensional convergent-divergent nozzles [NASA-CR-195050] p 273 N95-23183
- COOLING FINNS**
- Base drag prediction on missile configurations [BTN-95-EIX95152583256] p 266 A95-73557
- COPPER**
- Cu deposition using a permanent magnet electron cyclotron resonance microwave plasma source [DE94-017768] p 304 N95-23981
- COPPER OXIDES**
- Phonon characteristics of high (T sub c) superconductors from neutron Doppler broadening measurements [DE95-003703] p 324 N95-24076
- CORROSION**
- Corrosion detection and management of advanced airframe materials [AGARD-CP-565] p 302 N95-23496
- The corrosion and protection of advanced aluminum - lithium airframe alloys p 302 N95-23497
- Corrosion of landing gear steels p 302 N95-23500
- Double pass retroreflection for corrosion detection in aircraft structures p 323 N95-23503
- Non-destructive detection of corrosion for life management p 314 N95-23505
- Health and usage monitoring systems: Corrosion surveillance p 262 N95-23506
- Eddy current detection of pitting corrosion around fastener holes p 315 N95-23507
- In-situ detection of surface passivation or activation and of localized corrosion: Experiences and prospectives in aircraft p 302 N95-23508
- Test method and test results for environmental assessment of aircraft materials p 302 N95-23509
- New nondestructive techniques for the detection and quantification of corrosion in aircraft structures p 315 N95-23512
- Corrosion detection and monitoring of aircraft structures: An overview p 303 N95-23515
- Experience of in-service corrosion on military aircraft p 303 N95-23516
- US Navy operating experience with new aircraft construction materials p 303 N95-23517
- Corrosion in service experience with aircraft in France p 303 N95-23518
- Oklahoma City air logistics center (USAF) aging aircraft corrosion program p 262 N95-23519
- CORROSION PREVENTION**
- Corrosion detection and management of advanced airframe materials [AGARD-CP-565] p 302 N95-23496
- The corrosion and protection of advanced aluminum - lithium airframe alloys p 302 N95-23497
- Corrosion protection measures for CFC/metal joints of fuel integral tank structures of advanced military aircraft p 303 N95-23510
- Organic coating technology for the protection of aircraft against corrosion p 303 N95-23513
- Corrosion detection and monitoring of aircraft structures: An overview p 303 N95-23515
- Experience of in-service corrosion on military aircraft p 303 N95-23516
- US Navy operating experience with new aircraft construction materials p 303 N95-23517
- Corrosion in service experience with aircraft in France p 303 N95-23518
- CORROSION RESISTANCE**
- In-situ detection of surface passivation or activation and of localized corrosion: Experiences and prospectives in aircraft p 302 N95-23508
- CORROSION TESTS**
- Corrosion detection and management of advanced airframe materials [AGARD-CP-565] p 302 N95-23496
- Corrosion of landing gear steels p 302 N95-23500
- Eddy current detection of pitting corrosion around fastener holes p 315 N95-23507
- Test method and test results for environmental assessment of aircraft materials p 302 N95-23509
- Corrosion protection measures for CFC/metal joints of fuel integral tank structures of advanced military aircraft p 303 N95-23510
- New nondestructive techniques for the detection and quantification of corrosion in aircraft structures p 315 N95-23512
- US Navy operating experience with new aircraft construction materials p 303 N95-23517
- COST REDUCTION**
- Containing military autotest cost growth through the use of commercial standard equipment architectures [BTN-95-EIX95172595295] p 287 A95-75717
- Maintenance challenges and trends [BTN-95-EIX95182617808] p 261 A95-75753
- COTTON**
- A comparison of some aerodynamic resistance methods using measurements over cotton and grass from the 1991 California ozone deposition experiment [HTN-95-11295] p 319 A95-77000
- COUNTER ROTATION**
- Flow structure in the wake of a wishbone vortex generator [BTN-95-EIX95142553044] p 304 A95-73454
- COWLINGS**
- The use of cowl camber and taper to reduce rotor/stator interaction noise [NASA-CR-195421] p 323 N95-22675
- CRACK PROPAGATION**
- Growth of multiple cracks and their linkup in a fuselage lap joint [BTN-95-EIX95142553047] p 286 A95-73451
- Multiple site fatigue damage in fuselage skin splices: Experimental simulation and theoretical prediction [BTN-95-EIX95152584676] p 276 A95-73588
- Residual strength of thin panels with cracks p 311 N95-23311

CRACKS

CRACKS

- Growth of multiple cracks and their linkup in a fuselage lap joint
[BTN-95-EIX95142553047] p 286 A95-73451
Multiple site fatigue damage in fuselage skin splices: Experimental simulation and theoretical prediction
[BTN-95-EIX95152584676] p 276 A95-73588
Transient analysis of a cracked rotor passing through critical speed
[BTN-94-EIX94401360022] p 306 A95-74702
Residual strength of thin panels with cracks
p 311 N95-23311

CRASHES

- Aircraft fires, smoke toxicity, and survival: An overview
[DOT/FAA/AM-95/8] p 277 N95-24024
A multibody/finite element analysis approach for modeling of crash dynamic responses
[NIAR-94-3] p 277 N95-24050

CRASHWORTHINESS

- A multibody/finite element analysis approach for modeling of crash dynamic responses
[NIAR-94-3] p 277 N95-24050

CREEP PROPERTIES

- Evolution of oxidation and creep damage mechanisms in HIPed silicon nitride materials
[DE95-001360] p 300 N95-22689

CREEP TESTS

- Evolution of oxidation and creep damage mechanisms in HIPed silicon nitride materials
[DE95-001360] p 300 N95-22689

CRITICAL VELOCITY

- Transient analysis of a cracked rotor passing through critical speed
[BTN-94-EIX94401360022] p 306 A95-74702

CROSS FLOW

- Flow structure in the wake of a wishbone vortex generator
[BTN-95-EIX95142553044] p 304 A95-73454
Experimental investigation of the flowfield about an upswept afterbody
[BTN-95-EIX95152582321] p 265 A95-73524
Crossflow instability control on a swept-wing: Preliminary studies
p 274 N95-23283

CRYOGENIC FLUIDS

- Cavitation modeling in Euler and Navier-Stokes codes
p 315 N95-23630

CURING

- Development and verification of a resin film infusion/resin transfer molding simulation model for fabrication of advanced textile composites
[NASA-CR-197439] p 301 N95-23179

CURVATURE

- Influence of streamwise curvature on longitudinal vortices imbedded in turbulent boundary layers
[BTN-94-EIX94401378820] p 307 A95-76489
Effect of curvature in the numerical simulation of an electrothermal de-icer pad
[BTN-95-EIX95182619219] p 276 A95-76645

CYCLOTRON RESONANCE

- Cu deposition using a permanent magnet electron cyclotron resonance microwave plasma source
[DE94-017768] p 304 N95-23981

D

DAMAGE

- Multiaxis pilot ratings for damaged aircraft
[BTN-95-EIX95182619128] p 269 A95-76605
Rationale for the Modular Air-system Vulnerability Estimation Network (MAVEN) methodology
[AD-A285797] p 284 N95-22510
Residual strength of thin panels with cracks
p 311 N95-23311
Double pass retroreflection for corrosion detection in aircraft structures
p 323 N95-23503
POD assessment of NDI procedures using a round robin test
[AGARD-R-809] p 315 N95-23602

DAMAGE ASSESSMENT

- Mechanical system reliability and risk assessment
[BTN-95-EIX95142553046] p 304 A95-73452
Validation of an effective flat cruciform-shaped specimen to study CFRP composite laminates under biaxial loading
[BTN-95-EIX95152584677] p 282 A95-73589
POD assessment of NDI procedures using a round robin test
[AGARD-R-809] p 315 N95-23602
Aircraft accident report. Runway overrun following rejected takeoff. Continental Airlines flight 795, McDonnell Douglas MD-82, N18835, LaGuardia Airport, Flushing, NY, 2 March 1994
[PB95-910401] p 277 N95-23609

DATA ACQUISITION

- Condition monitoring and diagnostics
[BTN-95-EIX95182617811] p 261 A95-75756

DATA BASES

- Compendium of NASA data base for the Global Tropospheric Experiment's Pacific Exploratory Mission West-A (PEM West-A)
[NASA-TM-109177] p 320 N95-23009
Impeller flow field characterization with a laser two-focus velocimeter
p 313 N95-23440

DATA LINKS

- Differential GPS and system integration of the Low Visibility Landing and Surface Operations (LVLASO) demonstration
p 280 N95-23318

DATA PROCESSING

- On-line analysis capabilities developed to support the active flexible wing wind-tunnel tests
[BTN-95-EIX95182619213] p 296 A95-76639
Enhancement of F/A-18 operational flight measurements: Data report for phase 1
[DSTO-TR-0049] p 286 N95-23666
Calculation of satellite drag coefficients
[AD-A285118] p 300 N95-23781
AVIRIS and TIMS data processing and distribution at the land processes distributed active archive center
p 325 N95-23872

DATA STORAGE

- Holographic interferometric tomography for reconstructing flow fields
p 310 N95-23287
AVIRIS and TIMS data processing and distribution at the land processes distributed active archive center
p 325 N95-23872

DATA TRANSFER (COMPUTERS)

- AVIRIS and TIMS data processing and distribution at the land processes distributed active archive center
p 325 N95-23872

DEFECTS

- New nondestructive techniques for the detection and quantification of corrosion in aircraft structures
p 315 N95-23512

DEFENSE PROGRAM

- Report to the Secretary of Defense. Unmanned aerial vehicles: No more Hunter systems should be bought until problems are fixed
[GAO/NSIAD-95-52] p 286 N95-24091

DEFORMATION

- Dynamic analysis of bearingless tail rotor blades based on nonlinear shell modes
[BTN-95-EIX95152582338] p 281 A95-73540
Static aeroelastic characteristics of a composite wing
[BTN-95-EIX95152582340] p 282 A95-73542

DEGRADATION

- Evolution of oxidation and creep damage mechanisms in HIPed silicon nitride materials
[DE95-001360] p 300 N95-22689
Non-destructive detection of corrosion for life management
p 314 N95-23505
In-situ detection of surface passivation or activation and of localized corrosion: Experiences and perspectives in aircraft
p 302 N95-23508
Oklahoma City air logistics center (USAF) aging aircraft corrosion program
p 262 N95-23519

DEGREES OF FREEDOM

- Functional dependence of trajectory dispersion on initial condition errors
[BTN-95-EIX95152583263] p 298 A95-73564
Improving prediction: The incorporation of simplified rotor dynamics in a mathematical model of the bell 412HP
[BTN-95-EIX95152584679] p 282 A95-73591
Identification of higher order helicopter dynamics using linear modeling methods
[HTN-95-80851] p 290 A95-75093

DEICERS

- Effect of curvature in the numerical simulation of an electrothermal de-icer pad
[BTN-95-EIX95182619219] p 276 A95-76645

DEICING

- Effect of curvature in the numerical simulation of an electrothermal de-icer pad
[BTN-95-EIX95182619219] p 276 A95-76645

DELTA WINGS

- Effects of spatial order of accuracy on the computation of vortical flowfields
[BTN-95-EIX95152577604] p 305 A95-73479
Unstructured grid solutions to a wing/pylon/store configuration
[BTN-95-EIX95152582322] p 265 A95-73525
Navier-Stokes prediction of large-amplitude delta-wing roll oscillations
[BTN-95-EIX95152582329] p 281 A95-73531
Further analysis of high-rate rolling experiments of a 65-deg delta wing
[BTN-95-EIX95152582331] p 281 A95-73533

- Analytic prediction of lift for delta wings with partial leading-edge thrust
[BTN-95-EIX95152582345] p 266 A95-73547

- Effect of leeward flow dividers on the wing rock of a delta wing
[BTN-95-EIX95152582347] p 282 A95-73549

- Wing vertical position effects on wing-body carryover for noncircular missiles
[BTN-95-EIX95182617462] p 268 A95-75733

- Transient structure of vortex breakdown on a delta wing
[BTN-95-EIX95182619073] p 268 A95-75758

- Natural laminar flow wing concept for supersonic transports
[BTN-95-EIX95182619226] p 308 A95-76652

- A study of the vortex flow over 76/40-deg double-delta wing
[NASA-CR-195032] p 314 N95-23466

DEPOSITION

- A comparison of some aerodynamic resistance methods using measurements over cotton and grass from the 1991 California ozone deposition experiment
[HTN-95-11295] p 319 A95-77000
Cu deposition using a permanent magnet electron cyclotron resonance microwave plasma source
[DE94-017768] p 304 N95-23981

DEPTH

- Evaluation of advanced aerospace materials by depth sensing indentation and scratch methods
[BTN-95-EIX95152584678] p 282 A95-73590

DESIGN ANALYSIS

- Mechanical system reliability and risk assessment
[BTN-95-EIX95142553046] p 304 A95-73452
Efficient sensitivity analysis for rotary-wing aeromechanical problems
[BTN-95-EIX95152577585] p 264 A95-73497
Design constraints in the payload-range diagram of ultrahigh capacity transport airplanes
[BTN-95-EIX95152582319] p 276 A95-73522
Structural acoustic calculations in the low-frequency range
[BTN-95-EIX95152582336] p 323 A95-73538
Aerodynamic design of pegasus: Concept to flight with computational fluid dynamics
[BTN-95-EIX95182617463] p 298 A95-75734
Euler technology assessment for preliminary aircraft design employing OVERFLOW code with multiblock structured-grid method
[NASA-CR-4651] p 273 N95-23095
Aerodynamic design optimization with sensitivity analysis and computational fluid dynamics
[NASA-CR-197419] p 274 N95-23218
Design of a GaAs/Ge solar array for unmanned aerial vehicles
[NASA-TM-106870] p 320 N95-23259
Inner loop flight control for the High-Speed Civil Transport
p 293 N95-23314
Enhanced analysis and users manual for radial-inflow turbine conceptual design code RTD
[NASA-CR-195454] p 275 N95-23462

DETECTION

- Evaluation of neutron techniques for illicit substance detection
[DE95-002988] p 300 N95-22764
Health and usage monitoring systems: Corrosion surveillance
p 262 N95-23506
In-situ detection of surface passivation or activation and of localized corrosion: Experiences and perspectives in aircraft
p 302 N95-23508
New nondestructive techniques for the detection and quantification of corrosion in aircraft structures
p 315 N95-23512
Corrosion detection and monitoring of aircraft structures: An overview
p 303 N95-23515
Experience of in-service corrosion on military aircraft
p 303 N95-23516

DETERIORATION

- Non-destructive detection of corrosion for life management
p 314 N95-23505

DIAGNOSIS

- Condition monitoring and diagnostics
[BTN-95-EIX95182617811] p 261 A95-75756

DIFFERENTIAL EQUATIONS

- Three-dimensional structure of a supersonic jet impinging on an inclined plate
[BTN-95-EIX95152583259] p 267 A95-73560

DIGITAL SYSTEMS

- Multiple-function digital controller system for active flexible wing wind-tunnel model
[BTN-95-EIX95182619212] p 322 A95-76638

DIRECT LIFT CONTROLS

- Direct-lift design strategy for longitudinal control of hypersonic aircraft
[BTN-95-EIX95182619131] p 291 A95-76608

DIRECTIONAL CONTROL

Feedback control laws for highly maneuverable aircraft
[NASA-CR-197944] p 295 N95-23410

DISCONTINUITY

Application of a control-volume-based finite-element formulation to the shock tube problem
[BTN-95-EIX95182619099] p 295 A95-76584

DISORIENTATION

A review of civil aviation fatal accidents in which lost/disoriented was a cause/factor: 1981-1990
[DOT/FAA/AM-95/1] p 278 N95-24071

DISPERSIONS

Functional dependence of trajectory dispersion on initial condition errors
[BTN-95-EIX95152583263] p 298 A95-73564

DISPLAY DEVICES

Flight-deck displays on the Boeing 777
[BTN-95-EIX95142562402] p 286 A95-73438
Virtual reality flight control display with six-degree-of-freedom controller and spherical orientation overlay
[NASA-CASE-NPO-18733-1-CU] p 288 N95-22578
Automation technology using Geographic Information System (GIS) p 324 N95-23284
Differential GPS and system integration of the Low Visibility Landing and Surface Operations (LVLASO) demonstration p 280 N95-23318

DISTILLATION

Airborne rotary air separator study
[NASA-CR-189099] p 290 N95-24053

DISTRIBUTED PROCESSING

AVIRIS and TIMS data processing and distribution at the land processes distributed active archive center p 325 N95-23872

DISTRIBUTION FUNCTIONS

Determination of wall boundary conditions for high-speed-ratio direct simulation Monte Carlo calculations
[BTN-95-EIX95182617457] p 267 A95-75728

DIURNAL VARIATIONS

Diurnal variation of lee vortices in Taiwan and the surrounding area
[HTN-95-91363] p 318 A95-76394
A comparison of some aerodynamic resistance methods using measurements over cotton and grass from the 1991 California ozone deposition experiment
[HTN-95-11295] p 319 A95-77000

DIVIDERS

Effect of leeward flow dividers on the wing rock of a delta wing
[BTN-95-EIX95152582347] p 282 A95-73549

DOPPLER RADAR

2 micron LIDAR for laser-based remote sensing: Flight demonstration and application survey
[BTN-95-EIX95212641072] p 319 A95-76737
Maximum-likelihood spectral estimation and adaptive filtering techniques with application to airborne Doppler weather radar
[NASA-CR-197699] p 316 N95-23670

DRAG

Shock tunnel measurements of hypervelocity blunted cone drag
[BTN-95-EIX95152577606] p 305 A95-73477
Separation control on high-lift airfoils via micro-vortex generators
[BTN-95-EIX95152582326] p 265 A95-73529

DRAG REDUCTION

Effect of underwing frost on a transport aircraft airfoil at flight Reynolds number
[BTN-95-EIX95152582334] p 276 A95-73536
Numerical investigation of supersonic flows around a spiked blunt body
[BTN-95-EIX95212645690] p 271 A95-76742

DROP SIZE

Study of the droplet spray characteristics of a subsonic wind tunnel
[BTN-95-EIX95182619235] p 271 A95-76661

DROPS (LIQUIDS)

Study of the droplet spray characteristics of a subsonic wind tunnel
[BTN-95-EIX95182619235] p 271 A95-76661

DRUGS

Evaluation of neutron techniques for illicit substance detection
[DE95-002988] p 300 N95-22764

DUCTED FLOW

Flutter of an infinitely long panel in a duct
[BTN-95-EIX95182619087] p 291 A95-75772

DUCTS

The use of cowl camber and taper to reduce rotor/stator interaction noise
[NASA-CR-195421] p 323 N95-22675

DURABILITY

Interlaminar shear test method development for long term durability testing of composites p 301 N95-23300

DUST

Erosion of dust-filtered helicopter turbine engines. Part 1: Basic theoretical considerations
[BTN-95-EIX95182619222] p 288 A95-76648
Erosion of dust-filtered helicopter turbine engines. Part 2: Erosion reduction
[BTN-95-EIX95182619223] p 289 A95-76649
Life prediction of helicopter engines fitted with dust filters
[BTN-95-EIX95182619224] p 289 A95-76650

DUST COLLECTORS

Erosion of dust-filtered helicopter turbine engines. Part 2: Erosion reduction
[BTN-95-EIX95182619223] p 289 A95-76649
Life prediction of helicopter engines fitted with dust filters
[BTN-95-EIX95182619224] p 289 A95-76650

DYNAMIC CHARACTERISTICS

Analytical aeropropulsive/aeroelastic hypersonic-vehicle model with dynamic analysis
[BTN-95-EIX95182619138] p 269 A95-76615

DYNAMIC LOADS

Enhancement of F/A-18 operational flight measurements: Data report for phase 1
[DSTO-TR-0049] p 286 N95-23666

DYNAMIC MODELS

Flutter analysis of composite box beams
[NASA-CR-197931] p 294 N95-23392

DYNAMIC RESPONSE

Effects of AMB parameters on the dynamic stability of the rotor
[BTN-94-EIX94381353450] p 323 A95-75494
Response of a nonrotating rotor blade to lateral turbulence. Part 1: Theory
[BTN-95-EIX95182619228] p 284 A95-76654
Dynamic response tests of inertial and optical wind-tunnel model attitude measurement devices
[NASA-TM-109182] p 296 N95-23011
Influence of backup bearings and support structure dynamics on the behavior of rotors with active supports
[NASA-CR-197438] p 310 N95-23190
A multibody/finite element analysis approach for modeling of crash dynamic responses
[NIAR-94-3] p 277 N95-24050

DYNAMIC STABILITY

Dynamical instability of the aerogravity assist maneuver
[BTN-95-EIX95152583282] p 298 A95-73583
Effects of AMB parameters on the dynamic stability of the rotor
[BTN-94-EIX94381353450] p 323 A95-75494
Handling qualities of the High Speed Civil Transport p 294 N95-23325

DYNAMIC STRUCTURAL ANALYSIS

Postinstability behavior of a two-dimensional airfoil with a structural nonlinearity
[BTN-95-EIX95152582337] p 266 A95-73539
Integrated aerodynamic/dynamic/structural optimization of helicopter rotor blades using multilevel decomposition
[NASA-TP-3465] p 285 N95-22953
Thin tailored composite wing for civil tiltrotor p 285 N95-23317

Flutter analysis of composite box beams
[NASA-CR-197931] p 294 N95-23392

DYNAMIC TESTS

Measurement of particle emissions from clean room gas-handling components
[BTN-94-EIX94381359040] p 295 A95-74554

DYNAMICAL SYSTEMS

Nonlinear system guidance in the presence of transmission zero dynamics
[NASA-TM-4661] p 309 N95-22804

E**EARTH ORBITS**

Effects of satellite bunching on the probability of collision in geosynchronous orbit
[BTN-95-EIX95152583276] p 298 A95-73577

EARTH SURFACE

Thundercloud electric field modeling for the ionosphere-Earth region. 1: Dependence on cloud charge distribution
[HTN-95-41223] p 317 A95-75035
MAX-91: Polarimetric SAR results on Montespertoli site p 320 N95-23940

ECONOMIC ANALYSIS

Design constraints in the payload-range diagram of ultrahigh capacity transport airplanes
[BTN-95-EIX95152582319] p 276 A95-73522

EDDY CURRENTS

Eddy current detection of pitting corrosion around fastener holes p 315 N95-23507

EDDY VISCOSITY

Adaptive finite element method for turbulent flow near a propeller
[BTN-95-EIX95142553038] p 305 A95-73460

EDUCATION

ATE enabling technologies p 287 A95-75718
1994 NASA-HU American Society for Engineering Education (ASEE) Summer Faculty Fellowship Program
[NASA-CR-194972] p 325 N95-23276
Preparation of course materials: Elementary mathematics of powered flight p 324 N95-23320

EIGENVALUES

Eigenanalysis of unsteady flows about airfoils, cascades, and wings
[BTN-95-EIX95152577597] p 305 A95-73486

ELASTIC BENDING

Residual strength of thin panels with cracks p 311 N95-23311
Thin tailored composite wing for civil tiltrotor p 285 N95-23317

ELECTRIC FIELDS

Thundercloud electric field modeling for the ionosphere-Earth region. 1: Dependence on cloud charge distribution
[HTN-95-41223] p 317 A95-75035

ELECTRIC MOTORS

Motor drive technologies for the power-by-wire (PBW) program: Options, trends and tradeoffs
[NASA-TM-106885] p 295 N95-23671

ELECTRIFICATION

Collaborative research on aircraft icing and charging processes in ice
[AD-A285102] p 276 N95-23201

ELECTROCHEMICAL CORROSION

Corrosion protection measures for CFC/metal joints of fuel integral tank structures of advanced military aircraft p 303 N95-23510

ELECTROCHEMISTRY

Health and usage monitoring systems: Corrosion surveillance p 262 N95-23506
In-situ detection of surface passivation or activation and of localized corrosion: Experiences and prospectives in aircraft p 302 N95-23508
Test method and test results for environmental assessment of aircraft materials p 302 N95-23509

ELECTROMAGNETIC INTERFERENCE

US Navy operating experience with new aircraft construction materials p 303 N95-23517

ELECTROMAGNETS

Cu deposition using a permanent magnet electron cyclotron resonance microwave plasma source
[DE94-017768] p 304 N95-23981

ELECTRONIC EQUIPMENT

Differential GPS and system integration of the Low Visibility Landing and Surface Operations (LVLASO) demonstration p 280 N95-23318

ELECTRONIC EQUIPMENT TESTS

CASS: Design for supportability
[BTN-95-EIX95172595296] p 287 A95-75716

ENERGY BUDGETS

Diurnal variation of lee vortices in Taiwan and the surrounding area
[HTN-95-91363] p 318 A95-76394

ENGINE AIRFRAME INTEGRATION

Flow study of supersonic wing-nacelle configuration
[BTN-95-EIX95152582344] p 266 A95-73546
Integrated flight/propulsion control for helicopters
[HTN-95-80854] p 290 A95-75096

ENGINE ANALYZERS

Gearbox vibration diagnostic analyzer
[NASA-CR-189141] p 316 N95-23792

ENGINE DESIGN

Lycoming to test new engine core
[HTN-95-41393] p 288 A95-76389
Aerodynamic design and analysis of a highly loaded turbine exhaust p 312 N95-23435
Phase 2: HGM air flow tests in support of HEX vane investigation p 312 N95-23438

ENGINE INLETS

A new type of simulator for simulating the flow-field distortion of engine inlet
[BTN-95-EIX95202638963] p 289 A95-76673
Integrated design of hypersonic waveriders including inlets and tailfins
[BTN-95-EIX95212645692] p 271 A95-76744

ENGINE MONITORING INSTRUMENTS

Gearbox vibration diagnostic analyzer
[NASA-CR-189141] p 316 N95-23792

ENGINE NOISE

The use of cowl camber and taper to reduce rotor/stator interaction noise
[NASA-CR-195421] p 323 N95-22675

- Supersonic jet noise reductions predicted with increased jet spreading rate
[NASA-TM-106872] p 323 N95-23178
- ENGINE PARTS**
- Compliant interlayer
[BTN-95-EIX95142562401] p 304 A95-73439
- Influence of backup bearings and support structure dynamics on the behavior of rotors with active supports
[NASA-CR-197438] p 310 N95-23190
- Evaluation of thermal barrier and PS-200 self-lubricating coatings in an air-cooled rotary engine
[NASA-CR-195445] p 289 N95-23222
- ENGINE TESTS**
- Phase 2: HGM air flow tests in support of HEX vane investigation p 312 N95-23438
- Impeller flow field characterization with a laser two-focus velocimeter p 313 N95-23440
- ENGINEERING**
- 1994 NASA-HU American Society for Engineering Education (ASEE) Summer Faculty Fellowship Program [NASA-CR-194972] p 325 N95-23276
- ENTHALPY**
- Shock tunnel measurements of hypervelocity blunted cone drag
[BTN-95-EIX95152577606] p 305 A95-73477
- ENTRY GUIDANCE (STS)**
- Shuttle entry guidance revisited using nonlinear geometric methods
[BTN-95-EIX95182619144] p 299 A95-76621
- ENVIRONMENT EFFECTS**
- Modeling aerosol emissions from the combustion of composite materials p 301 N95-23038
- ENVIRONMENT PROTECTION**
- Aircraft stripping and painting
[BTN-95-EIX95182617810] p 300 A95-75755
- Corrosion in service experience with aircraft in France p 303 N95-23518
- ENVIRONMENT SIMULATION**
- Hypersonic convective heat transfer over 140-deg blunt cones in different gases
[BTN-95-EIX95152583253] p 306 A95-73554
- EQUATIONS OF MOTION**
- Functional dependence of trajectory dispersion on initial condition errors
[BTN-95-EIX95152583263] p 298 A95-73564
- Analytical solution and parameter estimation of projectile dynamics
[BTN-95-EIX9512645695] p 272 A95-76747
- Moving mass trim control for aerospace vehicles
[DE95-002602] p 299 N95-23532
- EQUATIONS OF STATE**
- Application of a control-volume-based finite-element formulation to the shock tube problem
[BTN-95-EIX95182619099] p 295 A95-76584
- On-line, adaptive state estimator for active noise control p 322 N95-23308
- EROSION**
- Erosion of dust-filtered helicopter turbine engines. Part 1: Basic theoretical considerations
[BTN-95-EIX95182619222] p 288 A95-76648
- Erosion of dust-filtered helicopter turbine engines. Part 2: Erosion reduction
[BTN-95-EIX95182619223] p 289 A95-76649
- Life prediction of helicopter engines fitted with dust filters
[BTN-95-EIX95182619224] p 289 A95-76650
- ERROR ANALYSIS**
- Enhancing filter robustness in cascaded GPS-INS integrations
[BTN-95-EIX95142555475] p 278 A95-73435
- Covariance analysis of strapdown INS considering gyrocompass characteristics
[BTN-95-EIX95202637592] p 279 A95-76697
- ERROR CORRECTING CODES**
- Improved version of the Naval Surface Warfare Center aeroprediction code (AP93)
[BTN-95-EIX95152583260] p 267 A95-73561
- ESTIMATING**
- Improving prediction: The incorporation of simplified rotor dynamics in a mathematical model of the bell 412HP
[BTN-95-EIX95152584679] p 282 A95-73591
- Real-time estimation of atmospheric turbulence severity from in-situ aircraft measurements
[BTN-95-EIX95182619231] p 319 A95-76657
- Rationale for the Modular Air-system Vulnerability Estimation Network (MAVEN) methodology
[AD-A285797] p 284 N95-22510
- EULER EQUATIONS OF MOTION**
- Limit cycle phenomena in computational transonic aerelasticity
[BTN-95-EIX95152582317] p 264 A95-73520
- Aeroacoustic model for weak shock waves based on Burgers equation
[BTN-95-EIX95182619076] p 269 A95-75761
- Euler Technology Assessment program for preliminary aircraft design employing SPLITFLOW code with Cartesian unstructured grid method
[NASA-CR-4649] p 273 N95-22917
- Euler technology assessment for preliminary aircraft design employing OVERFLOW code with multiblock structured-grid method
[NASA-CR-4651] p 273 N95-23095
- An assessment of viscous effects in computational simulation of benign and burst vortex flows on generic fighter wind-tunnel models using TEAM code
[NASA-CR-4650] p 273 N95-23185
- Convergence acceleration of implicit schemes in the presence of high aspect ratio grid cells p 313 N95-23446
- Cavitation modeling in Euler and Navier-Stokes codes p 315 N95-23630
- User's guide for ECAP2D: An Euler unsteady aerodynamic and aeroelastic analysis program for two dimensional oscillating cascades, version 1.0
[NASA-CR-189146] p 316 N95-24189
- EUROPEAN AIRBUS**
- Automatic riveting cell for commercial aircraft floor grid assembly
[BTN-95-EIX95182617807] p 261 A95-75752
- EXCITATION**
- SEM representation of the early and late time fields scattered from wire targets
[BTN-94-EIX94381353142] p 306 A95-74496
- EXHAUST DIFFUSERS**
- Design of a variable area diffuser for a 15-inch Mach 6 open-jet tunnel p 297 N95-23309
- EXHAUST EMISSION**
- Trajectory modeling of emissions from lower stratospheric aircraft
[HTN-95-41219] p 317 A95-75031
- EXHAUST GASES**
- Predicting exhaust plume boundaries with supersonic external flows
[BTN-95-EIX95152583258] p 297 A95-73559
- In situ observations in aircraft exhaust plumes in the lower stratosphere at midaltitudes
[HTN-95-A0862] p 318 A95-76266
- Sensitivity of two-dimensional model predictions of ozone response to stratospheric aircraft: An update
[HTN-95-A0863] p 318 A95-76267
- NTS-spill test facility wind tunnel exhaust plume characterization
[DE95-003630] p 297 N95-24019
- EXHAUST SYSTEMS**
- Aerodynamic design and analysis of a highly loaded turbine exhaust p 312 N95-23435
- EXHAUST VELOCITY**
- Aerodynamic design and analysis of a highly loaded turbine exhaust p 312 N95-23435
- EXPANSION**
- Effects of expansions on a supersonic boundary layer: Surface pressure measurements
[BTN-95-EIX95142553036] p 263 A95-73462
- EXPERT SYSTEMS**
- Artificial intelligence for turboprop engine maintenance
[BTN-95-EIX95182617812] p 288 A95-75757
- EXPOSURE**
- The corrosion and protection of advanced aluminum - lithium airframe alloys p 302 N95-23497
- Corrosion protection measures for CFC/metal joints of fuel integral tank structures of advanced military aircraft p 303 N95-23510
- EXTERNAL STORE SEPARATION**
- A CFD study of complex missile and store configurations in relative motion
[NASA-CR-197912] p 285 N95-22949
- EXTERNAL STORES**
- Aerodynamic characteristics of external store configurations at low speeds
[BTN-95-EIX95182619230] p 271 A95-76656
- EXTRACTION**
- On-line, adaptive state estimator for active noise control p 322 N95-23308
- EXTREMELY HIGH FREQUENCIES**
- Flight test evaluation of a 35 GHz forward looking altimeter for terrain avoidance
[BTN-95-EIX95212641071] p 287 A95-76736
- Enhancement of F/A-18 operational flight measurements: Data report for phase 1
[DSTO-TR-0049] p 286 N95-23666
- FABRICATION**
- Idealized textile composites for experimental/analytical correlation p 301 N95-23277
- FAIL-SAFE SYSTEMS**
- Residual strength of thin panels with cracks p 311 N95-23311
- FAILURE ANALYSIS**
- New failure detection approach and its application to GPS autonomous integrity monitoring
[BTN-95-EIX95202637613] p 279 A95-76676
- Handling qualities of the High Speed Civil Transport p 294 N95-23325
- FAILURE MODES**
- Mechanical system reliability and risk assessment
[BTN-95-EIX95142553046] p 304 A95-73452
- Residual strength of thin panels with cracks p 311 N95-23311
- FAN BLADES**
- H-76B fantail demonstrator composite fan blade fabrication
[HTN-95-80856] p 283 A95-75098
- FAST NEUTRONS**
- Evaluation of neutron techniques for illicit substance detection
[DE95-002988] p 300 N95-22764
- FASTENERS**
- Eddy current detection of pitting corrosion around fastener holes p 315 N95-23507
- FATIGUE (MATERIALS)**
- Growth of multiple cracks and their linkup in a fuselage lap joint
[BTN-95-EIX95142553047] p 286 A95-73451
- Validation of an effective flat cruciform-shaped specimen to study CFRP composite laminates under biaxial loading
[BTN-95-EIX95152584677] p 282 A95-73589
- Evaluation of advanced aerospace materials by depth sensing indentation and scratch methods
[BTN-95-EIX95152584678] p 282 A95-73590
- Review of aeronautical fatigue investigation in the Netherlands during the period March 1991-March 1993
[PB95-139184] p 285 N95-23161
- Review of some results of the author's fatigue investigations with applications in engineering and material science
[TAE-698] p 316 N95-23662
- FATIGUE LIFE**
- Growth of multiple cracks and their linkup in a fuselage lap joint
[BTN-95-EIX95142553047] p 286 A95-73451
- Review of some results of the author's fatigue investigations with applications in engineering and material science
[TAE-698] p 316 N95-23662
- FATIGUE TESTS**
- Growth of multiple cracks and their linkup in a fuselage lap joint
[BTN-95-EIX95142553047] p 286 A95-73451
- Validation of an effective flat cruciform-shaped specimen to study CFRP composite laminates under biaxial loading
[BTN-95-EIX95152584677] p 282 A95-73589
- Evaluation of advanced aerospace materials by depth sensing indentation and scratch methods
[BTN-95-EIX95152584678] p 282 A95-73590
- Fatigue strength of high-temperature alloys under conditions of cyclic temperature variation. Communication 1: Experimental procedure and results
[BTN-94-EIX94401363884] p 307 A95-75516
- FAULT DETECTION**
- Evaluation of advanced aerospace materials by depth sensing indentation and scratch methods
[BTN-95-EIX95152584678] p 282 A95-73590
- ATE enabling technologies
[BTN-95-EIX95172595294] p 287 A95-75718
- Condition monitoring and diagnostics
[BTN-95-EIX95182617811] p 261 A95-75756
- New failure detection approach and its application to GPS autonomous integrity monitoring
[BTN-95-EIX95202637613] p 279 A95-76676
- FAULT TREES**
- Rationale for the Modular Air-system Vulnerability Estimation Network (MAVEN) methodology
[AD-A285797] p 284 N95-22510
- FEASIBILITY ANALYSIS**
- Inner loop flight control for the High-Speed Civil Transport p 293 N95-23314
- FEEDBACK CONTROL**
- Dynamical instability of the aerogravity assist maneuver
[BTN-95-EIX95152583282] p 298 A95-73583

F

F-18 AIRCRAFT

- Forebody flow control on a full-scale F/A-18 aircraft
[BTN-95-EIX95152582333] p 281 A95-73535
- Analysis of the longitudinal handling qualities and pilot-induced-oscillation tendencies of the High-Angle-of-Attack Research Vehicle (HARV)
p 293 N95-23297

Analytical solution for controls, heats, and states of flight trajectories
[BTN-95-EIX95152583286] p 282 A95-73587

Real-time navigation using the global positioning system
[BTN-95-EIX95172595298] p 279 A95-75714

Aeroelastic vehicle multivariable control synthesis with analytical robustness evaluation
[BTN-95-EIX95182619115] p 321 A95-76592

Multivariable stability and robustness of sequentially designed feedback systems
[BTN-95-EIX95182619125] p 322 A95-76602

H-infinity helicopter flight control law design with and without rotor state feedback
[BTN-95-EIX95182619129] p 291 A95-76606

Performance of the 0.3-meter transonic cryogenic tunnel with air, nitrogen, and sulfur hexafluoride media under closed loop automatic control
[NASA-CR-195052] p 310 N95-23257

System identification of the Large-Angle Magnetic Suspension Test Fixture (LAMSTF)
[BTN-95-EIX95182619125] p 296 N95-23299

On-line, adaptive state estimator for active noise control
[BTN-95-EIX95182619125] p 322 N95-23308

Feedback control laws for highly maneuverable aircraft
[NASA-CR-197944] p 295 N95-23410

FIBER COMPOSITES

Validation of an effective flat cruciform-shaped specimen to study CFRP composite laminates under biaxial loading
[BTN-95-EIX95152584677] p 282 A95-73589

Corrosion protection measures for CFC/metal joints of fuel integral tank structures of advanced military aircraft
p 303 N95-23510

FIELD OF VIEW

Design of wide angle head up displays for synthetic vision
[BTN-95-EIX95212641070] p 287 A95-76735

FIGHTER AIRCRAFT

Method for the prediction of the onset of wing rock
[BTN-95-EIX95152582342] p 282 A95-73544

Design and multifunction tests of a frequency domain-based active flutter suppression system
[BTN-95-EIX95182619215] p 292 A95-76641

Application of Navier-Stokes aerodynamic methods to improve fighter wing maneuver performance
[BTN-95-EIX95182619218] p 284 A95-76644

An assessment of viscous effects in computational simulation of benign and burst vortex flows on generic fighter wind-tunnel models using TEAM code
[NASA-CR-4650] p 273 N95-23185

FILTRATION

Erosion of dust-filtered helicopter turbine engines. Part 1: Basic theoretical considerations
[BTN-95-EIX95182619222] p 288 A95-76648

Erosion of dust-filtered helicopter turbine engines. Part 2: Erosion reduction
[BTN-95-EIX95182619223] p 289 A95-76649

Life prediction of helicopter engines fitted with dust filters
[BTN-95-EIX95182619224] p 289 A95-76650

FINITE DIFFERENCE THEORY

Higher-order viscous shock-layer solutions for high-altitude flows
[BTN-95-EIX95152583255] p 306 A95-73556

Aeroacoustic model for weak shock waves based on Burgers equation
[BTN-95-EIX95182619076] p 269 A95-75761

FINITE ELEMENT METHOD

Adaptive finite element method for turbulent flow near a propeller
[BTN-95-EIX95142553038] p 305 A95-73460

Coupled FEM-BEM approach for mean flow effects on vibro-acoustic behavior of planar structures
[BTN-95-EIX95152577587] p 263 A95-73495

Static aeroelastic characteristics of a composite wing
[BTN-95-EIX95152582340] p 282 A95-73542

Thermal force modeling for global positioning system satellites using the finite element method
[BTN-95-EIX95152583270] p 278 A95-73571

Finite element model for a flexible non-symmetric rotor on distributed bearing: A stability study
[BTN-94-EIX9438135212] p 306 A95-74612

Application of a control-volume-based finite-element formulation to the shock tube problem
[BTN-95-EIX95182619099] p 295 A95-76584

Effect of curvature in the numerical simulation of an electrothermal de-icer pad
[BTN-95-EIX95182619219] p 276 A95-76645

Idealized textile composites for experimental/analytical correlation
p 301 N95-23277

Residual strength of thin panels with cracks
p 311 N95-23311

A multibody/finite element analysis approach for modeling of crash dynamic responses
[NIAR-94-3] p 277 N95-24050

FINITE VOLUME METHOD

A time-accurate finite volume method valid at all flow velocities
p 314 N95-23447

FINS

Integrated design of hypersonic waveriders including inlets and tailfins
[BTN-95-EIX95212645692] p 271 A95-76744

FIRES

Rationale for the Modular Air-system Vulnerability Estimation Network (MAVEN) methodology
[AD-A285797] p 284 N95-22510

Aircraft fires, smoke toxicity, and survival: An overview
[DOT/FAA/AM-95/8] p 277 N95-24024

FLAPS (CONTROL SURFACES)

Study of an airfoil with a flap and spoiler
[BTN-95-EIX95152582327] p 265 A95-73530

FLAT PLATES

Coupled FEM-BEM approach for mean flow effects on vibro-acoustic behavior of planar structures
[BTN-95-EIX95152577587] p 263 A95-73495

Three-dimensional structure of a supersonic jet impinging on an inclined plate
[BTN-95-EIX95152583259] p 267 A95-73560

Crossflow instability control on a swept-wing: Preliminary studies
p 274 N95-23283

FLAT SURFACES

Validation of an effective flat cruciform-shaped specimen to study CFRP composite laminates under biaxial loading
[BTN-95-EIX95152584677] p 282 A95-73589

FLEXIBLE WINGS

Experimental evaluation of a box beam specifically tailored for chordwise deformation
[BTN-95-EIX95182619088] p 283 A95-75773

Summary of an active flexible wing program
[BTN-95-EIX95182619209] p 283 A95-76635

Application of transonic small disturbance theory to the active flexible wing model
[BTN-95-EIX95182619210] p 270 A95-76636

Simulation and model reduction for the active flexible wing program
[BTN-95-EIX95182619211] p 295 A95-76637

Multiple-function digital controller system for active flexible wing wind-tunnel model
[BTN-95-EIX95182619212] p 322 A95-76638

On-line analysis capabilities developed to support the active flexible wing wind-tunnel tests
[BTN-95-EIX95182619213] p 296 A95-76639

Flutter suppression control law design and testing for the active flexible wing
[BTN-95-EIX95182619214] p 292 A95-76640

Flutter suppression for the active flexible wing: A classical design
[BTN-95-EIX95182619216] p 292 A95-76642

Rolling maneuver load alleviation using active controls
[BTN-95-EIX95182619217] p 270 A95-76643

Response of a nonrotating rotor blade to lateral turbulence. Part 1: Theory
[BTN-95-EIX95182619228] p 284 A95-76654

Flutter analysis of composite box beams
[NASA-CR-197931] p 294 N95-23392

FLIGHT ALTITUDE

Aerodynamic characteristics of a hypersonic viscous optimized waverider at high altitudes
[BTN-95-EIX95152583251] p 266 A95-73552

FLIGHT CHARACTERISTICS

Polar Patrol Balloon
[BTN-95-EIX95152582318] p 316 A95-73521

Analytical solution for controls, heats, and states of flight trajectories
[BTN-95-EIX95152583286] p 282 A95-73587

Real-time estimation of atmospheric turbulence severity from in-situ aircraft measurements
[BTN-95-EIX95182619231] p 319 A95-76657

Flight test of the X-29A at high angle of attack: Flight dynamics and controls
[NASA-TP-3537] p 284 N95-22806

Analysis of the longitudinal handling qualities and pilot-induced-oscillation tendencies of the High-Angle-of-Attack Research Vehicle (HARV)
p 293 N95-23297

Preparation of course materials: Elementary mathematics of powered flight
p 324 N95-23320

Handling qualities of the High Speed Civil Transport
p 294 N95-23325

FLIGHT CONDITIONS

Direct adaptive performance optimization of subsonic transports: A periodic perturbation technique
[NASA-TM-4676] p 284 N95-22829

Control of flow separation in airfoil/wing design applications
p 274 N95-23294

FLIGHT CONTROL

Dynamical instability of the aerogravity assist maneuver
[BTN-95-EIX95152583282] p 298 A95-73583

Identification of higher order helicopter dynamics using linear modeling methods
[HTN-95-80851] p 290 A95-75093

Effects of high order dynamics on helicopter flight control law design
[HTN-95-80852] p 290 A95-75094

Investigation of the effects of bandwidth and time delay on helicopter roll-axis handling qualities
[HTN-95-80853] p 290 A95-75095

Integrated flight/propulsion control for helicopters
[HTN-95-80854] p 290 A95-75096

Cypher moves toward autonomous flight
[HTN-95-41394] p 283 A95-76390

Functional agility metrics and optimal trajectory analysis
[BTN-95-EIX95182619121] p 321 A95-76598

H-infinity helicopter flight control law design with and without rotor state feedback
[BTN-95-EIX95182619129] p 291 A95-76606

Automatic guidance and control for helicopter obstacle avoidance
[BTN-95-EIX95182619130] p 291 A95-76607

Direct-lift design strategy for longitudinal control of hypersonic aircraft
[BTN-95-EIX95182619131] p 291 A95-76608

Shuttle entry guidance revisited using nonlinear geometric methods
[BTN-95-EIX95182619144] p 299 A95-76621

Attainable moments for the constrained control allocation problem
[BTN-95-EIX95182619149] p 322 A95-76626

Application of Navier-Stokes aerodynamic methods to improve fighter wing maneuver performance
[BTN-95-EIX95182619218] p 284 A95-76644

Robustly stable preliminary control systems design for the YF-16 CCV aircraft
[BTN-95-EIX95202637608] p 292 A95-76681

Virtual reality flight control display with six-degree-of-freedom controller and spherical orientation overlay
[NASA-CASE-NPO-18733-1-CU] p 288 N95-22578

Flight test of the X-29A at high angle of attack: Flight dynamics and controls
[NASA-TP-3537] p 284 N95-22806

Analysis of the longitudinal handling qualities and pilot-induced-oscillation tendencies of the High-Angle-of-Attack Research Vehicle (HARV)
p 293 N95-23297

Inner loop flight control for the High-Speed Civil Transport
p 293 N95-23314

Differential GPS and system integration of the Low Visibility Landing and Surface Operations (LVLASO) demonstration
p 280 N95-23318

Engines-only flight control system
[NASA-CASE-ARC-11944-1] p 294 N95-23389

Aerodynamic surface distension system for high angle of attack forebody vortex control
[NASA-CASE-ARC-11979-1] p 286 N95-23390

Feedback control laws for highly maneuverable aircraft
[NASA-CR-197944] p 295 N95-23410

Aerodynamic flight control to increase payload capability of future launch vehicles
[NASA-CR-197704] p 300 N95-24032

FLIGHT CREWS

Aircraft accident report. Runway overrun following rejected takeoff. Continental Airlines flight 795, McDonnell Douglas MD-82, N18835, LaGuardia Airport, Flushing, NY, 2 March 1994
[PB95-910401] p 277 N95-23609

FLIGHT HAZARDS

Thundercloud electric field modeling for the ionosphere-Earth region. 1: Dependence on cloud charge distribution
[HTN-95-41223] p 317 A95-75035

Optimal lateral-escape maneuvers for microburst encounters during final approach
[BTN-95-EIX95182619127] p 276 A95-76604

FLIGHT INSTRUMENTS

Design of wide angle head up displays for synthetic vision
[BTN-95-EIX95212641070] p 287 A95-76735

TRISTAR 1: Evaluation methods for testing head-up display (HUD) flight symbology
[NASA-TM-4665] p 288 N95-24030

FLIGHT MANAGEMENT SYSTEMS

Pilot Weather Advisor system
[BTN-95-EIX95152582314] p 316 A95-73517

FLIGHT MECHANICS

Functional dependence of trajectory dispersion on initial condition errors
[BTN-95-EIX95152583263] p 298 A95-73564

Aerodynamics of the Shuttle Orbiter at high altitudes
[BTN-95-EIX95182617454] p 298 A95-75725

Kinematics and aerodynamics of velocity-vector roll
[BTN-95-EIX95182619126] p 291 A95-76603

FLIGHT OPERATIONS

- Pilot Weather Advisor system
[BTN-95-EIX95152582314] p 316 A95-73517
- Guidance and control requirements for high-speed
Rollout and Turnoff (ROTO)
[NASA-CR-195026] p 292 N95-22674
- Oceanic operations: An authoritative guide to oceanic
operations
[FAA-AFS-550] p 277 N95-24065

FLIGHT PATHS

- Trajectory modeling of emissions from lower
stratospheric aircraft
[HTN-95-41219] p 317 A95-75031
- Optimal lateral-escape maneuvers for microburst
encounters during final approach
[BTN-95-EIX95182619127] p 276 A95-76604
- Analytical solution and parameter estimation of projectile
dynamics
[BTN-95-EIX95212645695] p 272 A95-76747
- Nonlinear system guidance in the presence of
transmission zero dynamics
[NASA-TM-4661] p 309 N95-22804
- Engines-only flight control system
[NASA-CASE-ARC-11944-1] p 294 N95-23389

FLIGHT RECORDERS

- The role of flight progress strips in en route air traffic
control: A time-series analysis
[DOT/FAA/AM-95/4] p 280 N95-23565

FLIGHT SAFETY

- Automatic guidance and control for helicopter obstacle
avoidance
[BTN-95-EIX95182619130] p 291 A95-76607
- Additional improvements to the NASA Lewis ice
accretion code LEWICE
[NASA-TM-106849] p 309 N95-22669
- Oklahoma City air logistics center (USAF) aging aircraft
corrosion program
p 262 N95-23519
- A multibody/finite element analysis approach for
modeling of crash dynamic responses
[NIAR-94-3] p 277 N95-24050

FLIGHT SIMULATION

- Virtual reality flight control display with
six-degree-of-freedom controller and spherical orientation
overlay
[NASA-CASE-NPO-18733-1-CU] p 288 N95-22578
- Direct adaptive performance optimization of subsonic
transports: A periodic perturbation technique
[NASA-TM-4676] p 284 N95-22829
- Review of aeronautical fatigue investigation in the
Netherlands during the period March 1991-March 1993
[PB95-139184] p 285 N95-23161
- Development of qualification guidelines for personal
computer-based aviation training devices
[DOT/FAA/AM-95/6] p 323 N95-23603

FLIGHT SIMULATORS

- Simulation of turbulent fluctuations
[BTN-95-EIX95142553041] p 304 A95-73457

FLIGHT TESTS

- Flight test evaluation of a 35 GHz forward looking
altimeter for terrain avoidance
[BTN-95-EIX95212641071] p 287 A95-76736
- 2 micron LIDAR for laser-based remote sensing: Flight
demonstration and application survey
[BTN-95-EIX95212641072] p 319 A95-76737
- Flight test of the X-29A at high angle of attack: Flight
dynamics and controls
[NASA-TP-3537] p 284 N95-22806
- High-lift flow-physics flight experiments on a subsonic
civil transport aircraft (B737-100)
p 275 N95-23333
- TRISTAR 1: Evaluation methods for testing head-up
display (HUD) flight symbology
[NASA-TM-4665] p 288 N95-24030

FLIGHT TRAINING

- Development of qualification guidelines for personal
computer-based aviation training devices
[DOT/FAA/AM-95/6] p 323 N95-23603

FLOORS

- Automatic riveting cell for commercial aircraft floor grid
assembly
[BTN-95-EIX95182617807] p 261 A95-75752

FLOW CHARACTERISTICS

- Impeller flow field characterization with a laser two-focus
velocimeter
p 313 N95-23440

FLOW DISTORTION

- A new type of simulator for simulating the flow-field
distortion of engine inlet
[BTN-95-EIX95202638963] p 289 A95-76673

FLOW DISTRIBUTION

- Experimental investigation of the flowfield about an
upswept afterbody
[BTN-95-EIX95152582321] p 265 A95-73524
- Convective and radiative heat transfer analysis for the
fire 2 forebody
[BTN-95-EIX95182617460] p 268 A95-75731

- Supersonic near-wake afterbody boattailing effects on
axisymmetric bodies
[BTN-95-EIX95182617465] p 268 A95-75736

- Transient structure of vortex breakdown on a delta
wing
[BTN-95-EIX95182619073] p 268 A95-75758

- Observations on using experimental data as boundary
conditions for computations
[BTN-95-EIX95182619103] p 321 A95-76588

- Simple method of supersonic flow visualization using
watertable
[BTN-95-EIX95182619105] p 269 A95-76590

- Tracking of raindrops in flow over an airfoil
[BTN-95-EIX95182619221] p 308 A95-76647

- Aerodynamics of a finite wing with simulated ice
[BTN-95-EIX95182619227] p 270 A95-76653

- Neural network prediction of three-dimensional unsteady
separated flowfields
[BTN-95-EIX95182619232] p 308 A95-76658

- Flow visualization studies of VTOL aircraft models during
Hover in ground effect
[NASA-TM-108860] p 272 N95-22666

- A CFD study of complex missile and store configurations
in relative motion
[NASA-CR-197912] p 285 N95-22949

- Mach 10 computational study of a three-dimensional
scramjet inlet flow field
[NASA-TM-4602] p 309 N95-23015

- Experimental results for a hypersonic nozzle/afterbody
flow field
[NASA-TM-4638] p 274 N95-23250

- Holographic interferometric tomography for
reconstructing flow fields
p 310 N95-23287

- Three-dimensional unsteady flow calculations in an
advanced gas generator turbine
p 312 N95-23425

- A study of the vortex flow over 76/40-deg double-delta
wing
[NASA-CR-195032] p 314 N95-23466

- Validation of a Computational Fluid Dynamics (CFD)
code for supersonic axisymmetric base flow
p 315 N95-23652

FLOW MEASUREMENT

- Time-of-flight mass spectrometer for impulse facilities
[BTN-95-EIX95142553057] p 262 A95-73441

- Flow structure in the wake of a wishbone vortex
generator
[BTN-95-EIX95142553044] p 304 A95-73454

- Real-time estimation of atmospheric turbulence severity
from in-situ aircraft measurements
[BTN-95-EIX95182619231] p 319 A95-76657

- Impeller flow field characterization with a laser two-focus
velocimeter
p 313 N95-23440

FLOW STABILITY

- A time-accurate finite volume method valid at all flow
velocities
p 314 N95-23447

FLOW VELOCITY

- Flow structure in the wake of a wishbone vortex
generator
[BTN-95-EIX95142553044] p 304 A95-73454

- Simulation of turbulent fluctuations
[BTN-95-EIX95142553041] p 304 A95-73457

- Effects of expansions on a supersonic boundary layer:
Surface pressure measurements
[BTN-95-EIX95142553036] p 263 A95-73462

- Supersonic axisymmetric conical flow solutions for
different ratios of specific heats
[BTN-95-EIX95152583283] p 306 A95-73584

- Real-time estimation of atmospheric turbulence severity
from in-situ aircraft measurements
[BTN-95-EIX95182619231] p 319 A95-76657

- Phase 2: HGM air flow tests in support of HEX vane
investigation
p 312 N95-23438

- Impeller flow field characterization with a laser two-focus
velocimeter
p 313 N95-23440

- A time-accurate finite volume method valid at all flow
velocities
p 314 N95-23447

FLOW VISUALIZATION

- Flow visualization studies on sidewall effects in
two-dimensional transonic airfoil testing
[BTN-95-EIX95152582313] p 264 A95-73516

- Experimental investigation of the flowfield about an
upswept afterbody
[BTN-95-EIX95152582321] p 265 A95-73524

- Simple method of supersonic flow visualization using
watertable
[BTN-95-EIX95182619105] p 269 A95-76590

- Aerodynamic characteristics of external store
configurations at low speeds
[BTN-95-EIX95182619230] p 271 A95-76656

- Flow visualization studies of VTOL aircraft models during
Hover in ground effect
[NASA-TM-108860] p 272 N95-22666

- Experimental results for a hypersonic nozzle/afterbody
flow field
[NASA-TM-4638] p 274 N95-23250

FLUID BOUNDARIES

- Predicting exhaust plume boundaries with supersonic
external flows
[BTN-95-EIX95152583258] p 297 A95-73559

FLUID DYNAMICS

- Possible effects of CO2 increase on the high-speed civil
transport impact on ozone
[HTN-95-60779] p 317 A95-75976

- Transport of exhaust products in the near trail of a jet
engine under atmospheric conditions
[HTN-95-91421] p 319 A95-77334

- High-lift flow-physics flight experiments on a subsonic
civil transport aircraft (B737-100)
p 275 N95-23333

FLUID FLOW

- Holographic interferometric tomography for
reconstructing flow fields
p 310 N95-23287

- Phase 2: HGM air flow tests in support of HEX vane
investigation
p 312 N95-23438

- A time-accurate finite volume method valid at all flow
velocities
p 314 N95-23447

FLUID-SOLID INTERACTIONS

- Structural acoustic calculations in the low-frequency
range
[BTN-95-EIX95152582336] p 323 A95-73538

FLUTTER

- Postinstability behavior of a two-dimensional airfoil with
a structural nonlinearity
[BTN-95-EIX95152582337] p 266 A95-73539

- Flutter of an infinitely long panel in a duct
[BTN-95-EIX95182619087] p 291 A95-75772

- Multirate flutter suppression system design for a model
wing
[BTN-95-EIX95182619132] p 292 A95-76609

- Summary of an active flexible wing program
[BTN-95-EIX95182619209] p 283 A95-76635

- Multiple-function digital controller system for active
flexible wing wind-tunnel model
[BTN-95-EIX95182619212] p 322 A95-76638

- Flutter suppression control law design and testing for
the active flexible wing
[BTN-95-EIX95182619214] p 292 A95-76640

- Flutter suppression for the active flexible wing: A
classical design
[BTN-95-EIX95182619216] p 292 A95-76642

- Flutter analysis of composite box beams
[NASA-CR-197931] p 294 N95-23392

FLUTTER ANALYSIS

- Application of transonic small disturbance theory to the
active flexible wing model
[BTN-95-EIX95182619210] p 270 A95-76636

- Flutter analysis of composite box beams
[NASA-CR-197931] p 294 N95-23392

FOIL BEARINGS

- Influence of backup bearings and support structure
dynamics on the behavior of rotors with active supports
[NASA-CR-197438] p 310 N95-23190

FOREBODIES

- Forebody flow control on a full-scale F/A-18 aircraft
[BTN-95-EIX95152582333] p 281 A95-73535

- Convective and radiative heat transfer analysis for the
fire 2 forebody
[BTN-95-EIX95182617460] p 268 A95-75731

- Review and development of base pressure and base
heating correlations in supersonic flow
[BTN-95-EIX95212645688] p 271 A95-76740

- Aerodynamic surface distension system for high angle
of attack forebody vortex control
[NASA-CASE-ARC-11979-1] p 286 N95-23390

FRAGMENTS

- Rationale for the Modular Air-system Vulnerability
Estimation Network (MAVEN) methodology
[AD-A285797] p 284 N95-22510

FREE FLOW

- Aerodynamic shape optimization using preconditioned
conjugate gradient methods
[BTN-95-EIX95142553033] p 263 A95-73465

- Unstructured grid solutions to a wing/pylon/store
configuration
[BTN-95-EIX95152582322] p 265 A95-73525

- Hypersonic nonequilibrium Navier-Stokes solutions over
an ablating graphite nosetip
[BTN-95-EIX95152583252] p 305 A95-73553

- Comparison of linear stability results with flight transition
data
[BTN-95-EIX95182619097] p 283 A95-76582

FREE JETS

- Main features of overexpanded triple jets
[BTN-95-EIX95142553040] p 304 A95-73458

FREQUENCY RESPONSE

- Real-time navigation using the global positioning
system
[BTN-95-EIX95172595298] p 279 A95-75714

FREQUENCY STABILITY

- Sensitivity of combustion-acoustic instabilities to boundary conditions for premixed gas turbine combustors
[NASA-TM-106890] p 289 N95-23550

FROST

- Effect of underwing frost on a transport aircraft airfoil at flight Reynolds number
[BTN-95-EIX95152582334] p 276 A95-73536

FUEL CONSUMPTION

- Fuel-optimal bank-angle control for lunar-return aerocapture
[BTN-95-EIX9512645706] p 299 A95-76758

FUSELAGES

- Growth of multiple cracks and their linkup in a fuselage lap joint
[BTN-95-EIX95142553047] p 286 A95-73451
- Efficient sensitivity analysis for rotary-wing aeromechanical problems
[BTN-95-EIX95152577585] p 264 A95-73497
- Experimental investigation of the flowfield about an upswept afterbody
[BTN-95-EIX95152582321] p 265 A95-73524
- Multiple site fatigue damage in fuselage skin splices: Experimental simulation and theoretical prediction
[BTN-95-EIX95152584676] p 276 A95-73588
- An analytical and experimental investigation of the response of the curved, composite frame/skin specimens
[HTN-95-80857] p 283 A95-75099
- Residual strength of thin panels with cracks
p 311 N95-23311

G

GALLIUM ARSENIDES

- Design of a GaAs/Ge solar array for unmanned aerial vehicles
[NASA-TM-106870] p 320 N95-23259

GAS DYNAMICS

- Measurement of particle emissions from clean room gas-handling components
[BTN-94-EIX94381359040] p 295 A95-74554
- Measurement of moisture and total hydrocarbon contributions by valves used in clean room gas-delivery systems
[BTN-94-EIX94381359041] p 295 A95-74629
- High-performance parallel analysis of coupled problems for aircraft propulsion
[NASA-CR-197440] p 289 N95-23088

GAS FLOW

- High-performance parallel analysis of coupled problems for aircraft propulsion
[NASA-CR-197440] p 289 N95-23088

GAS GENERATORS

- Three-dimensional unsteady flow calculations in an advanced gas generator turbine
p 312 N95-23425

GAS HEATING

- Hypersonic nonequilibrium Navier-Stokes solutions over an ablating graphite nosetip
[BTN-95-EIX95152583252] p 305 A95-73553

GAS INJECTION

- Simulation of transverse gas injection in turbulent supersonic air flows
[BTN-95-EIX95182619080] p 269 A95-75765

GAS JETS

- Mach wave emission from a high-temperature supersonic jet
[BTN-95-EIX95152577586] p 264 A95-73496

GAS MIXTURES

- Hypersonic convective heat transfer over 140-deg blunt cones in different gases
[BTN-95-EIX95152583253] p 306 A95-73554

GAS STREAMS

- Experimental results for a hypersonic nozzle/afterbody flow field
[NASA-TM-4638] p 274 N95-23250

GAS TURBINE ENGINES

- Fatigue strength of high-temperature alloys under conditions of cyclic temperature variation. Communication 1: Experimental procedure and results
[BTN-94-EIX94401363884] p 307 A95-75516
- Erosion of dust-filtered helicopter turbine engines. Part 2: Erosion reduction
[BTN-95-EIX95182619223] p 289 A95-76649
- Evolution of oxidation and creep damage mechanisms in HIPed silicon nitride materials
[DE95-001360] p 300 N95-22689

GAS TURBINES

- Sensitivity of combustion-acoustic instabilities to boundary conditions for premixed gas turbine combustors
[NASA-TM-106890] p 289 N95-23550

GAS-SOLID INTERACTIONS

- Three-dimensional structure of a supersonic jet impinging on an inclined plate
[BTN-95-EIX95152583259] p 267 A95-73560

GEARS

- Gearbox vibration diagnostic analyzer
[NASA-CR-189141] p 316 N95-23792

GENERAL OVERVIEWS

- Aircraft fires, smoke toxicity, and survival: An overview
[DOT/FAA/AM-95/8] p 277 N95-24024

GEOGRAPHIC INFORMATION SYSTEMS

- Pilot Weather Advisor system
[BTN-95-EIX95152582314] p 316 A95-73517
- Automation technology using Geographic Information System (GIS)
p 324 N95-23284

GEOIDS

- Geoid lineations of 1000 km wavelength over the central Pacific
[HTN-95-11304] p 319 A95-77009

GEOMETRIC DILUTION OF PRECISION

- On the exact solutions of pseudorange equations
[BTN-95-EIX95142555477] p 278 A95-73433

GEOSYNCHRONOUS ORBITS

- Effects of satellite bunching on the probability of collision in geosynchronous orbit
[BTN-95-EIX95152583276] p 298 A95-73577

GERMANIUM ALLOYS

- Design of a GaAs/Ge solar array for unmanned aerial vehicles
[NASA-TM-106870] p 320 N95-23259

GLOBAL POSITIONING SYSTEM

- On the exact solutions of pseudorange equations
[BTN-95-EIX95142555477] p 278 A95-73433
- Enhancing filter robustness in cascaded GPS-INS integrations
[BTN-95-EIX95142555475] p 278 A95-73435
- Thermal force modeling for global positioning system satellites using the finite element method
[BTN-95-EIX95152583270] p 278 A95-73571
- Real-time navigation using the global positioning system
[BTN-95-EIX95172595298] p 279 A95-75714
- New failure detection approach and its application to GPS autonomous integrity monitoring
[BTN-95-EIX95202637613] p 279 A95-76676
- Description of a GNSS availability model and its use in developing requirements
[BTN-95-EIX95202637603] p 308 A95-76686
- Differential GPS and system integration of the Low Visibility Landing and Surface Operations (LVLASO) demonstration
p 280 N95-23318

GRAPHICAL USER INTERFACE

- TIGER: A user-friendly interactive grid generation system for complicated turbomachinery and axis-symmetric configurations
p 322 N95-23419

GRAPHITE

- Hypersonic nonequilibrium Navier-Stokes solutions over an ablating graphite nosetip
[BTN-95-EIX95152583252] p 305 A95-73553

GRAPHITE-EPOXY COMPOSITES

- An analytical and experimental investigation of the response of the curved, composite frame/skin specimens
[HTN-95-80857] p 283 A95-75099

GRASSLANDS

- A comparison of some aerodynamic resistance methods using measurements over cotton and grass from the 1991 California ozone deposition experiment
[HTN-95-11295] p 319 A95-77000

GRAVITATIONAL EFFECTS

- Airborne rotary air separator study
[NASA-CR-189099] p 290 N95-24053

GRID GENERATION (MATHEMATICS)

- CFD optimization of a theoretical minimum-drag body
[BTN-95-EIX95182619234] p 308 A95-76660
- Euler Technology Assessment program for preliminary aircraft design employing SPLITFLOW code with Cartesian unstructured grid method
[NASA-CR-4649] p 273 N95-22917
- A CFD study of complex missile and store configurations in relative motion
[NASA-CR-197912] p 285 N95-22949
- High-performance parallel analysis of coupled problems for aircraft propulsion
[NASA-CR-197440] p 289 N95-23088
- Euler technology assessment for preliminary aircraft design employing OVERFLOW code with multiblock structured-grid method
[NASA-CR-4651] p 273 N95-23095
- TIGER: A user-friendly interactive grid generation system for complicated turbomachinery and axis-symmetric configurations
p 322 N95-23419
- CFD analysis of turbopump volutes
p 312 N95-23436

GROUND EFFECT (AERODYNAMICS)

- The influence of alternate inter-blade connections on ground resonance
[HTN-95-80859] p 267 A95-75101

- Stability derivatives of a flapped plate in unsteady ground effect
[BTN-95-EIX95182619225] p 270 A95-76651

- Unsteady ground effects on aerodynamic coefficients of finite wings with camber
[BTN-95-EIX95182619233] p 271 A95-76659

- Flow visualization studies of VTOL aircraft models during Hover in ground effect
[NASA-TM-108860] p 272 N95-22666

GROUND RESONANCE

- The influence of alternate inter-blade connections on ground resonance
[HTN-95-80859] p 267 A95-75101

GUIDANCE (MOTION)

- Moving mass trim control for aerospace vehicles
[DE95-002602] p 299 N95-23532

GULF OF MEXICO

- Oceanic operations: An authoritative guide to oceanic operations
[FAA-AFS-550] p 277 N95-24065

GULF STREAM

- Assimilation of altimeter data in a quasi-geostrophic model of the Gulf Stream system: A dynamical perspective
[NASA-CR-196313] p 320 N95-23766

GUST LOADS

- Response of a nonrotating rotor blade to lateral turbulence. Part 2: Experiment
[BTN-95-EIX95182619229] p 284 A95-76655
- Review of aeronautical fatigue investigation in the Netherlands during the period March 1991-March 1993
[PB95-139184] p 285 N95-23161

GYROCOMPASSES

- Covariance analysis of strapdown INS considering gyrocompass characteristics
[BTN-95-EIX95202637592] p 279 A95-76697

H

H-INFINITY CONTROL

- H-infinity helicopter flight control law design with and without rotor state feedback
[BTN-95-EIX95182619129] p 291 A95-76606
- Stable H(infinity) controller design for the longitudinal dynamics of an aircraft
[NASA-TM-106847] p 293 N95-22954
- Feedback control laws for highly maneuverable aircraft
[NASA-CR-197944] p 295 N95-23410

HARDNESS

- Evaluation of advanced aerospace materials by depth sensing indentation and scratch methods
[BTN-95-EIX95152584678] p 282 A95-73590

HARMONIC CONTROL

- Analysis of a higher harmonic control test to reduce blade vortex interaction noise
[BTN-95-EIX95152582330] p 265 A95-73532

HAZARDS

- Mishap risk control for advanced aerospace/composite materials
p 301 N95-23031

HEAD-UP DISPLAYS

- Design of wide angle head up displays for synthetic vision
[BTN-95-EIX95212641070] p 287 A95-76735
- TRISTAR 1: Evaluation methods for testing head-up display (HUD) flight symbology
[NASA-TM-4665] p 288 N95-24030

HEAT EXCHANGERS

- Base drag prediction on missile configurations
[BTN-95-EIX95152583256] p 266 A95-73557
- Phase 2: HGM air flow tests in support of HEX vane investigation
p 312 N95-23438

HEAT OF SOLUTION

- Analytical solution for controls, heats, and states of flight trajectories
[BTN-95-EIX95152583286] p 282 A95-73587

HEAT RESISTANT ALLOYS

- Fatigue strength of high-temperature alloys under conditions of cyclic temperature variation. Communication 1: Experimental procedure and results
[BTN-94-EIX94401363884] p 307 A95-75516

HEAT TRANSFER

- Comparison of linear stability results with flight transition data
[BTN-95-EIX95182619097] p 283 A95-76582
- Application of a control-volume-based finite-element formulation to the shock tube problem
[BTN-95-EIX95182619099] p 295 A95-76584
- Simulating heat addition via mass addition in constant area compressible flows
[BTN-95-EIX95182619100] p 307 A95-76585

- Development and verification of a resin film infusion/resin transfer molding simulation model for fabrication of advanced textile composites
[NASA-CR-197439] p 301 N95-23179
- HELICOPTER CONTROL**
Identification of higher order helicopter dynamics using linear modeling methods
[HTN-95-80851] p 290 A95-75093
Effects of high order dynamics on helicopter flight control law design
[HTN-95-80852] p 290 A95-75094
Investigation of the effects of bandwidth and time delay on helicopter roll-axis handling qualities
[HTN-95-80853] p 290 A95-75095
Integrated flight/propulsion control for helicopters
[HTN-95-80854] p 290 A95-75096
H-infinity helicopter flight control law design with and without rotor state feedback
[BTN-95-EIX95182619129] p 291 A95-76606
Automatic guidance and control for helicopter obstacle avoidance
[BTN-95-EIX95182619130] p 291 A95-76607
An investigation of helicopter dynamic coupling using an analytical model
[NASA-CR-197420] p 285 N95-23217
- HELICOPTER DESIGN**
Integrated flight/propulsion control for helicopters
[HTN-95-80854] p 290 A95-75096
H-76B fantail demonstrator composite fan blade fabrication
[HTN-95-80856] p 283 A95-75098
- HELICOPTER ENGINES**
Erosion of dust-filtered helicopter turbine engines. Part 1: Basic theoretical considerations
[BTN-95-EIX95182619222] p 288 A95-76648
Erosion of dust-filtered helicopter turbine engines. Part 2: Erosion reduction
[BTN-95-EIX95182619223] p 289 A95-76649
Life prediction of helicopter engines fitted with dust filters
[BTN-95-EIX95182619224] p 289 A95-76650
- HELICOPTER PERFORMANCE**
Investigation of the effects of bandwidth and time delay on helicopter roll-axis handling qualities
[HTN-95-80853] p 290 A95-75095
The influence of alternate inter-blade connections on ground resonance
[HTN-95-80859] p 267 A95-75101
- HELICOPTER PROPELLER DRIVE**
Gearbox vibration diagnostic analyzer
[NASA-CR-189141] p 316 N95-23792
- HELICOPTERS**
Static pressure distribution in the inlet of a helicopter turbine compressor
[BTN-95-EIX95152582339] p 266 A95-73541
Improving prediction: The incorporation of simplified rotor dynamics in a mathematical model of the bell 412HP
[BTN-95-EIX95152584679] p 282 A95-73591
Sensitivity of acoustic predictions to variation of input parameters
[HTN-95-80855] p 267 A95-75097
The influence of alternate inter-blade connections on ground resonance
[HTN-95-80859] p 267 A95-75101
An investigation of helicopter dynamic coupling using an analytical model
[NASA-CR-197420] p 285 N95-23217
Thin tailored composite wing for civil tiltrotor
p 285 N95-23317
- HEURISTIC METHODS**
Automatic guidance and control for helicopter obstacle avoidance
[BTN-95-EIX95182619130] p 291 A95-76607
- HIGH ALTITUDE**
Aerodynamic characteristics of a hypersonic viscous optimized waverider at high altitudes
[BTN-95-EIX95152583251] p 266 A95-73552
Higher-order viscous shock-layer solutions for high-altitude flows
[BTN-95-EIX95152583255] p 306 A95-73556
Aerodynamics of the Shuttle Orbiter at high altitudes
[BTN-95-EIX95182617454] p 298 A95-75725
Particle kinetic simulation of high altitude hypervelocity flight
[NASA-CR-197383] p 309 N95-22481
- HIGH ASPECT RATIO**
Convergence acceleration of implicit schemes in the presence of high aspect ratio grid cells
p 313 N95-23446
- HIGH RESOLUTION**
MAX-91: Polarimetric SAR results on Montespertoli site
p 320 N95-23940

- HIGH SPEED**
Possible effects of CO2 increase on the high-speed civil transport impact on ozone
[HTN-95-60779] p 317 A95-75976
Inner loop flight control for the High-Speed Civil Transport
p 293 N95-23314
- HIGH STRENGTH STEELS**
Test method and test results for environmental assessment of aircraft materials
p 302 N95-23509
- HIGH TEMPERATURE**
Evolution of oxidation and creep damage mechanisms in HIPed silicon nitride materials
[DE95-001360] p 300 N95-22689
Design of a variable area diffuser for a 15-inch Mach 6 open-jet tunnel
p 297 N95-23309
- HIGH TEMPERATURE GASES**
Mach wave emission from a high-temperature supersonic jet
[BTN-95-EIX95152577586] p 264 A95-73496
Phase 2: HGM air flow tests in support of HEX vane investigation
p 312 N95-23438
- HIGH TEMPERATURE SUPERCONDUCTORS**
Phonon characteristics of high (T sub c) superconductors from neutron Doppler broadening measurements
[DE95-003703] p 324 N95-24076
- HIGHLY MANEUVERABLE AIRCRAFT**
Feedback control laws for highly maneuverable aircraft
[NASA-CR-197944] p 295 N95-23410
- HISTORIES**
Development of aeronautical mobile satellite services over the past thirty years
[BTN-95-EIX95152589458] p 305 A95-73498
- HOLES (MECHANICS)**
Eddy current detection of pitting corrosion around fastener holes
p 315 N95-23507
POD assessment of NDI procedures using a round robin test
[AGARD-R-809] p 315 N95-23602
- HOLOGRAPHIC INTERFEROMETRY**
Holographic interferometric tomography for reconstructing flow fields
p 310 N95-23287
- HOMING**
Switched bias proportional navigation for homing guidance against highly maneuvering targets
[BTN-95-EIX95182619145] p 279 A95-76622
- HONEYCOMB STRUCTURES**
Minimum-mass design of sandwich aerobrakes for a lunar transfer vehicle
[BTN-95-EIX9512645707] p 299 A95-76759
- HORIZONTAL FLIGHT**
Response of a nonrotating rotor blade to lateral turbulence. Part 1: Theory
[BTN-95-EIX95182619228] p 284 A95-76654
- HOT ISOSTATIC PRESSING**
Evolution of oxidation and creep damage mechanisms in HIPed silicon nitride materials
[DE95-001360] p 300 N95-22689
- HOVERING**
H-infinity helicopter flight control law design with and without rotor state feedback
[BTN-95-EIX95182619129] p 291 A95-76606
Flow visualization studies of VTOL aircraft models during hover in ground effect
[NASA-TM-108860] p 272 N95-22666
- HUBS**
NASA low-speed axial compressor for fundamental research
[NASA-TM-4635] p 296 N95-23192
- HUMAN FACTORS ENGINEERING**
TRISTAR 1: Evaluation methods for testing head-up display (HUD) flight symbology
[NASA-TM-4665] p 288 N95-24030
- HUMIDITY**
Corrosion of landing gear steels
p 302 N95-23500
- HYDRAULIC ANALOGIES**
Simple method of supersonic flow visualization using watertable
[BTN-95-EIX95182619105] p 269 A95-76590
- HYDROCARBONS**
Measurement of moisture and total hydrocarbon contributions by valves used in clean room gas-delivery systems
[BTN-94-EIX94381359041] p 295 A95-74629
- HYDRODYNAMICS**
Numerical study of sound generation due to a spinning vortex pair
[BTN-95-EIX95182619075] p 307 A95-75760
- HYDROGRAPHY**
Assimilation of altimeter data in a quasi-geostrophic model of the Gulf Stream system: A dynamical perspective
[NASA-CR-196313] p 320 N95-23766
- HYPERBOLIC DIFFERENTIAL EQUATIONS**
On the exact solutions of pseudorange equations
[BTN-95-EIX95142555477] p 278 A95-73433

- HYPERSONIC AIRCRAFT**
Direct-lift design strategy for longitudinal control of hypersonic aircraft
[BTN-95-EIX95182619131] p 291 A95-76608
- HYPERSONIC BOUNDARY LAYER**
Analytical study of the neutral stability of a model hypersonic boundary layer
[BTN-95-EIX95152577589] p 263 A95-73493
- HYPERSONIC FLIGHT**
Shock tunnel measurements of hypervelocity blunted cone drag
[BTN-95-EIX95152577606] p 305 A95-73477
Analytical solution for controls, heats, and states of flight trajectories
[BTN-95-EIX95152583286] p 282 A95-73587
Direct-lift design strategy for longitudinal control of hypersonic aircraft
[BTN-95-EIX95182619131] p 291 A95-76608
Particle kinetic simulation of high altitude hypervelocity flight
[NASA-CR-197383] p 309 N95-22481
- HYPERSONIC FLOW**
Time-of-flight mass spectrometer for impulse facilities
[BTN-95-EIX95142553057] p 262 A95-73441
Analytical study of the neutral stability of a model hypersonic boundary layer
[BTN-95-EIX95152577589] p 263 A95-73493
Hypersonic rarefied flow past spheres including wake structure
[BTN-95-EIX95152583250] p 305 A95-73551
Application of the multigrid solution technique to hypersonic entry vehicles
[BTN-95-EIX95152583254] p 306 A95-73555
Zonally decoupled direct simulation Monte Carlo solutions of hypersonic blunt-body wake flows
[BTN-95-EIX95182617458] p 268 A95-75729
Scaling of incipient separation in supersonic/transonic speed laminar flows
[BTN-95-EIX95182619104] p 269 A95-76589
Review and development of base pressure and base heating correlations in supersonic flow
[BTN-95-EIX95212645688] p 271 A95-76740
Numerical analysis of hypersonic low-density scramjet inlet flow
[BTN-95-EIX95212645694] p 272 A95-76746
Laser velocimetry seed-particle behavior in shear layers at Mach 12
[BTN-95-EIX95212645712] p 272 A95-76764
Experimental results for a hypersonic nozzle/afterbody flow field
[NASA-TM-4638] p 274 N95-23250
Design of a variable area diffuser for a 15-inch Mach 6 open-jet tunnel
p 297 N95-23309
- HYPERSONIC HEAT TRANSFER**
Hypersonic convective heat transfer over 140-deg blunt cones in different gases
[BTN-95-EIX95152583253] p 306 A95-73554
- HYPERSONIC INLETS**
Optimization of contoured hypersonic scramjet inlets with a least-squares parabolized Navier-Stokes procedure
[HTN-95-20976] p 261 A95-74042
Numerical analysis of hypersonic low-density scramjet inlet flow
[BTN-95-EIX95212645694] p 272 A95-76746
- HYPERSONIC NOZZLES**
Optimized design of a hypersonic nozzle
p 297 N95-23304
- HYPERSONIC SPEED**
Mach 10 computational study of a three-dimensional scramjet inlet flow field
[NASA-TM-4602] p 309 N95-23015
Mach 10 computational study of a three-dimensional scramjet inlet flow field
[NASA-TM-4602] p 310 N95-23210
Design of a variable area diffuser for a 15-inch Mach 6 open-jet tunnel
p 297 N95-23309
- HYPERSONIC VEHICLES**
Computational study of plume-induced separation on a hypersonic powered model
[BTN-95-EIX95152582346] p 266 A95-73548
Application of the multigrid solution technique to hypersonic entry vehicles
[BTN-95-EIX95152583254] p 306 A95-73555
Analytical aeropropulsive/aeroelastic hypersonic-vehicle model with dynamic analysis
[BTN-95-EIX95182619138] p 269 A95-76615
Integrated design of hypersonic waveriders including inlets and tailfins
[BTN-95-EIX95212645692] p 271 A95-76744
Particle kinetic simulation of high altitude hypervelocity flight
[NASA-CR-197383] p 309 N95-22481

HYPERSONIC WAKES

- Zonally decoupled direct simulation Monte Carlo solutions of hypersonic blunt-body wake flows
[BTN-95-EIX95182617458] p 268 A95-75729

HYPERSONIC WIND TUNNELS

- Time-of-flight mass spectrometer for impulse facilities
[BTN-95-EIX95142553057] p 262 A95-73441
Optimized design of a hypersonic nozzle
p 297 N95-23304

HYPERSONICS

- Computational study of plume-induced separation on a hypersonic powered model
[BTN-95-EIX95152582346] p 266 A95-73548
Aerodynamic characteristics of a hypersonic viscous optimized waverider at high altitudes
[BTN-95-EIX95152583251] p 266 A95-73552
Hypersonic nonequilibrium Navier-Stokes solutions over an ablating graphite nose tip
[BTN-95-EIX95152583252] p 305 A95-73553

HYSTERESIS

- Computation of oscillating airfoil flows with one- and two-equation turbulence models
[BTN-95-EIX95152577588] p 263 A95-73494

ICE

- Collaborative research on aircraft icing and charging processes in ice
[AD-A285102] p 276 N95-23201

IMAGE ANALYSIS

- Scientific and technical photography at NASA Langley Research Center
p 310 N95-23290
Statistics of multi-look AIRSAR imagery: A comparison of theory with measurements
p 320 N95-23947

IMAGE PROCESSING

- Simple method of supersonic flow visualization using water table
[BTN-95-EIX95182619105] p 269 A95-76590
AVIRIS and TIMS data processing and distribution at the land processes distributed active archive center
p 325 N95-23872
Statistics of multi-look AIRSAR imagery: A comparison of theory with measurements
p 320 N95-23947

IMAGING TECHNIQUES

- Scientific and technical photography at NASA Langley Research Center
p 310 N95-23290
AIRSAR deployment in Australia, September 1993: Management and objectives
p 321 N95-23948

IMPACT TESTS

- Measurement of particle emissions from clean room gas-handling components
[BTN-94-EIX94381359040] p 295 A95-74554

IN SITU MEASUREMENT

- In situ observations in aircraft exhaust plumes in the lower stratosphere at midlatitudes
[HTN-95-A0862] p 318 A95-76266
Real-time estimation of atmospheric turbulence severity from in-situ aircraft measurements
[BTN-95-EIX95182619231] p 319 A95-76657

IN-FLIGHT MONITORING

- Enhancement of F/A-18 operational flight measurements: Data report for phase 1
[DSTO-TR-0049] p 286 N95-23666

INCENDIARY AMMUNITION

- Rationale for the Modular Air-system Vulnerability Estimation Network (MAVEN) methodology
[AD-A285797] p 284 N95-22510

INCOMPRESSIBLE FLOW

- Two-equation turbulence model for unsteady separated flows around airfoils
[BTN-95-EIX95142553054] p 262 A95-73444
Adaptive finite element method for turbulent flow near a propeller
[BTN-95-EIX95142553038] p 305 A95-73460
Eigenanalysis of unsteady flows about airfoils, cascades, and wings
[BTN-95-EIX95152577597] p 305 A95-73486
Progress in high-lift aerodynamic calculations
[BTN-95-EIX95152582315] p 264 A95-73518
Sidewash on the vertical tail in subsonic and supersonic flows
[BTN-95-EIX95152582316] p 264 A95-73519
Postinstability behavior of a two-dimensional airfoil with a structural nonlinearity
[BTN-95-EIX95152582337] p 266 A95-73539
Grid refinement test of time-periodic flows over bluff bodies
[BTN-94-EIX94401378822] p 307 A95-76491
Aerodynamic characteristics of external store configurations at low speeds
[BTN-95-EIX95182619230] p 271 A95-76656
Study of the droplet spray characteristics of a subsonic wind tunnel
[BTN-95-EIX95182619235] p 271 A95-76661

- Simulation on the 3-D turbulent flow in the passages of finocyl grain
[BTN-95-EIX95202638962] p 279 A95-76674

INDENTATION

- Evaluation of advanced aerospace materials by depth sensing indentation and scratch methods
[BTN-95-EIX95152584678] p 282 A95-73590

INDUCTION MOTORS

- Motor drive technologies for the power-by-wire (PBW) program: Options, trends and tradeoffs
[NASA-TM-106885] p 295 N95-23671

INERTIAL NAVIGATION

- Enhancing filter robustness in cascaded GPS-INS integrations
[BTN-95-EIX95142555475] p 278 A95-73435
Covariance analysis of strapdown INS considering gyrocompass characteristics
[BTN-95-EIX95202637592] p 279 A95-76697

INERTIAL PLATFORMS

- Dynamic response tests of inertial and optical wind-tunnel model attitude measurement devices
[NASA-TM-109182] p 296 N95-23011

INFILTRATION

- Development and verification of a resin film infusion/resin transfer molding simulation model for fabrication of advanced textile composites
[NASA-CR-197439] p 301 N95-23179

INFORMATION SYSTEMS

- Automation technology using Geographic Information System (GIS)
p 324 N95-23284

INFRARED IMAGERY

- AVIRIS and TIMS data processing and distribution at the land processes distributed active archive center
p 325 N95-23872

INFRARED LASERS

- 2 micron LIDAR for laser-based remote sensing: Flight demonstration and application survey
[BTN-95-EIX95212641072] p 319 A95-76737

INFRARED SPECTRA

- AVIRIS and TIMS data processing and distribution at the land processes distributed active archive center
p 325 N95-23872

INGESTION (ENGINES)

- Erosion of dust-filtered helicopter turbine engines. Part 1: Basic theoretical considerations
[BTN-95-EIX95182619222] p 288 A95-76648
Erosion of dust-filtered helicopter turbine engines. Part 2: Erosion reduction
[BTN-95-EIX95182619223] p 289 A95-76649
Life prediction of helicopter engines fitted with dust filters
[BTN-95-EIX95182619224] p 289 A95-76650

INLET FLOW

- Static pressure distribution in the inlet of a helicopter turbine compressor
[BTN-95-EIX95152582339] p 266 A95-73541
A new type of simulator for simulating the flow-field distortion of engine inlet
[BTN-95-EIX95202638963] p 289 A95-76673
Numerical analysis of hypersonic low-density scramjet inlet flow
[BTN-95-EIX95212645694] p 272 A95-76746
Flow visualization studies of VTOL aircraft models during Hover in ground effect
[NASA-TM-108860] p 272 N95-22666
Mach 10 computational study of a three-dimensional scramjet inlet flow field
[NASA-TM-4602] p 309 N95-23015
Mach 10 computational study of a three-dimensional scramjet inlet flow field
[NASA-TM-4602] p 310 N95-23210
Three-dimensional Navier-Stokes analysis and redesign of an imbedded bellmouth nozzle in a turbine cascade inlet section
p 311 N95-23423
Supersonic flow and shock formation in turbine tip gaps
p 312 N95-23429

INORGANIC COMPOUNDS

- Estimates of total organic and inorganic chlorine in the lower stratosphere from in situ and flask measurements during AASE 2
[HTN-95-A0861] p 317 A95-76265

INSPECTION

- Double pass retroreflection for corrosion detection in aircraft structures
p 323 N95-23503
Non-destructive detection of corrosion for life management
p 314 N95-23505
Health and usage monitoring systems: Corrosion surveillance
p 262 N95-23506
Eddy current detection of pitting corrosion around fastener holes
p 315 N95-23507
Corrosion detection and monitoring of aircraft structures: An overview
p 303 N95-23515
Experience of in-service corrosion on military aircraft
p 303 N95-23516

- POD assessment of NDI procedures using a round robin test
[AGARD-R-809] p 315 N95-23602

INTAKE SYSTEMS

- Static pressure distribution in the inlet of a helicopter turbine compressor
[BTN-95-EIX95152582339] p 266 A95-73541

INTEGRAL EQUATIONS

- Coupled FEM-BEM approach for mean flow effects on vibro-acoustic behavior of planar structures
[BTN-95-EIX95152577587] p 263 A95-73495

INTEGRATED CIRCUITS

- Cu deposition using a permanent magnet electron cyclotron resonance microwave plasma source
[DE94-017768] p 304 N95-23981

INTEGRATED LIBRARY SYSTEMS

- AVIRIS and TIMS data processing and distribution at the land processes distributed active archive center
p 325 N95-23872

INTERACTIONAL AERODYNAMICS

- Wing vertical position effects on wing-body carryover for noncircular missiles
[BTN-95-EIX95182617462] p 268 A95-75733

INTERLAYERS

- Compliant interlayer
[BTN-95-EIX95142562401] p 304 A95-73439

INTERNAL FLOW

- Main features of overexpanded triple jets
[BTN-95-EIX95142553040] p 304 A95-73458
Mach 10 computational study of a three-dimensional scramjet inlet flow field
[NASA-TM-4602] p 309 N95-23015
NASA low-speed axial compressor for fundamental research
[NASA-TM-4635] p 296 N95-23192
CFD analysis of turbopump volutes
p 312 N95-23436
Impeller flow field characterization with a laser two-focus velocimeter
p 313 N95-23440

INTERNAL PRESSURE

- Residual strength of thin panels with cracks
p 311 N95-23311

INTERNATIONAL TRADE

- Overview of AlliedSignal's avionics development in the CIS
[BTN-95-EIX95212641069] p 287 A95-76734

INTERPLANETARY SPACECRAFT

- Fourth-generation Mars vehicle concepts
[BTN-95-EIX95152583267] p 298 A95-73568

INTERPOLATION

- Application of a control-volume-based finite-element formulation to the shock tube problem
[BTN-95-EIX95182619099] p 295 A95-76584
On-line, adaptive state estimator for active noise control
p 322 N95-23308

INVISCID FLOW

- Aerodynamic shape optimization using preconditioned conjugate gradient methods
[BTN-95-EIX95142553033] p 263 A95-73465
Effects of spatial order of accuracy on the computation of vortical flowfields
[BTN-95-EIX95152577604] p 305 A95-73479
Sidewash on the vertical tail in subsonic and supersonic flows
[BTN-95-EIX95152582316] p 264 A95-73519
Unstructured grid solutions to a wing/pylon/store configuration
[BTN-95-EIX95152582322] p 265 A95-73525
Three-dimensional structure of a supersonic jet impinging on an inclined plate
[BTN-95-EIX95152583259] p 267 A95-73560

ION CYCLOTRON RADIATION

- Cu deposition using a permanent magnet electron cyclotron resonance microwave plasma source
[DE94-017768] p 304 N95-23981

IONOSPHERES

- Thundercloud electric field modeling for the ionosphere-Earth region. 1: Dependence on cloud charge distribution
[HTN-95-41223] p 317 A95-75035

ISENTROPIC PROCESSES

- Trajectory modeling of emissions from lower stratospheric aircraft
[HTN-95-41219] p 317 A95-75031

ITERATIVE SOLUTION

- Preconditioned domain decomposition scheme for three-dimensional aerodynamic sensitivity analysis
[BTN-95-EIX95152577612] p 321 A95-73471

J

JET AIRCRAFT NOISE

- Supersonic jet noise reductions predicted with increased jet spreading rate
[NASA-TM-106872] p 323 N95-23178

JET ENGINES

JET ENGINES

Transport of exhaust products in the near trail of a jet engine under atmospheric conditions
[HTN-95-91421] p 319 A95-77334
High-performance parallel analysis of coupled problems for aircraft propulsion
[NASA-CR-197440] p 289 N95-23088

JET EXHAUST

Transport of exhaust products in the near trail of a jet engine under atmospheric conditions
[HTN-95-91421] p 319 A95-77334

JET FLOW

Pneumatic concept for tip-stall control of cranked-arrow wings
[BTN-95-EIX95152582335] p 281 A95-73537

JET IMPINGEMENT

Three-dimensional structure of a supersonic jet impinging on an inclined plate
[BTN-95-EIX95152583259] p 267 A95-73560

JET MIXING FLOW

Supersonic jet noise reductions predicted with increased jet spreading rate
[NASA-TM-106872] p 323 N95-23178

K

K-EPSILON TURBULENCE MODEL

Computation of the poststall behavior of a circulation controlled airfoil
[BTN-95-EIX95152582320] p 264 A95-73523
Application of wall functions to generalized nonorthogonal curvilinear coordinate systems
[BTN-95-EIX95182619077] p 307 A95-75762
Numerical computation of aerodynamics and heat transfer in a turbine cascade and a turn-around duct using advanced turbulence models p 313 N95-23444

KALMAN FILTERS

Enhancing filter robustness in cascaded GPS-INS integrations
[BTN-95-EIX9514255475] p 278 A95-73435
Real-time navigation using the global positioning system
[BTN-95-EIX95172595298] p 279 A95-75714
New failure detection approach and its application to GPS autonomous integrity monitoring
[BTN-95-EIX95202637613] p 279 A95-76676

KNUDSEN FLOW

Hypersonic rarefied flow past spheres including wake structure
[BTN-95-EIX95152583250] p 305 A95-73551
Aerodynamic characteristics of a hypersonic viscous optimized waverider at high altitudes
[BTN-95-EIX95152583251] p 266 A95-73552
Aerodynamics of the Shuttle Orbiter at high altitudes
[BTN-95-EIX95182617454] p 298 A95-75725
Numerical analysis of hypersonic low-density scramjet inlet flow
[BTN-95-EIX95212645694] p 272 A95-76746

KUTTA-JOUKOWSKI CONDITION

Laplace interaction law for the computation of viscous airfoil flow in low- and high-speed aerodynamics
[BTN-95-EIX95142553037] p 263 A95-73461

L

LABORATORIES

Labs behind Boeing's new 777
[BTN-95-EIX95142562403] p 280 A95-73437

LAMINAR BOUNDARY LAYER

Review and development of base pressure and base heating correlations in supersonic flow
[BTN-95-EIX95212645688] p 271 A95-76740

LAMINAR FLOW

Effect of ambient turbulence intensity on sphere wakes at intermediate Reynolds numbers
[BTN-95-EIX95182619101] p 308 A95-76586
Scaling of incipient separation in supersonic/transonic speed laminar flows
[BTN-95-EIX95182619104] p 269 A95-76589
High-lift flow-physics flight experiments on a subsonic civil transport aircraft (B737-100) p 275 N95-23333
Supersonic laminar flow control research
[NASA-CR-197938] p 275 N95-23669

LAMINAR FLOW AIRFOILS

Natural laminar flow wing concept for supersonic transports
[BTN-95-EIX95182619226] p 308 A95-76652

LAMINAR WAKES

Effect of ambient turbulence intensity on sphere wakes at intermediate Reynolds numbers
[BTN-95-EIX95182619101] p 308 A95-76586

LAMINATES

MIL-HDBK-5 design allowables for fibre/metal laminates: ARALL 2 and ARALL 3
[BTN-94-EIX94371346933] p 300 A95-73345
Dynamic analysis of bearingless tail rotor blades based on nonlinear shell modes
[BTN-95-EIX95152582338] p 281 A95-73540
Validation of an effective flat cruciform-shaped specimen to study CFRP composite laminates under biaxial loading
[BTN-95-EIX95152584677] p 282 A95-73589
Interlaminar shear test method development for long term durability testing of composites p 301 N95-23300
New nondestructive techniques for the detection and quantification of corrosion in aircraft structures p 315 N95-23512

LANDING AIDS

Guidance and control requirements for high-speed Rollout and Turnoff (ROTO)
[NASA-CR-195026] p 292 N95-22674

LANDING GEAR

Corrosion of landing gear steels p 302 N95-23500

LANTHANUM OXIDES

Phonon characteristics of high (T sub c) superconductors from neutron Doppler broadening measurements
[DE95-003703] p 324 N95-24076

LAP JOINTS

Growth of multiple cracks and their linkup in a fuselage lap joint
[BTN-95-EIX95142553047] p 286 A95-73451

LAPLACE TRANSFORMATION

Laplace interaction law for the computation of viscous airfoil flow in low- and high-speed aerodynamics
[BTN-95-EIX95142553037] p 263 A95-73461

LASER APPLICATIONS

2 micron LIDAR for laser-based remote sensing: Flight demonstration and application survey
[BTN-95-EIX95212641072] p 319 A95-76737

LASER DOPPLER VELOCIMETERS

Laser velocimetry seed-particle behavior in shear layers at Mach 12
[BTN-95-EIX95212645712] p 272 A95-76764
Impeller flow field characterization with a laser two-focus velocimeter p 313 N95-23440

LASER SPECTROMETERS

AIRSAF deployment in Australia, September 1993: Management and objectives p 321 N95-23948

LATERAL CONTROL

Pneumatic concept for tip-stall control of cranked-arrow wings
[BTN-95-EIX95152582335] p 281 A95-73537
H-infinity helicopter flight control law design with and without rotor state feedback
[BTN-95-EIX95182619129] p 291 A95-76606
Fuel-optimal bank-angle control for lunar-return aerocapture
[BTN-95-EIX95212645706] p 299 A95-76758
Aerodynamic surface distension system for high angle of attack forebody vortex control
[NASA-CASE-ARC-11979-1] p 286 N95-23390
Feedback control laws for highly maneuverable aircraft
[NASA-CR-197944] p 295 N95-23410

LAUNCH VEHICLES

Aerodynamic flight control to increase payload capability of future launch vehicles
[NASA-CR-197704] p 300 N95-24032
Airborne rotary air separator study
[NASA-CR-189099] p 290 N95-24053

LAVAL NUMBER

Main features of overexpanded triple jets
[BTN-95-EIX95142553040] p 304 A95-73458

LEADING EDGE FLAPS

Natural laminar flow wing concept for supersonic transports
[BTN-95-EIX95182619226] p 308 A95-76652
Wing pressure distributions from subsonic tests of a high-wing transport model --- in the Langley 14- by 22-Foot Subsonic Wind Tunnel
[NASA-TM-4583] p 272 N95-22802

LEADING EDGE SLATS

Lift enhancing tabs for airfoils
[NASA-CASE-ARC-11990-1] p 286 N95-23395

LEADING EDGE THRUST

Analytic prediction of lift for delta wings with partial leading-edge thrust
[BTN-95-EIX95152582345] p 266 A95-73547

LEADING EDGES

Pneumatic concept for tip-stall control of cranked-arrow wings
[BTN-95-EIX95152582335] p 281 A95-73537

LEAST SQUARES METHOD

Optimization of contoured hypersonic scramjet inlets with a least-squares parabolized Navier-Stokes procedure
[HTN-95-20976] p 261 A95-74042

LEE WAVES

Diurnal variation of lee vortices in Taiwan and the surrounding area
[HTN-95-91363] p 318 A95-76394

LENGTH

Numerical investigation of supersonic flows around a spiked blunt body
[BTN-95-EIX95212645690] p 271 A95-76742

LENTICULAR BODIES

Evolution of oxidation and creep damage mechanisms in HIPed silicon nitride materials
[DE95-001360] p 300 N95-22689

LIFE (DURABILITY)

Test method and test results for environmental assessment of aircraft materials p 302 N95-23509

LIFT

Laplace interaction law for the computation of viscous airfoil flow in low- and high-speed aerodynamics
[BTN-95-EIX95142553037] p 263 A95-73461
Progress in high-lift aerodynamic calculations
[BTN-95-EIX95152582315] p 264 A95-73518
Separation control on high-lift airfoils via micro-vortex generators
[BTN-95-EIX95152582326] p 265 A95-73529
Study of an airfoil with a flap and spoiler
[BTN-95-EIX95152582327] p 265 A95-73530
Pneumatic concept for tip-stall control of cranked-arrow wings
[BTN-95-EIX95152582335] p 281 A95-73537
High-lift flow-physics flight experiments on a subsonic civil transport aircraft (B737-100) p 275 N95-23333
Lift enhancing tabs for airfoils
[NASA-CASE-ARC-11990-1] p 286 N95-23395

LIFTOFF (LAUNCHING)

Fourth-generation Mars vehicle concepts
[BTN-95-EIX95152583267] p 298 A95-73568

LINEAR EQUATIONS

Analytical study of the neutral stability of a model hypersonic boundary layer
[BTN-95-EIX95152577589] p 263 A95-73493
Neural network prediction of three-dimensional unsteady separated flowfields
[BTN-95-EIX95182619232] p 308 A95-76658

LINEAR QUADRATIC GAUSSIAN CONTROL

Effects of high order dynamics on helicopter flight control law design
[HTN-95-80852] p 290 A95-75094
Flutter suppression control law design and testing for the active flexible wing
[BTN-95-EIX95182619214] p 292 A95-76640

LINEAR QUADRATIC REGULATOR

Aeroelastic vehicle multivariable control synthesis with analytical robustness evaluation
[BTN-95-EIX95182619115] p 321 A95-76592
System identification of the Large-Angle Magnetic Suspension Test Fixture (LAMSTF) p 296 N95-23299

LINEAR VIBRATION

Active control of panel vibrations induced by a boundary layer flow
[NASA-CR-197867] p 273 N95-23182

LINEARITY

Comparison of linear stability results with flight transition data
[BTN-95-EIX95182619097] p 283 A95-76582

LINEARIZATION

Dynamical instability of the aerogravity assist maneuver
[BTN-95-EIX95152583282] p 298 A95-73583
Design of high performance multivariable control systems for supermaneuverable aircraft at high angle of attack
[NASA-CR-197661] p 293 N95-22908

LIQUID CRYSTALS

Flow visualization studies on sidewall effects in two-dimensional transonic airfoil testing
[BTN-95-EIX95152582313] p 264 A95-73516

LIQUID NITROGEN

Performance of the 0.3-meter transonic cryogenic tunnel with air, nitrogen, and sulfur hexafluoride media under closed loop automatic control
[NASA-CR-195052] p 310 N95-23257

LIQUID ROCKET PROPELLANTS

Fourth-generation Mars vehicle concepts
[BTN-95-EIX95152583267] p 298 A95-73568

LOAD CARRYING CAPACITY

An analytical and experimental investigation of the response of the curved, composite frame/skin specimens
[HTN-95-80857] p 283 A95-75099

LOAD TESTS

- Experimental evaluation of a box beam specifically tailored for chordwise deformation
[BTN-95-EIX95182619088] p 283 A95-75773

LOADING MOMENTS

- Rolling maneuver load alleviation using active controls
[BTN-95-EIX95182619217] p 270 A95-76643

LONGITUDINAL CONTROL

- H-infinity helicopter flight control law design with and without rotor state feedback
[BTN-95-EIX95182619129] p 291 A95-76606

- Direct-lift design strategy for longitudinal control of hypersonic aircraft
[BTN-95-EIX95182619131] p 291 A95-76608

- Robustly stable preliminary control systems design for the YF-16 CCV aircraft
[BTN-95-EIX95202637608] p 292 A95-76681

- Analysis of the longitudinal handling qualities and pilot-induced-oscillation tendencies of the High-Angle-of-Attack Research Vehicle (HARV)
p 293 N95-23297

- Aerodynamic surface distension system for high angle of attack forebody vortex control
[NASA-CASE-ARC-11979-1] p 286 N95-23390

LOW DENSITY FLOW

- Higher-order viscous shock-layer solutions for high-altitude flows
[BTN-95-EIX95152583255] p 306 A95-73556

- Numerical analysis of hypersonic low-density scramjet inlet flow
[BTN-95-EIX95212645694] p 272 A95-76746

LOW SPEED

- Aerodynamic characteristics of a canard-controlled missile at high angles of attack
[BTN-95-EIX95152583257] p 267 A95-73558

- Viscous-inviscid interaction method for unsteady low-speed airfoil flows
[BTN-95-EIX95182619093] p 269 A95-75778

- Aerodynamic characteristics of external store configurations at low speeds
[BTN-95-EIX95182619230] p 271 A95-76656

- NASA low-speed axial compressor for fundamental research
[NASA-TM-4635] p 296 N95-23192

- Handling qualities of the High Speed Civil Transport
p 294 N95-23325

LOW TURBULENCE

- Separation control on high-lift airfoils via micro-vortex generators
[BTN-95-EIX95152582326] p 265 A95-73529

LOW VISIBILITY

- Differential GPS and system integration of the Low Visibility Landing and Surface Operations (LVLASO) demonstration
p 280 N95-23318

LUMBAR REGION

- A multibody/finite element analysis approach for modeling of crash dynamic responses
[NIAR-94-3] p 277 N95-24050

LUNAR SPACECRAFT

- Minimum-mass design of sandwich aerobrakes for a lunar transfer vehicle
[BTN-95-EIX95212645707] p 299 A95-76759

M

MACH NUMBER

- Main features of overexpanded triple jets
[BTN-95-EIX95142553040] p 304 A95-73458

- Analytical study of the neutral stability of a model hypersonic boundary layer
[BTN-95-EIX95152577589] p 263 A95-73493

- Mach wave emission from a high-temperature supersonic jet
[BTN-95-EIX95152577586] p 264 A95-73496

- Improved version of the Naval Surface Warfare Center aeroprediction code (AP93)
[BTN-95-EIX95152583260] p 267 A95-73561

- Flutter of an infinitely long panel in a duct
[BTN-95-EIX95182619087] p 291 A95-75772

- Scaling of incipient separation in supersonic/transonic speed laminar flows
[BTN-95-EIX95182619104] p 269 A95-76589

- Natural laminar flow wing concept for supersonic transports
[BTN-95-EIX95182619226] p 308 A95-76652

- Numerical investigation of supersonic flows around a spiked blunt body
[BTN-95-EIX95212645690] p 271 A95-76742

- Calculation of wing-alone aerodynamics to high angles of attack
[BTN-95-EIX95212645713] p 261 A95-76765

- Wing pressure distributions from subsonic tests of a high-wing transport model --- in the Langley 14- by 22-Foot Subsonic Wind Tunnel
[NASA-TM-4583] p 272 N95-22802

- Performance of the 0.3-meter transonic cryogenic tunnel with air, nitrogen, and sulfur hexafluoride media under closed loop automatic control
[NASA-CR-195052] p 310 N95-23257

- Design of a variable area diffuser for a 15-inch Mach 6 open-jet tunnel
p 297 N95-23309

- MACHINE TOOLS**
Automatic riveting cell for commercial aircraft floor grid assembly
[BTN-95-EIX95182617807] p 261 A95-75752

- MAGNETIC BEARINGS**
Effects of AMB parameters on the dynamic stability of the rotor
[BTN-94-EIX94381353450] p 323 A95-75494

- Influence of backup bearings and support structure dynamics on the behavior of rotors with active supports
[NASA-CR-197438] p 310 N95-23190

- MAGNETIC EFFECTS**
Effects of AMB parameters on the dynamic stability of the rotor
[BTN-94-EIX94381353450] p 323 A95-75494

- MAGNETIC SUSPENSION**
System identification of the Large-Angle Magnetic Suspension Test Fixture (LAMSTF)
p 296 N95-23299

- MAN MACHINE SYSTEMS**
Flight-deck displays on the Boeing 777
[BTN-95-EIX95142562402] p 286 A95-73438

- MANAGEMENT INFORMATION SYSTEMS**
AVIRIS and TIMS data processing and distribution at the land processes distributed active archive center
p 325 N95-23872

- MANAGEMENT PLANNING**
Maintenance programs
[BTN-95-EIX95182617809] p 261 A95-75754

- MANEUVERABILITY**
Dynamical instability of the aerogravity assist maneuver
[BTN-95-EIX95152583282] p 298 A95-73583

- Multiaxis pilot ratings for damaged aircraft
[BTN-95-EIX95182619128] p 269 A95-76605

- Solutions of generalized proportional navigation with maneuvering and nonmaneuvering targets
[BTN-95-EIX95202637606] p 279 A95-76683

- MANIFOLDS**
Aerodynamic design and analysis of a highly loaded turbine exhaust
p 312 N95-23435

- Phase 2: HGM air flow tests in support of HEX vane investigation
p 312 N95-23438

- MANUALS**
Rationale for the Modular Air-system Vulnerability Estimation Network (MAVEN) methodology
[AD-A285797] p 284 N95-22510

- MANUFACTURING**
Automatic riveting cell for commercial aircraft floor grid assembly
[BTN-95-EIX95182617807] p 261 A95-75752

- MAPS**
Automation technology using Geographic Information System (GIS)
p 324 N95-23284

- MARITIME SATELLITES**
Development of aeronautical mobile satellite services over the past thirty years
[BTN-95-EIX95152569458] p 305 A95-73498

- MARKET RESEARCH**
The airline quality report, 1994
[NIAR-94-11] p 277 N95-24012

- MARS (PLANET)**
Fourth-generation Mars vehicle concepts
[BTN-95-EIX95152583267] p 298 A95-73568

- MARS EXPLORATION**
Fourth-generation Mars vehicle concepts
[BTN-95-EIX95152583267] p 298 A95-73568

- MASS FLOW**
Simulating heat addition via mass addition in constant area compressible flows
[BTN-95-EIX95182619100] p 307 A95-76585

- MASS SPECTROMETERS**
Time-of-flight mass spectrometer for impulse facilities
[BTN-95-EIX95142553057] p 262 A95-73441

- MASS TRANSFER**
Simulating heat addition via mass addition in constant area compressible flows
[BTN-95-EIX95182619100] p 307 A95-76585

- MATERIALS HANDLING**
Measurement of particle emissions from clean room gas-handling components
[BTN-94-EIX94381359040] p 295 A95-74554

- MATHEMATICAL MODELS**
On the exact solutions of pseudorange equations
[BTN-95-EIX95142555477] p 278 A95-73433

- Mechanical system reliability and risk assessment
[BTN-95-EIX95142553046] p 304 A95-73452

- Simulation of turbulent fluctuations
[BTN-95-EIX95142553041] p 304 A95-73457

- Effects of expansions on a supersonic boundary layer: Surface pressure measurements
[BTN-95-EIX95142553036] p 263 A95-73462

- Aerodynamic shape optimization using preconditioned conjugate gradient methods
[BTN-95-EIX95142553033] p 263 A95-73465

- Analytical study of the neutral stability of a model hypersonic boundary layer
[BTN-95-EIX95152577589] p 263 A95-73493

- Efficient sensitivity analysis for rotary-wing aeromechanical problems
[BTN-95-EIX95152577585] p 264 A95-73497

- Limit cycle phenomena in computational transonic aeroelasticity
[BTN-95-EIX95152582317] p 264 A95-73520

- Hypersonic rarefied flow past spheres including wake structure
[BTN-95-EIX95152583250] p 305 A95-73551

- Aerodynamic characteristics of a hypersonic viscous optimized waverider at high altitudes
[BTN-95-EIX95152583251] p 266 A95-73552

- Hypersonic nonequilibrium Navier-Stokes solutions over an ablating graphite nosetip
[BTN-95-EIX95152583252] p 305 A95-73553

- Hypersonic convective heat transfer over 140-deg blunt cones in different gases
[BTN-95-EIX95152583253] p 306 A95-73554

- Application of the multigrad solution technique to hypersonic entry vehicles
[BTN-95-EIX95152583254] p 306 A95-73555

- Higher-order viscous shock-layer solutions for high-altitude flows
[BTN-95-EIX95152583255] p 306 A95-73556

- Base drag prediction on missile configurations
[BTN-95-EIX95152583256] p 266 A95-73557

- Aerodynamic characteristics of a canard-controlled missile at high angles of attack
[BTN-95-EIX95152583257] p 267 A95-73558

- Predicting exhaust plume boundaries with supersonic external flows
[BTN-95-EIX95152583258] p 297 A95-73559

- Three-dimensional structure of a supersonic jet impinging on an inclined plate
[BTN-95-EIX95152583259] p 267 A95-73560

- Functional dependence of trajectory dispersion on initial condition errors
[BTN-95-EIX95152583263] p 298 A95-73564

- Thermal force modeling for global positioning system satellites using the finite element method
[BTN-95-EIX95152583270] p 278 A95-73571

- Supersonic axisymmetric conical flow solutions for different ratios of specific heats
[BTN-95-EIX95152583283] p 306 A95-73584

- Improving prediction: The incorporation of simplified rotor dynamics in a mathematical model of the bell 412HP
[BTN-95-EIX95152584679] p 282 A95-73591

- Finite element model for a flexible non-symmetric rotor on distributed bearing: A stability study
[BTN-94-EIX94381352212] p 306 A95-74612

- Flutter of an infinitely long panel in a duct
[BTN-95-EIX95182619087] p 291 A95-75772

- Observations on using experimental data as boundary conditions for computations
[BTN-95-EIX95182619103] p 321 A95-76588

- Aeroelastic vehicle multivariable control synthesis with analytical robustness evaluation
[BTN-95-EIX95182619115] p 321 A95-76592

- Analytical aeropropulsive/aeroelastic hypersonic-vehicle model with dynamic analysis
[BTN-95-EIX95182619138] p 269 A95-76615

- Drag function modeling for air traffic simulation
[BTN-95-EIX95182619154] p 279 A95-76631

- Application of transonic small disturbance theory to the active flexible wing model
[BTN-95-EIX95182619210] p 270 A95-76636

- Simulation and model reduction for the active flexible wing program
[BTN-95-EIX95182619211] p 295 A95-76637

- Erosion of dust-filtered helicopter turbine engines. Part 1: Basic theoretical considerations
[BTN-95-EIX95182619222] p 288 A95-76648

- Stability derivatives of a flapped plate in unsteady ground effect
[BTN-95-EIX95182619225] p 270 A95-76651

- Response of a nonrotating rotor blade to lateral turbulence. Part 1: Theory
[BTN-95-EIX95182619228] p 284 A95-76654

- Response of a nonrotating rotor blade to lateral turbulence. Part 2: Experiment
[BTN-95-EIX95182619229] p 284 A95-76655

- Aerodynamic characteristics of external store configurations at low speeds
[BTN-95-EIX95182619230] p 271 A95-76656

- Neural network prediction of three-dimensional unsteady separated flowfields
[BTN-95-EIX95182619232] p 308 A95-76658
- Unsteady ground effects on aerodynamic coefficients of finite wings with camber
[BTN-95-EIX95182619233] p 271 A95-76659
- CFD optimization of a theoretical minimum-drag body
[BTN-95-EIX95182619234] p 308 A95-76660
- A comparison of some aerodynamic resistance methods using measurements over cotton and grass from the 1991 California ozone deposition experiment
[HTN-95-11295] p 319 A95-77000
- Particle kinetic simulation of high altitude hypervelocity flight
[NASA-CR-197383] p 309 N95-22481
- Modeling aerosol emissions from the combustion of composite materials
p 301 N95-23038
- Supersonic jet noise reductions predicted with increased jet spreading rate
[NASA-TM-106872] p 323 N95-23178
- Development and verification of a resin film infusion/resin transfer molding simulation model for fabrication of advanced textile composites
[NASA-CR-197439] p 301 N95-23179
- An approximate theoretical method for modeling the static thrust performance of non-axisymmetric two-dimensional convergent-divergent nozzles
[NASA-CR-195050] p 273 N95-23193
- An investigation of helicopter dynamic coupling using an analytical model
[NASA-CR-197420] p 285 N95-23217
- Idealized textile composites for experimental/analytical correlation
p 301 N95-23277
- Inner loop flight control for the High-Speed Civil Transport
p 293 N95-23314
- Preparation of course materials: Elementary mathematics of powered flight
p 324 N95-23320
- Aerodynamic design and analysis of a highly loaded turbine exhaust
p 312 N95-23435
- Phase 2: HGM air flow tests in support of HEX vane investigation
p 312 N95-23438
- Moving mass trim control for aerospace vehicles
[DE95-002602] p 299 N95-23532
- Assimilation of altimeter data in a quasi-geostrophic model of the Gulf Stream system: A dynamical perspective
[NASA-CR-196313] p 320 N95-23766
- Statistics of multi-look AIRSAR imagery: A comparison of theory with measurements
p 320 N95-23947
- A multibody/finite element analysis approach for modeling of crash dynamic responses
[NIAR-94-3] p 277 N95-24050
- MATRIX MATERIALS**
US Navy operating experience with new aircraft construction materials
p 303 N95-23517
- MAXIMUM LIKELIHOOD ESTIMATES**
Maximum-likelihood spectral estimation and adaptive filtering techniques with application to airborne Doppler weather radar
[NASA-CR-197699] p 316 N95-23670
- MECHANICAL PROPERTIES**
Idealized textile composites for experimental/analytical correlation
p 301 N95-23277
- MESOMETEOROLOGY**
Diurnal variation of lee vortices in Taiwan and the surrounding area
[HTN-95-91363] p 318 A95-76394
- METAL COATINGS**
Cu deposition using a permanent magnet electron cyclotron resonance microwave plasma source
[DE94-017768] p 304 N95-23981
- METAL FATIGUE**
Multiple site fatigue damage in fuselage skin splices: Experimental simulation and theoretical prediction
[BTN-95-EIX95152584676] p 276 A95-73588
- Fatigue strength of high-temperature alloys under conditions of cyclic temperature variation. Communication 1: Experimental procedure and results
[BTN-94-EIX94401363884] p 307 A95-75516
- METAL FIBERS**
Compliant interlayer
[BTN-95-EIX95142562401] p 304 A95-73439
- METAL MATRIX COMPOSITES**
Mil-HDBK-5 design allowables for fibre/metal laminates: ARALL 2 and ARALL 3
[BTN-94-EIX94371346933] p 300 A95-73345
- METEOROLOGICAL BALLOONS**
Polar Patrol Balloon
[BTN-95-EIX95152582318] p 316 A95-73521
- METEOROLOGICAL INSTRUMENTS**
A new generation of instruments for flying laboratories
[BTN-94-EIX94401363947] p 317 A95-75532
- METEOROLOGICAL PARAMETERS**
Compendium of NASA data base for the Global Tropospheric Experiment's Pacific Exploratory Mission West-A (PEM West-A)
[NASA-TM-109177] p 320 N95-23009
- METEOROLOGICAL RADAR**
Maximum-likelihood spectral estimation and adaptive filtering techniques with application to airborne Doppler weather radar
[NASA-CR-197699] p 316 N95-23670
- METEOROLOGICAL SATELLITES**
Calculation of satellite drag coefficients
[AD-A285118] p 300 N95-23781
- METEOROLOGY**
A new generation of instruments for flying laboratories
[BTN-94-EIX94401363947] p 317 A95-75532
- MICROBURSTS (METEOROLOGY)**
Optimal lateral-escape maneuvers for microburst encounters during final approach
[BTN-95-EIX95182619127] p 276 A95-76604
- MICROWAVES**
Cu deposition using a permanent magnet electron cyclotron resonance microwave plasma source
[DE94-017768] p 304 N95-23981
- MIMO (CONTROL SYSTEMS)**
Multirate flutter suppression system design for a model wing
[BTN-95-EIX95182619132] p 292 A95-76609
- Design and multifunction tests of a frequency domain-based active flutter suppression system
[BTN-95-EIX95182619215] p 292 A95-76641
- MINIMUM DRAG**
CFD optimization of a theoretical minimum-drag body
[BTN-95-EIX95182619234] p 308 A95-76660
- Control of flow separation in airfoil/wing design applications
p 274 N95-23294
- MISSILE BODIES**
Wing vertical position effects on wing-body carryover for noncircular missiles
[BTN-95-EIX95182617462] p 268 A95-75733
- MISSILE CONFIGURATIONS**
Base drag prediction on missile configurations
[BTN-95-EIX95152583256] p 266 A95-73557
- Aerodynamic characteristics of a canard-controlled missile at high angles of attack
[BTN-95-EIX95152583257] p 267 A95-73558
- MISSILE CONTROL**
Switched bias proportional navigation for homing guidance against highly maneuvering targets
[BTN-95-EIX95182619145] p 279 A95-76622
- Moving mass trim control for aerospace vehicles
[DE95-002602] p 299 N95-23532
- MISSILE TRAJECTORIES**
A CFD study of complex missile and store configurations in relative motion
[NASA-CR-197912] p 285 N95-22949
- MISSILES**
Aerodynamic characteristics of a canard-controlled missile at high angles of attack
[BTN-95-EIX95152583257] p 267 A95-73558
- Wing vertical position effects on wing-body carryover for noncircular missiles
[BTN-95-EIX95182617462] p 268 A95-75733
- Supersonic near-wake afterbody boattailing effects on axisymmetric bodies
[BTN-95-EIX95182617465] p 268 A95-75736
- MOBILE COMMUNICATION SYSTEMS**
Development of aeronautical mobile satellite services over the past thirty years
[BTN-95-EIX95152569458] p 305 A95-73498
- MODULUS OF ELASTICITY**
Evaluation of advanced aerospace materials by depth sensing indentation and scratch methods
[BTN-95-EIX95152584678] p 282 A95-73590
- Interlaminar shear test method development for long term durability testing of composites
p 301 N95-23300
- MOISTURE**
Measurement of moisture and total hydrocarbon contributions by valves used in clean room gas-delivery systems
[BTN-94-EIX94381359041] p 295 A95-74629
- MOISTURE CONTENT**
Study of the droplet spray characteristics of a subsonic wind tunnel
[BTN-95-EIX95182619235] p 271 A95-76661
- MOLECULES**
Determination of wall boundary conditions for high-speed-ratio direct simulation Monte Carlo calculations
[BTN-95-EIX95182617457] p 267 A95-75728
- MONTE CARLO METHOD**
Hypersonic rarefied flow past spheres including wake structure
[BTN-95-EIX95152583250] p 305 A95-73551

- Aerodynamic characteristics of a hypersonic viscous optimized waverider at high altitudes
[BTN-95-EIX95152583251] p 266 A95-73552
- Higher-order viscous shock-layer solutions for high-altitude flows
[BTN-95-EIX95152583255] p 306 A95-73556
- Functional dependence of trajectory dispersion on initial condition errors
[BTN-95-EIX95152583263] p 298 A95-73564
- Determination of wall boundary conditions for high-speed-ratio direct simulation Monte Carlo calculations
[BTN-95-EIX95182617457] p 267 A95-75728
- Zonally decoupled direct simulation Monte Carlo solutions of hypersonic blunt-body wake flows
[BTN-95-EIX95182617458] p 268 A95-75729
- Numerical analysis of hypersonic low-density scramjet inlet flow
[BTN-95-EIX9512645694] p 272 A95-76746
- Particle kinetic simulation of high altitude hypervelocity flight
[NASA-CR-197383] p 309 N95-22481
- MOON-EARTH TRAJECTORIES**
Fuel-optimal bank-angle control for lunar-return aerocapture
[BTN-95-EIX9512645706] p 299 A95-76758
- MULTIGRID METHODS**
Application of the multigrid solution technique to hypersonic entry vehicles
[BTN-95-EIX95152583254] p 306 A95-73555
- MULTIPHASE FLOW**
Effect of ambient turbulence intensity on sphere wakes at intermediate Reynolds numbers
[BTN-95-EIX95182619101] p 308 A95-76586
- MULTIVARIABLE CONTROL**
Aeroelastic vehicle multivariable control synthesis with analytical robustness evaluation
[BTN-95-EIX95182619115] p 321 A95-76592
- Multivariable stability and robustness of sequentially designed feedback systems
[BTN-95-EIX95182619125] p 322 A95-76602
- Derivation of system matrices from nonlinear dynamic simulation of jet engines
[BTN-95-EIX95182619139] p 288 A95-76616
- Design of high performance multivariable control systems for supermaneuverable aircraft at high angle of attack
[NASA-CR-197661] p 293 N95-22908

N

- NAP-OF-THE-EARTH NAVIGATION**
Automatic guidance and control for helicopter obstacle avoidance
[BTN-95-EIX95182619130] p 291 A95-76607
- NASA PROGRAMS**
1994 NASA-HU American Society for Engineering Education (ASEE) Summer Faculty Fellowship Program
[NASA-CR-194972] p 325 N95-23276
- Research and Technology, 1994
[NASA-TM-106764] p 262 N95-24025
- NASTRAN**
Thin tailored composite wing for civil tiltrotor
p 285 N95-23317
- NAVIER-STOKES EQUATION**
Preconditioned domain decomposition scheme for three-dimensional aerodynamic sensitivity analysis
[BTN-95-EIX95152577612] p 321 A95-73471
- Effects of spatial order of accuracy on the computation of vortical flowfields
[BTN-95-EIX95152577604] p 305 A95-73479
- Computation of oscillating airfoil flows with one- and two-equation turbulence models
[BTN-95-EIX95152577588] p 263 A95-73494
- Computation of the poststall behavior of a circulation controlled airfoil
[BTN-95-EIX95152582320] p 264 A95-73523
- Navier-Stokes prediction of large-amplitude delta-wing roll oscillations
[BTN-95-EIX95152582329] p 281 A95-73531
- Computational study of plume-induced separation on a hypersonic powered model
[BTN-95-EIX95152582346] p 266 A95-73548
- Hypersonic rarefied flow past spheres including wake structure
[BTN-95-EIX95152583250] p 305 A95-73551
- Hypersonic nonequilibrium Navier-Stokes solutions over an ablating graphite nosetip
[BTN-95-EIX95152583252] p 305 A95-73553
- Hypersonic convective heat transfer over 140-deg blunt cones in different gases
[BTN-95-EIX95152583253] p 306 A95-73554
- Application of the multigrid solution technique to hypersonic entry vehicles
[BTN-95-EIX95152583254] p 306 A95-73555

Higher-order viscous shock-layer solutions for high-altitude flows
[BTN-95-EIX95152583255] p 306 A95-73556

Optimization of contoured hypersonic scramjet inlets with a least-squares parabolized Navier-Stokes procedure
[HTN-95-20976] p 261 A95-74042

Convective and radiative heat transfer analysis for the fire 2 forebody
[BTN-95-EIX95182617460] p 268 A95-75731

Turbulent transonic airflow flow simulation using a pressure-based algorithm
[BTN-95-EIX95182619078] p 269 A95-75763

Simulation of transverse gas injection in turbulent supersonic air flows
[BTN-95-EIX95182619080] p 269 A95-75765

Viscous-inviscid interaction method for unsteady low-speed airflow flows
[BTN-95-EIX95182619093] p 269 A95-75778

Influence of streamwise curvature on longitudinal vortices imbedded in turbulent boundary layers
[BTN-94-EIX94401378820] p 307 A95-76489

Grid refinement test of time-periodic flows over bluff bodies
[BTN-94-EIX94401378822] p 307 A95-76491

Numerical investigation of supersonic flows around a spiked blunt body
[BTN-95-EIX95212645690] p 271 A95-76742

An assessment of viscous effects in computational simulation of benign and burst vortex flows on generic fighter wind-tunnel models using TEAM code
[NASA-CR-4650] p 273 N95-23185

Mach 10 computational study of a three-dimensional scramjet inlet flow field
[NASA-TM-4602] p 310 N95-23210

Numerical computation of aerodynamics and heat transfer in a turbine cascade and a turn-around duct using advanced turbulence models
p 313 N95-23444

Convergence acceleration of implicit schemes in the presence of high aspect ratio grid cells
p 313 N95-23446

A time-accurate finite volume method valid at all flow velocities
p 314 N95-23447

Cavitation modeling in Euler and Navier-Stokes codes
p 315 N95-23630

NAVIGATION

Switched bias proportional navigation for homing guidance against highly maneuvering targets
[BTN-95-EIX95182619145] p 279 A95-76622

New failure detection approach and its application to GPS autonomous integrity monitoring
[BTN-95-EIX95202637613] p 279 A95-76676

Solutions of generalized proportional navigation with maneuvering and nonmaneuvering targets
[BTN-95-EIX95202637606] p 279 A95-76683

NAVIGATION AIDS

Cueing light configuration for aircraft navigation
[NASA-CASE-ARC-11982-1] p 280 N95-23393

TRISTAR 1: Evaluation methods for testing head-up display (HUD) flight symbology
[NASA-TM-4665] p 288 N95-24030

NAVIGATION SATELLITES

Description of a GNSS availability model and its use in developing requirements
[BTN-95-EIX95202637603] p 308 A95-76686

NEAR INFRARED RADIATION

2 micron LIDAR for laser-based remote sensing: Flight demonstration and application survey
[BTN-95-EIX95212641072] p 319 A95-76737

AVIRIS and TIMS data processing and distribution at the land processes distributed active archive center
p 325 N95-23872

NEAR WAKES

Supersonic near-wake afterbody boattailing effects on axisymmetric bodies
[BTN-95-EIX95182617465] p 268 A95-75736

NETHERLANDS

Review of aeronautical fatigue investigation in the Netherlands during the period March 1991-March 1993
[PB95-139184] p 285 N95-23181

NEURAL NETS

Artificial intelligence for turboprop engine maintenance
[BTN-95-EIX95182617812] p 288 A95-75757

Neural network prediction of three-dimensional unsteady separated flowfields
[BTN-95-EIX95182619232] p 308 A95-76658

On-line, adaptive state estimator for active noise control
p 322 N95-23308

NEUTRONS

Phonon characteristics of high (T sub c) superconductors from neutron Doppler broadening measurements
[DE95-003703] p 324 N95-24076

NOISE (SOUND)

Mach wave emission from a high-temperature supersonic jet
[BTN-95-EIX95152577586] p 264 A95-73496

NOISE PREDICTION

Analysis of a higher harmonic control test to reduce blade vortex interaction noise
[BTN-95-EIX95152582330] p 265 A95-73532

NOISE PREDICTION (AIRCRAFT)

Supersonic jet noise reductions predicted with increased jet spreading rate
[NASA-TM-106872] p 323 N95-23178

NOISE REDUCTION

Analysis of a higher harmonic control test to reduce blade vortex interaction noise
[BTN-95-EIX95152582330] p 265 A95-73532

The use of cowl camber and taper to reduce rotor/stator interaction noise
[NASA-CR-195421] p 323 N95-22675

Supersonic jet noise reductions predicted with increased jet spreading rate
[NASA-TM-106872] p 323 N95-23178

On-line, adaptive state estimator for active noise control
p 322 N95-23308

NONDESTRUCTIVE TESTS

Double pass retroreflection for corrosion detection in aircraft structures
p 323 N95-23503

Non-destructive detection of corrosion for life management
p 314 N95-23505

New nondestructive techniques for the detection and quantification of corrosion in aircraft structures
p 315 N95-23512

POD assessment of NDI procedures using a round robin test
[AGARD-R-809] p 315 N95-23602

NONEQUILIBRIUM FLOW

Hypersonic nonequilibrium Navier-Stokes solutions over an ablating graphite nosetip
[BTN-95-EIX95152583252] p 305 A95-73553

Higher-order viscous shock-layer solutions for high-altitude flows
[BTN-95-EIX95152583255] p 306 A95-73556

NONINTRUSIVE MEASUREMENT

Impeller flow field characterization with a laser two-focus velocimeter
p 313 N95-23440

NONLINEAR EQUATIONS

Neural network prediction of three-dimensional unsteady separated flowfields
[BTN-95-EIX95182619232] p 308 A95-76658

Moving mass trim control for aerospace vehicles
[DE95-002602] p 299 N95-23532

NONLINEAR FEEDBACK

Design of high performance multivariable control systems for supermaneuverable aircraft at high angle of attack
[NASA-CR-197661] p 293 N95-22908

NONLINEAR SYSTEMS

Nonlinear system guidance in the presence of transmission zero dynamics
[NASA-TM-4661] p 309 N95-22804

NONLINEARITY

Analytical solution for controls, heats, and states of flight trajectories
[BTN-95-EIX95152583286] p 282 A95-73587

NORTHERN HEMISPHERE

Trajectory modeling of emissions from lower stratospheric aircraft
[HTN-95-41219] p 317 A95-75031

NOSE CONES

Shock tunnel measurements of hypervelocity blunted cone drag
[BTN-95-EIX95152577606] p 305 A95-73477

NOSE TIPS

Hypersonic nonequilibrium Navier-Stokes solutions over an ablating graphite nosetip
[BTN-95-EIX95152583252] p 305 A95-73553

NOTCH TESTS

Interlaminar shear test method development for long term durability testing of composites
p 301 N95-23300

NOZZLE DESIGN

An approximate theoretical method for modeling the static thrust performance of non-axisymmetric two-dimensional convergent-divergent nozzles
[NASA-CR-195050] p 273 N95-23193

Optimized design of a hypersonic nozzle
p 297 N95-23304

Design of a variable area diffuser for a 15-inch Mach 6 open-jet tunnel
p 297 N95-23309

Three-dimensional Navier-Stokes analysis and redesign of an imbedded bellmouth nozzle in a turbine cascade inlet section
p 311 N95-23423

NOZZLE EFFICIENCY

An approximate theoretical method for modeling the static thrust performance of non-axisymmetric two-dimensional convergent-divergent nozzles
[NASA-CR-195050] p 273 N95-23193

NOZZLE FLOW

Predicting exhaust plume boundaries with supersonic external flows
[BTN-95-EIX95152583258] p 297 A95-73559

Simulation on the 3-D turbulent flow in the passages of finocyl grain
[BTN-95-EIX95202638962] p 279 A95-76674

An approximate theoretical method for modeling the static thrust performance of non-axisymmetric two-dimensional convergent-divergent nozzles
[NASA-CR-195050] p 273 N95-23193

Experimental results for a hypersonic nozzle/afterbody flow field
[NASA-TM-4638] p 274 N95-23250

NOZZLE WALLS

Supersonic laminar flow control research
[NASA-CR-197938] p 275 N95-23669

**OBLIQUE SHOCK WAVES**

Scaling of incipient separation in supersonic/transonic speed laminar flows
[BTN-95-EIX95182619104] p 269 A95-76589

Supersonic flow and shock formation in turbine tip gaps
p 312 N95-23429

OBSTACLE AVOIDANCE

Optimal lateral-escape maneuvers for microburst encounters during final approach
[BTN-95-EIX95182619127] p 276 A95-76604

Automatic guidance and control for helicopter obstacle avoidance
[BTN-95-EIX95182619130] p 291 A95-76607

OCEAN BOTTOM

Geoid lineations of 1000 km wavelength over the central Pacific
[HTN-95-11304] p 319 A95-77009

OCEAN MODELS

Assimilation of altimeter data in a quasi-geostrophic model of the Gulf Stream system: A dynamical perspective
[NASA-CR-196313] p 320 N95-23766

OCEAN SURFACE

Assimilation of altimeter data in a quasi-geostrophic model of the Gulf Stream system: A dynamical perspective
[NASA-CR-196313] p 320 N95-23766

ON-LINE SYSTEMS

On-line analysis capabilities developed to support the active flexible wing wind-tunnel tests
[BTN-95-EIX95182619213] p 296 A95-76639

On-line, adaptive state estimator for active noise control
p 322 N95-23308

ONE DIMENSIONAL FLOW

Simulating heat addition via mass addition in constant area compressible flows
[BTN-95-EIX95182619100] p 307 A95-76585

OPERATING COSTS

Design constraints in the payload-range diagram of ultrahigh capacity transport airplanes
[BTN-95-EIX95152582319] p 276 A95-73522

Containing military autotest cost growth through the use of commercial standard equipment architectures
[BTN-95-EIX95172595295] p 287 A95-75717

OPTICAL MEASUREMENT

Dynamic response tests of inertial and optical wind-tunnel model attitude measurement devices
[NASA-TM-109182] p 296 N95-23011

OPTICAL RADAR

2 micron LIDAR for laser-based remote sensing: Flight demonstration and application survey
[BTN-95-EIX95212641072] p 319 A95-76737

OPTIMAL CONTROL

Aeroelastic vehicle multivariable control synthesis with analytical robustness evaluation
[BTN-95-EIX95182619115] p 321 A95-76592

Functional agility metrics and optimal trajectory analysis
[BTN-95-EIX95182619121] p 321 A95-76598

Design and multifunction tests of a frequency domain-based active flutter suppression system
[BTN-95-EIX95182619215] p 292 A95-76641

Fuel-optimal bank-angle control for lunar-return aerocapture
[BTN-95-EIX95212645706] p 299 A95-76758

Active control of panel vibrations induced by a boundary layer flow
[NASA-CR-197867] p 273 N95-23182

OPTIMIZATION

Aerodynamic shape optimization using preconditioned conjugate gradient methods
[BTN-95-EIX95142553033] p 263 A95-73465

Improved version of the Naval Surface Warfare Center aeroprediction code (AP93)
[BTN-95-EIX95152583260] p 267 A95-73561

- Optimization of contoured hypersonic scramjet inlets with a least-squares parabolized Navier-Stokes procedure
[HTN-95-20976] p 261 A95-74042
- CFD optimization of a theoretical minimum-drag body
[BTN-95-EIX95182619234] p 308 A95-76660
- Direct adaptive performance optimization of subsonic transports: A periodic perturbation technique
[NASA-TM-4676] p 284 N95-22829
- Integrated aerodynamic/dynamic/structural optimization of helicopter rotor blades using multilevel decomposition
[NASA-TP-3465] p 285 N95-22953
- Aerodynamic design optimization with sensitivity analysis and computational fluid dynamics
[NASA-CR-197419] p 274 N95-23218
- ORBIT CALCULATION**
- Thermal force modeling for global positioning system satellites using the finite element method
[BTN-95-EIX95152583270] p 278 A95-73571
- Aerodynamics of the Shuttle Orbiter at high altitudes
[BTN-95-EIX95182617454] p 298 A95-75725
- ORBIT PERTURBATION**
- Thermal force modeling for global positioning system satellites using the finite element method
[BTN-95-EIX95152583270] p 278 A95-73571
- ORBIT TRANSFER VEHICLES**
- Minimum-mass design of sandwich aerobrakes for a lunar transfer vehicle
[BTN-95-EIX95212645707] p 299 A95-76759
- ORGANIC COMPOUNDS**
- Estimates of total organic and inorganic chlorine in the lower stratosphere from in situ and flask measurements during AASE 2
[HTN-95-A0861] p 317 A95-76265
- ORGANIC MATERIALS**
- Organic coating technology for the protection of aircraft against corrosion
p 303 N95-23513
- OSCILLATIONS**
- Further analysis of high-rate rolling experiments of a 65-deg delta wing
[BTN-95-EIX95152582331] p 281 A95-73533
- Postinstability behavior of a two-dimensional airfoil with a structural nonlinearity
[BTN-95-EIX95152582337] p 266 A95-73539
- OXIDATION**
- Evolution of oxidation and creep damage mechanisms in HIPed silicon nitride materials
[DE95-001360] p 300 N95-22689
- OXYGEN**
- Evolution of oxidation and creep damage mechanisms in HIPed silicon nitride materials
[DE95-001360] p 300 N95-22689
- OZONE**
- Sensitivity of two-dimensional model predictions of ozone response to stratospheric aircraft: An update
[HTN-95-A0863] p 318 A95-76267
- A comparison of some aerodynamic resistance methods using measurements over cotton and grass from the 1991 California ozone deposition experiment
[HTN-95-11295] p 319 A95-77000
- Compendium of NASA data base for the Global Tropospheric Experiment's Pacific Exploratory Mission West-A (PEM West-A)
[NASA-TM-109177] p 320 N95-23009
- OZONE DEPLETION**
- Trajectory modeling of emissions from lower stratospheric aircraft
[HTN-95-41219] p 317 A95-75031
- Possible effects of CO₂ increase on the high-speed civil transport impact on ozone
[HTN-95-60779] p 317 A95-75976
- Estimates of total organic and inorganic chlorine in the lower stratosphere from in situ and flask measurements during AASE 2
[HTN-95-A0861] p 317 A95-76265
- In situ observations in aircraft exhaust plumes in the lower stratosphere at midlatitudes
[HTN-95-A0862] p 318 A95-76266
- Sensitivity of two-dimensional model predictions of ozone response to stratospheric aircraft: An update
[HTN-95-A0863] p 318 A95-76267
- P**
- PACIFIC OCEAN**
- Geoid lineations of 1000 km wavelength over the central Pacific
[HTN-95-11304] p 319 A95-77009
- Oceanic operations: An authoritative guide to oceanic operations
[FAA-AFS-550] p 277 N95-24065
- PAINTS**
- Aircraft stripping and painting
[BTN-95-EIX95182617810] p 300 A95-75755

PANEL METHOD (FLUID DYNAMICS)

- Viscous-inviscid interaction method for unsteady low-speed airfoil flows
[BTN-95-EIX95182619093] p 269 A95-75778
- PANELS**
- Flutter of an infinitely long panel in a duct
[BTN-95-EIX95182619087] p 291 A95-75772
- Active control of panel vibrations induced by a boundary layer flow
[NASA-CR-197867] p 273 N95-23182
- Residual strength of thin panels with cracks
p 311 N95-23311
- PARACHUTE DESCENT**
- Dynamic investigation of the angular motion of a rotating body-parachute system
[BTN-95-EIX95182619220] p 270 A95-76646
- PARACHUTES**
- Dynamic investigation of the angular motion of a rotating body-parachute system
[BTN-95-EIX95182619220] p 270 A95-76646
- PARALLEL PROCESSING (COMPUTERS)**
- High-performance parallel analysis of coupled problems for aircraft propulsion
[NASA-CR-197440] p 289 N95-23088
- PARAMETER IDENTIFICATION**
- Improving prediction: The incorporation of simplified rotor dynamics in a mathematical model of the bell 412HP
[BTN-95-EIX95152584679] p 282 A95-73591
- Analytical solution and parameter estimation of projectile dynamics
[BTN-95-EIX95212645695] p 272 A95-76747
- PARTICLE EMISSION**
- Measurement of particle emissions from clean room gas-handling components
[BTN-95-EIX94381359040] p 295 A95-74554
- PARTICLE IMAGE VELOCIMETRY**
- Transient structure of vortex breakdown on a delta wing
[BTN-95-EIX95182619073] p 268 A95-75758
- Laser velocimetry seed-particle behavior in shear layers at Mach 12
[BTN-95-EIX95212645712] p 272 A95-76764
- PARTICLE SIZE DISTRIBUTION**
- Erosion of dust-filtered helicopter turbine engines. Part 1: Basic theoretical considerations
[BTN-95-EIX95182619222] p 288 A95-76648
- PARTICLE TRAJECTORIES**
- Tracking of raindrops in flow over an airfoil
[BTN-95-EIX95182619221] p 308 A95-76647
- Study of the droplet spray characteristics of a subsonic wind tunnel
[BTN-95-EIX95182619235] p 271 A95-76661
- PARTICULATES**
- Laser velocimetry seed-particle behavior in shear layers at Mach 12
[BTN-95-EIX95212645712] p 272 A95-76764
- PASSENGERS**
- A multibody/finite element analysis approach for modeling of crash dynamic responses
[NIAR-94-3] p 277 N95-24050
- PASSIVITY**
- In-situ detection of surface passivation or activation and of localized corrosion: Experiences and perspectives in aircraft
p 302 N95-23508
- PAYLOADS**
- Design constraints in the payload-range diagram of ultrahigh capacity transport airplanes
[BTN-95-EIX95152582319] p 276 A95-73522
- Dynamic investigation of the angular motion of a rotating body-parachute system
[BTN-95-EIX95182619220] p 270 A95-76646
- Aerodynamic flight control to increase payload capability of future launch vehicles
[NASA-CR-197704] p 300 N95-24032
- PENETRATION**
- Rationale for the Modular Air-system Vulnerability Estimation Network (MAVEN) methodology
[AD-A285797] p 284 N95-22510
- PERFORMANCE PREDICTION**
- Multiaxis pilot ratings for damaged aircraft
[BTN-95-EIX95182619128] p 269 A95-76605
- Drag function modeling for air traffic simulation
[BTN-95-EIX95182619154] p 279 A95-76631
- Life prediction of helicopter engines fitted with dust filters
[BTN-95-EIX95182619224] p 289 A95-76650
- An approximate theoretical method for modeling the static thrust performance of non-axisymmetric two-dimensional convergent-divergent nozzles
[NASA-CR-195050] p 273 N95-23193
- PERFORMANCE TESTS**
- Labs behind Boeing's new 777
[BTN-95-EIX95142562403] p 280 A95-73437

- Containing military autotest cost growth through the use of commercial standard equipment architectures
[BTN-95-EIX95172595295] p 287 A95-75717
- Flight test evaluation of a 35 GHz forward looking altimeter for terrain avoidance
[BTN-95-EIX95212641071] p 287 A95-76736
- Performance of the 0.3-meter transonic cryogenic tunnel with air, nitrogen, and sulfur hexafluoride media under closed loop automatic control
[NASA-CR-195052] p 310 N95-23257
- Report to the Secretary of Defense. Unmanned aerial vehicles: No more Hunter systems should be bought until problems are fixed
[GAO/NSIAD-95-52] p 286 N95-24091
- PERIODIC VARIATIONS**
- Grid refinement test of time-periodic flows over bluff bodies
[BTN-94-EIX94401378822] p 307 A95-76491
- PERMANENT MAGNETS**
- Cu deposition using a permanent magnet electron cyclotron resonance microwave plasma source
[DE94-017768] p 304 N95-23981
- PERSONAL COMPUTERS**
- New commercial off-the-shelf testers are automatic and intelligent
[BTN-95-EIX95172595292] p 287 A95-75720
- Development of qualification guidelines for personal computer-based aviation training devices
[DOT/FAA/AM-95/6] p 323 N95-23603
- PERSONNEL**
- CASS: Design for supportability
[BTN-95-EIX95172595296] p 287 A95-75716
- ATE enabling technologies
[BTN-95-EIX95172595294] p 287 A95-75718
- PERTURBATION**
- Direct adaptive performance optimization of subsonic transports: A periodic perturbation technique
[NASA-TM-4676] p 284 N95-22829
- PERTURBATION THEORY**
- Analytical study of the neutral stability of a model hypersonic boundary layer
[BTN-95-EIX95152577589] p 263 A95-73493
- Application of transonic small disturbance theory to the active flexible wing model
[BTN-95-EIX95182619210] p 270 A95-76636
- PHASE LOCKED SYSTEMS**
- Real-time navigation using the global positioning system
[BTN-95-EIX95172595298] p 279 A95-75714
- PHASE SHIFT**
- Real-time navigation using the global positioning system
[BTN-95-EIX95172595298] p 279 A95-75714
- PHONONS**
- Phonon characteristics of high (T sub c) superconductors from neutron Doppler broadening measurements
[DE95-003703] p 324 N95-24076
- PHOTOCHEMICAL REACTIONS**
- Possible effects of CO₂ increase on the high-speed civil transport impact on ozone
[HTN-95-60779] p 317 A95-75976
- Estimates of total organic and inorganic chlorine in the lower stratosphere from in situ and flask measurements during AASE 2
[HTN-95-A0861] p 317 A95-76265
- PHOTOGRAPHS**
- Simple method of supersonic flow visualization using watertable
[BTN-95-EIX95182619105] p 269 A95-76590
- Scientific and technical photography at NASA Langley Research Center
p 310 N95-23290
- PHOTOGRAPHY**
- Scientific and technical photography at NASA Langley Research Center
p 310 N95-23290
- PILOT INDUCED OSCILLATION**
- Analysis of the longitudinal handling qualities and pilot-induced-oscillation tendencies of the High-Angle-of-Attack Research Vehicle (HARV)
p 293 N95-23297
- PILOT PERFORMANCE**
- TRISTAR 1: Evaluation methods for testing head-up display (HUD) flight symbology
[NASA-TM-4665] p 288 N95-24030
- A review of civil aviation fatal accidents in which lost/disoriented was a cause/factor: 1981-1990
[DOT/FAA/AM-95/1] p 278 N95-24071
- PILOTLESS AIRCRAFT**
- Design of a GaAs/Ge solar array for unmanned aerial vehicles
[NASA-TM-106870] p 320 N95-23259
- Report to the Secretary of Defense. Unmanned aerial vehicles: No more Hunter systems should be bought until problems are fixed
[GAO/NSIAD-95-52] p 286 N95-24091

PITCH (INCLINATION)

- Identification of higher order helicopter dynamics using linear modeling methods
[HTN-95-80851] p 290 A95-75093
- Sensitivity of acoustic predictions to variation of input parameters
[HTN-95-80855] p 267 A95-75097

PITCHING MOMENTS

- Kinematics and aerodynamics of velocity-vector roll
[BTN-95-EIX95182619126] p 291 A95-76603

PITTING

- Eddy current detection of pitting corrosion around fastener holes p 315 N95-23507

PLANFORMS

- A study of the vortex flow over 76/40-deg double-delta wing
[NASA-CR-195032] p 314 N95-23466

PLASMAS (PHYSICS)

- Cu deposition using a permanent magnet electron cyclotron resonance microwave plasma source
[DE94-017768] p 304 N95-23981

PLATE THEORY

- Idealized textile composites for experimental/analytical correlation p 301 N95-23277

PLATES (STRUCTURAL MEMBERS)

- Stability derivatives of a flapped plate in unsteady ground effect
[BTN-95-EIX95182619225] p 270 A95-76651

PLUMES

- Predicting exhaust plume boundaries with supersonic external flows
[BTN-95-EIX95152583258] p 297 A95-73559
- In situ observations in aircraft exhaust plumes in the lower stratosphere at midaltitudes
[HTN-95-A0862] p 318 A95-76266
- NTS-spill test facility wind tunnel exhaust plume characterization
[DE95-003630] p 297 N95-24019

PNEUMATIC CONTROL

- Forebody flow control on a full-scale F/A-18 aircraft
[BTN-95-EIX95152582333] p 281 A95-73535
- Pneumatic concept for tip-stall control of cranked-arrow wings
[BTN-95-EIX95152582335] p 281 A95-73537

POLAR REGIONS

- Oceanic operations: An authoritative guide to oceanic operations
[FAA-AFS-550] p 277 N95-24065

POLARIMETRY

- MAX-91: Polarimetric SAR results on Montespertoli site p 320 N95-23940
- Statistics of multi-look AIRSAR imagery: A comparison of theory with measurements p 320 N95-23947

POLICIES

- Mishap risk control for advanced aerospace/composite materials p 301 N95-23031

POLLUTION MONITORING

- Modeling aerosol emissions from the combustion of composite materials p 301 N95-23038

POLLUTION TRANSPORT

- Trajectory modeling of emissions from lower stratospheric aircraft
[HTN-95-41219] p 317 A95-75031
- Transport of exhaust products in the near trail of a jet engine under atmospheric conditions
[HTN-95-91421] p 319 A95-77334

POLYMER MATRIX COMPOSITES

- Validation of an effective flat cruciform-shaped specimen to study CFRP composite laminates under biaxial loading
[BTN-95-EIX95152584677] p 282 A95-73589
- Mishap risk control for advanced aerospace/composite materials p 301 N95-23031
- Technology reinvestment project's focus area: Affordable polymer matrix composites for airframe structures
[PB95-136032] p 324 N95-23168

POPULATIONS

- Effects of satellite bunching on the probability of collision in geosynchronous orbit
[BTN-95-EIX95152583276] p 298 A95-73577

POSITION (LOCATION)

- Description of a GNSS availability model and its use in developing requirements
[BTN-95-EIX95202637603] p 308 A95-76686

POSITION ERRORS

- Dynamical instability of the aerogravity assist maneuver
[BTN-95-EIX95152583282] p 298 A95-73583

POSITION INDICATORS

- TRISTAR 1: Evaluation methods for testing head-up display (HUD) flight symbology
[NASA-TM-4665] p 288 N95-24030

POTENTIAL FLOW

- Viscous-inviscid interaction method for unsteady low-speed airfoil flows
[BTN-95-EIX95182619093] p 269 A95-75778
- Study of the droplet spray characteristics of a subsonic wind tunnel
[BTN-95-EIX95182619235] p 271 A95-76661

POWERED MODELS

- Computational study of plume-induced separation on a hypersonic powered model
[BTN-95-EIX95152582346] p 266 A95-73548

PRECIPITATION (METEOROLOGY)

- Diurnal variation of lee vortices in Taiwan and the surrounding area
[HTN-95-91363] p 318 A95-76394

PRECONDITIONING

- Aerodynamic shape optimization using preconditioned conjugate gradient methods
[BTN-95-EIX95142553033] p 263 A95-73465

PREDICTION ANALYSIS TECHNIQUES

- Analytic prediction of lift for delta wings with partial leading-edge thrust
[BTN-95-EIX95152582345] p 266 A95-73547
- Aerodynamic characteristics of a hypersonic viscous optimized waverider at high altitudes
[BTN-95-EIX95152583251] p 266 A95-73552
- Base drag prediction on missile configurations
[BTN-95-EIX95152583256] p 266 A95-73557
- Aerodynamic characteristics of a canard-controlled missile at high angles of attack
[BTN-95-EIX95152583257] p 267 A95-73558
- Predicting exhaust plume boundaries with supersonic external flows
[BTN-95-EIX95152583258] p 297 A95-73559
- Improved version of the Naval Surface Warfare Center aeroprediction code (AP93)
[BTN-95-EIX95152583260] p 267 A95-73561
- Multiple site fatigue damage in fuselage skin splices: Experimental simulation and theoretical prediction
[BTN-95-EIX95152584676] p 276 A95-73588
- Improving prediction: The incorporation of simplified rotor dynamics in a mathematical model of the bell 412HP
[BTN-95-EIX95152584679] p 282 A95-73591
- Comparison of linear stability results with flight transition data
[BTN-95-EIX95182619097] p 283 A95-76582
- Real-time estimation of atmospheric turbulence severity from in-situ aircraft measurements
[BTN-95-EIX95182619231] p 319 A95-76657
- Neural network prediction of three-dimensional unsteady separated flowfields
[BTN-95-EIX95182619232] p 308 A95-76658
- Additional improvements to the NASA Lewis ice accretion code LEWICE
[NASA-TM-106849] p 309 N95-22669
- Development and verification of a resin film infusion/resin transfer molding simulation model for fabrication of advanced textile composites
[NASA-CR-197439] p 301 N95-23179

PREDICTIONS

- The use of cowl camber and taper to reduce rotor/stator interaction noise
[NASA-CR-195421] p 323 N95-22675

PREMIXED FLAMES

- Sensitivity of combustion-acoustic instabilities to boundary conditions for premixed gas turbine combustors
[NASA-TM-106890] p 289 N95-23550

PRESSURE

- Effects of expansions on a supersonic boundary layer: Surface pressure measurements
[BTN-95-EIX95142553036] p 263 A95-73462
- Neural network prediction of three-dimensional unsteady separated flowfields
[BTN-95-EIX95182619232] p 308 A95-76658

PRESSURE DISTRIBUTION

- Aerodynamics of a finite wing with simulated ice
[BTN-95-EIX95182619227] p 270 A95-76653
- Aerodynamic characteristics of external store configurations at low speeds
[BTN-95-EIX95182619230] p 271 A95-76656
- Neural network prediction of three-dimensional unsteady separated flowfields
[BTN-95-EIX95182619232] p 308 A95-76658
- Wing pressure distributions from subsonic tests of a high-wing transport model --- in the Langley 14- by 22-Foot Subsonic Wind Tunnel
[NASA-TM-4583] p 272 N95-22802
- Three-dimensional unsteady flow calculations in an advanced gas generator turbine p 312 N95-23425

PRESSURE DRAG

- Application of Navier-Stokes aeroelastic methods to improve fighter wing maneuver performance
[BTN-95-EIX95182619218] p 284 A95-76644

PRESSURE EFFECTS

- Main features of overexpanded triple jets
[BTN-95-EIX95142553040] p 304 A95-73458
- Effects of expansions on a supersonic boundary layer: Surface pressure measurements
[BTN-95-EIX95142553036] p 263 A95-73462
- Experimental investigation of the flowfield about an upswep afterbody
[BTN-95-EIX95152582321] p 265 A95-73524

PRESSURE GRADIENTS

- Turbulent transonic airfoil flow simulation using a pressure-based algorithm
[BTN-95-EIX95182619078] p 269 A95-75763
- Simulating heat addition via mass addition in constant area compressible flows
[BTN-95-EIX95182619100] p 307 A95-76585

PRESSURE MEASUREMENT

- Separation control on high-lift airfoils via micro-vortex generators
[BTN-95-EIX95152582326] p 265 A95-73529

PRESSURE OSCILLATIONS

- Active control of panel vibrations induced by a boundary layer flow
[NASA-CR-197867] p 273 N95-23182

PRESSURE PULSES

- System for determining aerodynamic imbalance
[NASA-CASE-ARC-11913-1] p 311 N95-23377

PRESSURE SENSORS

- Impeller flow field characterization with a laser two-focus velocimeter p 313 N95-23440

PRIMERS (COATINGS)

- Organic coating technology for the protection of aircraft against corrosion p 303 N95-23513

PROBABILITY DENSITY FUNCTIONS

- Statistics of multi-look AIRSAR imagery: A comparison of theory with measurements p 320 N95-23947

PROBABILITY THEORY

- Effects of satellite bunching on the probability of collision in geosynchronous orbit
[BTN-95-EIX95152583276] p 298 A95-73577

PROBLEM SOLVING

- On the exact solutions of pseudorange equations
[BTN-95-EIX9514255477] p 278 A95-73433
- Application of a control-volume-based finite-element formulation to the shock tube problem
[BTN-95-EIX95182619099] p 295 A95-76584
- Empirical results on scheduling and dynamic backtracking p 299 N95-23761

PROCEDURES

- Scientific and technical photography at NASA Langley Research Center p 310 N95-23290

PRODUCT DEVELOPMENT

- New commercial off-the-shelf testers are automatic and intelligent
[BTN-95-EIX95172595292] p 287 A95-75720

PROGRAM VERIFICATION (COMPUTERS)

- Response of a nonrotating rotor blade to lateral turbulence. Part 2: Experiment
[BTN-95-EIX95182619229] p 284 A95-76655

PROPELLANT GRAINS

- Simulation on the 3-D turbulent flow in the passages of finocyl grain
[BTN-95-EIX95202638962] p 279 A95-76674

PROPELLER BLADES

- System for determining aerodynamic imbalance
[NASA-CASE-ARC-11913-1] p 311 N95-23377

PROPELLERS

- Adaptive finite element method for turbulent flow near a propeller
[BTN-95-EIX95142553038] p 305 A95-73460

PROPULSION

- Analytical aeropropulsive/aeroelastic hypersonic-vehicle model with dynamic analysis
[BTN-95-EIX95182619138] p 269 A95-76615
- Airborne rotary air separator study
[NASA-CR-189099] p 290 N95-24053
- Mechanical system reliability and risk assessment
[BTN-95-EIX95142553046] p 304 A95-73452
- Integrated flight/propulsion control for helicopters
[HTN-95-80854] p 290 A95-75096
- An unmanned air vehicle concept with tipjet drive
[HTN-95-80858] p 283 A95-75100

PROTECTIVE COATINGS

- Evaluation of advanced aerospace materials by depth sensing indentation and scratch methods
[BTN-95-EIX95152584678] p 282 A95-73590
- Evaluation of thermal barrier and PS-200 self-lubricating coatings in an air-cooled rotary engine
[NASA-CR-195445] p 289 N95-23222
- Corrosion protection measures for CFC/metal joints of fuel integral tank structures of advanced military aircraft p 303 N95-23510

PROTON RESONANCE

- Phonon characteristics of high (T sub c) superconductors from neutron Doppler broadening measurements
[DE95-003703] p 324 N95-24076
- PUMP IMPELLERS**
Impeller flow field characterization with a laser two-focus velocimeter p 313 N95-23440

Q

QUADRUPOLES

- Numerical study of sound generation due to a spinning vortex pair
[BTN-95-EIX95182619075] p 307 A95-75760

QUALITY

- The airline quality report, 1994
[NIAR-94-11] p 277 N95-24012

QUANTITATIVE ANALYSIS

- Simple method of supersonic flow visualization using watertable
[BTN-95-EIX95182619105] p 269 A95-76590
- Evaluation of neutron techniques for illicit substance detection
[DE95-002988] p 300 N95-22764

R

RADAR DATA

- Statistics of multi-look AIRSAR imagery: A comparison of theory with measurements p 320 N95-23947

RADAR IMAGERY

- Statistics of multi-look AIRSAR imagery: A comparison of theory with measurements p 320 N95-23947
- AIRSAR deployment in Australia, September 1993: Management and objectives p 321 N95-23948

RADAR MAPS

- Differential GPS and system integration of the Low Visibility Landing and Surface Operations (LVLASO) demonstration p 280 N95-23318
- MAX-91: Polarimetric SAR results on Montespertoli site p 320 N95-23940

RADIAL FLOW

- Enhanced analysis and users manual for radial-inflow turbine conceptual design code RTD
[NASA-CR-195454] p 275 N95-23462

RADIATIVE HEAT TRANSFER

- Convective and radiative heat transfer analysis for the fire 2 forebody
[BTN-95-EIX95182617460] p 268 A95-75731
- Possible effects of CO2 increase on the high-speed civil transport impact on ozone
[HTN-95-60779] p 317 A95-75976

RADIO ALTIMETERS

- Flight test evaluation of a 35 GHz forward looking altimeter for terrain avoidance
[BTN-95-EIX95212641071] p 287 A95-76736

RADIO FREQUENCIES

- CASS: Design for supportability
[BTN-95-EIX95172595296] p 287 A95-75716

RAINDROPS

- Tracking of raindrops in flow over an airfoil
[BTN-95-EIX95182619221] p 308 A95-76647

RANDOM ERRORS

- Functional dependence of trajectory dispersion on initial condition errors
[BTN-95-EIX95152583263] p 298 A95-73564

RAREFIED GAS DYNAMICS

- Hypersonic rarefied flow past spheres including wake structure
[BTN-95-EIX95152583250] p 305 A95-73551
- Particle kinetic simulation of high altitude hypervelocity flight
[NASA-CR-197383] p 309 N95-22481

RATINGS

- The airline quality report, 1994
[NIAR-94-11] p 277 N95-24012

RATIOS

- Supersonic axisymmetric conical flow solutions for different ratios of specific heats
[BTN-95-EIX95152583283] p 306 A95-73584

REACTION KINETICS

- Sensitivity of combustion-acoustic instabilities to boundary conditions for premixed gas turbine combustors
[NASA-TM-106890] p 289 N95-23550

REAL TIME OPERATION

- Pilot Weather Advisor system
[BTN-95-EIX95152582314] p 316 A95-73517
- Real-time navigation using the global positioning system
[BTN-95-EIX95172595298] p 279 A95-75714

- Estimates of total organic and inorganic chlorine in the lower stratosphere from in situ and flask measurements during AASE 2
[HTN-95-A0861] p 317 A95-76265
- Real-time estimation of atmospheric turbulence severity from in-situ aircraft measurements
[BTN-95-EIX95182619231] p 319 A95-76657

RECOMMENDATIONS

- Aviation Accident Investigation Symposium, Volume 1: Industry recommendations and Safety Board responses
[PB94-917005] p 278 N95-24105

RECONSTRUCTION

- Holographic interferometric tomography for reconstructing flow fields p 310 N95-23287

RECTANGULAR WINGS

- Aerodynamics of a finite wing with simulated ice
[BTN-95-EIX95182619227] p 270 A95-76653

REENTRY TRAJECTORIES

- Shuttle entry guidance revisited using nonlinear geometric methods
[BTN-95-EIX95182619144] p 299 A95-76621

REENTRY VEHICLES

- Functional dependence of trajectory dispersion on initial condition errors
[BTN-95-EIX95152583263] p 298 A95-73564
- Moving mass trim control for aerospace vehicles
[DE95-002602] p 299 N95-23532

REFRACTORY MATERIALS

- Compliant interlayer
[BTN-95-EIX95142562401] p 304 A95-73439

REINFORCING FIBERS

- Compliant interlayer
[BTN-95-EIX95142562401] p 304 A95-73439

REMOTE CONTROL

- Cypher moves toward autonomous flight
[HTN-95-41394] p 283 A95-76390

REMOTE SENSING

- AVIRIS and TIMS data processing and distribution at the land processes distributed active archive center p 325 N95-23872
- AIRSAR deployment in Australia, September 1993: Management and objectives p 321 N95-23948

REMOTELY PILOTED VEHICLES

- An unmanned air vehicle concept with tipjet drive
[HTN-95-80858] p 283 A95-75100
- Cypher moves toward autonomous flight
[HTN-95-41394] p 283 A95-76390

RESEARCH

- 1994 NASA-HU American Society for Engineering Education (ASEE) Summer Faculty Fellowship Program
[NASA-CR-194972] p 325 N95-23276
- Research and Technology, 1994
[NASA-TM-106764] p 262 N95-24025

RESEARCH AIRCRAFT

- Analysis of the longitudinal handling qualities and pilot-induced-oscillation tendencies of the High-Angle-of-Attack Research Vehicle (HARV)
p 293 N95-23297

RESEARCH VEHICLES

- Differential GPS and system integration of the Low Visibility Landing and Surface Operations (LVLASO) demonstration p 280 N95-23318

RESIDUAL STRENGTH

- Residual strength of thin panels with cracks
p 311 N95-23311

RESIN TRANSFER MOLDING

- Development and verification of a resin film infusion/resin transfer molding simulation model for fabrication of advanced textile composites
[NASA-CR-197439] p 301 N95-23179

RESONANT FREQUENCIES

- Phonon characteristics of high (T sub c) superconductors from neutron Doppler broadening measurements
[DE95-003703] p 324 N95-24076

RETROREFLECTION

- Double pass retroreflection for corrosion detection in aircraft structures p 323 N95-23503

REVERSED FLOW

- Aerodynamic characteristics of external store configurations at low speeds
[BTN-95-EIX95182619230] p 271 A95-76656

REYNOLDS EQUATION

- Influence of streamwise curvature on longitudinal vortices imbedded in turbulent boundary layers
[BTN-94-EIX94401378820] p 307 A95-76489

REYNOLDS NUMBER

- Effect of underwing frost on a transport aircraft airfoil at flight Reynolds number
[BTN-95-EIX95152582334] p 276 A95-73536
- Effect of ambient turbulence intensity on sphere wakes at intermediate Reynolds numbers
[BTN-95-EIX95182619101] p 308 A95-76586
- Wing pressure distributions from subsonic tests of a high-wing transport model --- in the Langley 14- by 22-Foot Subsonic Wind Tunnel
[NASA-TM-4583] p 272 N95-22802

- Design of a variable area diffuser for a 15-inch Mach 6 open-jet tunnel p 297 N95-23309

RISK

- Mechanical system reliability and risk assessment
[BTN-95-EIX95142553046] p 304 A95-73452

RIVETED JOINTS

- Growth of multiple cracks and their linkup in a fuselage lap joint
[BTN-95-EIX95142553047] p 286 A95-73451

RIVETING

- Automatic riveting cell for commercial aircraft floor grid assembly
[BTN-95-EIX95182617807] p 261 A95-75752

ROBOTICS

- Fourth-generation Mars vehicle concepts
[BTN-95-EIX95152583267] p 298 A95-73568

ROBOTS

- Automatic riveting cell for commercial aircraft floor grid assembly
[BTN-95-EIX95182617807] p 261 A95-75752

ROBUSTNESS (MATHEMATICS)

- Enhancing filter robustness in cascaded GPS-INS integrations
[BTN-95-EIX95142555475] p 278 A95-73435
- Identification of higher order helicopter dynamics using linear modeling methods
[HTN-95-80851] p 290 A95-75093
- Aeroelastic vehicle multivariable control synthesis with analytical robustness evaluation
[BTN-95-EIX95182619115] p 321 A95-76592
- Multivariable stability and robustness of sequentially designed feedback systems
[BTN-95-EIX95182619125] p 322 A95-76602
- Robustly stable preliminary control systems design for the YF-16 CCV aircraft
[BTN-95-EIX95202637608] p 292 A95-76681
- Design of high performance multivariable control systems for supermaneuverable aircraft at high angle of attack
[NASA-CR-197661] p 293 N95-22908

ROCKET ENGINES

- Fourth-generation Mars vehicle concepts
[BTN-95-EIX95152583267] p 298 A95-73568
- Impeller flow field characterization with a laser two-focus velocimeter p 313 N95-23440

ROLL

- Navier-Stokes prediction of large-amplitude delta-wing roll oscillations
[BTN-95-EIX95152582329] p 281 A95-73531
- Further analysis of high-rate rolling experiments of a 65-deg delta wing
[BTN-95-EIX95152582331] p 281 A95-73533
- Method for the prediction of the onset of wing rock
[BTN-95-EIX95152582342] p 282 A95-73544
- Investigation of the effects of bandwidth and time delay on helicopter roll-axis handling qualities
[HTN-95-80853] p 290 A95-75095
- Kinematics and aerodynamics of velocity-vector roll
[BTN-95-EIX95182619126] p 291 A95-76603
- Multiple-function digital controller system for active flexible wing wind-tunnel model
[BTN-95-EIX95182619212] p 322 A95-76638
- Rolling maneuver load alleviation using active controls
[BTN-95-EIX95182619217] p 270 A95-76643
- Feedback control laws for highly maneuverable aircraft
[NASA-CR-197944] p 295 N95-23410

ROLLING MOMENTS

- Effect of leeward flow dividers on the wing rock of a delta wing
[BTN-95-EIX95152582347] p 282 A95-73549
- Kinematics and aerodynamics of velocity-vector roll
[BTN-95-EIX95182619126] p 291 A95-76603

ROTARY ENGINES

- Evaluation of thermal barrier and PS-200 self-lubricating coatings in an air-cooled rotary engine
[NASA-CR-195445] p 289 N95-23222

ROTARY WING AIRCRAFT

- An unmanned air vehicle concept with tipjet drive
[HTN-95-80858] p 283 A95-75100
- Cypher moves toward autonomous flight
[HTN-95-41394] p 283 A95-76390
- System for determining aerodynamic imbalance
[NASA-CASE-ARC-11913-1] p 311 N95-23377

ROTARY WINGS

- Efficient sensitivity analysis for rotary-wing aeromechanical problems
[BTN-95-EIX95152577585] p 264 A95-73497
- Dynamic analysis of bearingless tail rotor blades based on nonlinear shell modes
[BTN-95-EIX95152582338] p 281 A95-73540
- Sensitivity of acoustic predictions to variation of input parameters
[HTN-95-80855] p 267 A95-75097

- The influence of alternate inter-blade connections on ground resonance
[HTN-95-80859] p 267 A95-75101
- Response of a nonrotating rotor blade to lateral turbulence. Part 1: Theory
[BTN-95-EIX95182619228] p 284 A95-76654
- Response of a nonrotating rotor blade to lateral turbulence. Part 2: Experiment
[BTN-95-EIX95182619229] p 284 A95-76655
- Integrated aerodynamic/dynamic/structural optimization of helicopter rotor blades using multilevel decomposition
[NASA-TP-3465] p 285 N95-22953
- System for determining aerodynamic imbalance
[NASA-CASE-ARC-11913-1] p 311 N95-23377
- ROTATING BODIES**
- Dynamic investigation of the angular motion of a rotating body-parachute system
[BTN-95-EIX95182619220] p 270 A95-76646
- ROTATING SHAFTS**
- Transient analysis of a cracked rotor passing through critical speed
[BTN-94-EIX94401360022] p 306 A95-74702
- ROTATION**
- Dynamic investigation of the angular motion of a rotating body-parachute system
[BTN-95-EIX95182619220] p 270 A95-76646
- ROTOR AERODYNAMICS**
- Efficient sensitivity analysis for rotary-wing aeromechanical problems
[BTN-95-EIX95152577585] p 264 A95-73497
- Effects of high order dynamics on helicopter flight control law design
[HTN-95-80852] p 290 A95-75094
- Sensitivity of acoustic predictions to variation of input parameters
[HTN-95-80855] p 267 A95-75097
- The influence of alternate inter-blade connections on ground resonance
[HTN-95-80859] p 267 A95-75101
- Response of a nonrotating rotor blade to lateral turbulence. Part 2: Experiment
[BTN-95-EIX95182619229] p 284 A95-76655
- ROTOR BLADES**
- Response of a nonrotating rotor blade to lateral turbulence. Part 2: Experiment
[BTN-95-EIX95182619229] p 284 A95-76655
- ROTOR BLADES (TURBOMACHINERY)**
- Efficient sensitivity analysis for rotary-wing aeromechanical problems
[BTN-95-EIX95152577585] p 264 A95-73497
- Analysis of a higher harmonic control test to reduce blade vortex interaction noise
[BTN-95-EIX95152582330] p 265 A95-73532
- Enhanced analysis and users manual for radial-inflow turbine conceptual design code RTD
[NASA-CR-195454] p 275 N95-23462
- ROTOR BODY INTERACTIONS**
- An investigation of helicopter dynamic coupling using an analytical model
[NASA-CR-197420] p 285 N95-23217
- ROTOR DYNAMICS**
- Improving prediction: The incorporation of simplified rotor dynamics in a mathematical model of the bell 412HP
[BTN-95-EIX95152584679] p 282 A95-73591
- Transient analysis of a cracked rotor passing through critical speed
[BTN-94-EIX94401360022] p 306 A95-74702
- Identification of higher order helicopter dynamics using linear modeling methods
[HTN-95-80851] p 290 A95-75093
- Effects of high order dynamics on helicopter flight control law design
[HTN-95-80852] p 290 A95-75094
- Integrated flight/propulsion control for helicopters
[HTN-95-80854] p 290 A95-75096
- Effects of AMB parameters on the dynamic stability of the rotor
[BTN-94-EIX94381353450] p 323 A95-75494
- Influence of backup bearings and support structure dynamics on the behavior of rotors with active supports
[NASA-CR-197438] p 310 N95-23190
- Evaluation of thermal barrier and PS-200 self-lubricating coatings in an air-cooled rotary engine
[NASA-CR-195445] p 289 N95-23222
- ROTOR SYSTEMS RESEARCH AIRCRAFT**
- H-76B fantail demonstrator composite fan blade fabrication
[HTN-95-80856] p 283 A95-75098
- ROTORS**
- Finite element model for a flexible non-symmetric rotor on distributed bearing: A stability study
[BTN-94-EIX94381352212] p 306 A95-74612
- Transient analysis of a cracked rotor passing through critical speed
[BTN-94-EIX94401360022] p 306 A95-74702
- Effects of AMB parameters on the dynamic stability of the rotor
[BTN-94-EIX94381353450] p 323 A95-75494
- Influence of backup bearings and support structure dynamics on the behavior of rotors with active supports
[NASA-CR-197438] p 310 N95-23190
- Thin tailored composite wing for civil tiltrotor
p 285 N95-23317
- RUNGE-KUTTA METHOD**
- Effects of spatial order of accuracy on the computation of vortical flowfields
[BTN-95-EIX95152577604] p 305 A95-73479
- Numerical computation of aerodynamics and heat transfer in a turbine cascade and a turn-around duct using advanced turbulence models
p 313 N95-23444
- RUNWAY CONDITIONS**
- Guidance and control requirements for high-speed Rollout and Turnoff (ROTO)
[NASA-CR-195026] p 292 N95-22674
- RUNWAYS**
- Aircraft accident report. Runway overrun following rejected takeoff. Continental airlines flight 795, McDonnell Douglas MD-82, N18835, LaGuardia Airport, Flushing, NY, 2 March 1994
[PB95-910401] p 277 N95-23609
- S**
- SABOT PROJECTILES**
- Analytical solution and parameter estimation of projectile dynamics
[BTN-95-EIX95212645695] p 272 A95-76747
- SAFETY**
- Mishap risk control for advanced aerospace/composite materials
p 301 N95-23031
- SAFETY FACTORS**
- Corrosion detection and monitoring of aircraft structures: An overview
p 303 N95-23515
- SAFETY MANAGEMENT**
- Maintenance programs
[BTN-95-EIX95182617809] p 261 A95-75754
- A review of civil aviation fatal accidents in which lost/disoriented was a cause/factor: 1981-1990
[DOT/FAA/AM-95/1] p 278 N95-24071
- Aviation Accident Investigation Symposium. Volume 1: Industry recommendations and Safety Board responses
[PB94-917005] p 278 N95-24105
- SALT BATHS**
- Corrosion of landing gear steels
p 302 N95-23500
- SALT SPRAY TESTS**
- Corrosion of landing gear steels
p 302 N95-23500
- SANDWICH STRUCTURES**
- Minimum-mass design of sandwich aerobrakes for a lunar transfer vehicle
[BTN-95-EIX95212645707] p 299 A95-76759
- SATELLITE COMMUNICATION**
- Development of aeronautical mobile satellite services over the past thirty years
[BTN-95-EIX95152569458] p 305 A95-73498
- Pilot Weather Advisor system
[BTN-95-EIX95152582314] p 316 A95-73517
- SATELLITE DRAG**
- Calculation of satellite drag coefficients
[AD-A285118] p 300 N95-23781
- SATELLITE ORBITS**
- Thermal force modeling for global positioning system satellites using the finite element method
[BTN-95-EIX95152583270] p 278 A95-73571
- SCALE MODELS**
- Aerodynamic characteristics of a canard-controlled missile at high angles of attack
[BTN-95-EIX95152583257] p 267 A95-73558
- SCALING LAWS**
- Scaling of incipient separation in supersonic/transonic speed laminar flows
[BTN-95-EIX95182619104] p 269 A95-76589
- SCANNING ELECTRON MICROSCOPY**
- SEM representation of the early and late time fields scattered from wire targets
[BTN-94-EIX94381353142] p 306 A95-74496
- SCHEDULING**
- Empirical results on scheduling and dynamic backtracking
p 299 N95-23761
- SECONDARY FLOW**
- Three-dimensional unsteady flow calculations in an advanced gas generator turbine
p 312 N95-23425
- SENSITIVITY**
- Preconditioned domain decomposition scheme for three-dimensional aerodynamic sensitivity analysis
[BTN-95-EIX95152577612] p 321 A95-73471
- Efficient sensitivity analysis for rotary-wing aeromechanical problems
[BTN-95-EIX95152577585] p 264 A95-73497
- SEPARATED FLOW**
- Two-equation turbulence model for unsteady separated flows around airfoils
[BTN-95-EIX95142553054] p 262 A95-73444
- Computation of oscillating airfoil flows with one- and two-equation turbulence models
[BTN-95-EIX95152577588] p 263 A95-73494
- Computational study of plume-induced separation on a hypersonic powered model
[BTN-95-EIX95152582346] p 266 A95-73548
- Simulating heat addition via mass addition in constant area compressible flows
[BTN-95-EIX95182619100] p 307 A95-76585
- Scaling of incipient separation in supersonic/transonic speed laminar flows
[BTN-95-EIX95182619104] p 269 A95-76589
- Neural network prediction of three-dimensional unsteady separated flowfields
[BTN-95-EIX95182619232] p 308 A95-76658
- SERVICE LIFE**
- Life prediction of helicopter engines fitted with dust filters
[BTN-95-EIX95182619224] p 289 A95-76650
- Oklahoma City air logistics center (USAF) aging aircraft corrosion program
p 262 N95-23519
- SHADOWGRAPH PHOTOGRAPHY**
- Simple method of supersonic flow visualization using watertable
[BTN-95-EIX95182619105] p 269 A95-76590
- SHAFTS (MACHINE ELEMENTS)**
- Finite element model for a flexible non-symmetric rotor on distributed bearing: A stability study
[BTN-94-EIX94381352212] p 306 A95-74612
- SHALLOW SHELLS**
- Dynamic analysis of bearingless tail rotor blades based on nonlinear shell modes
[BTN-95-EIX95152582338] p 281 A95-73540
- SHEAR**
- Finite element model for a flexible non-symmetric rotor on distributed bearing: A stability study
[BTN-94-EIX94381352212] p 306 A95-74612
- SHEAR FLOW**
- Adaptive finite element method for turbulent flow near a propeller
[BTN-95-EIX95142553038] p 305 A95-73460
- SHEAR LAYERS**
- Laser velocimetry seed-particle behavior in shear layers at Mach 12
[BTN-95-EIX95212645712] p 272 A95-76764
- SHEAR STRAIN**
- Finite element model for a flexible non-symmetric rotor on distributed bearing: A stability study
[BTN-94-EIX94381352212] p 306 A95-74612
- SHEAR STRENGTH**
- Interlaminar shear test method development for long term durability testing of composites
p 301 N95-23300
- SHEAR STRESS**
- Nonlinear angle of twist of advanced composite wing boxes under pure torsion
[BTN-95-EIX95152582323] p 281 A95-73526
- High-lift flow-physics flight experiments on a subsonic civil transport aircraft (B737-100)
p 275 N95-23333
- SHOCK HEATING**
- Application of the multigrid solution technique to hypersonic entry vehicles
[BTN-95-EIX95152583254] p 306 A95-73555
- SHOCK LAYERS**
- Higher-order viscous shock-layer solutions for high-altitude flows
[BTN-95-EIX95152583255] p 306 A95-73556
- SHOCK TUBES**
- Application of a control-volume-based finite-element formulation to the shock tube problem
[BTN-95-EIX95182619099] p 295 A95-76584
- SHOCK TUNNELS**
- Shock tunnel measurements of hypervelocity blunted cone drag
[BTN-95-EIX95152577606] p 305 A95-73477
- SHOCK WAVE INTERACTION**
- Flow study of supersonic wing-nacelle configuration
[BTN-95-EIX95152582344] p 266 A95-73546
- Scaling of incipient separation in supersonic/transonic speed laminar flows
[BTN-95-EIX95182619104] p 269 A95-76589
- Mach 10 computational study of a three-dimensional scramjet inlet flow field
[NASA-TM-4602] p 310 N95-23210
- Supersonic flow and shock formation in turbine tip gaps
p 312 N95-23429

SHOCK WAVE PROPAGATION

- Aeroacoustic model for weak shock waves based on Burgers equation
[BTN-95-EIX95182619076] p 269 A95-75761
- SHOCK WAVES**
Flow study of supersonic wing-nacelle configuration
[BTN-95-EIX95152582344] p 266 A95-73546
Application of the multigrid solution technique to hypersonic entry vehicles
[BTN-95-EIX95152583254] p 306 A95-73555
Three-dimensional structure of a supersonic jet impinging on an inclined plate
[BTN-95-EIX95152583259] p 267 A95-73560
Supersonic axisymmetric conical flow solutions for different ratios of specific heats
[BTN-95-EIX95152583283] p 306 A95-73584
Aeroacoustic model for weak shock waves based on Burgers equation
[BTN-95-EIX95182619076] p 269 A95-75761
Observations on using experimental data as boundary conditions for computations
[BTN-95-EIX95182619103] p 321 A95-76588
- SHUTTLE IMAGING RADAR**
AIRSAR deployment in Australia, September 1993: Management and objectives
[BTN-95-EIX95182619103] p 321 A95-76588
- SIDESLIP**
Method for the prediction of the onset of wing rock
[BTN-95-EIX95152582342] p 282 A95-73544
Effect of leeward flow dividers on the wing rock of a delta wing
[BTN-95-EIX95152582347] p 282 A95-73549
Wing pressure distributions from subsonic tests of a high-wing transport model --- in the Langley 14- by 22-Foot Subsonic Wind Tunnel
[NASA-TM-4583] p 272 N95-22802
- SIGNAL PROCESSING**
Simulation of turbulent fluctuations
[BTN-95-EIX95142553041] p 304 A95-73457
Maximum-likelihood spectral estimation and adaptive filtering techniques with application to airborne Doppler weather radar
[NASA-CR-197699] p 316 N95-23670
- SIKORSKY AIRCRAFT**
H-76B tailfin demonstrator composite fan blade fabrication
[HTN-95-80856] p 283 A95-75098
Cypher moves toward autonomous flight
[HTN-95-41394] p 283 A95-76390
- SILICON**
Cu deposition using a permanent magnet electron cyclotron resonance microwave plasma source
[DE94-017768] p 304 A95-23981
- SILICON NITRIDES**
Evolution of oxidation and creep damage mechanisms in HIPed silicon nitride materials
[DE95-001360] p 300 N95-22689
- SIMULATION**
Simulation and model reduction for the active flexible wing program
[BTN-95-EIX95182619211] p 295 A95-76637
Holographic interferometric tomography for reconstructing flow fields
[BTN-95-EIX95182619211] p 310 N95-23287
- SIMULATORS**
A new type of simulator for simulating the flow-field distortion of engine inlet
[BTN-95-EIX95202638963] p 289 A95-76673
- SINGULARITY (MATHEMATICS)**
A wall interference assessment/correction system
[NASA-CR-197421] p 309 N95-23183
- SITTING POSITION**
A multibody/finite element analysis approach for modeling of crash dynamic responses
[NIAR-94-3] p 277 N95-24050
- SKIN (STRUCTURAL MEMBER)**
Multiple site fatigue damage in fuselage skin splices: Experimental simulation and theoretical prediction
[BTN-95-EIX95152584676] p 276 A95-73588
An analytical and experimental investigation of the response of the curved, composite frame/skin specimens
[HTN-95-80857] p 283 A95-75099
- SLENDER CONES**
Shock tunnel measurements of hypervelocity blunted cone drag
[BTN-95-EIX95152577606] p 305 A95-73477
- SLOTS**
Forebody flow control on a full-scale F/A-18 aircraft
[BTN-95-EIX95152582333] p 281 A95-73535
Pneumatic concept for tip-stall control of cranked-arrow wings
[BTN-95-EIX95152582335] p 281 A95-73537
- SMOKE**
Modeling aerosol emissions from the combustion of composite materials
[DOT/FAA/AM-95/8] p 301 N95-23038
Aircraft fires, smoke toxicity, and survival: An overview
[DOT/FAA/AM-95/8] p 277 N95-24024

SOLAR ARRAYS

- Design of a GaAs/Ge solar array for unmanned aerial vehicles
[NASA-TM-106870] p 320 N95-23259
- SOLAR CELLS**
Design of a GaAs/Ge solar array for unmanned aerial vehicles
[NASA-TM-106870] p 320 N95-23259
- SOLID LUBRICANTS**
Evaluation of thermal barrier and PS-200 self-lubricating coatings in an air-cooled rotary engine
[NASA-CR-195445] p 289 N95-23222
- SOLID PROPELLANT ROCKET ENGINES**
Simulation on the 3-D turbulent flow in the passages of finocyl grain
[BTN-95-EIX95202638962] p 279 A95-76674
- SOLID STATE LASERS**
2 micron LIDAR for laser-based remote sensing: Flight demonstration and application survey
[BTN-95-EIX95212641072] p 319 A95-76737
- SONIC BOOMS**
Aeroacoustic model for weak shock waves based on Burgers equation
[BTN-95-EIX95182619076] p 269 A95-75761
- SOUND FIELDS**
Numerical study of sound generation due to a spinning vortex pair
[BTN-95-EIX95182619075] p 307 A95-75760
- SOUND WAVES**
Coupled FEM-BEM approach for mean flow effects on vibro-acoustic behavior of planar structures
[BTN-95-EIX95152577587] p 263 A95-73495
Mach wave emission from a high-temperature supersonic jet
[BTN-95-EIX95152577586] p 264 A95-73496
- SPACE PROCESSING**
Fourth-generation Mars vehicle concepts
[BTN-95-EIX95152583267] p 298 A95-73568
- SPACE SHUTTLE MAIN ENGINE**
Phase 2: HGM air flow tests in support of HEX vane investigation
[BTN-95-EIX95152583267] p 312 N95-23438
- SPACE SHUTTLE ORBITERS**
Aerodynamics of the Shuttle Orbiter at high altitudes
[BTN-95-EIX95182617454] p 298 A95-75725
Shuttle entry guidance revisited using nonlinear geometric methods
[BTN-95-EIX95182619144] p 299 A95-76621
- SPACECRAFT CONSTRUCTION MATERIALS**
Evaluation of advanced aerospace materials by depth sensing indentation and scratch methods
[BTN-95-EIX95152584678] p 282 A95-73590
- SPACECRAFT CONTROL**
Fuel-optimal bank-angle control for lunar-return aerocapture
[BTN-95-EIX95212645706] p 299 A95-76758
- SPACECRAFT LAUNCHING**
Fourth-generation Mars vehicle concepts
[BTN-95-EIX95152583267] p 298 A95-73568
- SPACECRAFT MODELS**
Thermal force modeling for global positioning system satellites using the finite element method
[BTN-95-EIX95152583270] p 278 A95-73571
- SPACECRAFT REENTRY**
Shuttle entry guidance revisited using nonlinear geometric methods
[BTN-95-EIX95182619144] p 299 A95-76621
- SPACECRAFT TRAJECTORIES**
Effects of satellite bunching on the probability of collision in geosynchronous orbit
[BTN-95-EIX95152583276] p 298 A95-73577
- SPACING**
Main features of overexpanded triple jets
[BTN-95-EIX95142553040] p 304 A95-73458
- SPALLATION**
Phonon characteristics of high (T sub c) superconductors from neutron Doppler broadening measurements
[DE95-003703] p 324 N95-24076
- SPATIAL DISTRIBUTION**
Thundercloud electric field modeling for the ionosphere-Earth region. 1: Dependence on cloud charge distribution
[HTN-95-41223] p 317 A95-75035
- SPATIAL FILTERING**
Simulation of turbulent fluctuations
[BTN-95-EIX95142553041] p 304 A95-73457
- SPECIFIC HEAT**
Supersonic axisymmetric conical flow solutions for different ratios of specific heats
[BTN-95-EIX95152583283] p 306 A95-73584
Review and development of base pressure and base heating correlations in supersonic flow
[BTN-95-EIX95212645688] p 271 A95-76740
- SPECIFICATIONS**
Handling qualities of the High Speed Civil Transport
[NASA-CR-195050] p 273 N95-23193

SPECTRAL SENSITIVITY

- Sensitivity of acoustic predictions to variation of input parameters
[HTN-95-80855] p 267 A95-75097
- SPECTRUM ANALYSIS**
Phonon characteristics of high (T sub c) superconductors from neutron Doppler broadening measurements
[DE95-003703] p 324 N95-24076
- SPHERES**
Hypersonic rarefied flow past spheres including wake structure
[BTN-95-EIX95152583250] p 305 A95-73551
- SPHERICAL COORDINATES**
Application of wall functions to generalized nonorthogonal curvilinear coordinate systems
[BTN-95-EIX95182619077] p 307 A95-75762
- SPHERICAL WAVES**
Effect of ambient turbulence intensity on sphere wakes at intermediate Reynolds numbers
[BTN-95-EIX95182619101] p 308 A95-76586
- SPIKES (AERODYNAMIC CONFIGURATIONS)**
Numerical investigation of supersonic flows around a spiked blunt body
[BTN-95-EIX95212645690] p 271 A95-76742
- SPIKE**
A multibody/finite element analysis approach for modeling of crash dynamic responses
[NIAR-94-3] p 277 N95-24050
- SPLASHING**
Tracking of raindrops in flow over an airfoil
[BTN-95-EIX95182619221] p 308 A95-76647
- SPlicing**
Multiple site fatigue damage in fuselage skin splices: Experimental simulation and theoretical prediction
[BTN-95-EIX95152584676] p 276 A95-73588
- SPOILERS**
Study of an airfoil with a flap and spoiler
[BTN-95-EIX95152582327] p 265 A95-73530
- SPRAY CHARACTERISTICS**
Study of the droplet spray characteristics of a subsonic wind tunnel
[BTN-95-EIX95182619235] p 271 A95-76661
- STABILITY**
Comparison of linear stability results with flight transition data
[BTN-95-EIX95182619097] p 283 A95-76582
Thin tailored composite wing for civil tiltrotor
[BTN-95-EIX95182619235] p 285 N95-23317
- STABILITY DERIVATIVES**
Attainable moments for the constrained control allocation problem
[BTN-95-EIX95182619149] p 322 A95-76626
Stability derivatives of a flapped plate in unsteady ground effect
[BTN-95-EIX95182619225] p 270 A95-76651
- STABILITY TESTS**
Functional dependence of trajectory dispersion on initial condition errors
[BTN-95-EIX95152583263] p 298 A95-73564
- STABILIZERS (FLUID DYNAMICS)**
Integrated design of hypersonic waveriders including inlets and tailfins
[BTN-95-EIX95212645692] p 271 A95-76744
- STAGNATION PRESSURE**
Main features of overexpanded triple jets
[BTN-95-EIX95142553040] p 304 A95-73458
- STATE ESTIMATION**
New failure detection approach and its application to GPS autonomous integrity monitoring
[BTN-95-EIX95202637613] p 279 A95-76676
- STATIC CHARACTERISTICS**
Static aeroelastic characteristics of a composite wing
[BTN-95-EIX95152582340] p 282 A95-73542
- STATIC PRESSURE**
Static pressure distribution in the inlet of a helicopter turbine compressor
[BTN-95-EIX95152582339] p 266 A95-73541
Aerodynamic characteristics of external store configurations at low speeds
[BTN-95-EIX95182619230] p 271 A95-76656
- STATIC STABILITY**
Handling qualities of the High Speed Civil Transport
[NASA-CR-195050] p 273 N95-23193
- STATIC TESTS**
Validation of an effective flat cruciform-shaped specimen to study CFRP composite laminates under biaxial loading
[BTN-95-EIX95152584677] p 282 A95-73589
Corrosion protection measures for CFC/metal joints of fuel integral tank structures of advanced military aircraft
[DOT/FAA/AM-95/8] p 303 N95-23510
- STATIC THRUST**
An approximate theoretical method for modeling the static thrust performance of non-axisymmetric two-dimensional convergent-divergent nozzles
[NASA-CR-195050] p 273 N95-23193

STATISTICAL ANALYSIS

- Effects of satellite bunching on the probability of collision in geosynchronous orbit
[BTN-95-EIX95152583276] p 298 A95-73577
- On-line, adaptive state estimator for active noise control
p 322 N95-23308
- POD assessment of NDI procedures using a round robin test
[AGARD-R-809] p 315 N95-23602

STATORS

- Enhanced analysis and users manual for radial-inflow turbine conceptual design code RTD
[NASA-CR-195454] p 275 N95-23462

STEADY FLOW

- Aerodynamic design and analysis of a highly loaded turbine exhaust
p 312 N95-23435

STEELS

- Corrosion of landing gear steels p 302 N95-23500

STIFFNESS

- Dynamic analysis of bearingless tail rotor blades based on nonlinear shell modes
[BTN-95-EIX95152582338] p 281 A95-73540
- Finite element model for a flexible non-symmetric rotor on distributed bearing: A stability study
[BTN-94-EIX94381352212] p 306 A95-74612
- Integrated aerodynamic/dynamic/structural optimization of helicopter rotor blades using multilevel decomposition
[NASA-TP-3465] p 285 N95-22953

STRAIN MEASUREMENT

- Shock tunnel measurements of hypervelocity blunted cone drag
[BTN-95-EIX95152577606] p 305 A95-73477

STRATOSPHERE

- Trajectory modeling of emissions from lower stratospheric aircraft
[HTN-95-41219] p 317 A95-75031
- Possible effects of CO₂ increase on the high-speed civil transport impact on ozone
[HTN-95-60779] p 317 A95-75976
- Estimates of total organic and inorganic chlorine in the lower stratosphere from in situ and flask measurements during AASE 2
[HTN-95-A0861] p 317 A95-76265
- In situ observations in aircraft exhaust plumes in the lower stratosphere at midlatitudes
[HTN-95-A0862] p 318 A95-76266
- Sensitivity of two-dimensional model predictions of ozone response to stratospheric aircraft: An update
[HTN-95-A0863] p 318 A95-76267

STRESS CORROSION CRACKING

- The corrosion and protection of advanced aluminium - lithium airframe alloys
p 302 N95-23497
- Corrosion of landing gear steels p 302 N95-23500

STRESS INTENSITY FACTORS

- Multiple site fatigue damage in fuselage skin splices: Experimental simulation and theoretical prediction
[BTN-95-EIX95152584676] p 276 A95-73588

STRIPPING

- Aircraft stripping and painting
[BTN-95-EIX95182617810] p 300 A95-75755

STRUCTURAL ANALYSIS

- Static aeroelastic characteristics of a composite wing
[BTN-95-EIX95152582340] p 282 A95-73542

STRUCTURAL DESIGN

- Minimum-mass design of sandwich aerobreaks for a lunar transfer vehicle
[BTN-95-EIX95212645707] p 299 A95-76759
- Integrated aerodynamic/dynamic/structural optimization of helicopter rotor blades using multilevel decomposition
[NASA-TP-3465] p 285 N95-22953

STRUCTURAL FAILURE

- An analytical and experimental investigation of the response of the curved, composite frame/skin specimens
[HTN-95-80857] p 283 A95-75099

STRUCTURAL STABILITY

- Finite element model for a flexible non-symmetric rotor on distributed bearing: A stability study
[BTN-94-EIX94381352212] p 306 A95-74612
- Flutter of an infinitely long panel in a duct
[BTN-95-EIX95182619087] p 291 A95-75772

STRUCTURAL STRAIN

- Dynamic analysis of bearingless tail rotor blades based on nonlinear shell modes
[BTN-95-EIX95152582338] p 281 A95-73540

STRUCTURAL VIBRATION

- Coupled FEM-BEM approach for mean flow effects on vibro-acoustic behavior of planar structures
[BTN-95-EIX95152577587] p 263 A95-73495
- Transient analysis of a cracked rotor passing through critical speed
[BTN-94-EIX94401360022] p 306 A95-74702

Analytical aeropropulsive/aeroelastic hypersonic-vehicle model with dynamic analysis

- [BTN-95-EIX95182619138] p 269 A95-76615
- Active control of panel vibrations induced by a boundary layer flow
[NASA-CR-197867] p 273 N95-23182
- Gearbox vibration diagnostic analyzer
[NASA-CR-189141] p 316 N95-23792

SUBSONIC FLOW

- Sidewash on the vertical tail in subsonic and supersonic flows
[BTN-95-EIX95152582316] p 264 A95-73519
- Analytic prediction of lift for delta wings with partial leading-edge thrust
[BTN-95-EIX95152582345] p 266 A95-73547
- Higher-order viscous shock-layer solutions for high-altitude flows
[BTN-95-EIX95152583255] p 306 A95-73556
- Comparison of linear stability results with flight transition data
[BTN-95-EIX95182619097] p 283 A95-76582
- Study of the droplet spray characteristics of a subsonic wind tunnel
[BTN-95-EIX95182619235] p 271 A95-76661
- Wing pressure distributions from subsonic tests of a high-wing transport model --- in the Langley 14- by 22-Foot Subsonic Wind Tunnel
[NASA-TM-4583] p 272 N95-22802

SUBSONIC FLUTTER

- Design and multifunction tests of a frequency domain-based active flutter suppression system
[BTN-95-EIX95182619215] p 292 A95-76641

SUBSONIC SPEED

- Computation of the poststall behavior of a circulation controlled airfoil
[BTN-95-EIX95152582320] p 264 A95-73523
- Aerodynamic characteristics of a canard-controlled missile at high angles of attack
[BTN-95-EIX95152583257] p 267 A95-73558
- Inner loop flight control for the High-Speed Civil Transport
p 293 N95-23314
- High-lift flow-physics flight experiments on a subsonic civil transport aircraft (B737-100)
p 275 N95-23333

SUBSONIC WIND TUNNELS

- Study of the droplet spray characteristics of a subsonic wind tunnel
[BTN-95-EIX95182619235] p 271 A95-76661

SUBSTRATES

- Evaluation of advanced aerospace materials by depth sensing indentation and scratch methods
[BTN-95-EIX95152584678] p 282 A95-73590

SUCTION

- Analytic prediction of lift for delta wings with partial leading-edge thrust
[BTN-95-EIX95152582345] p 266 A95-73547

SULFUR

- Compendium of NASA data base for the Global Tropospheric Experiment's Pacific Exploratory Mission West-A (PEM West-A)
[NASA-TM-109177] p 320 N95-23009

SULFUR HEXAFLUORIDE

- Performance of the 0.3-meter transonic cryogenic tunnel with air, nitrogen, and sulfur hexafluoride media under closed loop automatic control
[NASA-CR-195052] p 310 N95-23257

SUPERSONIC AIRCRAFT

- Mach wave emission from a high-temperature supersonic jet
[BTN-95-EIX95152577586] p 264 A95-73496
- Flow study of supersonic wing-nacelle configuration
[BTN-95-EIX95152582344] p 266 A95-73546

SUPERSONIC AIRFOILS

- Natural laminar flow wing concept for supersonic transports
[BTN-95-EIX95182619226] p 308 A95-76652

SUPERSONIC BOUNDARY LAYERS

- Effects of expansions on a supersonic boundary layer: Surface pressure measurements
[BTN-95-EIX95142553036] p 263 A95-73462

SUPERSONIC COMBUSTION

- Simulating heat addition via mass addition in constant area compressible flows
[BTN-95-EIX95182619100] p 307 A95-76585

SUPERSONIC COMBUSTION RAMJET ENGINES

- Computational study of plume-induced separation on a hypersonic powered model
[BTN-95-EIX95152582346] p 266 A95-73548
- Optimization of contoured hypersonic scramjet inlets with a least-squares parabolized Navier-Stokes procedure
[HTN-95-20976] p 261 A95-74042
- Numerical analysis of hypersonic low-density scramjet inlet flow
[BTN-95-EIX95212645694] p 272 A95-76746

- Mach 10 computational study of a three-dimensional scramjet inlet flow field
[NASA-TM-4602] p 309 N95-23015

- Mach 10 computational study of a three-dimensional scramjet inlet flow field
[NASA-TM-4602] p 310 N95-23210

SUPERSONIC DRAG

- CFD optimization of a theoretical minimum-drag body
[BTN-95-EIX95182619234] p 308 A95-76660

SUPERSONIC FLOW

- Main features of overexpanded triple jets
[BTN-95-EIX95142553040] p 304 A95-73458
- Sidewash on the vertical tail in subsonic and supersonic flows
[BTN-95-EIX95152582316] p 264 A95-73519
- Predicting exhaust plume boundaries with supersonic external flows
[BTN-95-EIX95152583258] p 297 A95-73559
- Supersonic axisymmetric conical flow solutions for different ratios of specific heats
[BTN-95-EIX95152583283] p 306 A95-73584
- Supersonic near-wake afterbody boattailing effects on axisymmetric bodies
[BTN-95-EIX95182617465] p 268 A95-75736
- Simulating heat addition via mass addition in constant area compressible flows
[BTN-95-EIX95182619100] p 307 A95-76585

- Observations on using experimental data as boundary conditions for computations
[BTN-95-EIX95182619103] p 321 A95-76588

- Scaling of incipient separation in supersonic/transonic speed laminar flows
[BTN-95-EIX95182619104] p 269 A95-76589

- Simple method of supersonic flow visualization using water table
[BTN-95-EIX95182619105] p 269 A95-76590

- CFD optimization of a theoretical minimum-drag body
[BTN-95-EIX95182619234] p 308 A95-76660

- Review and development of base pressure and base heating correlations in supersonic flow
[BTN-95-EIX95212645688] p 271 A95-76740

- Numerical investigation of supersonic flows around a spiked blunt body
[BTN-95-EIX95212645690] p 271 A95-76742

- Supersonic flow and shock formation in turbine tip gaps
p 312 N95-23429

- Validation of a Computational Fluid Dynamics (CFD) code for supersonic axisymmetric base flow
p 315 N95-23652

- Supersonic laminar flow control research
[NASA-CR-197938] p 275 N95-23669

SUPERSONIC INLETS

- Mach 10 computational study of a three-dimensional scramjet inlet flow field
[NASA-TM-4602] p 310 N95-23210
- Supersonic flow and shock formation in turbine tip gaps
p 312 N95-23429

SUPERSONIC JET FLOW

- Mach wave emission from a high-temperature supersonic jet
[BTN-95-EIX95152577586] p 264 A95-73496
- Three-dimensional structure of a supersonic jet impinging on an inclined plate
[BTN-95-EIX95152583259] p 267 A95-73560
- Simulation of transverse gas injection in turbulent supersonic air flows
[BTN-95-EIX95182619080] p 269 A95-75765
- Supersonic jet noise reductions predicted with increased jet spreading rate
[NASA-TM-106872] p 323 N95-23178

SUPERSONIC SPEED

- Simple method of supersonic flow visualization using water table
[BTN-95-EIX95182619105] p 269 A95-76590

SUPERSONIC TRANSPORTS

- Natural laminar flow wing concept for supersonic transports
[BTN-95-EIX95182619226] p 308 A95-76652
- Inner loop flight control for the High-Speed Civil Transport
p 293 N95-23314
- Preliminary identification of buffet problems in high speed civil transport
p 294 N95-23319
- Handling qualities of the High Speed Civil Transport
p 294 N95-23325

SUPERSONIC WIND TUNNELS

- Supersonic laminar flow control research
[NASA-CR-197938] p 275 N95-23669

SUPPORT SYSTEMS

- CASS: Design for supportability
[BTN-95-EIX95172595296] p 287 A95-75716

SURFACE DISTORTION

- Double pass retroreflection for corrosion detection in aircraft structures
p 323 N95-23503

SURFACE LAYERS

SURFACE LAYERS

Effects of expansions on a supersonic boundary layer:
Surface pressure measurements
[BTN-95-EIX95142553036] p 263 A95-73462

SURFACE PROPERTIES

Aerodynamic shape optimization using preconditioned conjugate gradient methods
[BTN-95-EIX95142553033] p 263 A95-73465
Guidance and control requirements for high-speed Rollout and Turnoff (ROTO)
[NASA-CR-195026] p 292 N95-22674

SURFACE REACTIONS

Hypersonic nonequilibrium Navier-Stokes solutions over an ablating graphite nosetip
[BTN-95-EIX95152583252] p 305 A95-73553
In-situ detection of surface passivation or activation and of localized corrosion: Experiences and perspectives in aircraft
p 302 N95-23508

SURFACE TEMPERATURE

Particle kinetic simulation of high altitude hypervelocity flight
[NASA-CR-197383] p 309 N95-22481

SURFACE TREATMENT

Experience of in-service corrosion on military aircraft
p 303 N95-23516

SURVIVAL

Aircraft fires, smoke toxicity, and survival: An overview
[DOT/FAA/AM-95/8] p 277 N95-24024

SWEPT FORWARD WINGS

Natural laminar flow wing concept for supersonic transports
[BTN-95-EIX95182619226] p 308 A95-76652
Flight test of the X-29A at high angle of attack: Flight dynamics and controls
[NASA-TP-3537] p 284 N95-22806

SWEPT WINGS

Limit cycle phenomena in computational transonic aerelasticity
[BTN-95-EIX95152582317] p 264 A95-73520
Method for the prediction of the onset of wing rock
[BTN-95-EIX95152582342] p 282 A95-73544
Aerodynamics of a finite wing with simulated ice
[BTN-95-EIX95182619227] p 270 A95-76653
Crossflow instability control on a swept-wing: Preliminary studies
p 274 N95-23283

SWIRLING

Aerodynamic design and analysis of a highly loaded turbine exhaust
p 312 N95-23435

SYMBOLS

TRISTAR 1: Evaluation methods for testing head-up display (HUD) flight symbology
[NASA-TM-4665] p 288 N95-24030

SYNTHETIC APERTURE RADAR

MAX-91: Polarimetric SAR results on Montespertoli site
p 320 N95-23940
Statistics of multi-look AIRSAR imagery: A comparison of theory with measurements
p 320 N95-23947
AIRSAR deployment in Australia, September 1993: Management and objectives
p 321 N95-23948

SYSTEM FAILURES

Mechanical system reliability and risk assessment
[BTN-95-EIX95142553046] p 304 A95-73452

SYSTEM IDENTIFICATION

System identification of the Large-Angle Magnetic Suspension Test Fixture (LAMSTF)
p 296 N95-23299

SYSTEMS ANALYSIS

CASS: Design for supportability
[BTN-95-EIX95172595296] p 287 A95-75716
Aerodynamic design of pegasus: Concept to flight with computational fluid dynamics
[BTN-95-EIX95182617463] p 298 A95-75734

SYSTEMS ENGINEERING

Aeroelastic vehicle multivariable control synthesis with analytical robustness evaluation
[BTN-95-EIX95182619115] p 321 A95-76592
Inner loop flight control for the High-Speed Civil Transport
p 293 N95-23314
Aerodynamic design and analysis of a highly loaded turbine exhaust
p 312 N95-23435

SYSTEMS INTEGRATION

Labs behind Boeing's new 777
[BTN-95-EIX95142562403] p 280 A95-73437
Automation technology using Geographic Information System (GIS)
p 324 N95-23284
Differential GPS and system integration of the Low Visibility Landing and Surface Operations (LVLASO) demonstration
p 280 N95-23318

SYSTEMS SIMULATION

Derivation of system matrices from nonlinear dynamic simulation of jet engines
[BTN-95-EIX95182619139] p 288 A95-76616

SYSTEMS STABILITY

Dynamical instability of the aerogravity assist maneuver
[BTN-95-EIX95152583282] p 298 A95-73583

T

TABS (CONTROL SURFACES)

Aerodynamic characteristics of a canard-controlled missile at high angles of attack
[BTN-95-EIX95152583257] p 267 A95-73558
Lift enhancing tabs for airfoils
[NASA-CASE-ARC-11990-1] p 286 N95-23395

TAIL ASSEMBLIES

Sidewash on the vertical tail in subsonic and supersonic flows
[BTN-95-EIX95152582316] p 264 A95-73519
Preliminary identification of buffet problems in high speed civil transport
p 294 N95-23319

TAIL ROTORS

Dynamic analysis of bearingless tail rotor blades based on nonlinear shell modes
[BTN-95-EIX95152582338] p 281 A95-73540

TAIWAN

Diurnal variation of lee vortices in Taiwan and the surrounding area
[HTN-95-91363] p 318 A95-76394

TAKEOFF

Progress in high-lift aerodynamic calculations
[BTN-95-EIX95152582315] p 264 A95-73518
Effect of underwing frost on a transport aircraft airfoil at flight Reynolds number
[BTN-95-EIX95152582334] p 276 A95-73536
Aircraft accident report. Runway overrun following rejected takeoff. Continental Airlines flight 795, McDonnell Douglas MD-82, N18835, LaGuardia Airport, Flushing, NY, 2 March 1994
[PB95-910401] p 277 N95-23609

TAPERING

The use of cowl camber and taper to reduce rotor/stator interaction noise
[NASA-CR-195421] p 323 N95-22675

TARGETS

SEM representation of the early and late time fields scattered from wire targets
[BTN-94-EIX94381353142] p 306 A95-74496

TECHNOLOGY ASSESSMENT

Euler Technology Assessment program for preliminary aircraft design employing SPLITFLOW code with Cartesian unstructured grid method
[NASA-CR-4649] p 273 N95-22917
Euler technology assessment for preliminary aircraft design employing OVERFLOW code with multiblock structured-grid method
[NASA-CR-4651] p 273 N95-23095
Motor drive technologies for the power-by-wire (PBW) program: Options, trends and tradeoffs
[NASA-TM-106885] p 295 N95-23671
Report to the Secretary of Defense. Unmanned aerial vehicles: No more Hunter systems should be bought until problems are fixed
[GAO/NSIAD-95-52] p 286 N95-24091

TECHNOLOGY TRANSFER

Technology reinvestment project's focus area: Affordable polymer matrix composites for airframe structures
[PB95-136032] p 324 N95-23168
Research and Technology, 1994
[NASA-TM-106764] p 262 N95-24025

TECHNOLOGY UTILIZATION

ATE enabling technologies
[BTN-95-EIX95172595294] p 287 A95-75718
Technology reinvestment project's focus area: Affordable polymer matrix composites for airframe structures
[PB95-136032] p 324 N95-23168

TEMPERATE REGIONS

In situ observations in aircraft exhaust plumes in the lower stratosphere at midlatitudes
[HTN-95-A0862] p 318 A95-76266

TENSILE CREEP

Evolution of oxidation and creep damage mechanisms in HIPed silicon nitride materials
[DE95-001360] p 300 N95-22689

TENSILE STRENGTH

Review of some results of the author's fatigue investigations with applications in engineering and material science
[TAE-698] p 316 N95-23662

TEST CHAMBERS

Design of a variable area diffuser for a 15-inch Mach 6 open-jet tunnel
p 297 N95-23309

TEST FACILITIES

Labs behind Boeing's new 777
[BTN-95-EIX95142562403] p 280 A95-73437
NASA low-speed axial compressor for fundamental research
[NASA-TM-4635] p 296 N95-23192
System identification of the Large-Angle Magnetic Suspension Test Fixture (LAMSTF)
p 296 N95-23299

TEXTILES

Development and verification of a resin film infusion/resin transfer molding simulation model for fabrication of advanced textile composites
[NASA-CR-197439] p 301 N95-23179

THERMAL MAPPING

AVIRIS and TIMS data processing and distribution at the land processes distributed active archive center
p 325 N95-23872

THEODORESEN TRANSFORMATION

Flutter analysis of composite box beams
[NASA-CR-197931] p 294 N95-23392

THERMAL ANALYSIS

Effect of curvature in the numerical simulation of an electrothermal de-icer pad
[BTN-95-EIX95182619219] p 276 A95-76645

THERMAL CONTROL COATINGS

Evaluation of thermal barrier and PS-200 self-lubricating coatings in an air-cooled rotary engine
[NASA-CR-195445] p 289 N95-23222

THERMAL CYCLING TESTS

Fatigue strength of high-temperature alloys under conditions of cyclic temperature variation. Communication 1: Experimental procedure and results
[BTN-94-EIX94401363884] p 307 A95-75516

THERMAL EMISSION

AVIRIS and TIMS data processing and distribution at the land processes distributed active archive center
p 325 N95-23872

THERMAL ENVIRONMENTS

Thermal force modeling for global positioning system satellites using the finite element method
[BTN-95-EIX95152583270] p 278 A95-73571

THERMAL FATIGUE

Fatigue strength of high-temperature alloys under conditions of cyclic temperature variation. Communication 1: Experimental procedure and results
[BTN-94-EIX94401363884] p 307 A95-75516

THERMAL PROTECTION

Minimum-mass design of sandwich aerobrakes for a lunar transfer vehicle
[BTN-95-EIX9512645707] p 299 A95-76759

THERMAL RADIATION

Thermal force modeling for global positioning system satellites using the finite element method
[BTN-95-EIX95152583270] p 278 A95-73571

THERMAL STRESSES

Minimum-mass design of sandwich aerobrakes for a lunar transfer vehicle
[BTN-95-EIX9512645707] p 299 A95-76759

THERMOSPHERE

Calculation of satellite drag coefficients
[AD-A285118] p 300 N95-23781

THIN WINGS

Static aeroelastic characteristics of a composite wing
[BTN-95-EIX95152582340] p 282 A95-73542
Unsteady ground effects on aerodynamic coefficients of finite wings with camber
[BTN-95-EIX95182619233] p 271 A95-76659
Thin tailored composite wing for civil tiltrotor
p 285 N95-23317

THREE DIMENSIONAL FLOW

Effects of spatial order of accuracy on the computation of vortical flowfields
[BTN-95-EIX95152577604] p 305 A95-73479
Influence of streamwise curvature on longitudinal vortices imbedded in turbulent boundary layers
[BTN-94-EIX94401378820] p 307 A95-76489
Comparison of linear stability results with flight transition data
[BTN-95-EIX95182619097] p 283 A95-76582
Neural network prediction of three-dimensional unsteady separated flowfields
[BTN-95-EIX95182619232] p 308 A95-76658
Unsteady ground effects on aerodynamic coefficients of finite wings with camber
[BTN-95-EIX95182619233] p 271 A95-76659
Study of the droplet spray characteristics of a subsonic wind tunnel
[BTN-95-EIX95182619235] p 271 A95-76661
Simulation on the 3-D turbulent flow in the passages of finocyl grain
[BTN-95-EIX95202638962] p 279 A95-76674
Mach 10 computational study of a three-dimensional scramjet inlet flow field
[NASA-TM-4602] p 309 N95-23015
Mach 10 computational study of a three-dimensional scramjet inlet flow field
[NASA-TM-4602] p 310 N95-23210
Holographic interferometric tomography for reconstructing flow fields
p 310 N95-23287
Three-dimensional unsteady flow calculations in an advanced gas generator turbine
p 312 N95-23425
Phase 2: HGM air flow tests in support of HEX vane investigation
p 312 N95-23438

THREE DIMENSIONAL MODELS

- Three-dimensional structure of a supersonic jet impinging on an inclined plate
[BTN-95-EIX95152583259] p 267 A95-73560
- Neural network prediction of three-dimensional unsteady separated flowfields
[BTN-95-EIX95182619232] p 308 A95-76658

THREE DIMENSIONAL MOTION

- Preconditioned domain decomposition scheme for three-dimensional aerodynamic sensitivity analysis
[BTN-95-EIX95152577612] p 321 A95-73471

THROATS

- Design of a variable area diffuser for a 15-inch Mach 6 open-jet tunnel p 297 N95-23309

THRUST CONTROL

- Analytical solution for controls, heats, and states of flight trajectories
[BTN-95-EIX95152583286] p 282 A95-73587

THUNDERSTORMS

- Thundercloud electric field modeling for the ionosphere-Earth region. 1: Dependence on cloud charge distribution
[HTN-95-41223] p 317 A95-75035
- Collaborative research on aircraft icing and charging processes in ice
[AD-A285102] p 276 N95-23201

TIME DEPENDENCE

- Grid refinement test of time-periodic flows over bluff bodies
[BTN-94-EIX94401378822] p 307 A95-76491

TIME LAG

- Investigation of the effects of bandwidth and time delay on helicopter roll-axis handling qualities
[HTN-95-80853] p 290 A95-75095

TIME OF FLIGHT SPECTROMETERS

- Time-of-flight mass spectrometer for impulse facilities
[BTN-95-EIX95142553057] p 262 A95-73441

TIME SERIES ANALYSIS

- The role of flight progress strips in en route air traffic control: A time-series analysis
[DOT/FAA/AM-95/4] p 280 N95-23565

TOMOGRAPHY

- Evaluation of neutron techniques for illicit substance detection
[DE95-002988] p 300 N95-22764

TOPOGRAPHY

- Geoid lineations of 1000 km wavelength over the central Pacific
[HTN-95-11304] p 319 A95-77009
- AVIRIS and TIMS data processing and distribution at the land processes distributed active archive center p 325 N95-23872

TOPOLOGY

- CFD analysis of turbopump volutes p 312 N95-23436

TORSION

- Nonlinear angle of twist of advanced composite wing boxes under pure torsion
[BTN-95-EIX95152582323] p 281 A95-73526

TORSIONAL VIBRATION

- Application of Navier-Stokes aeroelastic methods to improve fighter wing maneuver performance
[BTN-95-EIX95182619218] p 284 A95-76644

TOXICITY

- Modeling aerosol emissions from the combustion of composite materials p 301 N95-23038
- Aircraft fires, smoke toxicity, and survival: An overview
[DOT/FAA/AM-95/8] p 277 N95-24024

TRACKING (POSITION)

- Solutions of generalized proportional navigation with maneuvering and nonmaneuvering targets
[BTN-95-EIX95202637606] p 279 A95-76683

TRAILING EDGE FLAPS

- Natural laminar flow wing concept for supersonic transports
[BTN-95-EIX95182619226] p 308 A95-76652
- Wing pressure distributions from subsonic tests of a high-wing transport model --- in the Langley 14-by 22-Foot Subsonic Wind Tunnel
[NASA-TM-4583] p 272 N95-22802

TRAILING EDGES

- Computation of the poststall behavior of a circulation controlled airfoil
[BTN-95-EIX95152582320] p 264 A95-73523
- Lift enhancing tabs for airfoils
[NASA-CASE-ARC-11990-1] p 286 N95-23395

TRAINING DEVICES

- Virtual reality flight control display with six-degree-of-freedom controller and spherical orientation overlay
[NASA-CASE-NPO-18733-1-CU] p 288 N95-22578
- Development of qualification guidelines for personal computer-based aviation training devices
[DOT/FAA/AM-95/6] p 323 N95-23603

TRAJECTORIES

- Functional dependence of trajectory dispersion on initial condition errors
[BTN-95-EIX95152583263] p 298 A95-73564

TRAJECTORY ANALYSIS

- Trajectory modeling of emissions from lower stratospheric aircraft
[HTN-95-41219] p 317 A95-75031
- Functional agility metrics and optimal trajectory analysis
[BTN-95-EIX95182619121] p 321 A95-76598
- Analytical solution and parameter estimation of projectile dynamics
[BTN-95-EIX95212645695] p 272 A95-76747

TRAJECTORY CONTROL

- Dynamical instability of the aerogravity assist maneuver
[BTN-95-EIX95152583282] p 298 A95-73583
- Analytical solution for controls, heats, and states of flight trajectories
[BTN-95-EIX95152583286] p 282 A95-73587
- Functional agility metrics and optimal trajectory analysis
[BTN-95-EIX95182619121] p 321 A95-76598
- Nonlinear system guidance in the presence of transmission zero dynamics
[NASA-TM-4661] p 309 N95-22804

TRAJECTORY OPTIMIZATION

- Analytical solution for controls, heats, and states of flight trajectories
[BTN-95-EIX95152583286] p 282 A95-73587
- Optimal lateral-escape maneuvers for microburst encounters during final approach
[BTN-95-EIX95182619127] p 276 A95-76604

TRANSFER FUNCTIONS

- On-line, adaptive state estimator for active noise control p 322 N95-23308

TRANSIENT RESPONSE

- Transient analysis of a cracked rotor passing through critical speed
[BTN-94-EIX94401360022] p 306 A95-74702

TRANSITION FLOW

- Computation of oscillating airfoil flows with one- and two-equation turbulence models
[BTN-95-EIX95152577588] p 263 A95-73494
- Crossflow instability control on a swept-wing: Preliminary studies p 274 N95-23283

TRANSITION TEMPERATURE

- Phonon characteristics of high (T sub c) superconductors from neutron Doppler broadening measurements
[DE95-003703] p 324 N95-24076

TRANSONIC FLOW

- Aerodynamic shape optimization using preconditioned conjugate gradient methods
[BTN-95-EIX95142553033] p 263 A95-73465
- Flow visualization studies on sidewall effects in two-dimensional transonic airfoil testing
[BTN-95-EIX95152582313] p 264 A95-73516
- Improved version of the Naval Surface Warfare Center aeroprediction code (AP93)
[BTN-95-EIX95152583260] p 267 A95-73561
- Turbulent transonic airfoil flow simulation using a pressure-based algorithm
[BTN-95-EIX95182619078] p 269 A95-75763
- Scaling of incipient separation in supersonic/transonic speed laminar flows
[BTN-95-EIX95182619104] p 269 A95-76589

TRANSONIC FLUTTER

- Limit cycle phenomena in computational transonic aeroelasticity
[BTN-95-EIX95152582317] p 264 A95-73520
- Application of transonic small disturbance theory to the active flexible wing model
[BTN-95-EIX95182619210] p 270 A95-76636
- Rolling maneuver load alleviation using active controls
[BTN-95-EIX95182619217] p 270 A95-76643

TRANSONIC WIND TUNNELS

- Performance of the 0.3-meter transonic cryogenic tunnel with air, nitrogen, and sulfur hexafluoride media under closed loop automatic control
[NASA-CR-195052] p 310 N95-23257
- Three-dimensional Navier-Stokes analysis and redesign of an imbedded bellmouth nozzle in a turbine cascade inlet section p 311 N95-23423

TRANSPORT AIRCRAFT

- Design constraints in the payload-range diagram of ultrahigh capacity transport airplanes
[BTN-95-EIX95152582319] p 276 A95-73522
- Effect of underwing frost on a transport aircraft airfoil at flight Reynolds number
[BTN-95-EIX95152582334] p 276 A95-73536
- Possible effects of CO₂ increase on the high-speed civil transport impact on ozone
[HTN-95-60779] p 317 A95-75976

- Wing pressure distributions from subsonic tests of a high-wing transport model --- in the Langley 14-by 22-Foot Subsonic Wind Tunnel
[NASA-TM-4583] p 272 N95-22802

- Handling qualities of the High Speed Civil Transport p 294 N95-23325

- High-lift flow-physics flight experiments on a subsonic civil transport aircraft (B737-100) p 275 N95-23333

TRANSVERSE OSCILLATION

- Coupled FEM-BEM approach for mean flow effects on vibro-acoustic behavior of planar structures
[BTN-95-EIX95152577587] p 263 A95-73495

TROPOSPHERE

- Compendium of NASA data base for the Global Tropospheric Experiment's Pacific Exploratory Mission West-A (PEM West-A)
[NASA-TM-109177] p 320 N95-23009

TURBINE BLADES

- Fatigue strength of high-temperature alloys under conditions of cyclic temperature variation. Communication 1: Experimental procedure and results
[BTN-94-EIX94401363884] p 307 A95-75516
- Supersonic flow and shock formation in turbine tip gaps p 312 N95-23429

TURBINE ENGINES

- Erosion of dust-filtered helicopter turbine engines. Part 1: Basic theoretical considerations
[BTN-95-EIX95182619222] p 288 A95-76648

- Life prediction of helicopter engines fitted with dust filters
[BTN-95-EIX95182619224] p 289 A95-76650

TURBINE PUMPS

- CFD analysis of turbopump volutes p 312 N95-23436
- Phase 2: HGM air flow tests in support of HEX vane investigation p 312 N95-23438

TURBINES

- Static pressure distribution in the inlet of a helicopter turbine compressor
[BTN-95-EIX95152582339] p 266 A95-73541
- Three-dimensional unsteady flow calculations in an advanced gas generator turbine p 312 N95-23425
- Aerodynamic design and analysis of a highly loaded turbine exhaust p 312 N95-23435
- CFD analysis of turbopump volutes p 312 N95-23436

- Numerical computation of aerodynamics and heat transfer in a turbine cascade and a turn-around duct using advanced turbulence models p 313 N95-23444
- Enhanced analysis and users manual for radial-inflow turbine conceptual design code RTD
[NASA-CR-195454] p 275 N95-23462

TURBOCOMPRESSORS

- NASA low-speed axial compressor for fundamental research
[NASA-TM-4635] p 296 N95-23192

TURBOFAN ENGINES

- Lycoming to test new engine core
[HTN-95-41393] p 288 A95-76389
- Derivation of system matrices from nonlinear dynamic simulation of jet engines
[BTN-95-EIX95182619139] p 288 A95-76616

TURBOJET ENGINE CONTROL

- Derivation of system matrices from nonlinear dynamic simulation of jet engines
[BTN-95-EIX95182619139] p 288 A95-76616

TURBOPROP ENGINES

- Artificial intelligence for turboprop engine maintenance
[BTN-95-EIX95182617812] p 288 A95-75757
- Lycoming to test new engine core
[HTN-95-41393] p 288 A95-76389

TURBOSHAPTS

- Lycoming to test new engine core
[HTN-95-41393] p 288 A95-76389

TURBULENCE

- Navier-Stokes prediction of large-amplitude delta-wing roll oscillations
[BTN-95-EIX95152582329] p 281 A95-73531
- Flow study of supersonic wing-nacelle configuration
[BTN-95-EIX95152582344] p 266 A95-73546
- Observations on using experimental data as boundary conditions for computations
[BTN-95-EIX95182619103] p 321 A95-76588
- Response of a nonrotating rotor blade to lateral turbulence. Part 1: Theory
[BTN-95-EIX95182619228] p 284 A95-76654

TURBULENCE EFFECTS

- Effect of ambient turbulence intensity on sphere wakes at intermediate Reynolds numbers
[BTN-95-EIX95182619101] p 308 A95-76586

TURBULENCE MODELS

- Two-equation turbulence model for unsteady separated flows around airfoils
[BTN-95-EIX95142553054] p 262 A95-73444

- Flow structure in the wake of a wishbone vortex generator
[BTN-95-EIX95142553044] p 304 A95-73454
Adaptive finite element method for turbulent flow near a propeller
[BTN-95-EIX95142553038] p 305 A95-73460
Laplace interaction law for the computation of viscous airfoil flow in low- and high-speed aerodynamics
[BTN-95-EIX95142553037] p 263 A95-73461
Computation of oscillating airfoil flows with one- and two-equation turbulence models
[BTN-95-EIX95152577588] p 263 A95-73494
Progress in high-lift aerodynamic calculations
[BTN-95-EIX95152582315] p 264 A95-73518
Computation of the poststall behavior of a circulation controlled airfoil
[BTN-95-EIX95152582320] p 264 A95-73523
Transport of exhaust products in the near trail of a jet engine under atmospheric conditions
[HTN-95-91421] p 319 A95-77334
Numerical computation of aerodynamics and heat transfer in a turbine cascade and a turn-around duct using advanced turbulence models p 313 A95-23444
- TURBULENT BOUNDARY LAYER**
Flow structure in the wake of a wishbone vortex generator
[BTN-95-EIX95142553044] p 304 A95-73454
Effects of expansions on a supersonic boundary layer: Surface pressure measurements
[BTN-95-EIX95142553036] p 263 A95-73462
Influence of streamwise curvature on longitudinal vortices imbedded in turbulent boundary layers
[BTN-94-EIX94401378820] p 307 A95-76489
Review and development of base pressure and base heating correlations in supersonic flow
[BTN-95-EIX95212645688] p 271 A95-76740
- TURBULENT DIFFUSION**
Transport of exhaust products in the near trail of a jet engine under atmospheric conditions
[HTN-95-91421] p 319 A95-77334
- TURBULENT FLOW**
Two-equation turbulence model for unsteady separated flows around airfoils
[BTN-95-EIX95142553054] p 262 A95-73444
Flow structure in the wake of a wishbone vortex generator
[BTN-95-EIX95142553044] p 304 A95-73454
Simulation of turbulent fluctuations
[BTN-95-EIX95142553041] p 304 A95-73457
Adaptive finite element method for turbulent flow near a propeller
[BTN-95-EIX95142553038] p 305 A95-73460
Laplace interaction law for the computation of viscous airfoil flow in low- and high-speed aerodynamics
[BTN-95-EIX95142553037] p 263 A95-73461
Effects of expansions on a supersonic boundary layer: Surface pressure measurements
[BTN-95-EIX95142553036] p 263 A95-73462
Computation of oscillating airfoil flows with one- and two-equation turbulence models
[BTN-95-EIX95152577588] p 263 A95-73494
Mach wave emission from a high-temperature supersonic jet
[BTN-95-EIX95152577586] p 264 A95-73496
Base drag prediction on missile configurations
[BTN-95-EIX95152583256] p 266 A95-73557
Turbulent transonic airfoil flow simulation using a pressure-based algorithm
[BTN-95-EIX95182619078] p 269 A95-75763
Simulation of transverse gas injection in turbulent supersonic air flows
[BTN-95-EIX95182619080] p 269 A95-75765
Multigrid solution of compressible turbulent flow on unstructured meshes using a two-equation model
[BTN-94-EIX94401378794] p 307 A95-76484
Influence of streamwise curvature on longitudinal vortices imbedded in turbulent boundary layers
[BTN-94-EIX94401378820] p 307 A95-76489
Effect of ambient turbulence intensity on sphere wakes at intermediate Reynolds numbers
[BTN-95-EIX95182619101] p 308 A95-76586
Real-time estimation of atmospheric turbulence severity from in-situ aircraft measurements
[BTN-95-EIX95182619231] p 319 A95-76657
Simulation on the 3-D turbulent flow in the passages of finocyl grain
[BTN-95-EIX95202638962] p 279 A95-76674
Crossflow instability control on a swept-wing: Preliminary studies p 274 A95-23283
High-lift flow-physics flight experiments on a subsonic civil transport aircraft (B737-100) p 275 A95-23333
Numerical computation of aerodynamics and heat transfer in a turbine cascade and a turn-around duct using advanced turbulence models p 313 A95-23444
- Convergence acceleration of implicit schemes in the presence of high aspect ratio grid cells p 313 A95-23446
- TURBULENT WAKES**
Flow structure in the wake of a wishbone vortex generator
[BTN-95-EIX95142553044] p 304 A95-73454
Adaptive finite element method for turbulent flow near a propeller
[BTN-95-EIX95142553038] p 305 A95-73460
- TURNING FLIGHT**
Efficient sensitivity analysis for rotary-wing aeromechanical problems
[BTN-95-EIX95152577585] p 264 A95-73497
Functional agility metrics and optimal trajectory analysis
[BTN-95-EIX95182619121] p 321 A95-76598
Optimal lateral-escape maneuvers for microburst encounters during final approach
[BTN-95-EIX95182619127] p 276 A95-76604
- TVD SCHEMES**
Three-dimensional structure of a supersonic jet impinging on an inclined plate
[BTN-95-EIX95152583259] p 267 A95-73560
- TWISTED WINGS**
Nonlinear angle of twist of advanced composite wing boxes under pure torsion
[BTN-95-EIX95152582323] p 281 A95-73526
- TWISTING**
Application of Navier-Stokes aeroelastic methods to improve fighter wing maneuver performance
[BTN-95-EIX95182619218] p 284 A95-76644
- TWO DIMENSIONAL BOUNDARY LAYER**
Influence of streamwise curvature on longitudinal vortices imbedded in turbulent boundary layers
[BTN-94-EIX94401378820] p 307 A95-76489
- TWO DIMENSIONAL FLOW**
Predicting exhaust plume boundaries with supersonic external flows
[BTN-95-EIX95152583258] p 297 A95-73559
Comparison of linear stability results with flight transition data
[BTN-95-EIX95182619097] p 283 A95-76582
Observations on using experimental data as boundary conditions for computations
[BTN-95-EIX95182619103] p 321 A95-76588
Study of the droplet spray characteristics of a subsonic wind tunnel
[BTN-95-EIX95182619235] p 271 A95-76661
User's guide for ECAP2D: An Euler unsteady aerodynamic and aeroelastic analysis program for two dimensional oscillating cascades, version 1.0
[NASA-CR-189146] p 316 A95-24189
- TWO DIMENSIONAL MODELS**
Predicting exhaust plume boundaries with supersonic external flows
[BTN-95-EIX95152583258] p 297 A95-73559
Sensitivity of two-dimensional model predictions of ozone response to stratospheric aircraft: An update
[HTN-95-A0863] p 318 A95-76267
Observations on using experimental data as boundary conditions for computations
[BTN-95-EIX95182619103] p 321 A95-76588
- TWO PHASE FLOW**
Simulation of transverse gas injection in turbulent supersonic air flows
[BTN-95-EIX95182619080] p 269 A95-75765
- UNIVERSITIES**
1994 NASA-HU American Society for Engineering Education (ASEE) Summer Faculty Fellowship Program
[NASA-CR-194972] p 325 A95-23276
- UNSTEADY AERODYNAMICS**
Neural network prediction of three-dimensional unsteady separated flowfields
[BTN-95-EIX95182619232] p 308 A95-76658
Unsteady ground effects on aerodynamic coefficients of finite wings with camber
[BTN-95-EIX95182619233] p 271 A95-76659
Flutter analysis of composite box beams
[NASA-CR-197931] p 294 A95-23392
User's guide for ECAP2D: An Euler unsteady aerodynamic and aeroelastic analysis program for two dimensional oscillating cascades, version 1.0
[NASA-CR-189146] p 316 A95-24189
- UNSTEADY FLOW**
Two-equation turbulence model for unsteady separated flows around airfoils
[BTN-95-EIX95142553054] p 262 A95-73444
Eigenanalysis of unsteady flows about airfoils, cascades, and wings
[BTN-95-EIX95152577597] p 305 A95-73486

- Computation of oscillating airfoil flows with one- and two-equation turbulence models
[BTN-95-EIX95152577588] p 263 A95-73494
Limit cycle phenomena in computational transonic aeroelasticity
[BTN-95-EIX95152582317] p 264 A95-73520
Moving wall effect in relation to other dynamic stall flow mechanisms
[BTN-95-EIX95152582324] p 265 A95-73527
Numerical study of sound generation due to a spinning vortex pair
[BTN-95-EIX95182619075] p 307 A95-75760
Viscous-inviscid interaction method for unsteady low-speed airfoil flows
[BTN-95-EIX95182619093] p 269 A95-75778
Stability derivatives of a flapped plate in unsteady ground effect
[BTN-95-EIX95182619225] p 270 A95-76651
Response of a nonrotating rotor blade to lateral turbulence. Part 1: Theory
[BTN-95-EIX95182619228] p 284 A95-76654
Neural network prediction of three-dimensional unsteady separated flowfields
[BTN-95-EIX95182619232] p 308 A95-76658
Unsteady ground effects on aerodynamic coefficients of finite wings with camber
[BTN-95-EIX95182619233] p 271 A95-76659
A CFD study of complex missile and store configurations in relative motion
[NASA-CR-197912] p 285 A95-22949
Holographic interferometric tomography for reconstructing flow fields
[BTN-95-EIX95182619232] p 310 A95-23287
Three-dimensional unsteady flow calculations in an advanced gas generator turbine
[BTN-95-EIX95182619233] p 312 A95-23425
Aerodynamic design and analysis of a highly loaded turbine exhaust
[BTN-95-EIX95182619233] p 312 A95-23435
A time-accurate finite volume method valid at all flow velocities p 314 A95-23447

UPPER ATMOSPHERE

- Particle kinetic simulation of high altitude hypervelocity flight
[NASA-CR-197383] p 309 A95-22481

UPWIND SCHEMES (MATHEMATICS)

- Application of the multigrid solution technique to hypersonic entry vehicles
[BTN-95-EIX95152583254] p 306 A95-73555

USER MANUALS (COMPUTER PROGRAMS)

- Enhanced analysis and users manual for radial-inflow turbine conceptual design code RTD
[NASA-CR-195454] p 275 A95-23462
User's guide for ECAP2D: An Euler unsteady aerodynamic and aeroelastic analysis program for two dimensional oscillating cascades, version 1.0
[NASA-CR-189146] p 316 A95-24189

USER REQUIREMENTS

- Real-time navigation using the global positioning system
[BTN-95-EIX95172595298] p 279 A95-75714

V**V-22 AIRCRAFT**

- Thin tailored composite wing for civil tiltrotor
p 285 A95-23317

VALVES

- Measurement of moisture and total hydrocarbon contributions by valves used in clean room gas-delivery systems
[BTN-94-EIX94381359041] p 295 A95-74629

VANES

- Phase 2: HGM air flow tests in support of HEX vane investigation p 312 A95-23438

VAPORS

- NTS-spill test facility wind tunnel exhaust plume characterization
[DE95-003630] p 297 A95-24019

VARIATIONS

- Simulation of turbulent fluctuations
[BTN-95-EIX95142553041] p 304 A95-73457

VELOCITY

- A comparison of some aerodynamic resistance methods using measurements over cotton and grass from the 1991 California ozone deposition experiment
[HTN-95-11295] p 319 A95-77000

VELOCITY DISTRIBUTION

- Determination of wall boundary conditions for high-speed-ratio direct simulation Monte Carlo calculations
[BTN-95-EIX95182617457] p 267 A95-75728

VELOCITY MEASUREMENT

- Impeller flow field characterization with a laser two-focus velocimeter p 313 A95-23440

VERTICAL DISTRIBUTION

- Sensitivity of two-dimensional model predictions of ozone response to stratospheric aircraft: An update
[HTN-95-A0863] p 318 A95-76267

VERTICAL LANDING

- Flow visualization studies of VTOL aircraft models during Hover in ground effect
[NASA-TM-108860] p 272 N95-22666

VERTICAL TAKEOFF

- Flow visualization studies of VTOL aircraft models during Hover in ground effect
[NASA-TM-108860] p 272 N95-22666

VERTICAL TAKEOFF AIRCRAFT

- Cypher moves toward autonomous flight
[HTN-95-41394] p 283 A95-76390
- Flow visualization studies of VTOL aircraft models during Hover in ground effect
[NASA-TM-108860] p 272 N95-22666

VIBRATION DAMPING

- Multirate flutter suppression system design for a model wing
[BTN-95-EIX95182619132] p 292 A95-76609
- Summary of an active flexible wing program
[BTN-95-EIX95182619209] p 283 A95-76635
- Multiple-function digital controller system for active flexible wing wind-tunnel model
[BTN-95-EIX95182619212] p 322 A95-76638
- Flutter suppression control law design and testing for the active flexible wing
[BTN-95-EIX95182619214] p 292 A95-76640
- Design and multifunction tests of a frequency domain-based active flutter suppression system
[BTN-95-EIX95182619215] p 292 A95-76641
- Flutter suppression for the active flexible wing: A classical design
[BTN-95-EIX95182619216] p 292 A95-76642
- Active control of panel vibrations induced by a boundary layer flow
[NASA-CR-197867] p 273 N95-23182

VIBRATION MODE

- Application of Navier-Stokes aeroelastic methods to improve lighter wing maneuver performance
[BTN-95-EIX95182619218] p 284 A95-76644

VIKING LANDER SPACECRAFT

- Fourth-generation Mars vehicle concepts
[BTN-95-EIX95152583267] p 298 A95-73568

VIRTUAL REALITY

- Virtual reality flight control display with six-degree-of-freedom controller and spherical orientation overlay
[NASA-CASE-NPO-18733-1-CU] p 288 N95-22578

VISCOSITY

- Development and verification of a resin film infusion/resin transfer molding simulation model for fabrication of advanced textile composites
[NASA-CR-197439] p 301 N95-23179

VISCOS FLOW

- Laplace interaction law for the computation of viscous airflow flow in low- and high-speed aerodynamics
[BTN-95-EIX95142553037] p 263 A95-73461
- Aerodynamic characteristics of a hypersonic viscous optimized waverider at high altitudes
[BTN-95-EIX95152583251] p 266 A95-73552
- Higher-order viscous shock-layer solutions for high-altitude flows
[BTN-95-EIX95152583255] p 306 A95-73556
- Viscous-inviscid interaction method for unsteady low-speed airflow flows
[BTN-95-EIX95182619093] p 269 A95-75778
- CFD optimization of a theoretical minimum-drag body
[BTN-95-EIX95182619234] p 308 A95-76660
- An assessment of viscous effects in computational simulation of benign and burst vortex flows on generic fighter wind-tunnel models using TEAM code
[NASA-CR-4650] p 273 N95-23185

VISUAL SIGNALS

- Cueing light configuration for aircraft navigation
[NASA-CASE-ARC-11982-1] p 280 N95-23393

VORTEX BREAKDOWN

- Transient structure of vortex breakdown on a delta wing
[BTN-95-EIX95182619073] p 268 A95-75758

VORTEX GENERATORS

- Flow structure in the wake of a wishbone vortex generator
[BTN-95-EIX95142553044] p 304 A95-73454
- Separation control on high-lift airfoils via micro-vortex generators
[BTN-95-EIX95152582326] p 265 A95-73529

VORTEX LATTICE METHOD

- Sidewash on the vertical tail in subsonic and supersonic flows
[BTN-95-EIX95152582316] p 264 A95-73519
- Static aeroelastic characteristics of a composite wing
[BTN-95-EIX95152582340] p 282 A95-73542

VORTICES

- Flow structure in the wake of a wishbone vortex generator
[BTN-95-EIX95142553044] p 304 A95-73454
- Effects of spatial order of accuracy on the computation of vortical flowfields
[BTN-95-EIX95152577604] p 305 A95-73479
- Experimental investigation of the flowfield about an upswept afterbody
[BTN-95-EIX95152582321] p 265 A95-73524
- Navier-Stokes prediction of large-amplitude delta-wing roll oscillations
[BTN-95-EIX95152582329] p 281 A95-73531
- Forebody flow control on a full-scale F/A-18 aircraft
[BTN-95-EIX95152582333] p 281 A95-73535
- Pneumatic concept for tip-stall control of cranked-arrow wings
[BTN-95-EIX95152582335] p 281 A95-73537
- Effect of leeward flow dividers on the wing rock of a delta wing
[BTN-95-EIX95152582347] p 282 A95-73549
- Transient structure of vortex breakdown on a delta wing
[BTN-95-EIX95182619073] p 268 A95-75758
- Numerical study of sound generation due to a spinning vortex pair
[BTN-95-EIX95182619075] p 307 A95-75760
- Diurnal variation of lee vortices in Taiwan and the surrounding area
[HTN-95-91363] p 318 A95-76394
- Influence of streamwise curvature on longitudinal vortices imbedded in turbulent boundary layers
[BTN-94-EIX94401378820] p 307 A95-76489
- Euler technology assessment for preliminary aircraft design employing OVERFLOW code with multiblock structured-grid method
[NASA-CR-4651] p 273 N95-23095
- An assessment of viscous effects in computational simulation of benign and burst vortex flows on generic fighter wind-tunnel models using TEAM code
[NASA-CR-4650] p 273 N95-23185
- Crossflow instability control on a swept-wing: Preliminary studies
[BTN-95-EIX95152582326] p 274 N95-23283
- Preliminary identification of buffet problems in high speed civil transport
[NASA-CASE-ARC-11979-1] p 286 N95-23390
- Aerodynamic surface distension system for high angle of attack forebody vortex control
[NASA-CASE-ARC-11979-1] p 286 N95-23390
- Three-dimensional Navier-Stokes analysis and redesign of an imbedded bellmouth nozzle in a turbine cascade inlet section
[BTN-95-EIX95182619127] p 311 N95-23423
- A study of the vortex flow over 76/40-deg double-delta wing
[NASA-CR-195032] p 314 N95-23466

VULNERABILITY

- Rationale for the Modular Air-system Vulnerability Estimation Network (MAVEN) methodology
[AD-A285797] p 284 N95-22510

W

WAKES

- Experimental investigation of the flowfield about an upswept afterbody
[BTN-95-EIX95152582321] p 265 A95-73524
- Separation control on high-lift airfoils via micro-vortex generators
[BTN-95-EIX95152582326] p 265 A95-73529
- Hypersonic rarefied flow past spheres including wake structure
[BTN-95-EIX951525823250] p 305 A95-73551

WALL FLOW

- Main features of overexpanded triple jets
[BTN-95-EIX95142553040] p 304 A95-73458
- Effects of expansions on a supersonic boundary layer: Surface pressure measurements
[BTN-95-EIX95142553036] p 263 A95-73462
- Flow visualization studies on sidewall effects in two-dimensional transonic airflow testing
[BTN-95-EIX95152582313] p 264 A95-73516
- Moving wall effect in relation to other dynamic stall flow mechanisms
[BTN-95-EIX95152582324] p 265 A95-73527
- Application of wall functions to generalized nonorthogonal curvilinear coordinate systems
[BTN-95-EIX95182619077] p 307 A95-75762
- Observations on using experimental data as boundary conditions for computations
[BTN-95-EIX95182619103] p 321 A95-76588
- A wall interference assessment/correction system
[NASA-CR-197421] p 309 N95-23183

WALL PRESSURE

- A wall interference assessment/correction system
[NASA-CR-197421] p 309 N95-23183

WATER

- Study of the droplet spray characteristics of a subsonic wind tunnel
[BTN-95-EIX95182619235] p 271 A95-76661
- Airborne rotary air separator study
[NASA-CR-189099] p 290 N95-24053

WATER TABLES

- Simple method of supersonic flow visualization using water table
[BTN-95-EIX95182619105] p 269 A95-76590

WAVE SCATTERING

- SEM representation of the early and late time fields scattered from wire targets
[BTN-94-EIX94381353142] p 306 A95-74496

WAVELENGTHS

- Geoid lineations of 1000 km wavelength over the central Pacific
[HTN-95-11304] p 319 A95-77009

WAVERIDERS

- Aerodynamic characteristics of a hypersonic viscous optimized waverider at high altitudes
[BTN-95-EIX95152583251] p 266 A95-73552
- Integrated design of hypersonic waveriders including inlets and tailfins
[BTN-95-EIX95212645692] p 271 A95-76744

WEAPON SYSTEMS

- Improved version of the Naval Surface Warfare Center aeroprediction code (AP93)
[BTN-95-EIX95152583260] p 267 A95-73561

WEAR TESTS

- Evaluation of thermal barrier and PS-200 self-lubricating coatings in an air-cooled rotary engine
[NASA-CR-195445] p 289 N95-23222

WEATHER FORECASTING

- Pilot Weather Advisor system
[BTN-95-EIX95152582314] p 316 A95-73517

WEIGHT REDUCTION

- Minimum-mass design of sandwich aerobrakes for a lunar transfer vehicle
[BTN-95-EIX95212645707] p 299 A95-76759

WEIGHTING FUNCTIONS

- On-line, adaptive state estimator for active noise control
[BTN-95-EIX95152582314] p 322 N95-23308

WENTZEL-KRAMER-BRILLOUIN METHOD

- Analytical study of the neutral stability of a model hypersonic boundary layer
[BTN-95-EIX95152577589] p 263 A95-73493

WIND SHEAR

- Optimal lateral-escape maneuvers for microburst encounters during final approach
[BTN-95-EIX95182619127] p 276 A95-76604
- Maximum-likelihood spectral estimation and adaptive filtering techniques with application to airborne Doppler weather radar
[NASA-CR-197699] p 316 N95-23670

WIND TUNNEL APPARATUS

- Time-of-flight mass spectrometer for impulse facilities
[BTN-95-EIX95142553057] p 262 A95-73441

WIND TUNNEL MODELS

- Application of transonic small disturbance theory to the active flexible wing model
[BTN-95-EIX95182619210] p 270 A95-76636
- Multiple-function digital controller system for active flexible wing wind-tunnel model
[BTN-95-EIX95182619212] p 322 A95-76638
- Flutter suppression control law design and testing for the active flexible wing
[BTN-95-EIX95182619214] p 292 A95-76640
- Design and multifunction tests of a frequency domain-based active flutter suppression system
[BTN-95-EIX95182619215] p 292 A95-76641
- Flutter suppression for the active flexible wing: A classical design
[BTN-95-EIX95182619216] p 292 A95-76642
- Dynamic response tests of inertial and optical wind-tunnel model attitude measurement devices
[NASA-TM-109182] p 296 N95-23011

WIND TUNNEL NOZZLES

- Optimized design of a hypersonic nozzle
[BTN-95-EIX95182619210] p 297 N95-23304
- Three-dimensional Navier-Stokes analysis and redesign of an imbedded bellmouth nozzle in a turbine cascade inlet section
[BTN-95-EIX95182619127] p 311 N95-23423
- Supersonic laminar flow control research
[NASA-CR-197938] p 275 N95-23669

WIND TUNNEL TESTS

- Main features of overexpanded triple jets
[BTN-95-EIX95142553040] p 304 A95-73458
- Separation control on high-lift airfoils via micro-vortex generators
[BTN-95-EIX95152582326] p 265 A95-73529
- Analysis of a higher harmonic control test to reduce blade vortex interaction noise
[BTN-95-EIX95152582330] p 265 A95-73532
- Forebody flow control on a full-scale F/A-18 aircraft
[BTN-95-EIX95152582333] p 281 A95-73535

- Effect of underwing frost on a transport aircraft airfoil at flight Reynolds number
[BTN-95-EIX95152582334] p 276 A95-73536
- Pneumatic concept for tip-stall control of cranked-arrow wings
[BTN-95-EIX95152582335] p 281 A95-73537
- Flow study of supersonic wing-nacelle configuration
[BTN-95-EIX95152582344] p 266 A95-73546
- Computational study of plume-induced separation on a hypersonic powered model
[BTN-95-EIX95152582346] p 266 A95-73548
- Base drag prediction on missile configurations
[BTN-95-EIX95152583256] p 266 A95-73557
- Aerodynamic characteristics of a canard-controlled missile at high angles of attack
[BTN-95-EIX95152583257] p 267 A95-73558
- Some aspects of the aerodynamics of separating strap-ons
[BTN-95-EIX95182617464] p 298 A95-75735
- Comparison of linear stability results with flight transition data
[BTN-95-EIX95182619097] p 283 A95-76582
- Effect of ambient turbulence intensity on sphere wakes at intermediate Reynolds numbers
[BTN-95-EIX95182619101] p 308 A95-76586
- Observations on using experimental data as boundary conditions for computations
[BTN-95-EIX95182619103] p 321 A95-76588
- Simulation and model reduction for the active flexible wing program
[BTN-95-EIX95182619211] p 295 A95-76637
- On-line analysis capabilities developed to support the active flexible wing wind-tunnel tests
[BTN-95-EIX95182619213] p 296 A95-76639
- Flutter suppression control law design and testing for the active flexible wing
[BTN-95-EIX95182619214] p 292 A95-76640
- Design and multifunction tests of a frequency domain-based active flutter suppression system
[BTN-95-EIX95182619215] p 292 A95-76641
- Flutter suppression for the active flexible wing: A classical design
[BTN-95-EIX95182619216] p 292 A95-76642
- Rolling maneuver load alleviation using active controls
[BTN-95-EIX95182619217] p 270 A95-76643
- Dynamic investigation of the angular motion of a rotating body-parachute system
[BTN-95-EIX95182619220] p 270 A95-76646
- Natural laminar flow wing concept for supersonic transports
[BTN-95-EIX95182619226] p 308 A95-76652
- Aerodynamic characteristics of external store configurations at low speeds
[BTN-95-EIX95182619230] p 271 A95-76656
- Study of the droplet spray characteristics of a subsonic wind tunnel
[BTN-95-EIX95182619235] p 271 A95-76661
- Laser velocimetry seed-particle behavior in shear layers at Mach 12
[BTN-95-EIX95212645712] p 272 A95-76764
- Wing pressure distributions from subsonic tests of a high-wing transport model --- in the Langley 14- by 22-Foot Subsonic Wind Tunnel
[NASA-TM-4583] p 272 N95-22802
- Dynamic response tests of inertial and optical wind-tunnel model attitude measurement devices
[NASA-TM-109182] p 296 N95-23011
- Experimental results for a hypersonic nozzle/afterbody flow field
[NASA-TM-4638] p 274 N95-23250
- Performance of the 0.3-meter transonic cryogenic tunnel with air, nitrogen, and sulfur hexafluoride media under closed loop automatic control
[NASA-CR-195052] p 310 N95-23257
- Crossflow instability control on a swept-wing: Preliminary studies
[NASA-CR-195052] p 274 N95-23283
- Preliminary identification of buffet problems in high speed civil transport
[NASA-CR-195052] p 294 N95-23319
- A study of the vortex flow over 76/40-deg double-delta wing
[NASA-CR-195032] p 314 N95-23466
- WIND TUNNEL WALLS**
A wall interference assessment/correction system
[NASA-CR-197421] p 309 N95-23183
- WIND TUNNELS**
NTS-spill test facility wind tunnel exhaust plume characterization
[DE95-003630] p 297 N95-24019
- WIND VELOCITY**
NTS-spill test facility wind tunnel exhaust plume characterization
[DE95-003630] p 297 N95-24019
- WING FLAPS**
Stability derivatives of a flapped plate in unsteady ground effect
[BTN-95-EIX95182619225] p 270 A95-76651

WING LOADING

- Summary of an active flexible wing program
[BTN-95-EIX95182619209] p 283 A95-76635
- Multiple-function digital controller system for active flexible wing wind-tunnel model
[BTN-95-EIX95182619212] p 322 A95-76638
- Rolling maneuver load alleviation using active controls
[BTN-95-EIX95182619217] p 270 A95-76643
- Aerodynamics of a finite wing with simulated ice
[BTN-95-EIX95182619227] p 270 A95-76653
- WING NACELLE CONFIGURATIONS**
Flow study of supersonic wing-nacelle configuration
[BTN-95-EIX95152582344] p 266 A95-73546

WINGS

- Eigenanalysis of unsteady flows about airfoils, cascades, and wings
[BTN-95-EIX95152577597] p 305 A95-73486
- Sidewash on the vertical tail in subsonic and supersonic flows
[BTN-95-EIX95152582316] p 264 A95-73519
- Nonlinear angle of twist of advanced composite wing boxes under pure torsion
[BTN-95-EIX95152582323] p 281 A95-73526
- Moving wall effect in relation to other dynamic stall flow mechanisms
[BTN-95-EIX95152582324] p 265 A95-73527
- Study of an airfoil with a flap and spoiler
[BTN-95-EIX95152582327] p 265 A95-73530
- Effect of underwing frost on a transport aircraft airfoil at flight Reynolds number
[BTN-95-EIX95152582334] p 276 A95-73536
- Pneumatic concept for tip-stall control of cranked-arrow wings
[BTN-95-EIX95152582335] p 281 A95-73537
- Method for the prediction of the onset of wing rock
[BTN-95-EIX95152582342] p 282 A95-73544
- Multirate flutter suppression system design for a model wing
[BTN-95-EIX95182619132] p 292 A95-76609
- Application of Navier-Stokes aeroelastic methods to improve fighter wing maneuver performance
[BTN-95-EIX95182619218] p 284 A95-76644
- Calculation of wing-alone aerodynamics to high angles of attack
[BTN-95-EIX95212645713] p 261 A95-76765
- Wing pressure distributions from subsonic tests of a high-wing transport model --- in the Langley 14- by 22-Foot Subsonic Wind Tunnel
[NASA-TM-4583] p 272 N95-22802
- Control of flow separation in airfoil/wing design applications
[NASA-TM-4583] p 274 N95-23294
- High-lift flow-physics flight experiments on a subsonic civil transport aircraft (B737-100)
[NASA-TM-4583] p 275 N95-23333
- Lift enhancing tabs for airfoils
[NASA-CASE-ARC-11990-1] p 286 N95-23395

WIRE

- SEM representation of the early and late time fields scattered from wire targets
[BTN-94-EIX94381353142] p 306 A95-74496

WOVEN COMPOSITES

- Idealized textile composites for experimental/analytical correlation
[NASA-TM-4583] p 301 N95-23277

X**X RAY INSPECTION**

- POD assessment of NDI procedures using a round robin test
[AGARD-R-809] p 315 N95-23602

X-29 AIRCRAFT

- Flight test of the X-29A at high angle of attack: Flight dynamics and controls
[NASA-TP-3537] p 284 N95-22806

Y**YAW**

- Forebody flow control on a full-scale F/A-18 aircraft
[BTN-95-EIX95152582333] p 281 A95-73535
- Method for the prediction of the onset of wing rock
[BTN-95-EIX95152582342] p 282 A95-73544
- Feedback control laws for highly maneuverable aircraft
[NASA-CR-197944] p 295 N95-23410

YAWING MOMENTS

- Forebody flow control on a full-scale F/A-18 aircraft
[BTN-95-EIX95152582333] p 281 A95-73535

YF-16 AIRCRAFT

- Robustly stable preliminary control systems design for the YF-16 CCV aircraft
[BTN-95-EIX95202637608] p 292 A95-76681

YTTRIUM

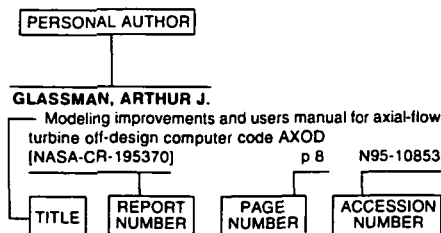
- Evolution of oxidation and creep damage mechanisms in HIPed silicon nitride materials
[DE95-001360] p 300 N95-22689

PERSONAL AUTHOR INDEX

AERONAUTICAL ENGINEERING / A Continuing Bibliography (Supplement 319)

July 1995

Typical Personal Author Index Listing



Listings in this index are arranged alphabetically by personal author. The title of the document is used to provide a brief description of the subject matter. The report number helps to indicate the type of document (e.g., NASA report, translation, NASA contractor report). The page and accession numbers are located beneath and to the right of the title. Under any one author's name the accession numbers are arranged in sequence.

A

- AARONSON, PHILIP**
CFD optimization of a theoretical minimum-drag body
[BTN-95-EIX95182619234] p 308 A95-76660
- ABEL, JONATHAN**
On the exact solutions of pseudorange equations
[BTN-95-EIX9514255477] p 278 A95-73433
- ABUSALI, P. A. M.**
Thermal force modeling for global positioning system satellites using the finite element method
[BTN-95-EIX95152583270] p 278 A95-73571
- ACHARYA, A.**
Airborne rotary air separator study
[NASA-CR-189099] p 290 N95-24053
- ADAMS, DANIEL O.**
Idealized textile composites for experimental/analytical correlation
p 301 N95-23277
- ADAMS, WILLIAM M., JR.**
Design and multifunction tests of a frequency domain-based active flutter suppression system
[BTN-95-EIX95182619215] p 292 A95-76641
- ADELMAN, HOWARD M.**
Integrated aerodynamic/dynamic/structural optimization of helicopter rotor blades using multilevel decomposition
[NASA-TP-3465] p 285 N95-22953
- AGARWALA, V. S.**
Corrosion detection and monitoring of aircraft structures: An overview
p 303 N95-23515
- AKIYAMA, HIROMITSU**
Polar Patrol Balloon
[BTN-95-EIX95152582318] p 316 A95-73521
- AL-GARNI, AHMED Z.**
Analytical solution for controls, heats, and states of flight trajectories
[BTN-95-EIX95152583286] p 282 A95-73587
- ALIGHANBARI, H.**
Postinstability behavior of a two-dimensional airfoil with a structural nonlinearity
[BTN-95-EIX95152582337] p 266 A95-73539
- ALMSTED, LARRY D.**
Flight test evaluation of a 35 GHz forward looking altimeter for terrain avoidance
[BTN-95-EIX9512641071] p 287 A95-76736

- AMBUR, DAMODAR R.**
Experimental evaluation of a box beam specifically tailored for chordwise deformation
[BTN-95-EIX95182619088] p 283 A95-75773
- ANDERSON, MARK R.**
Drag function modeling for air traffic simulation
[BTN-95-EIX95182619154] p 279 A95-76631
- APONSO, BIMAL L.**
Identification of higher order helicopter dynamics using linear modeling methods
[HTN-95-80851] p 290 A95-75093
- APPLIN, ZACHARY T.**
Wing pressure distributions from subsonic tests of a high-wing transport model
[NASA-TM-4583] p 272 N95-22802
- ARNETTE, STEPHEN A.**
Effects of expansions on a supersonic boundary layer: Surface pressure measurements
[BTN-95-EIX95142553036] p 263 A95-73462
- ARNOLD, F.**
Laplace interaction law for the computation of viscous airflow flow in low- and high-speed aerodynamics
[BTN-95-EIX95142553037] p 263 A95-73461
- ASCOLI, EDWARD P.**
CFD analysis of turbopump volutes
p 312 N95-23436
- ASLAN, A. R.**
Aerodynamic characteristics of external store configurations at low speeds
[BTN-95-EIX95182619230] p 271 A95-76656
- ATALLA, NOUREDDINE**
Coupled FEM-BEM approach for mean flow effects on vibro-acoustic behavior of planar structures
[BTN-95-EIX95152577587] p 263 A95-73495
- ATLAS, E. L.**
Estimates of total organic and inorganic chlorine in the lower stratosphere from in situ and flask measurements during AASE 2
[HTN-95-A0861] p 317 A95-76265
- ATLURI, SATYA N.**
Growth of multiple cracks and their linkup in a fuselage lap joint
[BTN-95-EIX95142553047] p 286 A95-73451
- AUSLENDER, A. H.**
Optimization of contoured hypersonic scramjet inlets with a least-squares parabolized Navier-Stokes procedure
[HTN-95-20976] p 261 A95-74042
- AYDIN, N. H.**
Aerodynamic characteristics of external store configurations at low speeds
[BTN-95-EIX95182619230] p 271 A95-76656

B

- BACON, BARTON**
Simulation and model reduction for the active flexible wing program
[BTN-95-EIX95182619211] p 295 A95-76637
- BAILLIE, STEWART**
Improving prediction: The incorporation of simplified rotor dynamics in a mathematical model of the bell 412HP
[BTN-95-EIX95152584679] p 282 A95-73591
- BALAKRISHNA, S.**
Performance of the 0.3-meter transonic cryogenic tunnel with air, nitrogen, and sulfur hexafluoride media under closed loop automatic control
[NASA-CR-195052] p 310 N95-23257
- BALAS, GARY J.**
Feedback control laws for highly maneuverable aircraft
[NASA-CR-197944] p 295 N95-23410
- BANG, ERIC S.**
Flight-deck displays on the Boeing 777
[BTN-95-EIX95142562402] p 286 A95-73438
- BARING, T. J.**
Estimates of total organic and inorganic chlorine in the lower stratosphere from in situ and flask measurements during AASE 2
[HTN-95-A0861] p 317 A95-76265
- BARONTI, S.**
MAX-91: Polarimetric SAR results on Montespetoli site
p 320 N95-23940
- BARTLETT, D. L.**
The corrosion and protection of advanced aluminium-lithium airframe alloys
p 302 N95-23497
- BATY, ROY S.**
Functional dependence of trajectory dispersion on initial condition errors
[BTN-95-EIX95152583263] p 298 A95-73564
- BAUCHAU, OLIVIER A.**
Dynamic analysis of bearingless tail rotor blades based on nonlinear shell modes
[BTN-95-EIX95152582338] p 281 A95-73540
- BAUER, JEFFREY E.**
Flight test of the X-29A at high angle of attack: Flight dynamics and controls
[NASA-TP-3537] p 284 N95-22806
- BAYSAL, OKTAY**
Aerodynamic shape optimization using preconditioned conjugate gradient methods
[BTN-95-EIX95142553033] p 263 A95-73465
- BECKMAN, BRIAN C.**
Preconditioned domain decomposition scheme for three-dimensional aerodynamic sensitivity analysis
[BTN-95-EIX95152577612] p 321 A95-73471
- BECKER, ROBERT C.**
A CFD study of complex missile and store configurations in relative motion
[NASA-CR-197912] p 285 N95-22949
- BECKER, ROBERT C.**
Aerodynamic design optimization with sensitivity analysis and computational fluid dynamics
[NASA-CR-197419] p 274 N95-23218
- BECKER, ROBERT C.**
Flight test evaluation of a 35 GHz forward looking altimeter for terrain avoidance
[BTN-95-EIX9512641071] p 287 A95-76736
- BELLINGER, N. C.**
Virtual reality flight control display with six-degree-of-freedom controller and spherical orientation overlay
[NASA-CASE-NPO-18733-1-CU] p 288 N95-22578
- BELLINGER, N. C.**
Double pass retroreflection for corrosion detection in aircraft structures
p 323 N95-23503
- BENDIKSEN, ODDVAR O.**
Limit cycle phenomena in computational transonic aeroelasticity
[BTN-95-EIX95152582317] p 264 A95-73520
- BENNETT, J.**
Enhancement of F/A-18 operational flight measurements: Data report for phase 1
[DSTO-TR-0049] p 286 N95-23666
- BENNETT, ROBERT M.**
Application of transonic small disturbance theory to the active flexible wing model
[BTN-95-EIX95182619210] p 270 A95-76636
- BENTS, DAVID J.**
Design of a GaAs/Ge solar array for unmanned aerial vehicles
[NASA-TM-106870] p 320 N95-23259
- BERG, MARTIN C.**
Multirate flutter suppression system design for a model wing
[BTN-95-EIX95182619132] p 292 A95-76609
- BERRICHE, R.**
Evaluation of advanced aerospace materials by depth sensing indentation and scratch methods
[BTN-95-EIX95152584678] p 282 A95-73590
- BERRY, L. A.**
Cu deposition using a permanent magnet electron cyclotron resonance microwave plasma source
[DE94-017768] p 304 N95-23981
- BHAGAT, P. K.**
Corrosion detection and monitoring of aircraft structures: An overview
p 303 N95-23515
- BHAT, THONSE R. S.**
Mach wave emission from a high-temperature supersonic jet
[BTN-95-EIX95152577586] p 264 A95-73496
- BIBER, KASIM**
Flow study of supersonic wing-nacelle configuration
[BTN-95-EIX95152582344] p 266 A95-73546

- BIDWELL, COLIN S.**
Additional improvements to the NASA Lewis ice accretion code LEWICE
[NASA-TM-106849] p 309 N95-22669
- BIEZAD, DANIEL J.**
Direct-lift design strategy for longitudinal control of hypersonic aircraft
[BTN-95-EIX95182619131] p 291 A95-76608
- BIRCH, STUART**
Aircraft stripping and painting
[BTN-95-EIX95182617810] p 300 A95-75755
- BISWAS, K. K.**
Some aspects of the aerodynamics of separating strap-ons
[BTN-95-EIX95182617464] p 298 A95-75735
- BLANCHARD, ROBERT E.**
Development of qualification guidelines for personal computer-based aviation training devices
[DOT/FAA/AM-95/6] p 323 N95-23603
- BLANKEN, CHRIS L.**
Investigation of the effects of bandwidth and time delay on helicopter roll-axis handling qualities
[HTN-95-80853] p 290 A95-75095
- BODDY, MARK S.**
Empirical results on scheduling and dynamic backtracking
p 299 N95-23761
- BOERING, K. A.**
In situ observations in aircraft exhaust plumes in the lower stratosphere at midlatitudes
[HTN-95-A0862] p 318 A95-76266
- BOITNOTT, RICHARD L.**
An analytical and experimental investigation of the response of the curved, composite frame/skin specimens
[HTN-95-80857] p 283 A95-75099
- BOODEY, J. B.**
Corrosion of landing gear steels
p 302 N95-23500
- BOOTH, EARL R., JR.**
Analysis of a higher harmonic control test to reduce blade vortex interaction noise
[BTN-95-EIX95152582330] p 265 A95-73532
- BOSE, B.**
Simple method of supersonic flow visualization using watertable
[BTN-95-EIX95182619105] p 269 A95-76590
- BOWEN, BRENT D.**
The airline quality report, 1994
[NIAR-94-11] p 277 N95-24012
- BOWER, DANIEL R.**
Analytical study of the neutral stability of a model hypersonic boundary layer
[BTN-95-EIX95152577589] p 263 A95-73493
- BOYD, D. DOUGLAS, JR.**
Analysis of a higher harmonic control test to reduce blade vortex interaction noise
[BTN-95-EIX95152582330] p 265 A95-73532
- BOYD, IAIN**
Particle kinetic simulation of high altitude hypervelocity flight
[NASA-CR-197383] p 309 N95-22481
- BOZKURT, Y.**
Aerodynamic characteristics of external store configurations at low speeds
[BTN-95-EIX95182619230] p 271 A95-76656
- BRAGG, M. B.**
Effect of underwing frost on a transport aircraft airfoil at flight Reynolds number
[BTN-95-EIX95152582334] p 276 A95-73536
- BRAGG, MICHAEL B.**
Aerodynamics of a finite wing with simulated ice
[BTN-95-EIX95182619227] p 270 A95-76653
- BRAGG, MICHAEL B.**
Study of the droplet spray characteristics of a subsonic wind tunnel
[BTN-95-EIX95182619235] p 271 A95-76661
- BRAZA, M.**
Two-equation turbulence model for unsteady separated flows around airfoils
[BTN-95-EIX95142553054] p 262 A95-73444
- BRENTNER, KENNETH S.**
Sensitivity of acoustic predictions to variation of input parameters
[HTN-95-80855] p 267 A95-75097
- BRIDGES, DAVID H.**
Crossflow instability control on a swept-wing: Preliminary studies
p 274 N95-23283
- BRINKER, DAVID J.**
Design of a GaAs/Ge solar array for unmanned aerial vehicles
[NASA-TM-106870] p 320 N95-23259
- BROOKS, CYNTHIA L.**
Automation technology using Geographic Information System (GIS)
p 324 N95-23284
- BROOKS, THOMAS F.**
Analysis of a higher harmonic control test to reduce blade vortex interaction noise
[BTN-95-EIX95152582330] p 265 A95-73532

- BROWN, ART**
Labs behind Boeing's new 777
[BTN-95-EIX95142562403] p 280 A95-73437
- BROWNE, G. T.**
US Navy operating experience with new aircraft construction materials
p 303 N95-23517
- BROZOWSKI, L. A.**
Impeller flow field characterization with a laser two-focus velocimeter
p 313 N95-23440
- BRUCE, DAVID A.**
Non-destructive detection of corrosion for life management
p 314 N95-23505
- BUCH, A.**
Review of some results of the author's fatigue investigations with applications in engineering and material science
[TAE-698] p 316 N95-23662
- BUEHLE, R. D.**
Dynamic response tests of inertial and optical wind-tunnel model attitude measurement devices
[NASA-TM-109182] p 296 N95-23011
- BUELOW, B. E. O.**
Convergence acceleration of implicit schemes in the presence of high aspect ratio grid cells
p 313 N95-23446
- BURCHAM, FRANK W.**
Engines-only flight control system
[NASA-CASE-ARC-11944-1] p 294 N95-23389
- BURGEE, GREG W.**
Aerodynamic shape optimization using preconditioned conjugate gradient methods
[BTN-95-EIX95142553033] p 263 A95-73465
- BURKEN, JOHN J.**
Flight test of the X-29A at high angle of attack: Flight dynamics and controls
[NASA-TP-3537] p 284 N95-22806
- BURLEY, CASEY L.**
Sensitivity of acoustic predictions to variation of input parameters
[HTN-95-80855] p 267 A95-75097
- BURNER, A. W.**
Dynamic response tests of inertial and optical wind-tunnel model attitude measurement devices
[NASA-TM-109182] p 296 N95-23011
- BUSTO, MARIO**
Nonlinear angle of twist of advanced composite wing boxes under pure torsion
[BTN-95-EIX95152582323] p 281 A95-73526
- BUTTRILL, CAREY**
Simulation and model reduction for the active flexible wing program
[BTN-95-EIX95182619211] p 295 A95-76637
- C**
- CAI, TIMIN**
Simulation on the 3-D turbulent flow in the passages of finocyl grain
[BTN-95-EIX95202638962] p 279 A95-76674
- CALCAGNO, P.**
Geoid lineations of 1000 km wavelength over the central Pacific
[HTN-95-11304] p 319 A95-77009
- CALDWELL, D. J.**
Modeling aerosol emissions from the combustion of composite materials
p 301 N95-23038
- CAPOTONDI, ANTONIETTA**
Assimilation of altimeter data in a quasi-geostrophic model of the Gulf Stream system: A dynamical perspective
[NASA-CR-196313] p 320 N95-23766
- CARBONARO, MARIO C.**
Experimental investigation of the flowfield about an upswep afterbody
[BTN-95-EIX95152582321] p 265 A95-73524
- CARTER, DALE**
Flow visualization studies of VTOL aircraft models during Hover in ground effect
[NASA-TM-108860] p 272 N95-22666
- CARUSO, STEVEN C.**
Aerodynamic design of pegasus: Concept to flight with computational fluid dynamics
[BTN-95-EIX95182617463] p 298 A95-75734
- CAUDRON, F.**
Experimental investigation of the flowfield about an upswep afterbody
[BTN-95-EIX95152582321] p 265 A95-73524
- CAZENAVE, A.**
Geoid lineations of 1000 km wavelength over the central Pacific
[HTN-95-11304] p 319 A95-77009
- CELLI, ROBERTO**
Efficient sensitivity analysis for rotary-wing aeromechanical problems
[BTN-95-EIX95152577585] p 264 A95-73497

- Effects of high order dynamics on helicopter flight control law design
[HTN-95-80852] p 290 A95-75094
- CHA, SOYOUNG S.**
Holographic interferometric tomography for reconstructing flow fields
p 310 N95-23287
- CHADERJIAN, NEAL M.**
Navier-Stokes prediction of large-amplitude delta-wing roll oscillations
[BTN-95-EIX95152582329] p 281 A95-73531
- CHAFFEE, JAMES**
On the exact solutions of pseudorange equations
[BTN-95-EIX9514255477] p 278 A95-73433
- CHAN, DANIEL C.**
CFD analysis of turbopump volutes
p 312 N95-23436
- CHANG, KEUN-SHIK**
Three-dimensional structure of a supersonic jet impinging on an inclined plate
[BTN-95-EIX95152583259] p 267 A95-73560
- CHANG, STEPHEN**
Experimental evaluation of a box beam specifically tailored for chordwise deformation
[BTN-95-EIX95182619088] p 283 A95-75773
- CHATURVEDI, ARVIND K.**
Aircraft fires, smoke toxicity, and survival: An overview
[DOT/FAA/AM-95/8] p 277 N95-24024
- CHAVEZ, FRANK R.**
Analytical aeropropulsive/aeroelastic hypersonic-vehicle model with dynamic analysis
[BTN-95-EIX95182619138] p 269 A95-76615
- CHEN, GUANGREN**
Development of aeronautical mobile satellite services over the past thirty years
[BTN-95-EIX95152569458] p 305 A95-73498
- CHEN, P.-S.**
High-performance parallel analysis of coupled problems for aircraft propulsion
[NASA-CR-197440] p 289 N95-23088
- CHEN, Y. K.**
Hypersonic convective heat transfer over 140-deg blunt cones in different gases
[BTN-95-EIX95152583253] p 306 A95-73554
- CHEN, Y.-K.**
Hypersonic nonequilibrium Navier-Stokes solutions over an ablating graphite nosetip
[BTN-95-EIX95152583252] p 305 A95-73553
- CHENG, VICTOR H. L.**
Automatic guidance and control for helicopter obstacle avoidance
[BTN-95-EIX95182619130] p 291 A95-76607
- CHERN, JIUN-DAR**
Diurnal variation of lee vortices in Taiwan and the surrounding area
[HTN-95-91363] p 318 A95-76394
- CHEUNG, BENNY K.**
System for determining aerodynamic imbalance
[NASA-CASE-ARC-11913-1] p 311 N95-23377
- CHEUNG, SAMSON**
CFD optimization of a theoretical minimum-drag body
[BTN-95-EIX95182619234] p 308 A95-76660
- CHIANG, WUYING**
Dynamic analysis of bearingless tail rotor blades based on nonlinear shell modes
[BTN-95-EIX95152582338] p 281 A95-73540
- CHIU, CHYIN-SHAN**
Sidewash on the vertical tail in subsonic and supersonic flows
[BTN-95-EIX95152582316] p 264 A95-73519
- CHOBOTOV, V. A.**
Effects of satellite bunching on the probability of collision in geosynchronous orbit
[BTN-95-EIX95152583276] p 298 A95-73577
- CHOW, PAO-LIU**
Active control of panel vibrations induced by a boundary layer flow
[NASA-CR-197867] p 273 N95-23182
- CHRISTILF, DAVID M.**
Design and multifunction tests of a frequency domain-based active flutter suppression system
[BTN-95-EIX95182619215] p 292 A95-76641
- CHUNG, CHAN H.**
Numerical analysis of hypersonic low-density scramjet inlet flow
[BTN-95-EIX9512645694] p 272 A95-76746
- CHURCHILL, GARY B.**
System for determining aerodynamic imbalance
[NASA-CASE-ARC-11913-1] p 311 N95-23377
- CLARKE, ROBERT**
Flight test of the X-29A at high angle of attack: Flight dynamics and controls
[NASA-TP-3537] p 284 N95-22806
- CLAYTON, A. C.**
Measurement of particle emissions from clean room gas-handling components
[BTN-94-EIX94381359040] p 295 A95-74554

- COCHRAN, JOHN E., JR.**
Aerodynamic flight control to increase payload capability of future launch vehicles
[NASA-CR-197704] p 300 N95-24032
- COLE, STANLEY R.**
Summary of an active flexible wing program
[BTN-95-EIX95182619209] p 283 A95-76635
- COLLINS, FRANK G.**
Determination of wall boundary conditions for high-speed-ratio direct simulation Monte Carlo calculations
[BTN-95-EIX95182617457] p 267 A95-75728
- COLLINS, WILLIAM E.**
A review of civil aviation fatal accidents in which lost/disoriented was a cause/factor: 1981-1990
[DOT/FAA/AM-95/11] p 278 N95-24071
- COLOZZA, ANTHONY J.**
Design of a GaAs/Ge solar array for unmanned aerial vehicles
[NASA-TM-106870] p 320 N95-23259
- CONLEY, JOSEPH L.**
Engines-only flight control system
[NASA-CASE-ARC-11944-1] p 294 N95-23389
- CONSIDINE, DAVID B.**
Sensitivity of two-dimensional model predictions of ozone response to stratospheric aircraft: An update
[HTN-95-A0863] p 318 A95-76267
- CORNMAN, LARRY B.**
Real-time estimation of atmospheric turbulence severity from in-situ aircraft measurements
[BTN-95-EIX95182619231] p 319 A95-76657
- COUILLAUD, STEPHANE**
Flow visualization studies of VTOL aircraft models during Hover in ground effect
[NASA-TM-108860] p 272 N95-22666
- COX, G. B., JR.**
Phase 2: HGM air flow tests in support of HEX vane investigation
p 312 N95-23438
- CRABILL, NORMAN L.**
Pilot Weather Advisor system
[BTN-95-EIX95152582314] p 316 A95-73517
- CRAGGS, A.**
Finite element model for a flexible non-symmetric rotor on distributed bearing: A stability study
[BTN-94-EIX94381352212] p 306 A95-74612
- CRAMER, K. E.**
New nondestructive techniques for the detection and quantification of corrosion in aircraft structures
p 315 N95-23512
- CRANE, JEAN M.**
Flight-deck displays on the Boeing 777
[BTN-95-EIX95142562402] p 286 A95-73438
- CRUSE, T. A.**
Mechanical system reliability and risk assessment
[BTN-95-EIX95142553046] p 304 A95-73452
- CUERNO, CRISTINA**
Design constraints in the payload-range diagram of ultrahigh capacity transport airplanes
[BTN-95-EIX95152582319] p 276 A95-73522
- CUNNING, GARY**
Real-time estimation of atmospheric turbulence severity from in-situ aircraft measurements
[BTN-95-EIX95182619231] p 319 A95-76657

D

- D'AZZO, J. J.**
Automatic formation flight control
[BTN-95-EIX95182619153] p 292 A95-76630
- DA, REN**
New failure detection approach and its application to GPS autonomous integrity monitoring
[BTN-95-EIX95202637613] p 279 A95-76676
- DAHL, MILO D.**
Supersonic jet noise reductions predicted with increased jet spreading rate
[NASA-TM-106872] p 323 N95-23178
- DARGAN, J. L.**
Automatic formation flight control
[BTN-95-EIX95182619153] p 292 A95-76630
- DARIAN, ARMEN**
CFD analysis of turbopump volutes
p 312 N95-23436
- DARLING, DOUGLAS**
Sensitivity of combustion-acoustic instabilities to boundary conditions for premixed gas turbine combustors
[NASA-TM-106890] p 289 N95-23550
- DAUBE, B. C.**
In situ observations in aircraft exhaust plumes in the lower stratosphere at midlatitudes
[HTN-95-A0862] p 318 A95-76266
- DAVIDHAZY, ANDREW**
Scientific and technical photography at NASA Langley Research Center
p 310 N95-23290

- DAVIDSON, LARS**
Turbulent transonic airfoil flow simulation using a pressure-based algorithm
[BTN-95-EIX95182619078] p 269 A95-75763
- DAVIS, SANFORD S.**
Aeroacoustic model for weak shock waves based on Burgers equation
[BTN-95-EIX95182619076] p 269 A95-75761
- DAWSON, JONATHAN A.**
Effects of expansions on a supersonic boundary layer: Surface pressure measurements
[BTN-95-EIX95142553036] p 263 A95-73462
- DEAN, JEFFREY S.**
ATE enabling technologies
[BTN-95-EIX95172595294] p 287 A95-75718
- DEATON, JERRY W.**
Development and verification of a resin film infusion/resin transfer molding simulation model for fabrication of advanced textile composites
[NASA-CR-197439] p 301 N95-23179
- DECKER, RAND A.**
Tracking of raindrops in flow over an airfoil
[BTN-95-EIX95182619221] p 308 A95-76647
- DEJONGE, J. B.**
Review of aeronautical fatigue investigation in the Netherlands during the period March 1991-March 1993
[PB95-139184] p 285 N95-23161
- DELANY, A.**
A comparison of some aerodynamic resistance methods using measurements over cotton and grass from the 1991 California ozone deposition experiment
[HTN-95-11295] p 319 A95-77000
- DEMMA, NICK**
2 micron LIDAR for laser-based remote sensing: Flight demonstration and application survey
[BTN-95-EIX95212641072] p 319 A95-76737
- DEROSA, S.**
Structural acoustic calculations in the low-frequency range
[BTN-95-EIX95152582336] p 323 A95-73538
- DESHAPANDE, MANISH**
Cavitation modeling in Euler and Navier-Stokes codes
p 315 N95-23630
- DESSLER, A. E.**
In situ observations in aircraft exhaust plumes in the lower stratosphere at midlatitudes
[HTN-95-A0862] p 318 A95-76266
- DEWITT, KENNETH J.**
Effect of curvature in the numerical simulation of an electrothermal de-icer pad
[BTN-95-EIX95182619219] p 276 A95-76645
- Numerical analysis of hypersonic low-density scramjet inlet flow
[BTN-95-EIX95212645694] p 272 A95-76746
- DEXTER, H. BENSON**
Development and verification of a resin film infusion/resin transfer molding simulation model for fabrication of advanced textile composites
[NASA-CR-197439] p 301 N95-23179
- DILLENIUS, MARNIX F. E.**
Aerodynamic design of pegasus: Concept to flight with computational fluid dynamics
[BTN-95-EIX95182617463] p 298 A95-75734
- DISIMILE, PETER J.**
Observations on using experimental data as boundary conditions for computations
[BTN-95-EIX95182619103] p 321 A95-76588
- DOGRA, VIRENDRA K.**
Hypersonic rarefied flow past spheres including wake structure
[BTN-95-EIX95152583250] p 305 A95-73551
- Zonally decoupled direct simulation Monte Carlo solutions of hypersonic blunt-body wake flows
[BTN-95-EIX95182617458] p 268 A95-75729
- DOHERR, KARL-FRIEDRICH**
Analytical solution and parameter estimation of projectile dynamics
[BTN-95-EIX95212645695] p 272 A95-76747
- DONOVAN, R. P.**
Measurement of particle emissions from clean room gas-handling components
[BTN-94-EIX94381359040] p 295 A95-74554
- Measurement of moisture and total hydrocarbon contributions by valves used in clean room gas-delivery systems
[BTN-94-EIX94381359041] p 295 A95-74629
- DORENBURG, FRANK M. G.**
Overview of AlliedSignal's avionics development in the CIS
[BTN-95-EIX95212641069] p 287 A95-76734
- DOUGLASS, ANNE R.**
Trajectory modeling of emissions from lower stratospheric aircraft
[HTN-95-41219] p 317 A95-75031

- Sensitivity of two-dimensional model predictions of ozone response to stratospheric aircraft: An update
[HTN-95-A0863] p 318 A95-76267
- DOWELL, E. H.**
Response of a nonrotating rotor blade to lateral turbulence. Part 1: Theory
[BTN-95-EIX95182619228] p 284 A95-76654
- Response of a nonrotating rotor blade to lateral turbulence. Part 2: Experiment
[BTN-95-EIX95182619229] p 284 A95-76655
- DOWELL, EARL H.**
Flutter of an infinitely long panel in a duct
[BTN-95-EIX95182619087] p 291 A95-75772
- DOWNING, DAVID R.**
Functional agility metrics and optimal trajectory analysis
[BTN-95-EIX95182619121] p 321 A95-76598
- DURHAM, WAYNE C.**
Kinematics and aerodynamics of velocity-vector roll
[BTN-95-EIX95182619126] p 291 A95-76603
- Attainable moments for the constrained control allocation problem
[BTN-95-EIX95182619149] p 322 A95-76626
- DUTTON, J. C.**
Supersonic near-wake afterbody boattailing effects on axisymmetric bodies
[BTN-95-EIX95182617465] p 268 A95-75736

E

- EASTAUGH, GRAEME F.**
Multiple site fatigue damage in fuselage skin splices: Experimental simulation and theoretical prediction
[BTN-95-EIX95152584676] p 276 A95-73588
- EDWARDS, MARK B.**
The role of flight progress strips in en route air traffic control: A time-series analysis
[DOT/FAA/AM-95/4] p 280 N95-23565
- EDWARDS, THOMAS**
CFD optimization of a theoretical minimum-drag body
[BTN-95-EIX95182619234] p 308 A95-76660
- EISENHART, D. W.**
Phase 2: HGM air flow tests in support of HEX vane investigation
p 312 N95-23438
- EKATERINARIS, J. A.**
Effects of spatial order of accuracy on the computation of vortical flowfields
[BTN-95-EIX95152577604] p 305 A95-73479
- Computation of oscillating airfoil flows with one- and two-equation turbulence models
[BTN-95-EIX95152577588] p 263 A95-73494
- EKATERINARIS, JOHN A.**
Viscous-inviscid interaction method for unsteady low-speed airfoil flows
[BTN-95-EIX95182619093] p 269 A95-75778
- EKSUZIAN, D. J.**
TRISTAR 1: Evaluation methods for testing head-up display (HUD) flight symbology
[NASA-TM-4665] p 288 N95-24030
- EL-SHERIEF, HOSSNY**
Real-time navigation using the global positioning system
[BTN-95-EIX95172595298] p 279 A95-75714
- ELBULUK, MALIK E.**
Motor drive technologies for the power-by-wire (PBW) program: Options, trends and tradeoffs
[NASA-TM-106885] p 295 N95-23671
- ELESHAKY, MOHAMED E.**
Preconditioned domain decomposition scheme for three-dimensional aerodynamic sensitivity analysis
[BTN-95-EIX95152577612] p 321 A95-73471
- ELKINS, J. W.**
Estimates of total organic and inorganic chlorine in the lower stratosphere from in situ and flask measurements during AASE 2
[HTN-95-A0861] p 317 A95-76265
- ENG, ANTHONY T.**
Organic coating technology for the protection of aircraft against corrosion
p 303 N95-23513
- ENSOR, D. S.**
Measurement of particle emissions from clean room gas-handling components
[BTN-94-EIX94381359040] p 295 A95-74554
- Measurement of moisture and total hydrocarbon contributions by valves used in clean room gas-delivery systems
[BTN-94-EIX94381359041] p 295 A95-74629
- EPSTEIN, RONALD J.**
Experimental investigation of the flowfield about an upswept afterbody
[BTN-95-EIX95152582321] p 265 A95-73524
- Flutter of an infinitely long panel in a duct
[BTN-95-EIX95182619087] p 291 A95-75772

ERCOLINE, W. R.

TRISTAR 1: Evaluation methods for testing head-up display (HUD) flight symbology
[NASA-TM-4665] p 288 N95-24030

ERICSSON, LARS E.

Moving wall effect in relation to other dynamic stall flow mechanisms
[BTN-95-EIX95152582324] p 265 A95-73527
Further analysis of high-rate rolling experiments of a 65-deg delta wing
[BTN-95-EIX95152582331] p 281 A95-73533

ESPANA, MARTIN D.

Direct adaptive performance optimization of subsonic transports: A periodic perturbation technique
[NASA-TM-4676] p 284 N95-22829

EST, BRIAN E.

Wing vertical position effects on wing-body carryover for noncircular missiles
[BTN-95-EIX95182617462] p 268 A95-75733

EVANS, R. H.

TRISTAR 1: Evaluation methods for testing head-up display (HUD) flight symbology
[NASA-TM-4665] p 288 N95-24030

F

FAETH, G. M.

Effect of ambient turbulence intensity on sphere wakes at intermediate Reynolds numbers
[BTN-95-EIX95182619101] p 308 A95-76586

FAHEY, D. W.

Estimates of total organic and inorganic chlorine in the lower stratosphere from in situ and flask measurements during AASE 2
[HTN-95-A0861] p 317 A95-76265
In situ observations in aircraft exhaust plumes in the lower stratosphere at midlatitudes
[HTN-95-A0862] p 318 A95-76266

FALASCO, THOMAS

H-76B fantail demonstrator composite fan blade fabrication
[HTN-95-80856] p 283 A95-75098

FALLER, WILLIAM E.

Neural network prediction of three-dimensional unsteady separated flowfields
[BTN-95-EIX95182619232] p 308 A95-76658

FARHAT, C.

High-performance parallel analysis of coupled problems for aircraft propulsion
[NASA-CR-197440] p 289 N95-23088

FELIPPA, C. A.

High-performance parallel analysis of coupled problems for aircraft propulsion
[NASA-CR-197440] p 289 N95-23088

FENG, JINZHANG

Cavitation modeling in Euler and Navier-Stokes codes
p 315 N95-23630

FENTRESS, MICHAEL L.

Experimental evaluation of a box beam specifically tailored for chordwise deformation
[BTN-95-EIX95182619088] p 283 A95-75773

FERBER, M. K.

Evolution of oxidation and creep damage mechanisms in HIPed silicon nitride materials
[DE95-001360] p 300 N95-22689

FERGUSON, T. V.

Impeller flow field characterization with a laser two-focus velocimeter
p 313 N95-23440

FINK, C. L.

Evaluation of neutron techniques for illicit substance detection
[DE95-002988] p 300 N95-22764

FINLEY, DENNIS B.

Euler Technology Assessment program for preliminary aircraft design employing SPLITFLOW code with Cartesian unstructured grid method
[NASA-CR-4649] p 273 N95-22917

FINLEY, T. D.

Dynamic response tests of inertial and optical wind-tunnel model attitude measurement devices
[NASA-TM-109182] p 296 N95-23011

FLOWERS, GEORGE T.

Influence of backup bearings and support structure dynamics on the behavior of rotors with active supports
[NASA-CR-197438] p 310 N95-23190

FREEMAN, L. MICHAEL

Predicting exhaust plume boundaries with supersonic external flows
[BTN-95-EIX95152583258] p 297 A95-73559

FRINK, NEAL T.

Unstructured grid solutions to a wing/pylon/store configuration
[BTN-95-EIX95152582322] p 265 A95-73525

FRULLA, GIACOMO

Nonlinear angle of twist of advanced composite wing boxes under pure torsion
[BTN-95-EIX95152582323] p 281 A95-73526

FRUSTIE, M. J.

Corrosion in service experience with aircraft in France
p 303 N95-23518

FUJII, KOZO

Numerical investigation of supersonic flows around a spiked blunt body
[BTN-95-EIX9512645690] p 271 A95-76742

FULLER, DANA

The role of flight progress strips in en route air traffic control: A time-series analysis
[DOT/FAA/AM-95/4] p 280 N95-23565

FULLERTON, CHARLES G.

Engines-only flight control system
[NASA-CASE-ARC-11944-1] p 294 N95-23389

G

GALLY, THOMAS A.

Control of flow separation in airfoil/wing design applications
p 274 N95-23294

GAO, R. S.

In situ observations in aircraft exhaust plumes in the lower stratosphere at midlatitudes
[HTN-95-A0862] p 318 A95-76266

GAPOSHCHIN, EDWARD M.

Calculation of satellite drag coefficients
[AD-A285118] p 300 N95-23781

GARG, SANJAY

Stable H(infinity) controller design for the longitudinal dynamics of an aircraft
[NASA-TM-106847] p 293 N95-22954

GARRARD, WILLIAM L.

Feedback control laws for highly maneuverable aircraft
[NASA-CR-197944] p 295 N95-23410

GAUTHIER, P.

Corrosion in service experience with aircraft in France
p 303 N95-23518

GENTRY, GARL L., JR.

Wing pressure distributions from subsonic tests of a high-wing transport model
[NASA-TM-4583] p 272 N95-22802

GERHARDT, HEINZ A.

Natural laminar flow wing concept for supersonic transports
[BTN-95-EIX95182619226] p 308 A95-76652

GIBSON, BERRY T.

Natural laminar flow wing concept for supersonic transports
[BTN-95-EIX95182619226] p 308 A95-76652

GIEL, P. W.

Three-dimensional Navier-Stokes analysis and redesign of an imbedded bellmouth nozzle in a turbine cascade inlet section
p 311 N95-23423

GILPIN, T. M.

Estimates of total organic and inorganic chlorine in the lower stratosphere from in situ and flask measurements during AASE 2
[HTN-95-A0861] p 317 A95-76265

GILYARD, GLENN

Direct adaptive performance optimization of subsonic transports: A periodic perturbation technique
[NASA-TM-4676] p 284 N95-22829

GILYARD, GLENN B.

Engines-only flight control system
[NASA-CASE-ARC-11944-1] p 294 N95-23389

GLASSMAN, ARTHUR J.

Enhanced analysis and users manual for radial-inflow turbine conceptual design code RTD
[NASA-CR-195454] p 275 N95-23462

GOLDMAN, ROBERT P.

Empirical results on scheduling and dynamic backtracking
p 299 N95-23761

GOLDTHORPE, STEVE H.

Guidance and control requirements for high-speed Rollout and Turnoff (ROTO)
[NASA-CR-195026] p 292 N95-22674

GOLDWIRE, H.

NTS-spill test facility wind tunnel exhaust plume characterization
[DE95-003630] p 297 N95-24019

GORBATKIN, S. M.

Cu deposition using a permanent magnet electron cyclotron resonance microwave plasma source
[DE94-017768] p 304 N95-23981

GOTTSMANN, C. F.

Airborne rotary air separator study
[NASA-CR-189099] p 290 N95-24053

GOULD, R. W.

Double pass retroreflection for corrosion detection in aircraft structures
p 323 N95-23503

GRASSO, F.

Simulation of transverse gas injection in turbulent supersonic air flows
[BTN-95-EIX95182619080] p 269 A95-75765

GRAY, J. A.

The corrosion and protection of advanced aluminum-lithium airframe alloys
p 302 N95-23497

GREENDYKE, ROBERT B.

Convective and radiative heat transfer analysis for the fire 2 forebody
[BTN-95-EIX95182617460] p 268 A95-75731

GREENE, FRANCIS A.

Application of the multigrid solution technique to hypersonic entry vehicles
[BTN-95-EIX95152583254] p 306 A95-73555

GREENMAN, MATTHEW

Flutter analysis of composite box beams
[NASA-CR-197931] p 294 N95-23392

GREGORY, G. L.

Compendium of NASA data base for the Global Tropospheric Experiment's Pacific Exploratory Mission West-A (PEM West-A)
[NASA-TM-109177] p 320 N95-23009

GRIFFIN, O. HAYDEN, JR.

An analytical and experimental investigation of the response of the curved, composite frame/skin specimens
[HTN-95-80857] p 283 A95-75099

GRYZANOV, B. A.

Fatigue strength of high-temperature alloys under conditions of cyclic temperature variation. Communication 1: Experimental procedure and results
[BTN-95-EIX94401363884] p 307 A95-75516

GUMASTE, U.

High-performance parallel analysis of coupled problems for aircraft propulsion
[NASA-CR-197440] p 289 N95-23088

GUPTA, ROOP N.

Higher-order viscous shock-layer solutions for high-altitude flows
[BTN-95-EIX95152583255] p 306 A95-73556

H

HAAS, BRIAN L.

Particle kinetic simulation of high altitude hypervelocity flight
[NASA-CR-197383] p 309 N95-22481

HAGENIERS, O. L.

Double pass retroreflection for corrosion detection in aircraft structures
p 323 N95-23503

HALL, KENNETH C.

Eigenanalysis of unsteady flows about airfoils, cascades, and wings
[BTN-95-EIX95152577597] p 305 A95-73486

HAMM, CLAUD D.

Corrosion protection measures for CFC/metal joints of fuel integral tank structures of advanced military aircraft
p 303 N95-23510

HAMMADI, MUNIR AL

Study of an airfoil with a flap and spoiler
[BTN-95-EIX95152582327] p 265 A95-73530

HANFF, ERNEST S.

Further analysis of high-rate rolling experiments of a 65-deg delta wing
[BTN-95-EIX95152582331] p 281 A95-73533

HANGE, CRAIG

Flow visualization studies of VTOL aircraft models during Hover in ground effect
[NASA-TM-108860] p 272 N95-22666

HARDY, G. L.

Corrosion detection and monitoring of aircraft structures: An overview
p 303 N95-23515

HARRIS, BRENDA W.

An assessment of viscous effects in computational simulation of benign and burst vortex flows on generic fighter wind-tunnel models using TEAM code
[NASA-CR-4650] p 273 N95-23185

HARTEL, MARTIN C.

Flight-deck displays on the Boeing 777
[BTN-95-EIX95142562402] p 286 A95-73438

HARTUNG, LIN C.

Convective and radiative heat transfer analysis for the fire 2 forebody
[BTN-95-EIX95182617460] p 268 A95-75731

HASKO, GREGORY H.

Development and verification of a resin film infusion/resin transfer molding simulation model for fabrication of advanced textile composites
[NASA-CR-197439] p 301 N95-23179

HAWORTH, L. A.

TRISTAR 1: Evaluation methods for testing head-up display (HUD) flight symbology
[NASA-TM-4665] p 288 N95-24030

- HE, HONGQING**
Simulation on the 3-D turbulent flow in the passages of finocyl grain
[BTN-95-EIX95202638962] p 279 A95-76674
- HEADLEY, DEAN E.**
The airline quality report, 1994
[NIAR-94-11] p 277 N95-24012
- HEBBAR, SHESHAGIRI**
Aerodynamic characteristics of a canard-controlled missile at high angles of attack
[BTN-95-EIX95152583257] p 267 A95-73558
- HEEG, JENNIFER**
Simulation and model reduction for the active flexible wing program
[BTN-95-EIX95182619211] p 295 A95-76637
- HEGEDUS, CHARLES R.**
Organic coating technology for the protection of aircraft against corrosion
p 303 N95-23513
- HEIDA, J. H.**
Eddy current detection of pitting corrosion around fastener holes
p 315 N95-23507
- HEIDT, L. E.**
Estimates of total organic and inorganic chlorine in the lower stratosphere from in situ and flask measurements during AASE 2
[HTN-95-A0861] p 317 A95-76265
- HEINRICH, D. C.**
Effect of underwing frost on a transport aircraft airfoil at flight Reynolds number
[BTN-95-EIX95152582334] p 276 A95-73536
- HEISER, W. H.**
Simulating heat addition via mass addition in constant area compressible flows
[BTN-95-EIX95182619100] p 307 A95-76585
- HENLINE, W. D.**
Hypersonic nonequilibrium Navier-Stokes solutions over an ablating graphite nosetip
[BTN-95-EIX95152583252] p 305 A95-73553
- HERRIN, J. L.**
Supersonic near-wake afterbody boattailing effects on axisymmetric bodies
[BTN-95-EIX95182617465] p 268 A95-75736
- HESS, RONALD A.**
Analysis of the longitudinal handling qualities and pilot-induced-oscillation tendencies of the High-Angle-of-Attack Research Vehicle (HARV)
p 293 N95-23297
- HETU, JEAN-FRANCOIS**
Adaptive finite element method for turbulent flow near a propeller
[BTN-95-EIX95142553038] p 305 A95-73460
- HIGASHINO, FUMIO**
Numerical investigation of supersonic flows around a spiked blunt body
[BTN-95-EIX95212645690] p 271 A95-76742
- HILL, S. D.**
Enhancement of F/A-18 operational flight measurements: Data report for phase 1
[DSTO-TR-0049] p 286 N95-23666
- HINGST, W. R.**
Flow structure in the wake of a wishbone vortex generator
[BTN-95-EIX95142553044] p 304 A95-73454
- HINTSA, E. J.**
In situ observations in aircraft exhaust plumes in the lower stratosphere at midlatitudes
[HTN-95-A0862] p 318 A95-76266
- HOADLEY, SHERWOOD T.**
Multiple-function digital controller system for active flexible wing wind-tunnel model
[BTN-95-EIX95182619212] p 322 A95-76638
On-line analysis capabilities developed to support the active flexible wing wind-tunnel tests
[BTN-95-EIX95182619213] p 296 A95-76639
Rolling maneuver load alleviation using active controls
[BTN-95-EIX95182619217] p 270 A95-76643
- HODGE, B. K.**
Supersonic axisymmetric conical flow solutions for different ratios of specific heats
[BTN-95-EIX95152583283] p 306 A95-73584
- HODGES, DEWEY H.**
Flutter analysis of composite box beams
[NASA-CR-197931] p 294 N95-23392
- HOLLAND, SCOTT D.**
Mach 10 computational study of a three-dimensional scramjet inlet flow field
[NASA-TM-4602] p 309 N95-23015
Mach 10 computational study of a three-dimensional scramjet inlet flow field
[NASA-TM-4602] p 310 N95-23210
- HOPPEL, K. W.**
Statistics of multi-look AIRSAR imagery: A comparison of theory with measurements
p 320 N95-23947
- HOUCK, JACOB**
Simulation and model reduction for the active flexible wing program
[BTN-95-EIX95182619211] p 295 A95-76637
- HSU, SHIH-CHE**
Solutions of generalized proportional navigation with maneuvering and nonmaneuvering targets
[BTN-95-EIX95202637606] p 279 A95-76683
- HSU, WAYNE W.**
CFD analysis of turbopump volutes
p 312 N95-23436
- HUANG, J. R.**
Effect of curvature in the numerical simulation of an electrothermal de-icer pad
[BTN-95-EIX95182619219] p 276 A95-76645
- HUANG, JEN-KUANG**
System identification of the Large-Angle Magnetic Suspension Test Fixture (LAMSTF)
p 296 N95-23299
- HUANG, Q.**
Mechanical system reliability and risk assessment
[BTN-95-EIX95142553046] p 304 A95-73452
- HUBER, F. W.**
Aerodynamic design and analysis of a highly loaded turbine exhaust
p 312 N95-23435
- HUEBNER, L. D.**
Computational study of plume-induced separation on a hypersonic powered model
[BTN-95-EIX95152582346] p 266 A95-73548
- HUGHES, T. C.**
TRISTAR 1: Evaluation methods for testing head-up display (HUD) flight symbology
[NASA-TM-4665] p 288 N95-24030
- HUI, FRANK C. L.**
Experimental results for a hypersonic nozzle/afterbody flow field
[NASA-TM-4638] p 274 N95-23250
- HUI, KENNETH**
Improving prediction: The incorporation of simplified rotor dynamics in a mathematical model of the bell 412HP
[BTN-95-EIX95152584679] p 282 A95-73591
- HUMM, P.**
Evaluation of neutron techniques for illicit substance detection
[DE95-002988] p 300 N95-22764
- HUNT, L. R.**
Nonlinear system guidance in the presence of transmission zero dynamics
[NASA-TM-4661] p 309 N95-22804
- HUNTER, CRAIG A.**
An approximate theoretical method for modeling the static thrust performance of non-axisymmetric two-dimensional convergent-divergent nozzles
[NASA-CR-195050] p 273 N95-23193
- HYMER, T.**
Base drag prediction on missile configurations
[BTN-95-EIX95152583256] p 266 A95-73557
Improved version of the Naval Surface Warfare Center aeroprediction code (AP93)
[BTN-95-EIX95152583260] p 267 A95-73561
- IFJU, PETER G.**
Interlaminar shear test method development for long term durability testing of composites
p 301 N95-23300
- ILINCA, FLORIN**
Adaptive finite element method for turbulent flow near a propeller
[BTN-95-EIX95142553038] p 305 A95-73460
- INGER, GEORGE R.**
Scaling of incipient separation in supersonic/transonic speed laminar flows
[BTN-95-EIX95182619104] p 269 A95-76589
- INGLE, STEVEN J.**
Effects of high order dynamics on helicopter flight control law design
[HTN-95-80852] p 290 A95-75094
- JACKMAN, CHARLES H.**
Sensitivity of two-dimensional model predictions of ozone response to stratospheric aircraft: An update
[HTN-95-A0863] p 318 A95-76267
- JARRABET, G. P.**
Compliant interlayer
[BTN-95-EIX95142562401] p 304 A95-73439
- JENG, YAUG-FAE**
Multiaxis pilot ratings for damaged aircraft
[BTN-95-EIX95182619128] p 269 A95-76605
- JENKINS, L. N.**
A study of the vortex flow over 76/40-deg double-delta wing
[NASA-CR-195032] p 314 N95-23466
- JIN, G.**
Two-equation turbulence model for unsteady separated flows around airfoils
[BTN-95-EIX95142553054] p 262 A95-73444
- JOHNSON, C. G.**
Effects of satellite bunching on the probability of collision in geosynchronous orbit
[BTN-95-EIX95152583276] p 298 A95-73577
- JOHNSON, WALTER A.**
Identification of higher order helicopter dynamics using linear modeling methods
[HTN-95-80851] p 290 A95-75093
- JOHNSON, WALTER J.**
Cueing light configuration for aircraft navigation
[NASA-CASE-ARC-11982-1] p 280 N95-23393
- JOHNSTON, DONALD E.**
Identification of higher order helicopter dynamics using linear modeling methods
[HTN-95-80851] p 290 A95-75093
- JOHNSTON, P. H.**
New nondestructive techniques for the detection and quantification of corrosion in aircraft structures
p 315 N95-23512

K

- KAISER, MARY K.**
Cueing light configuration for aircraft navigation
[NASA-CASE-ARC-11982-1] p 280 N95-23393
- KANDA, HIROSHI**
Flow visualization studies on sidewall effects in two-dimensional transonic airfoil testing
[BTN-95-EIX95152582313] p 264 A95-73516
- KANDEBO, STANLEY W.**
Lycoming to test new engine core
[HTN-95-41393] p 288 A95-76389
Cypher moves toward autonomous flight
[HTN-95-41394] p 283 A95-76390
- KANKAM, M. DAVID**
Motor drive technologies for the power-by-wire (PBW) program: Options, trends and tradeoffs
[NASA-TM-106885] p 295 N95-23671
- KARATSINIDES, SPIRO P.**
Enhancing filter robustness in cascaded GPS-INS integrations
[BTN-95-EIX95142555475] p 278 A95-73435
- KARCHER, B.**
Transport of exhaust products in the near trail of a jet engine under atmospheric conditions
[HTN-95-91421] p 319 A95-77334
- KARIMIAN, S. M. H.**
Application of a control-volume-based finite-element formulation to the shock tube problem
[BTN-95-EIX95182619099] p 295 A95-76584
- KARPALA, F.**
Double pass retroreflection for corrosion detection in aircraft structures
p 323 N95-23503
- KEENER, EARL R.**
Experimental results for a hypersonic nozzle/afterbody flow field
[NASA-TM-4638] p 274 N95-23250
- KEIM, E. R.**
In situ observations in aircraft exhaust plumes in the lower stratosphere at midlatitudes
[HTN-95-A0862] p 318 A95-76266
- KEITH, THEO G., JR.**
Effect of curvature in the numerical simulation of an electrothermal de-icer pad
[BTN-95-EIX95182619219] p 276 A95-76645
- KELLER, JEFFREY D.**
An investigation of helicopter dynamic coupling using an analytical model
[NASA-CR-197420] p 285 N95-23217
- KERN, S. B.**
A study of the vortex flow over 76/40-deg double-delta wing
[NASA-CR-195032] p 314 N95-23466
- KERNIK, ALAN C.**
Guidance and control requirements for high-speed Rollout and Turnoff (ROTO)
[NASA-CR-195026] p 292 N95-22674
- KERR, R.**
NTS-spill test facility wind tunnel exhaust plume characterization
[DE95-003630] p 297 N95-24019
- KERR, S. A.**
Moving mass trim control for aerospace vehicles
[DE95-002602] p 299 N95-23532

KESSLER, G. K.

TRISTAR 1: Evaluation methods for testing head-up display (HUD) flight symbology
[NASA-TM-4665] p 288 N95-24030

KHODADOUST, A.

Aerodynamics of a finite wing with simulated ice
[BTN-95-EIX95182619227] p 270 A95-76653

KHODADOUST, ABDOLLAH

Study of the droplet spray characteristics of a subsonic wind tunnel
[BTN-95-EIX95182619235] p 271 A95-76661

KILGORE, W. ALLEN

Performance of the 0.3-meter transonic cryogenic tunnel with air, nitrogen, and sulfur hexafluoride media under closed loop automatic control
[NASA-CR-195052] p 310 N95-23257

KIM, KYOUNG-HO

Three-dimensional structure of a supersonic jet impinging on an inclined plate
[BTN-95-EIX95152583259] p 267 A95-73560

KIM, S.-W.

A time-accurate finite volume method valid at all flow velocities
p 314 N95-23447

KIM, SEUNG-HO

Static aeroelastic characteristics of a composite wing
[BTN-95-EIX95152582340] p 282 A95-73542

KIM, SUK C.

Numerical analysis of hypersonic low-density scramjet inlet flow
[BTN-95-EIX9512645694] p 272 A95-76746

KIM, W. J.

Influence of streamwise curvature on longitudinal vortices imbedded in turbulent boundary layers
[BTN-94-EIX94401378820] p 307 A95-76489

KINARD, TIM A.

An assessment of viscous effects in computational simulation of benign and burst vortex flows on generic fighter wind-tunnel models using TEAM code
[NASA-CR-4650] p 273 N95-23185

KIRKLAND, LARRY V.

ATE enabling technologies
[BTN-95-EIX95172595294] p 287 A95-75718

KIRKLAND, T. P.

Evolution of oxidation and creep damage mechanisms in HIPed silicon nitride materials
[DE95-001360] p 300 N95-22689

KMETEC, JEFFREY D.

2 micron LIDAR for laser-based remote sensing: Flight demonstration and application survey
[BTN-95-EIX9512641072] p 319 A95-76737

KNOFF, R. E.

Containing military autotest cost growth through the use of commercial standard equipment architectures
[BTN-95-EIX95172595295] p 287 A95-75717

KNOX, E. C.

Determination of wall boundary conditions for high-speed-ratio direct simulation Monte Carlo calculations
[BTN-95-EIX95182617457] p 267 A95-75728

KOENIG, KEITH

Supersonic axisymmetric conical flow solutions for different ratios of specific heats
[BTN-95-EIX95152583283] p 306 A95-73584

KOKUBUN, S.

Polar Patrol Balloon
[BTN-95-EIX95152582318] p 316 A95-73521

KOMOROWSKI, J. P.

Double pass retroreflection for corrosion detection in aircraft structures
p 323 N95-23503

KOO, SAM OK

Numerical study of sound generation due to a spinning vortex pair
[BTN-95-EIX95182619075] p 307 A95-75760

KORTE, J. J.

Optimization of contoured hypersonic scramjet inlets with a least-squares parabolized Navier-Stokes procedure
[HTN-95-20976] p 261 A95-74042

KOUNTZ, JOHN

Effect of leeward flow dividers on the wing rock of a delta wing
[BTN-95-EIX95152582347] p 282 A95-73549

KOUSEN, KENNETH A.

Limit cycle phenomena in computational transonic aeroelasticity
[BTN-95-EIX95152582317] p 264 A95-73520

KOZOL, J.

Corrosion of landing gear steels
p 302 N95-23500

KREMER, JEAN-PAUL

Shuttle entry guidance revisited using nonlinear geometric methods
[BTN-95-EIX95182619144] p 299 A95-76621

KRISHNAKUMAR, S.

Double pass retroreflection for corrosion detection in aircraft structures
p 323 N95-23503

KRISHNAMURTHY, RAMESH

Optimized design of a hypersonic nozzle
p 297 N95-23304

KRISHNAN, C. G.

Some aspects of the aerodynamics of separating strap-ons
[BTN-95-EIX95182617464] p 298 A95-75735

KUBE, ROLAND

Analysis of a higher harmonic control test to reduce blade vortex interaction noise
[BTN-95-EIX95152582330] p 265 A95-73532

KUBO, TRACY S.

2 micron LIDAR for laser-based remote sensing: Flight demonstration and application survey
[BTN-95-EIX9512641072] p 319 A95-76737

KUHLMANN, K. J.

Modeling aerosol emissions from the combustion of composite materials
p 301 N95-23038

KUHN, GARY D.

Aerodynamic design of pegasus: Concept to flight with computational fluid dynamics
[BTN-95-EIX95182617463] p 298 A95-75734

KWEI, G. H.

Phonon characteristics of high (T sub c) superconductors from neutron Doppler broadening measurements
[DE95-003703] p 324 N95-24076

L

LABONTE, S.

Validation of an effective flat cruciform-shaped specimen to study CFRP composite laminates under biaxial loading
[BTN-95-EIX95152584677] p 282 A95-73589

LAFARGE, ROBERT A.

Functional dependence of trajectory dispersion on initial condition errors
[BTN-95-EIX95152583263] p 298 A95-73564

LAFORGE, LEO G.

Overview of AlliedSignal's avionics development in the CIS
[BTN-95-EIX9512641069] p 287 A95-76734

LAI, JONATHAN Y.

Maximum-likelihood spectral estimation and adaptive filtering techniques with application to airborne Doppler weather radar
[NASA-CR-197699] p 316 N95-23670

LAIT, LESLIE R.

Trajectory modeling of emissions from lower stratospheric aircraft
[HTN-95-41219] p 317 A95-75031

LAKSHMINARAYANA, B.

Numerical computation of aerodynamics and heat transfer in a turbine cascade and a turn-around duct using advanced turbulence models
p 313 N95-23444

LALLO, ART

H-76B fantail demonstrator composite fan blade fabrication
[HTN-95-80856] p 283 A95-75098

LAM, T.

Automatic guidance and control for helicopter obstacle avoidance
[BTN-95-EIX95182619130] p 291 A95-76607

LAMB, J. PARKER

Review and development of base pressure and base heating correlations in supersonic flow
[BTN-95-EIX9512645688] p 271 A95-76740

LANSER, WENDY R.

Forebody flow control on a full-scale F/A-18 aircraft
[BTN-95-EIX95152582333] p 281 A95-73535

LAPIN, MARK

Labs behind Boeing's new 777
[BTN-95-EIX95142562403] p 280 A95-73437

LECCE, L.

Structural acoustic calculations in the low-frequency range
[BTN-95-EIX95152582336] p 323 A95-73538

LEE, B. H. K.

Postinstability behavior of a two-dimensional airfoil with a structural nonlinearity
[BTN-95-EIX95152582337] p 266 A95-73539

LEE, DUCK JOO

Numerical study of sound generation due to a spinning vortex pair
[BTN-95-EIX95182619075] p 307 A95-75760

LEE, E. U.

Corrosion of landing gear steels
p 302 N95-23500

LEE, IN

Static aeroelastic characteristics of a composite wing
[BTN-95-EIX95152582340] p 282 A95-73542

LEE, J. S.

Statistics of multi-look AIRSAR imagery: A comparison of theory with measurements
p 320 N95-23947

LEE, JANG GYU

Covariance analysis of strapdown INS considering gyrocompass characteristics
[BTN-95-EIX95202637592] p 279 A95-76697

LEE, KAM-PU

Higher-order viscous shock-layer solutions for high-altitude flows
[BTN-95-EIX95152583255] p 306 A95-73556

LEFEBVRE, D.

Validation of an effective flat cruciform-shaped specimen to study CFRP composite laminates under biaxial loading
[BTN-95-EIX95152584677] p 282 A95-73589

LEOINNE, M.

High-performance parallel analysis of coupled problems for aircraft propulsion
[NASA-CR-197440] p 289 N95-23088

LESIEUTRE, DANIEL J.

Aerodynamic design of pegasus: Concept to flight with computational fluid dynamics
[BTN-95-EIX95182617463] p 298 A95-75734

LEVIN, D.

Dynamic investigation of the angular motion of a rotating body-parachute system
[BTN-95-EIX95182619220] p 270 A95-76646

LIEBST, BRAD S.

Method for the prediction of the onset of wing rock
[BTN-95-EIX95152582342] p 282 A95-73544

LIM, TAE W.

On-line, adaptive state estimator for active noise control
p 322 N95-23308

LIN, CHING-FANG

New failure detection approach and its application to GPS autonomous integrity monitoring
[BTN-95-EIX95202637613] p 279 A95-76676

LIN, I. J.

Sidewash on the vertical tail in subsonic and supersonic flows
[BTN-95-EIX95152582316] p 264 A95-73519

LIN, J.-C.

Transient structure of vortex breakdown on a delta wing
[BTN-95-EIX95182619073] p 268 A95-75758

LIN, JOHN C.

Separation control on high-lift airfoils via micro-vortex generators
[BTN-95-EIX95152582326] p 265 A95-73529

LIN, SHEAM-CHYUN

Integrated design of hypersonic waveriders including inlets and tailfins
[BTN-95-EIX9512645692] p 271 A95-76744

LINTON, SAMUEL W.

Computation of the poststall behavior of a circulation controlled airfoil
[BTN-95-EIX95152582320] p 264 A95-73523

LITNETSKIJ, A. V.

A new generation of instruments for flying laboratories
[BTN-94-EIX94401363947] p 317 A95-75532

LIU, CHING SHI

Analytical study of the neutral stability of a model hypersonic boundary layer
[BTN-95-EIX95152577589] p 263 A95-73493

LIU, YU

Simulation on the 3-D turbulent flow in the passages of finocyl grain
[BTN-95-EIX95202638962] p 279 A95-76674

LO, C. F.

A wall interference assessment/correction system
[NASA-CR-197421] p 309 N95-23183

Supersonic laminar flow control research
[NASA-CR-197938] p 275 N95-23669

LOHMANN, R. P.

In situ observations in aircraft exhaust plumes in the lower stratosphere at midlatitudes
[HTN-95-A0862] p 318 A95-76266

LONEY, NORMAN W.

Design of a variable area diffuser for a 15-inch Mach 6 open-jet tunnel
p 297 N95-23309

LOOS, ALFRED C.

Development and verification of a resin film infusion/resin transfer molding simulation model for fabrication of advanced textile composites
[NASA-CR-197439] p 301 N95-23179

LUCIANI, S.

MAX-91: Polarimetric SAR results on Montespetoli site
p 320 N95-23940

LUO, J.

Numerical computation of aerodynamics and heat transfer in a turbine cascade and a turn-around duct using advanced turbulence models
p 313 N95-23444

LUO, YU-SHAN

Integrated design of hypersonic waveriders including inlets and tailfins
[BTN-95-EIX9512645692] p 271 A95-76744

M

- LUTTGES, MARVIN W.**
Neural network prediction of three-dimensional unsteady separated flowfields
[BTN-95-EIX95182619232] p 308 A95-76658
- LUTZE, FREDERICK H.**
Kinematics and aerodynamics of velocity-vector roll
[BTN-95-EIX95182619126] p 291 A95-76603
- LYNN, J. E.**
Phonon characteristics of high (T sub c) superconductors from neutron Doppler broadening measurements
[DE95-003703] p 324 A95-24076
- MA, DEREN**
A multibody/finite element analysis approach for modeling of crash dynamic responses
[NIAR-94.3] p 277 N95-24050
- MA, JIAJU**
A new type of simulator for simulating the flow-field distortion of engine inlet
[BTN-95-EIX95202638963] p 289 A95-76673
- MACRAE, JOHN DOUGLAS**
Development and verification of a resin film infusion/resin transfer molding simulation model for fabrication of advanced textile composites
[NASA-CR-197439] p 301 N95-23179
- MADENCI, ERDOGAN**
Residual strength of thin panels with cracks
p 311 N95-23311
- MAGDELANEO, RAYMOND E.**
Identification of higher order helicopter dynamics using linear modeling methods
[HTN-95-80851] p 290 A95-75093
- MAGI, V.**
Simulation of transverse gas injection in turbulent supersonic air flows
[BTN-95-EIX95182619080] p 269 A95-75765
- MAH, G. R.**
AVIRIS and TIMS data processing and distribution at the land processes distributed active archive center
p 325 N95-23872
- MAHADEVAN, S.**
Mechanical system reliability and risk assessment
[BTN-95-EIX95142553046] p 304 A95-73452
- MALIK, M. R.**
Comparison of linear stability results with flight transition data
[BTN-95-EIX95182619097] p 283 A95-76582
- MANGO, S. A.**
Statistics of multi-look AIRSAR imagery: A comparison of theory with measurements
p 320 N95-23947
- MANNING, CAROL A.**
The role of flight progress strips in en route air traffic control: A time-series analysis
[DOT/FAA/AM-95/4] p 280 N95-23565
- MANTAY, WAYNE R.**
Integrated aerodynamic/dynamic/structural optimization of helicopter rotor blades using multilevel decomposition
[NASA-TP-3465] p 285 N95-22953
- MARCOLINI, MICHAEL A.**
Sensitivity of acoustic predictions to variation of input parameters
[HTN-95-80855] p 267 A95-75097
- MARGASON, RICHARD J.**
Flow visualization studies of VTOL aircraft models during Hover in ground effect
[NASA-TM-108860] p 272 N95-22666
- MARTIN, M. M.**
Evaluation of neutron techniques for illicit substance detection
[DE95-002988] p 300 N95-22764
- MARTINEZ-VAL, RODRIGO**
Design constraints in the payload-range diagram of ultrahigh capacity transport airplanes
[BTN-95-EIX95152582319] p 276 A95-73522
- MARTINEZ, R.**
The use of cowl camber and taper to reduce rotor/stator interaction noise
[NASA-CR-195421] p 323 N95-22675
- MARULO, F.**
Structural acoustic calculations in the low-frequency range
[BTN-95-EIX95152582336] p 323 A95-73538
- MASAD, J. A.**
Comparison of linear stability results with flight transition data
[BTN-95-EIX95182619097] p 283 A95-76582
- MASON, GREGORY S.**
Multirate flutter suppression system design for a model wing
[BTN-95-EIX95182619132] p 292 A95-76609
- MASON, WILLIAM**
Kinematics and aerodynamics of velocity-vector roll
[BTN-95-EIX95182619126] p 291 A95-76603
- MASSMAN, W. J.**
A comparison of some aerodynamic resistance methods using measurements over cotton and grass from the 1991 California ozone deposition experiment
[HTN-95-11295] p 319 A95-77000
- MATHEW, JOSEPH**
Study of an airfoil with a flap and spoiler
[BTN-95-EIX95152582327] p 265 A95-73530
- MATINELLI, L.**
Multigrid solution of compressible turbulent flow on unstructured meshes using a two-equation model
[BTN-94-EIX94401378794] p 307 A95-76484
- MATSUNO, KENICHI**
Flow visualization studies on sidewall effects in two-dimensional transonic airfoil testing
[BTN-95-EIX95152582313] p 264 A95-73516
- MAURICE, M. S.**
Laser velocimetry seed-particle behavior in shear layers at Mach 12
[BTN-95-EIX95212645712] p 272 A95-76764
- MAVRILIS, D. J.**
Multigrid solution of compressible turbulent flow on unstructured meshes using a two-equation model
[BTN-94-EIX94401378794] p 307 A95-76484
- MCBEE, LARRY S.**
Guidance and control requirements for high-speed Rollout and Turnoff (ROTO)
[NASA-CR-195026] p 292 N95-22674
- MCCLURE, W. B.**
Simulating heat addition via mass addition in constant area compressible flows
[BTN-95-EIX95182619100] p 307 A95-76585
- MCQHUE, R. J.**
Effect of underwing frost on a transport aircraft airfoil at flight Reynolds number
[BTN-95-EIX95152582334] p 276 A95-73536
- MCQHUE, ROBERT J.**
Separation control on high-lift airfoils via micro-vortex generators
[BTN-95-EIX95152582326] p 265 A95-73529
- MCGRAW, SANDRA M.**
Multiple-function digital controller system for active flexible wing wind-tunnel model
[BTN-95-EIX95182619212] p 322 A95-76638
On-line analysis capabilities developed to support the active flexible wing wind-tunnel tests
[BTN-95-EIX95182619213] p 296 A95-76639
- MCINNER, COLIN R.**
Dynamical instability of the aerogravity assist maneuver
[BTN-95-EIX95152583282] p 298 A95-73583
- MCINVILLE, R.**
Improved version of the Naval Surface Warfare Center aeroprediction code (AP93)
[BTN-95-EIX95152583260] p 267 A95-73561
- MCINVILLE, R. M.**
Calculation of wing-alone aerodynamics to high angles of attack
[BTN-95-EIX95212645713] p 261 A95-76765
- MEASE, KENNETH D.**
Shuttle entry guidance revisited using nonlinear geometric methods
[BTN-95-EIX95182619144] p 299 A95-76621
- MEE, D. J.**
Shock tunnel measurements of hypervelocity blunted cone drag
[BTN-95-EIX95152577606] p 305 A95-73477
- MEGGERS, K.**
Phonon characteristics of high (T sub c) superconductors from neutron Doppler broadening measurements
[DE95-003703] p 324 A95-24076
- MEHTA, S.**
Mechanical system reliability and risk assessment
[BTN-95-EIX95142553046] p 304 A95-73452
- MENA, ANDREW C.**
CASS: Design for supportability
[BTN-95-EIX95172595296] p 287 A95-75716
- MENDENHALL, MICHAEL R.**
Aerodynamic design of pegasus: Concept to flight with computational fluid dynamics
[BTN-95-EIX95182617463] p 298 A95-75734
- MENDOZA, JOEL**
Flow study of supersonic wing-nacelle configuration
[BTN-95-EIX95152582344] p 266 A95-73546
- MENGALI, GIOVANNI**
Simulation of turbulent fluctuations
[BTN-95-EIX95142553041] p 304 A95-73457
- MENTER, F. R.**
Computation of oscillating airfoil flows with one- and two-equation turbulence models
[BTN-95-EIX95152577588] p 263 A95-73494
- MERKLE, C. L.**
Convergence acceleration of implicit schemes in the presence of high aspect ratio grid cells
p 313 N95-23446
- MERKLE, CHARLES L.**
Cavitation modeling in Euler and Navier-Stokes codes
[NASA-TM-4661] p 309 N95-22804
- MEYER, G.**
Nonlinear system guidance in the presence of transmission zero dynamics
[NASA-TM-4661] p 309 N95-22804
- MEYER, J. L.**
Fuel-optimal bank-angle control for lunar-return aerocapture
[BTN-95-EIX95212645706] p 299 A95-76758
- MEYN, LARRY A.**
Forebody flow control on a full-scale F/A-18 aircraft
[BTN-95-EIX95152582333] p 281 A95-73535
- MICHEL, MARCO**
Simulation of turbulent fluctuations
[BTN-95-EIX95142553041] p 304 A95-73457
- MICKLICH, B. J.**
Evaluation of neutron techniques for illicit substance detection
[DE95-002988] p 300 N95-22764
- MILLER, GERALD D.**
Summary of an active flexible wing program
[BTN-95-EIX95182619209] p 283 A95-76635
- MILLER, MATT**
Labs behind Boeing's new 777
[BTN-95-EIX95142562403] p 280 A95-73437
- MILNE, A. K.**
AIRSAR deployment in Australia, September 1993: Management and objectives
p 321 N95-23948
- MITCHELTREE, ROBERT A.**
Zonally decoupled direct simulation Monte Carlo solutions of hypersonic blunt-body wake flows
[BTN-95-EIX95182617458] p 268 A95-75729
- MIURA, HIROKAZU**
Static aeroelastic characteristics of a composite wing
[BTN-95-EIX95152582340] p 282 A95-73542
- MOAS, EDUARDO**
An analytical and experimental investigation of the response of the curved, composite frame/skin specimens
[HTN-95-80857] p 283 A95-75099
- MOLLER, PAUL S.**
Evaluation of thermal barrier and PS-200 self-lubricating coatings in an air-cooled rotary engine
[NASA-CR-195445] p 289 N95-23222
- MONTESEDECA, X. A.**
Aerodynamic design and analysis of a highly loaded turbine exhaust
p 312 N95-23435
- MOORE, F. G.**
Base drag prediction on missile configurations
[BTN-95-EIX95152583256] p 266 A95-73557
Improved version of the Naval Surface Warfare Center aeroprediction code (AP93)
[BTN-95-EIX95152583260] p 267 A95-73561
Calculation of wing-alone aerodynamics to high angles of attack
[BTN-95-EIX95212645713] p 261 A95-76765
- MOORE, JOHN**
Supersonic flow and shock formation in turbine tip gaps
p 312 N95-23429
- MOORE, TOM**
Labs behind Boeing's new 777
[BTN-95-EIX95142562403] p 280 A95-73437
- MORE, K. L.**
Evolution of oxidation and creep damage mechanisms in HIPed silicon nitride materials
[DE95-001360] p 300 N95-22689
- MORETTI, S.**
MAX-91: Polarimetric SAR results on Montespertoli site
p 320 N95-23940
- MORRIS, PHILIP J.**
Supersonic jet noise reductions predicted with increased jet spreading rate
[NASA-TM-106872] p 323 N95-23178
- MORSE, CORINNE S.**
Real-time estimation of atmospheric turbulence severity from in-situ aircraft measurements
[BTN-95-EIX95182619231] p 319 A95-76657
- MOSS, JAMES M.**
Hypersonic rarefied flow past spheres including wake structure
[BTN-95-EIX95152583250] p 305 A95-73551
Zonally decoupled direct simulation Monte Carlo solutions of hypersonic blunt-body wake flows
[BTN-95-EIX95182617458] p 268 A95-75729
- MOURTOS, NIKOS J.**
Flow visualization studies of VTOL aircraft models during Hover in ground effect
[NASA-TM-108860] p 272 N95-22666

- MOUSTAFA, GAMAL H.**
Main features of overexpanded triple jets
[BTN-95-EIX95142553040] p 304 A95-73458
- MULLENBURG, DENNIS A.**
Euler technology assessment for preliminary aircraft design employing OVERFLOW code with multiblock structured-grid method
[NASA-CR-4651] p 273 N95-23095
- MUKHOPADHYAY, VIVEK**
Flutter suppression control law design and testing for the active flexible wing
[BTN-95-EIX95182619214] p 292 A95-76640
- MUNOZ, TOMAS**
Design constraints in the payload-range diagram of ultrahigh capacity transport airplanes
[BTN-95-EIX95152582319] p 276 A95-73522
- MYERS, J.**
AVIRIS and TIMS data processing and distribution at the land processes distributed active archive center
p 325 N95-23872

N

- NAGAMATSU, HENRY T.**
Numerical analysis of hypersonic low-density scramjet inlet flow
[BTN-95-EIX95212645694] p 272 A95-76746
- NAMKUNG, M.**
New nondestructive techniques for the detection and quantification of corrosion in aircraft structures
p 315 N95-23512
- NASH, KYLE L.**
Predicting exhaust plume boundaries with supersonic external flows
[BTN-95-EIX95152583258] p 297 A95-73559
- NAYANI, SUDHEER N.**
Higher-order viscous shock-layer solutions for high-altitude flows
[BTN-95-EIX95152583255] p 306 A95-73556
- NEIGHBORS, KEN**
Integrated flight/propulsion control for helicopters
[HTN-95-80854] p 290 A95-75096
- NELSON, H. F.**
Wing vertical position effects on wing-body carryover for noncircular missiles
[BTN-95-EIX95182617462] p 268 A95-75733
- NEWMAN, BRETT**
Aeroelastic vehicle multivariable control synthesis with analytical robustness evaluation
[BTN-95-EIX95182619115] p 321 A95-76592
Multivariable stability and robustness of sequentially designed feedback systems
[BTN-95-EIX95182619125] p 322 A95-76602
- NEWMAN, BRETT A.**
Inner loop flight control for the High-Speed Civil Transport
p 293 N95-23314
- NEWMAN, PAUL A.**
Trajectory modeling of emissions from lower stratospheric aircraft
[HTN-95-41219] p 317 A95-75031
- NEWMAN, R. L.**
TRISTAR 1: Evaluation methods for testing head-up display (HUD) flight symbology
[NASA-TM-4665] p 288 N95-24030
- NEWSOME, J. R.**
Measurement of moisture and total hydrocarbon contributions by valves used in clean room gas-delivery systems
[BTN-94-EIX94381359041] p 295 A95-74629
- NG, T. TERRY**
Effect of leeward flow dividers on the wing rock of a delta wing
[BTN-95-EIX95152582347] p 282 A95-73549
- NICOLAS, JEAN**
Coupled FEM-BEM approach for mean flow effects on vibro-acoustic behavior of planar structures
[BTN-95-EIX95152577587] p 263 A95-73495
- NIESER, DONALD E.**
Oklahoma City air logistics center (USAF) aging aircraft corrosion program
p 262 N95-23519
- NIESL, GEORG H.**
Analysis of a higher harmonic control test to reduce blade vortex interaction noise
[BTN-95-EIX95152582330] p 265 A95-73532
- NISHIMURA, JUN**
Polar Patrol Balloon
[BTN-95-EIX95152582318] p 316 A95-73521
- NOLAN, ROBERT C.**
Method for the prediction of the onset of wing rock
[BTN-95-EIX95152582342] p 282 A95-73544
- NOWOBILSKI, J. J.**
Airborne rotary air separator study
[NASA-CR-189099] p 290 N95-24053

- NUHAIT, A. O.**
Stability derivatives of a flapped plate in unsteady ground effect
[BTN-95-EIX95182619225] p 270 A95-76651
Unsteady ground effects on aerodynamic coefficients of finite wings with camber
[BTN-95-EIX95182619233] p 271 A95-76659
- NURICK, ALAN**
Static pressure distribution in the inlet of a helicopter turbine compressor
[BTN-95-EIX95152582339] p 266 A95-73541
Erosion of dust-filtered helicopter turbine engines. Part 1: Basic theoretical considerations
[BTN-95-EIX95182619222] p 288 A95-76648
Erosion of dust-filtered helicopter turbine engines. Part 2: Erosion reduction
[BTN-95-EIX95182619223] p 289 A95-76649
Life prediction of helicopter engines fitted with dust filters
[BTN-95-EIX95182619224] p 289 A95-76650

O

- OBERRAMPF, WILLIAM L.**
Review and development of base pressure and base heating correlations in supersonic flow
[BTN-95-EIX95212645688] p 271 A95-76740
- OEZBAY, HITAY**
Stable H(infinity) controller design for the longitudinal dynamics of an aircraft
[NASA-TM-106847] p 293 N95-22954
- OLSON, JOHN M.**
Mishap risk control for advanced aerospace/composite materials
p 301 N95-23031
- OLSSON, ERIK**
Turbulent transonic airfoil flow simulation using a pressure-based algorithm
[BTN-95-EIX95182619078] p 269 A95-75763
- OMAN, HENRY**
New commercial off-the-shelf testers are automatic and intelligent
[BTN-95-EIX95172595292] p 287 A95-75720
- ONCLEY, S. P.**
A comparison of some aerodynamic resistance methods using measurements over cotton and grass from the 1991 California ozone deposition experiment
[HTN-95-11295] p 319 A95-77000
- ORKWIS, PAUL D.**
Observations on using experimental data as boundary conditions for computations
[BTN-95-EIX95182619103] p 321 A95-76588
- OYEDIRAN, AYO**
Sensitivity of combustion-acoustic instabilities to boundary conditions for premixed gas turbine combustors
[NASA-TM-106890] p 289 N95-23550
- OZCAN, O.**
Aerodynamic characteristics of external store configurations at low speeds
[BTN-95-EIX95182619230] p 271 A95-76656

P

- PACHTER, M.**
Automatic formation flight control
[BTN-95-EIX95182619153] p 292 A95-76630
- PADRO, J.**
A comparison of some aerodynamic resistance methods using measurements over cotton and grass from the 1991 California ozone deposition experiment
[HTN-95-11295] p 319 A95-77000
- PAL, A. K.**
Simple method of supersonic flow visualization using watertable
[BTN-95-EIX95182619105] p 269 A95-76590
- PALOSCIA, S.**
MAX-91: Polarimetric SAR results on Montespetoli site
[BTN-95-EIX95202637592] p 320 N95-23940
- PARIKH, PARESH**
Unstructured grid solutions to a wing/pylon/store configuration
[BTN-95-EIX95152582322] p 265 A95-73525
- PARK, CHAN GOOK**
Covariance analysis of strapdown INS considering gyrocompass characteristics
[BTN-95-EIX95202637592] p 279 A95-76697
- PARK, HEUNG WON**
Covariance analysis of strapdown INS considering gyrocompass characteristics
[BTN-95-EIX95202637592] p 279 A95-76697
- PARK, JAI H.**
Growth of multiple cracks and their linkup in a fuselage lap joint
[BTN-95-EIX95142553047] p 286 A95-73451

- PARSONS, B.**
Geoid lineations of 1000 km wavelength over the central Pacific
[HTN-95-11304] p 319 A95-77009
- PATEL, BHAVESH B.**
Supersonic axisymmetric conical flow solutions for different ratios of specific heats
[BTN-95-EIX95152583283] p 306 A95-73584
- PATEL, V. C.**
Influence of streamwise curvature on longitudinal vortices imbedded in turbulent boundary layers
[BTN-94-EIX94401378820] p 307 A95-76489
- PAULL, A.**
Shock tunnel measurements of hypervelocity blunted cone drag
[BTN-95-EIX95152577606] p 305 A95-73477
- PAUSDER, HEINZ-JURGEN**
Investigation of the effects of bandwidth and time delay on helicopter roll-axis handling qualities
[HTN-95-80853] p 290 A95-75095
- PELLETIER, DOMINIQUE**
Adaptive finite element method for turbulent flow near a propeller
[BTN-95-EIX95142553038] p 305 A95-73460
- PENG, CHENGYI**
A new type of simulator for simulating the flow-field distortion of engine inlet
[BTN-95-EIX95202638963] p 289 A95-76673
- PEREZ, EMILIO**
Design constraints in the payload-range diagram of ultrahigh capacity transport airplanes
[BTN-95-EIX95152582319] p 276 A95-73522
- PERIASAMY, R.**
Measurement of particle emissions from clean room gas-handling components
[BTN-94-EIX94381359040] p 295 A95-74554
Measurement of moisture and total hydrocarbon contributions by valves used in clean room gas-delivery systems
[BTN-94-EIX94381359041] p 295 A95-74629
- PERRY, BOYD, III**
Summary of an active flexible wing program
[BTN-95-EIX95182619209] p 283 A95-76635
- PEZZULLO, G.**
Structural acoustic calculations in the low-frequency range
[BTN-95-EIX95152582336] p 323 A95-73538
- PIRZADEH, SHAHYAR**
Unstructured grid solutions to a wing/pylon/store configuration
[BTN-95-EIX95152582322] p 265 A95-73525
- PITARI, G.**
Possible effects of CO2 increase on the high-speed civil transport impact on ozone
[HTN-95-60779] p 317 A95-75976
- PLATZER, MAX F.**
Aerodynamic characteristics of a canard-controlled missile at high angles of attack
[BTN-95-EIX95152583257] p 267 A95-73558
Viscous-inviscid interaction method for unsteady low-speed airfoil flows
[BTN-95-EIX95182619093] p 269 A95-75778
- PLETCHER, RICHARD H.**
Application of wall functions to generalized nonorthogonal curvilinear coordinate systems
[BTN-95-EIX95182619077] p 307 A95-75762
- POLLACK, W. H.**
Estimates of total organic and inorganic chlorine in the lower stratosphere from in situ and flask measurements during AASE 2
[HTN-95-A0861] p 317 A95-76265
- PONTON, MICHAEL K.**
Mach wave emission from a high-temperature supersonic jet
[BTN-95-EIX95152577586] p 264 A95-73496
- POOR, WALTER A.**
Description of a GNSS availability model and its use in developing requirements
[BTN-95-EIX95202637603] p 308 A95-76686
- POPERNACK, T. G., JR.**
Dynamic response tests of inertial and optical wind-tunnel model attitude measurement devices
[NASA-TM-109182] p 296 N95-23011
- PORTER, L. M.**
Shock tunnel measurements of hypervelocity blunted cone drag
[BTN-95-EIX95152577606] p 305 A95-73477
- POTOTZKY, ANTHONY S.**
Rolling maneuver load alleviation using active controls
[BTN-95-EIX95182619217] p 270 A95-76643
- POURBAIX, A.**
In-situ detection of surface passivation or activation and of localized corrosion: Experiences and perspectives in aircraft
p 302 N95-23508
Test method and test results for environmental assessment of aircraft materials
p 302 N95-23509

- PRABHU, B. S.**
Transient analysis of a cracked rotor passing through critical speed
[BTN-94-EIX94401360022] p 306 A95-74702
- PRESTON, ORV W.**
Guidance and control requirements for high-speed Rollout and Turnoff (ROTO)
[NASA-CR-195026] p 292 N95-22674
- PRICE, JOSEPH M.**
Hypersonic rarefied flow past spheres including wake structure
[BTN-95-EIX95152583250] p 305 A95-73551
- PRICE, S. J.**
Postinstability behavior of a two-dimensional airfoil with a structural nonlinearity
[BTN-95-EIX95152582337] p 266 A95-73539
- PRITCHARD, JOCELYN I.**
Integrated aerodynamic/dynamic/structural optimization of helicopter rotor blades using multilevel decomposition
[NASA-TP-3465] p 285 N95-22953
- R**
- RADHAKRISHNAN, KRISHNAN**
Sensitivity of combustion-acoustic instabilities to boundary conditions for premixed gas turbine combustors
[NASA-TM-106890] p 289 N95-23550
- RAINWATER, B. A.**
Moving mass trim control for aerospace vehicles
[DE95-002602] p 299 N95-23532
- RAIS-ROHANI, MASOUD**
Thin tailored composite wing for civil tiltrotor
p 285 N95-23317
- RAJ, PRADEEP**
An assessment of viscous effects in computational simulation of benign and burst vortex flows on generic fighter wind-tunnel models using TEAM code
[NASA-CR-4650] p 273 N95-23185
- RANGWALLA, AKIL A.**
Three-dimensional unsteady flow calculations in an advanced gas generator turbine
p 312 N95-23425
- RANKIN, JAMES M.**
Differential GPS and system integration of the Low Visibility Landing and Surface Operations (LVLASO) demonstration
p 280 N95-23318
- RAO, DHANVADA M.**
Pneumatic concept for tip-stall control of cranked-arrow wings
[BTN-95-EIX95152582335] p 281 A95-73537
- RAULT, DIDIER F. G.**
Aerodynamic characteristics of a hypersonic viscous optimized waverider at high altitudes
[BTN-95-EIX95152583251] p 266 A95-73552
Aerodynamics of the Shuttle Orbiter at high altitudes
[BTN-95-EIX95182617454] p 298 A95-75725
- RAVINDRA, KRISHNASWAMY**
Preliminary identification of buffet problems in high speed civil transport
p 294 N95-23319
- RAVINDRABABU, K.**
Switched bias proportional navigation for homing guidance against highly maneuvering targets
[BTN-95-EIX95182619145] p 279 A95-76622
- RAWLINGS, J.**
NTS-spill test facility wind tunnel exhaust plume characterization
[DE95-003630] p 297 N95-24019
- READER, KENNETH R.**
An unmanned air vehicle concept with tipjet drive
[HTN-95-80858] p 283 A95-75100
- REDDY, T. S. R.**
User's guide for ECAP2D: An Euler unsteady aerodynamic and aeroelastic analysis program for two dimensional oscillating cascades, version 1.0
[NASA-CR-189146] p 316 N95-24189
- REHFIELD, LAWRENCE W.**
Experimental evaluation of a box beam specifically tailored for chordwise deformation
[BTN-95-EIX95182619088] p 283 A95-75773
- RHOADES, R. L.**
Cu deposition using a permanent magnet electron cyclotron resonance microwave plasma source
[DE94-017768] p 304 N95-23981
- RICHARDS, MICHAEL A.**
SEM representation of the early and late time fields scattered from wire targets
[BTN-94-EIX94381353142] p 306 A95-74496
- RIDDICK, J. C.**
Minimum-mass design of sandwich aerobrakes for a lunar transfer vehicle
[BTN-95-EIX95212645707] p 299 A95-76759
- RIDDLE, J.**
Measurement of particle emissions from clean room gas-handling components
[BTN-94-EIX94381359040] p 295 A95-74554
Measurement of moisture and total hydrocarbon contributions by valves used in clean room gas-delivery systems
[BTN-94-EIX94381359041] p 295 A95-74629
- ROACH, LISA K.**
Rationale for the Modular Air-system Vulnerability Estimation Network (MAVEN) methodology
[AD-A285797] p 284 N95-22510
- ROBINETT, R. D.**
Moving mass trim control for aerospace vehicles
[DE95-002602] p 299 N95-23532
- ROBINSON, STEPHEN K.**
Separation control on high-lift airfoils via micro-vortex generators
[BTN-95-EIX95152582326] p 265 A95-73529
- ROBSON, J.**
NTS-spill test facility wind tunnel exhaust plume characterization
[DE95-003630] p 297 N95-24019
- ROCHE, NIGEL R.**
Automatic riveting cell for commercial aircraft floor grid assembly
[BTN-95-EIX95182617807] p 261 A95-75752
- ROCK, STEPHEN M.**
Integrated light/pulsation control for helicopters
[HTN-95-80854] p 290 A95-75096
- ROCKWELL, D.**
Transient structure of vortex breakdown on a delta wing
[BTN-95-EIX95182619073] p 268 A95-75758
- ROGERS, ERNEST O.**
An unmanned air vehicle concept with tipjet drive
[HTN-95-80858] p 283 A95-75100
- ROGERS, STUART E.**
Progress in high-lift aerodynamic calculations
[BTN-95-EIX95152582315] p 264 A95-73518
- ROJAS, L.**
Impeller flow field characterization with a laser two-focus velocimeter
p 313 N95-23440
- ROMEO, GIULIO**
Nonlinear angle of twist of advanced composite wing boxes under pure torsion
[BTN-95-EIX95152582323] p 281 A95-73526
- ROOP, J. A.**
Modeling aerosol emissions from the combustion of composite materials
p 301 N95-23038
- ROSEN, A.**
The influence of alternate inter-blade connections on ground resonance
[HTN-95-80859] p 267 A95-75101
- ROSENFELD, MOSHE**
Grid refinement test of time-periodic flows over bluff bodies
[BTN-94-EIX94401378822] p 307 A95-76491
- ROSS, JAMES C.**
Lift enhancing tabs for airfoils
[NASA-Case-ARC-11990-1] p 286 N95-23395
- ROWEY, R. J.**
Aerodynamic design and analysis of a highly loaded turbine exhaust
p 312 N95-23435
- ROY, C.**
Validation of an effective flat cruciform-shaped specimen to study CFRP composite laminates under biaxial loading
[BTN-95-EIX95152584677] p 282 A95-73589
- RUBLEIN, GEORGE T.**
Preparation of course materials: Elementary mathematics of powered flight
p 324 N95-23320
- RYAN, GEORGE W., III**
Functional agility metrics and optimal trajectory analysis
[BTN-95-EIX95182619121] p 321 A95-76598
- S**
- SAGALOVSKY, L.**
Evaluation of neutron techniques for illicit substance detection
[DE95-002988] p 300 N95-22764
- SAMIMY, MO**
Effects of expansions on a supersonic boundary layer: Surface pressure measurements
[BTN-95-EIX95142553036] p 263 A95-73462
- SANDERS, DONALD C.**
Aircraft fires, smoke toxicity, and survival: An overview
[DOT/FAA/AM-95/8] p 277 N95-24024
- SARMA, I. G.**
Switched bias proportional navigation for homing guidance against highly maneuvering targets
[BTN-95-EIX95182619145] p 279 A95-76622
- SATO, MAMORU**
Flow visualization studies on sidewall effects in two-dimensional transonic airfoil testing
[BTN-95-EIX95152582313] p 264 A95-73516
- SAUNDERS, C. P.**
Collaborative research on aircraft icing and charging processes in ice
[AD-A285102] p 276 N95-23201
- SCHAB, DANIEL E.**
Drag function modeling for air traffic simulation
[BTN-95-EIX95182619154] p 279 A95-76631
- SCHAFER, T.**
NTS-spill test facility wind tunnel exhaust plume characterization
[DE95-003630] p 297 N95-24019
- SCHAUFFLER, S. M.**
Estimates of total organic and inorganic chlorine in the lower stratosphere from in situ and flask measurements during AASE 2
[HTN-95-A0861] p 317 A95-76265
- SCHEIMAN, DAVID A.**
Design of a GaAs/Ge solar array for unmanned aerial vehicles
[NASA-TM-106870] p 320 N95-23259
- SCHIAVON, G.**
MAX-91: Polarimetric SAR results on Montespertoli site
p 320 N95-23940
- SCHILLING, HARTMUT**
Analytical solution and parameter estimation of projectile dynamics
[BTN-95-EIX95212645695] p 272 A95-76747
- SCHMIDT, DAVID K.**
Aeroelastic vehicle multivariable control synthesis with analytical robustness evaluation
[BTN-95-EIX95182619115] p 321 A95-76592
Multivariable stability and robustness of sequentially designed feedback systems
[BTN-95-EIX95182619125] p 322 A95-76602
Analytical aeropropulsive/aeroelastic hypersonic-vehicle model with dynamic analysis
[BTN-95-EIX95182619138] p 269 A95-76615
- SCHMISSEUR, J. D.**
Laser velocimetry seed-particle behavior in shear layers at Mach 12
[BTN-95-EIX95212645712] p 272 A95-76764
- SCHNEIDER, G. E.**
Application of a control-volume-based finite-element formulation to the shock tube problem
[BTN-95-EIX95182619099] p 295 A95-76584
- SCHOEBERL, MARK R.**
Trajectory modeling of emissions from lower stratospheric aircraft
[HTN-95-41219] p 317 A95-75031
- SCHRECK, SCOTT J.**
Neural network prediction of three-dimensional unsteady separated flowfields
[BTN-95-EIX95182619232] p 308 A95-76658
- SCHULTZ, KLAUS-J.**
Analysis of a higher harmonic control test to reduce blade vortex interaction noise
[BTN-95-EIX95152582330] p 265 A95-73532
- SCHUSTER, DAVID M.**
Application of Navier-Stokes aeroelastic methods to improve fighter wing maneuver performance
[BTN-95-EIX95182619218] p 284 A95-76644
- SCHUTZ, BOB E.**
Thermal force modeling for global positioning system satellites using the finite element method
[BTN-95-EIX95152583270] p 278 A95-73571
- SCHWARTZ, ALAN W.**
An unmanned air vehicle concept with tipjet drive
[HTN-95-80858] p 283 A95-75100
- SCOTT, A. D., JR.**
Compendium of NASA data base for the Global Tropospheric Experiment's Pacific Exploratory Mission West-A (PEM West-A)
[NASA-TM-109177] p 320 N95-23009
- SEINER, JOHN M.**
Mach wave emission from a high-temperature supersonic jet
[BTN-95-EIX95152577586] p 264 A95-73496
- SEKHAR, A. S.**
Transient analysis of a cracked rotor passing through critical speed
[BTN-94-EIX94401360022] p 306 A95-74702
- SELA, N. M.**
The influence of alternate inter-blade connections on ground resonance
[HTN-95-80859] p 267 A95-75101
- SENYITKO, RICHARD G.**
NASA low-speed axial compressor for fundamental research
[NASA-TM-4635] p 296 N95-23192
- SEREGIN, YU. A.**
A new generation of instruments for flying laboratories
[BTN-94-EIX94401363947] p 317 A95-75532

- SETH, SHASHI**
Pilot Weather Advisor system
[BTN-95-EIX95152582314] p 316 A95-73517
- SGARD, FRANCK**
Coupled FEM-BEM approach for mean flow effects on vibro-acoustic behavior of planar structures
[BTN-95-EIX95152577587] p 263 A95-73495
- SHABIBI, ABDULLAH AL**
Study of an airfoil with a flap and spoiler
[BTN-95-EIX95152582327] p 265 A95-73530
- SHAW, R. H.**
A comparison of some aerodynamic resistance methods using measurements over cotton and grass from the 1991 California ozone deposition experiment
[HTN-95-11295] p 319 A95-77000
- SHERWOOD, BRENT**
Fourth-generation Mars vehicle concepts
[BTN-95-EIX95152583267] p 298 A95-73568
- SHIH, MING H.**
TIGER: A user-friendly interactive grid generation system for complicated turbomachinery and axis-symmetric configurations
p 322 N95-23419
- SHIVAKUMAR, K. N.**
Minimum-mass design of sandwich aerobrakes for a lunar transfer vehicle
[BTN-95-EIX9512645707] p 299 A95-76759
- SHPUND, Z.**
Dynamic investigation of the angular motion of a rotating body-parachute system
[BTN-95-EIX95182619220] p 270 A95-76646
- SIGSMONDI, S.**
MAX-91: Polarimetric SAR results on Montespetoli site
p 320 N95-23940
- SILVA, WALTER A.**
Application of transonic small disturbance theory to the active flexible wing model
[BTN-95-EIX95182619210] p 270 A95-76636
- SILVERBERG, L.**
Fuel-optimal bank-angle control for lunar-return aerocapture
[BTN-95-EIX9512645706] p 299 A95-76758
- SIMMONS, J. M.**
Shock tunnel measurements of hypervelocity blunted cone drag
[BTN-95-EIX95152577606] p 305 A95-73477
- SIMON, DAN**
Real-time navigation using the global positioning system
[BTN-95-EIX95172595298] p 279 A95-75714
- SIMPSON, DAVID L.**
Multiple site fatigue damage in fuselage skin splices: Experimental simulation and theoretical prediction
[BTN-95-EIX95152584676] p 276 A95-73588
- SINGH, RIPUDAMAN**
Growth of multiple cracks and their linkup in a fuselage lap joint
[BTN-95-EIX95142553047] p 286 A95-73451
- SIRBAUGH, J. R.**
Three-dimensional Navier-Stokes analysis and redesign of an imbedded bellmouth nozzle in a turbine cascade inlet section
p 311 N95-23423
- SKAFF, TONY**
Effect of leeward flow dividers on the wing rock of a delta wing
[BTN-95-EIX95152582347] p 282 A95-73549
- SKINNER, K. A.**
Time-of-flight mass spectrometer for impulse facilities
[BTN-95-EIX95142553057] p 262 A95-73441
- SMART, J. D.**
Health and usage monitoring systems: Corrosion surveillance
p 262 N95-23506
- SMITH, C. J. E.**
The corrosion and protection of advanced aluminium - lithium airframe alloys
p 302 N95-23497
- SMITH, D.**
NTS-spill test facility wind tunnel exhaust plume characterization
[DE95-003630] p 297 N95-24019
- SMITH, EDMUND H.**
Aerodynamic characteristics of a canard-controlled missile at high angles of attack
[BTN-95-EIX95152583257] p 267 A95-73558
- SOLIS, U. PETER**
Handling qualities of the High Speed Civil Transport
p 294 N95-23325
- SOLOMON, S.**
Estimates of total organic and inorganic chlorine in the lower stratosphere from in situ and flask measurements during AASE 2
[HTN-95-A0861] p 317 A95-76265
- SONDAK, DOUGLAS L.**
Application of wall functions to generalized nonorthogonal curvilinear coordinate systems
[BTN-95-EIX95182619077] p 307 A95-75762

- SONI, BHARAT K.**
TIGER: A user-friendly interactive grid generation system for complicated turbomachinery and axis-symmetric configurations
p 322 N95-23419
- SPADAFORA, STEPHEN J.**
Organic coating technology for the protection of aircraft against corrosion
p 303 N95-23513
- SPAUD, FRANK W.**
Experimental results for a hypersonic nozzle/afterbody flow field
[NASA-TM-4638] p 274 N95-23250
- SPARLING, LYNN C.**
Trajectory modeling of emissions from lower stratospheric aircraft
[HTN-95-41219] p 317 A95-75031
- SPENCE, ANNE MARIE**
Efficient sensitivity analysis for rotary-wing aeromechanical problems
[BTN-95-EIX95152577585] p 264 A95-73497
- SPENCER, JOHN H.**
1994 NASA-HU American Society for Engineering Education (ASCE) Summer Faculty Fellowship Program
[NASA-CR-194972] p 325 N95-23276
- SPLETTSTOEGER, WOLF R.**
Analysis of a higher harmonic control test to reduce blade vortex interaction noise
[BTN-95-EIX95152582330] p 265 A95-73532
- SRINATHKUMAR, S.**
Flutter suppression for the active flexible wing: A classical design
[BTN-95-EIX95182619216] p 292 A95-76642
- SRINIVASAN, RAMAKRISHNA**
Flutter of an infinitely long panel in a duct
[BTN-95-EIX95182619087] p 291 A95-75772
- STALKER, R. J.**
Time-of-flight mass spectrometer for impulse facilities
[BTN-95-EIX95142553057] p 262 A95-73441
- STEELE, L. L.**
Phase 2: HGM air flow tests in support of HEX vane investigation
p 312 N95-23438
- STERN, P.**
High-performance parallel analysis of coupled problems for aircraft propulsion
[NASA-CR-197440] p 289 N95-23088
- STEWART, D. A.**
Hypersonic convective heat transfer over 140-deg blunt cones in different gases
[BTN-95-EIX95152583253] p 306 A95-73554
- STEWART, JAMES F.**
Engines-only flight control system
[NASA-CASE-ARC-11944-1] p 294 N95-23389
- STRAZNICKY, PAUL V.**
Multiple site fatigue damage in fuselage skin splices: Experimental simulation and theoretical prediction
[BTN-95-EIX95152584676] p 276 A95-73588
- STREBY, OLIVIER**
Analysis of a higher harmonic control test to reduce blade vortex interaction noise
[BTN-95-EIX95152582330] p 265 A95-73532
- SU, R.**
Nonlinear system guidance in the presence of transmission zero dynamics
[NASA-TM-4661] p 309 N95-22804
- SUDANI, NORIKAZU**
Flow visualization studies on sidewall effects in two-dimensional transonic airfoil testing
[BTN-95-EIX95152582313] p 264 A95-73516
- SUGIYAMA, N.**
Derivation of system matrices from nonlinear dynamic simulation of jet engines
[BTN-95-EIX95182619139] p 288 A95-76616
- SUN, WEN-YIH**
Diurnal variation of lee vortices in Taiwan and the surrounding area
[HTN-95-91363] p 318 A95-76394
- SWAIM, ROBERT L.**
Multi-axis pilot ratings for damaged aircraft
[BTN-95-EIX95182619128] p 269 A95-76605
- SWAMY, K. N.**
Switched bias proportional navigation for homing guidance against highly maneuvering targets
[BTN-95-EIX95182619145] p 279 A95-76622
- TAKAHASHI, MARC D.**
H-infinity helicopter flight control law design with and without rotor state feedback
[BTN-95-EIX95182619129] p 291 A95-76606
- TAKALLU, M. A.**
Wing pressure distributions from subsonic tests of a high-wing transport model
[NASA-TM-4583] p 272 N95-22802

- TAM, CHUNG-JEN**
Observations on using experimental data as boundary conditions for computations
[BTN-95-EIX95182619103] p 321 A95-76588
- TANG, D. M.**
Response of a nonrotating rotor blade to lateral turbulence. Part 1: Theory
[BTN-95-EIX95182619228] p 284 A95-76654
- TANG, D. M.**
Response of a nonrotating rotor blade to lateral turbulence. Part 2: Experiment
[BTN-95-EIX95182619229] p 284 A95-76655
- TAPLEY, I. J.**
AIRSAR deployment in Australia, September 1993: Management and objectives
p 321 N95-23948
- TAYLOR, A. G.**
Finite element model for a flexible non-symmetric rotor on distributed bearing: A stability study
[BTN-95-EIX94381352212] p 306 A95-74612
- TCHENG, P.**
Dynamic response tests of inertial and optical wind-tunnel model attitude measurement devices
[NASA-TM-109182] p 296 N95-23011
- THART, W. G. J.**
Eddy current detection of pitting corrosion around fastener holes
p 315 N95-23507
- THIELE, F.**
Laplace interaction law for the computation of viscous airfoil flow in low- and high-speed aerodynamics
[BTN-95-EIX95142553037] p 263 A95-73461
- TONEV, PETER T.**
Thundercloud electric field modeling for the ionosphere-Earth region. 1: Dependence on cloud charge distribution
[HTN-95-41223] p 317 A95-75035
- TRAN, KEN**
CFD analysis of turbopump volutes
p 312 N95-23436
- TRAUB, LANCE W.**
Analytic prediction of lift for delta wings with partial leading-edge thrust
[BTN-95-EIX95152582345] p 266 A95-73547
- TREGO, LINDA E.**
Maintenance challenges and trends
[BTN-95-EIX95182617808] p 261 A95-75753
- TREGO, LINDA E.**
Maintenance programs
[BTN-95-EIX95182617809] p 261 A95-75754
- TREGO, LINDA E.**
Aircraft stripping and painting
[BTN-95-EIX95182617810] p 300 A95-75755
- TREIBER, DAVID A.**
Euler technology assessment for preliminary aircraft design employing OVERFLOW code with multiblock structured-grid method
[NASA-CR-4651] p 273 N95-23095
- TRELA, W. J.**
Phonon characteristics of high (T sub c) superconductors from neutron Doppler broadening measurements
[DE95-003703] p 324 N95-24076
- TRIPP, J. S.**
Dynamic response tests of inertial and optical wind-tunnel model attitude measurement devices
[NASA-TM-109182] p 296 N95-23011
- TROSHCHENKO, V. T.**
Fatigue strength of high-temperature alloys under conditions of cyclic temperature variation. Communication 1: Experimental procedure and results
[BTN-94-EIX94401363884] p 307 A95-75516
- TUCKER, P. KEVIN**
Validation of a Computational Fluid Dynamics (CFD) code for supersonic axisymmetric base flow
p 315 N95-23652
- TUNCER, ISMAIL H.**
Viscous-inviscid interaction method for unsteady low-speed airfoil flows
[BTN-95-EIX95182619093] p 269 A95-75778
- U**
- UNAL, M. F.**
Aerodynamic characteristics of external store configurations at low speeds
[BTN-95-EIX95182619230] p 271 A95-76656
- V**
- VALAREZO, W. O.**
Effect of underwing frost on a transport aircraft airfoil at flight Reynolds number
[BTN-95-EIX95152582334] p 276 A95-73536
- VALAREZO, WALTER O.**
Separation control on high-lift airfoils via micro-vortex generators
[BTN-95-EIX95152582326] p 265 A95-73529

VALAVANI, LENA

Design of high performance multivariable control systems for supermaneuverable aircraft at high angle of attack
[NASA-CR-197661] p 293 N95-22908

VALENTINE, JAMES R.

Tracking of raindrops in flow over an airfoil
[BTN-95-EIX95182619221] p 308 A95-76647

VANDAM, CORNELIS P.

High-lift flow-physics flight experiments on a subsonic civil transport aircraft (B737-100) p 275 N95-23333

VANDERWALT, JOHANNES P.

Static pressure distribution in the inlet of a helicopter turbine compressor
[BTN-95-EIX95152582339] p 266 A95-73541
Erosion of dust-filtered helicopter turbine engines. Part 1: Basic theoretical considerations
[BTN-95-EIX95182619222] p 288 A95-76648
Erosion of dust-filtered helicopter turbine engines. Part 2: Erosion reduction
[BTN-95-EIX95182619223] p 289 A95-76649
Life prediction of helicopter engines fitted with dust filters
[BTN-95-EIX95182619224] p 289 A95-76650

VELINOV, PETER I. Y.

Thundercloud electric field modeling for the ionosphere-Earth region. 1: Dependence on cloud charge distribution
[HTN-95-41223] p 317 A95-75035

VENKATESWARAN, S.

Convergence acceleration of implicit schemes in the presence of high aspect ratio grid cells
p 313 N95-23446

VERHAAGEN, N. G.

A study of the vortex flow over 76/40-deg double-delta wing
[NASA-CR-195032] p 314 N95-23466

VIGUE, YVONNE

Thermal force modeling for global positioning system satellites using the finite element method
[BTN-95-EIX95152583270] p 278 A95-73571

VISCONTI, G.

Possible effects of CO₂ increase on the high-speed civil transport impact on ozone
[HTN-95-60779] p 317 A95-75976

VISSER, H. G.

Optimal lateral-escape maneuvers for microburst encounters during final approach
[BTN-95-EIX95182619127] p 276 A95-76604

VOLKOV, V. V.

A new generation of instruments for flying laboratories
[BTN-94-EIX94401363947] p 317 A95-75532

VORTAC, O. U.

The role of flight progress strips in en route air traffic control: A time-series analysis
[DOT/FAA/AM-95/4] p 280 N95-23565

VOSS, H. J.

Experience of in-service corrosion on military aircraft
p 303 N95-23516

VU, PHUONG

Direct-lift design strategy for longitudinal control of hypersonic aircraft
[BTN-95-EIX95182619131] p 291 A95-76608

W**WAGENER, THOMAS J.**

2 micron LIDAR for laser-based remote sensing: Flight demonstration and application survey
[BTN-95-EIX9512641072] p 319 A95-76737

WALBERG, G. D.

Fuel-optimal bank-angle control for lunar-return aerocapture
[BTN-95-EIX9512645706] p 299 A95-76758

WALDMAN, J.

Corrosion of landing gear steels p 302 N95-23500

WALSH, JOANNE L.

Integrated aerodynamic/dynamic/structural optimization of helicopter rotor blades using multilevel decomposition
[NASA-TP-3465] p 285 N95-22953

WANG, HONGLI

Effects of AMB parameters on the dynamic stability of the rotor
[BTN-94-EIX94381353450] p 323 A95-75494

WARDWELL, DOUG

Flow visualization studies of VTOL aircraft models during hover in ground effect
[NASA-TM-108860] p 272 N95-22666

WASHBURN, A. E.

A study of the vortex flow over 76/40-deg double-delta wing
[NASA-CR-195032] p 314 N95-23466

WASSERBAUER, CHARLES A.

NASA low-speed axial compressor for fundamental research
[NASA-TM-4635] p 296 N95-23192

WASZAK, M. R.

Flutter suppression for the active flexible wing: A classical design
[BTN-95-EIX95182619216] p 292 A95-76642

WEAVER, CLARK J.

Trajectory modeling of emissions from lower stratospheric aircraft
[HTN-95-41219] p 317 A95-75031

WEAVER, HAROLD F.

NASA low-speed axial compressor for fundamental research
[NASA-TM-4635] p 296 N95-23192

WEETMAN, D. C.

Health and usage monitoring systems: Corrosion surveillance p 262 N95-23506

WEINSTEIN, L. F.

TRISTAR 1: Evaluation methods for testing head-up display (HUD) flight symbology
[NASA-TM-4665] p 288 N95-24030

WEISS, SUSANNE

Analytical solution and parameter estimation of projectile dynamics
[BTN-95-EIX9512645695] p 272 A95-76747

WENDT, B. J.

Flow structure in the wake of a wishbone vortex generator
[BTN-95-EIX95142553044] p 304 A95-73454

WERESZCZAK, A. A.

Evolution of oxidation and creep damage mechanisms in HIPed silicon nitride materials
[DE95-001360] p 300 N95-22689

WHITAKER, KEVIN W.

Predicting exhaust plume boundaries with supersonic external flows
[BTN-95-EIX95152583258] p 297 A95-73559

WIESEMAN, CAROL D.

On-line analysis capabilities developed to support the active flexible wing wind-tunnel tests
[BTN-95-EIX95182619213] p 296 A95-76639

WILCOX, F.

Base drag prediction on missile configurations
[BTN-95-EIX95152583256] p 266 A95-73557

WILLIAMS, KEVIN W.

Development of qualification guidelines for personal computer-based aviation training devices
[DOT/FAA/AM-95/6] p 323 N95-23603

WILMOTH, RICHARD G.

Hypersonic rarefied flow past spheres including wake structure
[BTN-95-EIX95152583250] p 305 A95-73551
Zonally decoupled direct simulation Monte Carlo solutions of hypersonic blunt-body wake flows
[BTN-95-EIX95182617458] p 268 A95-75729

WINFREE, W. P.

New nondestructive techniques for the detection and quantification of corrosion in aircraft structures
p 315 N95-23512

WISELY, PAUL L.

Design of wide angle head up displays for synthetic vision
[BTN-95-EIX9512641070] p 287 A95-76735

WOFSY, S. C.

In situ observations in aircraft exhaust plumes in the lower stratosphere at midlatitudes
[HTN-95-A0862] p 318 A95-76266

WOOD, C. W.

Simulating heat addition via mass addition in constant area compressible flows
[BTN-95-EIX95182619100] p 307 A95-76585

WOOD, DAVID

Simulation and model reduction for the active flexible wing program
[BTN-95-EIX95182619211] p 295 A95-76637

WOODBIDGE, E. L.

Estimates of total organic and inorganic chlorine in the lower stratosphere from in situ and flask measurements during AASE 2
[HTN-95-A0861] p 317 A95-76265

In situ observations in aircraft exhaust plumes in the lower stratosphere at midlatitudes
[HTN-95-A0862] p 318 A95-76266

WOODS-VEDELER, JESSICA A.

Rolling maneuver load alleviation using active controls
[BTN-95-EIX95182619217] p 270 A95-76643

WOODYATT, B. A.

Enhancement of F/A-18 operational flight measurements: Data report for phase 1
[DSTO-TR-0049] p 286 N95-23666

WRIGHT, WILLIAM B.

Additional improvements to the NASA Lewis ice accretion code LEWICE
[NASA-TM-106849] p 309 N95-22669

WU, H. F.

MIL-HDBK-5 design allowables for fibre/metal laminates: ARALL 2 and ARALL 3
[BTN-94-EIX94371346933] p 300 A95-73345

WU, J.-S.

Effect of ambient turbulence intensity on sphere wakes at intermediate Reynolds numbers
[BTN-95-EIX95182619101] p 308 A95-76586

WU, L. L.

MIL-HDBK-5 design allowables for fibre/metal laminates: ARALL 2 and ARALL 3
[BTN-94-EIX94371346933] p 300 A95-73345

WU, XINPING

Simulation on the 3-D turbulent flow in the passages of finocyl gran
[BTN-95-EIX95202638962] p 279 A95-76674

WU, ZHIQIANG

Effects of AMB parameters on the dynamic stability of the rotor
[BTN-94-EIX94381353450] p 323 A95-75494

X**XIONG, FUJIN**

Development of aeronautical mobile satellite services over the past thirty years
[BTN-95-EIX95152569458] p 305 A95-73498

Y**YAJIMA, NOBUYUKI**

Polar Patrol Balloon
[BTN-95-EIX95152582318] p 316 A95-73521

YAMAUCHI, MASAFUMI

Numerical investigation of supersonic flows around a spiked blunt body
[BTN-95-EIX9512645690] p 271 A95-76742

YAMSHANOV, YU. B.

Fatigue strength of high-temperature alloys under conditions of cyclic temperature variation. Communication 1: Experimental procedure and results
[BTN-94-EIX94401363884] p 307 A95-75516

YING, JUEFEEI

A new type of simulator for simulating the flow-field distortion of engine inlet
[BTN-95-EIX95202638963] p 289 A95-76673

YOUNG, C. P., JR.

Dynamic response tests of inertial and optical wind-tunnel model attitude measurement devices
[NASA-TM-109182] p 296 N95-23011

YOUNG, DEBORAH B.

1994 NASA-HU American Society for Engineering Education (ASEE) Summer Faculty Fellowship Program
[NASA-CR-194972] p 325 N95-23276

YOUNG, KATHERINE C.

Integrated aerodynamic/dynamic/structural optimization of helicopter rotor blades using multilevel decomposition
[NASA-TP-3465] p 285 N95-22953

YOUSSEF, Y.

Validation of an effective flat cruciform-shaped specimen to study CFRP composite laminates under biaxial loading
[BTN-95-EIX95152584677] p 282 A95-73589

YUAN, PIN-JAR

Solutions of generalized proportional navigation with maneuvering and nonmaneuvering targets
[BTN-95-EIX95202637606] p 279 A95-76683

YULE, T. J.

Evaluation of neutron techniques for illicit substance detection
[DE95-002988] p 300 N95-22764

Z**ZACHAR, EDWARD**

H-76B fantail demonstrator composite fan blade fabrication
[HTN-95-80856] p 283 A95-75098

ZEDAN, M. F.

Stability derivatives of a flapped plate in unsteady ground effect
[BTN-95-EIX95182619225] p 270 A95-76651

ZELL, PETER T.

Aerodynamic surface distension system for high angle of attack forebody vortex control
[NASA-CASE-ARC-11979-1] p 286 N95-23390

ZHOU, GANG

Turbulent transonic airfoil flow simulation using a pressure-based algorithm
[BTN-95-EIX95182619078] p 269 A95-75763

ZISCHKA, PETER J.

PERSONAL AUTHOR INDEX

ZISCHKA, PETER J.

Experimental evaluation of a box beam specifically
tailored for chordwise deformation

[BTN-95-EIX95182619088] p 283 A95-75773

ZOBY, ERNEST V.

Higher-order viscous shock-layer solutions for
high-altitude flows

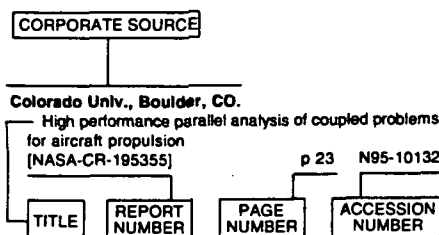
[BTN-95-EIX95152583255] p 306 A95-73556

CORPORATE SOURCE INDEX

AERONAUTICAL ENGINEERING / A Continuing Bibliography (Supplement 319)

July 1995

Typical Corporate Source Index Listing



Listings in this index are arranged alphabetically by corporate source. The title of the document is used to provide a brief description of the subject matter. The page number and the accession number are included in each entry to assist the user in locating the abstract in the abstract section. If applicable, a report number is also included as an aid in identifying the document.

A

- Advisory Group for Aeronautical Research and Development, Oxford (England).**
POD assessment of NDI procedures using a round robin test
[AGARD-R-809] p 315 N95-23602
- Advisory Group for Aerospace Research and Development, Neuilly-Sur-Seine (France).**
Corrosion detection and management of advanced airframe materials
[AGARD-CP-565] p 302 N95-23496
- Aerospatiale, Toulouse (France).**
Corrosion in service experience with aircraft in France
p 303 N95-23518
- Air Force Inst. of Tech., Wright-Patterson AFB, OH.**
Modeling aerosol emissions from the combustion of composite materials
p 301 N95-23038
- Air Force Systems Command, McClellan AFB, CA.**
Mishap risk control for advanced aerospace/composite materials
p 301 N95-23031
- Air Products and Chemicals, Inc., Allentown, PA.**
Organic coating technology for the protection of aircraft against corrosion
p 303 N95-23513
- Argonne National Lab., IL.**
Evaluation of neutron techniques for illicit substance detection
[DE95-002988] p 300 N95-22764
- Arizona Univ., Tucson, AZ.**
Residual strength of thin panels with cracks
p 311 N95-23311
- Arkansas Univ., Pine Bluff, AR.**
Automation technology using Geographic Information System (GIS)
p 324 N95-23284
- Army Research Lab., Watertown, MA.**
Rationale for the Modular Air-system Vulnerability Estimation Network (MAVEN) methodology
[AD-A285797] p 284 N95-22510

- Auburn Univ., AL.**
Influence of backup bearings and support structure dynamics on the behavior of rotors with active supports
[NASA-CR-197438] p 310 N95-23190
Aerodynamic flight control to increase payload capability of future launch vehicles
[NASA-CR-197704] p 300 N95-24032
- AVRO International Aerospace, Woodford (England).**
Health and usage monitoring systems: Corrosion surveillance
p 262 N95-23506

B

- Belgian Center for Corrosion Study, Brussels (Belgium).**
In-situ detection of surface passivation or activation and of localized corrosion: Experiences and prospects in aircraft
p 302 N95-23508
Test method and test results for environmental assessment of aircraft materials
p 302 N95-23509
- Boeing Defense and Space Group, Seattle, WA.**
Euler technology assessment for preliminary aircraft design employing OVERFLOW code with multiblock structured-grid method
[NASA-CR-4651] p 273 N95-23095

C

- California Univ., Davis, CA.**
Analysis of the longitudinal handling qualities and pilot-induced-oscillation tendencies of the High-Angle-of-Attack Research Vehicle (HARV)
p 293 N95-23297
High-lift flow-physics flight experiments on a subsonic civil transport aircraft (B737-100)
p 275 N95-23333
- Cambridge Acoustical Associates, Inc., Cambridge, MA.**
The use of cowl camber and taper to reduce rotor/stator interaction noise
[NASA-CR-195421] p 323 N95-22675
- Civil Aeromedical Inst., Oklahoma City, OK.**
The role of flight progress strips in en route air traffic control: A time-series analysis
[DOT/FAA/AM-95/4] p 280 N95-23565
Development of qualification guidelines for personal computer-based aviation training devices
[DOT/FAA/AM-95/6] p 323 N95-23603
Aircraft fires, smoke toxicity, and survival: An overview
[DOT/FAA/AM-95/8] p 277 N95-24024
A review of civil aviation fatal accidents in which lost/disoriented was a cause/factor: 1981-1990
[DOT/FAA/AM-95/1] p 278 N95-24071
- Clemson Univ., SC.**
Maximum-likelihood spectral estimation and adaptive filtering techniques with application to airborne Doppler weather radar
[NASA-CR-197699] p 316 N95-23670
- College of William and Mary, Williamsburg, VA.**
Preparation of course materials: Elementary mathematics of powered flight
p 324 N95-23320
- Colorado Univ., Boulder, CO.**
High-performance parallel analysis of coupled problems for aircraft propulsion
[NASA-CR-197440] p 289 N95-23088
- Consiglio Nazionale delle Ricerche, Rome (Italy).**
MAX-91: Polarimetric SAR results on Montespertoli site
p 320 N95-23940

D

- Defence Research Agency, Farnborough, Hampshire (England).**
The corrosion and protection of advanced aluminium - lithium airframe alloys
p 302 N95-23497
Non-destructive detection of corrosion for life management
p 314 N95-23505

- Defence Science and Technology Organisation, Melbourne (Australia).**
Enhancement of F/A-18 operational flight measurements: Data report for phase 1
[DSTO-TR-0049] p 286 N95-23666
- Defense Advanced Research Projects Agency, Arlington, VA.**
Technology reinvestment project's focus area: Affordable polymer matrix composites for airframe structures
[PB95-136032] p 324 N95-23168
- Department of the Air Force, Tinker AFB, OK.**
Oklahoma City air logistics center (USAF) aging aircraft corrosion program
p 262 N95-23519
- Deutsche Aerospace A.G., Munich (Germany).**
Corrosion protection measures for CFC/metal joints of fuel integral tank structures of advanced military aircraft
p 303 N95-23510
Experience of in-service corrosion on military aircraft
p 303 N95-23516

E

- Eloret Corp., Palo Alto, CA.**
Particle kinetic simulation of high altitude hypervelocity flight
[NASA-CR-197383] p 309 N95-22481

F

- Federal Aviation Administration, Washington, DC.**
Oceanic operations: An authoritative guide to oceanic operations
[FAA-AFS-550] p 277 N95-24065
- Florida Univ., Gainesville, FL.**
Interlaminar shear test method development for long term durability testing of composites
p 301 N95-23300

G

- General Accounting Office, Washington, DC.**
Report to the Secretary of Defense. Unmanned aerial vehicles: No more Hunter systems should be bought until problems are fixed
[GAO/NSIAD-95-52] p 286 N95-24091
- Georgia Tech Research Inst., Atlanta, GA.**
Flutter analysis of composite box beams
[NASA-CR-197931] p 294 N95-23392

H

- Hampton Univ., VA.**
1994 NASA-HU American Society for Engineering Education (ASEE) Summer Faculty Fellowship Program
[NASA-CR-194972] p 325 N95-23276
- Honeywell Technology Center, Minneapolis, MN.**
Empirical results on scheduling and dynamic backtracking
p 299 N95-23761

I

- Illinois Univ., Chicago, IL.**
Holographic interferometric tomography for reconstructing flow fields
p 310 N95-23287
- Institute for Aerospace Research, Ottawa (Ontario).**
Double pass retroreflection for corrosion detection in aircraft structures
p 323 N95-23503
- Institute for Computer Applications in Science and Engineering, Hampton, VA.**
A study of the vortex flow over 76/40-deg double-delta wing
[NASA-CR-195032] p 314 N95-23466
- Iowa State Univ. of Science and Technology, Ames, IA.**
Idealized textile composites for experimental/analytical correlation
p 301 N95-23277

SOURCE

J

Jet Propulsion Lab., California Inst. of Tech., Pasadena, CA.

Estimates of total organic and inorganic chlorine in the lower stratosphere from in situ and flask measurements during AASE 2

[HTN-95-A0861] p 317 A95-76265

In situ observations in aircraft exhaust plumes in the lower stratosphere at midlatitudes

[HTN-95-A0862] p 318 A95-76266

Virtual reality flight control display with six-degree-of-freedom controller and spherical orientation overlay

[NASA-CASE-NPO-18733-1-CU] p 288 N95-22578

Joint Inst. for Advancement of Flight Sciences, Hampton, VA.

An approximate theoretical method for modeling the static thrust performance of non-axisymmetric two-dimensional convergent-divergent nozzles

[NASA-CR-195050] p 273 N95-23193

K

Kansas Univ., Lawrence, KS.

On-line, adaptive state estimator for active noise control

p 322 N95-23308

L

Lockheed Aeronautical Systems Co., Marietta, GA.

An assessment of viscous effects in computational simulation of benign and burst vortex flows on generic fighter wind-tunnel models using TEAM code

[NASA-CR-4650] p 273 N95-23185

Lockheed-Fort Worth Co., Fort Worth, TX.

Euler Technology Assessment program for preliminary aircraft design employing SPLITFLOW code with Cartesian unstructured grid method

[NASA-CR-4649] p 273 N95-22917

Los Alamos National Lab., NM.

NTS-spill test facility wind tunnel exhaust plume characterization

[DE95-003630] p 297 N95-24019

Phonon characteristics of high (T sub c) superconductors from neutron Doppler broadening measurements

[DE95-003703] p 324 N95-24076

M

Manchester Univ. (England).

Collaborative research on aircraft icing and charging processes in ice

[AD-A285102] p 276 N95-23201

Massachusetts Inst. of Tech., Cambridge, MA.

Design of high performance multivariable control systems for supermaneuverable aircraft at high angle of attack

[NASA-CR-197661] p 293 N95-22908

Massachusetts Inst. of Tech., Lexington, MA.

Calculation of satellite drag coefficients

[AD-A285118] p 300 N95-23781

MCAT Inst., Moffett Field, CA.

Three-dimensional unsteady flow calculations in an advanced gas generator turbine

p 312 N95-23425

McDonnell-Douglas Aerospace, Long Beach, CA.

Guidance and control requirements for high-speed Rollout and Turnoff (ROTO)

[NASA-CR-195026] p 292 N95-22674

Minnesota Univ., Minneapolis, MN.

Feedback control laws for highly maneuverable aircraft

[NASA-CR-197944] p 295 N95-23410

Mississippi State Univ., Mississippi State, MS.

Crossflow instability control on a swept-wing: Preliminary studies

p 274 N95-23283

Thin tailored composite wing for civil tiltrotor

p 285 N95-23317

TIGER: A user-friendly interactive grid generation system for complicated turbomachinery and axis-symmetric configurations

p 322 N95-23419

Moller International, Inc., Davis, CA.

Evaluation of thermal barrier and PS-200 self-lubricating coatings in an air-cooled rotary engine

[NASA-CR-195445] p 289 N95-23222

N

National Aeronautics and Space Administration. Ames Research Center, Moffett Field, CA.

Progress in high-lift aerodynamic calculations

[BTN-95-EIX95152582315] p 264 A95-73518

Navier-Stokes prediction of large-amplitude delta-wing roll oscillations

[BTN-95-EIX95152582329] p 281 A95-73531

Forebody flow control on a full-scale F/A-18 aircraft

[BTN-95-EIX95152582333] p 281 A95-73535

Hypersonic nonequilibrium Navier-Stokes solutions over an ablating graphite nosetip

[BTN-95-EIX95152583252] p 305 A95-73553

Hypersonic convective heat transfer over 140-deg blunt cones in different gases

[BTN-95-EIX95152583253] p 306 A95-73554

Investigation of the effects of bandwidth and time delay on helicopter roll-axis handling qualities

[HTN-95-80853] p 290 A95-75095

Aeroacoustic model for weak shock waves based on Burgers equation

[BTN-95-EIX95182619076] p 269 A95-75761

Estimates of total organic and inorganic chlorine in the lower stratosphere from in situ and flask measurements during AASE 2

[HTN-95-A0861] p 317 A95-76265

In situ observations in aircraft exhaust plumes in the lower stratosphere at midlatitudes

[HTN-95-A0862] p 318 A95-76266

H-infinity helicopter flight control law design with and without rotor state feedback

[BTN-95-EIX95182619129] p 291 A95-76606

Automatic guidance and control for helicopter obstacle avoidance

[BTN-95-EIX95182619130] p 291 A95-76607

CFD optimization of a theoretical minimum-drag body

[BTN-95-EIX95182619234] p 308 A95-76660

Flow visualization studies of VTOL aircraft models during Hover in ground effect

[NASA-TM-108860] p 272 N95-22666

Nonlinear system guidance in the presence of transmission zero dynamics

[NASA-TM-4661] p 309 N95-22804

Experimental results for a hypersonic nozzle/afterbody flow field

[NASA-TM-4638] p 274 N95-23250

System for determining aerodynamic imbalance

[NASA-CASE-ARC-11913-1] p 311 N95-23377

Engines-only flight control system

[NASA-CASE-ARC-11944-1] p 294 N95-23389

Aerodynamic surface distension system for high angle of attack forebody vortex control

[NASA-CASE-ARC-11979-1] p 286 N95-23390

Cueing light configuration for aircraft navigation

[NASA-CASE-ARC-11982-1] p 280 N95-23393

Lift enhancing tabs for airfoils

[NASA-CASE-ARC-11990-1] p 286 N95-23395

AVIRIS and TIMS data processing and distribution at the land processes distributed active archive center

p 325 N95-23872

TRISTAR 1: Evaluation methods for testing head-up display (HUD) flight symbology

[NASA-TM-4665] p 288 N95-24030

National Aeronautics and Space Administration. Flight Research Center, Edwards, CA.

Flight test of the X-29A at high angle of attack: Flight dynamics and controls

[NASA-TP-3537] p 284 N95-22806

Direct adaptive performance optimization of subsonic transports: A periodic perturbation technique

[NASA-TM-4676] p 284 N95-22829

National Aeronautics and Space Administration. Goddard Space Flight Center, Greenbelt, MD.

Trajectory modeling of emissions from lower stratospheric aircraft

[HTN-95-41219] p 317 A95-75031

Sensitivity of two-dimensional model predictions of ozone response to stratospheric aircraft: An update

[HTN-95-A0863] p 318 A95-76267

National Aeronautics and Space Administration. Langley Research Center, Hampton, VA.

Mach wave emission from a high-temperature supersonic jet

[BTN-95-EIX95152577586] p 264 A95-73496

Separation control on high-lift airfoils via micro-vortex generators

[BTN-95-EIX95152582326] p 265 A95-73529

Analysis of a higher harmonic control test to reduce blade vortex interaction noise

[BTN-95-EIX95152582330] p 265 A95-73532

Computational study of plume-induced separation on a hypersonic powered model

[BTN-95-EIX95152582346] p 266 A95-73548

Aerodynamic characteristics of a hypersonic viscous optimized waverider at high altitudes

[BTN-95-EIX95152583251] p 266 A95-73552

Application of the multigrid solution technique to hypersonic entry vehicles

[BTN-95-EIX95152583254] p 306 A95-73555

Higher-order viscous shock-layer solutions for high-altitude flows

[BTN-95-EIX95152583255] p 306 A95-73556

Optimization of contoured hypersonic scramjet inlets with a least-squares parabolized Navier-Stokes procedure

[HTN-95-20976] p 261 A95-74042

Sensitivity of acoustic predictions to variation of input parameters

[HTN-95-80855] p 267 A95-75097

An analytical and experimental investigation of the response of the curved, composite frame/skin specimens

[HTN-95-80857] p 283 A95-75099

Aerodynamics of the Shuttle Orbiter at high altitudes

[BTN-95-EIX95182617454] p 298 A95-75725

Zonally decoupled direct simulation Monte Carlo solutions of hypersonic blunt-body wake flows

[BTN-95-EIX95182617458] p 268 A95-75729

Multigrid solution of compressible turbulent flow on unstructured meshes using a two-equation model

[BTN-95-EIX94401378794] p 307 A95-76484

Summary of an active flexible wing program

[BTN-95-EIX95182619209] p 283 A95-76635

Application of transonic small disturbance theory to the active flexible wing model

[BTN-95-EIX95182619210] p 270 A95-76636

Simulation and model reduction for the active flexible wing program

[BTN-95-EIX95182619211] p 295 A95-76637

Multiple-function digital controller system for active flexible wing wind-tunnel model

[BTN-95-EIX95182619212] p 322 A95-76638

On-line analysis capabilities developed to support the active flexible wing wind-tunnel tests

[BTN-95-EIX95182619213] p 296 A95-76639

Flutter suppression control law design and testing for the active flexible wing

[BTN-95-EIX95182619214] p 292 A95-76640

Design and multifunction tests of a frequency domain-based active flutter suppression system

[BTN-95-EIX95182619215] p 292 A95-76641

Flutter suppression for the active flexible wing: A classical design

[BTN-95-EIX95182619216] p 292 A95-76642

Rolling maneuver load alleviation using active controls

[BTN-95-EIX95182619217] p 270 A95-76643

Wing pressure distributions from subsonic tests of a high-wing transport model

[NASA-TM-4583] p 272 N95-22802

Integrated aerodynamic/dynamic/structural optimization of helicopter rotor blades using multilevel decomposition

[NASA-TP-3465] p 285 N95-22953

Compendium of NASA data base for the Global Tropospheric Experiment's Pacific Exploratory Mission West-A (PEM West-A)

[NASA-TM-109177] p 320 N95-23009

Dynamic response tests of inertial and optical wind-tunnel model attitude measurement devices

[NASA-TM-109182] p 296 N95-23011

Mach 10 computational study of a three-dimensional scramjet inlet flow field

[NASA-TM-4602] p 309 N95-23015

Mach 10 computational study of a three-dimensional scramjet inlet flow field

[NASA-TM-4602] p 310 N95-23210

New nondestructive techniques for the detection and quantification of corrosion in aircraft structures

p 315 N95-23512

National Aeronautics and Space Administration. Lewis Research Center, Cleveland, OH.

Flow structure in the wake of a wishbone vortex generator

[BTN-95-EIX95142553044] p 304 A95-73454

Integrated flight/propulsion control for helicopters

[HTN-95-80854] p 290 A95-75096

Numerical analysis of hypersonic low-density scramjet inlet flow

[BTN-95-EIX95212645694] p 272 A95-76746

Additional improvements to the NASA Lewis ice accretion code LEWICE

[NASA-TM-106849] p 309 N95-22669

Stable H(infinity) controller design for the longitudinal dynamics of an aircraft

[NASA-TM-106847] p 293 N95-22954

Supersonic jet noise reductions predicted with increased jet spreading rate

[NASA-TM-106872] p 323 N95-23178

NASA low-speed axial compressor for fundamental research

[NASA-TM-4635] p 296 N95-23192

Design of a GaAs/Ge solar array for unmanned aerial vehicles

[NASA-TM-106870] p 320 N95-23259

A time-accurate finite volume method valid at all flow velocities p 314 N95-23447
Sensitivity of combustion-acoustic instabilities to boundary conditions for premixed gas turbine combustors

[NASA-TM-106890] p 289 N95-23550

Motor drive technologies for the power-by-wire (PBW) program: Options, trends and tradeoffs
[NASA-TM-106885] p 295 N95-23671

Research and Technology, 1994
[NASA-TM-106764] p 262 N95-24025

National Aeronautics and Space Administration.

Marshall Space Flight Center, Huntsville, AL.

Validation of a Computational Fluid Dynamics (CFD) code for supersonic axisymmetric base flow
p 315 N95-23652

National Aeronautics and Space Administration.

Pasadena Office, CA.

Virtual reality flight control display with six-degree-of-freedom controller and spherical orientation overlay
[NASA-CASE-NPO-18733-1-CU] p 288 N95-22578

National Aerospace Lab., Amsterdam (Netherlands).

Review of aeronautical fatigue investigation in the Netherlands during the period March 1991-March 1993
[PB95-139184] p 285 N95-23161

Eddy current detection of pitting corrosion around fastener holes
p 315 N95-23507

National Transportation Safety Board, Washington, DC.

Report of proceedings: Aviation Accident Investigation Symposium. Volume 2: Participant presentations
[PB94-917007] p 277 N95-23598

Aircraft accident report. Runway overrun following rejected takeoff. Continental Airlines flight 795, McDonnell Douglas MD-82, N18835, LaGuardia Airport, Flushing, NY, 2 March 1994
[PB95-910401] p 277 N95-23609

Aviation Accident Investigation Symposium. Volume 1: Industry recommendations and Safety Board responses
[PB94-917005] p 278 N95-24105

Naval Air Station, Norfolk, VA.

US Navy operating experience with new aircraft construction materials
p 303 N95-23517

Naval Air Warfare Center, Warminster, PA.

Corrosion of landing gear steels p 302 N95-23500
Corrosion detection and monitoring of aircraft structures: An overview p 303 N95-23515

Naval Research Lab., Washington, DC.

Statistics of multi-look AIRSAR imagery: A comparison of theory with measurements
p 320 N95-23947

New Jersey Inst. of Tech., Newark, NJ.

Design of a variable area diffuser for a 15-inch Mach 6 open-jet tunnel
p 297 N95-23309

New South Wales Univ., Kensington (Australia).

AIRSAR deployment in Australia, September 1993: Management and objectives
p 321 N95-23948

O

Oak Ridge National Lab., TN.

Evolution of oxidation and creep damage mechanisms in HIPed silicon nitride materials
[DE95-001360] p 300 N95-22689

Cu deposition using a permanent magnet electron cyclotron resonance microwave plasma source
[DE94-017768] p 304 N95-23981

Old Dominion Coll., Norfolk, VA.

System identification of the Large-Angle Magnetic Suspension Test Fixture (LAMSTF) p 296 N95-23299

Optimized design of a hypersonic nozzle
p 297 N95-23304

Inner loop flight control for the High-Speed Civil Transport
p 293 N95-23314

Old Dominion Univ., Norfolk, VA.

A CFD study of complex missile and store configurations in relative motion
[NASA-CR-197912] p 285 N95-22949

Aerodynamic design optimization with sensitivity analysis and computational fluid dynamics
[NASA-CR-197419] p 274 N95-23218

P

Pennsylvania State Univ., State College, PA.

Cavitation modeling in Euler and Navier-Stokes codes
p 315 N95-23630

Pennsylvania State Univ., University Park, PA.

Numerical computation of aerodynamics and heat transfer in a turbine cascade and a turn-around duct using advanced turbulence models
p 313 N95-23444

Convergence acceleration of implicit schemes in the presence of high aspect ratio grid cells
p 313 N95-23446

Pratt and Whitney Aircraft, West Palm Beach, FL.

Aerodynamic design and analysis of a highly loaded turbine exhaust
p 312 N95-23435

Phase 2: HGM air flow tests in support of HEX vane investigation
p 312 N95-23438

Princeton Univ., NJ.

An investigation of helicopter dynamic coupling using an analytical model
[NASA-CR-197420] p 285 N95-23217

R

Rochester Univ., NY.

Scientific and technical photography at NASA Langley Research Center
p 310 N95-23290

Rockwell International Corp., Canoga Park, CA.

CFD analysis of turbopump volutes
p 312 N95-23436

Impeller flow field characterization with a laser two-focus velocimeter
p 313 N95-23440

S

Saint Cloud State Coll., MN.

Differential GPS and system integration of the Low Visibility Landing and Surface Operations (LVLASO) demonstration
p 280 N95-23318

Saint Louis Univ., Cahokia, IL.

Preliminary identification of buffet problems in high speed civil transport
p 294 N95-23319

Sandia National Labs., Albuquerque, NM.

Moving mass trim control for aerospace vehicles
[DE95-002602] p 299 N95-23532

Sverdrup Technology, Inc., Brook Park, OH.

Three-dimensional Navier-Stokes analysis and redesign of an imbedded bellmouth nozzle in a turbine cascade inlet section
p 311 N95-23423

T

Technion - Israel Inst. of Tech., Haifa (Israel).

Review of some results of the author's fatigue investigations with applications in engineering and material science
[TAE-698] p 316 N95-23662

Technology Integration and Development Group, Inc., Bedford, MA.

Gearbox vibration diagnostic analyzer
[NASA-CR-189141] p 316 N95-23792

Tennessee Univ., Tullahoma, TN.

A wall interference assessment/correction system
[NASA-CR-197421] p 309 N95-23183

Supersonic laminar flow control research
[NASA-CR-197938] p 275 N95-23669

Tennessee Univ. Space Inst., Tullahoma, TN.

Handling qualities of the High Speed Civil Transport
p 294 N95-23325

Texas A&M Univ., College Station, TX.

Control of flow separation in airfoil/wing design applications
p 274 N95-23294

Toledo Univ., OH.

Enhanced analysis and users manual for radial-inflow turbine conceptual design code RTD
[NASA-CR-195454] p 275 N95-23462

User's guide for ECAP2D: An Euler unsteady aerodynamic and aeroelastic analysis program for two dimensional oscillating cascades, version 1.0
[NASA-CR-189146] p 316 N95-24189

U

Union Carbide Industrial Gases, Inc., Tonawanda, NY.

Airborne rotary air separator study
[NASA-CR-189099] p 290 N95-24053

V

Vigyan Research Associates, Inc., Hampton, VA.

Performance of the 0.3-meter transonic cryogenic tunnel with air, nitrogen, and sulfur hexafluoride media under closed loop automatic control
[NASA-CR-195052] p 310 N95-23257

Virginia Polytechnic Inst., Blacksburg, VA.

Development and verification of a resin film infusion/resin transfer molding simulation model for fabrication of advanced textile composites
[NASA-CR-197439] p 301 N95-23179

Virginia Polytechnic Inst. and State Univ., Blacksburg, VA.

Supersonic flow and shock formation in turbine tip gaps
p 312 N95-23429

W

Wayne State Univ., Detroit, MI.

Active control of panel vibrations induced by a boundary layer flow
[NASA-CR-197867] p 273 N95-23182

Wichita State Univ., Wichita, KS.

The airline quality report, 1994
[NIAR-94-11] p 277 N95-24012

A multibody/finite element analysis approach for modeling of crash dynamic responses
[NIAR-94-3] p 277 N95-24050

Woods Hole Oceanographic Inst., MA.

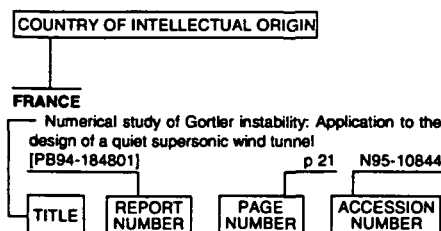
Assimilation of altimeter data in a quasi-geostrophic model of the Gulf Stream system: A dynamical perspective
[NASA-CR-196313] p 320 N95-23766

FOREIGN TECHNOLOGY INDEX

AERONAUTICAL ENGINEERING / A Continuing Bibliography (Supplement 319)

July 1995

Typical Foreign Technology Index Listing



Listings in this index are arranged alphabetically by country of intellectual origin. The title of the document is used to provide a brief description of the subject matter. The page number and accession number are included in each entry to assist the user in locating the abstract in the abstract section. If applicable, a report number is also included as an aid in identifying the document.

A

AUSTRALIA

- Time-of-flight mass spectrometer for impulse facilities
[BTN-95-EIX95142553057] p 262 A95-73441
- Shock tunnel measurements of hypervelocity blunted cone drag
[BTN-95-EIX95152577606] p 305 A95-73477
- Enhancement of F/A-18 operational flight measurements: Data report for phase 1
[DSTO-TR-0049] p 286 N95-23666
- AIRSAAR deployment in Australia, September 1993: Management and objectives p 321 N95-23948

B

BELGIUM

- Experimental investigation of the flowfield about an upswept afterbody
[BTN-95-EIX95152582321] p 265 A95-73524
- In-situ detection of surface passivation or activation and of localized corrosion: Experiences and perspectives in aircraft p 302 N95-23508
- Test method and test results for environmental assessment of aircraft materials p 302 N95-23509

BULGARIA

- Thundercloud electric field modeling for the ionosphere-Earth region. 1: Dependence on cloud charge distribution
[HTN-95-41223] p 317 A95-75035

C

CANADA

- Adaptive finite element method for turbulent flow near a propeller
[BTN-95-EIX95142553038] p 305 A95-73460

- Coupled FEM-BEM approach for mean flow effects on vibro-acoustic behavior of planar structures
[BTN-95-EIX95152577587] p 263 A95-73495
- Postinstability behavior of a two-dimensional airfoil with a structural nonlinearity
[BTN-95-EIX95152582337] p 266 A95-73539
- Multiple site fatigue damage in fuselage skin splices: Experimental simulation and theoretical prediction
[BTN-95-EIX95152584676] p 276 A95-73588
- Validation of an effective flat cruciform-shaped specimen to study CFRP composite laminates under biaxial loading
[BTN-95-EIX95152584677] p 282 A95-73589
- Evaluation of advanced aerospace materials by depth sensing indentation and scratch methods
[BTN-95-EIX95152584678] p 282 A95-73590
- Improving prediction: The incorporation of simplified rotor dynamics in a mathematical model of the bell 412HP
[BTN-95-EIX95152584679] p 282 A95-73591
- Finite element model for a flexible non-symmetric rotor on distributed bearing: A stability study
[BTN-94-EIX94381352212] p 306 A95-74612
- Application of a control-volume-based finite-element formulation to the shock tube problem
[BTN-95-EIX95182619099] p 295 A95-76584
- A comparison of some aerodynamic resistance methods using measurements over cotton and grass from the 1991 California ozone deposition experiment
[HTN-95-11295] p 319 A95-77000
- Double pass retroreflection for corrosion detection in aircraft structures p 323 N95-23503

CHINA

- Development of aeronautical mobile satellite services over the past thirty years
[BTN-95-EIX95152569458] p 305 A95-73498
- Effects of AMB parameters on the dynamic stability of the rotor
[BTN-94-EIX94381353450] p 323 A95-75494
- A new type of simulator for simulating the flow-field distortion of engine inlet
[BTN-95-EIX95202638963] p 289 A95-76673
- Simulation on the 3-D turbulent flow in the passages of finocyl grain
[BTN-95-EIX95202638962] p 279 A95-76674

E

EGYPT

- Main features of overexpanded triple jets
[BTN-95-EIX95142553040] p 304 A95-73458

F

FRANCE

- Two-equation turbulence model for unsteady separated flows around airfoils
[BTN-95-EIX95142553054] p 262 A95-73444
- Geoid lineations of 1000 km wavelength over the central Pacific
[HTN-95-11304] p 319 A95-77009
- Corrosion detection and management of advanced airframe materials
[AGARD-CP-565] p 302 N95-23496
- Corrosion in service experience with aircraft in France p 303 N95-23518

G

GERMANY

- Laplace interaction law for the computation of viscous airfoil flow in low- and high-speed aerodynamics
[BTN-95-EIX95142553037] p 263 A95-73461
- Analytical solution and parameter estimation of projectile dynamics
[BTN-95-EIX95212645695] p 272 A95-76747
- Transport of exhaust products in the near trail of a jet engine under atmospheric conditions
[HTN-95-91421] p 319 A95-77334

- Corrosion protection measures for CFC/metal joints of fuel integral tank structures of advanced military aircraft p 303 N95-23510
- Experience of in-service corrosion on military aircraft p 303 N95-23516

I

INDIA

- Transient analysis of a cracked rotor passing through critical speed
[BTN-94-EIX94401360022] p 306 A95-74702
- Some aspects of the aerodynamics of separating strap-ons
[BTN-95-EIX95182617464] p 298 A95-75735
- Simple method of supersonic flow visualization using watertable
[BTN-95-EIX95182619105] p 269 A95-76590
- Switched bias proportional navigation for homing guidance against highly maneuvering targets
[BTN-95-EIX95182619145] p 279 A95-76622

IRELAND

- The influence of alternate inter-blade connections on ground resonance
[HTN-95-80859] p 267 A95-75101

ISRAEL

- Grid refinement test of time-periodic flows over bluff bodies
[BTN-94-EIX94401378822] p 307 A95-76491
- Dynamic investigation of the angular motion of a rotating body-parachute system
[BTN-95-EIX95182619220] p 270 A95-76646
- Review of some results of the author's fatigue investigations with applications in engineering and material science
[TAE-698] p 316 N95-23662

ITALY

- Simulation of turbulent fluctuations
[BTN-95-EIX95142553041] p 304 A95-73457
- Structural acoustic calculations in the low-frequency range
[BTN-95-EIX95152582336] p 323 A95-73538
- Simulation of transverse gas injection in turbulent supersonic air flows
[BTN-95-EIX95182619080] p 269 A95-75765
- Possible effects of CO₂ increase on the high-speed civil transport impact on ozone
[HTN-95-60779] p 317 A95-75976
- MAX-91: Polarimetric SAR results on Montespetoli site p 320 N95-23940

J

JAPAN

- Flow visualization studies on sidewall effects in two-dimensional transonic airfoil testing
[BTN-95-EIX95152582313] p 264 A95-73516
- Polar Patrol Balloon
[BTN-95-EIX95152582318] p 316 A95-73521
- Derivation of system matrices from nonlinear dynamic simulation of jet engines
[BTN-95-EIX95182619139] p 288 A95-76616
- Numerical investigation of supersonic flows around a spiked blunt body
[BTN-95-EIX95212645690] p 271 A95-76742

K

KOREA, REPUBLIC OF

- Static aeroelastic characteristics of a composite wing
[BTN-95-EIX95152582340] p 282 A95-73542
- Numerical study of sound generation due to a spinning vortex pair
[BTN-95-EIX95182619075] p 307 A95-75760
- Covariance analysis of strapdown INS considering gyrocompass characteristics
[BTN-95-EIX95202637592] p 279 A95-76697

FOREIGN

N

NETHERLANDS

- Optimal lateral-escape maneuvers for microburst encounters during final approach
[BTN-95-EIX95182619127] p 276 A95-76604
- Review of aeronautical fatigue investigation in the Netherlands during the period March 1991-March 1993
[PB95-139184] p 285 N95-23161
- Eddy current detection of pitting corrosion around fastener holes p 315 N95-23507

Collaborative research on aircraft icing and charging processes in ice

- [AD-A285102] p 276 N95-23201
- The corrosion and protection of advanced aluminium - lithium airframe alloys p 302 N95-23497
- Non-destructive detection of corrosion for life management p 314 N95-23505
- Health and usage monitoring systems: Corrosion surveillance p 262 N95-23506
- POD assessment of NDI procedures using a round robin test
- [AGARD-R-809] p 315 N95-23602

O

OMAN

- Study of an airfoil with a flap and spoiler
[BTN-95-EIX95152582327] p 265 A95-73530

R

RUSSIA

- A new generation of instruments for flying laboratories
[BTN-94-EIX94401363947] p 317 A95-75532

S

SAUDI ARABIA

- Analytical solution for controls, heats, and states of flight trajectories
[BTN-95-EIX95152583286] p 282 A95-73587
- Stability derivatives of a flapped plate in unsteady ground effect
[BTN-95-EIX95182619225] p 270 A95-76651
- Unsteady ground effects on aerodynamic coefficients of finite wings with camber
[BTN-95-EIX95182619233] p 271 A95-76659

SOUTH AFRICA

- Static pressure distribution in the inlet of a helicopter turbine compressor
[BTN-95-EIX95152582339] p 266 A95-73541
- Analytic prediction of lift for delta wings with partial leading-edge thrust
[BTN-95-EIX95152582345] p 266 A95-73547
- Erosion of dust-filtered helicopter turbine engines. Part 1: Basic theoretical considerations
[BTN-95-EIX95182619222] p 268 A95-76648
- Erosion of dust-filtered helicopter turbine engines. Part 2: Erosion reduction
[BTN-95-EIX95182619223] p 289 A95-76649
- Life prediction of helicopter engines fitted with dust filters
[BTN-95-EIX95182619224] p 289 A95-76650

SPAIN

- Design constraints in the payload-range diagram of ultrahigh capacity transport airplanes
[BTN-95-EIX95152582319] p 276 A95-73522

SWEDEN

- Turbulent transonic airfoil flow simulation using a pressure-based algorithm
[BTN-95-EIX95182619078] p 269 A95-75763

T

TAIWAN, PROVINCE OF CHINA

- Sidewash on the vertical tail in subsonic and supersonic flows
[BTN-95-EIX95152582316] p 264 A95-73519
- Solutions of generalized proportional navigation with maneuvering and nonmaneuvering targets
[BTN-95-EIX95202637606] p 279 A95-76683
- Integrated design of hypersonic waveriders including inlets and tailfins
[BTN-95-EIX95212645692] p 271 A95-76744

TURKEY

- Aerodynamic characteristics of external store configurations at low speeds
[BTN-95-EIX95182619230] p 271 A95-76656

U

UKRAINE

- Fatigue strength of high-temperature alloys under conditions of cyclic temperature variation. Communication 1: Experimental procedure and results
[BTN-94-EIX94401363884] p 307 A95-75516

UNITED KINGDOM

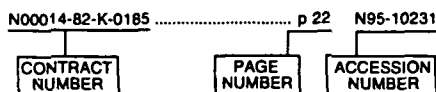
- Dynamical instability of the aerogravity assist maneuver
[BTN-95-EIX95152583282] p 298 A95-73583
- Design of wide angle head up displays for synthetic vision
[BTN-95-EIX95212641070] p 287 A95-76735

CONTRACT NUMBER INDEX

AERONAUTICAL ENGINEERING / A Continuing Bibliography (Supplement 319)

July 1995

Typical Contract Number Index Listing



Listings in this index are arranged alphanumerically by contract number. Under each contract number the accession numbers denoting documents that have been produced as a result of research done under the contract are shown. The accession number denotes the number by which the citation is identified in the abstract section. Preceding the accession number is the page number on which the citation may be found.

AF-AFOSR-0376-91 p 276 N95-23201
 DA PROJ. 1L1-6241-A-47-AB p 285 N95-22953
 DA PROJ. 1L1-62618-AH-80 p 284 N95-22510
 DAJA45-83-C-0011 p 302 N95-23509
 DAJA45-83-C-0041 p 302 N95-23509
 DE-AC04-94AL-85000 p 299 N95-23532
 DE-AC05-84OR-21400 p 300 N95-22689
 p 304 N95-23981
 F19628-90-C-0002 p 300 N95-23781
 JPL-958208 p 320 N95-23766
 NAG1-1088 p 293 N95-22908
 NAG1-1150 p 285 N95-22949
 NAG1-1175 p 273 N95-23182
 NAG1-1188 p 274 N95-23218
 NAG1-1380 p 295 N95-23410
 NAG1-19317 p 283 A95-75099
 NAG1-343 p 283 A95-75099
 p 301 N95-23179
 NAG1-928 p 316 N95-23670
 NAG2-561 p 285 N95-23217
 NAG2-733 p 309 N95-23183
 NAG2-881 p 275 N95-23669
 NAG3-1137 p 316 N95-24189
 NAG3-1165 p 275 N95-23462
 NAG3-1177 p 290 A95-75096
 NAG3-1273 p 289 N95-23088
 NAG3-1507 p 310 N95-23190
 NAS1-18762 p 273 N95-23095
 NAS1-19000 p 273 N95-22917
 p 273 N95-23185
 p 314 N95-23466
 NAS1-19480 p 310 N95-23257
 NAS1-19672 p 292 N95-22674
 NAS1-19703 p 296 N95-23192
 NAS3-25266 p 290 N95-24053
 NAS3-25560 p 316 N95-23792
 NAS3-26134 p 289 N95-23222
 NAS3-26309 p 309 N95-22669
 NAS3-27186 p 320 N95-23259
 p 289 N95-23550
 NAS3-27229 p 323 N95-22675
 NAS7-018 p 288 N95-22578
 NAS8-36801 p 312 N95-23438
 NAS8-38864 p 313 N95-23440
 NAS8-39131 p 300 N95-24032
 NCC1-14 p 273 N95-23193
 NCC1-24 p 273 N95-23193
 NCC2-582 p 309 N95-22481
 NGT-47-020-800 p 325 N95-23276
 NGT-50981 p 294 N95-23392
 N00019-87-C-0195 p 290 A95-75093

NSF ATMS-86-11729 p 318 A95-76394
 NSF ATMS-89-07881 p 318 A95-76394
 NSF CDR-88-03012 p 290 A95-75094
 RTOP 233-02-0A p 320 N95-23259
 RTOP 233-02-03 p 295 N95-23671
 RTOP 324-02-00 p 289 N95-23222
 RTOP 464-54-03-70 p 320 N95-23009
 RTOP 505-59-10-13 p 272 N95-22802
 RTOP 505-59-50-02 p 310 N95-23257
 RTOP 505-59-54-01 p 296 N95-23011
 RTOP 505-62-50 p 293 N95-22954
 RTOP 505-62-52 p 323 N95-23178
 p 296 N95-23192
 RTOP 505-63-36-06 p 285 N95-22953
 RTOP 505-63-36 p 316 N95-23792
 RTOP 505-64-30 p 284 N95-22806
 RTOP 505-64-36 p 288 N95-24030
 RTOP 505-64-52 p 309 N95-22804
 RTOP 505-68-10 p 309 N95-22669
 RTOP 505-68-30-03 p 273 N95-22917
 p 273 N95-23095
 p 273 N95-23185
 RTOP 505-68-32 p 272 N95-22666
 RTOP 505-69-10 p 284 N95-22829
 RTOP 505-69-50 p 275 N95-23462
 RTOP 505-70-62 p 274 N95-23250
 RTOP 505-90-52-01 p 314 N95-23466
 RTOP 506-40-41-02 p 309 N95-23015
 p 310 N95-23210
 RTOP 535-03-10 p 323 N95-22675
 RTOP 537-02-21 p 289 N95-23550
 RTOP 537-07-20 p 273 N95-23193
 RTOP 538-04-13-01 p 292 N95-22674
 RTOP 538-06-13 p 316 N95-24189
 W-31-109-ENG-38 p 300 N95-22764
 W-7405-ENG-36 p 324 N95-24076
 W-7405-ENG-48 p 297 N95-24019

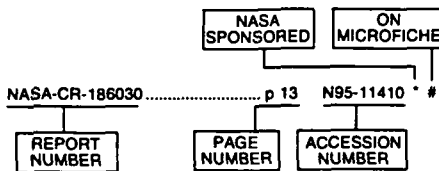
CONTRACT

REPORT NUMBER INDEX

AERONAUTICAL ENGINEERING / A Continuing Bibliography (Supplement 319)

July 1995

Typical Report Number Index Listing



Listings in this index are arranged alphanumerically by report number. The page number indicates the page on which the citation is located. The accession number denotes the number by which the citation is identified. An asterisk (*) indicates that the item is a NASA report. A pound sign (#) indicates that the item is available on microfiche.

A-94119	p 274	N95-23250	*	#
A-94141	p 288	N95-24030	*	#
A-95014	p 309	N95-22804	*	#
A-95025	p 272	N95-22666	*	#
AD-A279436	p 320	N95-23766	*	
AD-A285102	p 276	N95-23201	*	#
AD-A285118	p 300	N95-23781	*	#
AD-A285797	p 284	N95-22510	*	#
AGARD-CP-565	p 302	N95-23496	*	#
AGARD-R-809	p 315	N95-23602	*	#
AIAA PAPER 95-0560	p 314	N95-23466	*	#
AIAA PAPER 95-0752	p 309	N95-22669	*	#
AL-CF-TR-1994-0159	p 288	N95-24030	*	#
ANL/CD/CP-83462	p 300	N95-22764	*	#
AR-008-910	p 286	N95-23666	*	#
ARL-TR-518	p 285	N95-22953	*	#
ARL-TR-581	p 284	N95-22510	*	#
B-259256	p 286	N95-24091	*	#
BTN-94-EIX94371346933	p 300	A95-73345		
BTN-94-EIX94381352212	p 306	A95-74612		
BTN-94-EIX94381353142	p 306	A95-74496		
BTN-94-EIX94381353450	p 323	A95-75494		
BTN-94-EIX94381359040	p 295	A95-74554		
BTN-94-EIX94381359041	p 295	A95-74629		
BTN-94-EIX94401360022	p 306	A95-74702		
BTN-94-EIX94401363884	p 307	A95-75516		
BTN-94-EIX94401363947	p 317	A95-75532		
BTN-94-EIX94401378794	p 307	A95-76484		
BTN-94-EIX94401378820	p 307	A95-76489		
BTN-94-EIX94401378822	p 307	A95-76491		
BTN-95-EIX95142553043	p 263	A95-73465		
BTN-95-EIX95142553036	p 263	A95-73462		
BTN-95-EIX95142553037	p 263	A95-73461		
BTN-95-EIX95142553038	p 305	A95-73460		
BTN-95-EIX95142553040	p 304	A95-73458		
BTN-95-EIX95142553041	p 304	A95-73457		
BTN-95-EIX95142553044	p 304	A95-73454		
BTN-95-EIX95142553046	p 304	A95-73452		
BTN-95-EIX95142553047	p 286	A95-73451		
BTN-95-EIX95142553054	p 262	A95-73444		
BTN-95-EIX95142553057	p 262	A95-73441		
BTN-95-EIX95142555477	p 278	A95-73435		
BTN-95-EIX95142562401	p 278	A95-73433		
BTN-95-EIX95142562401	p 304	A95-73439		
BTN-95-EIX95142562402	p 286	A95-73438		

BTN-95-EIX95142562403	p 280	A95-73437	BTN-95-EIX95182619075	p 307	A95-75760
BTN-95-EIX95152569458	p 305	A95-73498	BTN-95-EIX95182619076	p 269	A95-75761
BTN-95-EIX95152577585	p 264	A95-73497	BTN-95-EIX95182619077	p 307	A95-75762
BTN-95-EIX95152577586	p 264	A95-73496	BTN-95-EIX95182619078	p 269	A95-75763
BTN-95-EIX95152577587	p 263	A95-73495	BTN-95-EIX95182619080	p 269	A95-75765
BTN-95-EIX95152577588	p 263	A95-73494	BTN-95-EIX95182619087	p 291	A95-75772
BTN-95-EIX95152577589	p 263	A95-73493	BTN-95-EIX95182619088	p 283	A95-75773
BTN-95-EIX95152577597	p 305	A95-73486	BTN-95-EIX95182619093	p 269	A95-75778
BTN-95-EIX95152577604	p 305	A95-73479	BTN-95-EIX95182619097	p 283	A95-75782
BTN-95-EIX95152577606	p 305	A95-73477	BTN-95-EIX95182619099	p 295	A95-75784
BTN-95-EIX95152577612	p 321	A95-73471	BTN-95-EIX95182619100	p 307	A95-75785
BTN-95-EIX95152582313	p 264	A95-73516	BTN-95-EIX95182619101	p 308	A95-75786
BTN-95-EIX95152582314	p 316	A95-73517	BTN-95-EIX95182619103	p 321	A95-75788
BTN-95-EIX95152582315	p 264	A95-73518	BTN-95-EIX95182619104	p 269	A95-75789
BTN-95-EIX95152582316	p 264	A95-73519	BTN-95-EIX95182619105	p 269	A95-75790
BTN-95-EIX95152582317	p 264	A95-73520	BTN-95-EIX95182619115	p 321	A95-75792
BTN-95-EIX95152582318	p 316	A95-73521	BTN-95-EIX95182619121	p 321	A95-75798
BTN-95-EIX95152582319	p 276	A95-73522	BTN-95-EIX95182619125	p 322	A95-76002
BTN-95-EIX95152582320	p 264	A95-73523	BTN-95-EIX95182619126	p 291	A95-76003
BTN-95-EIX95152582321	p 265	A95-73524	BTN-95-EIX95182619127	p 276	A95-76004
BTN-95-EIX95152582322	p 265	A95-73525	BTN-95-EIX95182619128	p 269	A95-76005
BTN-95-EIX95152582323	p 281	A95-73526	BTN-95-EIX95182619129	p 291	A95-76006
BTN-95-EIX95152582324	p 265	A95-73527	BTN-95-EIX95182619130	p 291	A95-76007
BTN-95-EIX95152582326	p 265	A95-73529	BTN-95-EIX95182619131	p 291	A95-76008
BTN-95-EIX95152582327	p 265	A95-73530	BTN-95-EIX95182619132	p 292	A95-76009
BTN-95-EIX95152582329	p 281	A95-73531	BTN-95-EIX95182619138	p 269	A95-76615
BTN-95-EIX95152582330	p 265	A95-73532	BTN-95-EIX95182619139	p 288	A95-76616
BTN-95-EIX95152582331	p 281	A95-73533	BTN-95-EIX95182619144	p 299	A95-76621
BTN-95-EIX95152582333	p 281	A95-73535	BTN-95-EIX95182619145	p 279	A95-76622
BTN-95-EIX95152582334	p 276	A95-73536	BTN-95-EIX95182619149	p 322	A95-76626
BTN-95-EIX95152582335	p 281	A95-73537	BTN-95-EIX95182619153	p 292	A95-76630
BTN-95-EIX95152582336	p 323	A95-73538	BTN-95-EIX95182619154	p 279	A95-76631
BTN-95-EIX95152582337	p 266	A95-73539	BTN-95-EIX95182619209	p 283	A95-76635
BTN-95-EIX95152582338	p 281	A95-73540	BTN-95-EIX95182619210	p 270	A95-76636
BTN-95-EIX95152582339	p 266	A95-73541	BTN-95-EIX95182619211	p 295	A95-76637
BTN-95-EIX95152582340	p 282	A95-73542	BTN-95-EIX95182619212	p 322	A95-76638
BTN-95-EIX95152582342	p 282	A95-73544	BTN-95-EIX95182619213	p 296	A95-76639
BTN-95-EIX95152582344	p 266	A95-73546	BTN-95-EIX95182619214	p 292	A95-76640
BTN-95-EIX95152582345	p 266	A95-73547	BTN-95-EIX95182619215	p 292	A95-76641
BTN-95-EIX95152582346	p 266	A95-73548	BTN-95-EIX95182619216	p 292	A95-76642
BTN-95-EIX95152582347	p 282	A95-73549	BTN-95-EIX95182619217	p 270	A95-76643
BTN-95-EIX95152583250	p 305	A95-73551	BTN-95-EIX95182619218	p 284	A95-76644
BTN-95-EIX95152583251	p 266	A95-73552	BTN-95-EIX95182619219	p 276	A95-76645
BTN-95-EIX95152583252	p 305	A95-73553	BTN-95-EIX95182619220	p 270	A95-76646
BTN-95-EIX95152583253	p 306	A95-73554	BTN-95-EIX95182619221	p 308	A95-76647
BTN-95-EIX95152583254	p 306	A95-73555	BTN-95-EIX95182619222	p 288	A95-76648
BTN-95-EIX95152583255	p 306	A95-73556	BTN-95-EIX95182619223	p 289	A95-76649
BTN-95-EIX95152583256	p 266	A95-73557	BTN-95-EIX95182619224	p 289	A95-76650
BTN-95-EIX95152583257	p 267	A95-73558	BTN-95-EIX95182619225	p 270	A95-76651
BTN-95-EIX95152583258	p 297	A95-73559	BTN-95-EIX95182619226	p 308	A95-76652
BTN-95-EIX95152583259	p 267	A95-73560	BTN-95-EIX95182619227	p 270	A95-76653
BTN-95-EIX95152583260	p 267	A95-73561	BTN-95-EIX95182619228	p 284	A95-76654
BTN-95-EIX95152583263	p 298	A95-73564	BTN-95-EIX95182619229	p 284	A95-76655
BTN-95-EIX95152583267	p 298	A95-73568	BTN-95-EIX95182619230	p 271	A95-76656
BTN-95-EIX95152583270	p 278	A95-73571	BTN-95-EIX95182619231	p 319	A95-76657
BTN-95-EIX95152583276	p 298	A95-73577	BTN-95-EIX95182619232	p 308	A95-76658
BTN-95-EIX95152583282	p 298	A95-73583	BTN-95-EIX95182619233	p 271	A95-76659
BTN-95-EIX95152583283	p 306	A95-73584	BTN-95-EIX95182619234	p 308	A95-76660
BTN-95-EIX95152583286	p 282	A95-73587	BTN-95-EIX95182619235	p 271	A95-76661
BTN-95-EIX95152584676	p 276	A95-73588	BTN-95-EIX95202637592	p 279	A95-76697
BTN-95-EIX95152584677	p 282	A95-73589	BTN-95-EIX95202637603	p 308	A95-76686
BTN-95-EIX95152584678	p 282	A95-73590	BTN-95-EIX95202637606	p 279	A95-76683
BTN-95-EIX95152584679	p 282	A95-73591	BTN-95-EIX95202637608	p 292	A95-76681
BTN-95-EIX95172595292	p 287	A95-75720	BTN-95-EIX95202637613	p 279	A95-76676
BTN-95-EIX95172595294	p 287	A95-75718	BTN-95-EIX95202638962	p 279	A95-76674
BTN-95-EIX95172595295	p 287	A95-75717	BTN-95-EIX95202638963	p 289	A95-76673
BTN-95-EIX95172595296	p 287	A95-75716	BTN-95-EIX95212641069	p 287	A95-76734
BTN-95-EIX95172595298	p 279	A95-75714	BTN-95-EIX95212641070	p 287	A95-76735
BTN-95-EIX95182617454	p 298	A95-75725	BTN-95-EIX95212641071	p 287	A95-76736
BTN-95-EIX95182617457	p 267	A95-75728	BTN-95-EIX95212641072	p 319	A95-76737
BTN-95-EIX95182617458	p 268	A95-75729	BTN-95-EIX95212645688	p 271	A95-76740
BTN-95-EIX95182617460	p 268	A95-75731	BTN-95-EIX95212645690	p 271	A95-76742
BTN-95-EIX95182617462	p 268	A95-75733	BTN-95-EIX95212645692	p 271	A95-76744
BTN-95-EIX95182617463	p 298	A95-75734	BTN-95-EIX95212645694	p 272	A95-76746
BTN-95-EIX95182617464	p 298	A95-75735	BTN-95-EIX95212645695	p 272	A95-76747
BTN-95-EIX95182617465	p 268	A95-75736	BTN-95-EIX95212645706	p 299	A95-76758
BTN-95-EIX95182617807	p 261	A95-75752	BTN-95-EIX95212645707	p 299	A95-76759
BTN-95-EIX95182617808	p 261	A95-75753	BTN-95-EIX95212645712	p 272	A95-76764
BTN-95-EIX95182617809	p 261	A95-75754	BTN-95-EIX95212645713	p 261	A95-76765
BTN-95-EIX95182617810	p 300	A95-75755			
BTN-95-EIX95182617811	p 261	A95-75756	CCMS-95-01	p 301	N95-23179 * #
BTN-95-EIX95182617812	p 288	A95-75757			
BTN-95-EIX95182619073	p 268	A95-75758	CONF-9404162-14	p 297	N95-24019 #

CONF-940440-5

CONF-940440-5 p 304 N95-23981 #
CONF-940865-4 p 300 N95-22689 #
CONF-9411142-4 p 299 N95-23532 #
CONF-941129-9 p 300 N95-22764 #
CONF-941144-14 p 324 N95-24076 #

CU-CAS-95-03 p 289 N95-23088 * #

DE94-017768 p 304 N95-23981 #
DE95-001360 p 300 N95-22689 #
DE95-002602 p 299 N95-23532 #
DE95-002988 p 300 N95-22764 #
DE95-003630 p 297 N95-24019 #
DE95-003703 p 324 N95-24076 #

DOT/FAA/AM-95/1 p 278 N95-24071 #
DOT/FAA/AM-95/4 p 280 N95-23565 #
DOT/FAA/AM-95/6 p 323 N95-23603 #
DOT/FAA/AM-95/8 p 277 N95-24024 #

DSTO-TR-0049 p 286 N95-23666 #

E-9016 p 296 N95-23192 * #
E-9207 p 262 N95-24025 * #
E-9364 p 323 N95-22675 * #
E-9421 p 293 N95-22954 * #
E-9425 p 309 N95-22669 * #
E-9489 p 320 N95-23259 * #
E-9491 p 323 N95-23178 * #
E-9493 p 289 N95-23222 * #
E-9521 p 295 N95-23671 * #
E-9530 p 289 N95-23550 * #
E-9538 p 275 N95-23462 * #
E-9552 p 316 N95-24189 * #
E-9583 p 290 N95-24053 * #
E-9589 p 316 N95-23792 * #

EOARD-TR-94-07 p 276 N95-23201 #

ESC-TR-93-293 p 300 N95-23781 #

FAA-AC-91-70 p 277 N95-24065 #

FAA-AFS-550 p 277 N95-24065 #

GAO/NSIAD-95-52 p 286 N95-24091 #

H-1984 p 284 N95-22806 * #
H-2040 p 284 N95-22829 * #

HTN-95-A0861 p 317 A95-76265 * #
HTN-95-A0862 p 318 A95-76266 * #
HTN-95-A0863 p 318 A95-76267 * #
HTN-95-11295 p 319 A95-77000 * #
HTN-95-11304 p 319 A95-77009 * #
HTN-95-20976 p 261 A95-74042 * #
HTN-95-41219 p 317 A95-75031 * #
HTN-95-41223 p 317 A95-75035 * #
HTN-95-41393 p 288 A95-76389 * #
HTN-95-41394 p 283 A95-76390 * #
HTN-95-60779 p 317 A95-75976 * #
HTN-95-80851 p 290 A95-75093 * #
HTN-95-80852 p 290 A95-75094 * #
HTN-95-80853 p 290 A95-75095 * #
HTN-95-80854 p 290 A95-75096 * #
HTN-95-80855 p 267 A95-75097 * #
HTN-95-80856 p 283 A95-75098 * #
HTN-95-80857 p 283 A95-75099 * #
HTN-95-80858 p 283 A95-75100 * #
HTN-95-80859 p 267 A95-75101 * #
HTN-95-91363 p 318 A95-76394 * #
HTN-95-91421 p 319 A95-77334 * #

ICASE-95-5 p 314 N95-23466 * #

INT-PATENT-CLASS-B64C-11/00 p 311 N95-23377 * #
INT-PATENT-CLASS-B64C-19/00 p 294 N95-23389 * #
INT-PATENT-CLASS-B64C-5/00 p 286 N95-23390 * #
INT-PATENT-CLASS-B64C-9/16 p 286 N95-23395 * #

INT-PATENT-CLASS-G08B-21/00 p 280 N95-23393 * #

ISBN-92-836-1010-5 p 315 N95-23602 #
ISBN-92-836-1011-3 p 302 N95-23496 #

L-17233 p 285 N95-22953 * #
L-17348 p 309 N95-23015 * #
L-17348 p 310 N95-23210 * #
L-17380 p 272 N95-22802 * #

LA-UR-94-3872 p 324 N95-24076 #

MIT-TR-998 p 300 N95-23781 #

NAS 1.15:106764 p 262 N95-24025 * #
NAS 1.15:106847 p 293 N95-22954 * #

NAS 1.15:106849 p 309 N95-22669 * #
NAS 1.15:106870 p 320 N95-23259 * #
NAS 1.15:106872 p 323 N95-23178 * #
NAS 1.15:106885 p 295 N95-23671 * #
NAS 1.15:106890 p 289 N95-23550 * #
NAS 1.15:108860 p 272 N95-22666 * #
NAS 1.15:109177 p 320 N95-23009 * #
NAS 1.15:109182 p 296 N95-23011 * #
NAS 1.15:4583 p 272 N95-22802 * #
NAS 1.15:4602 p 309 N95-23015 * #
NAS 1.15:4602 p 310 N95-23210 * #
NAS 1.15:4635 p 296 N95-23192 * #
NAS 1.15:4638 p 274 N95-23250 * #
NAS 1.15:4661 p 309 N95-22804 * #
NAS 1.15:4665 p 288 N95-24030 * #
NAS 1.15:4676 p 284 N95-22829 * #
NAS 1.26:189099 p 290 N95-24053 * #
NAS 1.26:189141 p 316 N95-23792 * #
NAS 1.26:189146 p 316 N95-24189 * #
NAS 1.26:194972 p 325 N95-23276 * #
NAS 1.26:195026 p 292 N95-22674 * #
NAS 1.26:195032 p 314 N95-23466 * #
NAS 1.26:195050 p 273 N95-23193 * #
NAS 1.26:195052 p 310 N95-23257 * #
NAS 1.26:195421 p 323 N95-22675 * #
NAS 1.26:195445 p 289 N95-23222 * #
NAS 1.26:195454 p 275 N95-23462 * #
NAS 1.26:196313 p 320 N95-23766 * #
NAS 1.26:197383 p 309 N95-22481 * #
NAS 1.26:197419 p 274 N95-23218 * #
NAS 1.26:197420 p 285 N95-23217 * #
NAS 1.26:197438 p 309 N95-23183 * #
NAS 1.26:197439 p 310 N95-23190 * #
NAS 1.26:197439 p 301 N95-23179 * #
NAS 1.26:197440 p 289 N95-23088 * #
NAS 1.26:197661 p 293 N95-22908 * #
NAS 1.26:197699 p 316 N95-23670 * #
NAS 1.26:197704 p 300 N95-24032 * #
NAS 1.26:197867 p 273 N95-23182 * #
NAS 1.26:197912 p 285 N95-22949 * #
NAS 1.26:197931 p 294 N95-23392 * #
NAS 1.26:197938 p 275 N95-23669 * #
NAS 1.26:197944 p 295 N95-23410 * #
NAS 1.26:4649 p 273 N95-22917 * #
NAS 1.26:4650 p 273 N95-23185 * #
NAS 1.26:4651 p 273 N95-23095 * #
NAS 1.60:3465 p 285 N95-22953 * #
NAS 1.60:3537 p 284 N95-22806 * #

NASA-CASE-ARC-11913-1 p 311 N95-23377 * #
NASA-CASE-ARC-11944-1 p 294 N95-23389 * #
NASA-CASE-ARC-11979-1 p 286 N95-23390 * #
NASA-CASE-ARC-11982-1 p 280 N95-23393 * #
NASA-CASE-ARC-11990-1 p 286 N95-23395 * #

NASA-CASE-NPO-18733-1-CU p 288 N95-22578 * #

NASA-CR-189099 p 290 N95-24053 * #
NASA-CR-189141 p 316 N95-23792 * #
NASA-CR-189146 p 316 N95-24189 * #
NASA-CR-194972 p 325 N95-23276 * #
NASA-CR-195026 p 292 N95-22674 * #
NASA-CR-195032 p 314 N95-23466 * #
NASA-CR-195050 p 273 N95-23193 * #
NASA-CR-195052 p 310 N95-23257 * #
NASA-CR-195421 p 323 N95-22675 * #
NASA-CR-195445 p 289 N95-23222 * #
NASA-CR-195454 p 275 N95-23462 * #
NASA-CR-196313 p 320 N95-23766 * #
NASA-CR-197383 p 309 N95-22481 * #
NASA-CR-197419 p 274 N95-23218 * #
NASA-CR-197420 p 285 N95-23217 * #
NASA-CR-197421 p 309 N95-23183 * #
NASA-CR-197438 p 310 N95-23190 * #
NASA-CR-197439 p 301 N95-23179 * #
NASA-CR-197440 p 289 N95-23088 * #
NASA-CR-197661 p 293 N95-22908 * #
NASA-CR-197699 p 316 N95-23670 * #
NASA-CR-197704 p 300 N95-24032 * #
NASA-CR-197867 p 273 N95-23182 * #
NASA-CR-197912 p 285 N95-22949 * #
NASA-CR-197931 p 294 N95-23392 * #
NASA-CR-197938 p 275 N95-23669 * #
NASA-CR-197944 p 295 N95-23410 * #
NASA-CR-4649 p 273 N95-22917 * #
NASA-CR-4650 p 273 N95-23185 * #
NASA-CR-4651 p 273 N95-23095 * #

NASA-TM-106764 p 262 N95-24025 * #
NASA-TM-106847 p 293 N95-22954 * #
NASA-TM-106849 p 309 N95-22669 * #
NASA-TM-106870 p 320 N95-23259 * #
NASA-TM-106872 p 323 N95-23178 * #
NASA-TM-106885 p 295 N95-23671 * #
NASA-TM-106890 p 289 N95-23550 * #
NASA-TM-108860 p 272 N95-22666 * #

NASA-TM-109177 p 320 N95-23009 * #
NASA-TM-109182 p 296 N95-23011 * #
NASA-TM-4583 p 272 N95-22802 * #
NASA-TM-4602 p 309 N95-23015 * #
NASA-TM-4602 p 310 N95-23210 * #
NASA-TM-4635 p 296 N95-23192 * #
NASA-TM-4638 p 274 N95-23250 * #
NASA-TM-4661 p 309 N95-22804 * #
NASA-TM-4665 p 288 N95-24030 * #
NASA-TM-4676 p 284 N95-22829 * #

NASA-TP-3465 p 285 N95-22953 * #
NASA-TP-3537 p 284 N95-22806 * #

NAWCADPAX-95-10-RTR p 288 N95-24030 * #

NIAR-94-11 p 277 N95-24012 #
NIAR-94-3 p 277 N95-24050 #

NLR-TP-93109-U p 285 N95-23161 #

NTSB/AAR-95/01 p 277 N95-23609 #

NTSB/RP-94/01-VOL-1 p 278 N95-24105 #
NTSB/RP-94/02-VOL-2 p 277 N95-23598 #

PB94-917005 p 278 N95-24105 #
PB94-917007 p 277 N95-23598 #
PB95-136032 p 324 N95-23168 #
PB95-139184 p 285 N95-23161 #
PB95-910401 p 277 N95-23609 #

SAND-94-2746C p 299 N95-23532 #

TAE-698 p 316 N95-23662 #

TII-R9201-001-RD p 316 N95-23792 * #

TR-112894-3570P p 316 N95-23670 * #
TR-94-A-019 p 288 N95-24030 * #

UCRL-JC-118476 p 297 N95-24019 #

US-PATENT-APPL-SN-014581 p 286 N95-23395 * #
US-PATENT-APPL-SN-014584 p 286 N95-23390 * #
US-PATENT-APPL-SN-056503 p 288 N95-22578 * #
US-PATENT-APPL-SN-689347 p 294 N95-23389 * #
US-PATENT-APPL-SN-926117 p 311 N95-23377 * #
US-PATENT-APPL-SN-935939 p 280 N95-23393 * #

US-PATENT-CLASS-244-182 p 294 N95-23389 * #
US-PATENT-CLASS-244-199 p 286 N95-23390 * #
US-PATENT-CLASS-244-215 p 286 N95-23395 * #
US-PATENT-CLASS-244-216 p 286 N95-23395 * #
US-PATENT-CLASS-244-51 p 294 N95-23389 * #
US-PATENT-CLASS-244-7R p 294 N95-23389 * #
US-PATENT-CLASS-244-75R p 294 N95-23389 * #
US-PATENT-CLASS-244-75R p 286 N95-23390 * #
US-PATENT-CLASS-340-946 p 280 N95-23393 * #
US-PATENT-CLASS-340-953 p 280 N95-23393 * #
US-PATENT-CLASS-340-961 p 280 N95-23393 * #
US-PATENT-CLASS-340-981 p 280 N95-23393 * #
US-PATENT-CLASS-345-8 p 288 N95-22578 * #
US-PATENT-CLASS-362-62 p 280 N95-23393 * #
US-PATENT-CLASS-364-578 p 288 N95-22578 * #
US-PATENT-CLASS-395-152 p 288 N95-22578 * #
US-PATENT-CLASS-416-34 p 311 N95-23377 * #
US-PATENT-CLASS-416-61 p 311 N95-23377 * #
US-PATENT-CLASS-434-307R p 288 N95-22578 * #
US-PATENT-CLASS-434-372 p 288 N95-22578 * #
US-PATENT-CLASS-434-38 p 288 N95-22578 * #
US-PATENT-CLASS-434-43 p 288 N95-22578 * #
US-PATENT-CLASS-73-178H p 280 N95-23393 * #

US-PATENT-5.294.080 p 286 N95-23395 * #
US-PATENT-5.315.296 p 280 N95-23393 * #
US-PATENT-5.326.050 p 286 N95-23390 * #
US-PATENT-5.330.131 p 294 N95-23389 * #
US-PATENT-5.352.090 p 311 N95-23377 * #
US-PATENT-5.388.990 p 288 N95-22578 * #

VPI-E-94-09 p 301 N95-23179 * #

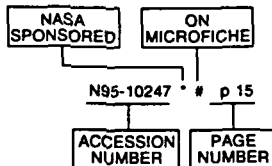
WHOI-93-29 p 320 N95-23766 *

ACCESSION NUMBER INDEX

AERONAUTICAL ENGINEERING / A Continuing Bibliography (Supplement 319)

July 1995

Typical Accession Number Index Listing



Listings in this index are arranged alphanumerically by accession number. The page number indicates the page on which the citation is located. The accession number denotes the number by which the citation is identified. An asterisk (*) indicates that the item is a NASA report. A pound sign (#) indicates that the item is available on microfiche.

A95-73345	p 300	A95-73548	p 266
A95-73433	p 278	A95-73549	p 282
A95-73435	p 278	A95-73551	p 305
A95-73437	p 280	A95-73552	p 266
A95-73438	p 286	A95-73553	p 305
A95-73439	p 304	A95-73554	p 306
A95-73441	p 262	A95-73555	p 306
A95-73444	p 262	A95-73556	p 306
A95-73451	p 286	A95-73557	p 266
A95-73452	p 304	A95-73558	p 267
A95-73454	p 304	A95-73559	p 297
A95-73457	p 304	A95-73560	p 267
A95-73458	p 304	A95-73561	p 267
A95-73460	p 305	A95-73564	p 298
A95-73461	p 263	A95-73568	p 298
A95-73462	p 263	A95-73571	p 278
A95-73465	p 263	A95-73577	p 298
A95-73471	p 321	A95-73583	p 298
A95-73477	p 305	A95-73584	p 306
A95-73479	p 305	A95-73587	p 282
A95-73486	p 305	A95-73588	p 276
A95-73493	p 263	A95-73589	p 282
A95-73494	p 263	A95-73590	p 282
A95-73495	p 263	A95-73591	p 282
A95-73496	p 264	A95-74042	p 261
A95-73497	p 264	A95-74496	p 306
A95-73498	p 305	A95-74554	p 295
A95-73516	p 264	A95-74612	p 306
A95-73517	p 316	A95-74629	p 295
A95-73518	p 264	A95-74702	p 306
A95-73519	p 264	A95-75031	p 317
A95-73520	p 264	A95-75035	p 317
A95-73521	p 316	A95-75093	p 290
A95-73522	p 276	A95-75094	p 290
A95-73523	p 264	A95-75095	p 290
A95-73524	p 265	A95-75096	p 290
A95-73525	p 265	A95-75097	p 267
A95-73526	p 281	A95-75098	p 283
A95-73527	p 265	A95-75099	p 283
A95-73529	p 265	A95-75100	p 283
A95-73530	p 265	A95-75101	p 267
A95-73531	p 281	A95-75494	p 323
A95-73532	p 265	A95-75516	p 307
A95-73533	p 281	A95-75532	p 317
A95-73535	p 281	A95-75714	p 279
A95-73536	p 276	A95-75716	p 287
A95-73537	p 281	A95-75717	p 287
A95-73538	p 323	A95-75718	p 287
A95-73539	p 266	A95-75720	p 287
A95-73540	p 281	A95-75725	p 298
A95-73541	p 266	A95-75728	p 267
A95-73542	p 282	A95-75729	p 268
A95-73544	p 282	A95-75731	p 268
A95-73546	p 266	A95-75733	p 268
A95-73547	p 266	A95-75734	p 298

A95-75735	p 298	A95-76686	p 308
A95-75736	p 268	A95-76697	p 279
A95-75752	p 261	A95-76734	p 287
A95-75753	p 261	A95-76735	p 287
A95-75754	p 261	A95-76736	p 287
A95-75755	p 300	A95-76737	p 319
A95-75756	p 261	A95-76740	p 271
A95-75757	p 288	A95-76742	p 271
A95-75758	p 268	A95-76744	p 271
A95-75760	p 307	A95-76746	p 272
A95-75761	p 269	A95-76747	p 272
A95-75762	p 307	A95-76758	p 299
A95-75763	p 269	A95-76759	p 299
A95-75765	p 269	A95-76764	p 272
A95-75772	p 291	A95-76765	p 261
A95-75773	p 283	A95-77000	p 319
A95-75778	p 269	A95-77009	p 319
A95-75976	p 317	A95-77334	p 319
A95-76265	p 317		
A95-76266	p 318	N95-22481	# p 309
A95-76267	p 318	N95-22510	# p 284
A95-76389	p 288	N95-22578	# p 288
A95-76390	p 283	N95-22666	# p 272
A95-76394	p 318	N95-22669	# p 309
A95-76484	p 307	N95-22674	# p 292
A95-76489	p 307	N95-22675	# p 323
A95-76491	p 307	N95-22689	# p 300
A95-76582	p 283	N95-22764	# p 300
A95-76584	p 295	N95-22802	# p 272
A95-76585	p 307	N95-22804	# p 309
A95-76586	p 308	N95-22806	# p 284
A95-76588	p 321	N95-22829	# p 284
A95-76589	p 269	N95-22908	# p 293
A95-76590	p 269	N95-22917	# p 273
A95-76592	p 321	N95-22949	# p 285
A95-76598	p 321	N95-22953	# p 285
A95-76602	p 322	N95-22954	# p 293
A95-76603	p 291	N95-23009	# p 320
A95-76604	p 276	N95-23011	# p 296
A95-76605	p 269	N95-23015	# p 309
A95-76606	p 291	N95-23031	# p 301
A95-76607	p 291	N95-23038	# p 301
A95-76608	p 291	N95-23088	# p 289
A95-76609	p 292	N95-23095	# p 273
A95-76615	p 269	N95-23161	# p 285
A95-76616	p 288	N95-23168	# p 324
A95-76621	p 299	N95-23178	# p 323
A95-76622	p 279	N95-23179	# p 301
A95-76626	p 322	N95-23182	# p 273
A95-76630	p 292	N95-23183	# p 309
A95-76631	p 279	N95-23185	# p 273
A95-76635	p 283	N95-23190	# p 310
A95-76636	p 270	N95-23192	# p 296
A95-76637	p 295	N95-23193	# p 273
A95-76638	p 322	N95-23201	# p 276
A95-76639	p 296	N95-23210	# p 310
A95-76640	p 292	N95-23217	# p 285
A95-76641	p 292	N95-23218	# p 274
A95-76642	p 292	N95-23222	# p 289
A95-76643	p 270	N95-23250	# p 274
A95-76644	p 284	N95-23257	# p 310
A95-76645	p 276	N95-23259	# p 320
A95-76646	p 270	N95-23276	# p 325
A95-76647	p 308	N95-23277	# p 301
A95-76648	p 288	N95-23283	# p 274
A95-76649	p 289	N95-23284	# p 324
A95-76650	p 289	N95-23287	# p 310
A95-76651	p 270	N95-23290	# p 310
A95-76652	p 308	N95-23294	# p 274
A95-76653	p 270	N95-23297	# p 293
A95-76654	p 284	N95-23299	# p 296
A95-76655	p 284	N95-23300	# p 301
A95-76656	p 271	N95-23304	# p 297
A95-76657	p 319	N95-23308	# p 322
A95-76658	p 308	N95-23309	# p 297
A95-76659	p 271	N95-23311	# p 311
A95-76660	p 308	N95-23314	# p 293
A95-76661	p 271	N95-23317	# p 285
A95-76673	p 289	N95-23318	# p 280
A95-76674	p 279	N95-23319	# p 294
A95-76676	p 279	N95-23320	# p 324
A95-76681	p 292	N95-23325	# p 294
A95-76683	p 279	N95-23333	# p 275

A95-76686	p 308	N95-23377	# p 311
A95-76697	p 279	N95-23389	# p 294
A95-76734	p 287	N95-23390	# p 286
A95-76735	p 287	N95-23392	# p 294
A95-76736	p 287	N95-23393	# p 280
A95-76737	p 319	N95-23395	# p 286
A95-76740	p 271	N95-23410	# p 295
A95-76742	p 271	N95-23419	# p 322
A95-76744	p 271	N95-23423	# p 311
A95-76746	p 272	N95-23425	# p 312
A95-76747	p 272	N95-23429	# p 312
A95-76758	p 299	N95-23435	# p 312
A95-76759	p 299	N95-23436	# p 312
A95-76764	p 272	N95-23438	# p 312
A95-76765	p 261	N95-23440	# p 313
A95-77000	p 319	N95-23444	# p 313
A95-77009	p 319	N95-23446	# p 313
A95-77334	p 319	N95-23447	# p 314
		N95-23462	# p 275
		N95-23466	# p 314
		N95-23496	# p 302
		N95-23497	# p 302
		N95-23500	# p 302
		N95-23503	# p 323
		N95-23505	# p 314
		N95-23506	# p 262
		N95-23507	# p 315
		N95-23508	# p 302
		N95-23509	# p 302
		N95-23510	# p 303
		N95-23512	# p 315
		N95-23513	# p 303
		N95-23515	# p 303
		N95-23516	# p 303
		N95-23517	# p 303
		N95-23518	# p 303
		N95-23519	# p 262
		N95-23532	# p 299
		N95-23550	# p 289
		N95-23565	# p 280
		N95-23598	# p 277
		N95-23602	# p 315
		N95-23603	# p 323
		N95-23609	# p 277
		N95-23630	# p 315
		N95-23652	# p 315
		N95-23662	# p 316
		N95-23666	# p 286
		N95-23669	# p 275
		N95-23670	# p 316
		N95-23671	# p 295
		N95-23761	# p 299
		N95-23766	# p 320
		N95-23781	# p 300
		N95-23792	# p 316
		N95-23872	# p 325
		N95-23940	# p 320
		N95-23947	# p 320
		N95-23948	# p 321
		N95-23981	# p 304
		N95-24012	# p 277
		N95-24019	# p 297
		N95-24024	# p 277
		N95-24025	# p 262
		N95-24030	# p 288
		N95-24032	# p 300
		N95-24050	# p 277
		N95-24053	# p 290
		N95-24065	# p 277
		N95-24071	# p 278
		N95-24076	# p 324
		N95-24091	# p 286
		N95-24105	# p 278
		N95-24189	# p 316

ACCESSION

AVAILABILITY OF CITED PUBLICATIONS

OPEN LITERATURE ENTRIES (A95-60000 Series)

Inquiries and requests should be addressed to NASA Center for AeroSpace Information, 800 Elkridge Landing Road, Linthicum Heights, MD 21090-2934. Orders are also taken by telephone, (301) 621-0390, e-mail, help@sti.nasa.gov, and fax, (301) 621-0134. Please refer to the accession number when requesting publications.

STAR ENTRIES (N95-10000 Series)

One or more sources from which a document announced in *STAR* is available to the public is ordinarily given on the last line of the citation. The most commonly indicated sources and their acronyms or abbreviations are listed below, and their addresses are listed on page APP-3. If the publication is available from a source other than those listed, the publisher and his address will be displayed on the availability line or in combination with the corporate source line.

Avail: CASI. Sold by the NASA Center for AeroSpace Information. Prices for hard copy (HC) and microfiche (MF) are indicated by a price code following the letters HC or MF in the *STAR* citation. Current values for the price codes are given in the tables on page APP-5.

NOTE ON ORDERING DOCUMENTS: When ordering publications from NASA CASI, use the N accession number or other report number. It is also advisable to cite the title and other bibliographic identification.

Avail: SOD (or GPO). Sold by the Superintendent of Documents, U.S. Government Printing Office, in hard copy.

Avail: BLL (formerly NLL): British Library Lending Division, Boston Spa, Wetherby, Yorkshire, England. Photocopies available from this organization at the price shown. (If none is given, inquiry should be addressed to the BLL.)

Avail: DOE Depository Libraries. Organizations in U.S. cities and abroad that maintain collections of Department of Energy reports, usually in microfiche form, are listed in *Energy Research Abstracts*. Services available from the DOE and its depositories are described in a booklet, *DOE Technical Information Center - Its Functions and Services* (TID-4660), which may be obtained without charge from the DOE Technical Information Center.

Avail: ESDU. Pricing information on specific data, computer programs, and details on Engineering Sciences Data Unit (ESDU) topic categories can be obtained from ESDU International Ltd. Requesters in North America should use the Virginia address while all other requesters should use the London address, both of which are on page APP-3.

Avail: Fachinformationszentrum Karlsruhe. Gesellschaft für wissenschaftlich-technische Information mbH 76344 Eggenstein-Leopoldshafen, Germany.

Avail: HMSO. Publications of Her Majesty's Stationery Office are sold in the U.S. by Pendragon House, Inc. (PHI), Redwood City, CA. The U.S. price (including a service and mailing charge) is given, or a conversion table may be obtained from PHI.

Avail: Issuing Activity, or Corporate Author, or no indication of availability. Inquiries as to the availability of these documents should be addressed to the organization shown in the citation as the corporate author of the document.

Avail: NASA Public Document Rooms. Documents so indicated may be examined at or purchased from the National Aeronautics and Space Administration (JBD-4), Public Documents Room (Room 1H23), Washington, DC 20546-0001, or public document rooms located at NASA installations, and the NASA Pasadena Office at the Jet Propulsion Laboratory.

Avail: NTIS. Sold by the National Technical Information Service. Initially distributed microfiche under the NTIS SRIM (Selected Research in Microfiche) are available. For information concerning this service, consult the NTIS Subscription Section, Springfield, VA 22161.

Avail: Univ. Microfilms. Documents so indicated are dissertations selected from *Dissertation Abstracts* and are sold by University Microfilms as xerographic copy (HC) and microfilm. All requests should cite the author and the Order Number as they appear in the citation.

Avail: US Patent and Trademark Office. Sold by Commissioner of Patents and Trademarks, U.S. Patent and Trademark Office, at the standard price of \$1.50 each, postage free.

Avail: (US Sales Only). These foreign documents are available to users within the United States from the National Technical Information Service (NTIS). They are available to users outside the United States through the International Nuclear Information Service (INIS) representative in their country, or by applying directly to the issuing organization.

Avail: USGS. Originals of many reports from the U.S. Geological Survey, which may contain color illustrations, or otherwise may not have the quality of illustrations preserved in the microfiche or facsimile reproduction, may be examined by the public at the libraries of the USGS field offices whose addresses are listed on page APP-3. The libraries may be queried concerning the availability of specific documents and the possible utilization of local copying services, such as color reproduction.

FEDERAL DEPOSITORY LIBRARY PROGRAM

In order to provide the general public with greater access to U.S. Government publications, Congress established the Federal Depository Library Program under the Government Printing Office (GPO), with 53 regional depositories responsible for permanent retention of material, inter-library loan, and reference services. At least one copy of nearly every NASA and NASA-sponsored publication, either in printed or microfiche format, is received and retained by the 53 regional depositories. A list of the regional GPO libraries, arranged alphabetically by state, appears on the inside back cover of this issue. These libraries are *not* sales outlets. A local library can contact a regional depository to help locate specific reports, or direct contact may be made by an individual.

PUBLIC COLLECTION OF NASA DOCUMENTS

An extensive collection of NASA and NASA-sponsored publications is maintained by the British Library Lending Division, Boston Spa, Wetherby, Yorkshire, England for public access. The British Library Lending Division also has available many of the non-NASA publications cited in *STAR*. European requesters may purchase facsimile copy or microfiche of NASA and NASA-sponsored documents, those identified by both the symbols # and * from ESA — Information Retrieval Service European Space Agency, 8-10 rue Mario-Nikis, 75738 CEDEX 15, France.

STANDING ORDER SUBSCRIPTIONS

NASA SP-7037 supplements and annual index are available from the NASA Center for AeroSpace Information (CASI) on standing order subscription. Standing order subscriptions do not terminate at the end of a year, as do regular subscriptions, but continue indefinitely unless specifically terminated by the subscriber.

ADDRESSES OF ORGANIZATIONS

British Library Lending Division
Boston Spa, Wetherby, Yorkshire
England

Commissioner of Patents and Trademarks
U.S. Patent and Trademark Office
Washington, DC 20231

Department of Energy
Technical Information Center
P.O. Box 62
Oak Ridge, TN 37830

European Space Agency-
Information Retrieval Service ESRIN
Via Galileo Galilei
00044 Frascati (Rome) Italy

Engineering Sciences Data Unit International
P.O. Box 1633
Manassas, VA 22110

Engineering Sciences Data Unit
International, Ltd.
251-259 Regent Street
London, W1R 7AD, England

Fachinformationszentrum Karlsruhe
Gesellschaft für wissenschaftlich-technische
Information mbH
76344 Eggenstein-Leopoldshafen, Germany

Her Majesty's Stationery Office
P.O. Box 569, S.E. 1
London, England

NASA Center for AeroSpace Information
800 Elkridge Landing Road
Linthicum Heights, MD 21090-2934

National Aeronautics and Space Administration
Scientific and Technical Information Office
(JT)
Washington, DC 20546-0001

National Technical Information Service
5285 Port Royal Road
Springfield, VA 22161

Pendragon House, Inc.
899 Broadway Avenue
Redwood City, CA 94063

Superintendent of Documents
U.S. Government Printing Office
Washington, DC 20402

University Microfilms
A Xerox Company
300 North Zeeb Road
Ann Arbor, MI 48106

University Microfilms, Ltd.
Tylers Green
London, England

U.S. Geological Survey Library National Center
MS 950
12201 Sunrise Valley Drive
Reston, VA 22092

U.S. Geological Survey Library
2255 North Gemini Drive
Flagstaff, AZ 86001

U.S. Geological Survey
345 Middlefield Road
Menlo Park, CA 94025

U.S. Geological Survey Library
Box 25046
Denver Federal Center, MS914
Denver, CO 80225

Page Intentionally Left Blank

NASA CASI PRICE CODE TABLE

(Effective January 1, 1995)

CASI PRICE CODE	NORTH AMERICAN PRICE	FOREIGN PRICE
A01	\$ 6.00	\$ 12.00
A02	9.00	18.00
A03	17.50	35.00
A04-A05	19.50	39.00
A06-A09	27.00	54.00
A10-A13	36.50	73.00
A14-A17	44.50	89.00
A18-A21	52.00	104.00
A22-A25	61.00	122.00
A99	Call For Price	Call For Price

IMPORTANT NOTICE

For users not registered at the NASA CASI, prepayment is required. Additionally, a shipping and handling fee of \$1.00 per document for delivery within the United States and \$9.00 per document for delivery outside the United States is charged.

For users registered at the NASA CASI, document orders may be invoiced at the end of the month, charged against a deposit account, or paid by check or credit card. NASA CASI accepts American Express, Diners' Club, MasterCard, and VISA credit cards. There are no shipping and handling charges. To register at the NASA CASI, please request a registration form through the NASA Access Help Desk at the numbers or addresses below.

RETURN POLICY

Effective June 1, 1995, the NASA Center for AeroSpace Information will gladly replace or make full refund on items you have requested if we have made an error in your order, if the item is defective, or if it was received in damaged condition and you contact us within 30 days of your original request. Just contact our NASA Access Help Desk at the numbers or addresses listed below.

NASA Center for AeroSpace Information
800 Elkridge Landing Road
Linthicum Heights, MD 21090-2934
Telephone: (301) 621-0390
E-mail: help@sti.nasa.gov
Fax: (301) 621-0134

REPORT DOCUMENT PAGE

1. Report No. NASA SP-7037 (319)	2. Government Accession No.	3. Recipient's Catalog No.	
4. Title and Subtitle Aeronautical Engineering A Continuing Bibliography (Supplement 319)		5. Report Date July 1995	
		6. Performing Organization Code JT	
7. Author(s)		8. Performing Organization Report No.	
		10. Work Unit No.	
9. Performing Organization Name and Address NASA Scientific and Technical Information Office		11. Contract or Grant No.	
		13. Type of Report and Period Covered Special Publication	
12. Sponsoring Agency Name and Address National Aeronautics and Space Administration Washington, DC 20546-0001		14. Sponsoring Agency Code	
		15. Supplementary Notes	
16. Abstract This report lists 349 reports, articles and other documents recently announced in the NASA STI Database.			
17. Key Words (Suggested by Author(s)) Aeronautical Engineering Aeronautics Bibliographies		18. Distribution Statement Unclassified - Unlimited Subject Category - 01	
19. Security Classif. (of this report) Unclassified	20. Security Classif. (of this page) Unclassified	21. No. of Pages 136	22. Price A07/HC

FEDERAL REGIONAL DEPOSITORY LIBRARIES

ALABAMA

AUBURN UNIV. AT MONTGOMERY LIBRARY
Documents Dept.
7300 University Dr.
Montgomery, AL 36117-3596
(205) 244-3650 Fax: (205) 244-0678

UNIV. OF ALABAMA

Amelia Gayle Gorgas Library
Govt. Documents
P.O. Box 870266
Tuscaloosa, AL 35487-0266
(205) 348-6046 Fax: (205) 348-0760

ARIZONA

DEPT. OF LIBRARY, ARCHIVES, AND PUBLIC RECORDS
Research Division
Third Floor, State Capitol
1700 West Washington
Phoenix, AZ 85007
(602) 542-3701 Fax: (602) 542-4400

ARKANSAS

ARKANSAS STATE LIBRARY
State Library Service Section
Documents Service Section
One Capitol Mall
Little Rock, AR 72201-1014
(501) 682-2053 Fax: (501) 682-1529

CALIFORNIA

CALIFORNIA STATE LIBRARY
Govt. Publications Section
P.O. Box 942837 - 914 Capitol Mall
Sacramento, CA 94337-0091
(916) 654-0069 Fax: (916) 654-0241

COLORADO

UNIV. OF COLORADO - BOULDER
Libraries - Govt. Publications
Campus Box 184
Boulder, CO 80309-0184
(303) 492-8834 Fax: (303) 492-1881

DENVER PUBLIC LIBRARY

Govt. Publications Dept. BSG
1357 Broadway
Denver, CO 80203-2165
(303) 640-8846 Fax: (303) 640-8817

CONNECTICUT

CONNECTICUT STATE LIBRARY
231 Capitol Avenue
Hartford, CT 06106
(203) 566-4971 Fax: (203) 566-3322

FLORIDA

UNIV. OF FLORIDA LIBRARIES
Documents Dept.
240 Library West
Gainesville, FL 32611-2048
(904) 392-0366 Fax: (904) 392-7251

GEORGIA

UNIV. OF GEORGIA LIBRARIES
Govt. Documents Dept.
Jackson Street
Athens, GA 30602-1645
(706) 542-8949 Fax: (706) 542-4144

HAWAII

UNIV. OF HAWAII
Hamilton Library
Govt. Documents Collection
2550 The Mall
Honolulu, HI 96822
(808) 948-8230 Fax: (808) 956-5968

IDAHO

UNIV. OF IDAHO LIBRARY
Documents Section
Rayburn Street
Moscow, ID 83844-2353
(208) 885-6344 Fax: (208) 885-6817

ILLINOIS

ILLINOIS STATE LIBRARY
Federal Documents Dept.
300 South Second Street
Springfield, IL 62701-1796
(217) 782-7596 Fax: (217) 782-6437

INDIANA

INDIANA STATE LIBRARY
Serials/Documents Section
140 North Senate Avenue
Indianapolis, IN 46204-2296
(317) 232-3679 Fax: (317) 232-3728

IOWA

UNIV. OF IOWA LIBRARIES
Govt. Publications
Washington & Madison Streets
Iowa City, IA 52242-1166
(319) 335-5926 Fax: (319) 335-5900

KANSAS

UNIV. OF KANSAS
Govt. Documents & Maps Library
6001 Malott Hall
Lawrence, KS 66045-2800
(913) 864-4660 Fax: (913) 864-3855

KENTUCKY

UNIV. OF KENTUCKY
King Library South
Govt. Publications/Maps Dept.
Patterson Drive
Lexington, KY 40506-0039
(606) 257-3139 Fax: (606) 257-3139

LOUISIANA

LOUISIANA STATE UNIV.
Middleton Library
Govt. Documents Dept.
Baton Rouge, LA 70803-3312
(504) 388-2570 Fax: (504) 388-6992

LOUISIANA TECHNICAL UNIV.

Prescott Memorial Library
Govt. Documents Dept.
Ruston, LA 71272-0046
(318) 257-4962 Fax: (318) 257-2447

MAINE

UNIV. OF MAINE
Raymond H. Fogler Library
Govt. Documents Dept.
Orono, ME 04469-5729
(207) 581-1673 Fax: (207) 581-1653

MARYLAND

UNIV. OF MARYLAND - COLLEGE PARK
McKeldin Library
Govt. Documents/Maps Unit
College Park, MD 20742
(301) 405-9165 Fax: (301) 314-9416

MASSACHUSETTS

BOSTON PUBLIC LIBRARY
Govt. Documents
666 Boylston Street
Boston, MA 02117-0286
(617) 536-5400, ext. 226
Fax: (617) 536-7758

MICHIGAN

DETROIT PUBLIC LIBRARY
5201 Woodward Avenue
Detroit, MI 48202-4093
(313) 833-1025 Fax: (313) 833-0156

LIBRARY OF MICHIGAN

Govt. Documents Unit
P.O. Box 30007
717 West Allegan Street
Lansing, MI 48909
(517) 373-1300 Fax: (517) 373-3381

MINNESOTA

UNIV. OF MINNESOTA
Govt. Publications
409 Wilson Library
309 19th Avenue South
Minneapolis, MN 55455
(612) 624-5073 Fax: (612) 626-9353

MISSISSIPPI

UNIV. OF MISSISSIPPI
J.D. Williams Library
106 Old Gym Bldg.
University, MS 38677
(601) 232-5857 Fax: (601) 232-7465

MISSOURI

UNIV. OF MISSOURI - COLUMBIA
106B Ellis Library
Govt. Documents Sect.
Columbia, MO 65201-5149
(314) 882-6733 Fax: (314) 882-8044

MONTANA

UNIV. OF MONTANA
Mansfield Library
Documents Division
Missoula, MT 59812-1195
(406) 243-6700 Fax: (406) 243-2060

NEBRASKA

UNIV. OF NEBRASKA - LINCOLN
D.L. Love Memorial Library
Lincoln, NE 68588-0410
(402) 472-2562 Fax: (402) 472-5131

NEVADA

THE UNIV. OF NEVADA LIBRARIES
Business and Govt. Information Center
Reno, NV 89557-0044
(702) 784-6579 Fax: (702) 784-1751

NEW JERSEY

NEWARK PUBLIC LIBRARY
Science Div. - Public Access
P.O. Box 630
Five Washington Street
Newark, NJ 07101-7812
(201) 733-7782 Fax: (201) 733-5648

NEW MEXICO

UNIV. OF NEW MEXICO
General Library
Govt. Information Dept.
Albuquerque, NM 87131-1466
(505) 277-5441 Fax: (505) 277-6019

NEW MEXICO STATE LIBRARY

325 Don Gaspar Avenue
Santa Fe, NM 87503
(505) 827-3824 Fax: (505) 827-3888

NEW YORK

NEW YORK STATE LIBRARY
Cultural Education Center
Documents/Gift & Exchange Section
Empire State Plaza
Albany, NY 12230-0001
(518) 474-5355 Fax: (518) 474-5786

NORTH CAROLINA

UNIV. OF NORTH CAROLINA - CHAPEL HILL
Walter Royal Davis Library
CB 3912, Reference Dept.
Chapel Hill, NC 27514-8890
(919) 962-1151 Fax: (919) 962-4451

NORTH DAKOTA

NORTH DAKOTA STATE UNIV. LIB.
Documents
P.O. Box 5599
Fargo, ND 58105-5599
(701) 237-8886 Fax: (701) 237-7138

UNIV. OF NORTH DAKOTA

Chester Fritz Library
University Station
P.O. Box 9000 - Centennial and University Avenue
Grand Forks, ND 58202-9000
(701) 777-4632 Fax: (701) 777-3319

OHIO

STATE LIBRARY OF OHIO
Documents Dept.
65 South Front Street
Columbus, OH 43215-4163
(614) 644-7051 Fax: (614) 752-9178

OKLAHOMA

OKLAHOMA DEPT. OF LIBRARIES
U.S. Govt. Information Division
200 Northeast 18th Street
Oklahoma City, OK 73105-3298
(405) 521-2502, ext. 253
Fax: (405) 525-7804

OKLAHOMA STATE UNIV.

Edmon Low Library
Stillwater, OK 74078-0375
(405) 744-6546 Fax: (405) 744-5183

OREGON

PORTLAND STATE UNIV.
Branford P. Millar Library
934 Southwest Harrison
Portland, OR 97207-1151
(503) 725-4123 Fax: (503) 725-4524

PENNSYLVANIA

STATE LIBRARY OF PENN.
Govt. Publications Section
116 Walnut & Commonwealth Ave.
Harrisburg, PA 17105-1601
(717) 787-3752 Fax: (717) 783-2070

SOUTH CAROLINA

CLEMSON UNIV.
Robert Muldrow Cooper Library
Public Documents Unit
P.O. Box 343001
Clemson, SC 29634-3001
(803) 656-5174 Fax: (803) 656-3025

UNIV. OF SOUTH CAROLINA

Thomas Cooper Library
Green and Sumter Streets
Columbia, SC 29208
(803) 777-4841 Fax: (803) 777-9503

TENNESSEE

UNIV. OF MEMPHIS LIBRARIES
Govt. Publications Dept.
Memphis, TN 38152-0001
(901) 678-2206 Fax: (901) 678-2511

TEXAS

TEXAS STATE LIBRARY
United States Documents
P.O. Box 12927 - 1201 Brazos
Austin, TX 78701-0001
(512) 463-5455 Fax: (512) 463-5436

TEXAS TECH. UNIV. LIBRARIES

Documents Dept.
Lubbock, TX 79409-0002
(806) 742-2282 Fax: (806) 742-1920

UTAH

UTAH STATE UNIV.
Merrill Library Documents Dept.
Logan, UT 84322-3000
(801) 797-2678 Fax: (801) 797-2677

VIRGINIA

UNIV. OF VIRGINIA
Alderman Library
Govt. Documents
University Ave. & McCormick Rd.
Charlottesville, VA 22903-2498
(804) 824-3133 Fax: (804) 924-4337

WASHINGTON

WASHINGTON STATE LIBRARY
Govt. Publications
P.O. Box 42478
16th and Water Streets
Olympia, WA 98504-2478
(206) 753-4027 Fax: (206) 586-7575

WEST VIRGINIA

WEST VIRGINIA UNIV. LIBRARY
Govt. Documents Section
P.O. Box 6069 - 1549 University Ave.
Morgantown, WV 26506-6069
(304) 293-3051 Fax: (304) 293-6638

WISCONSIN

ST. HIST. SOC. OF WISCONSIN LIBRARY
Govt. Publication Section
816 State Street
Madison, WI 53706
(608) 264-6525 Fax: (608) 264-6520

MILWAUKEE PUBLIC LIBRARY

Documents Division
814 West Wisconsin Avenue
Milwaukee, WI 53233
(414) 286-3073 Fax: (414) 286-8074

National Aeronautics and
Space Administration
Code JT
Washington, DC 20546-0001

Official Business
Penalty for Private Use \$300